



Burkhard Vogel

# Balanced Phono-Amps

An Extension to the  
'The Sound of Silence' Editions



 Springer

---

## Balanced Phono-Amps

---

Burkhard Vogel

# Balanced Phono-Amps

An Extension to the ‘The Sound  
of Silence’ Editions

Burkhard Vogel  
Lab 6-11  
Stuttgart  
Germany

Additional material to this book can be downloaded from <http://extras.springer.com>.

ISBN 978-3-319-18523-1                      ISBN 978-3-319-18524-8 (eBook)  
DOI 10.1007/978-3-319-18524-8

Library of Congress Control Number: 2015940724

Springer Cham Heidelberg New York Dordrecht London  
© Springer International Publishing Switzerland 2016

This work is subject to copyright. All rights are reserved by the Publisher, whether the whole or part of the material is concerned, specifically the rights of translation, reprinting, reuse of illustrations, recitation, broadcasting, reproduction on microfilms or in any other physical way, and transmission or information storage and retrieval, electronic adaptation, computer software, or by similar or dissimilar methodology now known or hereafter developed.

The use of general descriptive names, registered names, trademarks, service marks, etc. in this publication does not imply, even in the absence of a specific statement, that such names are exempt from the relevant protective laws and regulations and therefore free for general use.

The publisher, the authors and the editors are safe to assume that the advice and information in this book are believed to be true and accurate at the date of publication. Neither the publisher nor the authors or the editors give a warranty, express or implied, with respect to the material contained herein or for any errors or omissions that may have been made.

Printed on acid-free paper

Springer International Publishing AG Switzerland is part of Springer Science+Business Media  
([www.springer.com](http://www.springer.com))

*To Beate*

---

## Preface

In 2011, the second edition of my “The Sound of Silence” (TSOS-2) book appeared on the markets. The integration of a broad range of valve solutions became the main difference to the first edition (TSOS-1). In the July/August 2014 volume of their JAES publication, the Audio Engineering Society published an article about “The Vinyl Frontier”<sup>1</sup> showing remarkable sales quantities of vinyl LPs in the UK: from 200,000 in 2009 to 780,000 in 2013. At the same time, I read in US, French and German newspapers about an equally massive sales increase. Parallel to those increase in LP sales, very interesting newly developed turntables and phono-amplifiers of all kinds of technology entered (and still do) the markets. The price range is huge too and a price of  $\geq 15,000.00$  EUR/ $\geq 18,000.00$  \$ for a phono-amp or turntable is no longer impossible. Despite the still rather small overall quantities, vinyl is back again, and it produces reasonable revenues and profits.

Having studied the above-mentioned editions of my books, the observant reader might stumble over the fact that the design of a fully balanced RIAA phono-amp is missing. Finally, in these books, all mathematical- and design-oriented efforts led to the semi-balanced “RIAA Phono-Amp Engine I” that includes different modules of solid-state and triode-driven phono-amps; the triode module in the second edition first. Semi-balanced, because Engine I offers balanced and/or un-balanced inputs, followed by an un-balanced treatment of the RIAA transfer function creation—via feedback path in the solid-state environment, via one passive network between two triode gain stages. The outputs are balanced and un-balanced too.

The content of the herewith-presented TSOS-Extension<sup>2</sup> shall fill the obvious gap. No matter whether actively or passively configured, in this book on hand, fully balanced means that each phono-amp stage ends up in a balanced—or in other words symmetrical—solution, differentially amplified. Un-balanced/single-ended intermediate solutions are not in the scope.

---

<sup>1</sup>“The Vinyl Frontier”, Francis Rumsay, JAES Vol. 62, No. 7/8.

<sup>2</sup>= TSOS-E.

There are only two exceptions with un-balanced inputs:

1. In cases of input amplifiers for MM cartridges and the MM cartridge has a connection from one of its output leads to the case (eg many Shure cartridges), and
2. In cases of turntables that offer un-balanced connectors and the user does not want to install balanced cables.

In these cases, it makes sense to integrate un-balanced-in/balanced-out gain stages via an external input.

Consequently, I call the presented rather complex phono-amp solution “RIAA Phono-Amp Engine II”. It is thus a kind of platform fulfilling a high number of design goals, focused mainly on MC cartridge usage. Among these goals, Engine II offers the following:

- Many testing possibilities of very different active and/or passive amplifier technologies and cartridge/turntable combinations.
- The selection of a simple-mode Engine II for private use or of a complete test-purpose laboratory instrument.
- A deep insight into all design matters concerning electronic noise and stage circuitry through extensive example calculations with Mathcad worksheets.

These worksheets include signal-to-noise ratio (SN) calculation approaches, and all necessary calculation aspects concerning gain, input and output resistances, and frequency and phase response-settings.

The inclusion of the TSOS-1/-2 indexes should ease follow-ups across the different books. Like in TSOS-1/-2, the lowest noise results and an excellent sound production are still on top of my efforts.

Stuttgart, Germany  
March 2015

Burkhard Vogel

---

# Contents

## Part I The RIAA Phono-Amp Engine II

<b>1</b>	<b>The Complete Engine II—Overview</b>	3
1.1	Intro and Goals	3
1.2	General Concept	5
1.3	Basic Considerations	6
1.4	Pictures of Cases and PCBs	11
1.4.1	Cases	11
1.4.2	Printed Circuit Boards	12
1.4.3	Front and Rear of the Engine	13
1.5	Power Supplies	15
1.6	Mainboard	20
<b>2</b>	<b>The Triode Driven Central Amplifier Amp3</b>	21
2.1	General Design of Amp3	21
2.2	Gain and Noise Calculations	25
2.2.1	Gain of a DIF Followed by Two CFs	25
2.2.2	RIAA Transfer Function	26
2.2.3	Noise and SN Calculations According to Fig. 1.2	27
2.2.4	A Look into the Content of MCD-WS 3.1	29
<b>3</b>	<b>Mathcad Worksheets Amp3</b>	31
3.1	MCD-WS: The Triode Gain Stage Amp3 with RIAA Networks	32
<b>4</b>	<b>The Solid-State (Op-Amp) Driven Central Amplifier Amp4</b>	49
4.1	General Design of Amp4	49
4.2	Gain and CMRR	52
4.2.1	Gain	52
4.2.2	RIAA Transfer Function	54
4.2.3	CMRR	55
4.3	Noise Calculations	56
4.3.1	Output Noise Voltage of the Amp4 Input Gain Stage (2nd in Figs. 1.2 + 4.1) with OPs 3 & 4	58



4.3.2	Output Noise Voltage of the Amp4 Output Gain Stage (3rd in Figs. 1.2 + 4.1) with OPs 5 & 6 . . . . .	59
4.3.3	Total Input and Output Noise Voltages of Amp4 . . . . .	60
4.3.4	Noise and SN Calculations According to Fig. 1.2 . . . . .	60
4.3.5	A Look into the Content of MCD-WS 5.1 . . . . .	61
4.3.6	100 % Correlated Noise Voltages of Amp4 . . . . .	62
<b>5</b>	<b>Mathcad Worksheets Amp4 . . . . .</b>	<b>65</b>
5.1	MCD-WS: The Solid-State Gain Stage Amp4 with RIAA Networks . . . . .	66
<b>6</b>	<b>The Op-Amp and Transformer Driven Output Stage Amp5 . . . . .</b>	<b>83</b>
6.1	General Design and Gain of Amp5 . . . . .	83
6.2	Power Supply . . . . .	84
6.3	CMRR and Noise . . . . .	86
6.3.1	CMRR . . . . .	86
6.3.2	Noise and SNs . . . . .	86
6.4	Additional Remarks . . . . .	89
<b>7</b>	<b>Mathcad Worksheets Amp5 . . . . .</b>	<b>91</b>
7.1	MCD-WS: The Op-Amp + Transformer Driven Output Stage Amp5 . . . . .	92
<b>8</b>	<b>The Op-Amp and Transformer Driven Input Stage Amp1 . . . . .</b>	<b>101</b>
8.1	General Design and Gain of Amp1 . . . . .	101
8.2	CMRR and Noise . . . . .	103
8.2.1	CMRR . . . . .	103
8.2.2	Noise and SNs . . . . .	104
8.3	Measurement Results . . . . .	105
8.4	Additional Remarks . . . . .	108
8.4.1	DC Servo . . . . .	108
8.4.2	Wild Oscillation . . . . .	109
<b>9</b>	<b>Mathcad Worksheets Amp1 . . . . .</b>	<b>111</b>
9.1	MCD-WS: The Transformer + Op-Amp Driven Amp1 (Real Data) . . . . .	112
9.2	MCD-WS: The Transformer + Op-Amp Driven Amp1 (Data Sheet Data) . . . . .	119
<b>10</b>	<b>The BJT and Op-Amp Driven Input Amp2 . . . . .</b>	<b>125</b>
10.1	General Design and Gain of Amp2 . . . . .	125
10.2	CMRR . . . . .	127

10.3	Noise	127
10.3.1	General Noise Aspects	127
10.3.2	The BJT Noise Model Reloaded	128
10.3.3	In Search of the Slope Figures ‘x’ (2SC3329) and ‘y’ (2SA1316)	132
10.3.4	The SN Calculation Process	137
10.3.5	Results	140
10.4	Additional Remarks	141
10.4.1	Input Resistors R2, R3, R4	141
10.4.2	Wild Oscillation	141
<b>11</b>	<b>Mathcad Worksheets Amp2</b>	<b>143</b>
11.1	MCD-WS: Evaluation of the 1/f-Noise Corner Frequency of a 2SA1316 BJT	144
11.2	MCD-WS: Evaluation of the 1/f-Noise Corner Frequency of a 2SC3329 BJT	148
11.3	MCD-WS: Amp2 SN and Gain Calculations—1/f-Noise Based Version	152
<b>12</b>	<b>Engine II Performance</b>	<b>165</b>
12.1	Visible and Audible Effects	165
12.1.1	Visible Effects	165
12.1.2	Audible Effects	167
12.1.3	Test Records	168
12.1.4	Test Noise and Source Equipment	168
12.1.5	Loudspeaker Situation and Headphones	169
12.1.6	Listening Tests	169
12.2	Measurement Results	170
12.2.1	Noise	170
12.2.2	THD and IMD Matters, Left Channel	171
12.2.3	THD and IMD Matters, Right Channel	175
12.2.4	General THD and IMD Matters	176
12.2.5	Summary Tables and Graphs	176
12.3	Conclusions and Final Remarks	180
 <b>Part II Knowledge Transfer</b>		
<b>13</b>	<b>Selection of Draft Designs of Other Input Stages</b>	<b>187</b>
13.1	Intro	187
13.2	BJT/Op-Amps Driven MC Input Stage with Un-balanced Input and Balanced Output	188
13.3	BJT/Op-Amps Driven MC Input Stage with Balanced Transformer Input and Balanced Output	189

13.4	Fully Triode Driven MC/MM Pre-Amp with Transformer MC-Input and Balanced Output . . . . .	191
13.5	Other Development Examples. . . . .	195
13.5.1	The Joachim Gerhard Approach . . . . .	195
13.5.2	The Ovidiu Popa Approach . . . . .	197
13.5.3	The Bob Cordell Approach . . . . .	199
13.6	The Output Stage . . . . .	200
13.7	Summary of Results . . . . .	201
<b>14</b>	<b>Mathcad Worksheets Draft Designs . . . . .</b>	<b>205</b>
14.1	MCD-WS: BJT/Op-Amp Driven MC Input Stage with Un-Balanced Input and Balanced Output . . . . .	206
14.2	MCD-WS: BJT/Op-Amp Driven MC Input Stage with Balanced Transformer Input and Balanced Output . . . . .	215
14.3	MCD-WS: Fully Triode Driven MC/MM Pre-Amp with Transformer MC-Input and Balanced Output. . . . .	222
<b>15</b>	<b>Measurement Tools and Trimming . . . . .</b>	<b>233</b>
15.1	Computer Test Equipment . . . . .	233
15.1.1	Intro . . . . .	233
15.1.2	Signal-to-Noise Ratio . . . . .	234
15.1.3	Distortion (THD) . . . . .	236
15.1.4	IMD . . . . .	237
15.2	The Un-Balanced to Balanced Converter UBC . . . . .	239
15.2.1	Circuit. . . . .	239
15.2.2	F & P and SN Performance . . . . .	239
15.2.3	THD Performance. . . . .	241
15.2.4	Output Resistances . . . . .	243
15.3	RIAA Encoder and Trimming . . . . .	244
15.3.1	Encoder. . . . .	244
15.3.2	Trimming Actions. . . . .	244
<b>16</b>	<b>The Very Low-Noise Balanced Measurement Amp PMMA. . . . .</b>	<b>247</b>
16.1	Intro . . . . .	247
16.2	The Input Noise Voltage Density Question . . . . .	249
16.3	The Roles of the MA Input Resistance and Input Noise Current Density . . . . .	251
16.3.1	Influence of the DUT Output Resistance . . . . .	251
16.3.2	The Input Noise Current Density Question. . . . .	252
16.3.3	Conclusions . . . . .	254
16.4	The Final PMMA . . . . .	256
16.4.1	Principal Circuit Approach. . . . .	256
16.4.2	Gain Calculations . . . . .	258
16.4.3	Noise Calculations—Rule-of-Thumb SN Calculation Approach . . . . .	260

16.4.4	Noise Calculations—Detailed SN Calculation Approach . . . . .	261
16.5	The Complete PMMA Circuit . . . . .	264
16.6	PMMA Performance . . . . .	266
16.7	Practical Issues . . . . .	268
16.7.1	Ground Loop Avoidance and CMRR of a Following Amp . . . . .	268
16.7.2	Enclosure. . . . .	269
16.7.3	Room for Improvements . . . . .	269
16.8	Recommendations . . . . .	271
16.8.1	DUT Output Resistance $\leq 10 \Omega$ . . . . .	272
16.8.2	DUT Output Resistance $> 10 \Omega$ . . . . .	272
16.8.3	Summary of Recommendations. . . . .	273
16.9	Final Notes . . . . .	273
<b>17</b>	<b>The Galvanically Isolated Measurement Amp PFMA . . . . .</b>	<b>275</b>
17.1	Intro . . . . .	275
17.2	Ground Loop Avoidance . . . . .	275
17.3	Additional PFMA Data . . . . .	277
17.4	Gain and SN Calculations . . . . .	278
17.4.1	Gains . . . . .	278
17.4.2	Evaluation of Noise Voltages and SNs . . . . .	279
17.5	Enclosure. . . . .	281
<b>18</b>	<b>Mathcad Worksheets of Measurement Tools . . . . .</b>	<b>283</b>
18.1	MCD-WS: The UBC. . . . .	284
18.2	MCD-WS: The PMMA . . . . .	290
18.3	MCD-WS: The PFMA . . . . .	302
<b>19</b>	<b>A Unique MM Phono-Amp Noise Reduction Method . . . . .</b>	<b>307</b>
19.1	Intro . . . . .	307
19.2	The Un-Balanced Noise Reduction Approach. . . . .	307
19.2.1	Basics . . . . .	307
19.2.2	The M1 ELS . . . . .	310
19.2.3	The M2 ELS . . . . .	312
19.2.4	Results . . . . .	313
19.2.5	Consequences. . . . .	313
19.3	The Balanced Noise Reduction Approach . . . . .	314
19.3.1	Basics . . . . .	314
19.3.2	Results . . . . .	317
19.3.3	Consequences. . . . .	317
19.4	SN Calculations . . . . .	317

<b>20</b>	<b>Mathcad Worksheets of the MM Noise Reduction</b> . . . . .	319
20.1	MCD-WS: The Un-Balanced Version . . . . .	320
20.2	MCD-WS: The Balanced Version . . . . .	332
<b>21</b>	<b>BJT Circuits in CE Configuration</b> . . . . .	341
21.1	Intro . . . . .	341
21.2	BJT—Bipolar Junction Transistor—Basics . . . . .	341
21.2.1	Equations for Low Frequency Small Signal Calculations . . . . .	341
21.2.2	Circuit Parameter Based Formulae . . . . .	343
21.2.3	Noise of a BJT—Frequency Independent Version . . . . .	343
21.2.4	Noise of a BJT—Frequency Dependent Version . . . . .	344
21.2.5	Noise of a Resistor R . . . . .	345
21.2.6	Noise Factor & Noise Figure . . . . .	345
21.2.7	Signal-to-Noise Ratios SN . . . . .	346
21.3	Basic (b) CE <sub>b</sub> Circuit. . . . .	346
21.3.1	Idle Gains G <sub>b</sub> and G <sub>b,rot</sub> . . . . .	347
21.3.2	G <sub>b</sub> (RL) = RL Dependent Gain G <sub>b</sub> . . . . .	347
21.3.3	Input Resistance r <sub>i</sub> (O/P Open) . . . . .	347
21.3.4	Output Resistance r <sub>o,o</sub> (I/P = Open) . . . . .	347
21.3.5	Output Resistances r <sub>o,s</sub> and r <sub>o,s,rot</sub> (I/P = Shorted) . . . . .	348
21.3.6	Operating Gains G <sub>op</sub> (R0, RL) and G <sub>ops</sub> (f, R0, RL) . . . . .	348
21.3.7	Noise—Frequency Independent Version. . . . .	349
21.3.8	Noise—Frequency Dependent Version. . . . .	351
21.4	CE Circuit CE <sub>cf</sub> with Current Feedback . . . . .	351
21.4.1	Gains G <sub>cf</sub> and G <sub>cf,rot</sub> . . . . .	351
21.4.2	Input Resistances r <sub>i</sub> and r <sub>i,rot</sub> (O/P Open) . . . . .	352
21.4.3	Output Resistances r <sub>o,o</sub> and r <sub>o,o,rot</sub> (I/P = Open) . . . . .	353
21.4.4	Output Resistances r <sub>o,s</sub> and r <sub>o,s,rot</sub> (I/P = Shorted) . . . . .	353
21.4.5	Operating Gains G <sub>op</sub> (R0, RL) and G <sub>ops</sub> (f, R0, RL) . . . . .	353
21.4.6	Noise and SN. . . . .	355
21.5	CE Type 2 Circuit CE <sub>vcf2</sub> with Voltage Feedback and Current Feedback . . . . .	356
21.5.1	Gain G <sub>vcf2</sub> . . . . .	356
21.5.2	Input Resistance r <sub>i</sub> (O/P Open) . . . . .	357
21.5.3	Output Resistance r <sub>o,s</sub> (I/P Shorted) . . . . .	357
21.5.4	Output Resistance r <sub>o,o</sub> (I/P Open) . . . . .	358
21.5.5	Other Equations . . . . .	358
21.5.6	Noise and SN. . . . .	358
21.6	Correction of a TSOS-1 and TSOS-2 Gain Result. . . . .	359
21.7	The CE in Series Configuration with an Op-Amp . . . . .	360
21.7.1	Basics . . . . .	360
21.7.2	Noise and SN. . . . .	361

<b>22</b>	<b>Differential (DIF) Amps</b> . . . . .	365
22.1	Intro . . . . .	365
22.2	The DIFA-OPA . . . . .	366
22.2.1	Basics . . . . .	366
22.2.2	Noise Calculations Version 1 . . . . .	367
22.2.3	Noise Calculations Version 2 . . . . .	368
22.2.4	Noise Calculations Version with One Input Lead Grounded. . . . .	370
22.3	The DIFA-IC . . . . .	370
22.3.1	Basics . . . . .	370
22.3.2	Noise Calculations Version 1 . . . . .	371
22.3.3	Noise Calculations Version 2 . . . . .	372
<b>23</b>	<b>Mathcad Worksheets of DIF Amps</b> . . . . .	375
23.1	MCD-WS: DIFA-OPA . . . . .	376
23.2	MCD-WS: DIFA-IC . . . . .	380
<b>24</b>	<b>Old Stuff?</b> . . . . .	385
24.1	Intro . . . . .	385
24.2	The BRAUN Tracking Force Measurement Instrument . . . . .	387
24.3	Professional Test and Calibration Records . . . . .	387
24.4	Final Note . . . . .	390
	<b>Appendix 1: List of Mathcad Worksheets</b> . . . . .	391
	<b>Appendix 2: Useful Literature and Web Sites</b> . . . . .	393
	<b>Index TSOS-1</b> . . . . .	397
	<b>Index TSOS-2</b> . . . . .	403
	<b>Index TSOS-E</b> . . . . .	415

---

# Abbreviations and Symbols

(Expanded by the ones of TSOS-1 and TSOS-2)

A	Appendix
A	Amplitude (eg in an FFT diagram)
$\hat{A}$	Peak voltage of a voltage A
(A)	A-weighting (eg in dBV(A))
a	A-weighted (subscript)
a	Valve anode or plate
AC	Alternating current
ADC	Analog–digital converter
AES	Audio Engineering Society
Amp	Amplifier
amp	Amplifier (subscript)
ampx	Amplifier x
arm	Average metre reading
ass	Assuming (subscript)
b	Bypassed (subscript)
b	Balanced (subscript)
b	BJT base (subscript)
b'	BJT internal base (subscript)
$\beta$	Auxiliary symbol for the ratio of resistances
B	Bandwidth (in general)
B	BJT base
BE	Subscript of a resistance R formed by $BE = r_{bb}    RE$
BJT	Bipolar junction transistor
BNC	Standardised high-frequency connection system
boost	Booster
bp	Band-pass filter
BTFMI	BRAUN tracking force measurement instrument
Butt	Butterworth
bv	Big volume
C	BJT collector
c	BJT internal collector (subscript)
C	Capacitance or capacitor

---

c	Corner (subscript)
c	Valve cathode (also as subscript)
ca	Contribution allowed
calc	Calculated (subscript)
$C_c$	Cathode capacitance
CCA	CCS with CCG as anode load (also as subscript)
CCG	Constant current generator (also as subscript)
CCIR	Comité Consultatif International des Radiocommunications (became later-on ITU-R)
CCS	Common cathode gain stage (also as subscript)
CE	Common emitter configuration
CF	Cathode follower (also as subscript)
cf	Corner frequency
CGS	Common gate gain-stage (also as subscript)
Cheb	Chebyshev
Cinch	Audio connection system (equivalent to the RCA system)
CMRR	Common mode rejection ratio
$CMRR_c$	CMRR in [dB]
CMS	Computer (based) measurement system
c1	Proportional factor for RIAA network-type (E) calculations
D	FET drain
d	Decade (calculation of resistor excess noise)
dB	Decibel
DA	Digital-to-Analog
DC	Direct current
DCS	DC servo
dcs	DC servo (subscript)
DDR	Deutsche Demokratische Republik (see GDR, disappeared 1989)
dif	Differential (subscript)
diff	Difference, different
DIFA	Differential gain-stage
DIFA	Fully differential amplifier
DIN	Deutsche Industrie Norm (German Industrial Standard)
D/S	Douglas Self (author)
d.u.t.	Device under test
DUT	Device under test
dx	Distortion harmonic number x (subscript)
e	BJT internal emitter (subscript)
e	Noise voltage
e	$20 \cdot \log(xyz)$ (subscript)
E	BJT emitter
ein	Equivalent input noise voltage density
EIN	Equivalent rms input voltage
ENB	Equivalent noise bandwidth
ENCD	Equivalent noise current density



ENVD	Equivalent noise voltage density
eon	Output noise voltage density
EON	Output rms noise voltage
EU	Europe, European
EW	Electronics World (magazine)
EW&WW	Electronics World and Wireless World (older version of EW)
ex	Excess noise voltage (subscript)
ex	Excluding rumble (subscript)
f	Frequency
$f_c$	Corner frequency (eg $f_{c,e}$ = noise voltage based, $f_{c,i}$ = noise current based)
F	Frequency response
$F_c$	Worsening factor based on the low-frequency noise corner frequency
FET	Field-effect transistor
ffm	Frankfurt/Main (German financial hub)
FFT	Fast Fourier Transformation
Fig	Figure
FM	Flank modulation
$F_s$	FFT size
$f_s$	Sample rate
G	FET gate
G	Gain
g	Valve grid
$G_b$	Gain of the bypassed gain-stage
GDR	German democratic republic (disappeared 1989)
$g_m$	Mutual conductance
$G_0$	Idle gain
$G_u$	Gain of the un-bypassed gain-stage
$G_x$	Gain of stage x
HF	Hum figure
$h_{FE}$	BJT DC current gain
H&N	Hum and noise
HP	Unit width (of a 19" case)
hp	High-pass filter
HTGG-2	How to Gain Gain, 2nd ed
HU	Unit height (of a 19" case)
Hz	hertz = cycles per second (cps)
I	DC current
$I_a$	Anode DC current
i	AC current
i	in (subscript)
IC	Integrated circuit, also specifying a DIFA
$I_c$	Cathode DC current
id	Ideal
iL	Input load (subscript)

IMD	Intermodulation distortion
in	eg with $R_{in}$ = input resistance
i/p	Input
IN	Input load
ISCE	Institute of sound and communications engineers, UK
ITU-R	International Telecommunication Union—ITU Radiocommunication Sector (formerly CCIT and CCIR)
J	Jack
JAES	Journal of the Audio Engineering Society
JFET	Junction field-effect transistor
Jmp	Jumper (incl. header)
JT	Jensen transformers
K	Kelvin [K]
k	Boltzmann's constant
k	Kilo
L	Inductance
L	Left channel
L	Load (subscript)
lat.mod	Lateral modulated (subscript)
LB	TR of the ex-GDR
lin	Linear
LL	Lundahl
LM	Lateral modulation
log	Logarithmic
LP	Long play vinyl record
lp	Low-pass filter
LTE	Letter to the editor
LTP	Long-tailed pair
lv	Low volume
m	Measured (subscript)
m	Subscript of mutual conductance
MA	Measurement amplifier
MC	Moving coil (cartridge)
M/C	Motchenbacher/Connelly (authors)
MCD	Mathcad
mcd	Mathcad
meas	Measured (subscript)
MM	Moving magnet (cartridge)
mr	Metre reading (subscript)
MS	Measurement system
MSR	Maxi single vinyl record
N	Noise (as subscript mostly used to express "in $B_{20k}$ ")
N	Noise gain (subscript)
N	Noise of a valve (subscript of noise resistance)
n	Noise (as subscript mostly used to express "in $B_1$ ")

n	NPN (subscript)
n	Secondary trafo turns divided by primary turns, thus, tr becomes 1:n
$N_{fc}$	Nyquist frequency
NAB	National Association of Radio and Television Broadcasters (ex NARTB = a US organisation)
NCD	Noise current density
ne	Non-equalised (subscript)
NF	Noise factor
$NF_e$	Noise figure ( $20\log(NF)$ )
NI	Current noise index of resistors
NL	Noise level
nom	Nominal (subscript)
NVD	Noise voltage density
o	Out (also as subscript)
ocm	Common mode pin of DIFA-ICs
OP	Op-amp
op	Op-amp (subscript)
o/p	Output
OPA	Op-amp (also specifying a DIFA)
ops	Operating (subscript)
P	Phase response
P	Potentiometer
p	Peak (subscript)
p	Pentode (subscript)
p	PNP (subscript)
p	ponderé = weighted (subscript)
PA	Power amp
pa	Power amp (subscript)
par	Parallel
PFMA	Galvanically isolated measurement amp
pham	Valve phono-amp
PL	Plug
PMMA	Fully balanced measurement amp
ppa	Pre-preamp
Prof.	German title for a university professor
PSU	Power supply unit
q	Quasi peak (subscript)
R	Resistance or resistor (equivalent unit symbol for ohm [ $\Omega$ ])
R	Right channel
$R_a$	Anode resistor
$r_a$	Internal valve anode resistance
$r_{bb'}$	BJT base spreading resistance ( $r_{bb'}$ on MCD worksheets)
$r_c$	Internal valve cathode resistance
rc	Real case (subscript)
$R_c$	Cathode resistor

RCA	see Cinch
re	Real
real	Real (subscript)
ref	Reference, referenced to
Rel	Relay
res	Resolution (subscript)
Rf	Feedback resistance
RG	Gain setting resistance in DIFAs
R <sub>g</sub>	Bias setting grid resistor
R <sub>gg</sub>	Oscillation preventing grid resistor
RIAA	Radio Industry Association of America, a standard setting US organisation
riaa	dto. as subscript
rms	Root mean square (subscript)
r <sub>N</sub>	Valve (tube) equivalent noise resistance (white noise only) (also as subscript)
r <sub>Nc</sub>	Average equivalent noise resistance in a certain bandwidth that includes the valve's low-frequency noise (also as subscript)
R <sub>o</sub>	Output resistance
rot	Rule of thumb (subscript)
RP	Paralleled resistors
rpm	Rotations per minute
rt	Root
r1	Proportional factor for RIAA network-type (E) calculations
S	Sample (subscript)
S	S-filter (special noise measurement hp-filter)
S	Siemens
S	Source (subscript)
S	Source of a FET
s	Second
sec	Secondary
seq	Sequence or sequential
ser	Serial
SN	Signal-to-noise ratio
SN <sub>a</sub>	Improvement of white noise after A-weighting (-2.046 dB in B <sub>20k</sub> )
SN <sub>a</sub>	SN of a noise voltage after A-weighting
SN <sub>ar</sub>	Improvement of white noise after A-weighting and RIAA equalising (-7.935 dB in B <sub>20k</sub> )
SN <sub>ariaa</sub>	SN of a noise voltage after RIAA equalisation and A-weighting
SN <sub>ne</sub>	SN non-equalised and non-weighted
SN <sub>r</sub>	Improvement of white noise after RIAA equalising (-3.646 dB in B <sub>20k</sub> )
SN <sub>ra</sub>	Improvement of an RIAA equalised noise voltage after A-weighting (-4.289 dB in B <sub>20k</sub> = SN <sub>ar</sub> - SN <sub>r</sub> )
SN <sub>riaa</sub>	SN of a noise voltage after RIAA equalisation

SN <sub>sriaa</sub>	SN of a noise voltage after RIAA equalisation and S-weighting
sol	Solution
SR	Single vinyl record
SRPP	Shunt regulated push-pull
sst	Schallplatten-Schnitt (vinyl cut)
succ-app(s)	Successive approximation(s)
Sx	Switch number x
T	Transfer function
t	Triode (subscript)
T-BNC	BNC-based connection system for shielded twisted or paralleled wires
TC	Test and calibration
TCR	Test and calibration record
THD	Total harmonic distortion
tot	Total (subscript)
TR	Test record
tr	Transformer turns ratio (eg: 3:11)
trafo	Transformer
T/S	Tietze/Schenk (authors)
TSOS-1	The sound of silence, 1st ed
TSOS-2	The sound of silence, 2nd ed
TSOS-E	Balanced phono-amps, 1st ed. (E stands for extension to ....)
TSR	TC records 1005 and 1007
TT	Test terminal
Tx	Time constant x
u	Un-bypassed (subscript)
UBC	Un-balanced to balanced converter
ub	Un-balanced (subscript)
u0	Source signal voltage
v	Signal voltage
V <sub>a</sub>	Anode DC voltage between anode and cathode
V <sub>A</sub>	Early voltage
V <sub>c</sub>	Cathode DC voltage between cathode and ground or cold end of the grid resistor
V <sub>cc</sub>	DC supply voltage positive
V <sub>DC</sub>	DC voltage
V <sub>ee</sub>	DC supply voltage negative
VC-A	Voltage-to-current-amp
ver.mod	Vertical modulated (subscript)
VM	Vertical modulation
VR	Vinyl record
VV-A	Voltage-to-voltage-amp
Vx	Amplifying stage or device x
v0	Source signal voltage
WF <sub>c</sub>	SN worsening figure based on the 1/f-noise corner frequency

---

wn	White noise region (subscript)
WW	Wireless World (oldest version of EW magazine)
wyciwym	What you calculate is what you measure
$W_z$	SN worsening factor based on operating point setting components
$W_{z,e}$	SN worsening figure
x	BJT (NPN) noise current 1/f-noise slope power figure
XLR	Standardised balanced connection system
y	BJT (PNP) noise current 1/f-noise slope power figure
Z	Impedance formed of different components (R and/or C and/or L)
z	Indicates impedances, eg in $W_z$
Zf	Feedback impedance
Zi(n)	Input impedance
$Z_{iL}$	Input load impedance
$\mu$	Gain of a triode
$\mu F$	$\mu$ -follower (also as subscript)
0	Symbolises source, eg $R_0$ = source resistance
0	Source (subscript)
0s	Reference of a sound-programme level (here: 0 dBV)
1	Double-triode system one (subscript)
2	Double-triode system two (subscript), etc.
5	i/p load of 5 $\Omega$ (subscript)
10	10 Hz (subscript)
20	i/p load of 20 $\Omega$ (subscript)
33	33 1/3 rpm (vinyl record)
40	i/p load of 40 $\Omega$ (subscript)
43	i/p load of 43 $\Omega$ (subscript)
45	45 rpm (vinyl record)
1k	1 kHz (subscript)
1k	i/p load of 1 k $\Omega$ (subscript)
20k	Like 1 k
45°	Flank modulation
45°.mod	Flank modulated (subscript)
	Parallel

---

## Physical Constants and Mathematical Sizes

$B_1$	Bandwidth of 1 Hz
$B_{10k}$	Bandwidth of 10 kHz–20 kHz
$B_{20k}$	Bandwidth of 20 Hz–20 kHz (19,980 Hz)
$B_{22k}$	Bandwidth of 20 Hz–22 kHz
$B_{26k}$	Bandwidth of 20 Hz–26 kHz
$k$	$1.38065 \times 10^{-23} \text{ V}\cdot\text{A}\cdot\text{s K}^{-1}$ = Boltzmann's constant
$q$	$1.6022 \times 10^{-19} \text{ A}\cdot\text{s}$ = electron charge
$SN_{ne}$	Non-equalised ( <sub>ne</sub> ) SN of a white noise source
$SN_a$	-2.046 dB = SN improvement by A-weighting of $SN_{ne}$ in $B_{20k}$
$SN_{ar}$	-7.935 dB = SN improvement by RIAA equalising and A-weighting of $SN_{ne}$ in $B_{20k}$
$SN_r$	-3.646 dB: SN improvement by RIAA equalising of $SN_{ne}$ in $B_{20k}$
$SN_{ra}$	-4.289 dB: SN improvement by A-weighting of $SN_r$ in $B_{20k}$ ( $SN_r + SN_{ra} = SN_{ar}$ ) Note: These SN improvements work only in hum-free environments and with a white noise-based $SN_{ne}$
$T$	300 K for solid-state circuits
$T$	315 K inside valve amp cases
1k	FFT size $2^{10}$
2k	FFT size $2^{11}$
4k	FFT size $2^{12}$
8k	FFT size $2^{13}$
16k	FFT size $2^{14}$
32k	FFT size $2^{15}$
64k	FFT size $2^{16}$

# List of Figures

Figures on text pages and *on MCD Worksheets*

Figure 1.1	Block diagram of the Engine II . . . . .	4
Figure 1.2	RIAA transfer function creation and its insertion into an active and switchable amp chain . . . . .	7
Figure 1.3	Input alternative of Fig. 1.2. . . . .	8
Figure 1.4	75 $\mu$ s RIAA network at the input of Amps 3 & 4 . . . . .	8
Figure 1.5	Situation of the 318 $\mu$ s/3180 $\mu$ s RIAA network at the output of Amp3 . . . . .	10
Figure 1.6	Situation of the 318 $\mu$ s/3180 $\mu$ s RIAA network at the output of Amp4 . . . . .	11
Figure 1.7	Front of Engine II, <i>top</i> two fully equal engine channels L & R; <i>bottom left</i> and <i>right</i> two $\pm 21$ V/0.5 A PSU insertion units, <i>middle</i> one triode PSU with +200 V/75 mA, $2 \times 6.3$ V/1.5 A insertion unit . . . . .	11
Figure 1.8	Rear of Engine II. . . . .	12
Figure 1.9	Look on the fully equipped Mainboard of the right channel . . . . .	12
Figure 1.10	Rear and look into the case of one channel. . . . .	13
Figure 1.11	The first set of plug-in PCBs for Amp5 ( <i>fully left</i> ), Amp 2 ( <i>middle</i> ), and Amp1 ( <i>fully right</i> ). . . . .	14
Figure 1.12	Front of one channel . . . . .	14
Figure 1.13	Rear of one channel. . . . .	15
Figure 1.14	Main $\pm 21$ V power supply for all solid-state driven amps . . . . .	16
Figure 1.15	+200 V power supply for the triode driven section. . . . .	17
Figure 1.16	Two +6.3 V regulated triode heater power supplies . . . . .	18
Figure 1.17	Wiring on the Mainboard and to the outside world . . . . .	19
Figure 2.1	Amp3 without RIAA networks . . . . .	22
Figure 2.2	Output noise voltage density of the amp sequence Amp3 + Amp5 + Trafo with input shorted . . . . .	24
Figure 2.3	Calculated deviation from the exact RIAA transfer. . . . .	25
Figure 3.1	Triode driven Amp3 incl. RIAA networks . . . . .	32
Figure 3.2	Gain of Amp3 vs frequency. . . . .	34
Figure 3.3	T2 defining network . . . . .	35
Figure 3.4	Bode plot of $G_{T2}(f)$ . . . . .	35



Figure 3.5	<i>T1 &amp; T3 defining network</i> . . . . .	36
Figure 3.6	Bode plot of $G_{T1,3}(f)$ . . . . .	36
Figure 3.7	Normalized (1kHz at 0dB) RIAA transfer function . . . . .	37
Figure 3.8	Bode plot of the gain of the combined RIAA network . . . . .	37
Figure 3.9	Deviation from the exact RIAA transfer . . . . .	37
Figure 3.10	Bode plot of Amp3. . . . .	38
Figure 3.11	= Fig. 2.3. . . . .	38
Figure 3.12	Fig. 3.10's phase response . . . . .	38
Figure 3.13	Frequency response of the noise voltage density of the $T2(f)$ network . . . . .	40
Figure 3.14	Frequency response of the noise voltage density of the $T1(f) + T3(f)$ network . . . . .	41
Figure 3.15	<b>a</b> Amp3+Amp5 output noise voltage density with <i>i/p</i> shorted. <b>b</b> = Fig. 2.2 . . . . .	43
Figure 3.16	Comparison of the various output noise voltage densities vs. frequency (trace 3 is nearly hidden by trace 2) . . . . .	46
Figure 3.17	Deviation from the exact RIAA transfer of Amp1+Amp3+Amp5. . . . .	46
Figure 4.1	Amp4 without RIAA networks . . . . .	50
Figure 4.2	Output noise voltage density of the amp sequence Amp4 + Amp5 + Trafo with input shorted . . . . .	51
Figure 4.3	Calculated deviation from the exact RIAA transfer. . . . .	51
Figure 4.4	Two-op-amp fully differential amplifier . . . . .	52
Figure 4.5	Basic Amp4 circuit with input stage around OPs 3 & 4, output stage around OPs 5 & 6, and all relevant signal voltages. . . . .	53
Figure 4.6	Symbol for a fully differential amplifier with balanced electrometer input . . . . .	54
Figure 4.7	General noise voltage and current situation of the Amp4 input (2nd) gain stage. . . . .	57
Figure 4.8	General noise voltage and current situation of one Amp4 subtractor of the 3rd gain stage . . . . .	57
Figure 4.9	Detailed output noise voltage situation of the 2nd gain stage . . . . .	63
Figure 5.1	Op-amp driven Amp4 incl. RIAA networks . . . . .	66
Figure 5.2	$T2$ defining network . . . . .	67
Figure 5.3	Bode plot of $G_{T2}(f)$ . . . . .	68
Figure 5.4	$T1$ & $T3$ defining network. . . . .	68
Figure 5.5	Bode plot of $G_{T1}(f)$ & $G_{T3}(f)$ . . . . .	69
Figure 5.6	Normalized (1 kHz at 0 dB) RIAA transfer function . . . . .	69
Figure 5.7	Bode plot of the combined RIAA network . . . . .	70
Figure 5.8	Deviation from the exact RIAA transfer . . . . .	70

<i>Figure 5.9</i>	<i>Bode plot of Amp4 . . . . .</i>	70
<i>Figure 5.10</i>	<i>= Fig. 4.3 . . . . .</i>	71
<i>Figure 5.11</i>	<i>Fig. 5.9's phase response . . . . .</i>	71
<i>Figure 5.12</i>	<i>Noise voltage and current situation of the 2nd gain stage (OP3 &amp; OP4) . . . . .</i>	72
<i>Figure 5.13</i>	<i>Noise voltage and current situation of the 3rd gain stage (OP5 &amp; OP6) . . . . .</i>	72
<i>Figure 5.14</i>	<i>Frequency response of the noise voltage density of the T2(f) network . . . . .</i>	73
<i>Figure 5.15</i>	<i>Bode plot of the balanced o/p noise voltage density of the 2nd gain stage . . . . .</i>	74
<i>Figure 5.16</i>	<i>Frequency response of the noise voltage density of the T1(f)+T2(f) network . . . . .</i>	75
<i>Figure 5.17</i>	<i>a Amp4+Amp5 output noise voltage density with i/p shorted. b = Fig. 4.2 . . . . .</i>	76
<i>Figure 5.18</i>	<i>Comparison of the various output noise voltage densities vs. frequency (trace 3 is nearly hidden by trace 2) . . . . .</i>	79
<i>Figure 5.19</i>	<i>Deviation from the exact RIAA transfer of Amp1+Amp4+Amp5 . . . . .</i>	79
<i>Figure 5.20</i>	<i>Noise voltage densities at the output of the 2nd gain stage . . . . .</i>	81
<i>Figure 6.1</i>	<i>Circuit of the engine's output gain stage Amp5, also showing additional offset trim variants. . . . .</i>	84
<i>Figure 6.2</i>	<i>Plug-in connections between PCBs of Amps1, 2, 5 and the mainboard of Fig. 1.17 . . . . .</i>	85
<i>Figure 6.3</i>	<i>Solid-state gain stage <math>\pm 15</math> V PSU . . . . .</i>	85
<i>Figure 6.4</i>	<i>Noise sources of Amp5's input section (OPs 1 &amp; 2) . . . . .</i>	87
<i>Figure 6.5</i>	<i>Noise sources of Amp5's balanced output section (OPs 3 &amp; 4) . . . . .</i>	87
<i>Figure 6.6</i>	<i>Noise sources of Amp5's un-balanced output stage (OP5). . . . .</i>	88
<i>Figure 7.1</i>	<i>Op-amp driven Amp5 incl. balanced &amp; un-balanced output. . . . .</i>	92
<i>Figure 7.2</i>	<i>= Fig. 6.4 Noise voltage and current situation of the 1st gain stage (OP1 &amp; OP2) . . . . .</i>	94
<i>Figure 7.3</i>	<i>= Fig. 6.5 Noise voltage and current situation of the 2nd gain stage (OP3 stage &amp; the equivalent OP4 stage) . . . . .</i>	94
<i>Figure 7.4</i>	<i>Bode plot of the balanced o/p noise voltage density of the 1st gain stage. . . . .</i>	95
<i>Figure 7.5</i>	<i>= Fig. 6.6 Noise voltage and current situation of the un-balanced output gain stage (OP5) . . . . .</i>	96
<i>Figure 7.6</i>	<i>Amp5 output noise voltage density with i/p shorted . . . . .</i>	96

Figure 8.1	Input gain stage alternative Amp1 . . . . .	102
Figure 8.2	Noise sources of Amp1 . . . . .	104
Figure 8.3	Components of the Fig. 8.2 input load impedance $Z_i$ . . . . .	105
Figure 8.4	Frequency responses of Amp1, based on five different Amp1 input resistances $R_i$ (=S1–S4 settings) . . . . .	106
Figure 8.5	Phase responses of Amp1, based on five Amp1 input resistances $R_i$ (=S1–S4 settings) . . . . .	106
Figure 8.6	Output voltage frequency responses for five different Amp1 input voltages in 10 dB steps from $50 \mu V_{\text{rms}}$ to $5.0 \text{ mV}_{\text{rms}}$ in a 10 Hz–20 kHz band . . . . .	108
<i>Figure 9.1</i>	<i>= Fig. 8.1 . . . . .</i>	<i>112</i>
<i>Figure 9.2</i>	<i>= Fig. 8.2 Noise sources of Amp1 . . . . .</i>	<i>113</i>
<i>Figure 9.3</i>	<i>= Fig. 8.3 Components of the Fig. 9.2 input load <math>Z_i</math> . . . . .</i>	<i>113</i>
<i>Figure 9.4</i>	<i>Amp1 input noise voltage density with <math>R_0 = 20 \Omega</math> . . . . .</i>	<i>114</i>
<i>Figure 9.5</i>	<i>Amp1 input noise voltage density with <math>R_0 = 0 \Omega</math> . . . . .</i>	<i>115</i>
<i>Figure 9.6</i>	<i>Input referred and A-weighted SN vs. input load . . . . .</i>	<i>117</i>
<i>Figure 9.7</i>	<i>Zoomed Fig. 9.6 . . . . .</i>	<i>117</i>
<i>Figure 9.8</i>	<i>NF of Amp1 vs. <math>R_0</math> . . . . .</i>	<i>118</i>
<i>Figure 9.10</i>	<i>= Fig. 8.1 . . . . .</i>	<i>119</i>
<i>Figure 9.11</i>	<i>= Fig. 8.2 Noise sources of Amp1 . . . . .</i>	<i>120</i>
<i>Figure 9.12</i>	<i>= Fig. 8.3 Components of the Fig. 9.11 input load <math>Z_i</math> . . . . .</i>	<i>120</i>
<i>Figure 9.13</i>	<i>Amp1 input noise voltage density with <math>R_0 = 20 \Omega</math> . . . . .</i>	<i>121</i>
<i>Figure 9.14</i>	<i>Amp1 input noise voltage density with <math>R_0 = 0 \Omega</math> . . . . .</i>	<i>122</i>
<i>Figure 9.15</i>	<i>NF of Amp1 vs. <math>R_0</math> . . . . .</i>	<i>124</i>
Figure 10.1	Input gain stage alternative Amp2 . . . . .	126
Figure 10.2	Booster for insertion into Fig. 10.1's points A + A' and B + B' . . . . .	127
Figure 10.3	SSM2210 noise voltage density versus frequency and collector current. . . . .	129
Figure 10.4	SSM2210 noise current density versus frequency and collector current. . . . .	129
Figure 10.5	General simplified BJT noise model for the audio band . . . . .	129
Figure 10.6	Transfer of the Fig. 10.5 model into a strictly input referred one . . . . .	130
Figure 10.7	Transfer of the Fig.10.6 noise model into the final BJT noise model with only two equivalent noise sources in place . . . . .	130
Figure 10.8	NF of 2SC3329 at 10 Hz . . . . .	132
Figure 10.9	NF of 2SC3329 at 1 kHz . . . . .	133
Figure 10.10	NF of 2SA1316 at 10 Hz . . . . .	134
Figure 10.11	NF of 2SA1316 at 1 kHz . . . . .	135

Figure 10.12	Amp2 with all noise calculation relevant active and passive components . . . . .	136
Figure 10.13	Input load situation of a BJT. . . . .	136
Figure 10.14	Upper (N) half of Amp2 (excl. input network $Z_1(f,R_0)$ ), showing all relevant noise sources (frequency independent) . . . . .	138
Figure 10.15	Input resistor alternatives (input Cs not shown) . . . . .	141
Figure 11.1	2SA1316 current noise density curve and its tangents, after succ-apps and the chosen input load . . . . .	145
Figure 11.2	2SA1316 voltage noise density curve and its tangents, after succ-apps and the chosen input load . . . . .	145
Figure 11.3	2SC3329 current noise density curve and its tangents, after succ-apps and the chosen input load . . . . .	149
Figure 11.4	2SC3329 voltage noise density curve and its tangents, after succ-apps and the chosen input load . . . . .	149
Figure 11.5	= Fig. 10.12 . . . . .	152
Figure 11.6	Impedance of the input network $Z_{iL}(f)$ . . . . .	154
Figure 11.7	Input impedances $Z_i(f)$ & $Z_{in}(f)$ . . . . .	155
Figure 11.8	Noise situation of Amp2, transferred into the upper half of the amp and into the lower half, and vice versa . . . . .	156
Figure 11.9	= Fig. 10.14 . . . . .	159
Figure 11.10	Input referred noise voltage densities vs. frequency based on two different input loads . . . . .	160
Figure 11.11	Amp2 equivalent input noise voltage densities vs. $R_0$ based on two different frequencies . . . . .	160
Figure 11.12	Amp2 equivalent input noise voltage densities vs. frequency showing 1/f-noise based on two different input loads . . . . .	160
Figure 11.13	Noise Figure vs. $R_0$ . . . . .	161
Figure 11.14	Amp2 output noise voltage densities vs. frequency RIAA-equalized + A-weighted + un-weighted . . . . .	163
Figure 11.15	Input referred un-weighted + A-weighted & RIAA-equalized SN vs. $R_0$ . . . . .	163
Figure 12.1	<b>a</b> Frequency and phase response of the left channel's Amps 1 & 2 via Amp3 and Amp5 + Trafo, fed by a generator output resistance of 10.8 $\Omega$ . <b>b</b> Frequency and phase response of the left channel's Amp1 via Amp3 and Amp4 and Amp5 + Trafo, fed by a generator output resistance of appr. 0 $\Omega$ . . . . .	166
Figure 12.2	Engine II output noise voltage density curve of the left channel, input loaded with 20 $\Omega$ and Amp1 + Amp4 + Amp5 + Trafo . . . . .	167

Figure 12.3	Engine II output noise voltage density curve of the left channel, input loaded with $20\ \Omega$ and Amp2 + Amp3 + Amp5 + Trafo . . . . .	171
Figure 12.4	Engine II output noise voltage density curve of the left channel, external input shorted and Amp3 + Amp5 + Trafo. . .	172
Figure 12.5	Left channel's Amp1 + Amp3 + Amp5 + Trafo distortion measurement result of a 1 kHz signal via the central triode path . . . . .	173
Figure 12.6	Left channel's Amp1 + Amp4 + Amp5 + Trafo distortion measurement result of a 1 kHz signal via the central op-amp path. . . . .	174
Figure 12.7	Same as Fig. 12.5, however, Amp1 is replaced by Amp2 . . .	174
Figure 12.8	Same as Fig. 12.6, however, Amp3 is replaced by Amp4 . . .	175
Figure 12.9	Frequency and phase responses of Amp1 via Amps 3 & 4, fed by a generator with an output resistance of $0\ \Omega$ . . . . .	181
Figure 12.10	Frequency and phase responses of Amp1 via Amps 3 & 4, fed by a generator with an output resistance of $10.8\ \Omega$ . . . . .	182
Figure 12.11	Frequency and phase responses of Amp2 via Amps 3 & 4, fed by a generator with an output resistance of $10.8\ \Omega$ . . . . .	183
Figure 13.1	BJT driven input stage alternative for MC purposes . . . . .	188
Figure 13.2	Balanced transformer input and BJT/Op-Amp driven input stage alternative for low-output MC cartridges. . . . .	190
Figure 13.3	Fully triode driven MC/MM input stage alternative with transformer (Lundahl LL9226) MC-input and balanced output . . . . .	192
Figure 13.4	Noise model of the Fig. 13.3 MC input stage . . . . .	194
Figure 13.5	Principal Joachim Gerhard design with high-Z (Principally, Mr. Gerhard's low-Z input approach looks the same; details see footnote 11) voltage driven input, turned into a linear input amp for Engine II purposes. . . . .	196
Figure 13.6	Principal Ovidiu Popa design with additional and new output stage, turned into a linear input amp for Engine II purposes. . . . .	198
Figure 13.7	Principal Bob Cordell design with an additional and new output stage . . . . .	199
Figure 14.1	= Fig. 13.1 . . . . .	206
Figure 14.2	Impedance of the input network $Z_I(f)$ . . . . .	207
Figure 14.3	<b>a</b> Frequency dependent gain. <b>b</b> Phase response of the gain . . .	208
Figure 14.4	Input impedance $Z_{in}(f)$ . . . . .	209
Figure 14.5	Frequency and $R_0$ dependent equivalent input noise voltage density for two different input loads . . . . .	212
Figure 14.6	Frequency and $R_0$ dependent equivalent output noise voltage density for two different input loads . . . . .	212

Figure 14.7	<i>RO dependent average input noise voltage density</i> . . . . .	213
Figure 14.8	<i>RO dependent, A-weighted, and RIAA equalized output referred SNs</i> . . . . .	214
Figure 14.9	= Fig. 13.2 . . . . .	215
Figure 14.10	<i>Input referred noise voltage density based on two different input loads</i> . . . . .	219
Figure 14.11	<i>RO dependent average input noise voltage density</i> . . . . .	220
Figure 14.12	<i>RO dependent, A-weighted, and RIAA equalized output referred SNs</i> . . . . .	221
Figure 14.17	= Fig. 13.6 . . . . .	222
Figure 14.18	= Fig. 13.7 . . . . .	226
Figure 14.19	<i>Output referred A-weighted and RIAA equalized SN vs. RO of the MC input stage</i> . . . . .	230
Figure 14.20	<i>Output noise voltage densities of the two phono-amp input stage versions, inputs loaded</i> . . . . .	231
Figure 15.1	<i>Input referred noise voltage density curve of the Clio 8.5 measurement system, balanced input shorted</i> . . . . .	234
Figure 15.2	Same as Fig. 15.1, however, smoothed by $\frac{1}{2}$ Octave . . . . .	235
Figure 15.3	<i>Worsening figure <math>W_c(B)</math> as function of the difference B of two SNs</i> . . . . .	236
Figure 15.4	<i>Zoomed Fig. 15.3 with <math>B \leq 5</math> dB</i> . . . . .	236
Figure 15.5	<i>Clio's 1 kHz 0 dBV signal and its distortion artefacts in <math>B_{20k}</math></i> . . . . .	237
Figure 15.6	<i>The Clio IMD measurement result with 250 Hz/8 kHz and 4:1 signal levels</i> . . . . .	238
Figure 15.7	<i>The un-balanced to balanced converter UBC</i> . . . . .	239
Figure 15.8	<i>Booster alternatives for Fig. 15.7</i> . . . . .	240
Figure 15.9	<i>THD at UBC's PL01 output, fed by a 0 dBV/1 kHz signal</i> . . . . .	242
Figure 15.10	<i>THD at UBC's J03 output, fed by a 0 dBV/1 kHz signal</i> . . . . .	242
Figure 15.11	<i>THD at UBC's J03 output, fed by a -20 dBV/1 kHz signal</i> . . . . .	243
Figure 15.12	<i>Test-board case with Amp1</i> . . . . .	245
Figure 15.13	<i>Circuit of the test-board</i> . . . . .	245
Figure 15.14	<i>RIAA encoder for RIAA transfer function trimming actions via external input of the Engine II</i> . . . . .	246
Figure 16.1	<i>Output voltage noise density curve of the NAD M51</i> . . . . .	248
Figure 16.2	<b>a</b> <i>Worsening Figure <math>W_c(B)</math> as function of the difference B of two SNs. <b>b</b> Zoomed version of Fig. 16.2a for correction purposes of two SNs with values that are close together (<math>B \leq 5</math> dB)</i> . . . . .	250
Figure 16.3	<i>Noise voltage density situation with a corner frequency of 1 kHz (incl. tangents)</i> . . . . .	250
Figure 16.4	<i>General output situation of the DUT (left) and balanced input of measurement instrument (right)</i> . . . . .	252
Figure 16.5	<i>Effective output noise voltage of the DUT</i> . . . . .	253

Figure 16.6	The creation of the total input noise voltage of the measurement amp . . . . .	253
Figure 16.7	<b>a</b> DUT output resistance versus various MA total input noise voltage variants. <b>b</b> Zoomed version of Fig. 16.7a (for $R_{in,tot} = 18.182 \text{ k}\Omega$ only) . . . . .	255
Figure 16.8	Principal INA circuit . . . . .	256
Figure 16.9	Principal final MA. (+) and (-) at the <i>input</i> and <i>outputs</i> indicate the phase relationship . . . . .	257
Figure 16.10	Relevant circuits for the gain calculation process . . . . .	257
Figure 16.11	Circuit for rule-of-thumb SN calculation . . . . .	260
Figure 16.12	Noise model of one-half input stage (Amp A with OP1 and OP2) . . . . .	262
Figure 16.13	Noise model of one of the two summing stages (OP5 and OP6) . . . . .	262
Figure 16.14	Noise model of the balanced to un-balanced converter (OP7) . . . . .	263
Figure 16.15	Input load dependency of the output referred SN . . . . .	263
Figure 16.16	Complete MA circuit . . . . .	264
Figure 16.17	RG alternatives for gains of <b>a</b> $\times 10$ and <b>b</b> $\times 100$ (for only one input stage) . . . . .	265
Figure 16.18	Output noise voltage density curves, including input $C_s$ <i>lower trace</i> input shorted, <i>upper trace</i> input loaded with $1 \text{ k}\Omega$ . . . . .	267
Figure 16.19	Same as Fig. 16.18 with linear frequency range . . . . .	268
Figure 16.20	Frequency ( <i>top</i> ) and phase response ( <i>bottom</i> ) (bal in/bal out) . . . . .	269
Figure 16.21	The PMMA in its enclosure . . . . .	270
Figure 16.22	Plug-in input stages of the PMMA . . . . .	270
Figure 17.1	PFMA circuit . . . . .	276
Figure 17.2	Output noise voltage density of the PFMA, input shorted . . . . .	276
Figure 17.3	F & P of the PFMA . . . . .	277
Figure 17.4	Noise sources of the PFMA . . . . .	279
Figure 17.5	Evaluation of the OPI input load . . . . .	280
Figure 17.6	R0 dependency of the PFMA's input referred SN . . . . .	280
Figure 17.7	PFMA and its enclosure . . . . .	281
Figure 18.1	= Fig 15.7 . . . . .	284
Figure 18.2	UBC input impedance . . . . .	285
Figure 18.3	Output noise voltage density at PL01 . . . . .	286
Figure 18.4	= Fig. 16.15 . . . . .	290
Figure 18.5	= Fig. 16.12 . . . . .	291
Figure 18.6	Noise situation after paralleling of two i/p stages . . . . .	293
Figure 18.7	Output noise voltage density of the whole 1st stage . . . . .	294
Figure 18.8	= Fig. 16.13 . . . . .	294

<i>Figure 18.9 = Fig. 16.14</i> . . . . .	296
<i>Figure 18.10 = Fig. 16.15</i> . . . . .	297
<i>Figure 18.11 = Fig. 16.11</i> . . . . .	298
<i>Figure 18.12 Graph for interpolation purposes of the measurement correction figure D</i> . . . . .	299
<i>Figure 18.13 = Fig. 16.10</i> . . . . .	299
<i>Figure 18.14 = Fig. 17.1</i> . . . . .	302
<i>Figure 18.15 = Fig. 17.4</i> . . . . .	303
<i>Figure 18.16 = Fig. 17.5</i> . . . . .	303
<i>Figure 18.17 PFMA input noise voltage density vs. frequency</i> . . . . .	305
<i>Figure 18.18 Input referred R0 dependent SN</i> . . . . .	305
Figure 19.1 Principal situation of an MM cartridge attached to an un-balanced phono-amp input . . . . .	308
Figure 19.2 Noise model of Fig. 19.1 . . . . .	308
Figure 19.3 Principal situation of an MM cartridge attached to a balanced phono-amp input . . . . .	308
Figure 19.4 Noise model of Fig. 19.3 . . . . .	309
Figure 19.5 Test MM phono-amp à la Fig. 19.1 . . . . .	310
Figure 19.6 Standard Cartridge noise voltages at the input of the test phono-amp à la Fig. 19.5 . . . . .	310
Figure 19.7 R1 replaced by an M1 ELS. . . . .	311
Figure 19.8 R10 split into two sections to produce a virtual ground in-between them . . . . .	311
Figure 19.9 R1 replaced by an M2 ELS. . . . .	313
Figure 19.10 Input situation of a balanced phono-amp. . . . .	314
Figure 19.11 ELS of R1a + R1b. . . . .	315
<i>Figure 20.1 = Fig. 19.5</i> . . . . .	320
<i>Figure 20.2 = Fig. 19.7</i> . . . . .	320
<i>Figure 20.3 = Fig. 19.9</i> . . . . .	320
<i>Figure 20.4 Input impedance of the Fig. 20.1 phono-amp input load</i> . . . . .	322
<i>Figure 20.5 Phase of the Fig. 20.1 phono-amp input load</i> . . . . .	322
<i>Figure 20.6 Noise voltage density of the three different input voltage dividers</i> . . . . .	324
<i>Figure 20.7 = Fig. 19.6</i> . . . . .	324
<i>Figure 20.8 Total input noise voltage densities at the input of the phono-amp (A)</i> . . . . .	326
<i>Figure 20.9 Derivation sequence</i> . . . . .	330
<i>Figure 20.10 = Fig. 19.10</i> . . . . .	332
<i>Figure 20.11 = Fig. 19.11</i> . . . . .	332
<i>Figure 20.12 Input impedance of the Fig. 20.1 phono-amp input load</i> . . . . .	333
<i>Figure 20.13 Phase of the Fig. 20.12 phono-amp input load</i> . . . . .	333
<i>Figure 20.14 Noise voltage density of the three different input voltage dividers</i> . . . . .	335



<i>Figure 20.15 = Fig. 19.12</i> . . . . .	335
<i>Figure 20.16 Total input noise voltage densities at the input of the phono-amp (points A-B)</i> . . . . .	337
Figure 21.1 BJT model for low-frequency small signal calculation purposes . . . . .	342
Figure 21.2 BJT noise model . . . . .	343
Figure 21.3 Basic common emitter circuit CE. . . . .	346
Figure 21.4 CE <sub>b</sub> 's operational model . . . . .	348
Figure 21.5 Fig. 21.4 with all relevant noise sources . . . . .	350
Figure 21.6 Common emitter circuit CE <sub>cf</sub> with cf via RE. . . . .	351
Figure 21.7 CE <sub>cf</sub> 's operational model . . . . .	354
Figure 21.8 Noise model of Fig. 21.7 with all relevant noise sources. . . . .	355
Figure 21.9 Common emitter circuit CE <sub>vcf2</sub> with vf via R2 and cf via RE . . . . .	356
Figure 21.10 Derivation of the gain equation for Fig. 21.9. . . . .	357
Figure 21.11 Noise model of the Fig. 21.9 CE <sub>vcf2</sub> gain stage . . . . .	358
Figure 21.12 Principal circuit of a closed loop arrangement with a BJT followed by an op-amp . . . . .	360
Figure 21.13 Frequency independent noise model of the modified Fig. 21.12 amp . . . . .	362
Figure 22.1 Situation of the signal voltages in a DIFA . . . . .	366
Figure 22.2 General DIF-OPA circuit with input load . . . . .	366
Figure 22.3 Relevant noise sources of Fig. 22.2 . . . . .	368
Figure 22.4 Adapted Fig. 22.3 . . . . .	369
Figure 22.5 Typical amplifier circuit with a DIFA-IC . . . . .	370
Figure 22.6 DIFA-IC with input load . . . . .	371
Figure 22.7 Noise sources of a DIFA-IC . . . . .	372
<i>Figure 23.1 = Fig. 22.2</i> . . . . .	376
<i>Figure 23.2 = 22.3</i> . . . . .	377
<i>Figure 23.3 = Fig. 22.4</i> . . . . .	377
<i>Figure 23.4 Input referred and input loaded noise voltage densities of the fully differential input and the grounded input</i> . . . . .	378
<i>Figure 23.5 = 22.5</i> . . . . .	380
<i>Figure 23.6 = Fig. 22.6</i> . . . . .	380
<i>Figure 23.7 Input referred differential noise voltage density, input shorted or output resistance of preceding gain stage ~ 0R</i> . . . . .	381
Figure 24.1 BRAUN tracking force measurement instrument . . . . .	386
Figure 24.2 The BTFMI in action . . . . .	387

---

## List of Tables

Table 8.1	Detailed frequency and phase measurement results of Amp1, based on five Amp1 input resistances $R_i$ (= S1–S4 settings) . . .	107
Table 8.2	Figure 8.6 delta data at 10 Hz . . . . .	107
Table 10.1	Amp2 non-weighted SN results for two different input loads . . . . .	140
Table 10.2	Same as Table 10.1 after RIAA equalization and A-weighting . . . . .	140
Table 12.1	Relevant Engine II SN results . . . . .	177
Table 12.2	Relevant Engine II THD figures . . . . .	178
Table 12.3	Relevant Engine II IMD figures . . . . .	179
Table 12.4	Frequency and phase response measurement results of Amp1 and Amp2, fed by different generator output resistances . . . . .	180
Table 13.1	Draft design SNs compared with Engine II results . . . . .	202
Table 16.1	PMMA performance results . . . . .	267
Table 16.2	Increasing input loads yield increasing differences between measured and calculated output referred SNs . . . . .	271
Table 24.1	TCRs of the Deutsche Grammophon Gesellschaft . . . . .	388
Table 24.2	DIN TCRs . . . . .	389
Table 24.3	TCRs of the VEB-Deutsche Schallplatten . . . . .	389

---

**Part I**  
**The RIAA Phono-Amp Engine II**

Sometimes, the development of a very flexible fully balanced hybrid MC phono-amp solution may lead to rather unexpected and surprising results: Vive la différence?

---

## 1.1 Intro and Goals

My first RIAA Phono-Amp Engine (I) became an essential part of my books “The Sound of Silence” (TSOS-1/-2).<sup>1,2</sup> It became essential because with it, I could transfer all presented theory about electronic noise from math to a real thing. I could calculate it and I could measure it, with results that only show rather small deviations from the calculated values. However, I based the main amplifier chain design on an un-balanced RIAA transfer creation that additionally includes balanced/un-balanced inputs and outputs. The point I did not solve very elegantly was switching between the various input-output possibilities. Thus, the handling of quick comparisons between different cartridges and turntables became a hard job. In addition, I had to house the triode amplifier solution in a separate external case.

In contrast to my yesterday approach, the new Engine II design will deal with a much more elegant approach, expressed by several standards and goals as follows:

- A. Basically, the new engine should allow the user
1. to compare two different MC cartridges mounted on two turntables of the same type or on one turntable with two equal tonearms
  2. to compare two different turntables/tonearms (or one turntable with two different tonearms) equipped with the same type of MC cartridge
  3. to compare the sound of triode driven versus solid-state driven RIAA transfer creation stages

---

<sup>1</sup>“The Sound of Silence”, 1st ed.

<sup>2</sup>“The Sound of Silence”, 2nd ed.

4. to enhance the number of inputs by additional external amplifier stages for broader comparison needs, including MM cartridges and gain stages, with un-balanced inputs but always with balanced outputs
5. to test various technologies of balanced input and output gain stages, eg such as transformer or op-amp or JFET or BJT or valve driven ones

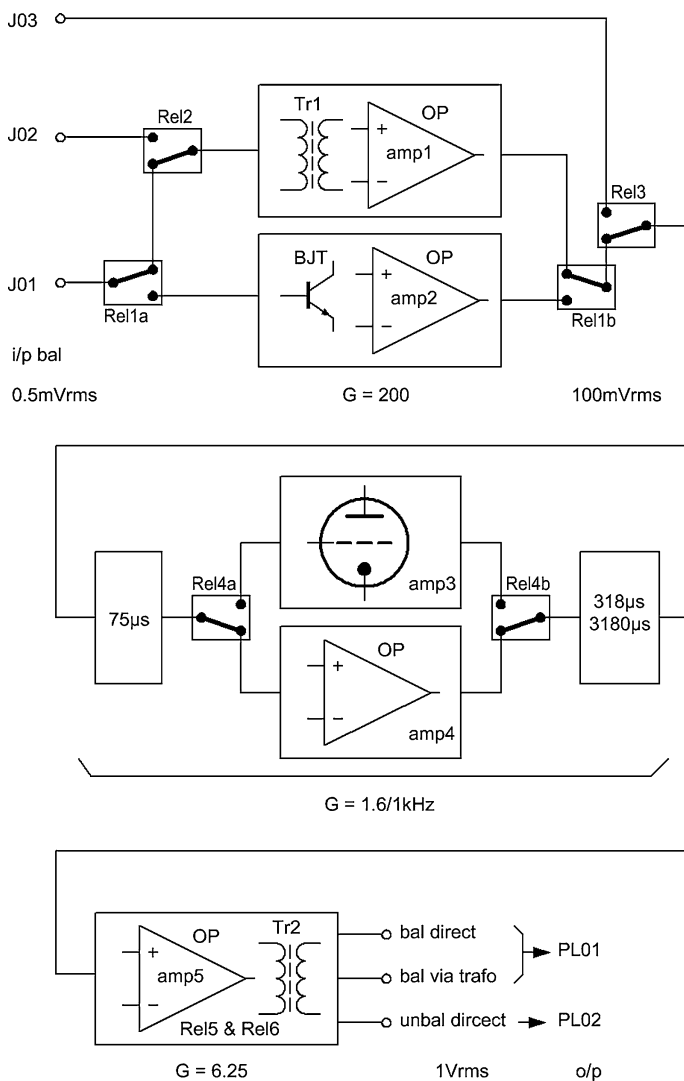


**Fig. 1.1** Block diagram of the Engine II

B. Additionally, the requirements concerning the chosen electronic solution should hit or become even better than the following points/goals:

1. Fully balanced from input to output—plus one un-balanced output
2. A-weighted input referred SN: better than or equal to  $-79$  dB(A) in  $B_{20k}$  (20 Hz–20 kHz), ref.  $0.5$  mV<sub>rms</sub>, input load =  $20$   $\Omega$   
 Note: the resulting A-weighted and RIAA equalized SN<sub>ariaa</sub> of an extremely low-noise LP vinyl record—eg DMM cut LPs with  $-72.5$  dB(A)—and the phono-amp would then become a combined and weighted SN of  $-71.6$  dB(A); the resulting SN<sub>ariaa</sub> of an average vinyl LP would become  $-70.5$  dB(A)<sup>3</sup>
3. Nominal output level balanced and un-balanced:  $0$  dBV  $\equiv$   $1$  V<sub>rms</sub>, but also changeable to  $0$  dBu to  $+6$  dBu
4. Nominal gain  $G_{nom} = 2000$  ( $+66$  dB) with trimming possibility for each channel: from min.  $700$  to max.  $3000$ , hence, the input sensitivity reaches from  $0.33$  to  $1.45$  mV<sub>rms</sub> referenced to DIN  $0$  dB ( $8$  cm/s/ $1$  kHz/flank mod.) or from  $0.2$  to  $0.9$  mV<sub>rms</sub> referenced to a velocity of  $5$  cm/s/ $1$  kHz/lateral modulated
5. Phase response in  $B_{20k}$ :  $\leq \pm 30^\circ$
6. Frequency response in  $B_{20k}$ :  $\leq \pm 0.1$  dB
7. RIAA transfer function creation: fully passive
8. With nominal gain overload margin  $\leq 20$  dB for all frequencies at all points of the signal chain; any change of the nominal gain by  $\pm x$  dB yields an overload margin of  $20$  dB  $\mp x$  dB
9. Slew rate  $> 1.8$   $\mu$ V/s
10. Easy change of input and output gain stages
11. Power supply:  $\pm 15$  V regulated for solid-state and  $+200$  V/ $+6.3$  V regulated for triode stages
12. Cases: one per channel, one for each PSU,  $19''$  format

Fulfilment of the above given points has led to the block diagram given in Fig. 1.1. The next chapters and sections will give the details.

---

## 1.2 General Concept

For MC purposes, the Fig. 1.1 input section (Amps 1 & 2) is composed of two low-noise and high gain linear amps of different or equal configuration and very flat frequency and phase response. In addition, their distortion level is rather low (more on distortion etc. see further down in Chap. 12—Engine II Performance). An external input allows the integration of additional linear amp stages. They may serve for MC or MM purposes with balanced or un-balanced inputs, however, always with balanced outputs.

---

<sup>3</sup>TSOS-2, Chap. 11, Fig. 11.5/TSOS-1, Chap. 3, Fig. 3.95.

The nominal signal level (100 mV) at the input section's output and center section's (Amps 3 & 4) input comes from two sources. Firstly, it's a level that allows the design of internal output stages of Amps 1 & 2 which practically do not hurt the noise level produced by the input stages of Amps 1 & 2, and secondly, the overload requirement can also sufficiently be fulfilled in the center section of Amps 3 (triodes) & 4 (op-amps).

Many comparisons of phono-amps suffer from the inequality of the components used to create and electronically handle the RIAA transfer function. I think that, besides a flat frequency & phase response and a certain distortion & intermodulation level, most of the amplifier's personal sound is created by these components and their application in the amp chain. Therefore, to ensure absolute equal conditions I have chosen only one 75  $\mu$ s network and only one 318  $\mu$ s & 3180  $\mu$ s network. These networks are switched by relays to the in- and outputs of Amps 3 & 4, the only amps that cannot be changed for further experiments. They are rather fast broadband linear valve or op-amp driven fully balanced amplifying devices, fixed on the main board, producing only minimal additional noise and THD & IMD. Their common mode rejection ratio is outstanding too.

I designed the output stage Amp5 as low-noise and as low-distortion as possible. Therefore, it works with rather expensive OPA627 op-amps plus a switchable 1:1 high-quality output transformer at its output. Its balanced and un-balanced paths have nearly no output resistance, very low THD & IMD, and very flat frequency and phase response in B<sub>20k</sub>. Additionally, Amp5 does not add neither noise nor hum to the noise level of the preceding gain stages Amps 1–4.

### 1.3 Basic Considerations

The way to produce the RIAA transfer function  $RIAA(f)^4$  form the main difference between the two engine versions:

$$RIAA(f) = \frac{\sqrt{1 + (2\pi f T3)^2}}{\sqrt{1 + (2\pi f T1)^2} + \sqrt{1 + (2\pi f T2)^2}} \quad (1.1)$$

$$T1 = 3180 \mu s$$

$$T2 = 75 \mu s$$

$$T3 = 318 \mu s$$

Engine I offers three solid-state solutions with creation of the transfer function via overall feedback plus a valve solution with only one passive network (2-pham<sup>5</sup> concept = two gain stages and the whole RIAA network in the middle).

<sup>4</sup>TSOS-2 Chap. 2, TSOS-1 Chap. 2.

<sup>5</sup>TSOS-2 Sect. 17.7.

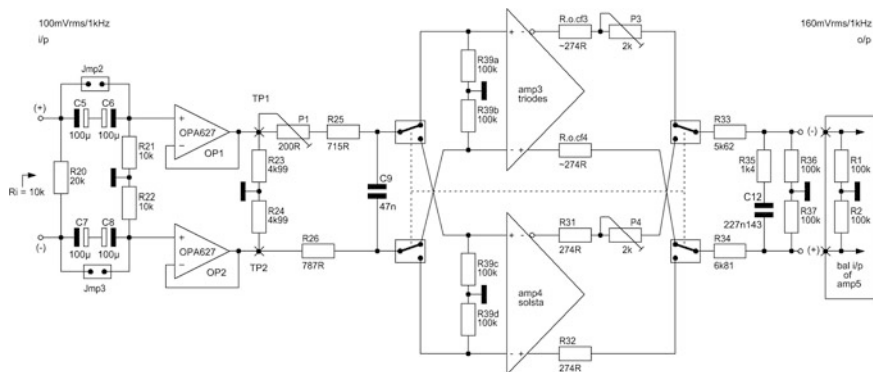


**Fig. 1.2** RIAA transfer function creation and its insertion into an active and switchable amp chain

No matter which type of amplification we use (valve or solid-state) Engine II always sets on a fully passive approach. We have the RIAA network split into two sub-networks (3-pham<sup>6</sup> concept = three gain stages with split RIAA networks between them). Hence, we have an input amp followed by the 75  $\mu$ s sub-net at the central amp's entrance, the 318  $\mu$ s & 3180  $\mu$ s sub-net at the central amp's output, loaded by an adequate output amp's input resistance, here the one of Amp5.

The chosen sequence is highly favourable according to the overload question: before the high frequencies (up to appr. +20 dB at 20 kHz) enter the central Amps 3 or 4 they got damped by the 75  $\mu$ s lp to the max. 100 mV<sub>rms</sub> level. In addition, it damps noise from the linear input Amps 1 & 2 too.

I have chosen the Fig. 1.2 design because it allows the RIAA transfer creation with utmost precision and it fulfils the overload goal in both signal paths.

Figure 1.3 shows an input alternative with fully galvanically isolated input connection via two 1:1/600  $\Omega$ :600  $\Omega$  transformers, however and after many checks, without disturbance of the overall picture of Fig. 1.2. Concerning external i/p-loads, it simply adds further flexibility.

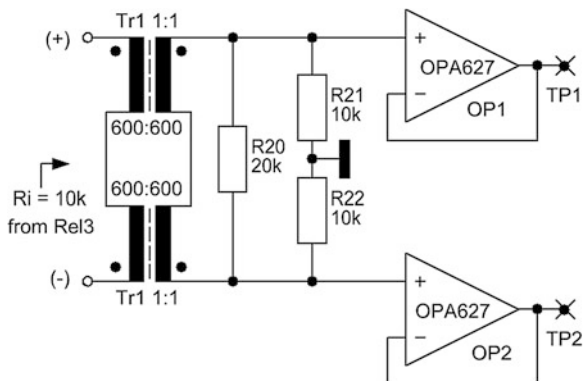
Trimming pot P1, C5, and (R25 + R26) form the 75  $\mu$ s network. In conjunction with C12, R35, (R36 + R77) || Amp5's (R1 + R2), and with trimming pots P3 (+ R<sub>o.cf3</sub> + R<sub>o.cf4</sub> = cathode follower output resistances) for the triode driven Amp3 and P4 + (R31 + R32) for the op-amp driven Amp4 we get the 318  $\mu$ s & 3180  $\mu$ s network. It only works perfect with the input resistance (R1 + R2) of the following output stage Amp5 taken into account. At the output of Amp4, we find R31 and R32. They stand for their output resistance counterparts R<sub>o.cf3</sub> and R<sub>o.cf4</sub> in the triode path.

The detailed calculation of the time constants follows next; the detailed calculation of the triode output resistances follows in the Amp3 chapter.

<sup>6</sup>TSOS-2 Sect. 17.7.



**Fig. 1.3** Input alternative of Fig. 1.2



Because of the given input resistances of Amps 3 & 4 ( $R_{39a-d}$ ) and their given equal balanced input capacitances  $C_{i,dif}$ , together with the nearly  $0 \Omega$  output resistance of OPs 1 & 2 (see  $R_{o,op1}$  &  $R_{o,op2}$  in Fig. 1.4), we obtain T2 for Amp3 and Amp4:

Amp3 ( $R_{o,op1} = R_{o,op2} = 0 \Omega$ ):

$$T2 = 75\mu s = (C9 + C_{i,dif}) \left[ \frac{(P1 + R25)R39a}{P1 + R25 + R39a} + \frac{R26R39b}{R26 + R39b} \right] \quad (1.2)$$

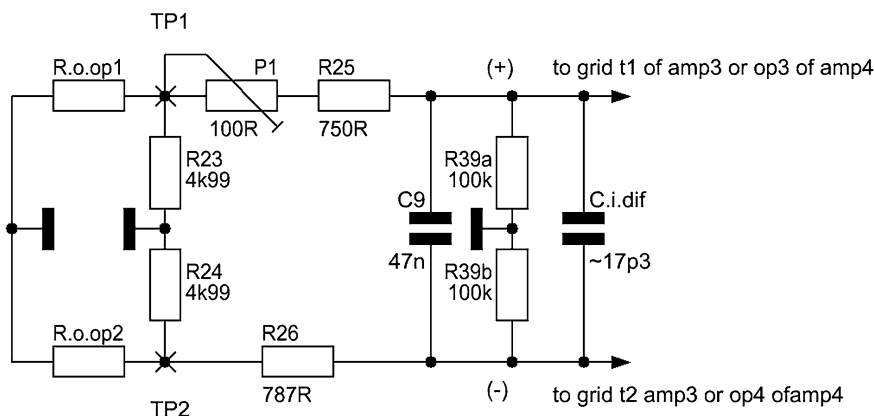


**Fig. 1.4** 75  $\mu s$  RIAA network at the input of Amps 3 & 4

Amp3 ( $R_{o.op1} = R_{o.op2} > 0 \Omega$ ):

$$T2 = 75 \mu s = (C9 + C_{i.dif}) \left[ \frac{(P1 + R25 + (R23 || R_{o.op1}))R39a}{P1 + R25 + (R23 || R_{o.op1}) + R39a} + \frac{(R26 + R24 || R_{o.op2})R39b}{(R26 + R24 || R_{o.op2}) + R39b} \right] \quad (1.3)$$

Amp4 ( $R_{o.op1} = R_{o.op2} = 0 \Omega$ ):

$$T2 = 75 \mu s = (C9 + C_{i.dif}) \left[ \frac{(P1 + R25)R39c}{P1 + R25 + R39c} + \frac{R26 R39d}{R26 + R39d} \right] \quad (1.4)$$

Amp4 ( $R_{o.op1} = R_{o.op2} > 0 \Omega$ ):

$$T2 = 75 \mu s = (C9 + C_{i.dif}) \left[ \frac{(P1 + R25 + (R23 || R_{o.op1}))R39c}{P1 + R25 + (R23 || R_{o.op1}) + R39c} + \frac{(R26 + R24 || R_{o.op2})R39d}{(R26 + R24 || R_{o.op2}) + R39d} \right] \quad (1.5)$$

Note: The Amp4 input capacitance  $C_{i.dif}$  ( $\sim 17.3$  pF) must physically be added to the Amp4 input. Here I propose the value of 15 pF ceramic, because the OPAs add their sequence connected input capacitances too.

With the given input resistance of Amp5 (=Amp5's  $R1 + R2$  in Figs. 1.2 and 1.5) we obtain the following equations for the other two time constants  $T1$  &  $T3$ :

Equal for both, Amps 3 & 4:

$$T3 = 318 \mu s = C12 R35 \quad (1.6)$$

Amp3 only (Fig. 1.5):

$$T1 = 3180 \mu s = \left| C12 \left\{ R35 + \left[ \frac{R_{T1.amp3}^{-1}(f)}{+ \left( \frac{R1_{amp5} R36}{R1_{amp5} + R36} + \frac{R2_{amp5} R37}{R2_{amp5} + R37} \right)^{-1}} \right]^{-1} \right\} \right| \quad (1.7)$$

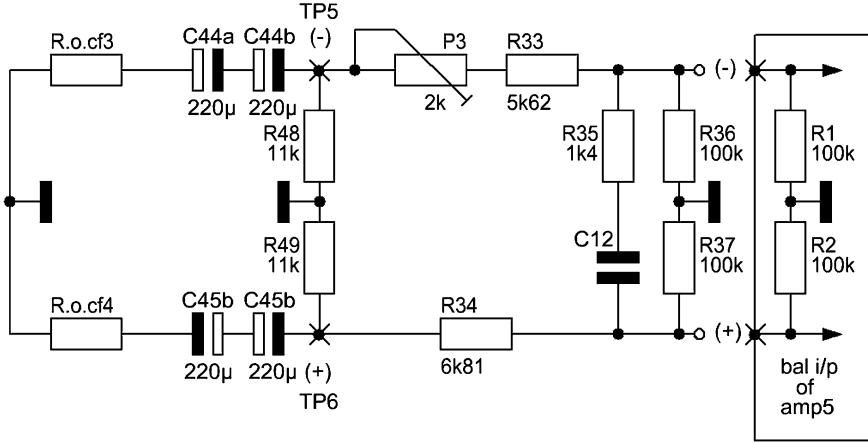


**Fig. 1.5** Situation of the 318  $\mu$ s/3180  $\mu$ s RIAA network at the output of Amp3

$$R_{T1.amp3}(f) = P3 + R_{o.cf.dif}(f) + R33 + R34 \quad (1.8)$$

The equation to calculate the frequency dependent output resistance  $R_{o.cf.dif}(f)$  of the triode driven Amp3 will be given further down in the Amp3 Chap. 2. If the capacitances in the signal path at the output of the triode cathode followers do not hurt a flat frequency and phase response, we can take the frequency independent value of the cathode follower's output resistance  $R_{o.cf.dif}$ . Hence, in (1.7) we could work without magnitude and  $R_{T1.Amp3}$ .

Amp4 only (Fig. 1.6):

$$T1 = 3180 \mu s = C12 \left\{ R35 + \left[ R_{T1.amp4}^{-1} + \left( \frac{R1_{amp5} R36}{R1_{amp5} + R36} + \frac{R2_{amp5} R37}{R2_{amp5} + R37} \right)^{-1} \right]^{-1} \right\} \quad (1.9)$$

$$R_{T1.amp4} = P4 + R31 + R32 + R33 + R34 \quad (1.10)$$

In contrast to the Amp3 output, we have no capacitances in the signal path. Therefore, the auxiliary resistance  $R_{T1.Amp4}$  is fully frequency independent. In cases of OP 5 & 6 output resistances  $>0 \Omega$  we must add these values to R31 and R32 in the above given equations.

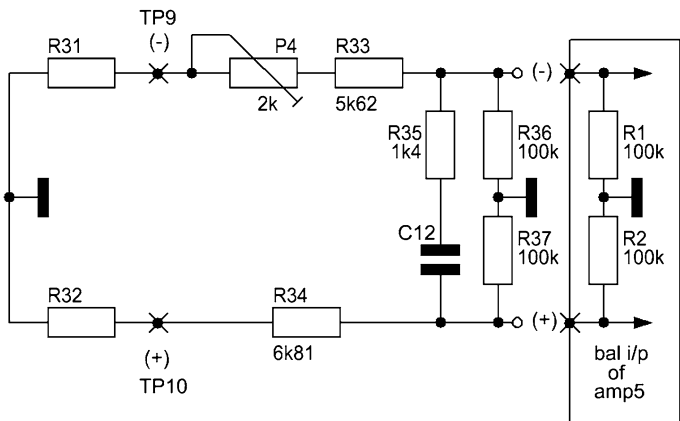


**Fig. 1.6** Situation of the 318  $\mu$ s/3180  $\mu$ s RIAA network at the output of Amp4

## 1.4 Pictures of Cases and PCBs

### 1.4.1 Cases

The Engine II is a rather complex and expensive approach: to get it done in 2013 I had to spend roughly 2500 EUR net. Therefore, some pics may give an idea about the many things that must work together and produce the shown results.

In the top 19" 3 UH-84 HP case of Fig. 1.7 we find the two engine amplifier channels for stereo use: green LEDs for the left channel, red LEDs for the right channel. Both channels are totally equal. They are housed in two 3 UH-42 HP fischer insertion cases (Fig. 1.8 shows the rear of Fig. 1.7).



**Fig. 1.7** Front of Engine II, *top* two fully equal engine channels L & R; *bottom left and right* two  $\pm 21$  V/0.5 A PSU insertion units, *middle* one triode PSU with +200 V/75 mA,  $2 \times 6.3$  V/1.5 A insertion unit



**Fig. 1.8** Rear of Engine II

In the bottom 19" 3 UH-84 HP case, together with the two  $\pm 21$  V PSU devices (cases: 3 UH-21 HP at the fully left and right sides) an Amp3 200 V plus  $2 \times 6.3$  V PSU (3 UH-42 HP case in the middle) is housed in a separate 19" 3 UH-84 HP case. The whole PSU case is located roughly 1 m away from the upper 19" 3 UH-84 HP case.

### 1.4.2 Printed Circuit Boards

Figure 1.9 gives a look on the completely equipped right channel main board before insertion into the case. From right to left side we find the plugged-in PCBs of

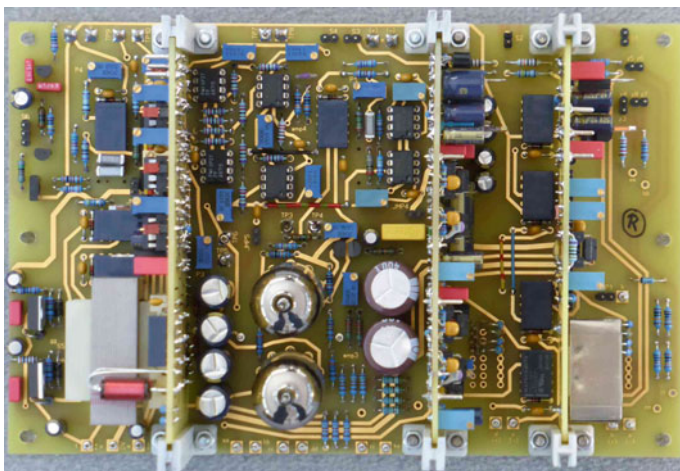


**Fig. 1.9** Look on the fully equipped Mainboard of the right channel

**Fig. 1.10** Rear and look into the case of one channel



Amp1, Amp2, and Amp5. In the top middle, there is Amp4 and the two double-triodes of the triode path Amp3 fill the lower part of the middle region.

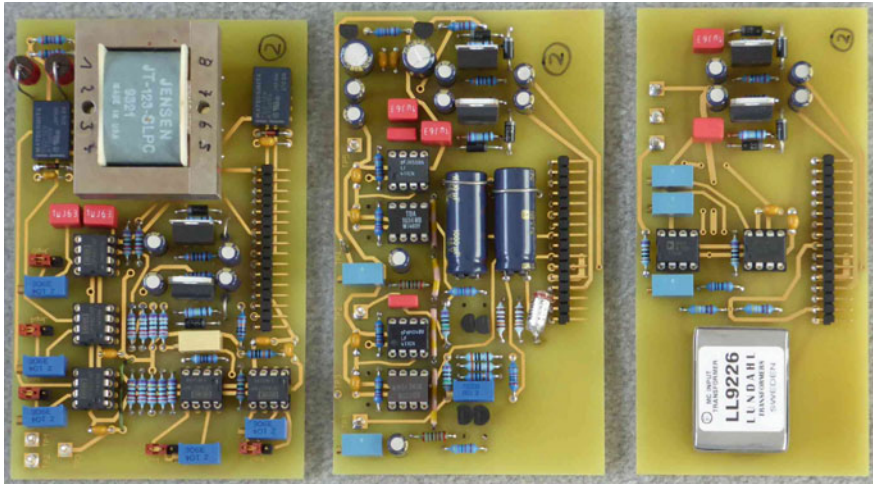
Figure 1.10 shows the rear of one channel. The observer also gets an impression about the crush inside the case. Nevertheless, many holes in the top and bottom metal plates ensure enough cooling.

Figure 1.11 gives an impression of the PCBs of the plug-in amps, the ones I used to create the measurement and listening results of this book. However, the shown Amps 1 & 2 versions need some improvements to overcome disadvantages I will describe in the following chapters.

### 1.4.3 Front and Rear of the Engine

The many switching possibilities of one chain need careful arrangement of the switches on the amplifier's front. I've chosen a set-up that follows—from left to right—the logic given in Fig. 1.1. Figure 1.12 presents the solution for the left channel. The right one looks the same with the exception of red LEDs.

The decision to design and further on to work with two fully separate channels comes from the fact that mono signals can easily be compared by application of



**Fig. 1.11** The first set of plug-in PCBs for Amp5 (*fully left*), Amp 2 (*middle*), and Amp1 (*fully right*)

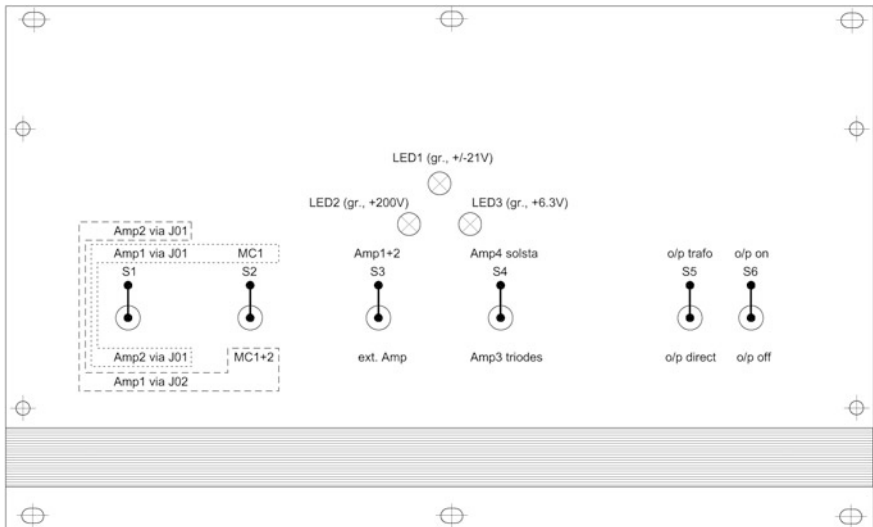


**Fig. 1.12** Front of one channel

- (a) two different triode operating point settings, or
- (b) different double-triodes, and/or
- (c) different op-amp types.

J04 at the rear offers  $\pm 21$  V for external solid-state input amp purposes. There is enough space to add female sockets for external triode anode and heater supply, if

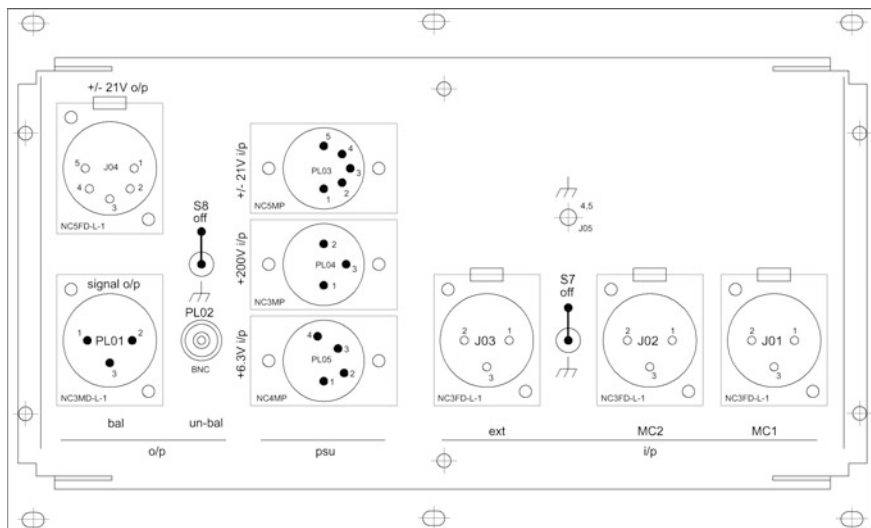


**Fig. 1.13** Rear of one channel

the triode PSU offers enough energy. Another solution for that could be extra PSUs for the external amps.

The front and rear of the PSU units are not shown in detail here. The placements of the sockets on each rear follow the logic of the needs of the two channels, as of Fig. 1.8. However, there is only one central mains socket for the triode PSU in the middle of Fig. 1.8. The mains connection for the two  $\pm 21$  V units comes from two additional and un-switched output sockets on the rear’s right side of the triode PSU.

In such a complex amp environment the right grounding is not easy to find. Therefore, at the rear of each channel and in the middle of the triode PSU rear we find ground lifts (see Figs. 1.8 and 1.13). The same applies to the motherboard with its numerous ground lift jumpers (see Fig. 1.17). Additional cable sockets on the rear of the channels allow further grounding actions between turntable(s), housing shields, and amps.

## 1.5 Power Supplies

I do not describe the different PSU units in detail here because the main emphasis lies on the amplifier action. However, here come the facts & figures on how the whole engine gets powered. In contrast to the findings of John Walton in L|A Vol. 4,<sup>7</sup> I always prefer 317 / 337 types. Each of the many solid-state amps, plug-in ones à la Fig. 1.11 as well as the ones on the main PCB, has its own stabilized

<sup>7</sup>“A comparative overview of power supply regulator designs with listening tests”, John Walton, Linear Audio Vol. 4, ISBN 978-949092905-3.



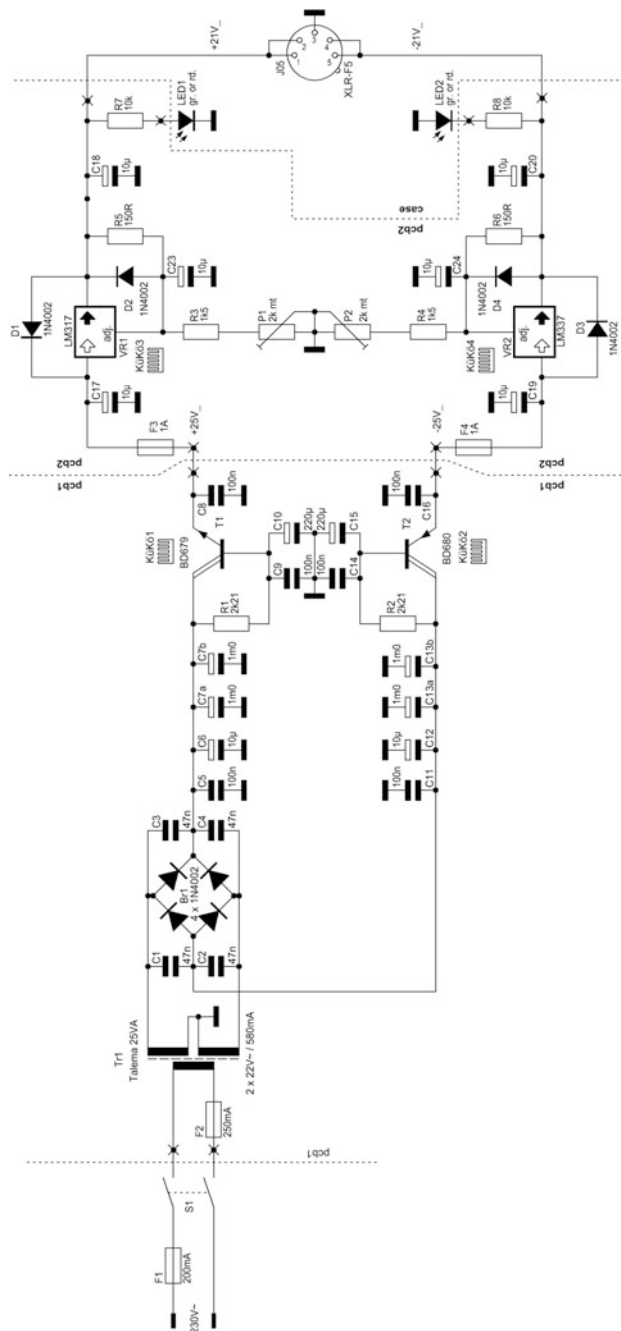


Fig. 1.14 Main  $\pm 21$  V power supply for all solid-state driven amps

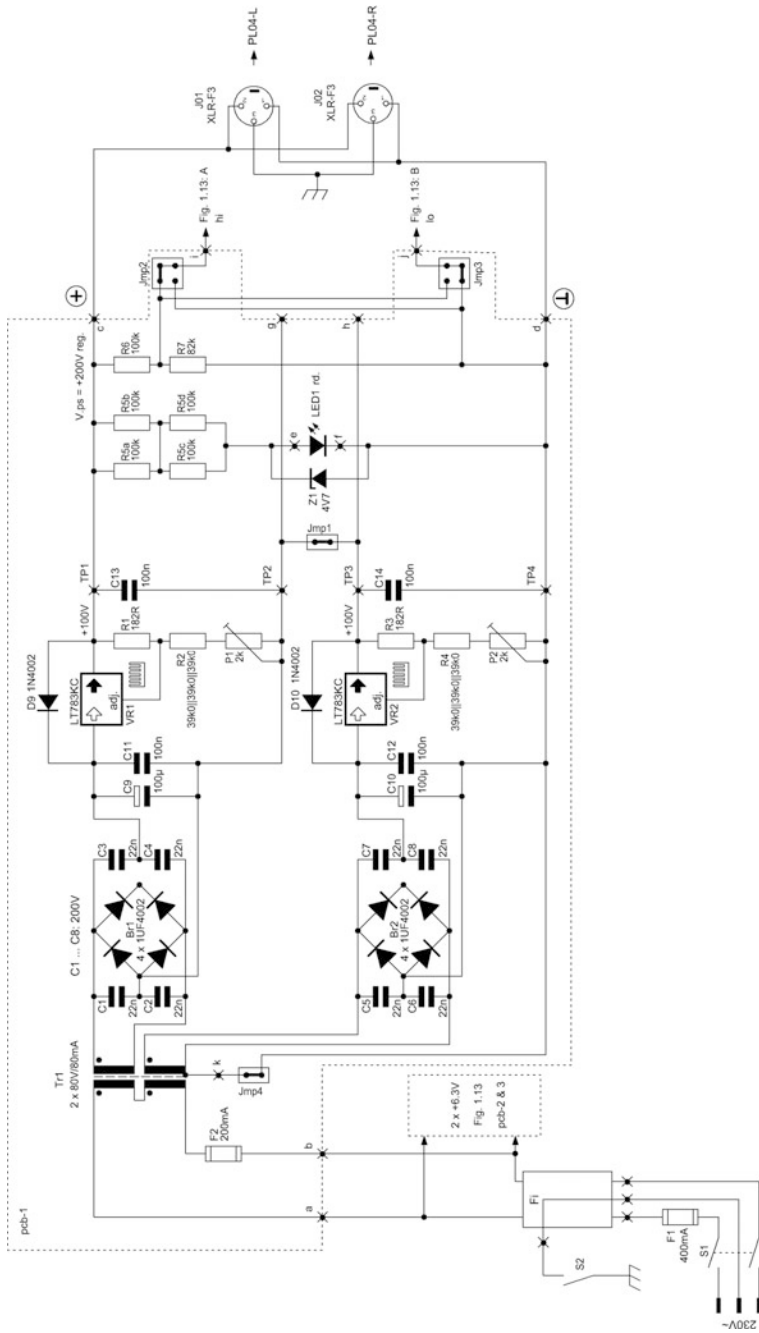
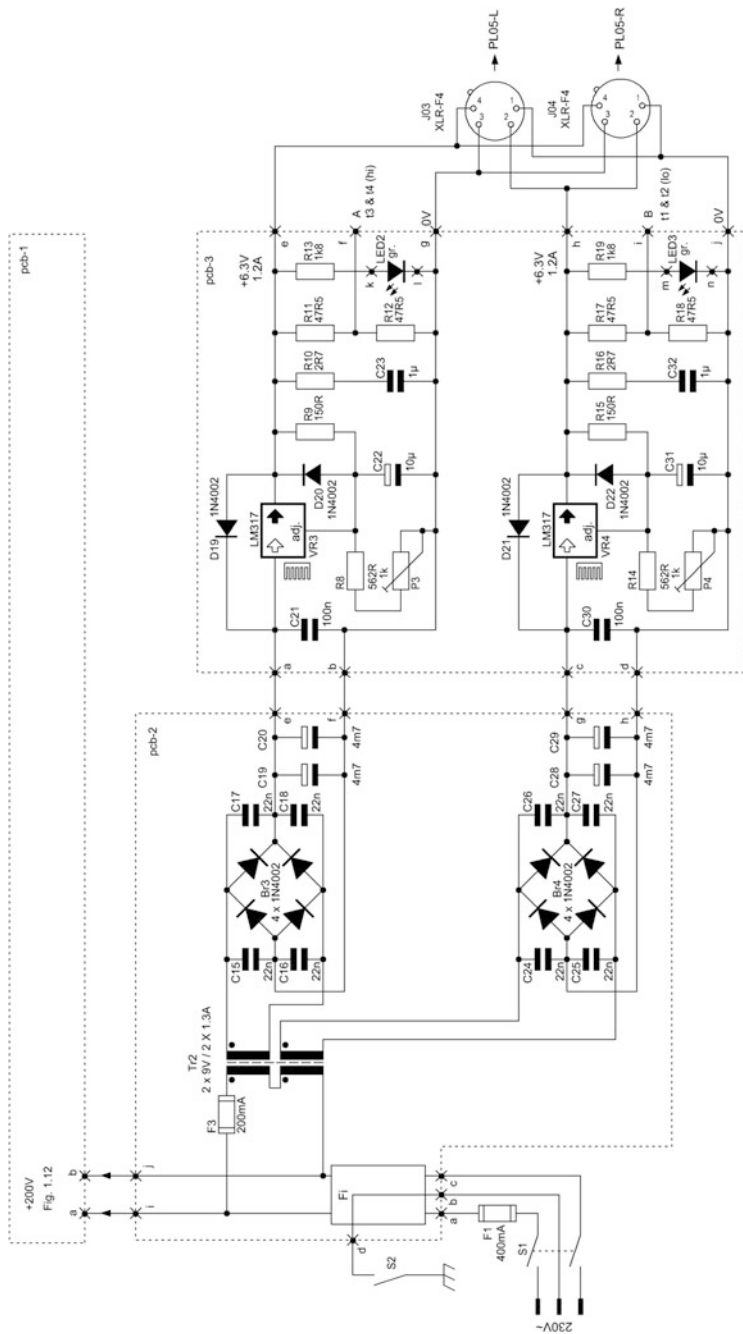


Fig. 1.15 +200 V power supply for the triode driven section



**Fig. 1.16** Two +6.3 V regulated triode heater supplies

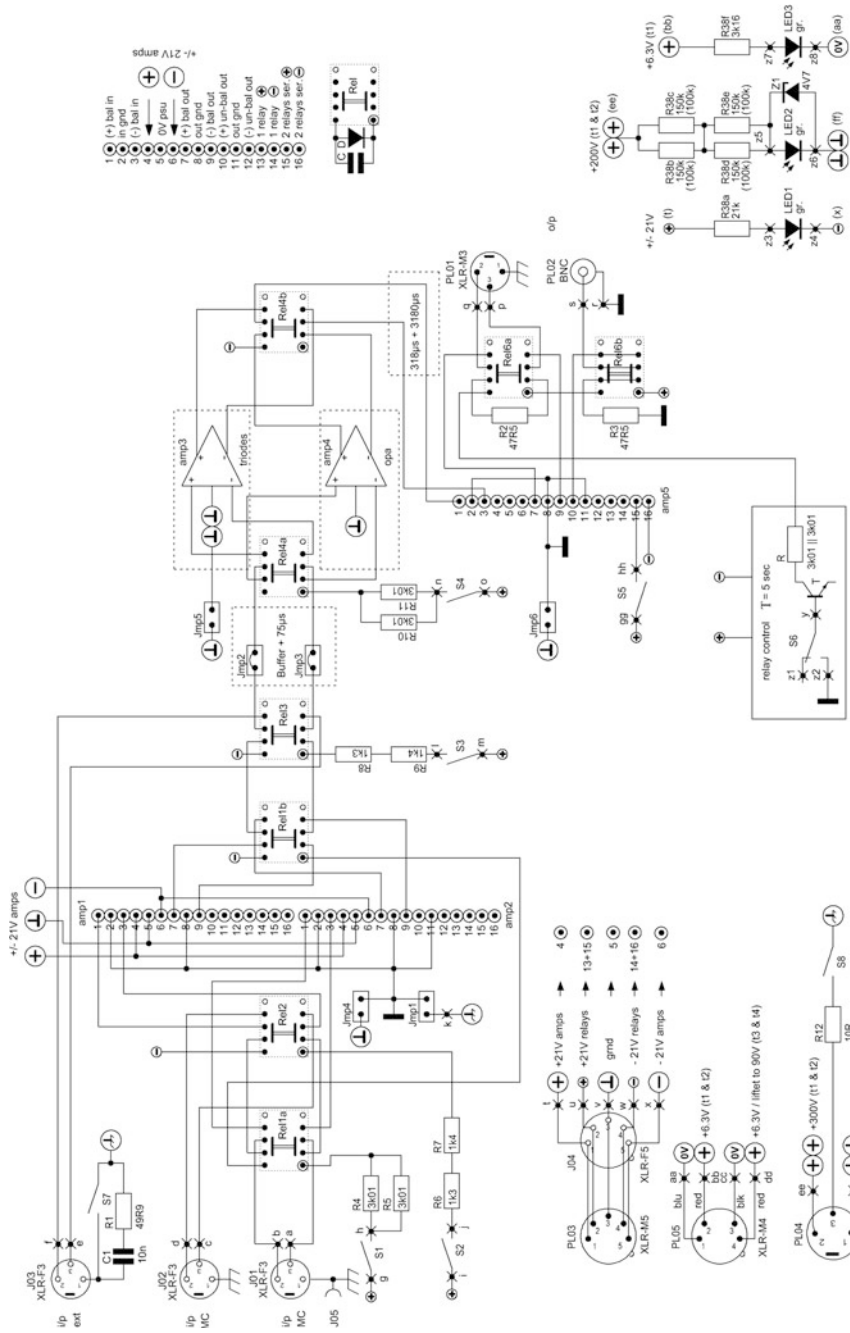


Fig. 1.17 Wiring on the Mainboard and to the outside world

$\pm 15$  V sub-PSU, each channel is fed by a  $\pm 21$  V main PSU, shown in Figs. 1.7 and 1.8 on the fully left and fully right side of the lower half. All op-amps have their blocking Cs located rather close to the IC. The  $\pm 21$  V circuit is given in Fig. 1.14.

A view words about the +200 V PSU. There is only one of them. I took a transformer with two 80 V/75 mA output windings. Each of them feeds a rectifier bridge followed by an integrated stabilizing circuit LT783KC with a trimmed output voltage of +100 V. Both output voltages stacked lead to a very stable and rather low-noise and low-hum output voltage of +200 V for both channels. There is no need of the same configuration for the other channel. One unit is enough here because there is a rather high filtering effect of the Amp3 anode voltage C-R-C chain. Between the two channels any interaction is cut down to an immeasurable level. Figure 1.15 shows the circuit.

In that unit I've also installed two 6.3 V heater supplies, one for the first double-triode's low heater potential around 0 V DC, the other one for the output triode with its heater potential around +90 V DC. Both heater voltages are regulated too. Figure 1.16 gives the details.

---

## 1.6 Mainboard

Figure 1.17 shows the circuit of the Mainboard. Its fully equipped version is shown in Fig. 1.9. Switches S1, S2, S7, S8 (and S2 on Figs. 1.15 and 1.16) are the before mentioned ground lifts that can be switched at the outside of the case rears. Depending on the hum amount represented in an output FFT diagram (with input shorted) jumpers Jmp1, Jmp4, Jmp5, and Jmp6 can be set to suppress most of the mains interferences on the ground lines. However, because of the fully balanced layout there should not be a need for that. I guess the rest of the circuit is self-explanatory.

---

## 2.1 General Design of Amp3

The two central Amps 3 & 4 are the heart of the whole amplifier arrangement. Therefore, I will start my explanations with these, followed by the output stage Amp5 and the two input stages Amps 1 & 2.

Before I entered into the here presented design of Fig. 2.1, I had some tests on the most useful balanced triode driven solution, however, always in conjunction with the placement of the RIAA network. In addition, the solution should be as low-noise as possible, thus, increasing the noise level of the preceding gain stage by not more than point B.2. of Chap. 1 would allow. On the other hand, it should have outstanding CMRR and easy balance trimming.

Based on the findings in the Differential Gain Stage (DIF) chapter of the 2nd edition of my How to Gain Gain book (HTGG-2)<sup>1</sup> I opted for a DIF input stage followed by a CF (cathode follower) output stage. The easy handling of a CCSCF gain stage (Common Cathode gain Stage CCS followed by a CF) led to the shown Fig. 2.1 configuration without RIAA networks. I used such a CCSCF as output stage in the triode driven Module 4 phono-amp of Engine I in TSOS-2.<sup>2</sup> To get a rather high CMRR the DIF stage's DC current comes from a solid-state current generator (a sink here), formed by two BJTs. It creates a very high dynamic resistance between t1 & t2 cathode and ground.

The input section is the DIF formed by a  $g_m$ -selected low-noise double-triode E88CC/6922 (E188CC/7308 work well too). In each triode system the anode current is equal and trimmed to 2 mA by P2 of the current sink T1 & T2 (480 mV between test points TP3 & TP4). Trimming of P5 optimizes CMRR further (calculated appr. 100 dB). It ensures equal signal levels at the cathodes of t4 & t3. Each of the following CF stages is powered by appr. 90 V/2 mA too. Here, instead of the shown

---

<sup>1</sup>“How to Gain Gain”, 2nd ed., B. Vogel, (HTGG-2), Chap. 30.

<sup>2</sup>TSOS-2, Chap. 17.

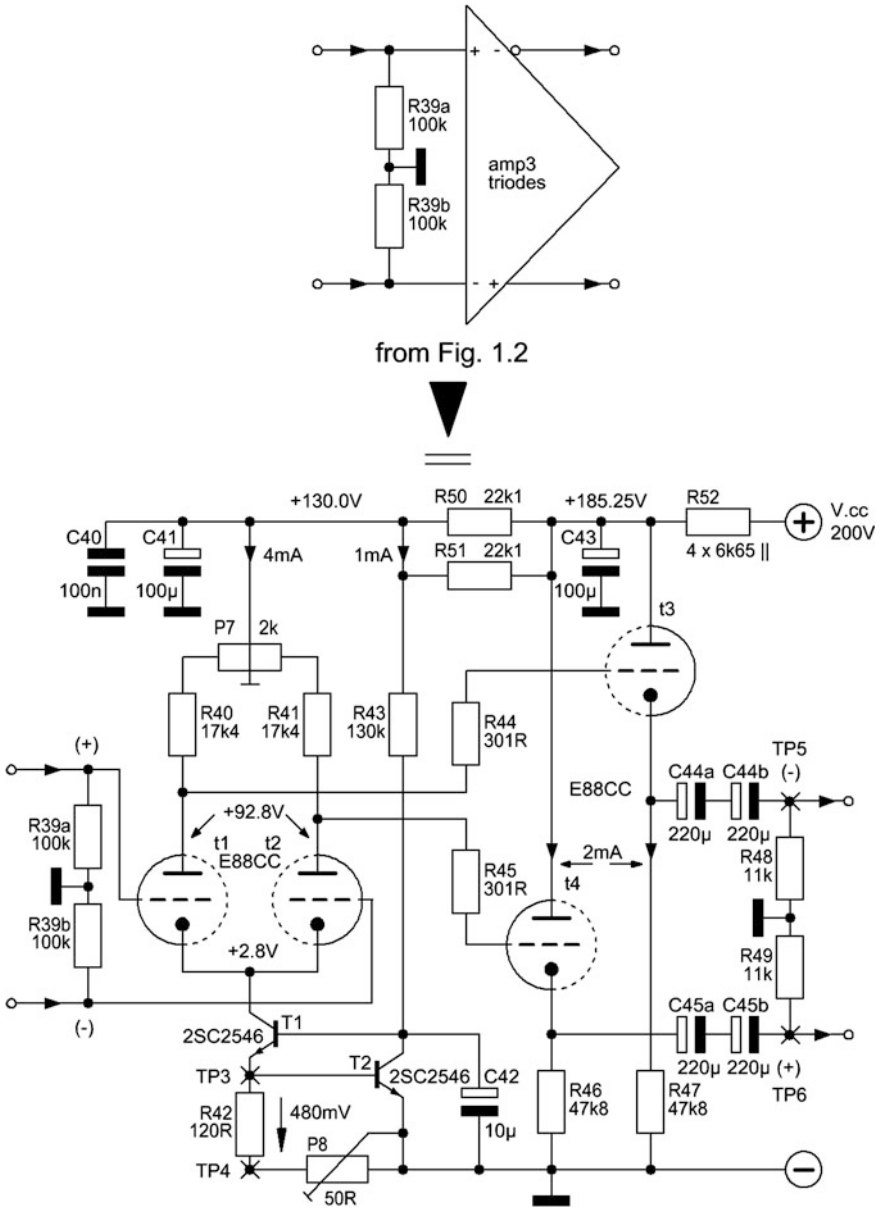


Fig. 2.1 Amp3 without RIAA networks

E88CC I also tried non-selected NOS 7308 s. Their noise level is rather low and their triode systems do not differ very much. Finally, I took the 7308 s.<sup>3</sup>

The gain  $G_{\text{amp3}}$  becomes measured appr. 16 and the whole design looks rather simple. In addition, with a perfect trim we can get a 1 kHz THD  $\leq 0.010\%$  (stronger d2 than d3) and IMD always  $< 0.010\%$  (I've measured 4 different 80 %/20 % frequency pairs). My Clio sinus generator offers a min. 1 kHz THD level of 0.002 % rounded<sup>4</sup> through my un-balanced to balanced converter (see Footnote 4), strictly THD only and not THD + N! I could calculate the real 1 kHz THD with distortion spike level figures taken from the FFT diagram: 0.00159 % (more about distortions etc. see Chap. 12—Engine II Performance).

The gain stage fulfils the overload goal. I measured 46  $V_{\text{pp}}$  before soft clipping. With an input signal level of 100 mV<sub>rms</sub> + 20 dB overload margin = 1 V<sub>rms</sub> and a gain of 16 we need a max. voltage swing of  $16 \text{ V} * 2 * \sqrt{2} = 45.255 \text{ V}_{\text{pp}}$ .

Based on the following considerations we can roughly check the extra-generated noise level of the sequence of Amp3 & Amp5: with input loaded by 20  $\Omega$ , Amp2 (its SN looks worse than the one of Amp1) alone generates a measured (<sub>m</sub>) output referred non-equalized (<sub>ne</sub>)  $\text{SN}_{\text{ne.o.m}} = -73.1 \text{ dB}$  ref. 100 mV/B<sub>20k</sub>, almost white noise. It includes a tiny amount of 1/f-noise.<sup>5</sup> Multiplication by 10 (theoretically through a no-noise amp-stage) leads to a total output referred  $\text{SN}_{\text{ne.o.tot}} = -73.1 \text{ dBV}$  at the engine's output. Now, after application of the B<sub>20k</sub> RIAA function and A-weighting SN-improvement figure  $\text{SN}_{\text{ar}} \approx -8 \text{ dB}$ <sup>6</sup> for purely white noise generating devices we obtain the guessed output referred A-weighted and equalized (<sub>ariaa</sub>)  $\text{SN}_{\text{ariaa.o}} = -81.1 \text{ dBV(A)}$ . With the sequence of 20  $\Omega$  + Amp2 + Amp3 + Amp5 + Trafo at the output of the Engine I've measured  $\text{SN}_{\text{ariaa.o.m}} = -79.9 \text{ dBV(A)}$  for the left channel and  $-80.2 \text{ dBV(A)}$  for the right one. With that, the goal of an input referred  $\text{SN}_{\text{ariaa.i}} = -79.0 \text{ dBV(A)}$  won't get into trouble.

Nevertheless, via shorted external input, the output referred SN of the amp sequence Amp3 + Amp5 + Trafo becomes measured (calculated)  $-99.0 \text{ dBV(A)}$  ( $-100.2 \text{ dBV(A)}$ ). Figure 2.2<sup>7</sup> shows the curve of the noise voltage density at the output of the before given sequence, based on data-sheet data. It also shows a kind of 1/f-noise characteristic. It is generated by two sources:

- (a) by an assumed 1/f-noise corner frequency of  $f_{\text{c.e1,2}} = 1 \text{ kHz}$  of the DIF input triodes (high influence on the overall noise voltage) and an  $f_{\text{c.e3,4}} = 10 \text{ kHz}$  of the two output CFs (rather low influence on the overall noise voltage), and

<sup>3</sup>I deeply have to thank my friend Klaus Burosch ([www.burosch.de](http://www.burosch.de)) for his courteous support concerning his huge collection of NOS and brand new valves. All used (and many more) valves had to pass the test arrangement I've presented in Jan Didden's Linear Audio Vol. 4 "The Glowing NoiseMaker—on the demystification of triode noise" or in HTGG-2, Sect. 2.3.

<sup>4</sup>Details see Chap. 15.

<sup>5</sup>Additionally see my remarks on Amp2's SN in Chapter 10.

<sup>6</sup>TSOS-2, Chapter 15, TSOS-1 Chapter 6.

<sup>7</sup>Details see next Chapter and MCD-WS 3.1.



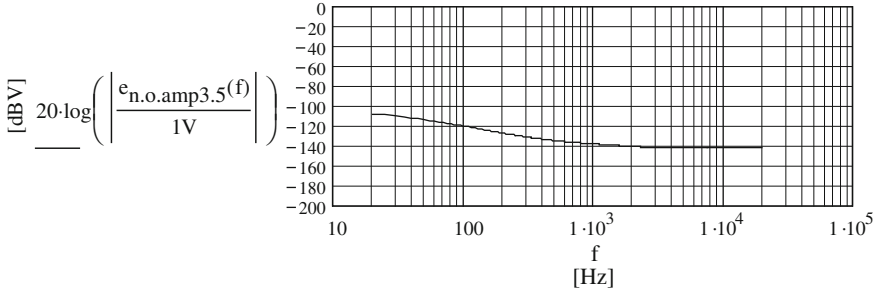


**Fig. 2.2** Output noise voltage density of the amp sequence Amp3 + Amp5 + Trafo with input shorted

- (b) by the RIAA network effect of the 318  $\mu$ s/3180  $\mu$ s network at the output of Amp3. The 75  $\mu$ s input network has practically no effect on the Amp3 noise generation. It only filters the incoming noise voltage from preceding gain stages.

To calculate the component values for the T1/T3 RIAA network we need the differential o/p resistance  $R_{o.cf,dif}(f)$  of t3 & t4 (see (1.6)–(1.8) in the previous chapter). Because of C44a–C45b it is frequency dependent and in consideration of R48 & R49 it is the sum of the equal o/p resistances  $R_{o.cf3}(f) + R_{o.cf4}(f)$ . The relevant equations look as follows:

$$\begin{aligned} R_{o.cf3}(f) &= R_{o.cf4}(f) \\ &= \left[ \frac{1}{R48} + \frac{1}{R_{o.cf3} + \left(2j\pi f \frac{C44a}{2}\right)^{-1}} \right]^{-1} \end{aligned} \quad (2.1)$$

$$R_{o.cf,dif}(f) = R_{o.cf3}(f) + R_{o.cf4}(f) \quad (2.2)$$

$$\begin{aligned} R_{o.cf3} &= \frac{r_{a3}R47}{r_{a3} + (1 + \mu_3)R47} \\ &= R_{o.cf4} \end{aligned} \quad (2.3)$$

According to the goals C44a–C45b must be chosen of a size that should not hurt a flat frequency and phase response in  $B_{20k}$ . Then, with  $r_{a3} = r_{a4} = 8.836 \text{ k}\Omega$ ,  $g_{m3} = g_{m4} = 3.5 \text{ mS}$ , and  $\mu_3 = \mu_4 = 29$  we'll get  $R_{o.cf,dif} = 549.2 \Omega$ . I've chosen Panasonic FC 63 V types. With them, the deviation from the flatness becomes a calculated  $-0.025 \text{ dB}/+0.2^\circ$  at 20 Hz only. Figure 2.3 shows the calculated deviation from the exact RIAA transfer if we would consider the RIAA networks. The measured frequency and phase response will be given in Chap. 12.

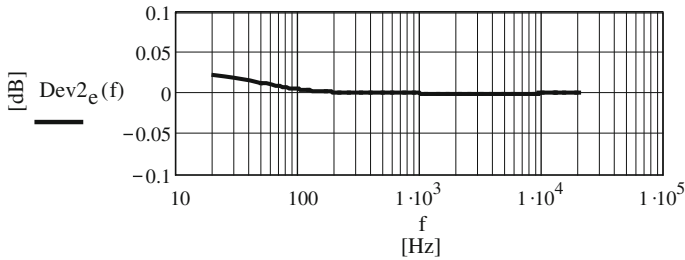


**Fig. 2.3** Calculated deviation from the exact RIAA transfer

Figure 2.1 also shows the constant current sink around BJTs T1 & T2. The actual noise voltage of this CCsi is of minor importance. What hits the DIF most is the noise current mainly produced by T1's collector current. Multiplied by the cathode input resistance of the DIF we have an enormous noise voltage that is amplified by the here effective grounded grid gain stages (CGS) formed by t1 & t2, in this case leading to 100 % correlated noise voltages of equal amplitude at the anodes of t1 & t2. Hence, at the differential output of Amp3 we find the CCsi generated noise voltage with a doubled level! To suppress it we need a following Amp5 with rather high CMRR. Chapter 6 gives the details of Amp5.

## 2.2 Gain and Noise Calculations

The Mathcad worksheet (MCD WS-3.1) of the next chapter gives all the details of a rather extensive calculation course. All results are based on data-sheet data. I've also gone through the calculation with actual data. Selected low-noise triodes should have very low  $1/f$ -noise corner frequencies and far better (higher)  $g_m$ -values than the ones of the data-sheets. Fortunately, they do not differ very much from the ones gained by application of data-sheet data together with the assumed data for the  $1/f$ -noise corner frequency. I guess it is clear that higher  $1/f$ -noise corner frequencies will automatically lead to worsened SNs.

The complete calculation of the gain and noise production of a DIF can easily be studied in HTGG-2, Chap. 30. However, for a better understanding I will repeat the equivalent circuit and the main equations here.

### 2.2.1 Gain of a DIF Followed by Two CFs

The DIF's idle gain  $G_{0,dif}$ :

$$G_{0,dif} = G_{0,t1,2} = -\mu_1 \frac{R40 + 0.5P7}{r_{a1} + R40 + 0.5P7} \quad (2.4)$$

The CF's frequency dependent gain with output load  $R_L(f)$  (because of its tiny influence here the impedance of Fig. 1.2's C12 is set to  $0 \Omega$ ):

$$G_{cf4}(f) = \mu_4 \frac{R47}{r_{a4} + (1 + \mu_4)R47 + \frac{r_{a4}R47}{R_{L,t4}(f)}} \quad (2.5)$$

$$R_{L,t4}(f) = \frac{1}{2j\pi f 0.5C44a} + \left[ \frac{1}{R48} + \frac{1}{R34 + \left( [0.5R35]^{-1} + R36^{-1} \right)^{-1}} \right]^{-1} \quad (2.6)$$

$$= R_{L,t3}(f)$$

$G_{0,dif}$  is the DIF's idle gain because its anode has an infinite load by the following t3/t4 grids.  $R_{L,t4}(f)$  is the frequency dependent load at the cathode of t4. The same applies to  $R_{L,t3}(f)$ .

$$G_{cf3}(f) = G_{cf4}(f) \quad (2.7)$$

$$G_{cf}(f) = G_{cf3}(f)G_{cf4}(f) \quad (2.8)$$

⇒ The frequency dependent DIFCF gain  $G_{difcf}(f)$  thus becomes:

$$G_{difcf}(f) = G_{0,dif}G_{cf}(f) \quad (2.9)$$

⇒ The balanced gain  $G_{op1,2}$  of the two op-amps OPs 1 & 2 is 1. Hence, the Amp3 gain  $G_{amp3}(f)$  without RIAA transfer becomes:

$$G_{amp3}(f) = G_{difcf}(f)G_{op1,2} \quad (2.10)$$

## 2.2.2 RIAA Transfer Function

From Figs. 1.4 and 1.5 and (2.1)–(2.3) we can derive the frequency dependent and RIAA transfer loaded gains  $G_{T2}(f)$  and  $G_{T1,3}(f)$  of the Amp3 input and output networks as follows:

$$G_{T2}(f) = \frac{M}{M + R25 + R26 + P1 + 2 \left( R_{o,op1}^{-1} + R23^{-1} \right)^{-1}} \quad (2.11)$$

$$M = \left[ 2j\pi f (C9 + C_{i,dif}) + (R39a + RR39b)^{-1} \right]^{-1}$$

$$G_{T1.3}(f) = \frac{\left[ \left( [2j\pi f C12]^{-1} + R35 \right)^{-1} + R_{L,dif}^{-1} \right]^{-1}}{\left[ \left( [2j\pi f C12]^{-1} + R35 \right)^{-1} + R_{L,dif}^{-1} \right]^{-1} + R_{T1,eff}(f)} \quad (2.12)$$

$$R_{L,dif} = \left( [R1_{amp5} + R2_{amp5}]^{-1} + [R36 + R37]^{-1} \right)^{-1} \quad (2.13)$$

$$R_{T1,eff}(f) = R_{o,cf,dif}(f) + P3 + R33 + R34 \quad (2.14)$$

⇒ With C9 and C12 carefully selected according to Figs. 1.4 and 1.5 the transfer function  $T_{amp3}(f)$  of the whole Amp3, including RIAA transfer function, thus becomes:

$$T_{amp3}(f) = G_{amp3}(f)G_{T2}(f)G_{T1.3}(f) \quad (2.15)$$

### 2.2.3 Noise and SN Calculations According to Fig. 1.2

The calculation of the noise voltage of the DIFCF alone makes no sense, as long as there are influential factors at its input (OPs 1 & 2 + T2(f)) and at its output (T1(f) + T3(f) + Amp5). All together, they generate a noise voltage that can be measured at the output of Amp5, and thus be compared with the calculated results. The calculation course follows the mathematical course given in MCD-WS 3.1, “6. Noise and SN calculations”. However, here comes the short version. It tackles the major factors.

To calculate the output noise voltage density  $e_{n.o.amp3.5}(f)$  at the o/p of Amp5 and with Amp3 input shorted the rather complex looking equation looks as follows:

$$e_{n.o.amp3.5}(f) = G_{amp5} \sqrt{\left[ \left[ \left[ \begin{array}{l} \left( e_{n.o.op1.2}(f)^2 G_{T2}(f)^2 \right) \\ + e_{n.z.T2}(f)^2 \\ + 2e_{n.rN1}(f)^2 \end{array} \right] |G_{0,dif}|^2 \right] G_{cf}(f)^2 \right] G_{T1.3}(f)^2 + \left( \frac{2e_{n.ccsi} G_{cgs.1} G_{cf}(f) G_{T1.3}(f)}{CMRR_{amp5}} \right)^2 + e_{n.z.T1.3}(f) + i_{n.i.amp5}^2 Z_{T1.3}(f)^2 + e_{n.i.amp5}^2 \right]} \quad (2.16)$$

$$G_{\text{cgs.1}} = (1 + \mu_1) \frac{R40 + 0.5P7}{r_{a1} + R40 + 0.5P7} \quad (2.17)$$

$$= G_{\text{cgs.2}}$$

According to (2.16), Figs. 1.2 and 2.1 it includes the following 100 % uncorrelated noise sources:

• OP1 & OP2 (frequency dependent = fd):	$e_{\text{n.o.op1.2}}(f)$
• T2(f) network (fd):	$e_{\text{n.Z.T2}}(f)$
• t1 & t2 noise (fd) <sup>a</sup> :	$e_{\text{n.rN1}}(f) = e_{\text{n.rN2}}(f)$
• $R_{\text{gg3}} = R44 + R45$ :	$e_{\text{n.Rgg3}}$
• $R_a = R40 + R41$ (incl. fd excess noise):	$e_{\text{n.Ra.eff}}(f)$
• t3 & t4 noise (fd) <sup>b</sup> :	$e_{\text{n.rN3}}(f) = e_{\text{n.rN4}}(f)$
• $R_c = R46 + R47$ (incl. fd excess noise):	$e_{\text{n.Rc.eff}}(f)$
• T1(f) & T3(f) network (fd):	$e_{\text{n.Z.T1.3}}(f) \& Z_{\text{T1.3}}(f)$
• Amp5 i/p noise current	$i_{\text{n.i.amp5}}$ (no 1/f-noise!)
• Amp5 input referred noise voltage:	$e_{\text{n.i.amp5}}$ (=average value in $B_{20k}$ )

<sup>a</sup>I've chosen a low-noise double-triode here that has, in both systems, a 1/f-noise corner frequency of 1 kHz; a change to 10 kHz would worsen the calculated output referred SN of  $-100.2$  dBV(A) by appr. 3.5 dB, a change to 100 Hz would improve SNs by appr. 0.6 dB

<sup>b</sup>For calculation purposes, I've chosen a noisy double-triode here that has in both systems a 1/f-noise corner frequency of 10 kHz; a change to 1 kHz would improve the result of (2.16) by 0.014 dB only

Note: By integration over  $B_{20k}$  and division by  $\sqrt{B_{20k}}$  the frequency dependency of the input referred noise voltage density of Amp5 (see respective MCD-WS in Chap. 7) can be turned into one single average density value. Hence, and in other words, we gain the rms value of the noise voltage in  $B_{20k}$  and after division by  $\sqrt{B_{20k}}$  we'll get the average density value, however, guilty in  $B_{20k}$  only!

- Generated by the noise current of the constant current sink CCsi and its BJTs T1 & T2 and multiplied by the equal gains  $G_{\text{cgs.1}}$  of the Common Grid Stages (CGS) t1 & t2 the 100 % correlated noise voltage  $e_{\text{n.ccsi}}$  is damped by the CMRR of Amp5 (see Chaps. 6 and 7). Because there is 100 % uncorrelation between this term and all the other ones, it is integrated into (2.16) too.

I must point out that some terms in (2.16) do not add significant values to the total sum underneath the root. Nevertheless, I keep them for universal usage with other than the chosen components.

The resulting noise voltage density multiplied by the A-weighting function, referenced to 1  $V_{\text{rms}}$  nominal signal output voltage, and integrated over the bandwidth of  $B_{20k}$ , will lead to the A-weighted output referred  $\text{SN}_{\text{a.o.amp3.5}}$  in  $B_{20k}$ , expressed in dBV(A).

With the exception of the DIF, the detailed calculation approaches of the different terms in (2.16) can completely be studied in TSOS-2. TSOS-1 is not a help at all because it doesn't cover the triode math approaches.

### 2.2.4 A Look into the Content of MCD-WS 3.1

MCD-WS 3.1 shows some additional interesting results:

- Very important for external amplifiers Point 6.5.2 shows the calculation of the Amp3 CMRR.
- Point 7. covers the math of an extremely low-noise input load of the Fig. 2.1 arrangement with Amp3. Here, I've chosen a pre-amp with a gain of 200, an i/p referred noise voltage density of 0.2 nV/rtHz and noise current density of only 2.4 pA/rtHz. The i/p load is 20  $\Omega$ . Now we can compare the A-weighted and RIAA equalized SN result ( $=-82.523$  dBV(A)) with the one of Point 8.
- Point 8. covers the math of the Point 7. low-noise Amp1, followed by a no-noise arrangement à la Fig. 2.1. The SN result becomes  $-82.582$  dBV(A).
- Hence, the difference is appr. 0.06 dB only. It is nothing else but the Noise Figure. In other words: a further chase for extremely low-noise solutions makes no sense for input loads  $\geq 20 \Omega$ . We will see later on in Chap. 10 what it will mean for input loads  $< 20 \Omega$ .
- Point 9. and 10. show calculations of the Noise Figure NF of the amp chain Amp3 + Amp5, fed by a lowest-noise input amp: 9. for MC and 10. for MM cartridge purposes. These NFs are all  $< 0.1$  dB. Hence, together with its input and output loads the noise impact of the here presented Amp3 is completely ignorable.
- Point 11. gives up the shorted input and replaces the shortage by an output resistance of a preceding gain stage, here 1 k $\Omega$ . Because of the 75  $\mu$ s lp at the input, the noise impact becomes marginal too.

## Contents

### 3.1 MCD-WS: The Triode Gain Stage Amp3 with RIAA Networks

**Note 1:** MCD 11 has no built-in unit “rtHz” or “ $\sqrt{\text{Hz}}$ ”. To get  $\sqrt{1 \text{ Hz}}$  based voltage noise and current noise densities the rms noise voltage and current in a specific frequency range  $B > 1 \text{ Hz}$  must be multiplied by  $\sqrt{1 \text{ Hz}}$  and divided by the root of that specific frequency range  $\sqrt{B}$ !

**Note 2:** MCD 11 offers no “dB” unit. This is available from MCD 13 on!

3.1 MCD-WS: The Triode Gain Stage Amp3 with RIAA Networks

Calculations of the triode driven Amp3 with T1/T3 RIAA network at the output, T2 RIAA network at the input, and based on triode data-sheet figures :

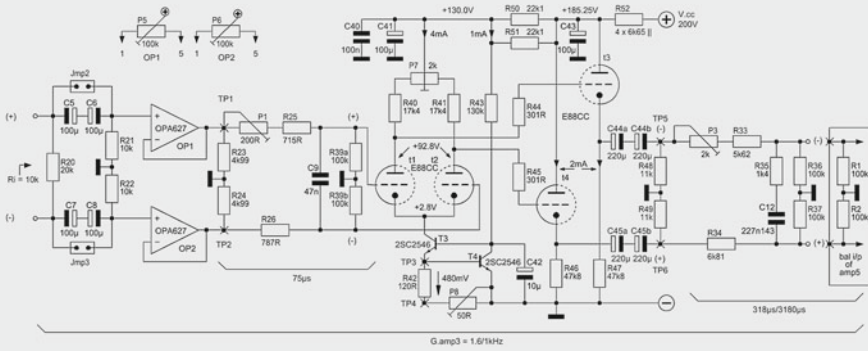


Fig. 3.1 Triode driven Amp3 incl. RIAA networks

1. General data :

DIF (t1+t2) with E88CC - 2x2mA:

2xCF (t3+t4) with E88CC - 2x2mA

At the triode stage input:

OP1 = OPA627      OP2 = OP1

$$k := 1.38065 \cdot 10^{-23} \text{V} \cdot \text{A} \cdot \text{s} \cdot \text{K}^{-1}$$

$$T := 315\text{K}$$

$$B_{20k} := 19980\text{Hz}$$

$$B_1 := 1\text{Hz}$$

$$f := 20\text{Hz}, 25\text{Hz}, 20000\text{Hz}$$

$$h := 1000\text{Hz}$$

Assumed:  $f_{c1} := 1000\text{Hz}$

$$f_{c2} := f_{c1}$$

$$f_{c3} := 10000\text{Hz}$$

$$f_{c4} := f_{c3}$$

$$F_{c1} := \frac{f_{c1} \cdot \ln(1000) + B_{20k}}{B_{20k}}$$

$$F_{c1} = 1.346$$

$$F_{c2} = F_{c1}$$

$$F_{c3} := \frac{f_{c3} \cdot \ln(1000) + B_{20k}}{B_{20k}}$$

$$F_{c3} = 4.457$$

$$F_{c4} = F_{c3}$$

$$\mu_1 := 29$$

$$\mu_2 := \mu_1$$

$$\mu_3 := 29$$

$$\mu_4 := \mu_3$$

$$g_{m1} := 3.5 \cdot 10^{-3} \text{S}$$

$$g_{m2} := g_{m1}$$

$$g_{m3} := 3.5 \cdot 10^{-3} \text{S}$$

$$g_{m4} := g_{m3}$$

$$r_{a1} := \frac{\mu_1}{g_{m1}} \quad r_{a1} = 8.286 \times 10^3 \Omega \quad r_{a2} := r_{a1}$$

$$r_{a3} := \frac{\mu_3}{g_{m3}} \quad r_{a4} := r_{a3}$$

$$V_{g1} := -2.8\text{V}$$

$$V_{g2} := V_{g1}$$

$$V_{g3} := -2.8\text{V}$$

$$V_{g4} := V_{g3}$$



## 3.1 MCD-WS: The Triode Gain Stage Amp3 with RIAA Networks

Page 2

$$\begin{array}{llll} V_{a1} := 90V & V_{a2} := V_{a1} & V_{a3} := 90V & V_{a4} := V_{a3} \\ I_{a1} := 2 \cdot 10^{-3} A & I_{a2} := I_{a1} & I_{a3} := 2 \cdot 10^{-3} A & I_{a4} := I_{a3} \end{array}$$

2. Gain stage (GS) component data :

$$\begin{array}{lllll} R20 := 20 \cdot 10^3 \Omega & R21 := 10 \cdot 10^3 \Omega & R22 := R21 & R23 := 4.99 \cdot 10^3 \Omega & R24 := R23 \\ R25 := 750 \Omega & R26 := 787 \Omega & R33 := 5.62 \cdot 10^3 \Omega & R34 := 6.81 \cdot 10^3 \Omega & R35 := 1.4 \cdot 10^3 \Omega \\ R36 := 100 \cdot 10^3 \Omega & R37 := R36 & R39a := 100 \cdot 10^3 \Omega & R39b := R39a & R40 := 18.4 \cdot 10^3 \Omega \\ R41 := R40 & R42 := 145 \Omega & R43 := 130 \cdot 10^3 \Omega & R44 := 301 \Omega & R45 := R44 \\ R46 := \frac{143 \cdot 10^3 \Omega}{3} & R46 = 47.667 \times 10^3 \Omega & R47 := R46 & R48 := 11 \cdot 10^3 \Omega & R49 := R48 \\ R50 := 22.1 \cdot 10^3 \Omega & R51 := R50 & R52 := \frac{6.65 \cdot 10^3 \Omega}{4} & R52 = 1.663 \times 10^3 \Omega & \\ \\ R1_{amp5} := 100 \cdot 10^3 \Omega & R2_{amp5} := R1_{amp5} & & & \\ C5 := 100 \cdot 10^{-6} F & C6 := C5 & C7 := C5 & C8 := C5 & \\ C9 := 47 \cdot 10^{-9} F & C12 := 227.143 \cdot 10^{-9} F & & & \\ C44a := 220 \cdot 10^{-6} F & C44b := C44a & C45a := C44a & C45b := C44a & \\ P5 := 20 \cdot 10^3 \Omega & P6 := P5 & P7 := 2 \cdot 10^3 \Omega & P8 := 50 \Omega & \end{array}$$

Note: For further calculation purposes only: R25 = R25+P1, R33 = R33+P3, R42 = R42+P8, R40&41 = R40&41+0.5\*P7  
Exact values for P1, P3, C9, C12 see further down

3. DIFCF = CCSCF in balanced mode :

## 3.1 DIF :

$$\begin{array}{ll} G_{0,dif} := -\mu_1 \frac{R40}{r_{a1} + R40} & G_{0,dif} = -19.996 \\ R_{o,dif} := 2 \cdot \frac{r_{a1} \cdot R40}{r_{a1} + R40} & R_{o,dif} = 11.426 \times 10^3 \Omega \\ R_{o,a1} := \frac{r_{a1} \cdot R40}{r_{a1} + R40} & R_{o,a1} = 5.713 \times 10^3 \Omega \\ C_{ga1} := 1.4 \cdot 10^{-12} F & C_{gc1} := 3.1 \cdot 10^{-12} F \\ C_{stray1} := 2 \cdot 10^{-12} F & \\ C_{i1} := \left( |G_{0,dif}| + 1 \right) \cdot C_{ga1} + C_{gc1} + C_{stray1} & C_{i1} = 34.494 \times 10^{-12} F \\ C_{i,dif} := 0.5 \cdot C_{i1} & C_{i,dif} = 17.247 \times 10^{-12} F \end{array}$$

3.1 MCD-WS: The Triode Gain Stage Amp3 with RIAA Networks

3.2 CF :

$$R_{L,t4}(f) := \frac{1}{2j \cdot \pi \cdot f \cdot 0.5 \cdot C44a} + \left[ \frac{1}{R48} + \frac{1}{R34 + \left( \frac{1}{0.5 \cdot R35} + \frac{1}{R36} \right)^{-1}} \right]^{-1} \quad |R_{L,t4}(h)| = 4.461 \times 10^3 \Omega$$

$$R_{L,t3}(f) := R_{L,t4}(f)$$

$$G_{cf,4}(f) := \mu_4 \cdot \frac{R47}{r_{a4} + (1 + \mu_4) \cdot R47 + \frac{r_{a4} \cdot R47}{R_{L,t4}(f)}} \quad |G_{cf,4}(h)| = 0.905$$

$$|G_{cf,4}(20Hz)| = 0.905$$

$$G_{cf,3}(f) := G_{cf,4}(f)$$

$$G_{cf}(f) := G_{cf,3}(f) \cdot G_{cf,4}(f) \quad |G_{cf}(h)| = 0.82$$

$$R_{o,cf,t4} := \frac{r_{a4} \cdot R47}{r_{a4} + (1 + \mu_4) \cdot R47} \quad R_{o,cf,t4} = 274.599 \Omega$$

$$R_{o,cf,t4,eff}(f) := \left[ \frac{1}{R_{o,cf,t4} + (2j \cdot \pi \cdot f \cdot 0.5 \cdot C44a)^{-1}} + \frac{1}{R48} \right]^{-1} \quad |R_{o,cf,t4,eff}(h)| = 267.915 \Omega$$

$$R_{o,cf,t3,eff}(f) := R_{o,cf,t4,eff}(f)$$

$$R_{o,cf,dif}(f) := R_{o,cf,t4,eff}(f) + R_{o,cf,t3,eff}(f) \quad |R_{o,cf,dif}(h)| = 535.83 \Omega$$

3.3 Gain of DIFCF :

$$G_{difcf}(f) := G_{0,dif} \cdot G_{cf}(f) \quad |G_{difcf}(h)| = 16.390411$$

3.4 Gain and  $R_o$  of i/p buffers OP1 and OP2 :  $G_{op1,2} := 1$       $R_{o,op1} := 0.1 \Omega$       $R_{o,op2} := R_{o,op1}$

3.5 Overall gain of Amp3 without RIAA network :

$$G_{amp3}(f) := G_{difcf}(f) \cdot G_{op1,2} \quad |G_{amp3}(h)| = 16.390411$$

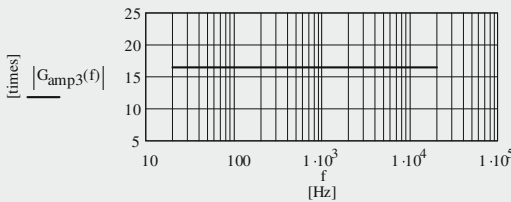


Fig. 3.2  
Gain of Amp3 vs frequency

3.1 MCD-WS: The Triode Gain Stage Amp3 with RIAA Networks

4. RIAA time constants T and transfer gains  $G_{T2}$ :

4.1  $T_2 = 75\mu s$  :  $P1 := 70.8 \cdot \Omega$

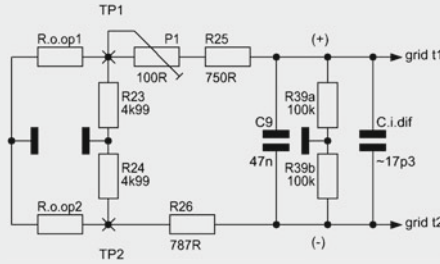


Fig. 3.3  
T2 defining network

succ-apps of P1 should bring in line the value of  $T_2$  with the RIAA network component values (because of the marginal influence the voltage divider respective effects of  $R_{o.op1}/R_{o.op2}$  and  $R23/R26$  are ignored here!)

$$T_2 := (C_9 + C_{i.dif}) \left[ \left[ \left[ (R_{o.op1}^{-1} + R23^{-1})^{-1} + R25 + P1 \right]^{-1} + R39a^{-1} \right]^{-1} \dots \right. \\ \left. + \left[ \left[ (R_{o.op2}^{-1} + R24^{-1})^{-1} + R26 \right]^{-1} + R39b^{-1} \right]^{-1} \right]$$

$$T_2 = 75 \times 10^{-6} s$$

$$G_{T2}(f) := \frac{\left[ 2j \cdot \pi \cdot f \cdot (C_9 + C_{i.dif}) + (R39a + R39b)^{-1} \right]^{-1}}{\left[ 2j \cdot \pi \cdot f \cdot (C_9 + C_{i.dif}) + (R39a + R39b)^{-1} \right]^{-1} + R25 + R26 + P1 + 2 \cdot (R_{o.op1}^{-1} + R23^{-1})^{-1}}$$

$$\left| G_{T2} \left( \frac{1}{2 \cdot \pi \cdot T_2} \right) \right| = 0.701$$

$$20 \cdot \log \left( \left| G_{T2} \left( \frac{1}{2 \cdot \pi \cdot T_2} \right) \right| \right) = -3.08 \quad [dB]$$

$$G_{T2,e}(f) := 20 \cdot \log \left( \left| G_{T2}(f) \right| \right)$$

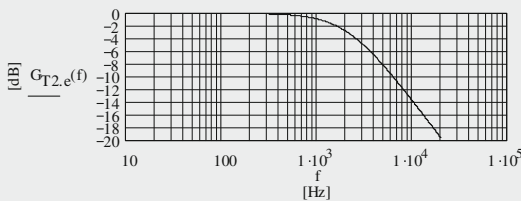


Fig. 3.4  
Bode plot of  $G_{T2}(f)$

3.1 MCD-WS: The Triode Gain Stage Amp3 with RIAA Networks

4.2  $T1 = 3180\mu s, T3 = 318\mu s : P3 := 1.450653 \cdot 10^3 \Omega \quad C12 := 227.1428575 \cdot 10^{-9} F$

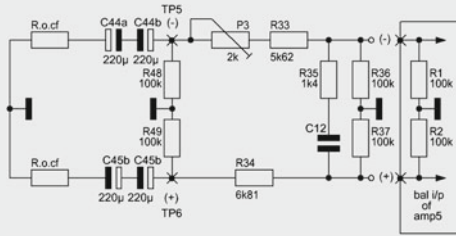


Fig. 3.5  
T1 & T3 defining network

succ-apps of 1.C12 & 2. P3 should bring in line the values of T1 & T3 with the required RIAA values

$T3 := C12 \cdot R35$

$T3 = 318 \times 10^{-6} s$

$R_{T1,eff}(f) := R_{o,cf,dif}(f) + P3 + R33 + R34$

$|R_{T1,eff}(h)| = 14.416 \times 10^3 \Omega$

$T1 := \left| C12 \cdot \left[ R35 + \left[ R_{T1,eff}(h)^{-1} + \left[ \left( R_{1,amp5}^{-1} + R36^{-1} \right)^{-1} + \left( R_{2,amp5}^{-1} + R37^{-1} \right)^{-1} \right]^{-1} \right]^{-1} \right|$

$T1 = 3.18 \times 10^{-3} s$

$R_{L,dif} := \left( \frac{1}{R_{1,amp5} + R_{2,amp5}} + \frac{1}{R36 + R37} \right)^{-1}$

$R_{L,dif} = 100 \times 10^3 \Omega$

$G_{T1,3}(f) := \frac{\left[ \left( \frac{1}{2j \cdot \pi \cdot f \cdot C12} + R35 \right)^{-1} + \frac{1}{R_{L,dif}} \right]^{-1}}{\left[ \left( \frac{1}{2j \cdot \pi \cdot f \cdot C12} + R35 \right)^{-1} + \frac{1}{R_{L,dif}} \right]^{-1} + R_{T1,eff}(f)}$

$|G_{T1,3}(h)| = 0.098$

$20 \cdot \log(|G_{T1,3}(20Hz)|) = -1.829 \quad [dB]$

$20 \cdot \log\left(|G_{T1,3}\left(\frac{1}{2 \cdot \pi \cdot T1}\right)|\right) = -4.15 \quad [dB]$

$20 \cdot \log\left(|G_{T1,3}\left(\frac{1}{2 \cdot \pi \cdot T3}\right)|\right) = -18.203 \quad [dB]$

$G_{T1,3,e}(f) := 20 \cdot \log(|G_{T1,3}(f)|)$

$20 \cdot \log(|G_{T1,3}(20kHz)|) = -21.167 \quad [dB]$

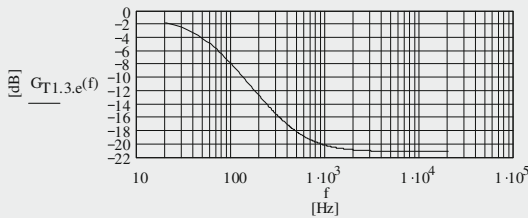


Fig. 3.6  
Bode plot of  $G_{T1,3}(f)$

3.1 MCD-WS: The Triode Gain Stage Amp3 with RIAA Networks

4.3 RIAA transfer :

$$G_{riaa}(f) := G_{T2}(f) \cdot G_{T1.3}(f) \qquad G_{riaa.e}(f) := 20 \cdot \log\left(\left|G_{riaa}(f) \cdot G_{riaa}(h)^{-1}\right|\right)$$

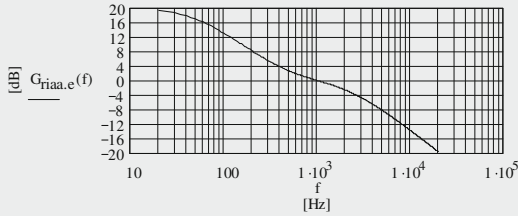


Fig. 3.7  
Normalized (1kHz at 0dB)  
RIAA transfer function

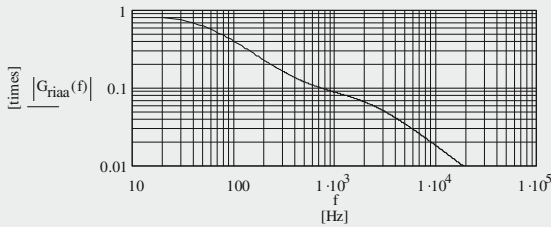


Fig. 3.8  
Bode plot of the gain of  
the combined RIAA network

$$R_{1000} := \frac{\sqrt{1 + (2 \cdot \pi \cdot h \cdot 318 \cdot 10^{-6} \cdot s)^2}}{\sqrt{1 + (2 \cdot \pi \cdot h \cdot 3180 \cdot 10^{-6} \cdot s)^2} \cdot \sqrt{1 + (2 \cdot \pi \cdot h \cdot 75 \cdot 10^{-6} \cdot s)^2}}$$

$$R_0(f) := \frac{\sqrt{1 + (2 \cdot \pi \cdot f \cdot 318 \cdot 10^{-6} \cdot s)^2}}{\sqrt{1 + (2 \cdot \pi \cdot f \cdot 3180 \cdot 10^{-6} \cdot s)^2} \cdot \sqrt{1 + (2 \cdot \pi \cdot f \cdot 75 \cdot 10^{-6} \cdot s)^2}} \cdot (R_{1000})^{-1}$$

$$Dev_{1e}(f) := 20 \cdot \log(R_0(f)) - G_{riaa.e}(f)$$

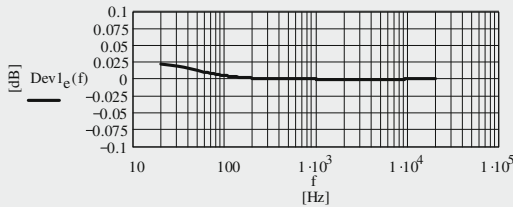


Fig. 3.9  
Deviation from the exact  
RIAA transfer

3.1 MCD-WS: The Triode Gain Stage Amp3 with RIAA Networks

5. Transfer function T(f) of Amp3

General assumption: the corner frequency of the  $\nu$ p hp R21, R22, C5 ... C8 is chosen that there is no influence on a flat phase and frequency response in B<sub>20k</sub> !

$$T_{amp3}(f) := G_{amp3}(h) \cdot G_{T2}(f) \cdot G_{T1.3}(f)$$

$$|T_{amp3}(h)| = 1.435716$$

$$T_{amp3,e}(f) := 20 \cdot \log(|T_{amp3}(f)|)$$

$$T_{amp3,e}(h) = 3.141371 \quad [dB]$$

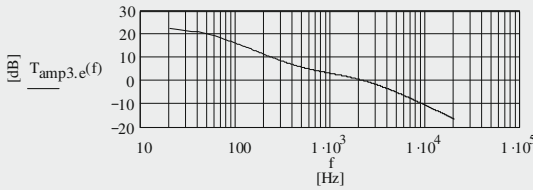


Fig. 3.10  
Bode plot of Amp3

$$Dev2_e(f) := 20 \cdot \log(R_0(f)) - 20 \cdot \log(|T_{amp3}(f) \cdot T_{amp3}(h)^{-1}|)$$

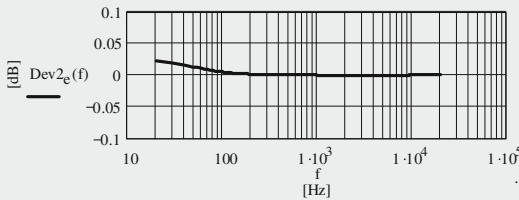


Fig. 3.11 = Fig. 2.3  
Fig. 3.10's deviation from the exact RIAA transfer

$$RIAA(f) := \frac{1 + 2j \cdot \pi \cdot f \cdot 318 \times 10^{-6} \cdot s}{(1 + 2j \cdot \pi \cdot f \cdot 3180 \times 10^{-6} \cdot s) \cdot (1 + 2j \cdot \pi \cdot f \cdot 75 \times 10^{-6} \cdot s)}$$

$$|RIAA(h)| = 101.03 \times 10^{-3}$$

$$\phi_{amp3}(f) := \text{atan} \left( \frac{\text{Im}(T_{amp3}(f) \cdot RIAA(f)^{-1})}{\text{Re}(T_{amp3}(f) \cdot RIAA(f)^{-1})} \right)$$

$$\phi_{amp3}(h) = 0$$

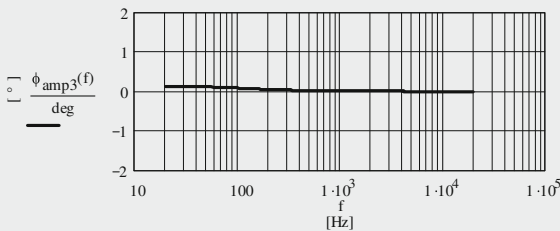


Fig. 3.12  
Fig. 3.10's phase response

3.1 MCD-WS: The Triode Gain Stage Amp3 with RIAA Networks

6. Noise and SN calculations :

6.1 General data :

$$v_{i.ref} := 100 \cdot 10^{-3} \text{V}$$

$$v_{o.ref} := v_{i.ref} |T_{amp3}(h)|$$

$$v_{o.ref} = 143.572 \times 10^{-3} \text{V}$$

$$v_{o.ref.m} := 152.8 \cdot 10^{-3} \text{V}$$

Op-amps:

$$e_{n.i.op1} := 4.8 \cdot 10^{-9} \text{V}$$

$$e_{n.i.op2} := e_{n.i.op1}$$

$$i_{n.i.op1} := 2.5 \cdot 10^{-15} \text{A}$$

$$i_{n.i.op2} := i_{n.i.op1}$$

$$f_{c.e.1} := 40 \text{Hz}$$

$$f_{c.i.1} < 0.1 \text{Hz}$$

$$e_{n.i.op1}(f) := e_{n.i.op1} \cdot \left( \sqrt{\frac{f_{c.e.1}}{f} + 1} \right)$$

$$e_{n.i.op2}(f) := e_{n.i.op1}(f)$$

Triodes:

$$r_{N1} := \frac{3.06}{g_{m1}}$$

$$r_{N1} = 874.286 \Omega$$

$$e_{n.rN1} := \sqrt{4 \cdot k \cdot T \cdot r_{N1} \cdot B_1}$$

$$e_{n.rN1} = 3.9 \times 10^{-9} \text{V}$$

$$r_{N2} := r_{N1}$$

$$e_{n.rN2} := e_{n.rN1}$$

$$r_{N3} := \frac{3.06}{g_{m1}}$$

$$r_{N3} = 874.286 \Omega$$

$$e_{n.rN3} := \sqrt{4 \cdot k \cdot T \cdot r_{N3} \cdot B_1}$$

$$e_{n.rN3} = 3.9 \times 10^{-9} \text{V}$$

$$r_{N4} := r_{N3}$$

$$e_{n.rN4} := e_{n.rN3}$$

$$e_{n.rN1}(f) := e_{n.rN1} \cdot \left( \sqrt{\frac{f_{c1}}{f} + 1} \right)$$

$$e_{n.rN1}(h) = 5.515 \times 10^{-9} \text{V}$$

$$e_{n.rN2}(f) := e_{n.rN1}(f)$$

$$e_{n.rN3}(f) := e_{n.rN3} \cdot \left( \sqrt{\frac{f_{c3}}{f} + 1} \right)$$

$$e_{n.rN3}(h) = 12.935 \times 10^{-9} \text{V}$$

$$e_{n.rN4}(f) := e_{n.rN3}(f)$$

Resistances:

$$R_a = R_{a1} = R_{a2}$$

$$R_c = R_{c3} = R_{c4}$$

$$NI_{e.a} := -24 \quad [\text{dB}]$$

$$NI_{e.c} := -24 \quad [\text{dB}]$$

$$R_a := R40$$

$$V_{Ra} := I_{a1} \cdot R_a$$

$$V_{Ra} = 36.8 \text{V}$$

$$e_{n.R40} := \sqrt{4 \cdot k \cdot T \cdot B_1 \cdot R40}$$

$$e_{n.R40} = 17.891 \times 10^{-9} \text{V}$$

$$e_{n.R40ex}(f) := \sqrt{\frac{NI_{e.a}}{10} \cdot \frac{10^{-12} V_{Ra}^2}{\ln(10)} \cdot \frac{1}{f} \cdot B_1}$$

$$e_{n.R40ex}(h) = 48.388 \times 10^{-9} \text{V}$$

3.1 MCD-WS: The Triode Gain Stage Amp3 with RIAA Networks

$$e_{n,Ra}(f) := \sqrt{e_{n,R40}^2 + e_{n,R40ex}(f)^2}$$

$$e_{n,Ra}(h) = 51.59 \times 10^{-9} V$$

$$e_{n,Ra,eff}(f) := e_{n,Ra}(f) \left( \frac{r_{a1}}{r_{a1} + R_a} \right)$$

$$e_{n,Ra,eff}(h) = 16.018 \times 10^{-9} V$$

$$R_{gg3} := R44$$

$$e_{n,Rgg3} := \sqrt{4 \cdot k \cdot T \cdot B_1 \cdot R44}$$

$$e_{n,Rgg3} = 2.288 \times 10^{-9} V$$

$$R_{gg4} := R_{gg3}$$

$$e_{n,Rgg4} := e_{n,Rgg3}$$

$$R_c := R46$$

$$V_{Rc} := I_{a1} \cdot R_c$$

$$V_{Rc} = 95.333 V$$

$$r_c = r_{c3} = r_{c4}$$

$$r_c := \frac{r_{a3}}{1 + \mu_1}$$

$$r_c = 276.19 \Omega$$

$$e_{n,R46} := \sqrt{4 \cdot k \cdot T \cdot B_1 \cdot R46}$$

$$e_{n,R46} = 28.796 \times 10^{-9} V$$

$$e_{n,R46ex}(f) := \sqrt{\frac{\frac{NI_{e,c}}{10} \cdot 10^{-12} \cdot V_{Rc}^2}{\ln(10)} \cdot \frac{1}{f}} \cdot B_1$$

$$e_{n,R46ex}(h) = 125.354 \times 10^{-9} V$$

$$e_{n,Rc}(f) := \sqrt{e_{n,R46}^2 + e_{n,R46ex}(f)^2}$$

$$e_{n,Rc}(h) = 128.619 \times 10^{-9} V$$

$$e_{n,Rc,eff}(f) := e_{n,Rc}(f) \cdot \frac{r_c}{R_c + r_c}$$

$$e_{n,Rc,eff}(h) = 740.95 \times 10^{-12} V$$

6.2 Noise Voltage of the T2 network :

$$Z_{T2} := \left[ (R25 + R26 + P1)^{-1} + (R39a + R39b)^{-1} \right]^{-1}$$

$$Z_{T2} = 1.595 \times 10^3 \Omega$$

$$e_{n,Z,T2}(f) := G_{T2}(f) \cdot \sqrt{4 \cdot k \cdot T \cdot B_1 \cdot Z_{T2}}$$

$$|e_{n,Z,T2}(h)| = 4.727 \times 10^{-9} V$$

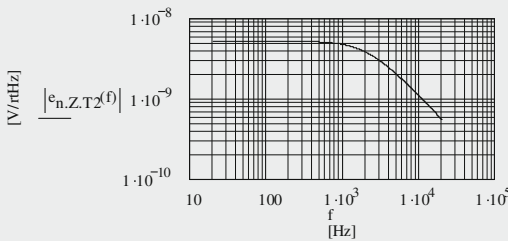


Fig. 3.13  
Frequency response of  
the noise voltage density  
of the T2(f) network

$$Z_{T2}(f) := Z_{T2} \cdot G_{T2}(f)$$



3.1 MCD-WS: The Triode Gain Stage Amp3 with RIAA Networks

6.3 Noise Voltage of the T1/T3 network at the o/p :

$$Z_{T1.3}(f) := \left( \frac{1}{R_{o.cf.dif}(f) + P3 + R33 + R34} + \frac{1}{R35 + \frac{1}{2j \cdot \pi \cdot f \cdot C12}} + \frac{1}{R_{L.dif}} \right)^{-1}$$

$$|Z_{T1.3}(h)| = 1.407 \times 10^3 \Omega$$

$$e_{n.Z.T1.3}(f) := |G_{T1.3}(f) \cdot \sqrt{4 \cdot k \cdot T \cdot B_1} \cdot |Z_{T1.3}(f)||$$

$$e_{n.Z.T1.3}(h) = 482.963 \times 10^{-12} V$$

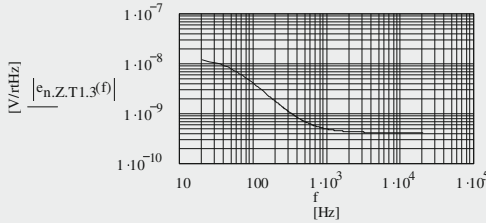


Fig. 3.14  
Frequency response of the noise voltage density of the T1(f)+T3(f) network

6.4 Relevant Amp5 data :

$$i_{n.i.amp5} := \frac{2.5}{\sqrt{2}} \cdot 10^{-15} A$$

average noise voltage in  $B_{20k}$  :

$$e_{n.i.amp5} := 8.103 \cdot 10^{-9} V$$

$$G_{amp5} := \frac{1 \cdot V}{v_{o.ref}}$$

$$G_{amp5} = 6.965$$

$$G_{cm.amp5} := 1.2 \cdot \frac{0.1}{200}$$

$$G_{cm.amp5} = 1 \times 10^{-3}$$

$$CMRR_{amp5} := \frac{G_{amp5}}{G_{cm.amp5}}$$

$$CMRR_{amp5} = 6.965 \times 10^3$$

$$CMRR_{amp5,e} := 20 \cdot \log(CMRR_{amp5})$$

$$CMRR_{amp5,e} = 76.859 \text{ [dB]}$$

6.5 Impact of the current sink CCsi of BJTs T1 and T2 and CMRR of the gain stage:

6.5.1 CCsi :

$$q := 1.6022 \cdot 10^{-19} A \cdot s$$

$$I_{C1} := 4 \cdot 10^{-3} A$$

$$V_{CE1} := 2.2V$$

$$V_{A1} := -100V$$

$$h_{fe1} := 500$$

$$R_E := R42 + P8$$

$$R_E = 195 \Omega$$

$$g_{mt1} := \frac{q \cdot I_{C1}}{k \cdot T}$$

$$g_{mt1} = 147.361 \times 10^{-3} S$$

$$r_{bb} := 13.74 \Omega$$

$$r_{ce1} := \frac{|V_{A1}|}{I_{C1}}$$

$$r_{ce1} = 25 \times 10^3 \Omega$$

$$r_{be1} := \frac{h_{fe1}}{g_{mt1}}$$

$$r_{be1} = 3.393 \times 10^3 \Omega$$

$$r_{c.1} := 0.5 \cdot \frac{r_{a1} + R40}{1 + \mu_1}$$

$$r_{c.1} = 444.762 \Omega$$

## 3.1 MCD-WS: The Triode Gain Stage Amp3 with RIAA Networks

Page 11

$$I_{C2} := 1 \cdot 10^{-3} \text{ A} \quad V_{CE2} := 1.2 \text{ V} \quad V_{A2} := -100 \text{ V} \quad h_{fe2} := 500$$

$$g_{m2} := \frac{q \cdot I_{C2}}{k \cdot T} \quad g_{m2} = 36.84 \times 10^{-3} \text{ S} \quad r_{ce2} := \frac{|V_{A2}|}{I_{C2}} \quad r_{ce2} = 100 \times 10^3 \Omega$$

$$r_{be2} := \frac{h_{fe2}}{g_{m2}} \quad r_{be2} = 13.572 \times 10^3 \Omega$$

$$r_{ccsi} := r_{ce1} \cdot \left[ 1 + \frac{h_{fe1} + \frac{r_{be1}}{r_{ce1}}}{1 + \frac{r_{be1}}{\left( \frac{R_E \cdot r_{be2}}{R_E + r_{be2}} \right)}} \right] \quad r_{ccsi} = 695.418 \times 10^3 \Omega$$

$$i_{n,C1} := \sqrt{2 \cdot q \cdot I_{C1} \cdot B_1}$$

$$i_{n,C1} = 35.802 \times 10^{-12} \text{ A}$$

$$G_{bjt} := -g_{m1} \cdot r_{c,1}$$

$$G_{bjt} = -65.541$$

$$e_{n,bjt} := \sqrt{\frac{2 \cdot k \cdot T^2}{q \cdot I_{C1}} \cdot B_1 + 4 \cdot k \cdot T \cdot B_1 \cdot (r_{bb} + R_E)}$$

$$e_{n,bjt} = 1.921 \times 10^{-9} \text{ V}$$

$$\sqrt{e_{n,bjt}^2 \cdot G_{bjt}^2 \cdot \left( \frac{r_{c,1}}{r_{c,1} + r_{ccsi}} \right)^2} = 80.472 \times 10^{-12} \text{ V}$$

$$i_{n,C1} \cdot r_{c,1} = 15.923 \times 10^{-9} \text{ V}$$

=&gt;

$$e_{n,ccsi} := \sqrt{(i_{n,C1} \cdot r_{c,1})^2 + e_{n,bjt}^2 \cdot G_{bjt}^2 \cdot \left( \frac{r_{c,1}}{r_{c,1} + r_{ccsi}} \right)^2}$$

$$e_{n,ccsi} = 15.923 \times 10^{-9} \text{ V}$$

$$G_{cgs,1} := (1 + \mu_1) \cdot \frac{R_{40}}{r_{a1} + R_{40}}$$

$$G_{cgs,1} = 20.685$$

## 6.5.2 CMRR of Amp3 :

$$CMRR_{amp3,rot} := r_{ccsi} \cdot g_{m1}$$

$$CMRR_{amp3,rot} = 2.434 \times 10^3$$

$$CMRR_{amp3,rot,e} := 20 \cdot \log(CMRR_{amp3,rot})$$

$$CMRR_{amp3,rot,e} = 67.726 \quad [\text{dB}]$$

$$CMRR_{amp3} := 1 + \frac{2 \cdot r_{ccsi}}{r_{a1} + R_a} + \mu_1 \cdot \frac{2 \cdot r_{ccsi}}{r_{a1} + R_a}$$

$$CMRR_{amp3} = 1.565 \times 10^3$$

$$CMRR_{amp3,e} := 20 \cdot \log(CMRR_{amp3})$$

$$CMRR_{amp3,e} = 63.888 \quad [\text{dB}]$$

3.1 MCD-WS: The Triode Gain Stage Amp3 with RIAA Networks

6.6 Output noise voltage of Amp3 + Amp5 with i/p shorted ( $amp_{3,5}$ ) :

$$e_{n.o.op1.2}(f) := G_{op1.2} \sqrt{e_{n.i.op1}(f)^2 + e_{n.i.op2}(f)^2} \quad e_{n.o.op1.2}(h) = 6.923 \times 10^{-9} \text{ V}$$

$$e_{n.o.amp3.5}(f) := G_{amp5} \sqrt{\left[ \left( \frac{e_{n.o.op1.2}(f)^2 \cdot G_{T2}(f)^2 + e_{n.Z.T2}(f)^2 \dots}{+ 2 \cdot e_{n.rN1}(f)^2} \right) \cdot (G_{0,dif})^2 \dots \right] \cdot G_{cf}(f)^2 \dots \cdot G_{T1.3}(f)^2 \dots + 2 \cdot e_{n.Rgg3}^2 + 2 \cdot e_{n.Ra.eff}(f)^2 + 2 \cdot e_{n.rN3}(f)^2 + 2 \cdot e_{n.Rc.eff}(f)^2 + \left( \frac{e_{n.ccsi}^2 \cdot G_{cgs.1} \cdot G_{cf}(f) \cdot G_{T1.3}(f)}{CMRR_{amp5}} \right)^2 \dots + e_{n.Z.T1.3}(f)^2 + i_{n.i.amp5}^2 \cdot Z_{T1.3}(f)^2 + e_{n.i.amp5}^2}$$

$$|e_{n.o.amp3.5}(h)| = 123.309 \times 10^{-9} \text{ V}$$

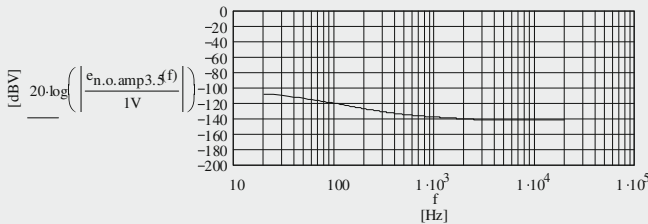
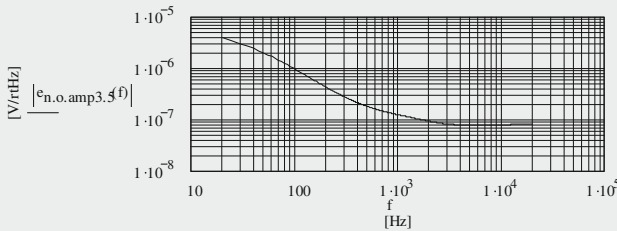


Fig. 3.15a & Fig. 3.15b = Fig. 2.3 Amp3+amp5 output noise voltage density with i/p shorted

$$e_{N.o.amp3.5} := \sqrt{\frac{1}{B_1} \cdot \int_{20\text{Hz}}^{2000\text{Hz}} (|e_{n.o.amp3.5}(f)|)^2 df} \quad e_{N.o.amp3.5} = 22.905 \times 10^{-6} \text{ V}$$

$$|T_{amp3}(h) \cdot G_{amp5}| = 10$$

$$e_{n.i.amp3.5}(f) := \frac{e_{n.o.amp3.5}(f)}{T_{amp3}(h) \cdot G_{amp5}} \quad |e_{n.i.amp3.5}(h)| = 12.331 \times 10^{-9} \text{ V}$$

3.1 MCD-WS: The Triode Gain Stage Amp3 with RIAA Networks

6.7 SNs of the sequence of Amp3 + Amp5 :

$$SN_{o,amp3.5} := 20 \cdot \log \left[ \frac{\sqrt{\frac{1}{B_1} \cdot \int_{20\text{Hz}}^{2000\text{Hz}} (|e_{n.o,amp3.5}(f)|)^2 df}}{1\text{V}} \right] \quad SN_{o,amp3.5} = -92.801 \quad [\text{dBV}]$$

measured with high CMRR instrument: -90.43 [dBV]

B(f) = A(f) = A-weighting transfer function

$$B(f) := \frac{1.259}{\left[ 1 + \left( \frac{20.6\text{Hz}}{f} \right)^2 \right] \cdot \sqrt{1 + \left( \frac{107.7\text{Hz}}{f} \right)^2} \cdot \sqrt{1 + \left( \frac{737.9\text{Hz}}{f} \right)^2} \cdot \left[ 1 + \left( \frac{f}{12200\text{Hz}} \right)^2 \right]}$$

$$SN_{a.o,amp3.5} := 20 \cdot \log \left[ \frac{\sqrt{\frac{1}{B_1} \cdot \int_{20\text{Hz}}^{2000\text{Hz}} (|e_{n.o,amp3.5}(f)|)^2 \cdot (|B(f)|)^2 df}}{1\text{V}} \right] \quad SN_{a.o,amp3.5} = -100.165 \quad [\text{dBV(A)}]$$

$$SN_{a.o,amp3.5,m} := -99.00 \quad [\text{dBV(A)}]$$

$$SN_{a.i,amp3.5} := 20 \cdot \log \left[ \frac{\sqrt{\frac{1}{B_1} \cdot \int_{20\text{Hz}}^{2000\text{Hz}} (|e_{n.i,amp3.5}(f)|)^2 \cdot (|B(f)|)^2 df}}{v_{i,ref}} \right] \quad SN_{a.i,amp3.5} = -100.165 \quad [\text{dB(A)}]$$

7. Amp3 + Amp5 with i/p loaded by the noise voltage of a preceding MC amp1 with extremely low input noise voltage & current density :

$$G_{amp1} := 200 \quad R_0 := 20\Omega \quad e_{n,i0} := 0.2 \cdot 10^{-9} \text{V} \cdot \sqrt{2} \quad i_{n,i0} := \frac{2.4 \cdot 10^{-12} \text{A}}{\sqrt{2}}$$

$$T := 315 \text{K} \quad v_{o,ref,mc} := 100 \cdot 10^{-3} \text{V} \quad v_{i,ref,mc} := 0.5 \cdot 10^{-3} \text{V}$$

$$e_{n,R0} := \sqrt{4 \cdot k \cdot T \cdot B_1 \cdot R_0} \quad e_{n,R0} = 589.851 \times 10^{-12} \text{V}$$

$$e_{n,i0,eff} := \sqrt{e_{n,i0}^2 + e_{n,R0}^2 + i_{n,i0}^2 \cdot R_0^2} \quad e_{n,i0,eff} = 655.039 \times 10^{-12} \text{V}$$

$$e_{n,o,amp1} := G_{amp1} \cdot e_{n,i0,eff} \quad e_{n,o,amp1} = 131.008 \times 10^{-9} \text{V}$$

$$e_{N,o,amp1} := e_{n,o,amp1} \cdot \sqrt{\frac{B_{20k}}{B_1}} \quad e_{N,o,amp1} = 18.518 \times 10^{-6} \text{V}$$

$$e_{n,o,mc}(f) := \sqrt{e_{n,o,amp1}^2 \cdot (|T_{amp3}(f)|)^2 \cdot G_{amp5}^2 + e_{n,o,amp3.5}(f)^2} \quad |e_{n,o,mc}(f)| = 1.313 \times 10^{-6} \text{V}$$

3.1 MCD-WS: The Triode Gain Stage Amp3 with RIAA Networks

$$e_{n.i.mc}(f) := \frac{e_{n.o.mc}(f)}{G_{amp1} \cdot T_{amp3}(h) \cdot G_{amp5}} \quad |e_{n.i.mc}(h)| = 656.468 \times 10^{-12} V$$

$$SN_{riaa.o.amp3.5.mc} := 20 \cdot \log \left[ \frac{\sqrt{\frac{1}{B_1} \cdot \int_{20Hz}^{2000Hz} (|e_{n.o.mc}(f)|)^2 df}}{1V} \right] \quad SN_{riaa.o.amp3.5.mc} = -78.201 \quad [dB]$$

$$SN_{ariaa.o.amp3.5.mc} := 20 \cdot \log \left[ \frac{\sqrt{\frac{1}{B_1} \cdot \int_{20Hz}^{2000Hz} (|e_{n.o.mc}(f)|)^2 \cdot (|B(f)|)^2 df}}{1V} \right] \quad SN_{ariaa.o.amp3.5.mc} = -82.523 \quad [dB(A)]$$

$$SN_{ariaa.i.amp3.5.mc} := 20 \cdot \log \left[ \frac{\sqrt{\frac{1}{B_1} \cdot \int_{20Hz}^{2000Hz} (|e_{n.i.mc}(f)|)^2 \cdot (|B(f)|)^2 df}}{v_{i.ref.mc}} \right] \quad SN_{ariaa.i.amp3.5.mc} = -82.523 \quad [dB(A)]$$

8. Preceding MC Amp1 alone and noise calculation up to the o/p of Amp5 :

$$e_{n.o.mc.eff}(f) := e_{n.o.amp1} \cdot T_{amp3}(f) \cdot G_{amp5} \quad |e_{n.o.mc.eff}(h)| = 1.31 \times 10^{-6} V$$

$$e_{n.i.mc.eff}(f) := \frac{e_{n.o.mc.eff}(f)}{T_{amp3}(h) \cdot G_{amp1} \cdot G_{amp5}} \quad |e_{n.i.mc.eff}(h)| = 655.039 \times 10^{-12} V$$

$$SN_{riaa.o.mc} := 20 \cdot \log \left[ \frac{\sqrt{\frac{1}{B_1} \cdot \int_{20Hz}^{2000Hz} (|e_{n.o.mc.eff}(f)|)^2 df}}{1V} \right] \quad SN_{riaa.o.mc} = -78.263 \quad [dB]$$

$$SN_{riaa.i.mc} := 20 \cdot \log \left[ \frac{\sqrt{\frac{1}{B_1} \cdot \int_{20Hz}^{2000Hz} (|e_{n.i.mc.eff}(f)|)^2 df}}{v_{i.ref.mc}} \right] \quad SN_{riaa.i.mc} = -78.263 \quad [dB]$$

$$SN_{ariaa.o.mc} := 20 \cdot \log \left[ \frac{\sqrt{\frac{1}{B_1} \cdot \int_{20Hz}^{2000Hz} (|e_{n.o.mc.eff}(f)|)^2 \cdot (|B(f)|)^2 df}}{1V} \right] \quad SN_{ariaa.o.mc} = -82.582 \quad [dBA]$$

$$SN_{ariaa.i.mc} := 20 \cdot \log \left[ \frac{\sqrt{\frac{1}{B_1} \cdot \int_{20Hz}^{2000Hz} (|e_{n.i.mc.eff}(f)|)^2 \cdot (|B(f)|)^2 df}}{v_{i.ref.mc}} \right] \quad SN_{ariaa.i.mc} = -82.582 \quad [dB(A)]$$

3.1 MCD-WS: The Triode Gain Stage Amp3 with RIAA Networks

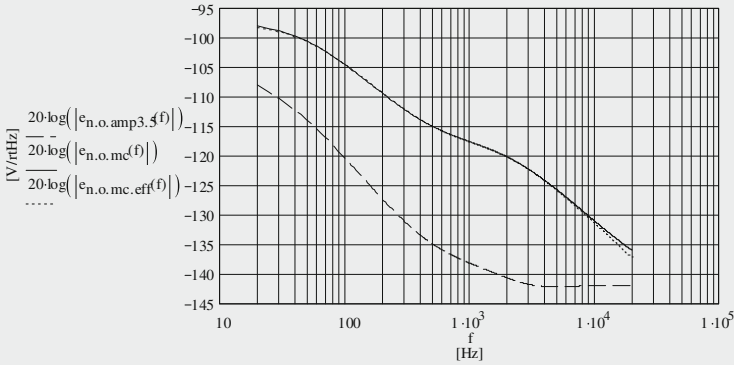


Fig. 3.16 Comparison of the various output noise voltage densities vs. frequency (trace 3 is nearly hidden by trace 2)

$$Dev_{3_e}(f) := 20 \cdot \log(R_0(f)) - 20 \cdot \log\left(\left|e_{n.o.mc.eff(f)} \cdot e_{n.o.mc.eff(h)}^{-1}\right|\right)$$

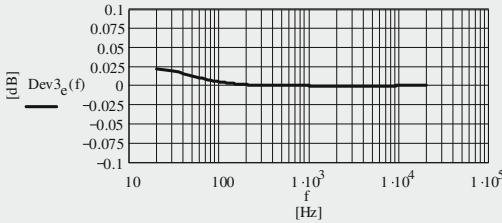


Fig. 3.17 Deviation from the exact RIAA transfer of Amp1+Amp3+Amp5

Mainly, the shown deviation comes from the chosen C44 & C45 values!

9. MC Amp1 noise worsening by additional noise from Amp3+Amp5:

$$NF_{e.mc12} := SN_{ariaa.o.amp3.5.mc} - SN_{ariaa.o.mc} \quad NF_{e.mc12} = 0.059 \quad [dB]$$

10. MM Amp noise worsening by additional noise from Amp3+Amp5:

$$SN_{ariaa.o.mm} := -80.5 \quad [dB(A) \text{ ref. } 100mV_{rms}]$$

$$SN_{ariaa.i.amp3.mm} := 20 \cdot \log\left(\sqrt{10 \frac{SN_{ariaa.o.mm}}{10} + 10 \frac{SN_{a.i.amp3.5}}{10}}\right) \quad SN_{ariaa.i.amp3.mm} = -80.453 \quad [dB(A)]$$

$$NF_{e.mm} := SN_{ariaa.i.amp3.mm} - SN_{ariaa.o.mm} \quad NF_{e.mm} = 0.047 \quad [dB]$$

3.1 MCD-WS: The Triode Gain Stage Amp3 with RIAA Networks

1.1. Amp3 with i/p loaded by the noise voltage of a 1k resistor and via o/p of Amp5:

$$R0 := 1000\Omega \quad T := 315K$$

$$e_{n,R0} := \sqrt{4 \cdot k \cdot T \cdot B_1 \cdot R0}$$

$$e_{n,R0} = 4.171 \times 10^{-9} V$$

$$e_{n,o.1k}(f) := \sqrt{e_{n,R0}^2 \cdot (|T_{amp3}(f)| \cdot G_{amp5})^2 + e_{n,o.amp3.5}(f)^2}$$

$$|e_{n,o.1k}(h)| = 127 \times 10^{-9} V$$

$$e_{n,i.1k}(f) := \frac{e_{n,o.1k}(f)}{G_{amp5} \cdot T_{amp3}(h)}$$

$$|e_{n,i.1k}(h)| = 127 \times 10^{-9} V$$

$$SN_{riaa.o.amp3.5.1k} := 20 \cdot \log \left[ \frac{\frac{1}{B_1} \cdot \int_{20Hz}^{2000Hz} (|e_{n,o.1k}(f)|)^2 df}{1V} \right]$$

$$SN_{riaa.o.amp3.5.1k} = -92.763 \quad [dBV]$$

$$SN_{ariaa.o.amp3.5.1k} := 20 \cdot \log \left[ \frac{\frac{1}{B_1} \cdot \int_{20Hz}^{2000Hz} (|e_{n,o.1k}(f)|)^2 \cdot (|B(f)|)^2 df}{1V} \right]$$

$$SN_{ariaa.o.amp3.5.1k} = -99.999 \quad [dBV(A)]$$

$$SN_{ariaa.i.amp3.5.1k} := 20 \cdot \log \left[ \frac{\frac{1}{B_1} \cdot \int_{20Hz}^{2000Hz} (|e_{n,i.1k}(f)|)^2 \cdot (|B(f)|)^2 df}{100mV} \right]$$

$$SN_{ariaa.i.amp3.5.1k} = -99.999 \quad [dB(A)]$$

## 4.1 General Design of Amp4

Outside the microphone amp world I rarely found a design configuration alike the one I have chosen for the Fig. 4.1 Amp4.<sup>1</sup> Together with low-noise and low-THD goals, the main development drivers are overload margin and CMRR. Low-noise means a noise level equal to the one of Amp3; hence, an input referred noise voltage density of appr. 10 nV/rtHz balanced should make it. The chosen input op-amp types assure very low THD in the main gain producing input gain stage of Amp4's OPs 3 & 4. They have Amp3-similar input current behaviour too. Figure 4.1 shows the central Amp4 without RIAA input and output networks.

The output stage (OPs 5 & 6) has a balanced gain of 2.<sup>2</sup> These two op-amps set the overload margin too. Their output voltage swing is  $\pm 12.3 V_p$  nominal.<sup>3</sup> Hence, the output voltage swing of such an amplifier becomes  $\pm 24.6 V_p = 49.2 V_{pp}$  nominal. With an input signal level of  $100 mV_{rms} + 20 \text{ dB}$  overload margin =  $1 V_{rms}$  and a gain of appr. 16 (set by P9) we need a max. voltage swing of  $16 V * 2 * \sqrt{2} = 45.255 V_{pp}$ . Without selection of OPs 5 & 6 and a very exact  $\pm 15V$  power supply, I measured clipping at a  $17.22 V_{rms} \equiv 48.71 V_{pp}$ .

High CMRR is important because neither the Amp1 & Amp2 alternatives show excellent CMRR nor the external amps will always produce it. The calculated<sup>4</sup> CMRR becomes appr. 16,000, hence, expressed in dB:  $CMRR_c \geq 20 * \log(16,000) = 84 \text{ dB}$ . Careful selection of the R9–R18 values to a 0.01 % tolerance level could improve  $CMRR_c$  to 104 dB.

The output stage's output resistance is very low. Thus, to get equal conditions for the RIAA network I've added R31 & R32 by taking their values equal to the calculated CF output resistances of Amp3. Replacement of  $R_{o,cf3}$  in (2.1) and

<sup>1</sup>“Schaltungstips für Vierfach Op-amps” (Hints for quadruple op-amps), Bob Atwell, Elektronik Nr. 20, 1988, p. 110ff. German language only.

<sup>2</sup>Further details see Sect. 4.2.1.

<sup>3</sup>Analog Devices data sheet.

<sup>4</sup>Further details see Sect. 4.2.3.



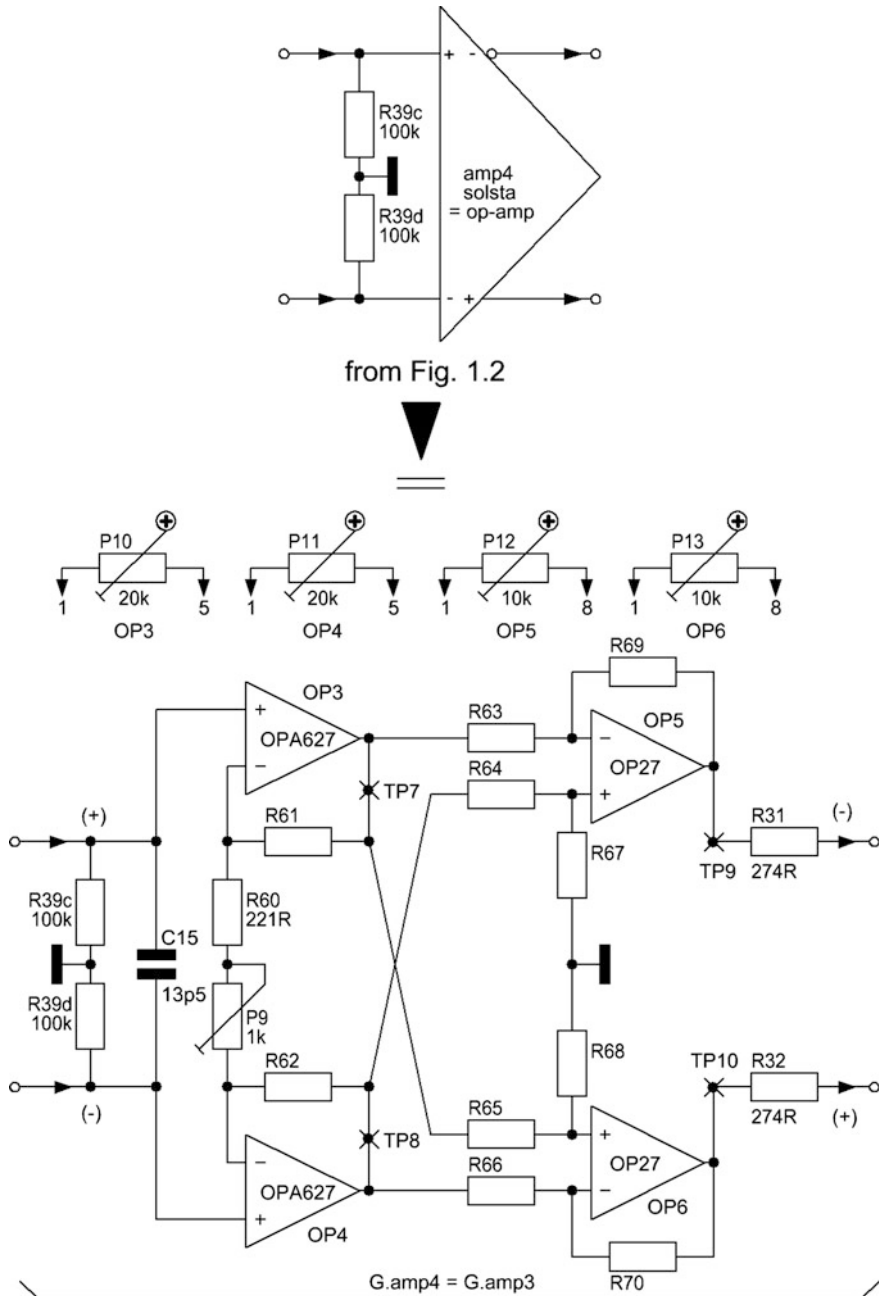
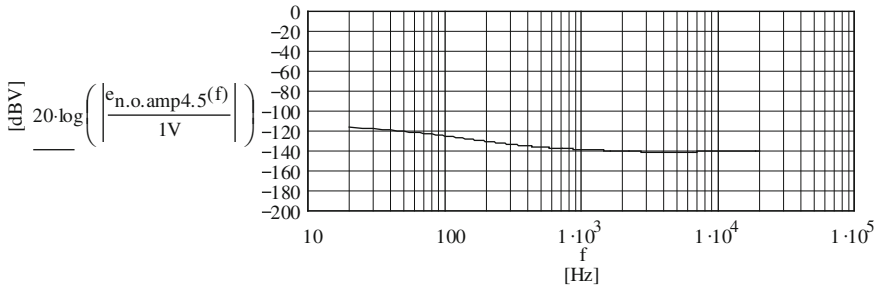
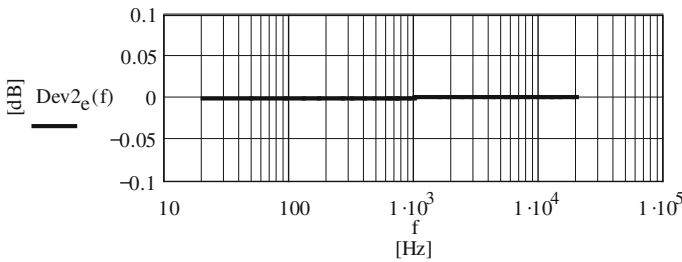


Fig. 4.1 Amp4 without RIAA networks



**Fig. 4.2** Output noise voltage density of the amp sequence Amp4 + Amp5 + Trafo with input shorted



**Fig. 4.3** Calculated deviation from the exact RIAA transfer

without frequency dependency by a capacitance inside the signal path we can calculate the RIAA voltage divider  $G_{T1.3}(f)$  (and thus the time constants T1 & T3) the same way we've done it for the Amp3 case. Section 4.2.2 gives the details, incl. the input voltage divider  $G_{T2}(f)$ .

My first design worked with  $4 \times$  OPA627. These op-amps are very expensive. I found out that in the output stage OP27s work equally well, without changing overall noise level, THD, IMD, etc.

With the CLIO signal generator<sup>5</sup> and depending on Amps 1 or 2 of this development, the 1 kHz THD-level of the Amp1/Amp2 + Amp4 + Amp5 + Trafo chain becomes always  $\leq 0.005 \%$ ,  $IMD \leq 0.002 \%$ . Via shorted external input, the amp sequence of Amp4 + Amp5 + Trafo produces a measured (calculated) A-weighted output referred  $SN_{a.o.amp4.5} = -100.8 \text{ dBV(A)}$  ( $-100.0 \text{ dBV(A)}$ )<sup>6</sup>. Figure 4.2 shows the calculated and corresponding output noise voltage density curve and Fig. 4.3 the calculated deviation from the exact RIAA transfer. Chapter 12 shows the measured curves.

<sup>5</sup>More on THD & IMD see Chaps. 12 and 15.

<sup>6</sup>See MCD-WS 5.1.

## 4.2 Gain and CMRR

### 4.2.1 Gain

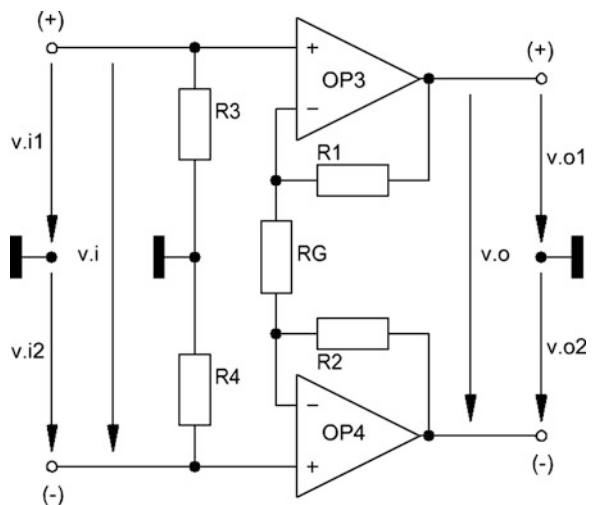
Normally,  $\pm 15$  V op-amps (also rail-to-rail) cannot produce higher output voltages than the used supply voltages would allow. However, the well-known two-op-amp balanced in/balanced out amplifier à la Fig. 4.4 creates higher output voltages, up to 2 times the output voltage of the single op-amp, paid for it by a disadvantage of rather lousy CMRR.

With equal values of  $R_1$  &  $R_2$  and with the input and output voltages  $v_{i1,2}$  and  $v_{o1,2}$  from lead to ground the differential gain equation for the Fig. 4.4 amplifier thus becomes (without any phase shift indicated by the (+) & (-) signs):

$$\begin{aligned} G_{\text{dif}} &= \frac{V_o}{V_i} = G_{\text{amp4.in}} \\ &= \frac{V_{o1} - V_{o2}}{V_{i1} - V_{i2}} \\ &= 1 + \frac{R_1 + R_2}{R_G} \end{aligned} \quad (4.1)$$

To get an increase in op-amp output voltage swing that exceeds the boundaries set by the op-amp supply voltage we could firstly load the op-amp by an additional high-voltage output stage with gain. However, CMRR would still become lousy. Secondly, if only doubling of the output voltage swing is enough, we could take the fully op-amp based solution shown in Fig. 4.5. It offers additional high common mode rejection by OPs 5 & 6, together with their corresponding circuitry.

**Fig. 4.4** Two-op-amp fully differential amplifier



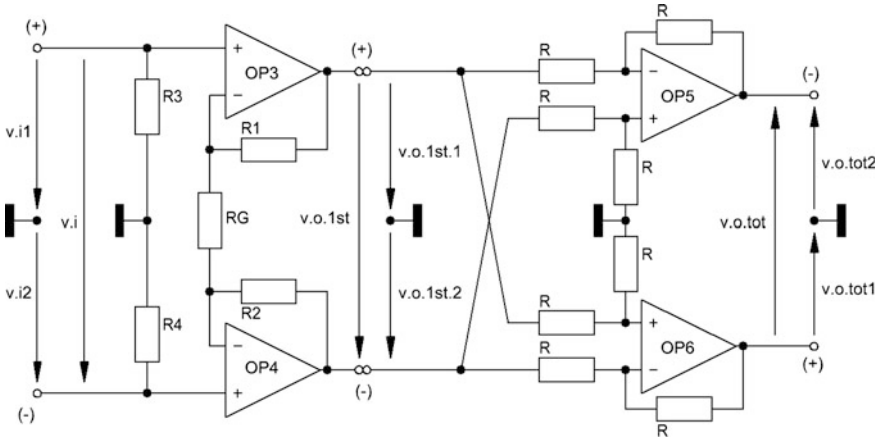


**Fig. 4.5** Basic Amp4 circuit with input stage around OPs 3 & 4, output stage around OPs 5 & 6, and all relevant signal voltages

Amp4 consists of two typical three-op-amp instrumentation amplifiers (INA) with OPs 3 & 4 as the only input stage and OPs 5 & 6 as two equal but differently connected subtractors working as output stages, hence, producing a 180° phase shift of the first gain stage’s output signal  $v_{o.1st}$ . With equal valued Rs we obtain the gain equation as follows:

1. In an instrumentation amplifier, the gain of the outputs stage is 1 as long as there are equal valued resistors R. Hence, the amps around OPs 5 & 6 have a gain of 1 each, thus, the whole output stage has a combined differential gain  $G_{amp4.out} = 2$ , as follows:

$$G_{amp4.out} = \frac{V_{o.tot}}{V_{o.1st}} = \frac{V_{o.tot1} - V_{o.tot2}}{V_{o.1st.1} - V_{o.1st.2}} \tag{4.2}$$

$$\begin{aligned} V_{o.tot1} &= [V_{o.1st.1} - (-V_{o.1st.2})]G_{op6} = V_{o.1st}G_{op6} \\ V_{o.tot2} &= -[V_{o.1st.1} - (-V_{o.1st.2})]G_{op5} = -V_{o.1st}G_{op5} \end{aligned} \tag{4.3}$$

$$G_{op5} = G_{op6} = 1 \tag{4.4}$$

$$\Rightarrow G_{amp4.out} = 2 \tag{4.5}$$

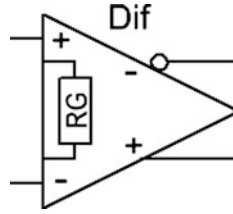


**Fig. 4.6** Symbol for a fully differential amplifier with balanced electrometer input

2. The input stage has the gain already given in (4.1)  $G_{\text{amp4.in}} = G_{\text{dif}}$ .
3. With the signal voltages shown in Fig. 4.5 the differential (=balanced) gain  $G_{\text{amp4}}$  of Amp4 thus becomes:

$$\begin{aligned}
 G_{\text{amp4}} &= \frac{V_{\text{o.tot}}}{V_i} \\
 &= G_{\text{amp4.in}} G_{\text{amp4.out}} \\
 &= \left(1 + \frac{R1 + R2}{RG}\right) 2
 \end{aligned} \tag{4.6}$$

With the shown op-amp arrangement, the output becomes a true differential one. The whole amp's circuit could be expressed by the Fig. 4.6 symbol.

Note: the Fig. 4.6 symbol is derived from another kind of fully differential amp's symbol: eg the OPA1632 with a different looking input arrangement alike the one of OPs 5 or 6 plus a fully differential output configuration.

## 4.2.2 RIAA Transfer Function

From Figs. 1.4 and 1.6 we can derive the frequency dependent and RIAA transfer loaded gains  $G_{T2}(f)$  and  $G_{T1.3}(f)$  of the Amp4 input and output networks as follows:

$$G_{T2}(f) = \frac{M}{M + R25 + R26 + P1 + 2 \left( R_{\text{o.op1}}^{-1} + R23^{-1} \right)^{-1}} \tag{4.7}$$

$$M = \left[ 2j\pi f (C9 + C_{\text{i.dif}}) + (R39c + R39d)^{-1} \right]^{-1}$$

$$G_{T1.3}(f) = \frac{\left[ \left( [2j\pi f C12]^{-1} + R35 \right)^{-1} + R_{\text{L.dif}}^{-1} \right]^{-1}}{\left[ \left( [2j\pi f C12]^{-1} + R35 \right)^{-1} + R_{\text{L.dif}}^{-1} \right]^{-1} + R_{T1.1.\text{eff}}} \tag{4.8}$$

$$R_{L.dif} = \left( [R1_{amp5} + R2_{amp5}]^{-1} + [R36 + R37]^{-1} \right)^{-1} \quad (4.9)$$

$$R_{T1.eff} = R31 + R32 + R33 + R34 + P4 \quad (4.10)$$

$$R_{o.op1} = R_{o.op2} \approx 0 \Omega \quad (4.11)$$

=> With C9 and C12 carefully selected according to Figs. 1.4 and 1.6 the transfer function  $T_{amp4}(f)$  of the whole Amp4, including RIAA transfer, thus becomes:

$$T_{amp4}(f) = G_{amp4}(f)G_{T2}(f)G_{T1.3}(f) \quad (4.12)$$

### 4.2.3 CMRR

The common mode gain  $G_{cm}$  of the Fig. 4.4 amp looks a bit different. With equal values of R1 & R2 it simply becomes:

$$G_{cm.in} = 1 \quad (4.13)$$

With equal voltages at the input leads (= the common mode input voltage) the signal current that flows through RG becomes 0; hence, RG's gain effective value looks like infinite, it has thus no effect on the amplification, and OPs 3 & 4 work as voltage followers only.

With (4.1) and (4.7) we obtain the common mode rejection ratio CMRR of the Fig. 4.4 amp as follows:

$$\begin{aligned} CMRR &= \frac{G_{dif}}{G_{cm.in}} \\ CMRR_e &= 20 \log(CMRR)[dB] \end{aligned} \quad (4.14)$$

However, the Fig. 4.5 CMRR situation looks very much different to the one for Fig. 4.4. The differential gain is given by (4.6). The common mode gain of an INA is mainly produced by its output stage. The details can be studied eg in,<sup>7</sup> however, expressed roughly and in short words: mainly, the tolerances of the resistors R in Fig. 4.5 set the value of the common mode gain, eg 1 % resistors would lead to a common mode gain of 1/200 or -46 dB, 0.1 % resistors produce a common mode gain of 1/2000 or -66 dB and so forth. We obtain thus the CMRR for the INAs with OPs 3 & 4 & 5 and/or OPs 3 & 4 & 6:

$$CMRR_{INA} = \frac{G_{INA}}{G_{cm.INA}} \quad (4.15)$$

<sup>7</sup>“Electronic Circuits”, 2nd ed. Tietze/Schenk, Springer, Heidelberg, ISBN 978-3-540-00429-5.

$$\begin{aligned} G_{\text{cm.INA}} &= G_{\text{cm.in}} G_{\text{cm.out}} \\ &= 1 * \frac{\text{tolerance} [\%]}{200 \%} \end{aligned} \quad (4.16)$$

and for Amp4:

$$\text{CMRR}_{\text{amp4}} = \frac{G_{\text{amp4}}}{G_{\text{amp4.cm}}} \quad (4.17)$$

$$\begin{aligned} G_{\text{amp4.cm}} &= G_{\text{cm.in}} G_{\text{cm.out}} \\ G_{\text{cm.in}} &= 1 \\ G_{\text{cm.out}} &= 2 \frac{\text{tolerance} [\%]}{200 \%} \end{aligned} \quad (4.18)$$

I must point out that, with the shown circuits, the CMRR results are best-case results only. Many influential factors may destroy the rather good-looking picture, eg hidden and/or unequal capacitances in the circuit lead to a decreasing CMRR with increasing frequency. However, to further improve CMRR there is a broad range of measures by eg adjustment of input capacitance of the subtractor and/or by trimming the resistor R between the subtractor's (+) input and ground, etc. Details can be studied in the application papers of the IC manufacturers.

---

### 4.3 Noise Calculations

The calculation of the noise production of Amp4 alone, and further on of Amp4 in conjunction with the RIAA transfer producing networks, becomes a rather complex task. The numbers of the gain stages follows the logic of Fig. 1.2: 1st gain stage = OPs 1 & 2, 2nd gain stage = OPs 3 & 4, 3rd gain stage = OPs 5 & 6. According to MCD-WS 5.1 we have to split the calculation approach into five different actions:

1. Calculation of the output noise voltage density  $e_{\text{n.o.2nd}}$  of Amp4's input stage with OPs 3 & 4 and input shorted or loaded by a resistance R0 (Fig. 4.7).
2. Calculation of the output noise voltage density  $e_{\text{n.o.5}}$  of the subtractor with OP5 and input of the subtractor shorted; the output noise voltage  $e_{\text{n.o.6}}$  of the subtractor OP6 equals the one with OP5, hence, by rms summing we can calculate the output noise voltage density  $e_{\text{n.o.3rd}}$  of the 3rd gain stage with input shorted (Fig. 4.8).
3. Calculation of Amp4's output noise voltage density  $e_{\text{n.o.tot}}$  and its input referred noise voltage density  $e_{\text{n.i.tot}}$ .

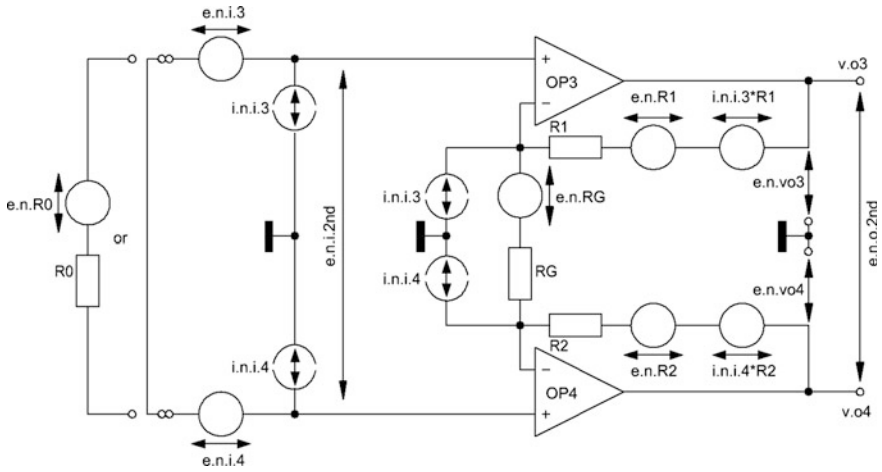


**Fig. 4.7** General noise voltage and current situation of the Amp4 input (2nd) gain stage

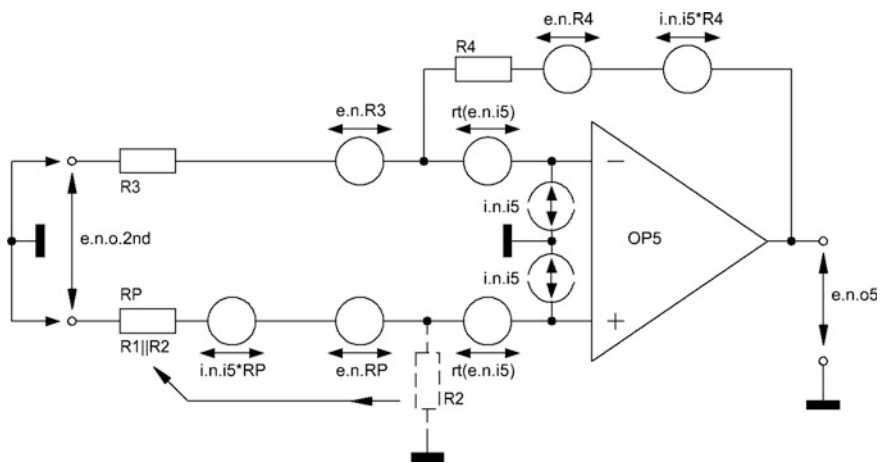


**Fig. 4.8** General noise voltage and current situation of one Amp4 subtractor of the 3rd gain stage

4. With  $e_{n.i.tot}$  and  $i_{n.i}$  on the table, we can now calculate any input load  $R0$  dependent input and/or output referred SN( $R0$ ).
5. Integration of the Fig. 1.2 input stage (OPs 1 & 2), the 75  $\mu s$  network, the output load with the 318  $\mu s$ /3180  $\mu s$  network, and the Amp5 input into the calculation course. Consequently, we obtain the output referred noise voltage density  $e_{n.o.amp4,5}(f)$  of the amp sequence Amp4 + Amp5 + Trafo, with input shorted.



### 4.3.1 Output Noise Voltage of the Amp4 Input Gain Stage (2nd in Figs. 1.2 + 4.1) with OPs 3 & 4

According to Fig. 4.7, with a balanced input load  $R_0$ , the output referred noise voltage density  $e_{n.o.2nd}$  can be calculated by a rather practical equation without big errors. Concerning a frequency independent version I changed Fred Floru's<sup>8</sup> math approach a bit by treating the noise voltage of  $RG$  in the shown different way. However, the calculated results do not differ much. It follows the math approach for single-ended op-amps I've already shown in TSOS-1, Chap. 3.5, and TSOS-2, Chap. 8. Hence, after many measurements with various kinds of op-amps, input loads, and gains, with  $R_1 = R_2$ ,  $e_{n.i.3} = e_{n.i.4}$ , and  $i_{n.i.3} = i_{n.i.4}$  I could obtain the below given frequency independent version of the output noise voltage density  $e_{n.o.2nd}$ : with

$$e_{n.i} = \sqrt{e_{n.i.3}^2 + e_{n.i.4}^2} \quad (4.19)$$

and

$$i_{n.i} = \sqrt{\left(\frac{1}{i_{n.i.3}^2} + \frac{1}{i_{n.i.4}^2}\right)^{-1}} \quad (4.20)$$

We obtain the  $R_0$  and  $RG$  dependent expression for  $e_{n.o.2nd}$ :

$$e_{n.o.2nd}(R_0, RG) = \sqrt{\frac{(e_{n.i}^2 + i_{n.i}^2 R_0^2 + e_{n.R0}^2) \left(1 + \frac{2R_1}{RG}\right)^2}{+2(i_{n.i.3}^2 R_1^2 + e_{n.R1}^2) + e_{n.RG}^2 \left(\frac{2R_1}{RG}\right)^2}} \quad (4.21)$$

Concerning a frequency dependent version by taking  $1/f$ -noise into account and in cases of  $1/f$ -noise corner frequencies  $f_c > 1$  Hz ( $f_{c,e}$  for voltages and  $f_{c,i}$  for currents) it makes sense to change to the frequency dependent version  $e_{n.o.2nd}(f, R_0, RG)$  by adequate integration of the following terms into (4.19)–(4.21):

<sup>8</sup>Improved Mic Preamp IC, Fred Floru, 2001, THAT Corp., (AES UK 103)

I found in the web the following THAT Corp. based design notes and AES lectures. They give an additional and rather deep look into the matter of balanced in/balanced out microphone amps:

- Designing Mic Preamps, Gary K. Herbert, 2010 (AES 129)
- De-integrating Integrated Circuit Preamps, Les Tyler, 2013
- Double Balanced Microphone Amplifier Notes, Graeme John Cohen, 2008
- Perform audio line receiver impedance balancing, Wayne Kirkwood.

$$\begin{aligned}
 e_{n.i.3}(f) &= e_{n.i.3} \sqrt{\frac{f_{c.e.3}}{f} + 1} \\
 i_{n.i.3}(f) &= i_{n.i.3} \sqrt{\frac{f_{c.i.3}}{f} + 1}
 \end{aligned}
 \tag{4.22}$$

### 4.3.2 Output Noise Voltage of the Amp4 Output Gain Stage (3rd in Figs. 1.2 + 4.1) with OPs 5 & 6

The 3rd gain stage around OPs 5 & 6 is composed by two subtractors with opposite connection of their input leads to the 2nd gain stage's output leads. By ignoring any noise voltage influence of the 3rd gain stage the effect of this arrangement leads to two 100 % correlated noise voltages at the outputs of OPs 5 & 6. Their sum would automatically lead to a stage gain factor of 2, as long as all Fig. 4.5 resistors R are chosen of equal value.

Nevertheless and rather important for low overall gains, we have to take the fully un-correlated noise voltage of the two halves of the 3rd gain stage into account too. The situation of all noise sources of one branch of the 3rd gain stage is given in Fig. 4.8.

In order to catch the equation to calculate the output noise voltage density  $e_{n.o.5}$  we shorten the input. Moreover, for general purposes we rename the Rs by  $R3 = R1$ ,  $R4 = R2$ , and  $RP = R1 \parallel R2$ . The output noise voltage density  $e_{n.o.5}$  at the output of OP5 thus becomes<sup>9</sup>:

$$e_{n.o.5} = \sqrt{2 \left( 1 + \frac{R4}{R3} \right)^2 \left( \frac{e_{n.i.5}^2}{2} + e_{n.RP}^2 + i_{n.i.5}^2 RP \right)}
 \tag{4.23}$$

In cases of 1/f-noise corner frequencies  $f_c > 1$  Hz ( $f_{c.e}$  for voltages and  $f_{c.i}$  for currents) it makes sense to change to the frequency dependent version  $e_{n.o.5}(f)$  by adequate integration of the following terms into (4.23):

$$\begin{aligned}
 e_{n.i.5}(f) &= e_{n.i.5} \sqrt{\frac{f_{c.e.5}}{f} + 1} \\
 i_{n.i.5}(f) &= i_{n.i.5} \sqrt{\frac{f_{c.i.5}}{f} + 1}
 \end{aligned}
 \tag{4.24}$$

<sup>9</sup>“Low-Noise Electronic System Design”, 1993, Motchenbacher/Connelly, Wiley-Interscience, N. Y., ISBN 0-471-57742-1.

### 4.3.3 Total Input and Output Noise Voltages of Amp4

With the rms sum  $e_{n.o.3rd}$  of the un-correlated subtractor output noise voltage densities  $e_{n.o.5}$  and  $e_{n.o.6}$

$$e_{n.o.6} = e_{n.o.5} \quad (4.25)$$

$$\Rightarrow e_{n.o.3rd} = \sqrt{2e_{n.o.5}^2} \quad (4.26)$$

the output noise voltage  $e_{n.o.tot}$  of Amp4 is the nothing else but the rms sum of the output noise voltage  $e_{n.o.3rd}$  of the 3rd gain stage plus the output noise voltage  $e_{n.o.2nd}$  of the 2nd gain stage multiplied by the gain of the 3rd gain stage (here, with equal  $R_s$  it's two), hence,  $e_{n.o.tot}$  becomes

$$e_{n.o.tot} = \sqrt{e_{n.o.2nd}^2 G_{3rd}^2 + e_{n.o.3rd}^2} \quad (4.27)$$

Consequently, we obtain Amp4's input referred noise voltage density  $e_{n.i.tot}$  as follows:

$$e_{n.i.tot} = \frac{e_{n.o.tot}}{G_{amp4}} \quad (4.28)$$

### 4.3.4 Noise and SN Calculations According to Fig. 1.2

The calculation of the noise voltage of Amp4 alone makes no sense, as long as there are influential factors not taken into account: the ones at its input (OPs 1 & 2 and  $T_2(f)$ ) and at its output ( $T_1(f) + T_3(f) + \text{Amp5}$ ). All together, they generate a noise voltage that can be measured at the output of Amp5, and thus be compared with the calculated results. The calculation course follows the mathematical course given in MCD-WS 5.1, "6. Noise and SN calculations". However, here comes the short version, tackling the major factors.

To calculate the output noise voltage density  $e_{n.o.amp4.5}(f)$  at the output of Amp5 with input shorted the rather extensive equation looks as follows<sup>10</sup>:

$$e_{n.o.amp4.5}(f) = \sqrt{[e_{n.o.2nd}(f)G_{3rd}]^2 + e_{n.o.3rd}(f)^2 + e_{n.Z.T1.3}(f)^2 + i_{n.i.amp5}^2 Z_{T1.3}(f)^2 + e_{n.i.amp5}^2} \quad (4.29)$$

<sup>10</sup>Impedances  $Z_{T1.3}(f)$  and  $Z_{T2}(f)$  and their respective noise voltages: see MCD-WS 5.1, Points 6.4ff.

$$e_{n.o.2nd}(f) = \sqrt{\left[ \begin{aligned} &e_{n.o.1st}(f)^2 G_{T2}(f)^2 + e_{n.Z.T2}(f)^2 \\ &+ 0.5i_{n.i.2nd}^2 Z_{T2}(f)^2 + 2e_{n.i.2nd}(f)^2 \end{aligned} \right] G_{2nd}^2 + i_{n.i.2nd}^2 (R61 + R62)^2 + e_{n.R61}^2 + e_{n.R62}^2 + e_{n.RG.o}^2} \quad (4.30)$$

$$e_{n.RG.o} = e_{n.RG}(G_{2nd} - 1) \quad (4.31)$$

$$e_{n.o.1st}(f) = \sqrt{\left[ e_{n.i.1}(f)^2 + e_{n.i.2}(f)^2 \right] G_{1st}^2} \quad (4.32)$$

$$e_{n.o.3rd}(f) = \sqrt{e_{n.o.5}(f)^2 + e_{n.o.6}(f)^2} \quad (4.33)$$

From the preceding sections, we can take the gain results as follows:

$$G_{1st} = 1 \quad (4.34)$$

$$G_{2nd} = G_{dif} = G_{amp4.in} \quad (4.35)$$

$$G_{3rd} = G_{amp4.out} \quad (4.36)$$

According to (4.29)–(4.36), Fig. 1.2, and Fig. 4.1  $e_{n.o.amp4.5}(f)$  includes 100 % uncorrelated noise sources only. The average input referred noise voltage density of Amp5 equals the one of Chap. 2 (see Note in Sect. 2.2.3).

I must point out that some terms in (4.29) and (4.30) do not add significant values to the total sum underneath the roots. Nevertheless, I keep them for universal usage with other than the chosen components.

The resulting noise voltage density multiplied by the A-weighting function, referenced to 1  $V_{rms}$  nominal signal output voltage, and integrated over the bandwidth of  $B_{20k}$ , will lead to the A-weighted output referred  $SN_{a.o.amp4.5}$  in  $B_{20k}$ , expressed in dBV(A).

The detailed calculation approaches of the different terms in (4.29) and (4.30) can be studied in TSOS-2 and TSOS-1.

### 4.3.5 A Look into the Content of MCD-WS 5.1

MCD-WS 5.1 shows some additional interesting results:

- Very important for external amplifiers Point 6.6.3 shows the calculation of the Amp4 CMRR.
- Point 7. covers the math of an extremely low-noise input load of the Fig. 2.1 arrangement with Amp4. Here, like in Chap. 2, I've also chosen a pre-amp with a gain of 200, an *i/p* referred noise voltage density of 0.2 nV/rHz and noise current density of only 2.4 pA/rHz. The *i/p* load is 20  $\Omega$ . Now we can compare

the A-weighted and RIAA equalized SN result ( $=-82.514$  dBV(A)) with the one of Point 8.

- Point 8. covers the math of the Point 7. low-noise Amp1, followed by a no-noise arrangement à la Fig. 2.1. The SN result becomes  $-82.582$  dBV(A).
- Hence, the difference is appr. 0.07 dB only. It is nothing else but the Noise Figure. In other words: a further chase for extremely low-noise solutions makes no sense for input loads  $\geq 20 \Omega$ . We will see later on in Chap. 10 what it will mean for input loads  $< 20 \Omega$ .
- Points 9 and 10. show calculations of the Noise Figure (NF) of the amp chain Amp4 + Amp5, fed by a lowest-noise input amp: 9. for MC and 10. for MM cartridge purposes. These NFs are all  $< 0.1$  dB. Hence, together with its input and output loads the noise impact of the here presented Amp4 is completely ignorable.
- Point 11. gives up the shorted input and replaces the shortage by an output resistance of a preceding gain stage, here 1 k $\Omega$ . Because of the 75  $\mu$ s lp at the input, the noise impact becomes marginal too.
- Point 12. tackles the 100 % correlated noise voltages; see also next section below!

### 4.3.6 100 % Correlated Noise Voltages of Amp4

The differences between the measurement results and the calculated ones look very good, always  $\leq 0.5$ – $1.0$  dB rounded for the balanced outputs of Amps 4 & 5.

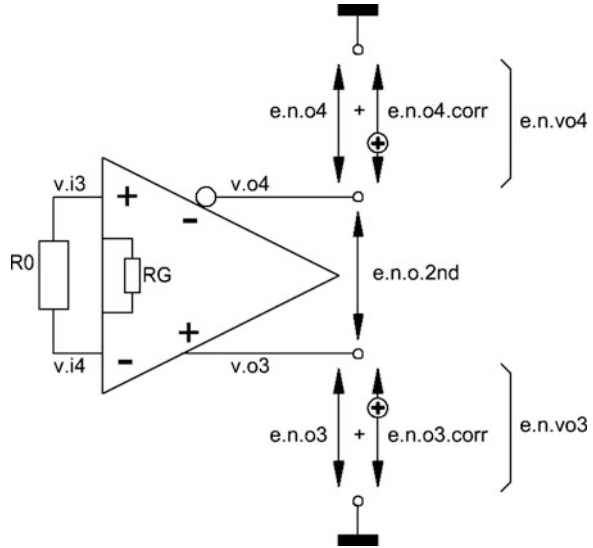
However, if we also measure the 2nd stage's un-balanced output noise voltages between the output leads and ground we'll find surprising results: they look nearly the same like the balanced output noise voltage results between the output leads, thus, the SNs follow the same track. This can only be the case if we assume two 100 % correlated noise voltage densities  $e_{n.o3,corr}$  &  $e_{n.o4,corr}$  and two uncorrelated ones  $e_{n.o3}$  &  $e_{n.o4}$  that form the output noise voltages from each output lead to ground. Hence, the following simplified frequency independent equations and Fig. 4.9 should describe this situation. The encircled "+" sign signals the phase relationship of the correlated noise voltage parts.

$$\begin{aligned}
 e_{n.vo3}^2 &= e_{n.o3}^2 + e_{n.o3,corr}^2 \\
 e_{n.vo4}^2 &= e_{n.o4}^2 + e_{n.o4,corr}^2 \\
 e_{n.vo3} &= e_{n.vo4}
 \end{aligned}
 \tag{4.37}$$

Consequently, with (4.37) and (4.21) the remaining un-correlated output noise voltage density  $e_{n.o3}$  ( $=e_{n.o4}$ ) becomes thus:

$$e_{n.o3} = \frac{e_{n.o,2nd}}{\sqrt{2}}
 \tag{4.38}$$

**Fig. 4.9** Detailed output noise voltage situation of the 2nd gain stage



and

$$e_{n.o.2nd} = \sqrt{e_{n.o3}^2 + e_{n.o4}^2} \tag{4.39}$$

Hence, both rms voltages  $e_{N.vo3} = e_{n.vo3}$  in  $B_{20k}$  and  $e_{N.vo4} = e_{n.vo4}$  in  $B_{20k}$  become always worse than the output rms voltage  $e_{N.o.2nd} = e_{n.o.2nd}$  in  $B_{20k}$  (approximately 1.6 dB measured and calculated) because  $e_{N.o3.corr}$  ( $=e_{n.o3.corr}$  in  $B_{20k}$ ) is always bigger than  $e_{N.o3}$  ( $=e_{n.o3}$  in  $B_{20k}$ ).

The way to get its rms voltage  $e_{N.o3.corr}$  in  $B_{20k}$  and the frequency dependent noise voltage density  $e_{n.o3.corr}$  look as follows:

$$e_{n.o3.corr}(f) = \sqrt{\left( e_{n.i.2nd}(f)^2 + i_{n.i.2nd}^2 R_0^2 + e_{n.R0}^2 \right) \left( 1 + \frac{2R_1}{RG} \right)^2 + i_{n.i.3}^2 R_1^2 + e_{n.R1}^2 + e_{n.RG}^2 \left( \frac{R_1}{RG} \right)^2} \tag{4.40}$$

$$= e_{n.o4.corr}(f)$$

$$e_{N.o3.corr} = \sqrt{\frac{1}{B_1} \int_{20Hz}^{20kHz} (|e_{n.o3.corr}(f)|)^2 df} \tag{4.41}$$

The following chapter’s Mathcad Worksheet 5.1 shows the respective calculations and comparisons under Point 12.

Note: This section's equations are of academic interest only because of the fact that most of the existing common mode voltages between the DIF amp's output leads and ground will be cancelled by the CMR of a following gain stage. They represent a first and rough attempt to mathematically describe the measured findings with Amp4. However, to bring them (or improved versions) in formats of general validity further investigations must be carried out.

## Contents

### 5.1 MCD-WS: The Solid-State Gain Stage Amp4 with RIAA Networks

**Note 1:** MCD 11 has no built-in unit “rtHz” or “ $\sqrt{\text{Hz}}$ ”. To get  $\sqrt{1 \text{ Hz}}$  based voltage noise and current noise densities the rms noise voltage and current in a specific frequency range  $B > 1 \text{ Hz}$  must be multiplied by  $\sqrt{1 \text{ Hz}}$  and divided by the root of that specific frequency range  $\sqrt{B}$ !

**Note 2:** MCD 11 offers no “dB” unit. This is available from MCD 13 on!



5.1 MCD-WS: The Solid-State Gain Stage Amp4 with RIAA Networks

Calculations of a solid-state (op-amp) driven Amp4 with T1/T3 RIAA network at the output, T2 RIAA network at the input, and based on data-sheet figures

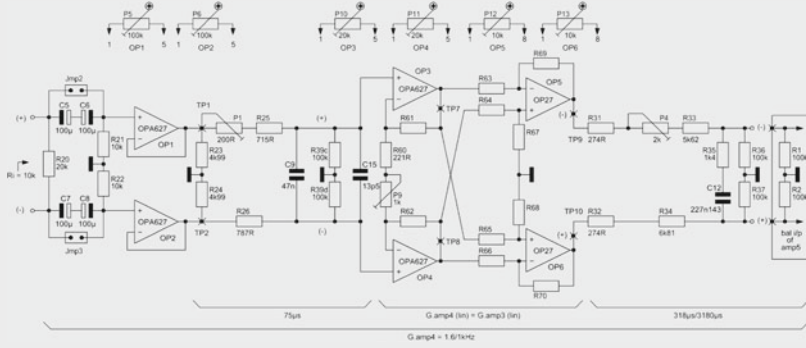


Fig. 5.1 Op-amp driven Amp4 incl. RIAA networks

1. General data :

OP1 = OPA627    OP2 = OP1    OP3 = OP1    OP4 = OP1    OP5 = OP27    OP6 = OP5

$k := 1.38065 \cdot 10^{-23} \text{V} \cdot \text{A} \cdot \text{s} \cdot \text{K}^{-1}$

$T := 315\text{K}$

$B_1 := 1\text{Hz}$

$B_{20k} := 19980\text{Hz}$

$f := 20\text{Hz}, 25\text{Hz}, 20000\text{Hz}$

$h := 1000\text{Hz}$

2. Gain stage component data :

$R_{20} := 20 \cdot 10^3 \Omega$      $R_{21} := 10 \cdot 10^3 \Omega$      $R_{22} := R_{21}$      $R_{23} := 4.99 \cdot 10^3 \Omega$      $R_{24} := R_{23}$

$R_{25} := 750 \Omega$      $R_{26} := 787 \Omega$      $R_{31} := 274 \Omega$      $R_{32} := R_{31}$      $R_{33} := 5.62 \cdot 10^3 \Omega$

$R_{34} := 6.81 \cdot 10^3 \Omega$      $R_{35} := 1.4 \cdot 10^3 \Omega$      $R_{36} := 100 \cdot 10^3 \Omega$      $R_{37} := R_{36}$      $R_{39c} := 100 \cdot 10^3 \Omega$

$R_{39d} := R_{39c}$      $R_{60} := 221 \Omega$      $R_{61} := 2.2 \cdot 10^3 \Omega$      $R_{62} := R_{61}$      $R_{63} := R_{61}$

$R_{64} := R_{63}$      $R_{65} := R_{63}$      $R_{66} := R_{63}$      $R_{67} := R_{63}$      $R_{68} := R_{63}$

$R_{69} := R_{63}$      $R_{70} := R_{63}$      $R_{1amp5} := 100 \cdot 10^3 \Omega$      $R_{2amp5} := R_{1amp5}$

R61 ... R70: 0.1%

$C_5 := 100 \cdot 10^{-6} \text{F}$      $C_6 := C_5$      $C_7 := C_5$      $C_8 := C_5$      $C_9 := 47 \cdot 10^{-9} \text{F}$

$C_{i,op1} := 8 \cdot 10^{-12} \text{F}$      $C_{15} := 13.5 \cdot 10^{-12} \text{F}$      $C_{i,op2} := C_{i,op1}$      $C_{i,dif} := C_{15} + 0.5 \cdot C_{i,op1}$

$C_{i,dif} := 17.5 \cdot 10^{-12} \text{F}$      $C_{12} := 227.143 \cdot 10^{-9} \text{F}$

$P_5 = 100\text{k}\Omega$      $P_6 = P_5$      $P_{10} = 20\text{k}\Omega$      $P_{11} = P_{10}$      $P_{12} = 10\text{k}\Omega$      $P_{13} = P_{12}$

5.1 MCD-WS: The Solid-State Gain Stage Amp4 with RIAA Networks

3. Gains and gain setting RG :

3.1 Gain setting :

$$R_G := 550\Omega \quad G := \left(1 + \frac{R61 + R62}{R_G}\right) \cdot \left(\frac{R69}{R63} + \frac{R70}{R66}\right) \quad G = 18$$

The idle gain  $G_0$  of the gain stage with OP3 ... OP6 equals that of the triode driven gain stage, hence,

$$G_{0,amp4} := 16.390411 \quad R60 + P9 = R_G$$

$G_{1st}$  = gain of OP1 & OP2 stage       $G_{2nd}$  = gain of OP3 & OP4 stage       $G_{3rd}$  = gain of OP5 & OP6 stage

$$G_{1st} := 1 \quad R_G := 4 \cdot \frac{R61 \cdot R69}{G_{0,amp4} \cdot R63 - 2 \cdot R69} \quad R_G = 611.518 \Omega \quad G_{3rd} := 2 \cdot \frac{R69}{R63}$$

$$R_{o,op1} := 0.003\Omega$$

$$R_{o,op2} := R_{o,op1} \quad G_{2nd} := 1 + \frac{2 \cdot R61}{R_G} \quad G_{2nd} = 8.195 \quad G_{3rd} = 2$$

3.2 Overall gain of Amp4 without RIAA network :

$$G_{amp4} := G_{1st} \cdot G_{2nd} \cdot G_{3rd} \quad G_{amp4} = 16.390411$$

$$P9 := R_G - R60 \quad P9 = 390.518 \Omega$$

4. RIAA time constants T and transfer gains  $G_T$  :

4.1  $T2 = 75\mu s$  :       $P1 := 70.975293 \cdot \Omega$

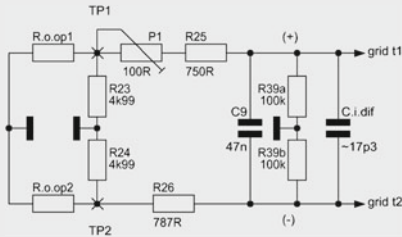


Fig. 5.2  
T2 defining network

Subc-apps of P1 should bring in line the value of T2 with the RIAA network component values (because of the marginal influence the voltage divider effects of  $R_{o,op1}/R_{o,op2}$  and  $R23/R26$  are ignored here!)

$$T2 := (C9 + C_{i,dif}) \cdot \left[ \left[ \left[ \left( R_{o,op1}^{-1} + R23^{-1} \right)^{-1} + R25 + P1 \right]^{-1} + R39c^{-1} \right]^{-1} \dots \right. \\ \left. + \left[ \left[ \left( R_{o,op2}^{-1} + R24^{-1} \right)^{-1} + R26 \right]^{-1} + R39d^{-1} \right]^{-1} \right]$$

5.1 MCD-WS: The Solid-State Gain Stage Amp4 with RIAA Networks

$$T2 = 75 \times 10^{-6} \text{ s}$$

$$G_{T2}(f) := \frac{\left[ 2j \cdot \pi \cdot f \cdot (C9 + C_{i,dif}) + (R39c + R39d)^{-1} \right]^{-1}}{\left[ 2j \cdot \pi \cdot f \cdot (C9 + C_{i,dif}) + (R39c + R39d)^{-1} \right]^{-1} + R25 + R26 + P1 + 2 \cdot \left( R_{o,op1}^{-1} + R23^{-1} \right)^{-1}}$$

$$\left| G_{T2} \left( \frac{1}{2 \cdot \pi \cdot T2} \right) \right| = 0.701$$

$$20 \cdot \log \left( \left| G_{T2} \left( \frac{1}{2 \cdot \pi \cdot T2} \right) \right| \right) = -3.08 \text{ [dB]}$$

$$G_{T2,e}(f) := 20 \cdot \log \left( \left| G_{T2}(f) \right| \right)$$

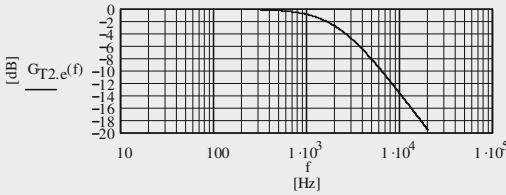


Fig. 5.3  
Bode plot of  $G_{T2}(f)$

4.2  $T1 = 3180 \mu\text{s}$ ,  $T3 = 318 \mu\text{s}$  :  $P4 := 1.438476 \cdot 10^3 \cdot \Omega$

$C12 := 227.142857143 \cdot 10^{-9} \text{ F}$

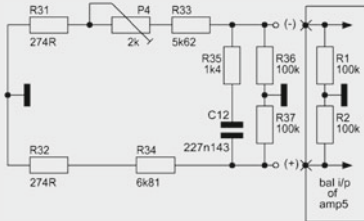


Fig. 5.4  
T1 & T3 defining network

Succ-apps of C12 & P4 should bring in line the values of T1 & T3 with the required RIAA network values:

$$T3 := C12 \cdot R35$$

$$T3 = 318 \times 10^{-6} \text{ s}$$

$$R_{T1,eff} := R31 + R32 + P4 + R33 + R34$$

$$R_{T1,eff} = 14.416 \times 10^3 \Omega$$

$$T1 := C12 \cdot \left[ R35 + \left[ R_{T1,eff}^{-1} + \left[ \left( R_{1,amp5}^{-1} + R36^{-1} \right)^{-1} + \left( R_{2,amp5}^{-1} + R37^{-1} \right)^{-1} \right]^{-1} \right]^{-1} \right]$$

$$T1 = 3.18 \times 10^{-3} \text{ s}$$

5.1 MCD-WS: The Solid-State Gain Stage Amp4 with RIAA Networks

$$R_{L,dif} := \left( \frac{1}{R1_{amp5} + R2_{amp5}} + \frac{1}{R36 + R37} \right)^{-1}$$

$$R_{L,dif} = 100 \times 10^3 \Omega$$

$$G_{T1.3}(f) := \frac{\left[ \left( \frac{1}{2j \cdot \pi \cdot f \cdot C12} + R35 \right)^{-1} + \frac{1}{R_{L,dif}} \right]^{-1}}{\left[ \left( \frac{1}{2j \cdot \pi \cdot f \cdot C12} + R35 \right)^{-1} + \frac{1}{R_{L,dif}} \right]^{-1} + R_{T1,eff}}$$

$$|G_{T1.3}(h)| = 0.098$$

$$20 \cdot \log(|G_{T1.3}(20Hz)|) = -1.806$$

$$20 \cdot \log\left(\left|G_{T1.3}\left(\frac{1}{2 \cdot \pi \cdot T1}\right)\right|\right) = -4.137$$

$$20 \cdot \log\left(\left|G_{T1.3}\left(\frac{1}{2 \cdot \pi \cdot T3}\right)\right|\right) = -18.203$$

$$G_{T1.3,e}(f) := 20 \cdot \log(|G_{T1.3}(f)|)$$

$$20 \cdot \log(|G_{T1.3}(20kHz)|) = -21.167$$

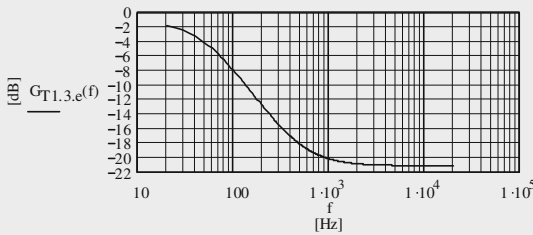


Fig. 5.5  
Bode plot of  $G_{T1}(f)$  &  $G_{T3}(f)$

4.3 RIAA transfer :

$$G_{riaa}(f) := G_{T2}(f) \cdot G_{T1.3}(f)$$

$$G_{riaa,e}(f) := 20 \cdot \log(|G_{riaa}(f) \cdot G_{riaa}(h)^{-1}|)$$

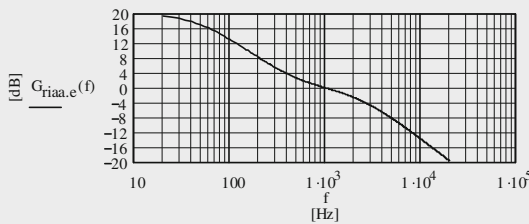


Fig. 5.6  
Normalized (1kHz at 0dB)  
RIAA transfer function

5.1 MCD-WS: The Solid-State Gain Stage Amp4 with RIAA Networks

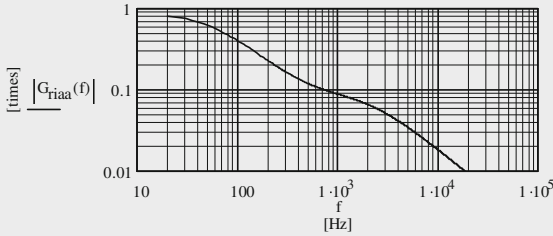


Fig. 5.7  
Bode plot of the combined RIAA network

$$R_{1000} := \frac{\sqrt{1 + (2 \cdot \pi \cdot h \cdot 318 \cdot 10^{-6} \text{ s})^2}}{\sqrt{1 + (2 \cdot \pi \cdot h \cdot 3180 \cdot 10^{-6} \text{ s})^2} \cdot \sqrt{1 + (2 \cdot \pi \cdot h \cdot 75 \cdot 10^{-6} \text{ s})^2}}$$

$$R_0(f) := \frac{\sqrt{1 + (2 \cdot \pi \cdot f \cdot 318 \cdot 10^{-6} \text{ s})^2}}{\sqrt{1 + (2 \cdot \pi \cdot f \cdot 3180 \cdot 10^{-6} \text{ s})^2} \cdot \sqrt{1 + (2 \cdot \pi \cdot f \cdot 75 \cdot 10^{-6} \text{ s})^2}} \cdot (R_{1000})^{-1}$$

$$\text{Dev}_{1e}(f) := 20 \cdot \log(R_0(f)) - G_{riaa,e}(f)$$

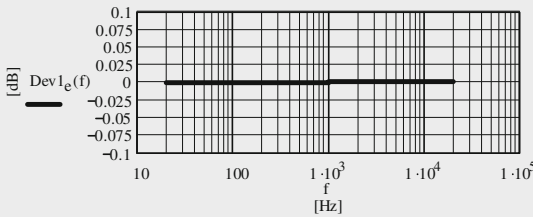


Fig. 5.8  
Deviation from the exact RIAA transfer

5. Transfer function  $T(f)$  of Amp4 :

General assumption: the corner frequency of the  $\dot{v}_p$  hp R21, R22, C5 ... C8 is chosen that there is no influence on a flat phase and frequency response in  $B_{20k}$  !

$$T_{amp4}(f) := G_{amp4} \cdot G_{T2}(f) \cdot G_{T1.3}(f)$$

$$|T_{amp4}(h)| = 1.435729$$

$$T_{amp4,e}(f) := 20 \cdot \log(|T_{amp4}(f)|)$$

$$T_{amp4,e}(h) = 3.141447 \quad [\text{dB}]$$

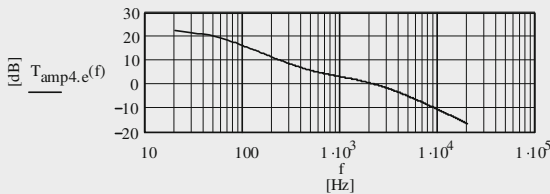


Fig. 5.9  
Bode plot of Amp4

$$\text{Dev}2_e(f) := 20 \cdot \log(R_0(f)) - 20 \cdot \log\left(\left|T_{\text{amp4}}(f) \cdot T_{\text{amp4}}(h)^{-1}\right|\right)$$

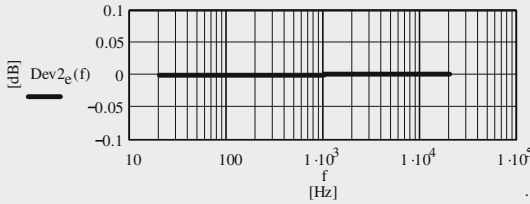


Fig. 5.10 = Fig. 4.3  
Fig. 5.9's deviation from the exact RIAA transfer

$$\text{RIAA}(f) := \frac{1 + 2j \cdot \pi \cdot f \cdot 318 \times 10^{-6} \cdot s}{(1 + 2j \cdot \pi \cdot f \cdot 3180 \times 10^{-6} \cdot s) \cdot (1 + 2j \cdot \pi \cdot f \cdot 75 \times 10^{-6} \cdot s)}$$

$$|\text{RIAA}(h)| = 101.03 \times 10^{-3}$$

$$\phi_{\text{amp4}}(f) := \text{atan}\left(\frac{\text{Im}\left(T_{\text{amp4}}(f) \cdot \text{RIAA}(f)^{-1}\right)}{\text{Re}\left(T_{\text{amp4}}(f) \cdot \text{RIAA}(f)^{-1}\right)}\right)$$

$$\phi_{\text{amp4}}(h) = -0$$

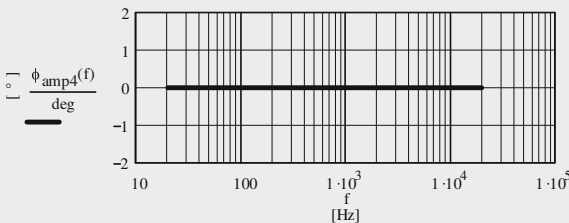


Fig. 5.11  
Fig. 5.9's phase response

**6. Noise and SN calculations :**

**6.1 General data :**

$$v_{i,\text{ref}} := 100 \cdot 10^{-3} \text{V}$$

$$v_{o,\text{ref}} := v_{i,\text{ref}} \cdot |T_{\text{amp4}}(h)|$$

$$v_{o,\text{ref}} = 143.573 \times 10^{-3} \text{V} \quad v_{o,\text{ref},m} = v_{o,\text{ref}}$$

$$\text{RP}_{3\text{rd},i} := \left(\frac{1}{R_{64}} + \frac{1}{R_{67}}\right)^{-1}$$

$$\text{RP}_{3\text{rd},i} = 1.1 \times 10^3 \Omega$$

$$\text{RP}_{3\text{rd},o} := \left(\frac{1}{R_{63}} + \frac{1}{R_{69}}\right)^{-1}$$

$$\text{RP}_{3\text{rd},o} = 1.1 \times 10^3 \Omega$$

$$\text{RP}_{3\text{rd},i} = \text{RP}_{3\text{rd},o} = \text{RP}_{3\text{rd}}$$

$$\text{RP}_{3\text{rd}} := \text{RP}_{3\text{rd},i}$$

$$e_{n,i,1} := 4.2 \cdot 10^{-9} \text{V} \quad e_{n,i,2} := e_{n,i,1} \quad e_{n,i,3} := e_{n,i,1} \quad e_{n,i,4} := e_{n,i,1} \quad e_{n,i,5} := 3.2 \cdot 10^{-9} \text{V} \quad e_{n,i,6} := e_{n,i,5}$$

$$i_{n,i,1} := 2.5 \cdot 10^{-15} \text{A} \quad i_{n,i,2} := i_{n,i,1} \quad i_{n,i,3} := i_{n,i,1} \quad i_{n,i,4} := i_{n,i,1} \quad i_{n,i,5} := 0.4 \cdot 10^{-12} \text{A} \quad i_{n,i,6} := i_{n,i,5}$$

$$f_{c,e,1} := 40 \text{Hz} \quad f_{c,i,1} < 0.1 \text{Hz} \quad f_{c,e,5} := 2.7 \text{Hz} \quad f_{c,i,5} := 140 \text{Hz}$$

5.1 MCD-WS: The Solid-State Gain Stage Amp4 with RIAA Networks

$$\begin{aligned}
 e_{n.i.1}(f) &:= e_{n.i.1} \cdot \left( \sqrt{\frac{f \cdot c.e.1}{f} + 1} \right) & e_{n.i.2}(f) &:= e_{n.i.1}(f) & e_{n.i.3}(f) &:= e_{n.i.1}(f) & e_{n.i.4}(f) &:= e_{n.i.1}(f) \\
 e_{n.i.5}(f) &:= e_{n.i.5} \cdot \left( \sqrt{\frac{f \cdot c.e.5}{f} + 1} \right) & e_{n.i.6}(f) &:= e_{n.i.5}(f) & i_{n.i.5}(f) &:= i_{n.i.5} \cdot \left( \sqrt{\frac{f \cdot c.i.5}{f} + 1} \right) & i_{n.i.6}(f) &:= i_{n.i.5}(f) \\
 e_{n.i.1st}(f) &:= e_{n.i.1}(f) & e_{n.i.2nd}(f) &:= e_{n.i.3}(f) & e_{n.i.3rd}(f) &:= e_{n.i.5}(f) \\
 i_{n.i.1st} &:= i_{n.i.1} & i_{n.i.2nd} &:= i_{n.i.3} & i_{n.i.3rd}(f) &:= i_{n.i.5}(f)
 \end{aligned}$$

6.2 Situation of the various noise sources :

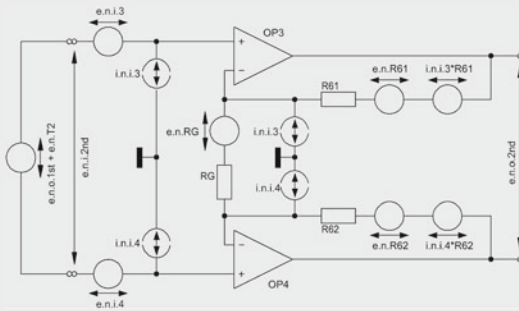


Fig. 5.12  
Noise voltage and current situation of the 2nd gain stage (OP3 & OP4)

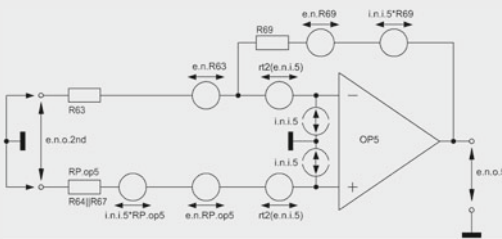


Fig. 5.13  
Noise voltage and current situation of the 3rd gain stage (OP5 & OP6)

$$e_{n.R25} := \sqrt{4 \cdot k \cdot T \cdot B_1 \cdot [(R25 + P1)^{-1} + R39c^{-1}]^{-1}}$$

$$e_{n.R25} = 3.764 \times 10^{-9} \text{ V}$$

$$e_{n.R26} := \sqrt{4 \cdot k \cdot T \cdot B_1 \cdot (R26^{-1} + R39d^{-1})^{-1}}$$

$$e_{n.R26} = 3.686 \times 10^{-9} \text{ V}$$

$$e_{n.R33} := \sqrt{4 \cdot k \cdot T \cdot B_1 \cdot (R31 + R33 + P4)}$$

$$e_{n.R33} = 11.294 \times 10^{-9} \text{ V}$$

5.1 MCD-WS: The Solid-State Gain Stage Amp4 with RIAA Networks

$$\begin{aligned}
 e_{n.R34} &:= \sqrt{4 \cdot k \cdot T \cdot B_1 \cdot (R34 + R32)} & e_{n.R34} &= 11.101 \times 10^{-9} \text{ V} \\
 e_{n.R61} &:= \sqrt{4 \cdot k \cdot T \cdot B_1 \cdot R61} & e_{n.R61} &= 6.186 \times 10^{-9} \text{ V} \\
 e_{n.R62} &:= e_{n.R61} \\
 e_{n.R63} &:= \sqrt{4 \cdot k \cdot T \cdot B_1 \cdot R63} & e_{n.R63} &= 6.186 \times 10^{-9} \text{ V} \\
 e_{n.R69} &:= e_{n.R63} \\
 e_{n.RP.3rd.i} &:= \sqrt{4 \cdot k \cdot T \cdot B_1 \cdot RP_{3rd.i}} & e_{n.RP.3rd.i} &= 4.374 \times 10^{-9} \text{ V} \\
 e_{n.RP.3rd.o} &:= \sqrt{4 \cdot k \cdot T \cdot B_1 \cdot RP_{3rd.o}} & e_{n.RP.3rd.o} &= 4.374 \times 10^{-9} \text{ V} \\
 e_{n.RP.3rd.i} &= e_{n.RP.3rd.o} = e_{n.RP.3rd} & e_{n.RP.3rd} &:= e_{n.RP.3rd.i}
 \end{aligned}$$

6.3 Output noise voltage of the 1st gain stage (OP1 & OP2) with i/p shorted :

$$e_{n.o.1st(f)} := \sqrt{e_{n.i.1st(f)}^2 \cdot G_{1st}^2} \quad |e_{n.o.1st(h)}| = 6.057 \times 10^{-9} \text{ V}$$

6.4 Output noise voltage of the 2nd gain stage (OP3 & OP4 & T2) with i/p of the 1st gain stage (OP1 & OP2) shorted :

6.4.1 Noise Voltage of the 2nd gain stage :

$$\begin{aligned}
 e_{n.RG} &:= \sqrt{4 \cdot k \cdot T \cdot B_1 \cdot RG} & e_{n.RG} &= 3.262 \times 10^{-9} \text{ V} \\
 e_{n.RG.o} &:= e_{n.RG} \cdot (G_{2nd} - 1) & e_{n.RG.o} &= 23.468 \times 10^{-9} \text{ V}
 \end{aligned}$$

6.4.2 Noise Voltage of the T2 network :

$$\begin{aligned}
 Z_{T2} &:= \left[ (R25 + R26 + P1)^{-1} + (R39c + R39d)^{-1} \right]^{-1} & Z_{T2} &= 1.595 \times 10^3 \Omega \\
 e_{n.Z.T2(f)} &:= G_{T2(f)} \cdot \sqrt{4 \cdot k \cdot T \cdot B_1 \cdot Z_{T2}} & |e_{n.Z.T2(h)}| &= 4.727 \times 10^{-9} \text{ V}
 \end{aligned}$$

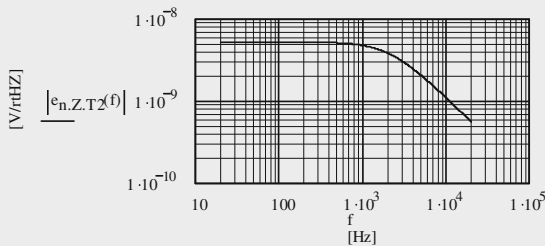


Fig. 5.14  
Frequency response of the noise voltage density of the T2(f) network



5.1 MCD-WS: The Solid-State Gain Stage Amp4 with RIAA Networks

$$Z_{T2}(f) := Z_{T2} \cdot G_{T2}(f)$$

6.4.3 Output noise voltage of 1st+2nd+T2 stages :

$$e_{n.o.2nd}(f) := \sqrt{\left( e_{n.o.1st}(f)^2 \cdot G_{T2}(f)^2 + e_{n.Z.T2}(f)^2 + \frac{i_{n.i.2nd}^2}{2} \cdot Z_{T2}(f)^2 \dots \cdot G_{2nd}^2 \dots \right. \\ \left. + 2 \cdot e_{n.i.2nd}(f)^2 \right. \\ \left. + i_{n.i.2nd}^2 \cdot (R61 + R62)^2 + e_{n.R61}^2 + e_{n.R62}^2 + e_{n.RG.o}^2 \right)}$$

$$|e_{n.o.2nd}(h)| = 77.147 \times 10^{-9} \text{V}$$

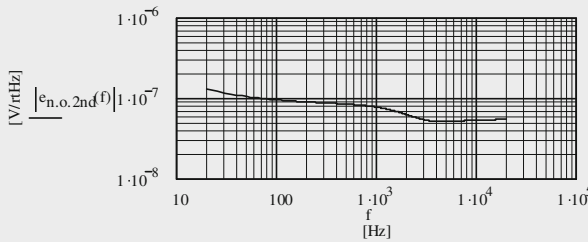


Fig. 5.15  
Bode plot of the balanced o/p noise voltage density of the 2nd gain stage

6.5 Output noise voltage of the 3rd gain stage with i/p shorted :

6.5.1 Noise Voltages of the OP5 and OP6 stages :

$$e_{n.o.5}(f) := \sqrt{2 \cdot \left( 1 + \frac{R69}{R63} \right)^2 \cdot \left( \frac{e_{n.i.3rd}(f)^2}{2} + e_{n.RP.3rd}^2 + i_{n.i.3rd}(f)^2 \cdot R_{P3rd}^2 \right)}$$

$$e_{n.o.5}(h) = 13.997 \times 10^{-9} \text{V}$$

$$e_{n.o.6}(f) := e_{n.o.5}(f)$$

6.5.2 Noise Voltage and SN of the whole 3rd gain stage :

$$e_{n.o.3rd}(f) := \sqrt{e_{n.o.5}(f)^2 + e_{n.o.6}(f)^2}$$

$$e_{n.o.3rd}(h) = 19.795 \times 10^{-9} \text{V}$$

$$SN_{ne.o.3rd} := 20 \cdot \log \left[ \frac{\frac{1}{B_1} \cdot \int_{20\text{Hz}}^{2000\text{Hz}} \left( |e_{n.o.3rd}(f)| \right)^2 df}{1\text{V}} \right]$$

$$SN_{ne.o.3rd} = -111.068 \text{ [dBV]}$$

measured: -110.51 dBV

5.1 MCD-WS: The Solid-State Gain Stage Amp4 with RIAA Networks Page 10

6.6 Output noise voltage of Amp4 + Amp5 with i/p shorted :

6.6.1 Noise Voltage of the T1/T3 network at the o/p of Amp4 :

$$Z_{T1,3}(f) := \left( \frac{1}{P4 + R31 + R32 + R33 + R34} + \frac{1}{R35 + \frac{1}{2j \cdot \pi \cdot f \cdot C12}} + \frac{1}{R_{L,dif}} \right)^{-1} \quad |Z_{T1,3}(h)| = 1.407 \times 10^3 \Omega$$

$$e_{n,Z.T1,3}(f) := G_{T1,3}(f) \cdot \sqrt{4 \cdot k \cdot T \cdot B_1 \cdot |Z_{T1,3}(f)|} \quad |e_{n,Z.T1,3}(h)| = 482.968 \times 10^{-12} V$$

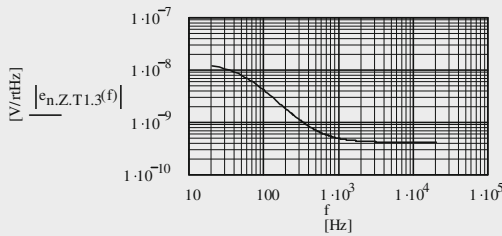


Fig. 5.16  
Frequency response of the noise voltage density of the T1(f)+T3(f) network

6.6.2 Relevant Amp5 data :

$i_{n,i.amp5} := \frac{2.5}{\sqrt{2}} \cdot 10^{-15} A$	average noise voltage in B <sub>20k</sub> :	$e_{n,i.amp5} := 8.103 \cdot 10^{-9} V$
$G_{amp5} := \frac{1 \cdot V}{V_{o.ref}}$		$G_{amp5} = 6.965$
$G_{cm.amp5} := 1.2 \cdot \frac{0.1}{200}$		$G_{cm.amp5} = 1 \times 10^{-3}$
$CMRR_{amp5} := \frac{G_{amp5}}{G_{cm.amp5}}$		$CMRR_{amp5} = 6.965 \times 10^3$
$CMRR_{amp5,e} := 20 \cdot \log(CMRR_{amp5})$		$CMRR_{amp5,e} = 76.859 \quad [dB]$

6.6.3 CMRR of Amp4 :

$G_{cm.amp4} := 1.2 \cdot \frac{0.1}{200}$	$G_{cm.amp4} = 1 \times 10^{-3}$
$CMRR_{amp4} := \frac{G_{amp4}}{G_{cm.amp4}}$	$CMRR_{amp4} = 16.39 \times 10^3$
$CMRR_{amp4,e} := 20 \cdot \log(CMRR_{amp4})$	$CMRR_{amp4,e} = 84.292$

5.1 MCD-WS: The Solid-State Gain Stage Amp4 with RIAA Networks Page 11

6.6.3 Total output noise voltage at the o/p of Amp5 (amp4,5) :

$$e_{n.o.amp4.5}(f) := G_{amp5} \cdot \sqrt{\left[ \left( e_{n.o.2nd}(f) \cdot G_{3rd} \right)^2 + e_{n.o.3rd}(f)^2 \right] \cdot G_{T1.3}(f)^2 \dots + e_{n.Z.T1.3}(f)^2 + i_{n.i.amp5}^2 \cdot Z_{T1.3}(f)^2 + e_{n.i.amp5}^2}$$

$$|e_{n.o.amp4.5}(h)| = 111.555 \times 10^{-9} V$$

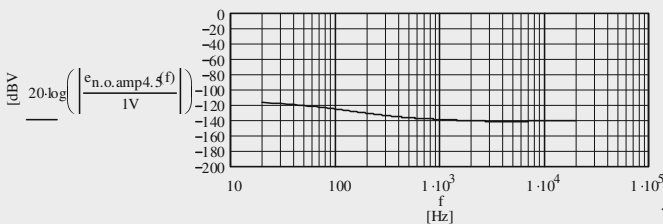
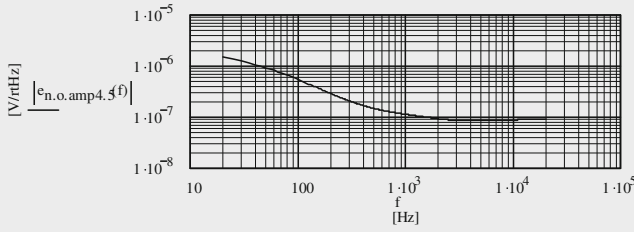


Fig. 5.17a & Fig. 5.17b = Fig. 4.2 Amp4+amp5 output noise voltage density with i/p shorted

$$e_{N.o.amp4.5} := \sqrt{\frac{1}{B_1} \int_{20Hz}^{20000Hz} \left( |e_{n.o.amp4.5}(f)| \right)^2 df}$$

$$e_{N.o.amp4.5} = 15.617 \times 10^{-6} V$$

$$|T_{amp4(h)} \cdot G_{amp5}| = 10$$

$$e_{n.i.amp4.5}(f) := \frac{e_{n.o.amp4.5}(f)}{T_{amp4(h)} \cdot G_{amp5}}$$

$$|e_{n.i.amp4.5}(h)| = 11.156 \times 10^{-9} V$$

6.7 SNs of the sequence of Amp4 + Amp5 :

$$SN_{o.amp4.5} := 20 \cdot \log \left[ \frac{\sqrt{\frac{1}{B_1} \int_{20Hz}^{20000Hz} \left( |e_{n.o.amp4.5}(f)| \right)^2 df}}{1V} \right]$$

$$SN_{o.amp4.5} = -96.128 \quad [dBV]$$

measured: -98.06 dBV

5.1 MCD-WS: The Solid-State Gain Stage Amp4 with RIAA Networks

B(f) = A(f) = A-weighting transfer function

$$B(f) := \frac{1.259}{\left[ 1 + \left( \frac{20.6\text{Hz}}{f} \right)^2 \right] \cdot \sqrt{1 + \left( \frac{107.7\text{Hz}}{f} \right)^2} \cdot \sqrt{1 + \left( \frac{737.9\text{Hz}}{f} \right)^2} \cdot \left[ 1 + \left( \frac{f}{12200\text{Hz}} \right)^2 \right]}$$

$$SN_{a.o.amp4.5} := 20 \cdot \log \left[ \frac{\sqrt{\frac{1}{B_1} \cdot \int_{20\text{Hz}}^{2000\text{Hz}} (|e_{n.o.amp4.5}(f)|)^2 \cdot (|B(f)|)^2 df}}{1V} \right] \quad SN_{a.o.amp4.5} = -99.962 \quad [\text{dBV(A)}]$$

measured: -100.82 dBV(A)

$$SN_{a.i.amp4.5} := 20 \cdot \log \left[ \frac{\sqrt{\frac{1}{B_1} \cdot \int_{20\text{Hz}}^{2000\text{Hz}} (|e_{n.i.amp4.5}(f)|)^2 \cdot (|B(f)|)^2 df}}{v_{i.ref}} \right] \quad SN_{a.i.amp4.5} = -99.962 \quad [\text{dB(A)}]$$

7. Amp4 + Amp5 with i/p loaded by the noise voltage of a preceding MC amp1 with extremely low input noise voltage & current density :

$G_{amp1} := 200$	$R0 := 20\Omega$	$e_{n.i.0} := 0.2 \cdot 10^{-9} V \sqrt{2}$	$i_{n.i.0} := \frac{2.4 \cdot 10^{-12} A}{\sqrt{2}}$
$T := 315K$		$v_{o.ref.mc} := 100 \cdot 10^{-3} V$	$v_{i.ref.mc} := 0.5 \cdot 10^{-3} V$
$e_{n.R0} := \sqrt{4 \cdot k \cdot T \cdot B_1 \cdot R0}$			$e_{n.R0} = 589.851 \times 10^{-12} V$
$e_{n.i.0.eff} := \sqrt{e_{n.i.0}^2 + e_{n.R0}^2 + i_{n.i.0}^2 \cdot R0^2}$			$e_{n.i.0.eff} = 655.039 \times 10^{-12} V$
$e_{n.o.amp1} := G_{amp1} \cdot e_{n.i.0.eff}$			$e_{n.o.amp1} = 131.008 \times 10^{-9} V$
$e_{N.o.amp1} := e_{n.o.amp1} \cdot \sqrt{\frac{B_{20k}}{B_1}}$			$e_{N.o.amp1} = 18.518 \times 10^{-6} V$
$e_{n.o.mc}(f) := \sqrt{e_{n.o.amp1}^2 \cdot ( T_{amp4}(f) )^2 \cdot G_{amp5}^2 + e_{n.o.amp4.5}(f)^2}$			$ e_{n.o.mc}(h)  = 1.312 \times 10^{-6} V$
$e_{n.i.mc}(f) := \frac{e_{n.o.mc}(f)}{G_{amp1} \cdot T_{amp4}(h) \cdot G_{amp5}}$			$ e_{n.i.mc}(h)  = 656.245 \times 10^{-12} V$

5.1 MCD-WS: The Solid-State Gain Stage Amp4 with RIAA Networks Page 13

$$SN_{riaa.o.amp4.5.mc} := 20 \cdot \log \left[ \frac{\sqrt{\frac{1}{B_1} \int_{20Hz}^{2000Hz} (|e_{n.o.mc}(f)|)^2 df}}{1V} \right] \quad SN_{riaa.o.amp4.5.mc} = -78.212 \quad [dB]$$

$$SN_{ariaa.o.amp4.5.mc} := 20 \cdot \log \left[ \frac{\sqrt{\frac{1}{B_1} \int_{20Hz}^{2000Hz} (|e_{n.o.mc}(f)|)^2 \cdot (|B(f)|)^2 df}}{1V} \right] \quad SN_{ariaa.o.amp4.5.mc} = -82.514 \quad [dB(A)]$$

$$SN_{ariaa.i.amp4.5.mc} := 20 \cdot \log \left[ \frac{\sqrt{\frac{1}{B_1} \int_{20Hz}^{2000Hz} (|e_{n.i.mc}(f)|)^2 \cdot (|B(f)|)^2 df}}{V_{i.ref.mc}} \right] \quad SN_{ariaa.i.amp4.5.mc} = -82.514 \quad [dB(A)]$$

8. Preceding MC Amp1 alone and noise calculation up to the o/p of Amp5 :

$$e_{n.o.mc.eff(f)} := e_{n.o.amp1} \cdot T_{amp4(f)} \cdot G_{amp5} \quad |e_{n.o.mc.eff(h)}| = 1.31 \times 10^{-6} V$$

$$e_{n.i.mc.eff(f)} := \frac{e_{n.o.mc.eff(f)}}{T_{amp4(h)} \cdot G_{amp1} \cdot G_{amp5}} \quad |e_{n.i.mc.eff(h)}| = 655.039 \times 10^{-12} V$$

$$SN_{riaa.o.mc} := 20 \cdot \log \left[ \frac{\sqrt{\frac{1}{B_1} \int_{20Hz}^{2000Hz} (|e_{n.o.mc.eff(f)}|)^2 df}}{1V} \right] \quad SN_{riaa.o.mc} = -78.256 \quad [dB]$$

$$SN_{riaa.i.mc} := 20 \cdot \log \left[ \frac{\sqrt{\frac{1}{B_1} \int_{20Hz}^{2000Hz} (|e_{n.i.mc.eff(f)}|)^2 df}}{V_{i.ref.mc}} \right] \quad SN_{riaa.i.mc} = -78.256 \quad [dB]$$

$$SN_{ariaa.o.mc} := 20 \cdot \log \left[ \frac{\sqrt{\frac{1}{B_1} \int_{20Hz}^{2000Hz} (|e_{n.o.mc.eff(f)}|)^2 \cdot (|B(f)|)^2 df}}{1V} \right] \quad SN_{ariaa.o.mc} = -82.582 \quad [dBA]$$

$$SN_{ariaa.i.mc} := 20 \cdot \log \left[ \frac{\sqrt{\frac{1}{B_1} \int_{20Hz}^{2000Hz} (|e_{n.i.mc.eff(f)}|)^2 \cdot (|B(f)|)^2 df}}{V_{i.ref.mc}} \right] \quad SN_{ariaa.i.mc} = -82.582 \quad [dB(A)]$$

5.1 MCD-WS: The Solid-State Gain Stage Amp4 with RIAA Networks

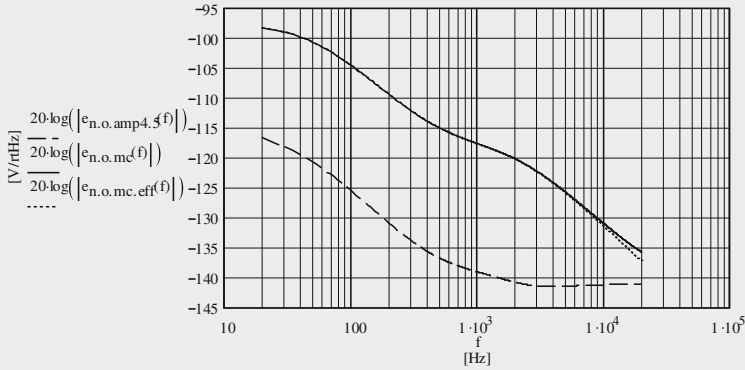


Fig. 5.18 Comparison of the various output noise voltage densities vs. frequency (trace 3 is nearly hidden by trace 2)

$$\text{Dev}_{3_e}(f) := 20 \cdot \log(R_0(f)) - 20 \cdot \log\left(\left|e_{n.o.mc,eff}(f) \cdot e_{n.o.mc,eff}(f)^{-1}\right|\right)$$

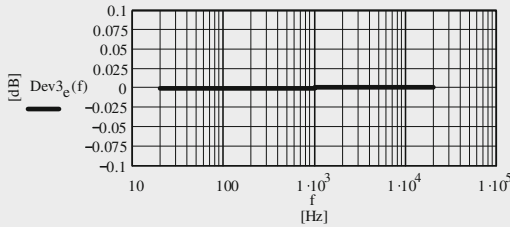


Fig. 5.19 Deviation from the exact RIAA transfer of Amp1+Amp4+Amp5

9. MC Amp1 noise worsening by additional noise from Amp4+Amp5:

$$NF_{e.mc12} := SN_{ariaa.o.amp4.5.mc} - SN_{ariaa.o.mc} \quad NF_{e.mc12} = 0.068 \quad [\text{dB}]$$

10. MM Amp noise worsening by additional noise from Amp4+Amp5:

$$SN_{ariaa.o.mm} := -80.5 \quad [\text{dB(A) ref. } 100\text{mV}_{rms}]$$

$$SN_{ariaa.i.amp4.mm} := 20 \cdot \log\left(\sqrt{10 \frac{SN_{ariaa.o.mm}}{10} + 10 \frac{SN_{a.i.amp4.5}}{10}}\right) \quad SN_{ariaa.i.amp4.mm} = -80.451 \quad [\text{dB(A)}]$$

$$NF_{e.mm} := SN_{ariaa.i.amp4.mm} - SN_{ariaa.o.mm} \quad NF_{e.mm} = 0.049 \quad [\text{dB}]$$

5.1 MCD-WS: The Solid-State Gain Stage Amp4 with RIAA Networks Page 15

11. Amp4 with i/p loaded by the noise voltage of a 1k resistor and via o/p of Amp5:

$$R0 := 1000\Omega \quad T := 315K$$

$$e_{n.R0} := \sqrt{4 \cdot k \cdot T \cdot B1 \cdot R0}$$

$$e_{n.R0} = 4.171 \times 10^{-9} V$$

$$e_{n.o.1k(f)} := \sqrt{e_{n.R0}^2 \cdot (|T_{amp4}(f)|)^2 \cdot G_{amp5}^2 + e_{n.o.amp4.5(f)}^2}$$

$$|e_{n.o.1k}(h)| = 115.796 \times 10^{-9} V$$

$$e_{n.i1k(f)} := \frac{e_{n.o.1k(f)}}{G_{amp5} \cdot T_{amp4}(h)}$$

$$|e_{n.i1k}(h)| = 11.58 \times 10^{-9} V$$

$$SN_{riaa.o.amp4.5.1k} := 20 \cdot \log \left[ \frac{\int_{20Hz}^{20000Hz} \left( \frac{1}{B1} \right) \cdot (|e_{n.o.1k}(f)|)^2 \cdot df}{1V} \right]$$

$$SN_{riaa.o.amp4.5.1k} = -96.042 \quad [dBV]$$

$$SN_{ariaa.o.amp4.5.1k} := 20 \cdot \log \left[ \frac{\int_{20Hz}^{20000Hz} \left( \frac{1}{B1} \right) \cdot (|e_{n.o.1k}(f)|)^2 \cdot (|B(f)|)^2 \cdot df}{1V} \right]$$

$$SN_{ariaa.o.amp4.5.1k} = -99.798 \quad [dBV(A)]$$

$$SN_{ariaa.i.amp4.5.1k} := 20 \cdot \log \left[ \frac{\int_{20Hz}^{20000Hz} \left( \frac{1}{B1} \right) \cdot (|e_{n.i1k}(f)|)^2 \cdot (|B(f)|)^2 \cdot df}{100mV} \right]$$

$$SN_{ariaa.i.amp4.5.1k} = -99.798 \quad [dB(A)]$$

12. Amp4's 100% correlated output noise voltage density at the output leads to ground :

$$e_{n.o3.corr(f)} := \sqrt{e_{n.i2nd(f)}^2 \cdot \left( 1 + 2 \cdot \frac{R61}{RG} \right)^2 + i_{n.i3}^2 \cdot R61^2 + e_{n.R61}^2 + e_{n.RG.o}^2}$$

$$e_{n.o4.corr(f)} := e_{n.o3.corr(f)}$$

$$e_{n.o3.corr}(h) = 55.256 \times 10^{-9} V$$

$$e_{n.o3(f)} := \frac{e_{n.o.2nd(f)}}{\sqrt{2}}$$

$$|e_{n.o3}(h)| = 54.551 \times 10^{-9} V$$

$$e_{n.vo3(f)} := \sqrt{e_{n.o3(f)}^2 + e_{n.o3.corr(f)}^2}$$

$$|e_{n.vo3}(h)| = 76.579 \times 10^{-9} V$$

5.1 MCD-WS: The Solid-State Gain Stage Amp4 with RIAA Networks Page 16

$$e_{N.o3.corr} := \sqrt{\frac{1}{B_1} \cdot \int_{20\text{Hz}}^{2000\text{Hz}} (|e_{n.o3.corr}(f)|)^2 df} \quad e_{N.o3.corr} = 7.731 \times 10^{-6} \text{V}$$

$$e_{N.o3} := \sqrt{\frac{1}{B_1} \cdot \int_{20\text{Hz}}^{2000\text{Hz}} (|e_{n.o3}(f)|)^2 df} \quad e_{N.o3} = 5.637 \times 10^{-6} \text{V}$$

$$e_{N.vo3} := \sqrt{\frac{1}{B_1} \cdot \int_{20\text{Hz}}^{2000\text{Hz}} (|e_{n.vo3}(f)|)^2 df} \quad e_{N.vo3} = 9.539 \times 10^{-6} \text{V}$$

$$e_{N.o.2nd} := \sqrt{\frac{1}{B_1} \cdot \int_{20\text{Hz}}^{2000\text{Hz}} (|e_{n.o.2nd}(f)|)^2 df} \quad e_{N.o.2nd} = 7.972 \times 10^{-6} \text{V}$$

$$SN_{o3.corr} := 20 \cdot \log \left[ \frac{\sqrt{\frac{1}{B_1} \cdot \int_{20\text{Hz}}^{2000\text{Hz}} (|e_{n.vo3}(f)|)^2 df}}{0.5\text{V}} \right] \quad SN_{o3.corr} = -94.39 \quad [\text{dB}]$$

$$SN_{o.2nd} := 20 \cdot \log \left[ \frac{\sqrt{\frac{1}{B_1} \cdot \int_{20\text{Hz}}^{2000\text{Hz}} (|e_{n.o.2nd}(f)|)^2 df}}{0.5\text{V}} \right] \quad SN_{o.2nd} = -95.948 \quad [\text{dB}]$$

$$SN_{o4.corr} := SN_{o3.corr} \quad SN_{o.2nd} - SN_{o3.corr} = -1.558 \quad [\text{dB}]$$

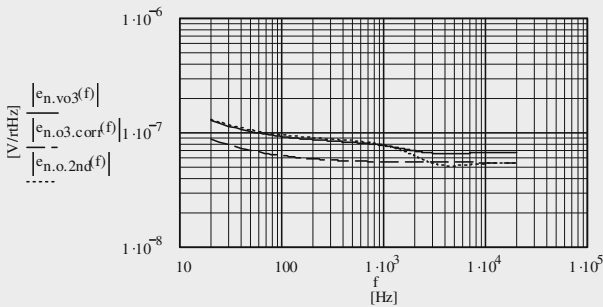


Fig. 5.20  
Noise voltage densities  
at the output of the 2nd  
gain stage



## 6.1 General Design and Gain of Amp5

With the T1 & T3 RIAA network included, the Amp5 gain stage must lift the output level of Amps 3 or 4 to a nominal output level of 0 dBu or 0 dBV or +6 dBu at 1 kHz, depending on ones own needs. Hence, we set on a nominal 0 dBV/1 kHz based gain of 6.25 here. In addition, this gain stage should be capable to drive a 1:1 output transformer. Generally, the overload margin should not be lost out of sight. However, it becomes less dramatic: with the +20 dB goal at the input we would get  $10V_{\text{rms}}$  at the output, which is much smaller than the maximal possible  $17.2V_{\text{rms}}$ .

Figures 6.1 and 6.2 show the solution. It follows the basic design of Amp4 with only one further gain stage to get an un-balanced output via OP5. This stage produces the same output level, but less good overload margin. P1 sets the gain of Amp5. Of course, to get higher gains R3 could be chosen smaller. The gain  $G_{\text{amp5}}$  of such an amplifying stage becomes:

$$\begin{aligned}
 G_{\text{amp5}} &= G_{1\text{st}}G_{2\text{nd}} \\
 &= \left(1 + \frac{R4 + R5}{RG}\right) \left(\frac{R10}{R6} + \frac{R13}{R9}\right) \\
 RG &= P1 + R3
 \end{aligned}
 \tag{6.1}$$

With equal valued resistors R6–R13 the gain  $G_{2\text{nd}}$  of the output stage (OPs 3 & 4) becomes 2. Thus, for a given  $G_{\text{amp5}}$  we obtain RG as follows:

$$RG = \frac{R4 + R5}{0.5G_{\text{amp5}} - 1}
 \tag{6.2}$$

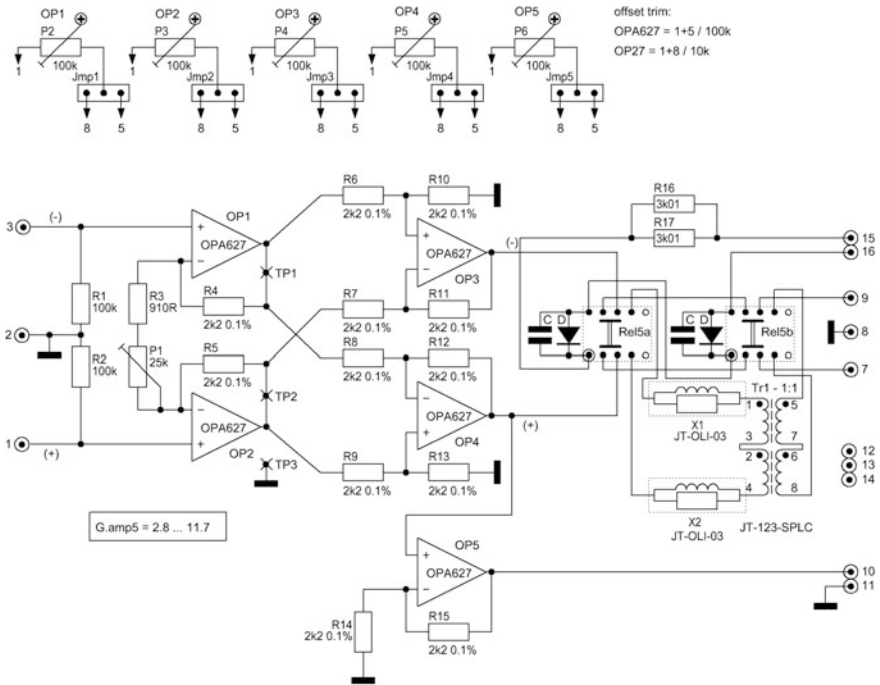


**Fig. 6.1** Circuit of the engine’s output gain stage Amp5, also showing additional offset trim variants

Hence, with  $G_{amp5} = 6.25$  P1 becomes:

$$\begin{aligned}
 P1 &= RG - R3 \\
 &= 1161 \Omega
 \end{aligned}
 \tag{6.3}$$

The transformer circuit follows the recommendations of Jensen Transformers Inc. Fortunately, switching the transformer in and out of the signal path does not lead to different signal levels. It also does not lower (or lift up) the overall frequency and phase response at the edges of  $B_{20k}$ .

On the Mainboard there are three female strip connectors for Amps 1 and 2 and 5. Figure 6.2 shows the connections to the Mainboard and to the plug-in PCBs.

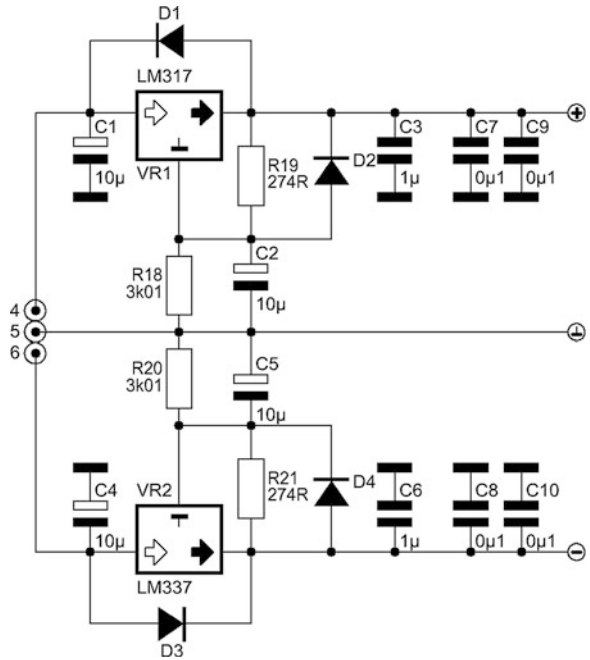
## 6.2 Power Supply

Each of the various solid-state gain stages has its own power supply, on plug-in PCBs (Amps 1, 2, and 5) as well as on the Mainboard (Amp4). Figure 6.3 shows the circuit. Because of tolerances of the IC reference voltages R18 and R20 may need additional trimming to get a rather exact  $\pm 15$  V output.

**Fig. 6.2** Plug-in connections between PCBs of Amps1, 2, 5 and the mainboard of Fig. 1.17

- 1 ● (+) bal in
  - 2 ● in gnd
  - 3 ● (-) bal in
  - 4 ● ← ⊕
  - 5 ● 0V psu
  - 6 ● ← ⊖
  - 7 ● (+) bal out
  - 8 ● out gnd
  - 9 ● (-) bal out
  - 10 ● (+) un-bal out
  - 11 ● out gnd
  - 12 ● (-) un-bal out
  - 13 ● ⊕
  - 14 ● ⊖
  - 15 ● ⊕
  - 16 ● ⊖
- +/- 21V amps

**Fig. 6.3** Solid-state gain stage ±15 V PSU



## 6.3 CMRR and Noise

### 6.3.1 CMRR

The CMRR reflections follow the remarks I've already made about Amp4, hence, with its nominal gain  $G_{amp5} = 6.25$   $CMRR_e$  of Amp5 becomes appr. 76 dB as follows:

$$CMRR_{amp5} = \frac{G_{amp5}}{G_{amp5.cm}} \quad (6.4)$$

$$\begin{aligned} G_{amp5.cm} &= 2 \frac{\text{tolerance}[\%]}{200\%} \\ &= \frac{2 * 0.1}{200} \\ &= 0.001 \end{aligned} \quad (6.5)$$

$$\begin{aligned} CMRR_{amp5} &= \frac{6.25}{0.001} \\ &= 6250 \end{aligned} \quad (6.6)$$

$$\begin{aligned} CMRR_{amp5.e} &= 20 \log(CMRR_{amp5}) \\ &= 75.92 \text{ dB} \end{aligned} \quad (6.7)$$

Concerning the Amp5 generated common mode noise voltage  $CM_{amp5}$  at the output of its solid-state section we have the same situation already described in Sect. 4.3.6. That's why it is important to have a well designed following gain stage with a CMRR that is capable to damp  $CM_{amp5}$  to an ignorable amount. The output transformer switched into the signal path produces a big additional  $CMRR_e$  portion >60 dB. In this context, a transformer is the most effective component.

The next chapter's Mathcad Worksheet gives the details on Amp5's CM noise voltage production.

### 6.3.2 Noise and SNs

The Mathcad Worksheet 7.1's noise and SN calculations follow Figs. 6.4 and 6.5 and the calculation course already described for Amp4. However, I'll repeat the main issues. Additionally, Fig. 6.6 shows the noise situation of the un-balanced output via OP5.

With input shorted and  $R4 = R5$ , the frequency dependent output noise voltage density  $e_{n.o.1st}(f)$  of the 1st gain stage with OPs 1 & 2 becomes:

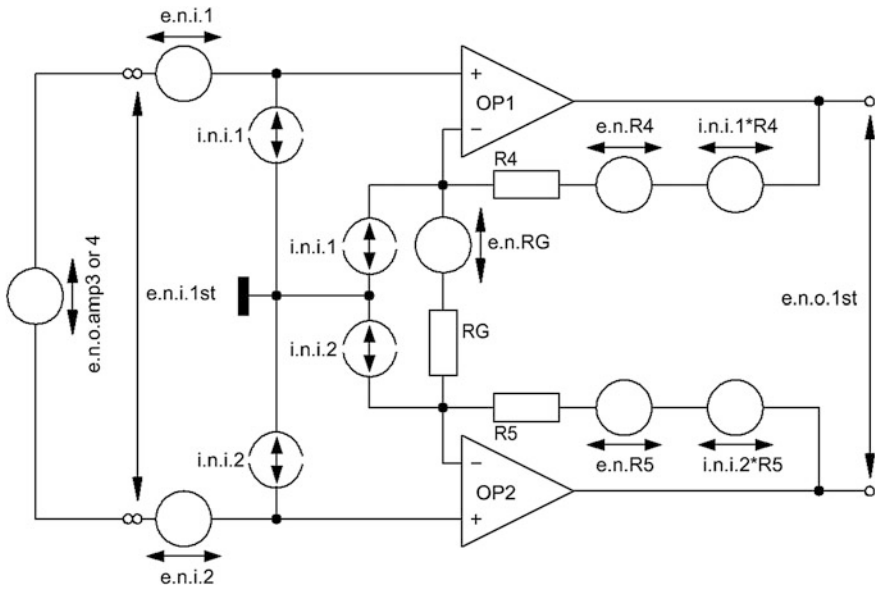


**Fig. 6.4** Noise sources of Amp5's input section (OPs 1 & 2)

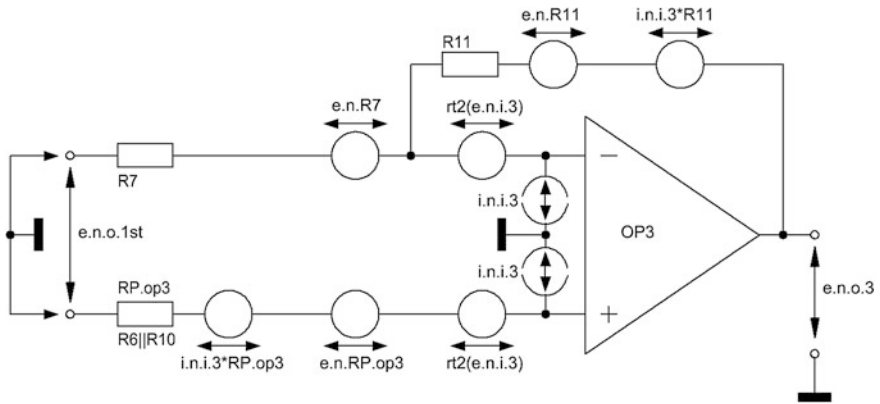


**Fig. 6.5** Noise sources of Amp5's balanced output section (OPs 3 & 4)

$$e_{n.o.1st}(f) = \sqrt{2 e_{n.i.1st}(f)^2 G_{1st}^2 + i_{n.i.1st}^2 (2R4)^2 + 2e_{n.R4}^2 + e_{n.RG.o}^2} \quad (6.8)$$

$$e_{n.RG.o} = e_{n.RG} \frac{2R4}{RG} \quad (6.9)$$

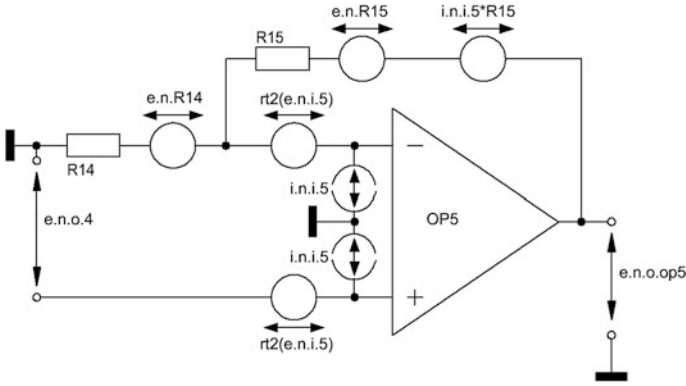


**Fig. 6.6** Noise sources of Amp5's un-balanced output stage (OP5)

With input shorted and R6–R13 with equal values, we obtain the frequency dependent output noise voltage density  $e_{n.o.3}(f)$  at the output of OP3:

$$e_{n.o.3}(f) = \sqrt{2 \left(1 + \frac{R11}{R7}\right) \left( \frac{e_{n.i.2nd}(f)^2}{2} + e_{n.RP.op3}^2 + i_{n.i.2nd}^2 RP_{op3}^2 \right)} \quad (6.10)$$

The same applies for the output noise of OP4,  $e_{n.o.4}(f)$ . Thus, the output noise voltage density of the 2nd gain stage (input shorted) becomes:

$$e_{n.o.2nd}(f) = \sqrt{e_{n.o.3}(f)^2 + e_{n.o.4}(f)^2} \quad (6.11)$$

Hence, Amp5's balanced output noise voltage density  $e_{n.o.amp5,bal}(f)$  looks as follows:

$$e_{n.o.amp5,bal}(f) = \sqrt{(e_{n.o.1st} G_{2nd})^2 + e_{n.o.2nd}(f)^2} \quad (6.12)$$

The noise situation of the un-balanced output looks a bit different.<sup>1</sup> With input shorted,  $RP_{op5} = R14 \parallel R15$ , and  $G_{op5} = 1 + R15/R14$  we obtain  $e_{n.o.5}(f)$ :

$$e_{n.o.5}(f) = G_{op5} \sqrt{e_{n.i.5}(f)^2 + i_{n.i.5}^2 RP_{op5}^2 + e_{n.RP.op5}^2} \quad (6.13)$$

<sup>1</sup>Details see TSOS-1, Sect. 3.5 or TSOS-2, Chap. 8.

We can now formulate the frequency dependent output noise voltage density  $e_{n.o.amp5.unbal}(f)$  at Amp5's un-balanced output, with input of Amp5 shorted:

$$e_{n.o.amp5.unbal}(f) = \sqrt{G_{op5}^2 \left( e_{n.o.1st}(f)^2 + e_{n.o.4}(f)^2 \right) + e_{n.o.5}(f)^2} \quad (6.14)$$

The noise level of Amp5's output stage is very low. The output transformer does not significantly add further noise to the active parts. With input shorted at the balanced output the A-weighted  $SN_{a.o.amp5.bal}$  becomes a measured (calculated)  $-103.50$  dBV(A) ( $-104.01$  dBV(A)) and the un-balanced output offers an  $SN_{a.o.amp5.unbal}$  of  $-102.90$  dBV(A) ( $-103.29$  dBV(A)). With these results we can completely ignore any Amp5 impact on the noise that comes in from the preceding gain stages.

---

## 6.4 Additional Remarks

Concerning THD and IMD Amp5, incl. or excl. output trafo, did not produce additional artefacts that could increase the CLIO generated levels.

A simpler Amp5 configuration would work too, eg OPs 1 & 2 in the typical balanced 2-op-amp configuration, however, without output trafo CMRR would be too low, the one we need here to kill the CM voltage generated by the Amp3 current sink.

## Contents

### 7.1 MCD-WS: The Op-Amp + Transformer Driven Output Stage Amp5

**Note 1:** MCD 11 has no built-in unit “rtHz” or “ $\sqrt{\text{Hz}}$ ”. To get  $\sqrt{1 \text{ Hz}}$  based voltage noise and current noise densities the rms noise voltage and current in a specific frequency range  $B > 1 \text{ Hz}$  must be multiplied by  $\sqrt{1 \text{ Hz}}$  and divided by the root of that specific frequency range  $\sqrt{B}$ !

**Note 2:** MCD 11 offers no “dB” unit. This is available from MCD 13 on!



7.1 MCD-WS: The Op-Amp + Transformer Driven Output Stage Amp5

Calculations of the op-amp driven Amp5:

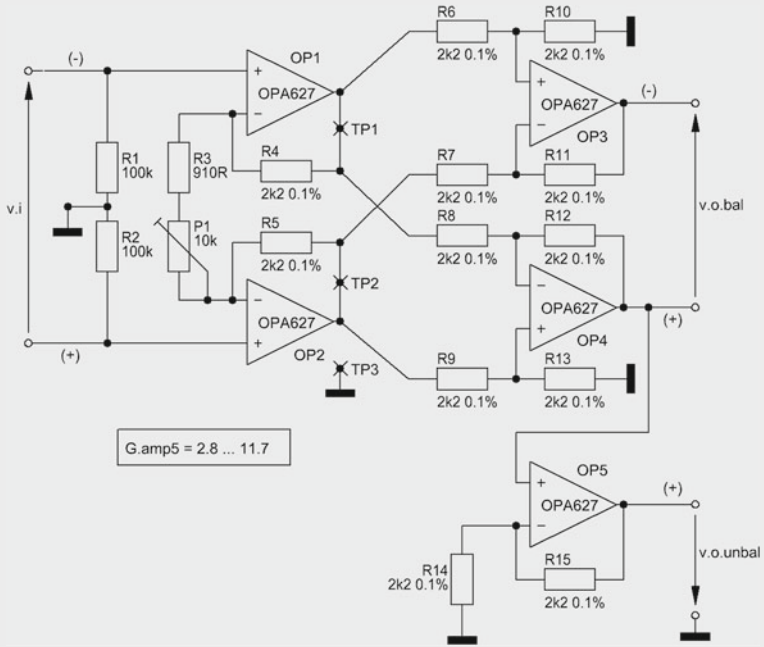


Fig. 7.1 Op-amp driven Amp5 incl. balanced & un-balanced output

1. General data :

$OP1 = OPA627$      $OP2 = OP1$      $OP3 = OPA627$      $OP4 = OP3$      $OP5 = OPA627$   
 $k := 1.38065 \cdot 10^{-23} \text{V} \cdot \text{A} \cdot \text{s} \cdot \text{K}^{-1}$      $T := 300\text{K}$      $B_1 := 1\text{Hz}$      $B_{20k} := 19980\text{Hz}$   
 $f := 20\text{Hz}, 25\text{Hz}, 20000\text{Hz}$      $h := 1000\text{Hz}$

2. Gain stage component data :

$R1 := 100 \cdot 10^3 \Omega$      $R2 := 100 \cdot 10^3 \Omega$      $R3 := 910 \Omega$      $R4 := 2.2 \cdot 10^3 \Omega$      $R5 := R4$   
 $R6 := 2.2 \cdot 10^3 \Omega$      $R7 := R6$      $R8 := R6$      $R9 := R8$      $R10 := R8$      $R11 := R8$   
 $R4 \dots R15: 0.1\%$      $R12 := R8$      $R13 := R8$      $R14 := R8$      $R15 := R8$

## 7.1 MCD-WS: The Op-Amp + Transformer Driven Output Stage Amp5

Page 2

3. Gains and gain setting RG :

## 3.1 Gain setting

$$P1 := 25000 \cdot \Omega$$

$$RG := R3 + P1$$

$$RG = 25.91 \times 10^3 \Omega$$

$$G := \left(1 + \frac{R4 + R5}{RG}\right) \cdot \left(\frac{R10}{R6} + \frac{R12}{R8}\right) \quad v_{i.ref} := 143.572 \cdot 10^{-3} \text{V} \quad G = 2.34$$

Depending on the nominal output voltage the gain  $G_{amp5}$  of the gain stage with OP1 ... OP5 can be trimmed by P1, hence, with  $1V_{rms}$  nominal output voltage and an input voltage of  $143.572mV_{rms}$  we'll obtain:

$$G_{amp5} = G_{1st} \cdot G_{2nd} \quad G_{amp5} := \frac{1.0V}{v_{i.ref}} \quad G_{amp5} = 6.965$$

$$G_{2nd} := 2 \cdot \frac{R10}{R6} \quad G_{2nd} = 2 \quad G_{1st} := \frac{G_{amp5}}{G_{2nd}} \quad G_{1st} = 3.483$$

$$RG := \frac{R4 + R5}{G_{1st} - 1} \quad RG = 1.772 \times 10^3 \Omega \quad P1 := RG - R3 \quad P1 = 862.355 \Omega$$

## 3.2 Actual overall gain of Amp5, bal &amp; un-bal :

$$G_{amp5} := G_{1st} \cdot G_{2nd} \quad G_{amp5} = 6.965$$

4. Noise and SN calculations :

## 4.1 General data :

$$v_{o.ref} := v_{i.ref} \cdot G_{amp5} \quad v_{o.ref} = 1 \text{V}$$

$$RP_{op3} := \left(\frac{1}{R6} + \frac{1}{R10}\right)^{-1} \quad RP_{op3} = 1.1 \times 10^3 \Omega$$

$$RP_{op4} := \left(\frac{1}{R9} + \frac{1}{R13}\right)^{-1} \quad RP_{op4} = 1.1 \times 10^3 \Omega$$

$$RP_{op5} := \left(\frac{1}{R14} + \frac{1}{R15}\right)^{-1} \quad RP_{op5} = 1.1 \times 10^3 \Omega$$

$$e_{n.i.1} := 4.2 \cdot 10^{-9} \text{V} \quad e_{n.i.2} := e_{n.i.1} \quad e_{n.i.3} := 4.2 \cdot 10^{-9} \text{V} \quad e_{n.i.4} := e_{n.i.3} \quad e_{n.i.5} := e_{n.i.3}$$

$$f_c := 40 \text{Hz} \quad e_{n.i.1} \text{ and } e_{n.i.3} \text{ at } 1 \text{MHz and according to the data sheet graphs}$$

$$e_{n.i.1}(f) := e_{n.i.1} \cdot \sqrt{\frac{f_c}{f} + 1} \quad e_{n.i.2}(f) := e_{n.i.1}(f) \quad e_{n.i.3}(f) := e_{n.i.3} \cdot \sqrt{\frac{f_c}{f} + 1} \quad e_{n.i.4}(f) := e_{n.i.3}(f) \quad e_{n.i.5}(f) := e_{n.i.3}(f)$$

7.1 MCD-WS: The Op-Amp + Transformer Driven Output Stage Amp5

$$\begin{aligned}
 i_{n.i.1} &:= 2.5 \cdot 10^{-15} \text{ A} & i_{n.i.2} &:= i_{n.i.1} & i_{n.i.3} &:= 0.05 \cdot 10^{-12} \text{ A} & i_{n.i.4} &:= i_{n.i.3} & i_{n.i.5} &:= i_{n.i.3} \\
 e_{n.i.1st}(f) &:= \sqrt{2} \cdot e_{n.i.1}(f) & e_{n.i.2nd}(f) &:= e_{n.i.3}(f) \\
 i_{n.i.1st} &:= \frac{i_{n.i.1}}{\sqrt{2}} & i_{n.i.2nd} &:= i_{n.i.3}
 \end{aligned}$$

4.2 Situation of the various noise sources :

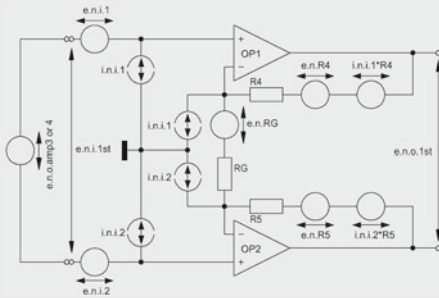


Fig. 7.2 = Fig. 6.4  
Noise voltage and current situation of the 1st gain stage (OP1 & OP2)

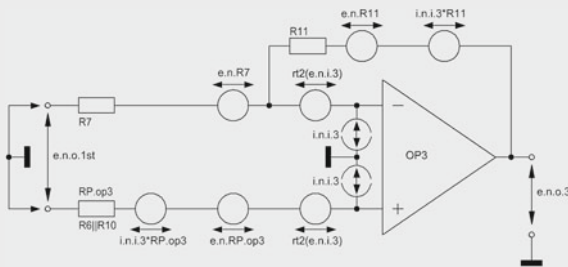


Fig. 7.3 = Fig. 6.5  
Noise voltage and current situation of the 2nd gain stage (OP3 stage & the equivalent OP4 stage)

$$\begin{aligned}
 e_{n.R4} &:= \sqrt{4 \cdot k \cdot T \cdot B_1 \cdot R4} & e_{n.R4} &= 6.037 \times 10^{-9} \text{ V} \\
 e_{n.R5} &:= e_{n.R4} \\
 e_{n.R7} &:= e_{n.R4} \\
 e_{n.R8} &:= e_{n.R4} \\
 e_{n.R11} &:= e_{n.R4} \\
 e_{n.R12} &:= e_{n.R4} \\
 e_{n.RP.op3} &:= \sqrt{4 \cdot k \cdot T \cdot B_1 \cdot RP_{op3}} & e_{n.RP.op3} &= 4.269 \times 10^{-9} \text{ V}
 \end{aligned}$$

7.1 MCD-WS: The Op-Amp + Transformer Driven Output Stage Amp5

$$e_{n.RP.op4} := \sqrt{4 \cdot k \cdot T \cdot B_1 \cdot RP_{op4}} \quad e_{n.RP.op4} = 4.269 \times 10^{-9} \text{ V}$$

$$e_{n.RP.op5} := \sqrt{4 \cdot k \cdot T \cdot B_1 \cdot RP_{op5}} \quad e_{n.RP.op5} = 4.269 \times 10^{-9} \text{ V}$$

4.3 Output noise voltage of Amp5 with i/p shorted :

At the bal o/p of the 1st gain stage (OPs 1 & 2 with i/p shorted) we'll get the balanced noise voltage density:

$$e_{n.RG} := \sqrt{4 \cdot k \cdot T \cdot B_1 \cdot RG} \quad e_{n.RG} = 5.419 \times 10^{-9} \text{ V}$$

$$e_{n.RG.o} := e_{n.RG} \cdot \frac{R4 + R5}{RG} \quad e_{n.RG.o} = 13.453 \times 10^{-9} \text{ V}$$

$$e_{n.o.1st}(f) := \sqrt{e_{n.i.1st}(f)^2 \cdot G_{1st}^2 + i_{n.i.1}^2 \cdot (R4 + R5)^2 + e_{n.R4}^2 + e_{n.R5}^2 + e_{n.RG.o}^2}$$

$$e_{n.o.1st}(h) = 26.436 \times 10^{-9} \text{ V}$$

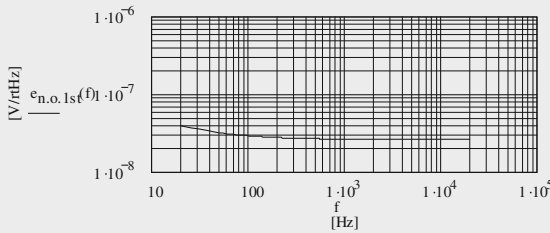


Fig. 7.4  
Bode plot of the balanced o/p noise voltage density of the 1st gain stage

At the bal o/p of the 2nd stage (OPs 3 & 4 with inputs of the 2nd gain stage shorted!) we'll get the un-correlated output noise density as follows:

$$e_{n.o.3}(f) := \sqrt{2 \cdot \left(1 + \frac{R11}{R7}\right)^2 \cdot \left(\frac{e_{n.i.2nd}(f)^2}{2} + e_{n.RP.op3}^2 + i_{n.i.2nd}^2 \cdot RP_{op3}^2\right)} \quad e_{n.o.3}(h) = 14.806 \times 10^{-9} \text{ V}$$

$$e_{n.o.4}(f) := e_{n.o.3}(f)$$

$$e_{n.o.2nd}(f) := \sqrt{e_{n.o.3}(f)^2 + e_{n.o.4}(f)^2} \quad e_{n.o.2nd}(h) = 20.938 \times 10^{-9} \text{ V}$$

$$SN_{ne.o.2nd} := 20 \cdot \log \left[ \frac{\sqrt{\left[ \frac{1}{B_1} \cdot \int_{20\text{Hz}}^{2000\text{Hz}} \left( |e_{n.o.2nd}(f)| \right)^2 df \right]}}{1\text{V}} \right]$$

$$SN_{ne.o.2nd} = -110.612 \text{ [dBV]}$$

$$\text{measured: } -110.1 \text{ [dBV]}$$

7.1 MCD-WS: The Op-Amp + Transformer Driven Output Stage Amp5

At the un-bal o/p of the 2nd stage (OP5 with inputs of the 2nd gain stage shorted!) we'll get the un-correlated output noise voltage density as follows:

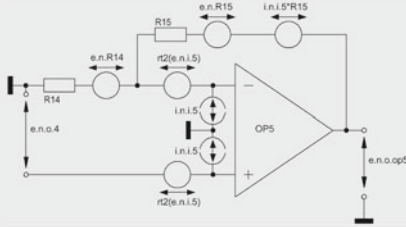


Fig. 7.5 = Fig. 6.6  
Noise voltage and current situation of the un-balanced output gain stage (OP5)

$$G_{op5} := 1 + \frac{R15}{R14}$$

$$G_{op5} = 2$$

$$e_{n.o.5}(f) := G_{op5} \cdot \sqrt{e_{n.i.5}(f)^2 + i_{n.i.5}^2 \cdot R_{P_{op5}}^2 + e_{n.RP.op5}^2}$$

$$e_{n.o.5}(h) = 12.095 \times 10^{-9} \text{ V}$$

Thus, the total o/p noise voltage density at the bal o/p becomes:

$$e_{n.o.amp5.baf}(f) := \sqrt{(e_{n.o.1st}(f) \cdot G_{2nd})^2 + e_{n.o.2nd}(f)^2}$$

$$e_{n.o.amp5.baf}(h) = 56.867 \times 10^{-9} \text{ V}$$

$$e_{n.i.amp5.baf}(f) := \frac{e_{n.o.amp5.baf}(f)}{|G_{amp5}|}$$

$$e_{n.i.amp5.baf}(h) = 8.165 \times 10^{-9} \text{ V}$$

$$\frac{\sqrt{\frac{1}{B_{20k}} \int_{20\text{Hz}}^{20000\text{Hz}} (e_{n.o.amp5.baf}(f))^2 df}}{|G_{amp5}|} = 8.103 \times 10^{-9} \text{ V}$$

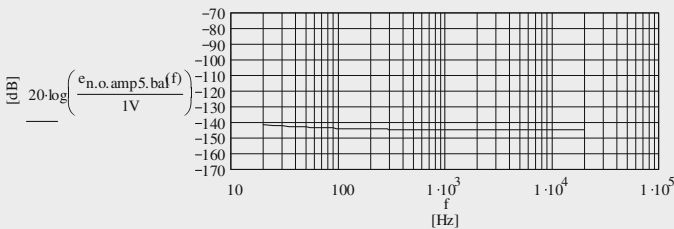


Fig. 7.6 Amp5 output noise voltage density with i/p shorted

7.1 MCD-WS: The Op-Amp + Transformer Driven Output Stage Amp5

Hence, the total o/p noise voltage density at the un-bal o/p becomes:

$$e_{n.o.op5}(f) := \sqrt{G_{Op5}^2 \cdot (e_{n.o.1st}(f)^2 + e_{n.o.4}(f)^2) + e_{n.o.5}(f)^2} \quad e_{n.o.op5}(h) = 61.795 \times 10^{-9} V$$

$$e_{n.o.amp5.unbal}(f) := e_{n.o.op5}(f)$$

4.4 SNs :

$$SN_{ne.o.amp5.bal} := 20 \cdot \log \left[ \frac{\sqrt{\frac{1}{B_1} \cdot \int_{20Hz}^{20000Hz} (|e_{n.o.amp5.bal}(f)|)^2 df}}{V_{o.ref}} \right] \quad SN_{ne.o.amp5.bal} = -101.963 \quad [dBV]$$

measured: -101.80 [dBV]

$$SN_{ne.i.amp5.bal} := 20 \cdot \log \left[ \frac{\sqrt{\frac{1}{B_1} \cdot \int_{20Hz}^{20000Hz} [ (|e_{n.i.amp5.bal}(f)|)^2 ] df}}{V_{i.ref}} \right] \quad SN_{ne.i.amp5.bal} = -101.963 \quad [dB]$$

$$SN_{ne.o.amp5.unbal} := 20 \cdot \log \left[ \frac{\sqrt{\frac{1}{B_1} \cdot \int_{20Hz}^{20000Hz} (|e_{n.o.amp5.unbal}(f)|)^2 df}}{V_{o.ref}} \right] \quad SN_{ne.o.amp5.unbal} = -101.237 \quad [dBV]$$

measured: -101.40 [dBV]

B(f) = A(f) = A – weighting transferfunction

$$B(f) := \frac{1.259}{\left[ 1 + \left( \frac{20.6Hz}{f} \right)^2 \right] \cdot \sqrt{1 + \left( \frac{107.7Hz}{f} \right)^2} \cdot \sqrt{1 + \left( \frac{737.9Hz}{f} \right)^2} \cdot \left[ 1 + \left( \frac{f}{12200Hz} \right)^2 \right]}$$

$$SN_{a.o.amp5.bal} := 20 \cdot \log \left[ \frac{\sqrt{\frac{1}{B_1} \cdot \int_{20Hz}^{20000Hz} (|e_{n.o.amp5.bal}(f)|)^2 \cdot (|B(f)|)^2 df}}{V_{o.ref}} \right] \quad SN_{a.o.amp5.bal} = -104.014 \quad [dBV(A)]$$

measured: -103.50 [dBV(A)]

7.1 MCD-WS: The Op-Amp + Transformer Driven Output Stage Amp5

$$SN_{a.i.amp5.bal} := 20 \cdot \log \left[ \frac{\int_{20\text{Hz}}^{20000\text{Hz}} \left( |e_{n.i.amp5.bal}(f)| \right)^2 \cdot (|B(f)|)^2 df}{v_{i.ref}} \right]$$

$SN_{a.i.amp5.bal} = -104.014 \quad [\text{dB(A)}]$

$$SN_{a.o.amp5.unbal} := 20 \cdot \log \left[ \frac{\int_{20\text{Hz}}^{20000\text{Hz}} \left( |e_{n.o.amp5.unbal}(f)| \right)^2 \cdot (|B(f)|)^2 df}{v_{o.ref}} \right]$$

$SN_{a.o.amp5.unbal} = -103.288 \quad [\text{dBV(A)}]$

measured:  $-102.90 \quad [\text{dBV(A)}]$

5. Amp3 & 4 noise worsening by additional noise from Amp5, i/p loaded with 20Ω :

$SN_{ariaa.o.mc} := -82.9 \quad [\text{dB}]$

$$SN_{ariaa.tot.mc} := 20 \cdot \log \left( \sqrt{10 \frac{SN_{a.i.amp5.bal}}{10} + 10 \frac{SN_{ariaa.o.mc}}{10}} \right)$$

$SN_{ariaa.tot.mc} = -82.867 \quad [\text{dBV(A)}]$

$W_{e.mc} := SN_{ariaa.tot.mc} - SN_{ariaa.o.mc}$

$W_{e.mc} = 0.033 \quad [\text{dB}]$

## 7.1 MCD-WS: The Op-Amp + Transformer Driven Output Stage Amp5

Page 8

6. Amp3 & 4 noise worsening by additional noise from Amp5, i/p loaded with ampMM and Standard cartridge :

$$SN_{ariaa.o.mm} := -80.5 \quad [\text{dB}]$$

$$SN_{ariaa.tot.mm} := 20 \cdot \log \left( \sqrt{10 \frac{SN_{a.i.amp5.bal}}{10} + 10 \frac{SN_{ariaa.o.mm}}{10}} \right) \quad SN_{ariaa.tot.mm} = -80.481 \quad [\text{dBV(A)}]$$

$$W_{e.mm} := SN_{ariaa.tot.mm} - SN_{ariaa.o.mm}$$

$$W_{e.mm} = p_0 \quad [\text{dB}]$$



## 8.1 General Design and Gain of Amp1

In the past, in order to get the required output level, I found very good sounding results in putting together an input transformer followed by an active gain stage.<sup>1</sup> However, these solutions always happened in the single ended world with balanced or un-balanced inputs. For frequency and phase response accuracy, the transformers I used became “handicapped” by the need to load them with an additional R-C network.

To ensure less complexity and for the Engine II purposes I was in search of an excellent 1:10 (nominal) input transformer that allows switching between various MC cartridge loads, eg 1 k $\Omega$ , 500  $\Omega$ , 200  $\Omega$ , 100  $\Omega$ , 50  $\Omega$ , hence, without inclusion of any kind of frequency and phase response flattening additional R-C network.<sup>2</sup>

I found a real good one, the Lundahl LL9226. Its coils offer outstanding low DC resistances too, thus, the generated noise<sup>3</sup> becomes extremely low. There are small disadvantages that come from the measured frequency and phase responses in B<sub>20k</sub> and from the measured turns ratios:

- Depending on Fig. 8.1’s setting of S1–S4 we find—with 0.5 mV input and/or 5 mV output level—at 20 Hz a deviation from a flat frequency and phase response of  $-0.3$  to  $-0.5$  dB/ $+13^\circ$  to  $+18^\circ$ ,<sup>4</sup> measured with the Fig. 8.1 circuit. Lundahl claims  $-1.5$  dB max./10 Hz at  $-10$  dBu output level/100 k $\Omega$  output load. Figure 8.6 shows what I’ve measured with transformer input (output) voltages of 0.5 mV<sub>rms</sub> (5.5 mV<sub>rms</sub>), 1.58 mV<sub>rms</sub> (17.38 mV<sub>rms</sub>), and 5 mV<sub>rms</sub> (55 mV<sub>rms</sub>) and 100 k $\Omega$  transformer output load.

<sup>1</sup>See TSOS-1 Chaps. 6 and 16, TSOS-2 Chaps. 5 and 28.

<sup>2</sup>See Sect. 8.3 for corresponding graphs.

<sup>3</sup>More on transformer noise calculations: TSOS-1 Sect. 3.7, TSOS-2 Chap. 10.

<sup>4</sup>See Sect. 8.3, Table 8.1.

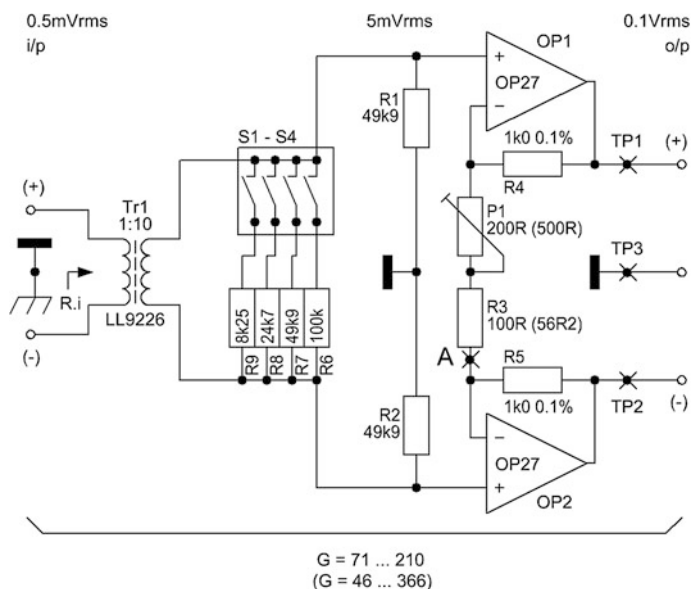


**Fig. 8.1** Input gain stage alternative Amp1

- I've measured 4 transformers: the first pair offers equal turns ratios, however, 11.00 instead of nominal 10, the second pair offers turns ratios with a tiny difference: 11.19 and 11.22. The measurement set-up looks like Fig. 8.1, however, with an interruption at point 'A'. Thus, the signal voltage at the circuit's output vs. the signal voltage at the transformer's input gives the turns ratio, here at 1 kHz and a transformer load of nearly 100 k $\Omega$  (99.8 k $\Omega$ ).

The calculation results of the two Mathcad Worksheets of Chap. 9 don't look rather close. However, the described disadvantages could be tolerated, as long as the listening tests of Chap. 12 won't create any negative indications. Without op-amp offset trim potentiometers and blocking Cs Fig. 8.1 shows all the details of the chosen circuit.

Formed by two OP27 op-amps a rather simple looking balanced stage follows the transformer. I've also tried LT1028 op-amps, however, with an input load of 20  $\Omega$  the improvement in SN became 0.8 dB measured. Although offering very low input noise voltage (0.95nV/rtHz) the rather high input noise current (1pA/rtHz) plus the 100 % correlated noise current as result of unequal loads at the op-amp's " + " and " - " inputs<sup>5</sup> does not create very much better RIAA- and A-weighted results, calculated and measured 0.8 dB(A) too.

<sup>5</sup>See Linear Technology LT1028 data sheet.

To get the above-mentioned different input resistances the resistors R6–R9 of the transformer's output load  $(R1 + R2) \parallel (R6–R9)$  can easily be set by the switch bank S1–S4. Division by the turns ratio squared leads to the effective MC cartridge load and Amp1 input resistances. Trimming of P1 sets the required gain. However, I must point out that the before mentioned actual transformer turns ratios of appr. 11 may lead to a recalculation of the R6–R9 values to get the required input resistances.

The gain  $G_{2nd}$  of such a balanced stage (=2nd gain stage of Amp1) becomes:

$$G_{2nd} = 1 + \frac{R4 + R5}{R3 + P1} \quad (8.1)$$

The gain  $G_{1st}$  of the transformer (=1st gain stage of Amp1) is mainly<sup>6</sup> set by its turns ratio  $tr = 1:n = 1:10$ . Hence, we can set:

$$G_{1st} = n = \text{nominal } 10 \quad (8.2)$$

Thus, with  $R4 = R5$  and  $RG = R3 + P1$  we obtain the Amp1 overall gain  $G_{amp1}$  as follows:

$$\begin{aligned} G_{amp1} &= G_{1st}G_{2nd} \\ &= 10 \left( 1 + \frac{2R4}{RG} \right) \end{aligned} \quad (8.3)$$

---

## 8.2 CMRR and Noise

### 8.2.1 CMRR

Because of the fact that the central amps Amp 3 and 4 offer very good CMRR this point is not a big issue for the input stages. Lundahl gives no data sheet indication, neither about the transformer's CMRR nor about its capacitances that influence CMRR most. Depending on the generator output resistance, normally very good input transformers show  $CMRR_e$  values better than 60 dB. I did not measure it, but I guess, theoretically with the op-amp stage's  $CMRR_{e,2nd} = 26$  dB the amp's  $CMRR_{e,amp1}$  becomes always >86 dB.

Concerning the common mode noise voltage  $CM_{amp1}$  generated by Amp1 we have the same situation already described in Sect. 4.3.6. That's why it is important to

---

<sup>6</sup>Mainly, because there is a gain loss  $G_{loss}$  coming from the voltage divider effect between input load resistance  $R0$  and the impedance  $Z_i$ , formed by the Amp1 input resistance (see the details in the next chapter's MCD Worksheets).

have a well designed following gain stage with a CMRR that is capable to damp  $CM_{amp1}$  to an ignorable amount. The next chapter's Mathcad Worksheet 9.1 /Point 8. gives the details.

### 8.2.2 Noise and SNs

With  $20 \Omega$  ( $43 \Omega$  for my DL-103 cartridge) input load and in consideration of the RIAA transfer, A-weighting, and the following gain stages, the outstanding input referred  $SN_{ariaa.i}$  becomes measured  $-81.8 \text{ dB(A)}$  ( $-79.3 \text{ dB(A)}$ ) and calculated  $-80.9 \text{ dB(A)}$  ( $-78.6 \text{ dB(A)}$ ).

The calculation process for the Amp1 output noise voltage density and its SNs is given in full detail in the next chapter's MCD-WS 9.1 and 9.2. In Chap. 9, I present two different worksheets because, after RIAA equalization and A-weighting, there is a considerable difference in the calculation results with real transformer data (MCD-WS 9.1) and with data from the data sheet (MCD-WS 9.2). However, I'll repeat the main equations as follows with Fig. 8.2 showing the circuit with all relevant noise sources in place and Fig. 8.3 gives the details about the input load  $Z_i$ .

$R_s$  in Fig. 8.3 is the transformer's secondary coil resistance,  $R_{p_{sec}}$  is its primary coil resistance transferred to the secondary side, and  $R_{0_{sec}}$  is the input load transferred to the secondary side too.

Amp1's frequency and  $R_0$  dependent output noise voltage density  $e_{n.o.amp1}(f, R_0)$  thus becomes:

$$e_{n.o.amp1}(f, R_0) = \sqrt{(e_{n.o.tr1}(f, R_0)^2 + e_{n.i.2nd}(f)^2)} G_{2nd}^2 \tag{8.4}$$

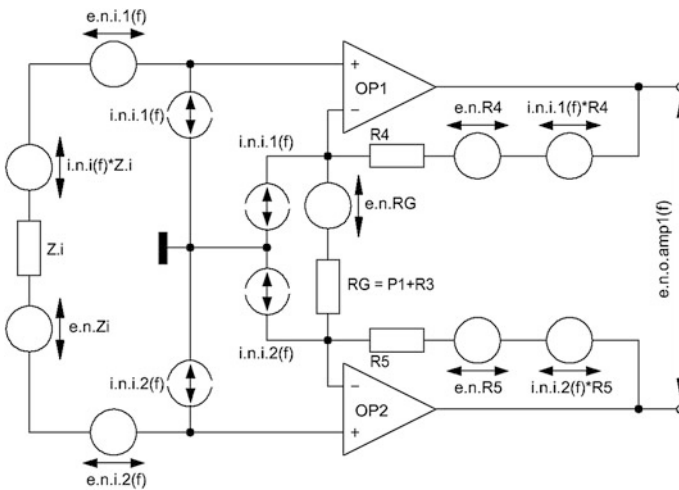
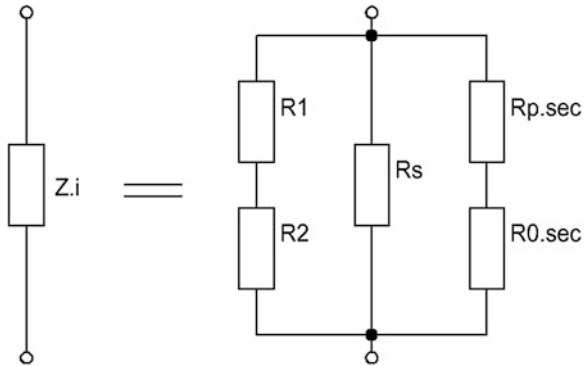


Fig. 8.2 Noise sources of Amp1

**Fig. 8.3** Components of the Fig. 8.2 input load impedance  $Z_i$



$$e_{n.o.tr1}(f) = \sqrt{e_{n.Zi}(R_0)^2 + i_{n,i}(f)^2 Z_i (R_0)^2} \tag{8.5}$$

$$e_{n.i.2nd}(f) = \frac{\sqrt{e_{n,i}(f)^2 G_{2nd}^2 + 2(e_{n,R4}^2 + i_{n,i.1}(f)^2 R_4^2) + e_{n,RG.o}^2}}{G_{2nd}} \tag{8.6}$$

$$e_{n,RG.o} = (G_{2nd} - 1) \sqrt{4kTB_1 (R_3 + P_1)} \tag{8.7}$$

Both Chap. 9 worksheets calculate the relevant SNs and Noise Figures NF in an input load dependent format. Figures 9.6, 9.7, 9.8 and 9.15 are the relevant graphs with the  $R_0$  dependent curves.

### 8.3 Measurement Results

The following graphs (Figs. 8.4 and 8.5) and tables show the Amp1 frequency and phase responses, measured with various input resistances (nominal: 1 k $\Omega$ , 500  $\Omega$ , 250  $\Omega$ , 125  $\Omega$ , 50  $\Omega$  and actual: 800  $\Omega$ , 400  $\Omega$ , 200  $\Omega$ , 100  $\Omega$ , 40  $\Omega$ ) and a generator output resistance of 10.8  $\Omega$ . The corresponding data are summed-up in Table 8.1. The phase results are corrected by the phase response of the used un-bal. to bal. converter UBC<sup>7</sup>: at 20 Hz: -0.05°, at 1 kHz: -0.07°, at 20 kHz: +1.42°.

Due to voltage divider effects at the 2nd stage's input the frequency responses show decreasing Amp1 output levels, exactly according to the input resistance. The differences (in [dB]) between the top frequency response (with highest  $R_i$ ) and the others indicate an SN reduction by roughly the same amount, because the 2nd gain stage must adequately increase its gain to reach Amp1's original gain of 200.

<sup>7</sup>Details see Sect. 15.2.

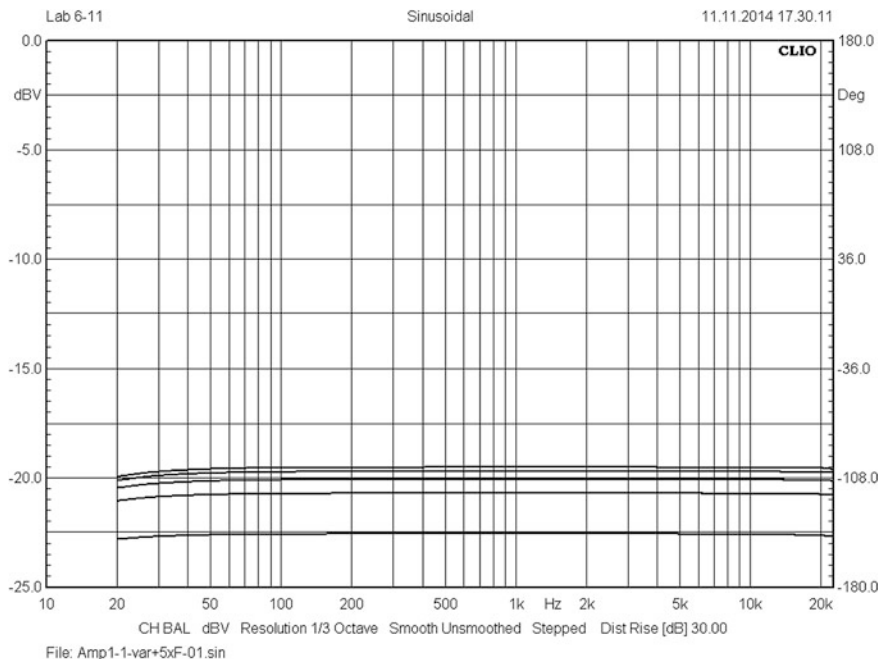


**Fig. 8.4** Frequency responses of Amp1, based on five different Amp1 input resistances  $R_i$ (=S1–S4 settings)

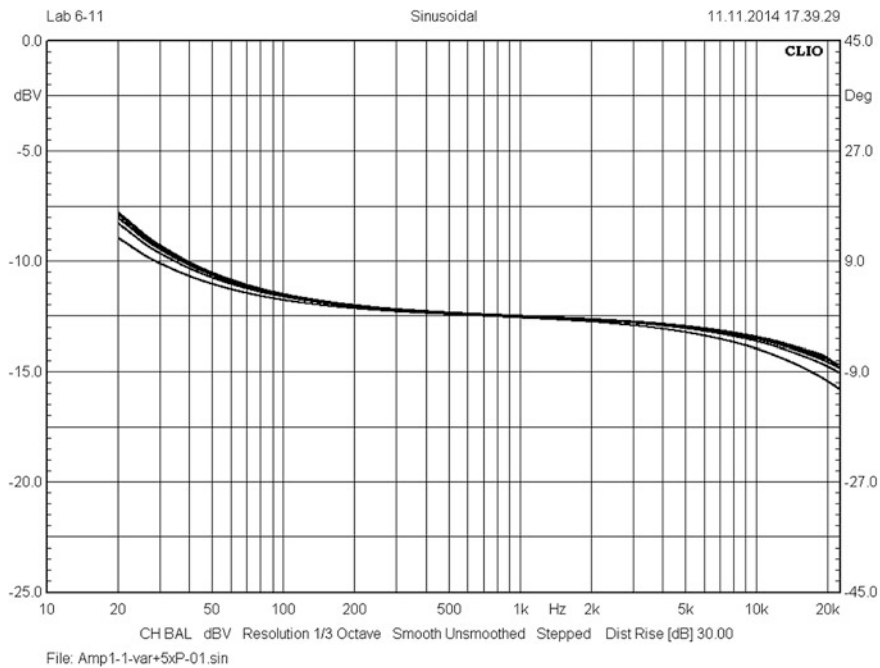


**Fig. 8.5** Phase responses of Amp1, based on five Amp1 input resistances  $R_i$ (=S1–S4 settings)

**Table 8.1** Detailed frequency and phase measurement results of Amp1, based on five Amp1 input resistances  $R_i$ (= S1–S4 settings)

1/A	B	C	D	E	F	G	H	I	J	K	L
2	$R_i$ [ $\Omega$ ] → nominal (actual)	1000 (800)		500 (400)		250 (200)		125 (100)		50 (40)	
3	f [Hz] ↓	o/p [dBV]	$\phi$ [°]	o/p [dBV]	$\phi$ [°]	o/p [dBV]	$\phi$ [°]	o/p [dBV]	$\phi$ [°]	o/p [dBV]	$\phi$ [°]
3	20	-20,062	17,89	-20,241	17,61	-20,526	17,10	-21,119	16,11	-22,872	13,57
4	1k	-19,598	-0,03	-19,792	-0,05	-20,101	-0,08	-20,742	-0,15	-22,602	-0,33
5	20k	-19,633	-5,26	-19,830	-5,59	-20,143	-6,02	-20,793	-6,78	-22,681	-9,21
6											
7	Delta o/p : 20Hz vs. 1kHz [dB]										
8	0,464		0,449		0,425		0,377		0,270		
9	Delta o/p : 20kHz vs. 1kHz [dB]										
10	0,035		0,038		0,042		0,051		0,079		
11											
12	Delta $\phi$ : 20Hz vs. 20kHz [°]										
13	23,15		23,20		23,12		22,89		22,78		
14											
16	nominal:	tr = 10		Rp = 5R		Rs = 260R					
17											
18	actual:	tr = 11.22		Rp = 4R3		Rs = 254R		Amp1-2-var1			
19											

**Table 8.2** Figure 8.6 delta data at 10 Hz

1.	Delta between 1 kHz and 10 Hz at ~ 0dBV: -0.76 dB
2.	Delta between 1 kHz and 10 Hz at ~ -10dBV: -1.26 dB
3.	Delta between 1 kHz and 10 Hz at ~ -20dBV: -1.48 dB
4.	Delta between 1 kHz and 10 Hz at ~ -30dBV: -1.52 dB
5.	Delta between 1 kHz and 10 Hz at ~ -40dBV: -1.52 dB

Note With a generator output resistance of 10.8  $\Omega$  in Fig. 8.6 Amp1’s 0 dBV output level equals a nominal (actual) transformer output voltage of 50 mV<sub>rms</sub> [-23.8 dBu] (55 mV<sub>rms</sub> [-23.0 dBu]), etc.

We can simulate the whole matter by changing R1 and R2 according to the chosen input resistance  $R_i$  and input load R0. Hence, with decreasing R1 + R2 the now additionally R1 + R2 dependent term  $G_{e.loss}(R0)$  in the next chapter’s worksheets becomes bigger, thus, worsening the SNs accordingly (Figs. 8.1 and 8.3).

Concerning the deviation from a flat frequency response in the range  $\leq 1$  kHz at the Amp1 output I’ve measured the following Table 8.2 delta data from Fig. 8.6.

These delta data look like being in line with the before mentioned Lundahl data for high input levels, the deltas keep their levels with decreasing input signal voltages  $< 0.5$  mV<sub>rms</sub> (=100 mV<sub>rms</sub> [-20dBV] output level). Points 3. ff of Table 8.2

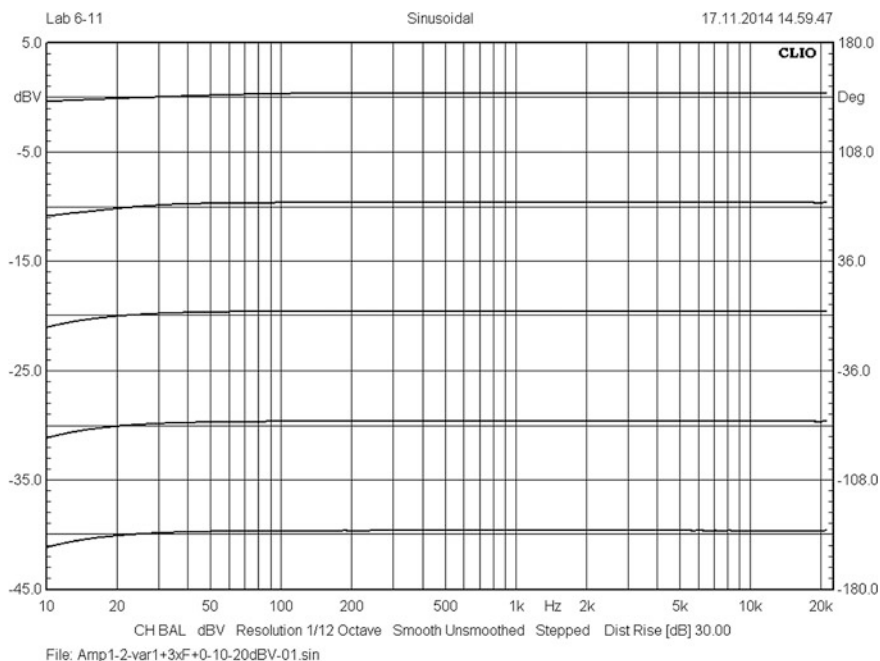


**Fig. 8.6** Output voltage frequency responses for five different Amp1 input voltages in 10 dB steps from 50  $\mu\text{V}_{\text{rms}}$  to 5.0  $\text{mV}_{\text{rms}}$  in a 10 Hz–20 kHz band

indicate why the overall frequency response of the Amp1 + Amp3 + Amp5 + Trafo chain in Fig. 12.1a shows the same low-frequency tendency of its flatness. Table 8.1, line 8, shows the deviations at 20 Hz: always  $<0.5$  dB.

Fully independent from the generator output resistance the responses at the upper end of  $B_{20\text{k}}$ —at 20 kHz—do not show these amounts of deviations (see Table 8.1, line 10, always  $<0.08$  dB).

## 8.4 Additional Remarks

### 8.4.1 DC Servo

It is not necessary to think about a DC servo. No matter which type of op-amp I've checked the circuit's DC conditions look very stable. Trimming the offset voltages of OPs 1 & 2 will sufficiently make it.



### **8.4.2 Wild Oscillation**

Another point is the prevention of wild oscillation. Depending on the location of the amp's PCB in the case there might be a tendency of ringing at very high frequencies  $>1$  MHz. Without touching the overall performance, a ceramic capacitance of approximately 100p–560p parallel to R4 or R5 or parallel to each resistor will sufficiently damp any oscillation. It's a trial and error approach.

## Contents

- 9.1 MCD-WS: The Transformer + Op-Amp Driven Amp1 (Real Data)
- 9.2 MCD-WS: The Transformer + Op-Amp Driven Amp1 (Data Sheet Data)

**Note 1:** MCD 11 has no built-in unit “rtHz” or “ $\sqrt{\text{Hz}}$ ”. To get  $\sqrt{1 \text{ Hz}}$  based voltage noise and current noise densities the rms noise voltage and current in a specific frequency range  $B > 1 \text{ Hz}$  must be multiplied by  $\sqrt{1 \text{ Hz}}$  and divided by the root of that specific frequency range  $\sqrt{B}$ !

**Note 2:** MCD 11 offers no “dB” unit. This is available from MCD 13 on!

9.1 MCD-WS: The Transformer + Op-Amp Driven Amp1 (Real Data)

Amp1 SN and gain calculations (Real data)

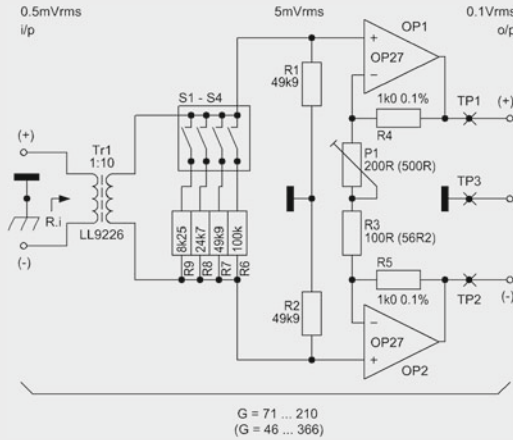


Fig. 9.1 = Fig. 8.1

1. Definition of all meaningful constants, components, etc. :

$T := 300\text{-K}$        $k := 1.38065 \cdot 10^{-23} \cdot \text{V} \cdot \text{A} \cdot \text{s} \cdot \text{K}^{-1}$        $v_{i, \text{nom}} := 0.5 \cdot 10^{-3} \text{V}$   
 $B_{20k} := 19980\text{-Hz}$        $B_1 := 1\text{Hz}$        $h := 1000\text{Hz}$        $f := 10\text{Hz}, 15\text{Hz}.. 100 \cdot 10^3\text{Hz}$

2. Gain stage component data :

$R0 := 20\Omega$        $R1 := 49.9 \cdot 10^3 \Omega$        $R2 := R1$        $R3 := 100\Omega$        $R4 := 1 \cdot 10^3 \Omega$        $R5 := R4$   
 $n := 11$        $G_{\text{tot}} := 200$        $G_{2\text{nd}} := \frac{G_{\text{tot}}}{n}$        $G_{2\text{nd}} = 18.182$   
 $G_{2\text{nd}} = 1 + \frac{R4 + R5}{RG}$        $RG := \frac{R4 + R5}{G_{2\text{nd}} - 1}$        $RG = 116.402 \Omega$        $P1 := RG - R3$        $P1 = 16.402 \Omega$   
 note: in this calculation course  $RG = R3 + P1!$

3. Calculation of the total input load  $Z_i$  :

Measured transformer values according to Lundahl's data sheet recommendation "C":

$R_p := 4.3\Omega$        $R_s := 254\Omega$   
 $R0_{\text{sec}} := R0 \cdot n^2$        $R0_{\text{sec}} = 2.42 \times 10^3 \Omega$

9.1 MCD-WS: The Transformer + Op-Amp Driven Amp1 (Real Data)

$$R_{p_{sec}} := R_p \cdot n^2 \quad R_{p_{sec}} = 520.3 \Omega$$

$$Z_{tr1} := R_{0_{sec}} + R_{p_{sec}} + R_s \quad Z_{tr1} = 3.194 \times 10^3 \Omega$$

$$Z_i := \frac{(R1 + R2) \cdot Z_{tr1}}{R1 + R2 + Z_{tr1}} \quad Z_i = 3.095 \times 10^3 \Omega$$

$$R_i := \frac{R1 + R2 + R_s}{n^2} + R_p \quad R_i = 831.193 \Omega$$

4. Calculation of the total noise voltage density at the input of Amp1 :

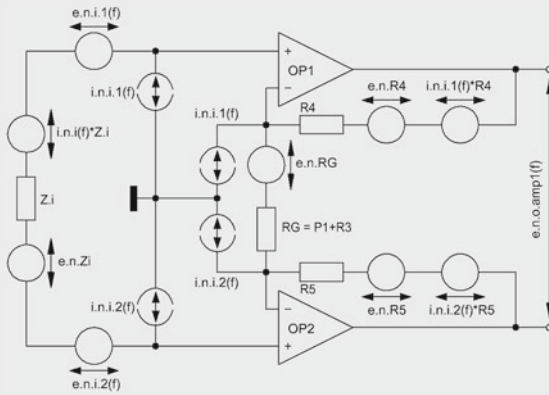


Fig. 9.2 = Fig. 8.2  
Noise sources of Amp1

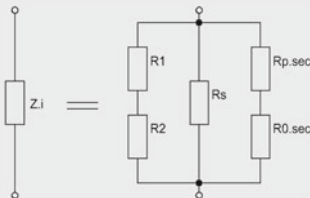


Fig. 9.3 = Fig. 8.3  
Components of the  
Fig. 9.2 input load Zi

4.1 Noise voltage density at the output of the 2nd stage (OPs 1 & 2) with input shorted :

$$e_{n,i1} := 3.0 \cdot 10^{-9} V \quad f_{c,e} := 2.7 Hz \quad i_{n,i1} := 0.4 \cdot 10^{-12} A \quad f_{c,i} := 120 Hz$$

$$e_{n,i2} := e_{n,i1} \quad i_{n,i2} := i_{n,i1}$$

$$e_{n,i1}(f) := e_{n,i1} \cdot \sqrt{\frac{f_{c,e}}{f} + 1} \quad e_{n,i2}(f) := e_{n,i1}(f) \quad i_{n,i1}(f) := i_{n,i1} \cdot \sqrt{\frac{f_{c,i}}{f} + 1} \quad i_{n,i2}(f) := i_{n,i1}(f)$$

9.1 MCD-WS: The Transformer + Op-Amp Driven Amp1 (Real Data)

$i_{n,i}(f) := \frac{i_{n,i,1}(f)}{\sqrt{2}}$	$i_{n,i}(h) = 299.333 \times 10^{-15} \text{ A}$
$e_{n,i}(f) := \sqrt{2} \cdot e_{n,i,1}(f)$	$e_{n,i}(h) = 4.248 \times 10^{-9} \text{ V}$
$e_{n,RG,o} := (G_{2nd} - 1) \cdot \sqrt{4 \cdot k \cdot T \cdot B_1 \cdot R_G}$	$e_{n,RG,o} = 23.861 \times 10^{-9} \text{ V}$
$e_{n,R4} := \sqrt{4 \cdot k \cdot T \cdot B_1 \cdot R4}$	$e_{n,R4} = 4.07 \times 10^{-9} \text{ V}$
$e_{n,o,2nd}(f) := \sqrt{e_{n,i}(f)^2 \cdot G_{2nd}^2 + 2 \cdot e_{n,R4}^2 + 2 \cdot i_{n,i,1}(f)^2 \cdot R4^2 + e_{n,RG,o}^2}$	$e_{n,o,2nd}(h) = 81.051 \times 10^{-9} \text{ V}$
$e_{n,i,2nd}(f) := \frac{e_{n,o,2nd}(f)}{G_{2nd}}$	$e_{n,i,2nd}(h) = 4.458 \times 10^{-9} \text{ V}$

4.2 Noise voltage density at the output of the 1st stage ( $Z_i$ ) with input loaded :

$e_{n,Zi} := \sqrt{4 \cdot k \cdot T \cdot B_1 \cdot Z_i}$	$e_{n,Zi} = 7.161 \times 10^{-9} \text{ V}$
$e_{n,o,tr1}(f) := \sqrt{e_{n,Zi}^2 + i_{n,i}(f)^2 \cdot Z_i^2}$	$e_{n,o,tr1}(h) = 7.221 \times 10^{-9} \text{ V}$

4.3 Noise voltage density at the output of Amp 1 with input loaded :

$e_{n,o,amp1}(f) := \sqrt{(e_{n,o,tr1}(f)^2 + e_{n,i,2nd}(f)^2) \cdot G_{2nd}^2}$	$e_{n,o,amp1}(h) = 154.29 \times 10^{-9} \text{ V}$
$e_{n,i,amp1}(f) := \frac{e_{n,o,amp1}(f)}{G_{tot}}$	$e_{n,i,amp1}(h) = 771.452 \times 10^{-12} \text{ V}$

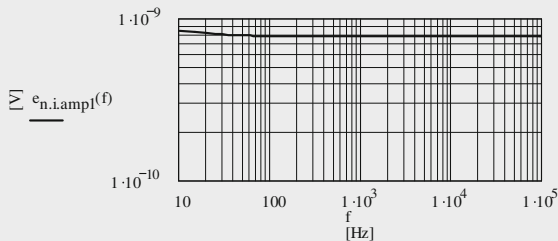


Fig. 9.4  
Amp1 input noise  
voltage density with  
 $R_0 = 20 \Omega$

5. Calculations of loss due to the cartridge load :

$G_{loss} := \frac{R1 + R2 + R_s + n^2 \cdot R_p + n^2 \cdot R_0}{R1 + R2}$	$G_{loss} = 1.032$
$G_{e,loss} := 20 \cdot \log(G_{loss})$	$G_{e,loss} = 0.274 \quad [\text{dB}]$

9.1 MCD-WS: The Transformer + Op-Amp Driven Amp1 (Real Data)

6. SN calculation (R0-dependent) :

$$\begin{aligned}
 R0_{sec}(R0) &:= R0 \cdot n^2 & Z_{tr1}(R0) &:= R0_{sec}(R0) + R_{p_{sec}} + R_s & Z_{tr1}(20\Omega) &= 3.194 \times 10^3 \Omega \\
 Z_1(R0) &:= \frac{(R1 + R2) \cdot Z_{tr1}(R0)}{R1 + R2 + Z_{tr1}(R0)} & Z_1(20\Omega) &= 3.095 \times 10^3 \Omega \\
 e_{n,Z1}(R0) &:= \sqrt{4 \cdot k \cdot T \cdot B_1 \cdot Z_1(R0)} & e_{n,Z1}(20\Omega) &= 7.161 \times 10^{-9} V \\
 e_{n,o.tr1}(f, R0) &:= \sqrt{e_{n,Z1}(R0)^2 + i_{n,i}(f)^2 \cdot Z_1(R0)^2} & e_{n,o.tr1}(h, 20\Omega) &= 7.221 \times 10^{-9} V \\
 e_{n,o.amp1}(f, R0) &:= \sqrt{(e_{n,o.tr1}(f, R0)^2 + e_{n,i.2nd}(f)^2) \cdot G_{2nd}^2} & e_{n,o.amp1}(h, 20\Omega) &= 154.29 \times 10^{-9} V \\
 e_{n,i.amp1}(f, R0) &:= \frac{e_{n,o.amp1}(f, R0)}{G_{2nd} \cdot n} & e_{n,i.amp1}(h, 20\Omega) &= 771.452 \times 10^{-12} V \\
 & & e_{n,i.amp1}(h, 0\Omega) &= 519.494 \times 10^{-12} V
 \end{aligned}$$

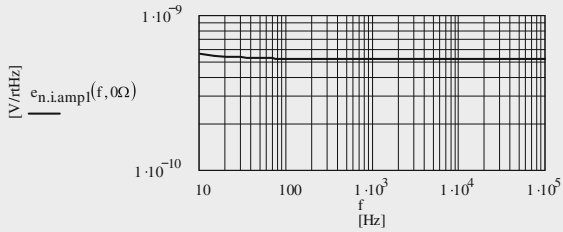


Fig. 9.5  
Amp1 input noise  
voltage density with  
R0 = 0Ω

$$\begin{aligned}
 G_{loss}(R0) &:= \frac{R1 + R2 + R_s + n^2 \cdot R_p + n^2 \cdot R0}{R1 + R2} & G_{loss}(20\Omega) &= 1.032 \\
 G_{e.loss}(R0) &:= 20 \cdot \log(G_{loss}(R0)) & G_{e.loss}(20\Omega) &= 0.274 \text{ [dB]}
 \end{aligned}$$

$$\begin{aligned}
 SN_{ne,i}(R0) &:= 20 \cdot \log \left[ \frac{\int_{20\text{Hz}}^{20000\text{Hz}} \left( \frac{1}{B_1} \right) \left( |e_{n,i.amp1}(f, R0)| \right)^2 df}{v_{i,nom}} \right] + G_{e.loss}(R0) \\
 SN_{ne,i}(20\Omega) &= -72.959 \text{ [dB]}
 \end{aligned}$$

## 9.1 MCD-WS: The Transformer + Op-Amp Driven Amp1 (Real Data)

Page 5

$$e_{in}(R0) := \sqrt{\frac{1}{B_{20k}} \cdot \int_{20\text{Hz}}^{2000\text{Hz}} \left( |e_{n.i.amp1}(f, R0)| \right)^2 df} \quad e_{in}(0\Omega) = 519.21 \times 10^{-12} \text{V}$$

$$A(f) := \frac{1.259}{1 + \left( \frac{20.6\text{Hz}}{f} \right)^2} \cdot \frac{1}{\sqrt{1 + \left( \frac{107.7\text{Hz}}{f} \right)^2}} \cdot \frac{1}{\sqrt{1 + \left( \frac{737.9\text{Hz}}{f} \right)^2}} \cdot \frac{1}{1 + \left( \frac{f}{12200\text{Hz}} \right)^2}$$

$$SN_{ne.i.a}(R0) := 20 \cdot \log \left[ \frac{\left[ \frac{1}{B_1} \cdot \int_{20\text{Hz}}^{2000\text{Hz}} \left( |e_{n.i.amp1}(f, R0)| \right)^2 \cdot (|A(f)|)^2 df \right]}{v_{i,nom}} \right] + G_{e.loss}(R0)$$

$$SN_{ne.i.a}(20\Omega) = -75.005 \quad [\text{dB(A)}]$$

$$R_{1000} := \left[ \frac{\sqrt{1 + (2 \cdot \pi \cdot 10^3 \text{Hz} \cdot 318 \cdot 10^{-6} \text{s})^2}}{\sqrt{1 + (2 \cdot \pi \cdot 10^3 \text{Hz} \cdot 3180 \cdot 10^{-6} \text{s})^2} \cdot \sqrt{1 + (2 \cdot \pi \cdot 10^3 \text{Hz} \cdot 75 \cdot 10^{-6} \text{s})^2}} \right]^{-1} \quad R_{1000} = 9.898$$

$$R(f) := \left[ \frac{\sqrt{1 + (2 \cdot \pi \cdot f \cdot 318 \cdot 10^{-6} \text{s})^2}}{\sqrt{1 + (2 \cdot \pi \cdot f \cdot 3180 \cdot 10^{-6} \text{s})^2} \cdot \sqrt{1 + (2 \cdot \pi \cdot f \cdot 75 \cdot 10^{-6} \text{s})^2}} \right] \cdot R_{1000}$$

$$SN_{riaa.f}(R0) := 20 \cdot \log \left[ \frac{\left[ \frac{1}{B_1} \cdot \int_{20\text{Hz}}^{2000\text{Hz}} \left( |e_{n.i.amp1}(f, R0)| \right)^2 \cdot (|R(f)|)^2 df \right]}{v_{i,nom}} \right] + G_{e.loss}(R0)$$

$$SN_{riaa.f}(20\Omega) = -76.477 \quad [\text{dB}]$$

$$SN_{ariaa.f}(R0) := 20 \cdot \log \left[ \frac{\left[ \frac{1}{B_1} \cdot \int_{20\text{Hz}}^{2000\text{Hz}} \left( |e_{n.i.amp1}(f, R0)| \right)^2 \cdot (|R(f)|)^2 \cdot (|A(f)|)^2 df \right]}{v_{i,nom}} \right] + G_{e.loss}(R0)$$

$$SN_{ariaa.f}(20\Omega) = -80.889 \quad [\text{dB(A)}]$$

measured via Amps 4 & 5 & trafo: -81.78 [dBV(A)]

9.1 MCD-WS: The Transformer + Op-Amp Driven Amp1 (Real Data)

$R0 := 0\Omega, 0.5\Omega \dots 100\Omega$

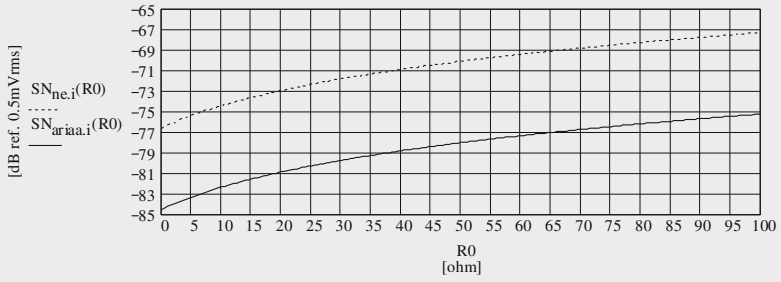


Fig. 9.6 Input referred and A-weighted SN vs. input load

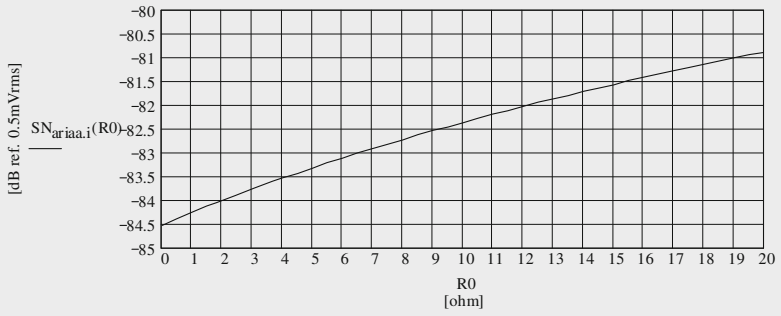


Fig. 9.7 Zoomed Fig. 9.6



9.1 MCD-WS: The Transformer + Op-Amp Driven Amp1 (Real Data)

7. NF calculation (R0-dependent) :

$$R0 := 1\Omega, 2\Omega \dots 1000\Omega$$

$$R_{iL}(R0) := \left( R_1^{-1} + R0^{-1} \right)^{-1}$$

$$i_{n,ieff}(f) := i_{n,i}(f) \cdot n$$

$$e_{n,ieff}(f) := \frac{e_{n,i}(f)}{n}$$

$$e_{n,RiL}(R0) := \sqrt{4 \cdot k \cdot T \cdot B_1 \cdot R_{iL}(R0)}$$

$$NF_e(R0) := 20 \cdot \log \left( \frac{\sqrt{e_{n,RiL}(R0)^2 + i_{n,ieff}(h)^2 \cdot R_{iL}(R0)^2 + e_{n,ieff}(h)^2}}{e_{n,RiL}(R0)} \right)$$

$R_{iL}(R0)$  = R0-dependent Amp1 input load

$$R_{iL}(20\Omega) = 19.53\Omega$$

$$i_{n,ieff}(h) = 3.293 \times 10^{-12} A$$

$$e_{n,ieff}(h) = 386.215 \times 10^{-12} V$$

$$e_{n,RiL}(20\Omega) = 568.832 \times 10^{-12} V$$

$$NF_e(20\Omega) = 1.684 \quad [dB]$$

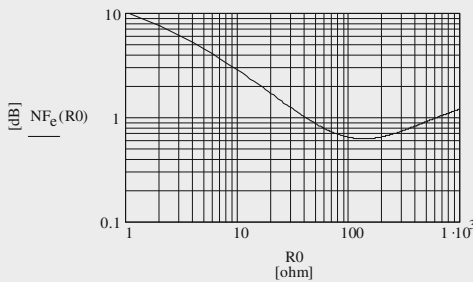


Fig. 9.8  
NF of Amp1 vs. R0

9.2 MCD-WS: The Transformer + Op-Amp Driven Amp1 (Data sheet data) Page 1

Amp1 SN and gain calculations (Data sheet data)

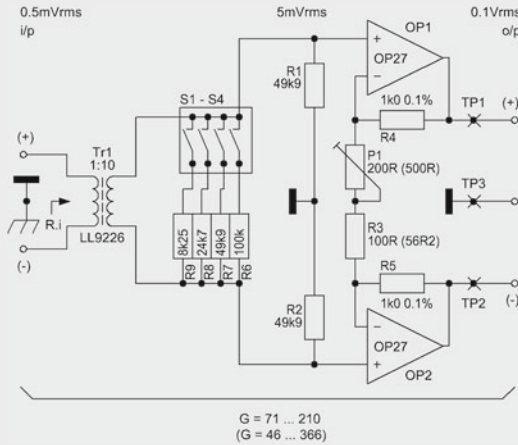


Fig. 9.10 = Fig. 8.1

1. Definition of all meaningful constants, components, etc. :

$T := 300 \cdot K$        $k := 1.38065 \cdot 10^{-23} \cdot V \cdot A \cdot s \cdot K^{-1}$        $v_{l,nom} := 0.5 \cdot 10^{-3} V$   
 $B_{20k} := 19980 \cdot Hz$        $B_1 := 1 Hz$        $h := 1000 Hz$        $f := 10 Hz, 15 Hz.. 100 \cdot 10^3 Hz$

2. Gain stage component data :

$R0 := 20 \Omega$        $R1 := 49.9 \cdot 10^3 \Omega$        $R2 := R1$        $R3 := 100 \Omega$        $R4 := 1 \cdot 10^3 \Omega$        $R5 := R4$   
 $n := 10$        $G_{tot} := 200$        $G_{2nd} := \frac{G_{tot}}{n}$        $G_{2nd} = 20$   
 $G_{2nd} = 1 + \frac{R4 + R5}{RG}$        $RG := \frac{R4 + R5}{G_{2nd} - 1}$        $RG = 105.263 \Omega$        $P1 = RG - R3$        $P1 = 5.263 \Omega$   
 note: in this calculation course  $RG = R3 + P1!$

3. Calculation of the total input load  $Z_i$  :

Measured transformer values according to Lundah's data sheet recommendation "C":

$R_p := 5 \Omega$        $R_s := 260 \Omega$   
 $R_{0,sec} := R_0 \cdot n^2$        $R_{sec} = 2 \times 10^3 \Omega$

9.2 MCD-WS: The Transformer + Op-Amp Driven Amp1 (Data sheet data) Page 2

$$R_{p,sec} := R_p \cdot n^2 \qquad R_{p,sec} = 500 \Omega$$

$$Z_{tr1} := R_{0,sec} + R_{p,sec} + R_s \qquad Z_{tr1} = 2.76 \times 10^3 \Omega$$

$$Z_i := \frac{(R1 + R2) \cdot Z_{tr1}}{R1 + R2 + Z_{tr1}} \qquad Z_i = 2.686 \times 10^3 \Omega$$

$$R_i := \frac{R1 + R2 + R_s}{n^2} + R_p \qquad R_i = 1005.6 \Omega$$

4. Calculation of the total noise voltage density at the input of Amp1 :

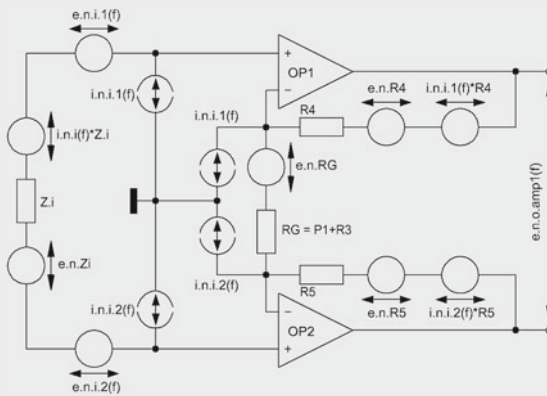


Fig. 9.11 = Fig. 8.2  
Noise sources of Amp1

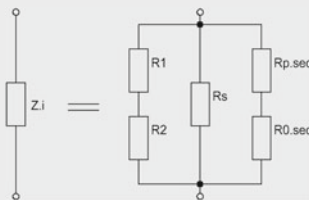


Fig. 9.12 = Fig. 8.3  
Components of the  
Fig. 9.11 input load Zi

4.1 Noise voltage density at the output of the 2nd stage (OPs 1 & 2) with input shorted :

$$e_{n,i1} := 3.0 \cdot 10^{-9} V \qquad f_{c,e} := 2.7 Hz \qquad i_{n,i1} := 0.4 \cdot 10^{-12} A \qquad f_{c,i} := 120 Hz$$

$$e_{n,i2} := e_{n,i1} \qquad i_{n,i2} := i_{n,i1}$$

$$e_{n,i1}(f) := e_{n,i1} \cdot \sqrt{\frac{f_{c,e}}{f} + 1} \qquad e_{n,i2}(f) := e_{n,i1}(f) \qquad i_{n,i1}(f) := i_{n,i1} \cdot \sqrt{\frac{f_{c,i}}{f} + 1} \qquad i_{n,i2}(f) := i_{n,i1}(f)$$

9.2 MCD-WS: The Transformer + Op-Amp Driven Amp1 (Data sheet data) Page 3

$$\begin{aligned}
 i_{n,i}(f) &:= \frac{i_{n,i,1}(f)}{\sqrt{2}} & i_{n,i}(h) &= 299.333 \times 10^{-15} \text{ A} \\
 e_{n,i}(f) &:= \sqrt{2} \cdot e_{n,i,1}(f) & e_{n,i}(h) &= 4.248 \times 10^{-9} \text{ V} \\
 e_{n,RG,o} &:= (G_{2nd} - 1) \cdot \sqrt{4 \cdot k \cdot T \cdot B_1 \cdot R_G} & e_{n,RG,o} &= 25.091 \times 10^{-9} \text{ V} \\
 e_{n,R4} &:= \sqrt{4 \cdot k \cdot T \cdot B_1 \cdot R4} & e_{n,R4} &= 4.07 \times 10^{-9} \text{ V} \\
 e_{n,o,2nd}(f) &:= \sqrt{e_{n,i}(f)^2 \cdot G_{2nd}^2 + 2 \cdot e_{n,R4}^2 + 2 \cdot i_{n,i,1}(f)^2 \cdot R4^2 + e_{n,RG,o}^2} & e_{n,o,2nd}(h) &= 88.784 \times 10^{-9} \text{ V} \\
 e_{n,i,2nd}(f) &:= \frac{e_{n,o,2nd}(f)}{G_{2nd}} & e_{n,i,2nd}(h) &= 4.439 \times 10^{-9} \text{ V}
 \end{aligned}$$

4.2 Noise voltage density at the output of the 1st stage ( $Z_i$ ) with input loaded :

$$\begin{aligned}
 e_{n,Z_i} &:= \sqrt{4 \cdot k \cdot T \cdot B_1 \cdot Z_i} & e_{n,Z_i} &= 6.671 \times 10^{-9} \text{ V} \\
 e_{n,o,tr1}(f) &:= \sqrt{e_{n,Z_i}^2 + i_{n,i}(f)^2 \cdot Z_i^2} & e_{n,o,tr1}(h) &= 6.719 \times 10^{-9} \text{ V}
 \end{aligned}$$

4.3 Noise voltage density at the output of Amp1 with input loaded :

$$\begin{aligned}
 e_{n,o,amp1}(f) &:= \sqrt{(e_{n,o,tr1}(f)^2 + e_{n,i,2nd}(f)^2) \cdot G_{2nd}^2} & e_{n,o,amp1}(h) &= 161.058 \times 10^{-9} \text{ V} \\
 e_{n,i,amp1}(f) &:= \frac{e_{n,o,amp1}(f)}{G_{tot}} & e_{n,i,amp1}(h) &= 805.29 \times 10^{-12} \text{ V}
 \end{aligned}$$

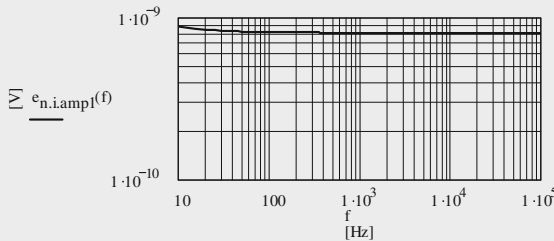


Fig. 9.13  
Amp1 input noise  
voltage density with  
 $R_0 = 20 \Omega$

5. Calculations of loss due to the cartridge load :

$$\begin{aligned}
 G_{loss} &:= \frac{R1 + R2 + R_s + n^2 \cdot R_p + n^2 \cdot R_0}{R1 + R2} & G_{loss} &= 1.028 \\
 G_{e,loss} &:= 20 \cdot \log(G_{loss}) & G_{e,loss} &= 0.237 \quad [\text{dB}]
 \end{aligned}$$

9.2 MCD-WS: The Transformer + Op-Amp Driven Amp1 (Data sheet data) Page 4

6. SN calculation (R0-dependent) :

$$\begin{aligned}
 R0_{sec}(R0) &:= R0 \cdot n^2 & Z_{tr1}(R0) &:= R0_{sec}(R0) + R_{p_{sec}} + R_s & Z_{tr1}(20\Omega) &= 2.76 \times 10^3 \Omega \\
 Z_1(R0) &:= \frac{(R1 + R2) \cdot Z_{tr1}(R0)}{R1 + R2 + Z_{tr1}(R0)} & Z_1(20\Omega) &= 2.686 \times 10^3 \Omega \\
 e_{n,Z1}(R0) &:= \sqrt{4 \cdot k \cdot T \cdot B_1 \cdot Z_1(R0)} & e_{n,Z1}(20\Omega) &= 6.671 \times 10^{-9} V \\
 e_{n.o.tr1}(f,R0) &:= \sqrt{e_{n,Z1}(R0)^2 + i_{n,i}(f)^2 \cdot Z_1(R0)^2} & e_{n.o.tr1}(h,20\Omega) &= 6.719 \times 10^{-9} V \\
 e_{n.o.amp1}(f,R0) &:= \sqrt{(e_{n.o.tr1}(f,R0)^2 + e_{n,i.2nd}(f)^2) \cdot G_{2nd}^{-2}} & e_{n.o.amp1}(h,20\Omega) &= 161.058 \times 10^{-9} V \\
 e_{n.i.amp1}(f,R0) &:= \frac{e_{n.o.amp1}(f,R0)}{G_{2nd} \cdot n} & e_{n.i.amp1}(h,20\Omega) &= 805.29 \times 10^{-12} V \\
 & & e_{n.i.amp1}(h,0\Omega) &= 567.923 \times 10^{-12} V
 \end{aligned}$$

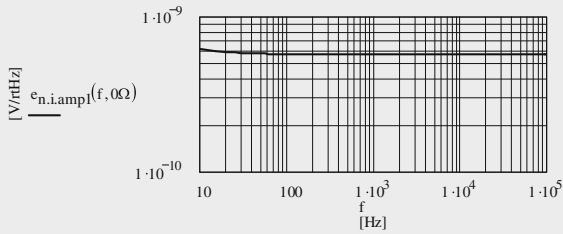


Fig. 9.14  
Amp1 input noise  
voltage density with  
R0 = 0Ω

$$\begin{aligned}
 G_{loss}(R0) &:= \frac{R1 + R2 + R_s + n^2 \cdot R_p + n^2 \cdot R0}{R1 + R2} & G_{loss}(20\Omega) &= 1.028 \\
 G_{e.loss}(R0) &:= 20 \cdot \log(G_{loss}(R0)) & G_{e.loss}(20\Omega) &= 0.237 \quad [dB] \\
 SN_{ne,i}(R0) &:= 20 \cdot \log \left[ \frac{\int_{20Hz}^{2000Hz} \left( \frac{1}{B_1} \cdot \left( |e_{n.i.amp1}(f,R0)| \right)^2 df \right)}{V_{i,nom}} \right] + G_{e.loss}(R0) \\
 SN_{ne,i}(0\Omega) &= -75.827 \quad [dB]
 \end{aligned}$$

9.2 MCD-WS: The Transformer + Op-Amp Driven Amp1 (Data sheet data) Page 5

$$e_{in}(R0) := \left[ \frac{1}{B_{20k}} \cdot \int_{20\text{Hz}}^{2000\text{Hz}} \left( |e_{n.i.amp1}(f, R0)| \right)^2 df \right] \quad e_{in}(0\Omega) = 567.61 \times 10^{-12}\text{V}$$

$$A(f) := \frac{1.259}{1 + \left( \frac{20.6\text{Hz}}{f} \right)^2} \cdot \frac{1}{\sqrt{1 + \left( \frac{107.7\text{Hz}}{f} \right)^2}} \cdot \frac{1}{\sqrt{1 + \left( \frac{737.9\text{Hz}}{f} \right)^2}} \cdot \frac{1}{1 + \left( \frac{f}{12200\text{Hz}} \right)^2}$$

$$SN_{ne.i.a}(R0) := 20 \cdot \log \left[ \frac{\left[ \frac{1}{B_1} \cdot \int_{20\text{Hz}}^{2000\text{Hz}} \left( |e_{n.i.amp1}(f, R0)| \right)^2 \cdot (|A(f)|)^2 df \right]}{v_{i,nom}} \right] + G_{e.loss}(R0) \quad SN_{ne.i.a}(20\Omega) = -74.669 \text{ [dB(A)]}$$

$$R_{1000} := \left[ \frac{\sqrt{1 + (2 \cdot \pi \cdot 10^3 \text{Hz} \cdot 318 \cdot 10^{-6} \text{s})^2}}{\sqrt{1 + (2 \cdot \pi \cdot 10^3 \text{Hz} \cdot 3180 \cdot 10^{-6} \text{s})^2} \cdot \sqrt{1 + (2 \cdot \pi \cdot 10^3 \text{Hz} \cdot 75 \cdot 10^{-6} \text{s})^2}} \right]^{-1} \quad R_{1000} = 9.898$$

$$R(f) := \left[ \frac{\sqrt{1 + (2 \cdot \pi \cdot f \cdot 318 \cdot 10^{-6} \text{s})^2}}{\sqrt{1 + (2 \cdot \pi \cdot f \cdot 3180 \cdot 10^{-6} \text{s})^2} \cdot \sqrt{1 + (2 \cdot \pi \cdot f \cdot 75 \cdot 10^{-6} \text{s})^2}} \right] \cdot R_{1000}$$

$$SN_{riaa.f}(R0) := 20 \cdot \log \left[ \frac{\left[ \frac{1}{B_1} \cdot \int_{20\text{Hz}}^{2000\text{Hz}} \left( |e_{n.i.amp1}(f, R0)| \right)^2 \cdot (|R(f)|)^2 df \right]}{v_{i,nom}} \right] + G_{e.loss}(R0) \quad SN_{riaa.f}(20\Omega) = -76.147 \text{ [dB]}$$

$$SN_{ariaa.f}(R0) := 20 \cdot \log \left[ \frac{\left[ \frac{1}{B_1} \cdot \int_{20\text{Hz}}^{2000\text{Hz}} \left( |e_{n.i.amp1}(f, R0)| \right)^2 \cdot (|R(f)|)^2 \cdot (|A(f)|)^2 df \right]}{v_{i,nom}} \right] + G_{e.loss}(R0) \quad SN_{ariaa.f}(0\Omega) = -83.757 \text{ [dB(A)]}$$

measured via Amps 4 & 5 & trafo: -81.78 [dBV(A)]

9.2 MCD-WS: The Transformer + Op-Amp Driven Amp1 (Data sheet data) Page 6

7. NF calculation (R0-dependent) :

$$R0 := 1\Omega, 2\Omega \dots 1000\Omega$$

$$R_{iL}(R0) := \left( R_i^{-1} + R0^{-1} \right)^{-1}$$

$$i_{n,ieff}(f) := i_{n,i}(f) \cdot n$$

$$e_{n,ieff}(f) := \frac{e_{n,i}(f)}{n}$$

$$e_{n,RiL}(R0) := \sqrt{4 \cdot k \cdot T \cdot B_1 \cdot R_{iL}(R0)}$$

$$NF_e(R0) := 20 \cdot \log \left( \frac{\sqrt{e_{n,RiL}(R0)^2 + i_{n,ieff}(h)^2 \cdot R_{iL}(R0)^2 + e_{n,ieff}(h)^2}}{e_{n,RiL}(R0)} \right)$$

$R_{iL}(R0)$  = R0-dependent Amp1 input load

$$R_{iL}(20\Omega) = 19.61\Omega$$

$$i_{n,ieff}(h) = 2.993 \times 10^{-12} A$$

$$e_{n,ieff}(h) = 424.836 \times 10^{-12} V$$

$$e_{n,RiL}(20\Omega) = 569.995 \times 10^{-12} V$$

$$NF_e(20\Omega) = 1.948 \quad [dB]$$

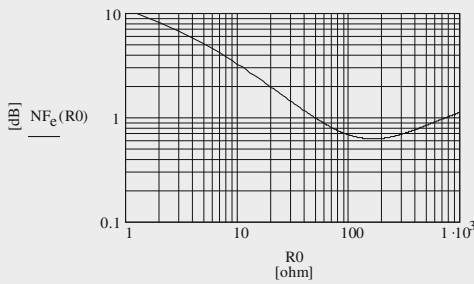


Fig. 9.15  
NF of Amp1 vs. R0

## 10.1 General Design and Gain of Amp2

The Amp2 circuit shown in Fig. 10.1 is nothing else but a kind of balanced version of Douglas Self’s original MC pre-amp,<sup>1</sup> however, forming a differential input, equipped with very low-noise complementary BJTs in the input stage, the Toshiba 2SC3329BL / 2SA1316BL ( $h_{fe} \sim 500$ ,  $r_{bb'} = 2 \Omega$ ). I used such an un-balanced gain stage as first stage of the TSOS-2 Chap. 15 and Module 2 phono-amp (TSOS-1 Chap. 6).

The exact equations to calculate the gain of the T1-T2 or T3-T4 stage are part of this book’s Chap. 21. However, Amp2’s overall gain  $G_{amp2}$  becomes:

$$G_{amp2} = 1 + \frac{R10 + R11}{R5} \tag{10.1}$$

Because of the very low resistive environment, I’ve composed R5 by the shown arrangement. T1–T4 work with 2.1–2.2 mA collector current each, set by R4, R6, R7 and the emitter resistors

$$R5 = (P3 || R5a) + (R5b || R5c || R5d) \tag{10.2}$$

With P3 trimmed to 0  $\Omega$ , P1 and P2 (P1 or P2 could be replaced by a 100  $\Omega$  resistor) set equal (but with opposite polarity) DC voltages at test points TP1 and TP2, roughly  $\pm 2$  to  $\pm 2.1$  mV. With P3 set to the nominal gain of 200, we should find appr.  $\pm 3$  to  $\pm 3.3$  mV at the test points. Generally, P3 can set overall gains in a range of 51–301 without significantly influencing the DC voltage and current situation of the input stage.

The feedback resistors R10 & R11 seem to be rather small. They are chosen very much smaller than the usually recommended min. 600  $\Omega$  output load for the 5534 or equivalent op-amp types. I guess the op-amps do not have big problems by driving

<sup>1</sup>“Small Signal Audio Design”, Douglas Self, 2010, Focal Press.



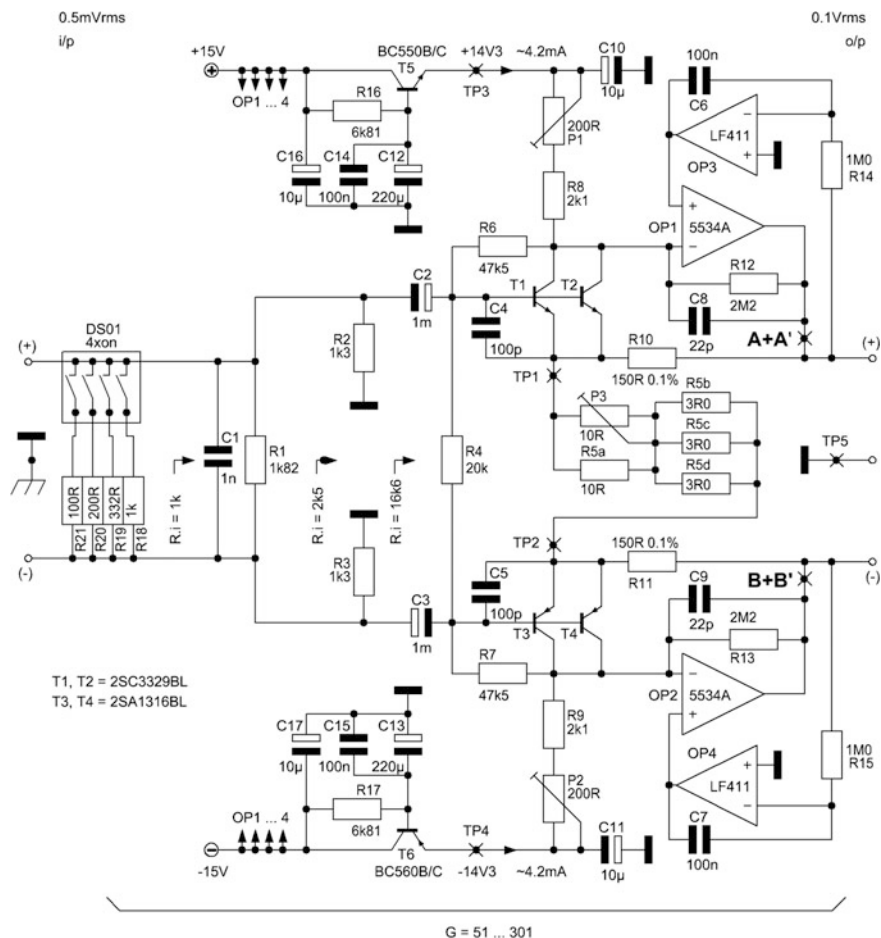


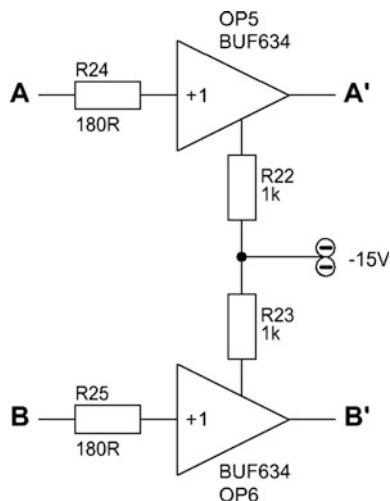
**Fig. 10.1** Input gain stage alternative Amp2

this output load with a maximal OPs 1 & 2 output voltage of nominal  $500 \text{ mV}_{\text{rms}}$  at 20 kHz. In this respect the only point here is the question what would happen with the op-amps if they would be forced into a +20 dB overload situation, hence  $5 \text{ V}_{\text{rms}}$  at 20 kHz.

Under normal conditions the Fig. 10.1 circuit works very well, hence, by feeding the MC cartridge with a 1 kHz / 0 dB DIN<sup>2</sup> signal we trim P3 to the gain that ensures a nominal  $100 \text{ mV}_{\text{rms}}$  at Amp2's balanced output. According to Fig. 10.2 and in cases of massive overload threat, I recommend the insertion of two boosters at points A + A' and B + B'. They do not negatively touch the excellent picture of

<sup>2</sup>See TSOS-2, Chap. 3.

**Fig. 10.2** Booster for insertion into Fig. 10.1's points A + A' and B + B'



the Fig. 10.1 Amp2 and they work well in the Module 2 phono-amps in both TSOS versions.

In contrast to all other switching actions switching from Amp1 to Amp2 leads to a tiny but audible transient phenomenon. I guess the high valued input Cs create it. The other way around does not create such a phenomenon.

## 10.2 CMRR

Compared with Amp1, we find a very much lower  $CMRR_c$  figure. With a common mode gain  $G_{cm} = 1$  and a differential gain  $G_{dif} = 200$  it becomes only  $46 \text{ dB} = 20 * \log(G_{dif}/G_{cm}) = 20 * \log(200)$ . We could drastically improve it (min. +60 dB) by integration of a gain x2 output stage à la Fig. 6.1's OPs 3 & 4 + R6–R13. Additionally, resistors R10 and R11 of Fig. 10.1 must then be reduced to  $75 \Omega$ .

## 10.3 Noise

### 10.3.1 General Noise Aspects

With an input load of  $20 \Omega$ , the input referred SN situation is not as good as the Amp1 solution, however, better than the goal from Chap. 1 and always better than most phono-amps on the market. Additionally, in contrast to the Amp1 SNs with input loads  $\leq 10 \Omega$  and compared with the calculated results Amp2 shows increasingly worse measured input referred RIAA- and A-weighted SN results. They are measured at the output of the Amp2 + Amp4 + Amp5 + Trafo chain. Hence, eg with i/p-load  $5 \Omega$ : Amp1 calculated  $SN_o = -84.0 \text{ dB(A)}$  versus Amp2

measured  $SN_o = -81.2 \text{ dB(A)}$ . Because of the rather complex SN calculations with unclear flicker-noise behaviour of the chosen BJTs and in conjunction with the next chapter's Mathcad Worksheets the following section should give satisfying answers.

In consideration of the RIAA transfer function, A-weighting, the subsequent gain stages, and with  $20 \Omega$  ( $43 \Omega$ ) input load the measured input referred SN via Amps 3 or 4 + Amp5 + Trafo shows a worst case  $SN_{ariaa.i.m} = -79.8 \text{ dB(A)}$  ( $-78.4 \text{ dB(A)}$ ), the calculated  $SN_{ariaa.i.calc} = -80.4 \text{ dB(A)}$  ( $-78.6 \text{ dB(A)}$ ). THD and IMD become  $<0.01\%$  each.

### 10.3.2 The BJT Noise Model Reloaded

In the past—and in my books too—I have been handling the analysis of the BJT noise creation in a way of hopefully easy usage, hence, mainly based on a white noise production of the BJTs. The reason lies in the Figs. 10.3 and 10.4 charts of the used input BJTs, the now obsolete Analog Devices SSM2210.<sup>3</sup> They show completely ignorable  $1/f$ -noise in the audio band  $B_{20k}$ . The  $1/f$ -noise corner frequencies will not change after paralleling the devices.

Hit by a surprising noise production mechanism the Amp2 SN results forced me to change my analysis approach from purely white noise to a flicker noise ( $1/f$ -noise) influenced one. With input loads  $R_0 > 45 \Omega$  Amp2's difference between a calculated and a measured input referred SN became always  $<1 \text{ dB}$ . The white noise based differences with input loads  $\leq 45 \Omega$  became  $>1 \text{ dB}$ , up to  $4.8 \text{ dB}$  at  $R_0 = 0 \Omega$ . If we accept a maximal deviation of  $1 \text{ dB}$  for  $R_0 \geq 1 \Omega$  we have to find a reasonable calculation method that includes  $1/f$ -noise effects. Thus, the BJT's noise currents and voltages have to be treated in a frequency dependent way.

According to the respective white noise based figures in TSOS-1 & TSOS-2 and with the hopefully self-explanatory evolution towards a simple BJT noise model of Figs. 10.5, 10.6 and 10.7, we can sum-up the noise sources of a BJT in a frequency dependent equivalent input referred noise voltage density  $e_{n,i}(f)$  and in an input referred noise current density  $i_{n,i}(f)$ .

Here, I talk about noise sources in  $B_{20k}$  only. Outside the band  $>20 \text{ kHz}$  we find another deviation from the white noise flatness. Based on most BJT's transit frequency  $f_T \gg 20 \text{ MHz}$  it's the current noise's increase by  $\sim f \equiv +6 \text{ dB/oct.}$  or  $+20 \text{ dB/dec.}$  after a 2nd corner frequency of  $\geq \sim f_T/h_{fe}$ . Fortunately, this behaviour lies far outside the audio band and it does not touch the here presented cases.

With the following equations and based on given operating conditions for the collector current  $I_C$ , the collector-emitter voltage  $V_{ce}$ , and thus the small signal

---

<sup>3</sup>See Analog Devices data sheet.

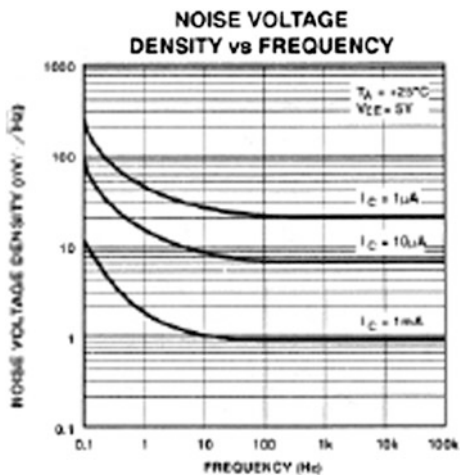


Fig. 10.3 SSM2210 noise voltage density versus frequency and collector current

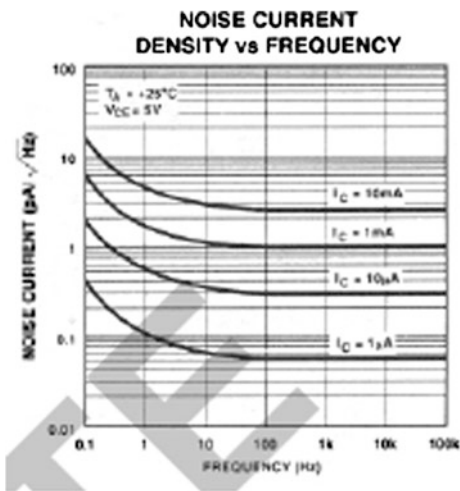


Fig. 10.4 SSM2210 noise current density versus frequency and collector current

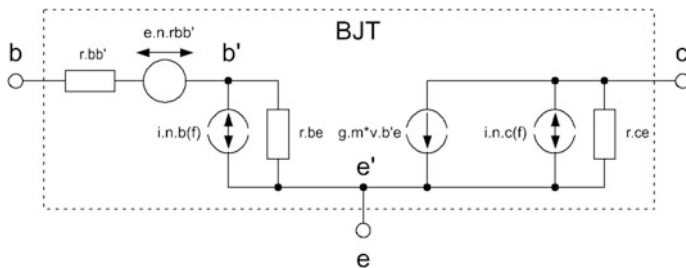
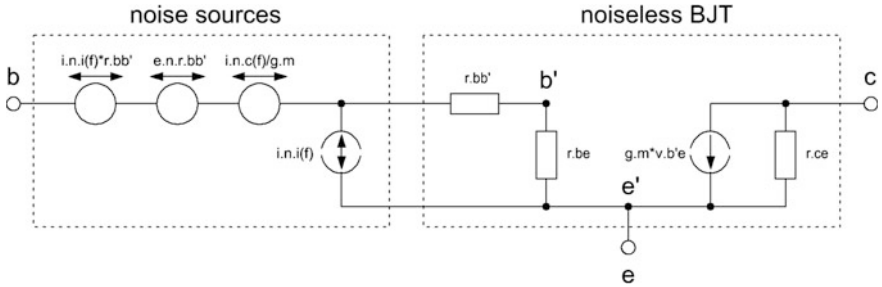
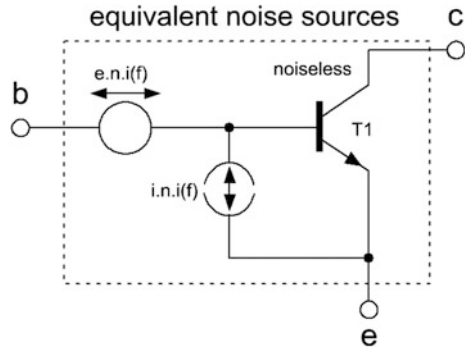


Fig. 10.5 General simplified BJT noise model for the audio band



**Fig. 10.6** Transfer of the Fig. 10.5 model into a strictly input referred one

**Fig. 10.7** Transfer of the Fig. 10.6 noise model into the final BJT noise model with only two equivalent noise sources in place



current gain  $h_{fe}$  ( $\approx h_{FE}$  = DC current gain), the operating temperature  $T$ , and hopefully a given base-spreading resistance  $r_{bb'}$ , we can now calculate Fig. 10.7's equivalent noise sources.

In a BJT the flicker noise (=1/f-noise region) and shot noise (=white noise region) production starts in the collector current  $I_C$ , hence, the noise current  $i_{n,c}(f)$  in density format becomes:

$$i_{n,c}(f) = \sqrt{2qI_C B_1} \left( 1 + \frac{f_{c,i}}{f} \right)^x \tag{10.3}$$

In (10.3)  $f_{c,i}$  is the 1/f-noise corner frequency of the  $I_C$  noise current and 'x' defines the slope of the noise current in the 1/f-noise region. Slope figure  $x = 0.5$  means that the slope decreases according to the square root of 1/f. With that, it equals pink noise with a slope of  $-10$  dB/decade or  $-3$  dB/octave. However, in the reality of low-noise BJTs  $x$  can show values between 0 (=purely white noise) and 1 (purely red noise). To find the right one in the next section we have to dive deep into the jungle of mostly vague or rough data-sheet data and their integration into a useful math.

The collector noise current transferred to the input shows two different noise relevant effects. It creates what I call the BJT kernel noise voltage density  $e_{n1}(f)$  and it is the source for the input referred noise current density  $i_{n,i}(f)$ :

$$e_{n1}(f) = \frac{i_{n,c}(f)}{g_m} \quad (10.4)$$

$$i_{n,i}(f) = \frac{i_{n,c}(f)}{h_{fe}} \quad (10.5)$$

With the BJT's mutual conductance (transconductance)  $g_m$

$$g_m = \frac{qI_C}{kT} \quad (10.6)$$

We'll get a useful expression for the kernel noise voltage density  $e_{n1}(f)$ :

$$e_{n1}(f) = \sqrt{2 \frac{k^2 T^2}{qI_C} B_1 \left(1 + \frac{f_{c,i}}{f}\right)^x} \quad (10.7)$$

The noise voltage density  $e_{n,rbb'}$  of the base spreading resistance  $r_{bb'}$  becomes:

$$e_{n,rbb'} = \sqrt{4kTr_{bb'}B_1} \quad (10.8)$$

We can take  $e_{n,rbb'}$  frequency independent in  $B_{20k}$ .<sup>4</sup> Thus, we obtain the general equation to calculate the frequency dependent input referred noise voltage density  $e_{n,i}(f)$  of Fig. 10.7 as follows:

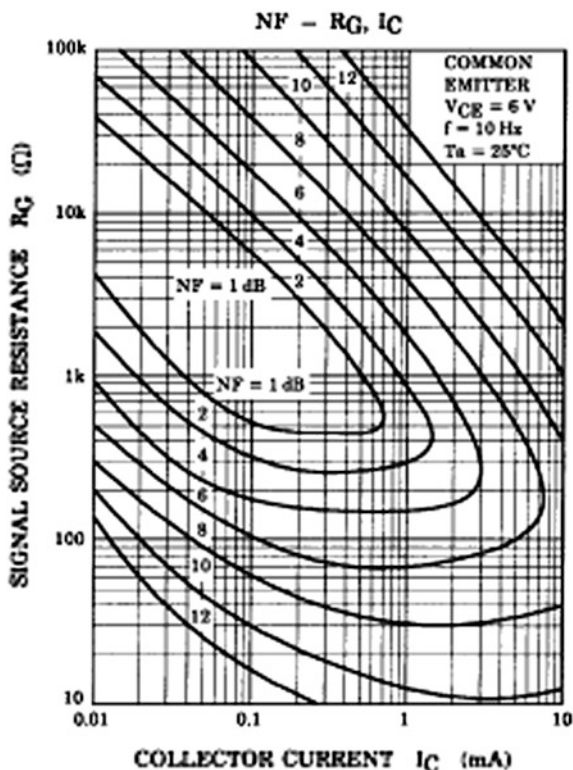
$$e_{n,i}(f) = \sqrt{e_{n1}(f)^2 + i_{n,i}(f)^2 r_{bb'}^2 + e_{n,rbb'}^2} \quad (10.9)$$

The BJT's kernel noise voltage density  $e_{n1}(f)$  is fully independent of any resistance that might disturb the nice looking picture of its decreasing value with increasing  $I_C$ . However, the bad boy in the BJT noise production game is the base-spreading resistance  $r_{bb'}$ , mostly not given in data-sheets and mostly too high for real lowest-noise purposes. The good news: in the past years more and more information about the  $r_{bb'}$  value of many BJTs came on the table and—among many alternatives—it becomes easier now to select the ones we need.

---

<sup>4</sup>See page xxv for further information on physical expressions and constants, etc.

**Fig. 10.8** NF of 2SC3329 at 10 Hz



### 10.3.3 In Search of the Slope Figures 'x' (2SC3329) and 'y' (2SA1316)

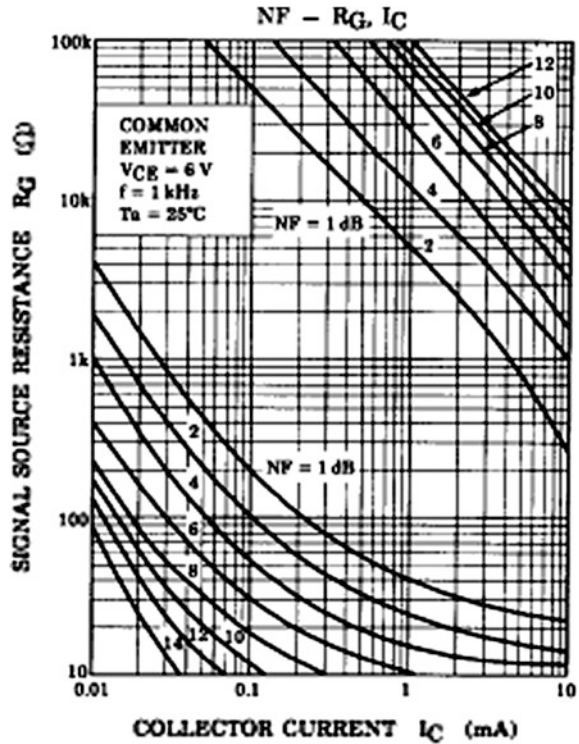
The BJTs in the input section of Amp2 show very interesting data for MC purposes and Toshiba claims low  $1/f$ -noise, low base spreading resistance of  $2\ \Omega$  (at 100 MHz!!!), and—without any further explanations—rather low input referred noise voltage density of typical  $0.6\ \text{nV}/\text{rtHz}$ .

Additional noise-concerning information come from the NF charts that show contours of various NF values in the source resistance  $R_G$  versus collector current  $I_C$  plane. The absence of charts like the ones of Figs. 2 and 3 triggers my suspicion that, by contrasting the manufacturer's claim, the BJTs produce a certain amount of  $1/f$ -noise too; however, I guess with lower than  $-10\ \text{dB}/\text{dec.}$  slopes, especially with input loaded by a resistance.

Figures 10.8, 10.9, 10.10 and 10.11<sup>5</sup> show the NF charts of the two devices. The operating current gain  $h_{fe}$  is not indicated, however, with a flat  $h_{fe}$  over most of the operating collector current ( $100\ \mu\text{A}$ – $10\ \text{mA}$ ) we can expect equal NF conditions for

<sup>5</sup>Toshiba data sheet.

**Fig. 10.9** NF of 2SC3329 at 1 kHz



the indicated  $h_{fe}$  range of 350–700. The chosen BJTs for Amp2 operate at a selected  $h_{fe} = 500$ .

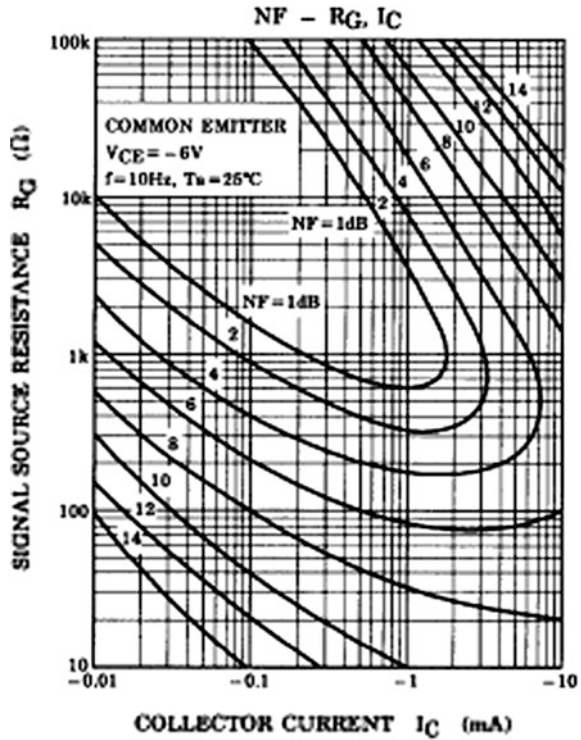
The first chart is taken at 10 Hz and the second one at 1 kHz. The data sheet’s table of Electrical Characteristics indicates NF values too, however, without any relevance for this section, because they show NF values for input loads  $\geq 100 \Omega$ .

The major disadvantage of the shown charts lies in the fact that all NF solutions are based on input loads  $\geq 10 \Omega$ . There is no indication for lower input loads and no one for the shorted input case. Hence, in order to get equivalent input noise voltages and currents I had to find an easy to use path out of the mud. Generally, my developed approach is based on the chosen operating collector current and an average input load of  $20 \Omega$ . Consequently, other than  $20 \Omega$  input loads will yield calculated results less close to the measured ones, as it will be the case with  $20 \Omega$ .

The Amp2 collector current  $I_C$  is set to 2.2 mA for each device. The collector-emitter voltage  $V_{CE}$  comes up with appr. 4.3 V. Now we must find ‘x’ and ‘y’ for the  $20 \Omega$  input load case. This means that each half of Amp2 (one half represents the input’s N channel, the other one represents the P channel) “sees” an input load of  $10 \Omega$ . Figure 10.12 shows the situation of Amp2 with all noise calculation relevant active and passive components.



**Fig. 10.10** NF of 2SA1316 at 10 Hz



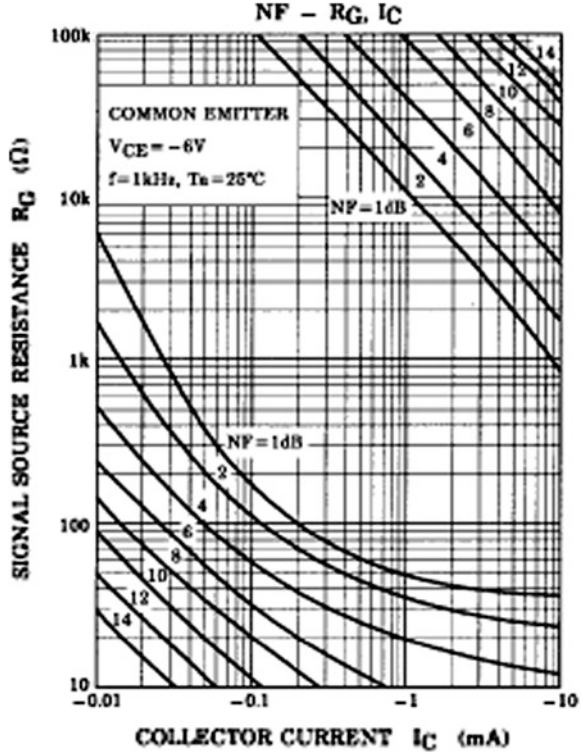
The search process for the N half follows the steps given below; the P half process looks the same. I add its results in brackets.

1. At 10 Hz: from a zoomed Fig. 10.8 (10.10) value pair 2.2 mA/10 Ω we'll get  $NF_{e,n.10} = 10.2$  dB (9.5 dB)
2. At 1 kHz: from a zoomed Fig. 10.9 (10.11) value pair 2.2 mA/10 Ω we'll get  $NF_{e,n.1k} = 5.0$  dB (5.0 dB)
3. For the NF calculation of a gain stage input with input load R0 and according to Fig. 10.13 the general equation looks as follows ("e" signals a noise factor NF expressed in the noise figure mode  $NF_e = 20 \log(NF)$  [dB]):

$$NF_e = 20 \log \left( \frac{\sqrt{e_{n,i}(f)^2 + e_{n,R0}^2 + i_{n,i}(f)^2 R0^2}}{e_{n,R0}} \right) \tag{10.10}$$

$$e_{n,R0} = \sqrt{4kTB_1 R0} \tag{10.11}$$

**Fig. 10.11** NF of 2SA1316 at 1 kHz



By inclusion of the above given frequency dependent Eqs. (10.5) and (10.9) for 10 Hz and 1 kHz into (10.10) we obtain the  $x$  and  $f_{c,i}$  dependent expressions for  $NF_{e,n,10}$  (at 10 Hz) and  $NF_{e,n,1k}$  (at 1 kHz):

$$\begin{aligned}
 NF_{e,n,10}(x, f_{c,i}) &= 10.2 \\
 &= 20 \log \left( \frac{\sqrt{e_{n,i}(10\text{Hz}, x, f_{c,i})^2 + e_{n,R0}^2} + i_{n,i}(10\text{Hz}, x, f_{c,i})^2 R_0^2}{e_{n,R0}} \right) \quad (10.12)
 \end{aligned}$$

$$\begin{aligned}
 NF_{e,n,1k}(x, f_{c,i}) &= 5 \\
 &= 20 \log \left( \frac{\sqrt{e_{n,i}(1\text{kHz}, x, f_{c,i})^2 + e_{n,R0}^2} + i_{n,i}(1\text{kHz}, x, f_{c,i})^2 R_0^2}{e_{n,R0}} \right) \quad (10.13)
 \end{aligned}$$

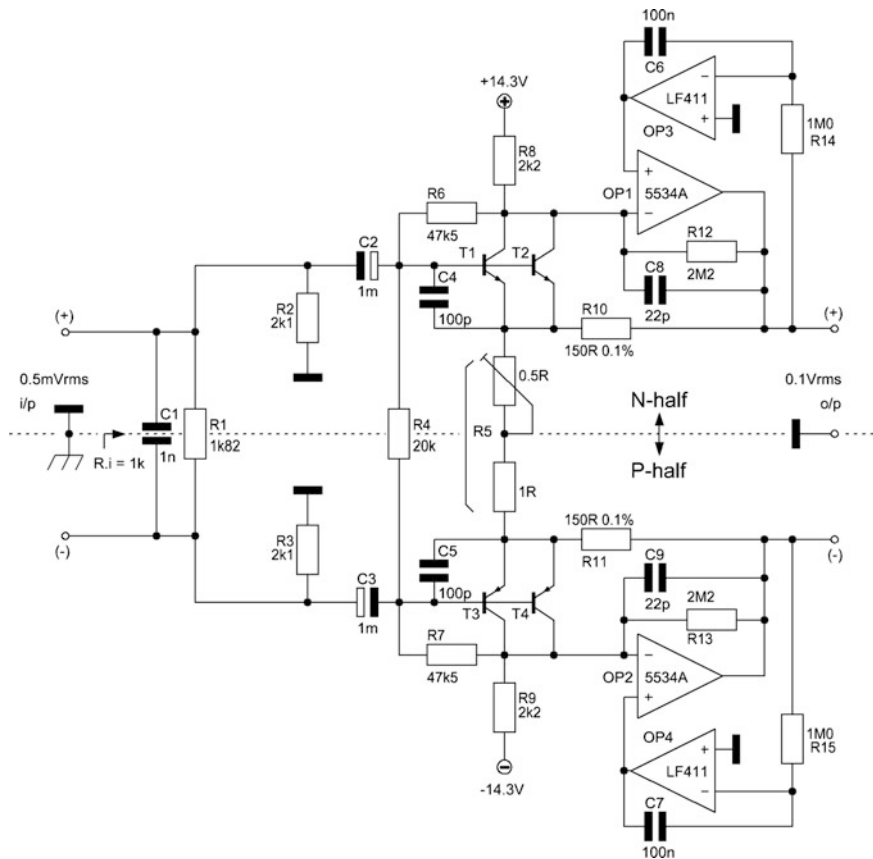
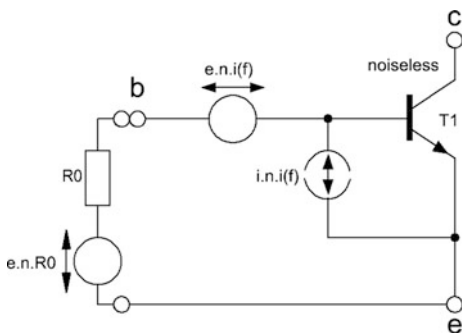


**Fig. 10.12** Amp2 with all noise calculation relevant active and passive components

**Fig. 10.13** Input load situation of a BJT



The P channel equations for  $NF_{e,p.10}(y,f_{c,i})$  and  $NF_{e,p.1k}(y,f_{c,i})$  look the same, however, with adapted NF values according to points 1 & 2 from above:

$$\begin{aligned} NF_{e,p.10}(y,f_{c,i}) &= 9.5 \\ NF_{e,p.1k}(y,f_{c,i}) &= 5 \end{aligned} \quad (10.14)$$

4. This step of the search process needs some patience. Without big math, I found the following successive approximation (succ-apps) approach rather easy to handle. Starting with guessed values for  $x$  and  $f_{c,i}$  in (10.12) and (10.13) further changes of  $0.1 < x (y) < 0.5$  and  $100 \text{ Hz} < f_{c,i} < 2 \text{ MHz}$  will gradually lead to the NF values required by the above given points 1 & 2

- The values for the N-BJT's become thus:  $x = 0.16965$  and  $f_{c,i} = 33,750 \text{ Hz}$ ;
- The values for the P-BJT's become thus:  $y = 0.1492$  and  $f_{c,i} = 55,650 \text{ Hz}$ ;

These specific 2SC3329 & 2SA1316 values of the input loaded circuit environment (that includes  $R_0 = 20 \Omega$ ) allow calculating Amp2's input referred SNs with  $10 \Omega < R_0 < 100 \Omega$  input load. Resulting SNs will show a  $< 1 \text{ dB}$  difference between measured and calculated values. SNs for input loads  $R_0 < 10 \Omega$  show deltas  $> 1 \text{ dB}$ , maximal  $1.5 \text{ dB}$  with  $R_0 = 0 \Omega$ .

Because of the BJT's application in an input load dependent connection to get noise figure values  $NF_e$  à la Figs. 10.8, 10.9, 10.10 and 10.11, they do not show the BJT's stand-alone  $1/f$ -noise corner frequency and slope of its current noise. It won't be possible to get them neither with the demonstrated approach nor by studying the data sheet.

Mathcad Worksheets 11.1 and 11.2 demonstrate the 'x' and 'y' search process.

Note: Because of the uncertainty of the NF-picking in points 1 & 2 we should not wear out the exactness of  $x$  and  $y$  and  $f_{c,i}$ : for  $x$ ,  $y$  two digits after the decimal point is exact enough, hence,  $x = 1.70$  and  $y = 1.50$  will make it in our case here, and  $f_{c,i} \pm 2 \%$  will work well too.

### 10.3.4 The SN Calculation Process

Generally, and in full length exercised on next chapter's Mathcad Worksheets 11.3 ( $x, y > 0$ ), the SN calculation process is split in many steps. It begins with the calculation of all relevant gain-creating aspects of the amp, such as the BJT's reduced mutual conductance  $g_{m,red}$ , its input resistances  $r_{be}$  and  $R_i$ , gain setting resistor  $R_5$ , total input load  $Z_1$ , etc. The noise voltage densities  $e_{n,i,n}$  &  $e_{n,i,p}$  represent the BJT input noise voltages, including their emitter loads. Then follow separate calculations for the closed-loop input referred noise voltages of the two halves of Amp2. Figure 10.14 shows the N-half of Amp2 with all relevant noise voltage and noise current sources. Of course, with polarities inversed the P-half looks the same.

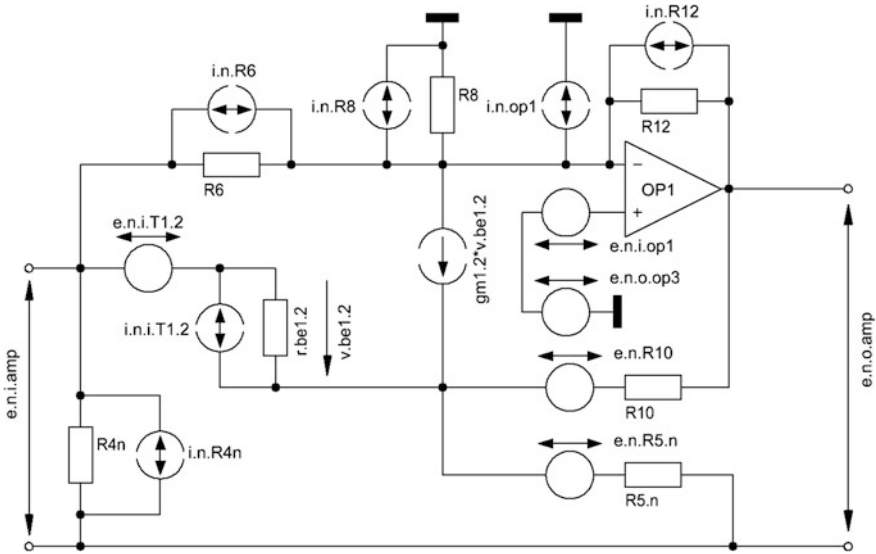


**Fig. 10.14** Upper (N) half of Amp2 (excl. input network Z1(f,R0)), showing all relevant noise sources (frequency independent)

In Fig. 10.14 “1.2” always indicates a relationship to the paralleled BJTs T1 and T2. The same applies to “3.4” for the not shown BJTs T3 & T4 in the P-half. The subscript “n” in the first place means noise, in the 2nd place means NPN. “i” in the first place means noise current, and as subscript it means “input related”.

The input referred noise voltages of both halves  $e_{n.i.amp,n}(f)$  &  $e_{n.i.amp,p}(f)$  include all relevant active and passive component’s noise sources, such as those of R8 (R9), R5n (R5p), R12 (R13), OP1 (OP2), and OP3 (OP4).

These input referred noise voltages have to be rms summed-up to form the input referred noise voltage  $e_{n.i.amp}(f)$  of the amp without input load.

$$e_{n.i.amp}(f) = \sqrt{e_{n.i.amp,n}(f)^2 + e_{n.i.amp,p}(f)^2} \tag{10.15}$$

The input referred noise currents of the halves have to be summed-up according to the rules of the summing of two series-connected noise current sources.<sup>6</sup> This noise current sum  $i_{n.i.amp}(f)$  is the input referred noise current of Amp2 too. Therefore, it needs no further treatment.

$$i_{n.i.amp}(f) = \sqrt{\left(\frac{1}{i_{n.i.n}(f)^2} + \frac{1}{i_{n.i.p}(f)^2}\right)^{-1}} \tag{10.16}$$

<sup>6</sup>See TSOS-1 Chap. 3 or TSOS-2 Chap. 4.

With the input referred noise current densities of the two pairs of BJTs ( $i_{n.T.b1.2}(f)$  &  $i_{n.T.b3.4}(f)$ ) the following two equations are given in the most practical form:

$$i_{n.i.n}(f) = \sqrt{i_{n.T.b1.2}(f)^2 + i_{n.R6}^2 + i_{n.R4n}^2} \quad (10.17)$$

$$i_{n.i.p}(f) = \sqrt{i_{n.T.b3.4}(f)^2 + i_{n.R7}^2 + i_{n.R4p}^2} \quad (10.18)$$

The additional inclusion of the frequency and R0 dependent input load impedance  $Z_{iL}(f, R0)$  yields the following equations:

$$Z_{iL}(f, R0) = \left| \begin{array}{c} \left( R0^{-1} + R1^{-1} + 2j\pi f C1 + (R2 + R3)^{-1} \right)^{-1} \\ + (2j\pi f C2)^{-1} + (2j\pi f C3)^{-1} \end{array} \right| \quad (10.19)$$

If C1, C2, and C3 are chosen of sizes that do not hurt a flat frequency and phase response in  $B_{20k}$  (10.22) could be simply written as frequency independent, but R0 dependent, impedance  $Z_{iL}(R0)$ :

$$Z_{iL}(R0) = \left( R0^{-1} + R1^{-1} + (R2 + R3)^{-1} \right)^{-1} \quad (10.20)$$

The output referred frequency and R0 dependent Amp2 noise voltage density  $e_{n.o.amp}(f, R0)$  thus becomes:

$$e_{n.o.amp}(f, R0) = G_{amp} \sqrt{\frac{e_{n.i.amp}(f)^2 + i_{n.i.amp}(f)^2 Z_{iL}(f, R0)^2}{+ e_{n.z.iL}(f, R0)^2}} \quad (10.21)$$

Now we can calculate the R0 dependent output referred non-equalized  $SN_{ne.o}(R0)$ :

$$SN_{ne.o}(R0) = 20 \log \left( \frac{\sqrt{\frac{1}{B_1} \int_{20Hz}^{20kHz} |e_{n.o.amp}(f, R0)|^2 df}}{v_{o,nom}} \right) \quad (10.22)$$

With  $v_{o,nom} = 100 \text{ mV}_{RMS}$ ,  $v_{i,nom} = 0.5 \text{ mV}_{RMS}$ , and  $G_{amp} = 200$  we can calculate the input referred  $SN_{ne.i}(R0)$  too. We will obtain the same result because  $v_{o,nom} / v_{i,nom} = G_{amp}$ .

**Table 10.1** Amp2 non-weighted SN results for two different input loads

1/A	B	C	D	E	F	G	H	I
2	R0	SN <sub>ne</sub>			Delta 1	Delta 2	Delta 3	Remarks
3		Calculated		Measured	E-D	E-C	D-C	
4		wn based	f <sub>c,i</sub> based					
5	Ω	dB ref. 0.5 V <sub>rms</sub>			dB	dB	dB	
6	0	-78.592	-75.768	-75.370	0.398	3.222	2.824	
7	20	-74.005	-72.801	-73.130	-0.329	0.875	1.204	See remarks for Table 10.2

**Table 10.2** Same as Table 10.1 after RIAA equalization and A-weighting

1/A	B	C	D	E	F	G	H	I
2	R0	SN <sub>ariaa</sub>			Delta 1	Delta 2	Delta 3	Remarks
3		Calculated		Measured	E-D	E-C	D-C	
4		wn based	f <sub>c,i</sub> based					
5	Ω	dB(A) ref. 0.5 V <sub>rms</sub>			dB	dB	dB	
6	0	-86.440	-83.095	-81.600	1.495	4.840	3.345	
7	5	-84.845	-82.283	-81.200	1.083	3.645	2.562	x, y, f <sub>c,i</sub> calculated for R0 = 10 Ω +10 Ω
8	10	-83.637	-81.571	-80.700	0.871	2.937	2.066	
9	20	-81.933	-80.431	-79.800	0.631	2.133	1.502	
10	43	-79.557	-78.612	-78.400	0.212	1.157	0.945	

### 10.3.5 Results

Based on two different input loads Table 10.1 shows the non-weighted output referred SN<sub>ne,o</sub> = SN<sub>ne,i</sub> of Amp2. The calculated column is split into two versions: wn in column C is based on white noise (x = 0 and y = 0) only, ‘f<sub>c,i</sub> based’ in column D includes the found x, y, and f<sub>c,i</sub> values of Sect. 10.3.3, Point 4. Column E shows the measured SN results. Delta values are given in columns F, G, and H. F indicates that the presented calculation approach works, whereas G gives a signal that it would be better not to set on a white noise approach only. Table 10.2’s column G shows why: A-weighted and RIAA equalized SN result differences increase stronger with decreasing R0s.

In Table 10.2 we find the more realistic measured and calculated A-weighted and RIAA equalized SNs for a broader range of input R0 s, from 0 Ω to 43 Ω (my DL-103). It shows the SNs of the outcome after adding low-noise RIAA stages à la Amps 3 & 4 & 5 and A-weighting to the Amp2 output, thus, SN<sub>ariaa,o</sub>(R0) = SN<sub>ariaa,i</sub>(R0).

Because of the rather vague NF picking process with a guessed error of ± 0.0–± 0.3 dB, we should set the SN exactness to one digit after the decimal point. According to the <1 dB goal from the beginning of this chapter we can see that down to 10 Ω input load the x, y, f<sub>c,i</sub> based math works quite well (columns D, E, & F).

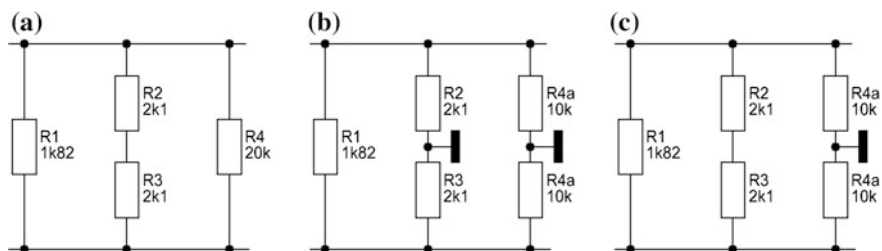


**Fig. 10.15** Input resistor alternatives (input Cs not shown)

Although the  $w_n$ -based results (C) look better, the deltas (G) don't look equally good and worse than the Table 10.1 ones.

Figure 12.1a shows a very flat frequency and phase response of Amp2, followed by Amp4 + Amp5 + Trafo.

## 10.4 Additional Remarks

### 10.4.1 Input Resistors R2, R3, R4

Additionally, I have checked three other alternatives with the input resistor's arrangements à la Fig. 10.15, however, without any audible change in sound and SN:

- Without connection to ground and cold ends of R2 and R3 tied together,
- Halving of R4 and connection of the newly created cold ends of R4a = 10 k $\Omega$  and R4b = 10 k $\Omega$  to ground,
- Both versions.

The switching transient phenomenon, mentioned at the end of Sect. 10.1, became worth with these alternatives in place.

### 10.4.2 Wild Oscillation

A measure to take care of is the prevention of wild oscillation. Depending on the location of the amp's PCB in the case there might be a tendency of ringing at very high frequencies >1 MHz. It can happen without producing any audible indication while listening to music or other signals.

Not touching the overall performance, a ceramic capacitance of approximately 100 p–1 n parallel to R10 or R11 or parallel to each resistor will sufficiently damp any oscillation. Like in the Amp1 case, it becomes a trial and error approach.



## Contents

- 11.1 MCD-WS: Evaluation of the 1/f-Noise Corner Frequency of a 2SA1316 BJT
- 11.2 MCD-WS: Evaluation of the 1/f-Noise Corner Frequency of a 2SC3329 BJT
- 11.3 MCD-WS: Amp2 SN and Gain Calculations—1/f-Noise Based Version

**Note 1:** MCD 11 has no built-in unit “rtHz” or “ $\sqrt{\text{Hz}}$ ”. To get  $\sqrt{1\text{Hz}}$  based voltage noise current noise densities the rms noise voltage current in a specific frequency range  $B > 1\text{ Hz}$  must be multiplied by  $\sqrt{1\text{Hz}}$  divided by the root of that specific frequency range  $\sqrt{B}$ !

**Note 2:** MCD 11 offers no “dB” unit. This is available from MCD 13 on!

## 11.1 MCD-WS: Evaluation of the 1/f-Noise Corner Frequency of a 2SA1316 BJT

Page 1

1/f-Noise Evaluation of 2SA1316 with  $R_0 = 10\Omega$  and  $I_C = 2.2\text{mA}$ 1. General data :

$$\begin{array}{lll}
 k := 1.38065 \cdot 10^{-23} \cdot \text{V} \cdot \text{A} \cdot \text{s} \cdot \text{K}^{-1} & q := 1.6021765 \cdot 10^{-19} \text{A} \cdot \text{s} & T := 300 \cdot \text{K} \\
 B_{20k} := 19980 \cdot \text{Hz} & B_1 := 1 \text{Hz} & h := 1000 \text{Hz} & f := 10 \text{Hz}, 20 \text{Hz}, 10^5 \text{Hz} \\
 r_{bb} := 2\Omega & e_{n,rbb} := \sqrt{4 \cdot k \cdot T \cdot B_1 \cdot r_{bb}} & e_{n,rbb} = 182.032 \times 10^{-12} \text{V} \\
 R_0 := 10\Omega & e_{n,R0} := \sqrt{4 \cdot k \cdot T \cdot B_1 \cdot R_0} & e_{n,R0} = 407.036 \times 10^{-12} \text{V} \\
 h_{fe} := 500 & I_C := 2.2 \cdot 10^{-3} \text{A} & g_m := \frac{q \cdot I_C}{k \cdot T}
 \end{array}$$

2. Evaluation of 'x' and the current noise density corner frequency 'f<sub>c,i</sub>':succ-apps of 'x' and 'f<sub>c,i</sub>' lead to the results of (1) & (2) further down in '3.3'!

$$\text{succ-apps of 'x':} \quad x := 0.1492 \quad \text{succ-apps of 'f}_{c,i}\text{':} \quad f_{c,i} := 55650 \text{Hz}$$

3. Density curves based on results of '2.' and relevant NF equations :

## 3.1 The current noise density curve :

$$i_{n,c}(f) := \sqrt{2 \cdot q \cdot I_C \cdot B_1} \cdot \left(1 + \frac{f_{c,i}}{f}\right)^x \quad i_{n,c}(h) = 48.491 \times 10^{-12} \text{A}$$

$$i_{n,i}(f) := \sqrt{\frac{2 \cdot q \cdot I_C}{h_{fe}} \cdot B_1} \cdot \left(1 + \frac{f_{c,i}}{f}\right)^x \quad i_{n,i}(h) = 2.169 \times 10^{-12} \text{A}$$

$$i_{n,il}(f) := \sqrt{\frac{2 \cdot q \cdot I_C}{h_{fe}} \cdot B_1} \quad i_{n,il}(f) := \sqrt{\frac{2 \cdot q \cdot I_C}{h_{fe}} \cdot B_1} \cdot \left(\frac{f_{c,i}}{f}\right)^x$$

$$i_{n,e1}(f) := \sqrt{2 \cdot q \cdot I_C \cdot B_1} \quad i_{n,e2}(f) := \sqrt{2 \cdot q \cdot I_C \cdot B_1} \cdot \left(\frac{f_{c,i}}{f}\right)^x$$

11.1 MCD-WS: Evaluation of the 1/f-Noise Corner Frequency of a 2SA1316 BJT

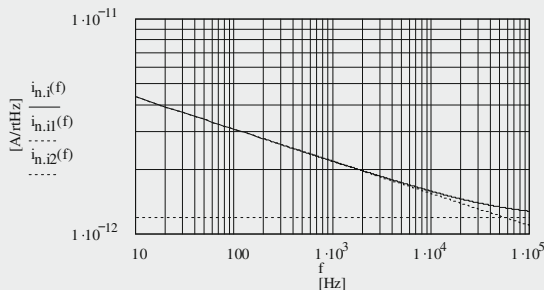


Fig. 11.1  
2SA1316 current noise density curve and its tangents, after succ-apps and the chosen input load

3.2 The voltage noise density curve :

$$e_{n,i}(f) := \sqrt{e_{n,rbb}^2 + i_{n,i}(f)^2 \cdot r_{bb}^2 + \frac{i_{n,c1}(f)^2}{g_m^2}} \quad e_{n,i}(h) = 598.196 \times 10^{-12} \text{V}$$

$$e_{n,il}(f) := \sqrt{e_{n,rbb}^2 + i_{n,il}(f)^2 \cdot r_{bb}^2 + \frac{i_{n,c1}(f)^2}{g_m^2}} \quad (3) \quad e_{n,i2}(f) := \sqrt{i_{n,i2}(f)^2 \cdot r_{bb}^2 + \frac{i_{n,c2}(f)^2}{g_m^2}} \quad (4)$$

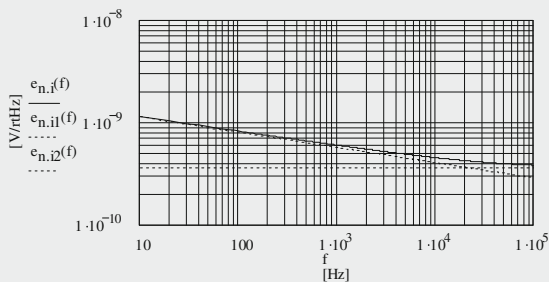


Fig. 11.2  
2SA1316 voltage noise density curve and its tangents, after succ-apps and the chosen input load

11.1 MCD-WS: Evaluation of the 1/f-Noise Corner Frequency of a 2SA1316 BJT

3.3 NF equations for succ-apps purposes :

**succ-apps goals :**       $NF(10Hz) = 9.5$       [dB]       $NF(1kHz) = 5$       [dB]

$$NF_{e,1k} := 20 \cdot \log \left( \frac{\sqrt{e_{n,R0}^2 + R0^2 \cdot i_{n,i}(h)^2 + e_{n,i}(h)^2}}{e_{n,R0}} \right) \quad NF_{e,1k} = 5.001 \quad [dB] \quad (1)$$

$$NF_{e,10} := 20 \cdot \log \left( \frac{\sqrt{e_{n,R0}^2 + R0^2 \cdot i_{n,i}(10Hz)^2 + e_{n,i}(10Hz)^2}}{e_{n,R0}} \right) \quad NF_{e,10} = 9.501 \quad [dB] \quad (2)$$

4. Evaluation of the voltage noise density corner frequency 'f<sub>c,e</sub>' :

From 3.2 and Fig. 11.2 we can arrange (3) and (4) as follows :

$$\sqrt{e_{n,rbb}^2 + i_{n,il}(f)^2 \cdot r_{bb}^2 + \frac{i_{n,cl}(f)^2}{g_m^2}} = \sqrt{i_{n,c2}(f)^2 \cdot r_{bb}^2 + \frac{i_{n,c2}(f)^2}{g_m^2}}$$

=>

$$\sqrt{e_{n,rbb}^2 + \frac{2 \cdot q \cdot I_C}{h_{fe}} \cdot B_1 \cdot r_{bb}^2 + \frac{(2 \cdot q \cdot I_C \cdot B_1)^2}{g_m^2}} - \sqrt{\left[ \frac{2 \cdot q \cdot I_C}{h_{fe}} \cdot B_1 \cdot \left( \frac{f_{c,i}}{f} \right)^x \right]^2 \cdot r_{bb}^2 + \frac{\left[ \sqrt{2 \cdot q \cdot I_C \cdot B_1} \cdot \left( \frac{f_{c,i}}{f} \right)^x \right]^2}{g_m^2}} = 0 \quad (5)$$

To get 'f' solving of (5) leads to 'f<sub>c,e</sub> = 20.85kHz'

f<sub>c,e</sub> := 20850Hz

## 11.1 MCD-WS: Evaluation of the 1/f-Noise Corner Frequency of a 2SA1316 BJT

Page 4

5. Slope of 'f<sub>c,i</sub>' (incl. a given R0) :

$$20 \cdot \log \left[ \frac{\left( \frac{f_{c,i}}{10\text{Hz}} \right)^x}{\left( \frac{f_{c,i}}{100\text{Hz}} \right)^x} \right] = 2.984 \Rightarrow \text{slope } i = -3.0\text{dB/dec or } -0.9\text{dB/oct.}$$

6. Slope of 'f<sub>c,e</sub>' (incl. a given R0) :

$$20 \cdot \log \left[ \frac{\left( \frac{f_{c,e}}{10\text{Hz}} \right)^x}{\left( \frac{f_{c,e}}{100\text{Hz}} \right)^x} \right] = 2.984 \Rightarrow \text{slope } e = -3.0\text{dB/dec or } -0.9\text{dB/oct.}$$

7. Input referred SN with the chosen input load R0 and based on the evaluated corner frequencies from above :

$$e_{n,i}(f) := \sqrt{e_{n,R0}^2 + R0^2 \cdot i_{n,i}(f)^2 + e_{n,i}(f)^2}$$

$$SN_i := 20 \cdot \log \left[ \frac{\sqrt{\frac{1}{B_1} \cdot \int_{20\text{Hz}}^{2000\text{Hz}} (|e_{n,i}(f)|)^2 df}}{0.5 \cdot 10^{-3} \text{V}} \right] \quad SN_i = -75.02 \quad [\text{dB}]$$

## 11.2 MCD-WS: Evaluation of the 1/f-Noise Corner Frequency of a 2SC3329 BJT

Page 1

1/f-Noise Evaluation of 2SC3329 with  $R_0 = 10\Omega$  and  $I_C = 2.2\text{mA}$ 1. General data :

$$\begin{array}{lll}
 k := 1.38065 \cdot 10^{-23} \cdot \text{V} \cdot \text{A} \cdot \text{s} \cdot \text{K}^{-1} & q := 1.6021765 \cdot 10^{-19} \text{A} \cdot \text{s} & T := 300 \cdot \text{K} \\
 B_{20k} := 19980 \cdot \text{Hz} & B_1 := 1 \text{Hz} & h := 1000 \text{Hz} & f := 10 \text{Hz}, 20 \text{Hz}, 10^5 \text{Hz} \\
 r_{bb} := 2\Omega & e_{n,rbb} := \sqrt{4 \cdot k \cdot T \cdot B_1 \cdot r_{bb}} & e_{n,rbb} = 182.032 \times 10^{-12} \text{V} \\
 R_0 := 10\Omega & e_{n,R0} := \sqrt{4 \cdot k \cdot T \cdot B_1 \cdot R_0} & e_{n,R0} = 407.036 \times 10^{-12} \text{V} \\
 h_{fe} := 500 & I_C := 2.2 \cdot 10^{-3} \text{A} & g_m := \frac{q \cdot I_C}{k \cdot T}
 \end{array}$$

2. Evaluation of 'x' and the current noise density corner frequency 'f<sub>c,i</sub>' :succ-apps of 'x' and 'f<sub>c,i</sub>' lead to the results of (1) & (2) further down in '3.3'!succ-apps of 'x':      x := 0.16965      succ-apps of 'f<sub>c,i</sub>':      f<sub>c,i</sub> := 33750 Hz3. Density curves based on results of '2.' and relevant NF equations :

## 3.1 The current noise density curve :

$$i_{n,c}(f) := \sqrt{2 \cdot q \cdot I_C \cdot B_1} \cdot \left(1 + \frac{f_{c,i}}{f}\right)^x \qquad i_{n,c}(h) = 48.474 \times 10^{-12} \text{A}$$

$$i_{n,i}(f) := \sqrt{\frac{2 \cdot q \cdot I_C}{h_{fe}} \cdot B_1} \cdot \left(1 + \frac{f_{c,i}}{f}\right)^x \qquad i_{n,i}(h) = 2.168 \times 10^{-12} \text{A}$$

$$i_{n,il}(f) := \sqrt{\frac{2 \cdot q \cdot I_C}{h_{fe}} \cdot B_1} \qquad i_{n,il}(f) := \sqrt{\frac{2 \cdot q \cdot I_C}{h_{fe}} \cdot B_1} \cdot \left(\frac{f_{c,i}}{f}\right)^x$$

$$i_{n,c1}(f) := \sqrt{2 \cdot q \cdot I_C \cdot B_1} \qquad i_{n,c2}(f) := \sqrt{2 \cdot q \cdot I_C \cdot B_1} \cdot \left(\frac{f_{c,i}}{f}\right)^x$$

11.2 MCD-WS: Evaluation of the 1/f-Noise Corner Frequency of a 2SC3329 BJT

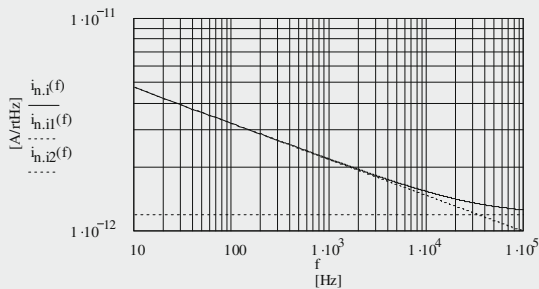


Fig. 11.3  
2SC3329 current noise density curve and its tangents, after succ-apps and the chosen input load

3.2 The voltage noise density curve :

$$e_{n,i}(f) := \sqrt{e_{n,rbb}^2 + i_{n,i}(f)^2 \cdot r_{bb}^2 + \frac{i_{n,c}(f)^2}{g_m^2}}$$

$$e_{n,i}(h) = 598.003 \times 10^{-12} \text{V}$$

$$e_{n,il}(f) := \sqrt{e_{n,rbb}^2 + i_{n,il}(f)^2 \cdot r_{bb}^2 + \frac{i_{n,c1}(f)^2}{g_m^2}} \quad (3)$$

$$e_{n,iz}(f) := \sqrt{i_{n,iz}(f)^2 \cdot r_{bb}^2 + \frac{i_{n,c2}(f)^2}{g_m^2}} \quad (4)$$

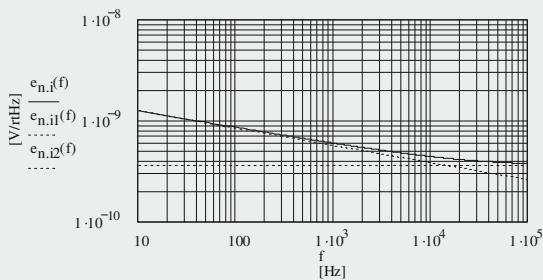


Fig. 11.4  
2SC3329 voltage noise density curve and its tangents, after succ-apps and the chosen input load





## 11.2 MCD-WS: Evaluation of the 1/f-Noise Corner Frequency of a 2SC3329 BJT

Page 4

5. Slope of 'f<sub>c,i</sub>' (incl. a given R0!):

$$20 \cdot \log \left[ \frac{\left( \frac{f_{c,i}}{10\text{Hz}} \right)^x}{\left( \frac{f_{c,i}}{100\text{Hz}} \right)^x} \right] = 3.393 \Rightarrow \text{slope } i = -3.4\text{dB/dec or } -1.1\text{dB/oct.}$$

6. Slope of 'f<sub>c,e</sub>' (incl. a given R0!):

$$20 \cdot \log \left[ \frac{\left( \frac{f_{c,e}}{10\text{Hz}} \right)^x}{\left( \frac{f_{c,e}}{100\text{Hz}} \right)^x} \right] = 3.393 \Rightarrow \text{slope } e = -3.4\text{dB/dec or } -1.1\text{dB/oct.}$$

7. Input referred SN with the chosen input load R0 and based on the evaluated corner frequencies from above:

$$e_{n,i}(f) := \sqrt{e_{n,R0}^2 + R0^2 \cdot i_{n,i}(f)^2 + e_{n,i}(f)^2}$$

$$SN_i := 20 \cdot \log \left[ \frac{\frac{1}{B_1} \cdot \int_{20\text{Hz}}^{20000\text{Hz}} (|e_{n,i}(f)|)^2 df}{0.5 \cdot 10^{-3} \text{V}} \right] \quad SN_i = -75.107 \quad [\text{dB}]$$

11.3 MCD-WS: Amp2 SN and Gain Calculations - 1/f-Noise Based Version

Amp2 SN and Gain Calculations - 1/f-Noise Based (x = 0.15, y = 0.17)

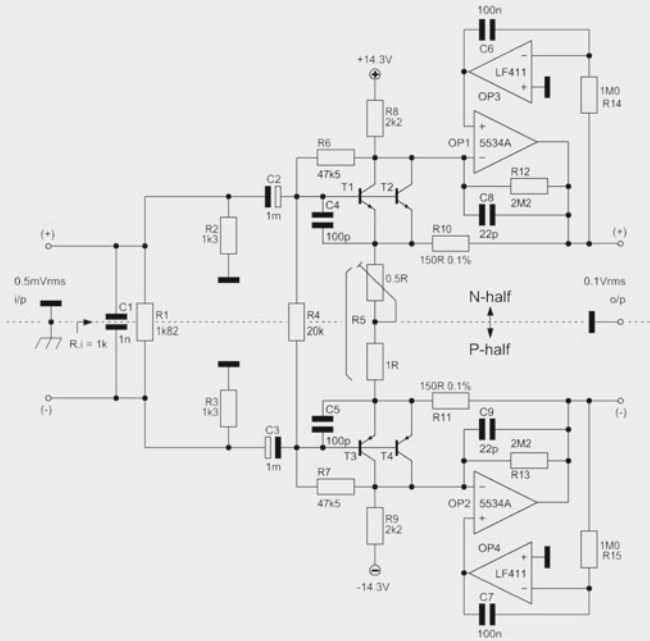


Fig. 11.5 = Fig. 10.12

1. Definition of all meaningful constants, components, gain setting resistance R5, etc. :

- |  |   |                                |                                    |
|--|---|--------------------------------|------------------------------------|
| $k := 1.38065 \cdot 10^{-23} \cdot V \cdot A \cdot s \cdot K^{-1}$ | $q := 1.6021765 \cdot 10^{-19} A \cdot s$ | $T := 300 \cdot K$             | $v_{i,nom} := 0.5 \cdot 10^{-3} V$ |
| $B_{20k} := 19980 \cdot Hz$  | $B_1 := 1Hz$                              | $h := 1000Hz$                  | $v_{o,nom} := 0.1V$                |
| $R0 := 20\Omega$   | $R1 := 1.82 \cdot 10^3 \Omega$            | $R2 := 1.3 \cdot 10^3 \Omega$  | $R3 := R2$                         |
| $R4 := 20 \cdot 10^3 \Omega$                                       | $R5 = tbd$                                | $R6 := 47.5 \cdot 10^3 \Omega$ | $R7 := R6$                         |
| $R8 := 2.2 \cdot 10^3 \Omega$                                      | $R9 := R8$                                | $R10 := 150\Omega$             | $R11 := R10$                       |
| $R12 := 2.2 \cdot 10^6 \Omega$                                     | $R13 = R12$                               | $R14 := 1 \cdot 10^6 \Omega$   | $R15 = R14$                        |
| $C1 := 1.0 \cdot 10^{-9} F$  | $C2 := 1 \cdot 10^{-3} F$                 | $C3 := C2$                     | $C4 := 100 \times 10^{-12} F$      |
| $C5 := C4$   | $C6 := 100 \cdot 10^{-9} F$               | $C7 := C6$                     |                                    |
| $C8 := 10 \cdot 10^{-12} F$  | $C9 := C8$                                |                                |                                    |

11.3 MCD-WS: Amp2 SN and Gain Calculations - 1/f-Noise Based Version

$$\begin{aligned}
 NI_e &:= -30 \text{ [dB]} & NI &:= 10^{\frac{NI_e}{20}} \cdot 10^{-6} & NI &= 31.623 \times 10^{-9} \\
 G_{amp} &:= 200 & & & & \\
 G_{amp} &:= \frac{R10 + R11}{R5} + 1 & R5 &:= \frac{R10 + R11}{G_{amp} - 1} & R5 &= 1.508 \Omega \\
 R5_n &:= 0.5 \cdot R5 & R5_n &= 753.769 \times 10^{-3} \Omega & R5_p &:= R5_n \\
 G_n &:= \frac{R10}{R5_n} + 1 & G_p &:= G_n & G_n &= 200 \\
 R0_n &:= R0 \cdot 0.5 & R1_n &:= R1 \cdot 0.5 & R2_n &:= R2 & R4_n &:= R4 \cdot 0.5 \\
 R0_p &:= R0_n & R1_p &:= R1_n & R3_p &:= R3 & R4_p &:= R4_n \\
 I_{C1.2} &:= 4.4 \cdot 10^{-3} \text{ A} & h_{fe1.2} &:= 500 & r_{bb1.2} &:= \frac{2 \Omega}{2} & V_{A,n} &:= -160 \text{ V} \\
 I_{C3.4} &:= -I_{C1.2} & h_{fe3.4} &:= h_{fe1.2} & r_{bb3.4} &:= r_{bb1.2} & V_{A,p} &:= 77 \text{ V} \\
 V_{DC.C1.2} &:= R8 \cdot I_{C1.2} & V_{DC.C1.2} &= 9.68 \text{ V} & V_{DC.E1.2} &:= I_{C1.2} \cdot \frac{R5}{2} & V_{DC.E1.2} &= 3.317 \times 10^{-3} \text{ V} \\
 V_{DC.C3.4} &:= R9 \cdot I_{C3.4} & V_{DC.C3.4} &= -9.68 \text{ V} & V_{DC.E3.4} &:= -V_{DC.E1.2} & & 
 \end{aligned}$$

2. Calculation of the amp's input resistance  $R_i$  :

$$\begin{aligned}
 r_{ce1.2n} &:= \frac{|V_{A,n}|}{I_{C1.2}} & r_{ce1.2n} &= 36.364 \times 10^3 \Omega & g_{m1.2} &:= \frac{q \cdot I_{C1.2}}{k \cdot T} & g_{m1.2} &= 170.199 \times 10^{-3} \text{ S} \\
 r_{be1.2} &:= \frac{h_{fe1.2}}{g_{m1.2}} & r_{be1.2} &= 2.938 \times 10^3 \Omega & & & & \\
 R_{i1.2} &:= \left[ \frac{1}{\left( r_{be1.2} + h_{fe1.2} \cdot R5_n \right) \left( 1 + g_{m1.2} \cdot R12 \cdot \frac{R5_n}{R10 + R5_n} \right)} + \frac{1}{R6 + \left( \frac{1}{R8} + \frac{1}{r_{ce1.2n}} \right)^{-1}} \right]^{-1} & & & & & & R_{i1.2} &= 49.182 \times 10^3 \Omega \\
 r_{ce3.4} &:= \frac{V_{A,p}}{I_{C1.2}} & r_{ce3.4} &= 17.5 \times 10^3 \Omega & g_{m3.4} &:= \frac{q \cdot |I_{C3.4}|}{k \cdot T} & g_{m3.4} &= 170.199 \times 10^{-3} \text{ S} \\
 r_{be3.4} &:= \frac{h_{fe3.4}}{g_{m3.4}} & r_{be3.4} &= 2.938 \times 10^3 \Omega & & & & R4_p &:= R4_n
 \end{aligned}$$

11.3 MCD-WS: Amp2 SN and Gain Calculations - 1/f-Noise Based Version

$$R_{i,3.4} := \left[ \frac{1}{\left( r_{be3.4} + h_{fe3.4} R_{5p} \right) \cdot \left( 1 + g_{m3.4} R_{13} \cdot \frac{R_{5p}}{R_{11} + R_{5p}} \right)} + \frac{1}{R_7 + \left( \frac{1}{R_9} + \frac{1}{r_{ce3.4}} \right)^{-1}} \right]^{-1}$$

$$R_{i,3.4} = 49.064 \times 10^3 \Omega$$

$$R_{i,tot,n} := \left( \frac{1}{R_{i,1.2}} + \frac{1}{R_{4n}} \right)^{-1}$$

$$R_{i,tot,n} = 8.31 \times 10^3 \Omega$$

$$R_{i,tot,p} := \left( \frac{1}{R_{i,3.4}} + \frac{1}{R_{4p}} \right)^{-1}$$

$$R_{i,tot,p} = 8.307 \times 10^3 \Omega$$

$$R_{i,tot} := \left( \frac{1}{R_4} + \frac{1}{R_{i,1.2} + R_{i,3.4}} \right)^{-1}$$

$$R_{i,tot} = 16.617 \times 10^3 \Omega$$

3. Evaluation of the impedance of the input network :

$R_0 := 0\Omega, 1\Omega, 100\Omega$   $f := 10\text{Hz}, 11\text{Hz}, 20000\text{Hz}$

$Z_{iL}$  incl.  $R_0$  is the total noise-relevant **input load**, composed by  $Z_{iL,n} + Z_{iL,p}$

$$Z_{iL,n}(f, R_0) := 0.5 \cdot \left[ R_0^{-1} + 2j \cdot \pi \cdot f \cdot C_1 + R_1^{-1} + (R_2 + R_3)^{-1} \right]^{-1} + (2j \cdot \pi \cdot f \cdot C_2)^{-1} + (2j \cdot \pi \cdot f \cdot C_3)^{-1}$$

$$Z_{iL,p}(f, R_0) := Z_{iL,n}(f, R_0) \quad Z_{iL}(f, R_0) := Z_{iL,n}(f, R_0) + Z_{iL,p}(f, R_0) \quad Z_{iL,n}(h, 20\Omega) = 9.818 \Omega$$

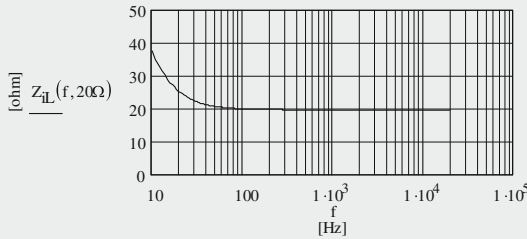


Fig. 11.6  
Impedance of the input network  $Z_{iL}(f)$

$Z_i(f)$  is the frequency dependent **input impedance** (~  $R_i$  from Fig. 11.5), composed by  $Z_{i,n}(f) + Z_{i,p}(f)$

$$Z_{i,n}(f) := 0.5 \cdot \left[ \left( 2j \cdot \pi \cdot f \cdot C_1 + \frac{1}{R_1} + \frac{1}{R_2 + R_3} \right)^{-1} + (2j \cdot \pi \cdot f \cdot C_2)^{-1} + (2j \cdot \pi \cdot f \cdot C_3)^{-1} \right]^{-1} + \frac{1}{R_{i,tot}}$$

$$Z_{i,n}(h) = 502.885 \Omega$$

$$Z_{i,p}(f) := Z_{i,n}(f) \quad Z_i(f) := Z_{i,n}(f) + Z_{i,p}(f) \quad Z_i(h) = 1005.771 \Omega$$

11.3 MCD-WS: Amp2 SN and Gain Calculations - 1/f-Noise Based Version

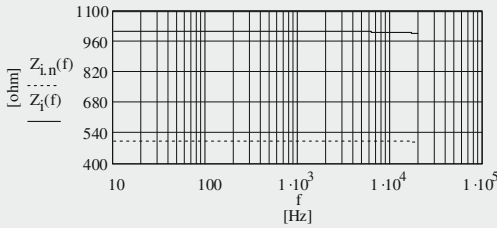


Fig. 11.7  
Input impedances  
 $Z_i(f)$  &  $Z_{i,n}(f)$

4. Gain evaluations : Gain equations for T1+T2 or T3+T4 : see Chapter 20

$$r_{ce1.2} := \frac{|V_{A,n}|}{I_{C1.2}} \quad r_{ce1.2} = 36.364 \times 10^3 \Omega$$

$$g_{m1.2,red} := \frac{g_{m1.2}(r_{ce1.2} + R8) \cdot \left( h_{fe1.2} - \frac{R5_n}{r_{ce1.2}} \right)}{h_{fe1.2}(r_{ce1.2} + R5_n + R8) + g_{m1.2} \cdot R5_n \cdot (h_{fe1.2} r_{ce1.2} + r_{ce1.2} + R8)}$$

$$g_{m1.2,red} = 151.795 \times 10^{-3} S$$

$$r_{ce3.4} := \frac{V_{A,p}}{|I_{C3.4}|} \quad r_{ce3.4} = 17.5 \times 10^3 \Omega$$

$$g_{m3.4,red} := \frac{g_{m3.4}(r_{ce3.4} + R9) \cdot \left( h_{fe3.4} - \frac{R5_p}{r_{ce3.4}} \right)}{h_{fe3.4}(r_{ce3.4} + R5_p + R9) + g_{m3.4} \cdot R5_p \cdot (h_{fe3.4} r_{ce3.4} + r_{ce3.4} + R9)}$$

$$g_{m3.4,red} = 152.747 \times 10^{-3} S$$

$$G_{1.2} := \left[ \frac{g_{m1.2,red} R6 - 1}{1 + R6 \cdot \left( \frac{1}{R8} + \frac{1}{r_{ce1.2}} \right)} \right]$$

$$G_{1.2} = -301.678$$

$$G_{1.2,e} := 20 \cdot \log(|G_{1.2}|)$$

$$G_{1.2,e} = 49.591 \quad [dB]$$

$$G_{3.4} := \left[ \frac{g_{m3.4,red} R7 - 1}{1 + R7 \cdot \left( \frac{1}{R9} + \frac{1}{r_{ce3.4}} \right)} \right]$$

$$G_{3.4} = -286.679$$

$$G_{3.4,e} := 20 \cdot \log(|G_{3.4}|)$$

$$G_{3.4,e} = 49.148 \quad [dB]$$

11.3 MCD-WS: Amp2 SN and Gain Calculations - 1/f-Noise Based Version

$$G_{0,n} := \xi_{m1.2} \cdot \text{red} \cdot R_{12}$$

$$G_{0,n} = 333.948 \times 10^3$$

$$G_{0,p} := \xi_{m3.4} \cdot \text{red} \cdot R_{13}$$

$$G_{0,p} = 336.043 \times 10^3$$

5. Calculation of the relevant noise currents and voltages of the whole amp

(<sub>n</sub> refers to the T1+T2 part, <sub>p</sub> refers to the T3+T4 part) :

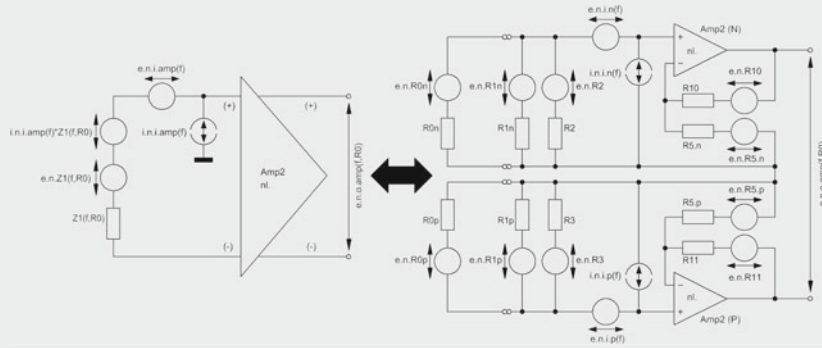


Fig. 11.8 Noise situation of Amp2, transferred into the upper half of the amp and into the lower half, and vice versa

5.1 BJT noise currents (for white-noise based calculations set  $x = 0$  &  $y = 0$ ) :

$$x := 0.16965$$

$$f_{c.i1.2} := 33.75 \cdot 10^3 \text{ Hz}$$

$$f_{c.e1.2} := 14.233 \cdot 10^3 \text{ Hz}$$

$$y := 0.1492$$

$$f_{c.i3.4} := 55.65 \cdot 10^3 \text{ Hz}$$

$$f_{c.e3.4} := 20.85 \cdot 10^3 \text{ Hz}$$

$$i_{h.T.c1.2}(f) := \sqrt{2 \cdot q \cdot |C_{1.2}| \cdot B_1} \cdot \left( \frac{f_{c.i1.2}}{f} + 1 \right)^x$$

$$i_{h.T.c1.2}(h) = 68.552 \times 10^{-12} \text{ A}$$

$$i_{h.T.b1.2}(f) := \sqrt{\frac{2 \cdot q \cdot |C_{1.2}|}{h_{fe1.2}}} \cdot B_1 \cdot \left( \frac{f_{c.i1.2}}{f} + 1 \right)^x$$

$$i_{h.T.b1.2}(h) = 3.066 \times 10^{-12} \text{ A}$$

$$i_{h.T.c3.4}(f) := \sqrt{2 \cdot q \cdot |C_{3.4}| \cdot B_1} \cdot \left( \frac{f_{c.i3.4}}{f} + 1 \right)^y$$

$$i_{h.T.c3.4}(h) = 68.576 \times 10^{-12} \text{ A}$$

$$i_{h.T.b3.4}(f) := \sqrt{\frac{2 \cdot q \cdot |C_{3.4}|}{h_{fe3.4}}} \cdot B_1 \cdot \left( \frac{f_{c.i3.4}}{f} + 1 \right)^y$$

$$i_{h.T.b3.4}(h) = 3.067 \times 10^{-12} \text{ A}$$

## 11.3 MCD-WS: Amp2 SN and Gain Calculations - 1/f-Noise Based Version

Page 6

## 5.2 Noise voltages and currents of resistors :

$$i_{n.R4.n} := \sqrt{\frac{4 \cdot k \cdot T \cdot B_1}{R_{4n}}}$$

$$i_{n.R4.p} := i_{n.R4.n}$$

$$i_{n.R4.n} = 1.287 \times 10^{-12} \text{ A}$$

$$i_{n.R5.n} := \sqrt{\frac{4 \cdot k \cdot T \cdot B_1}{R_{5n}}}$$

$$i_{n.R5.p} := i_{n.R5.n}$$

$$i_{n.R5.n} = 148.256 \times 10^{-12} \text{ A}$$

$$i_{n.R6} := \sqrt{\frac{4 \cdot k \cdot T \cdot B_1}{R_6}}$$

$$i_{n.R7} := i_{n.R6}$$

$$i_{n.R6} = 590.589 \times 10^{-15} \text{ A}$$

$$i_{n.R12} := \sqrt{\frac{4 \cdot k \cdot T \cdot B_1}{R_{12}}}$$

$$i_{n.R12} = 86.78 \times 10^{-15} \text{ A}$$

$$i_{n.R13} := \sqrt{\frac{4 \cdot k \cdot T \cdot B_1}{R_{12}}}$$

$$i_{n.R13} = 86.78 \times 10^{-15} \text{ A}$$

$$e_{Nex.R8(f)} := \sqrt{\left( \frac{NI_e}{10^{10} \cdot 10^{-12}} \right) \cdot \frac{(I_{C1.2} \cdot R_8)^2 \cdot B_1}{f}}$$

$$e_{Nex.R8(h)} = 6.379 \times 10^{-9} \text{ V}$$

$$e_{N.R8} := \sqrt{4 \cdot k \cdot T \cdot R_8 \cdot B_{20k}}$$

$$e_{N.R8} = 853.378 \times 10^{-9} \text{ V}$$

$$e_{N.R8.eff(f)} := \sqrt{e_{Nex.R8(f)}^2 + e_{N.R8}^2}$$

$$e_{N.R8.eff(h)} = 853.402 \times 10^{-9} \text{ V}$$

$$e_{n.R8.eff(f)} := e_{N.R8.eff(f)} \cdot \sqrt{\frac{B_1}{B_{20k}}}$$

$$e_{n.R9.eff(f)} := e_{n.R8.eff(f)}$$

$$e_{n.R8.eff(h)} = 6.037 \times 10^{-9} \text{ V}$$

$$i_{n.R8(f)} := \frac{e_{n.R8.eff(f)}}{R_8}$$

$$i_{n.R9(f)} := i_{n.R8(f)}$$

$$i_{n.R8(h)} = 2.744 \times 10^{-12} \text{ A}$$

$$e_{n.R14} := \sqrt{4 \cdot k \cdot T \cdot B_1 \cdot R_{14}}$$

$$e_{n.R15} := e_{n.R14}$$

$$e_{n.R14} = 128.716 \times 10^{-9} \text{ V}$$

$$e_{n.Z_{iL}(f,R0)} := \sqrt{4 \cdot k \cdot T \cdot B_1 \cdot Z_{iL}(f,R0)}$$

$$e_{n.Z_{iL}(h,20\Omega)} = 570.371 \times 10^{-12} \text{ V}$$

$$e_{n.R0(R0)} := \sqrt{4 \cdot k \cdot T \cdot B_1 \cdot R_0}$$

$$e_{n.R0(20\Omega)} = 575.635 \times 10^{-12} \text{ V}$$

$$R_{BE1.2} := r_{bb1.2} + \left( \frac{1}{R_{5n}} + \frac{1}{R_{10}} \right)^{-1}$$

$$R_{BE1.2} = 1.75 \Omega$$

$$R_{BE3.4} := r_{bb3.4} + \left( \frac{1}{R_{5p}} + \frac{1}{R_{11}} \right)^{-1}$$

$$R_{BE3.4} = 1.75 \Omega$$

$$e_{n.R.BE1.2} := \sqrt{4 \cdot k \cdot T \cdot B_1 \cdot R_{BE1.2}}$$

$$e_{n.R.BE1.2} = 170.275 \times 10^{-12} \text{ V}$$

$$e_{n.R.BE3.4} := \sqrt{4 \cdot k \cdot T \cdot B_1 \cdot R_{BE3.4}}$$

$$e_{n.R.BE3.4} = 170.275 \times 10^{-12} \text{ V}$$

## 11.3 MCD-WS: Amp2 SN and Gain Calculations - 1/f-Noise Based Version

Page 7

## 5.3 Noise of op-amps :

$$f_{c.e1} := 6\text{Hz}$$

$$f_{c.il} := 8\text{Hz}$$

$$f_{c.e3} := 0.1 \cdot 10^3 \text{Hz}$$

$$e_{n.i.op1} := 4 \cdot 10^{-9} \text{V}$$

$$e_{n.i.op1}(f) := e_{n.i.op1} \cdot \sqrt{\frac{f_{c.e1}}{f} + 1}$$

$$i_{n.i.op1} := 0.4 \cdot 10^{-12} \text{A}$$

$$i_{n.i.op1}(f) := i_{n.i.op1} \cdot \sqrt{\frac{f_{c.il}}{f} + 1}$$

$$e_{n.i.op2}(f) := e_{n.i.op1}(f)$$

$$i_{n.i.op2}(f) := i_{n.i.op1}(f)$$

$$e_{n.i.op3} := 25 \cdot 10^{-9} \text{V}$$

$$e_{n.i.op3}(f) := e_{n.i.op3} \cdot \sqrt{\frac{f_{c.e3}}{f} + 1}$$

$$e_{n.i.op4}(f) := e_{n.i.op3}(f)$$

$$i_{n.i.op3} := 0.01 \cdot 10^{-12} \text{A}$$

$$i_{n.i.op4} := i_{n.i.op3}$$

$$e_{n.o.op3}(f) := \sqrt{\left[ e_{n.R14} \frac{(2j \cdot \pi \cdot f \cdot C6)^{-1}}{R14} \right]^2 + e_{n.i.op3}(f)^2 \left[ 1 + \frac{(2j \cdot \pi \cdot f \cdot C6)^{-1}}{R14} \right]^2 + \left[ i_{n.i.op3} (2j \cdot \pi \cdot f \cdot C6)^{-1} \right]^2}$$

$$e_{n.o.op4}(f) := e_{n.o.op3}(f)$$

$$e_{n.o.op3}(h) = 26.219 \times 10^{-9} \text{V}$$

## 5.4 Input referred noise voltages of BJTs and Amp2 input :

$$e_{n.i.T1.2}(f) := \sqrt{\frac{i_{n.T.c1.2}(f)^2}{g_{m1.2}^2} + 4 \cdot k \cdot T \cdot r_{bb1.2} \cdot B_1}$$

$$e_{n.i.T1.2}(h) = 422.841 \times 10^{-12} \text{V}$$

$$e_{n.i.T3.4}(f) := \sqrt{\frac{i_{n.T.c3.4}(f)^2}{g_{m3.4}^2} + 4 \cdot k \cdot T \cdot r_{bb3.4} \cdot B_1}$$

$$e_{n.i.T3.4}(h) = 422.978 \times 10^{-12} \text{V}$$

$$e_{n.i.n}(f) := \sqrt{\frac{i_{n.T.c1.2}(f)^2}{g_{m1.2}^2} + e_{n.R.BE1.2}^2 + i_{n.T.b1.2}(f)^2 \cdot R_{BE1.2}^2}$$

$$e_{n.i.n}(h) = 437.321 \times 10^{-12} \text{V}$$

$$e_{n.i.p}(f) := \sqrt{\frac{i_{n.T.c3.4}(h)^2}{g_{m3.4}^2} + e_{n.R.BE3.4}^2 + i_{n.T.b3.4}(h)^2 \cdot R_{BE3.4}^2}$$

$$e_{n.i.p}(h) = 437.452 \times 10^{-12} \text{V}$$

$$i_{n.i.n}(f) := \sqrt{i_{n.T.b1.2}(f)^2 + i_{n.R6}^2 + i_{n.R4.n}^2}$$

$$i_{n.i.n}(h) = 3.377 \times 10^{-12} \text{A}$$

$$i_{n.i.p}(f) := \sqrt{i_{n.T.b3.4}(f)^2 + i_{n.R7}^2 + i_{n.R4.p}^2}$$

$$i_{n.i.p}(h) = 3.378 \times 10^{-12} \text{A}$$



11.3 MCD-WS: Amp2 SN and Gain Calculations - 1/f-Noise Based Version

**Note:** Because of the low DC voltage across R5+P1 (appr. 3 ...45 mV) any generated R5+P1-excess noise can fully be ignored.

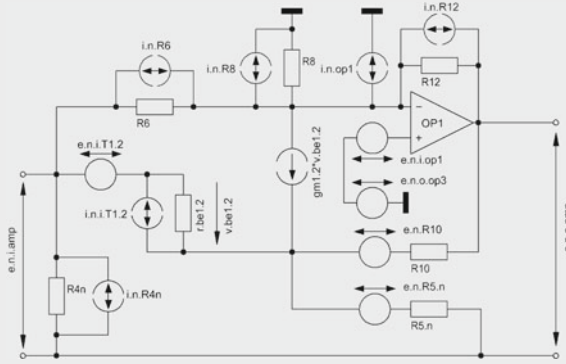


Fig. 11.9 = Fig. 10.14

$$e_{n.i.amp.f}(f) := \sqrt{\left[ e_{n.i.n}(f)^2 + \frac{e_{n.i.op1}(f)^2 + e_{n.o.op3}(f)^2}{(|G_{1.2}|)^2} \right] \dots} + \frac{i_{n.R8}(f)^2 + i_{n.i.op1}(f)^2 + i_{n.R12}(f)^2}{g_{m1.2}^2}$$

$$e_{n.i.amp.f}(h) = 446.369 \times 10^{-12}V$$

$$e_{n.i.amp.p}(f) := \sqrt{\left[ e_{n.i.p}(f)^2 + \frac{e_{n.i.op2}(f)^2 + e_{n.o.op4}(f)^2}{(|G_{3.4}|)^2} \right] \dots} + \frac{i_{n.R9}(f)^2 + i_{n.i.op1}(f)^2 + i_{n.R13}(f)^2}{g_{m3.4}^2}$$

$$e_{n.i.amp.p}(h) = 447.427 \times 10^{-12}V$$

5.5 Amp2's total input and output referred noise voltages incl. R0 :

$$e_{n.i.amp}(f) := \sqrt{e_{n.i.amp.f}(f)^2 + e_{n.i.amp.p}(f)^2}$$

$$e_{n.i.amp}(h) = 632.01 \times 10^{-12}V$$

$$e_{n.o.amp}(f) := e_{n.i.amp}(f) \cdot G_{amp}$$

$$e_{n.o.amp}(h) = 126.402 \times 10^{-9}V$$

$$i_{n.i.amp}(f) := \sqrt{\left( \frac{1}{i_{n.i.p}(f)^2} + \frac{1}{i_{n.i.n}(f)^2} \right)^{-1}}$$

$$i_{n.i.amp}(h) = 2.388 \times 10^{-12}A$$

$$e_{n.i.amp}(f, R0) := \sqrt{e_{n.i.amp}(f)^2 + i_{n.i.amp}(f)^2 \cdot (Z_{iL}(f, R0))^2 + e_{n.Z.iL}(f, R0)^2}$$

11.3 MCD-WS: Amp2 SN and Gain Calculations - 1/f-Noise Based Version

$$e_{n.i.amp}(h, 20\Omega) = 852.619 \times 10^{-12}V$$

$$e_{n.i.amp}(h, 10^{-6}\Omega) = 636.169 \times 10^{-12}V$$

$$e_{n.o.amp}(f, R0) := e_{n.i.amp}(f, R0) \cdot G_{amp}$$

$$e_{n.o.amp}(h, 20\Omega) = 170.524 \times 10^{-9}V$$

$$f := 10Hz, 20Hz.. 20 \cdot 10^3 Hz$$

$$R0 := 0\Omega, 1\Omega.. 100\Omega$$

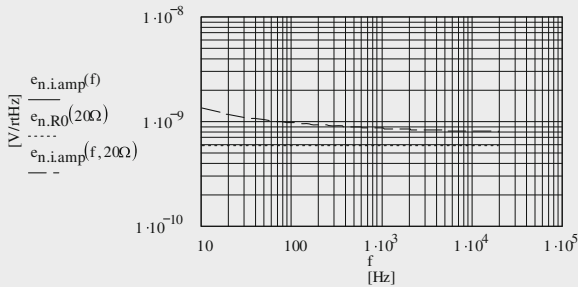


Fig. 11.10  
Input referred noise voltage densities vs. frequency based on two different input loads

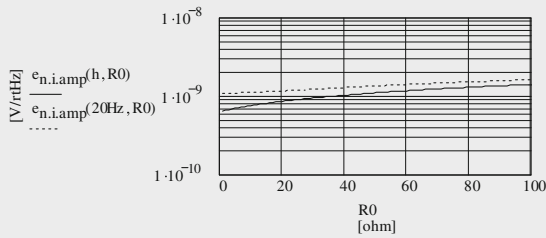


Fig. 11.11  
Amp2 equivalent input noise voltage densities vs. R0 based on two different frequencies

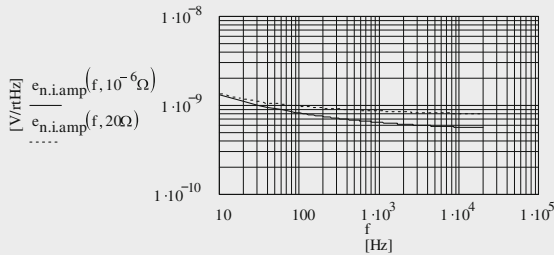


Fig. 11.12  
Amp2 equivalent input noise voltage densities vs. frequency showing 1/f-noise based on two different input loads

11.3 MCD-WS: Amp2 SN and Gain Calculations - 1/f-Noise Based Version

6. NF calculation :

$$NF_e(R0) := 20 \cdot \log \left( \frac{\sqrt{e_{n,Z.il}(h,R0)^2 + i_{n,i.amp}(h)^2 Z_{Ll}(h,R0)^2 + e_{n,i.amp}(h,R0)^2}}{e_{n,Z.il}(h,R0)} \right) \quad NF_e(20\Omega) = 5.107 \quad [dB]$$

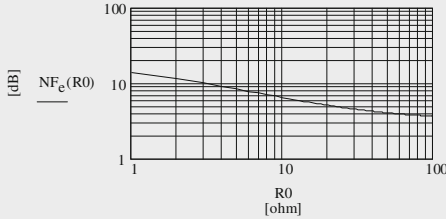


Fig. 11.13  
Noise Figure  
vs. R0

7. Evaluation of SNs with reference to  $B_{20k}$  and  $100mV_{rms}/1kHz$  nominal output voltage:

$$SN_{ne}(R0) := 20 \cdot \log \left[ \frac{\frac{1}{B_1} \int_{20Hz}^{20000Hz} (|e_{n.o.amp}(f,R0)|)^2 df}{v_{o.nom}} \right]$$

$$SN_{ne}(20\Omega) = -72.801 \quad [dB]$$

$$SN_{ne.m}(20\Omega) = -73.13 \quad [dB]$$

$$SN_{ne}(10^{-6}\Omega) = -75.768 \quad [dB]$$

$$SN_{ne.m}(10^{-6}\Omega) = -75.37 \quad [dB]$$

A-weighting by A(f) :

$$A(f) := \frac{1.259}{1 + \left(\frac{20.6Hz}{f}\right)^2} \cdot \frac{1}{\sqrt{1 + \left(\frac{107.7Hz}{f}\right)^2}} \cdot \frac{1}{\sqrt{1 + \left(\frac{737.9Hz}{f}\right)^2}} \cdot \frac{1}{1 + \left(\frac{f}{12200Hz}\right)^2}$$

$$SN_{ne.a}(R0) := 20 \cdot \log \left[ \frac{\frac{1}{B_1} \int_{20Hz}^{20000Hz} (|e_{n.o.amp}(f,R0)|)^2 \cdot (|A(f)|)^2 df}{v_{o.nom}} \right]$$

$$SN_{ne.a}(20\Omega) = -74.797 \quad [dB(A)]$$

$$SN_{ne.a.m}(20\Omega) = -75.22 \quad [dB(A)]$$

11.3 MCD-WS: Amp2 SN and Gain Calculations - 1/f-Noise Based Version

RIAA equalizing by R(f) :

$$R_{1000} := \left[ \frac{\sqrt{1 + (2 \cdot \pi \cdot 10^3 \text{ Hz} \cdot 318 \cdot 10^{-6} \text{ s})^2}}{\sqrt{1 + (2 \cdot \pi \cdot 10^3 \text{ Hz} \cdot 3180 \cdot 10^{-6} \text{ s})^2} \cdot \sqrt{1 + (2 \cdot \pi \cdot 10^3 \text{ Hz} \cdot 75 \cdot 10^{-6} \text{ s})^2}} \right]^{-1} \quad R_{1000} = 9.898$$

$$R(f) := \left[ \frac{\sqrt{1 + (2 \cdot \pi \cdot f \cdot 318 \cdot 10^{-6} \text{ s})^2}}{\sqrt{1 + (2 \cdot \pi \cdot f \cdot 3180 \cdot 10^{-6} \text{ s})^2} \cdot \sqrt{1 + (2 \cdot \pi \cdot f \cdot 75 \cdot 10^{-6} \text{ s})^2}} \right] \cdot R_{1000}$$

$$SN_{riaa}(R0) := 20 \cdot \log \left[ \frac{\int_{20\text{Hz}}^{2000\text{Hz}} \left( |e_{n.o.amp}(f, R0)| \right)^2 \cdot (|R(f)|)^2 \cdot df}{v_{o.nom}} \right]$$

$$SN_{riaa}(20\Omega) = -75.054 \quad [\text{dB}]$$

$$SN_{ariaa}(R0) := 20 \cdot \log \left[ \frac{\int_{20\text{Hz}}^{2000\text{Hz}} \left( |e_{n.o.amp}(f, R0)| \right)^2 \cdot (|A(f)|)^2 \cdot (|R(f)|)^2 \cdot df}{v_{o.nom}} \right]$$

Calculated and measured (m) results :

$$SN_{ariaa}(10^{-6}\Omega) = -83.095 \quad [\text{dB(A)}]$$

$$SN_{ariaa}(20\Omega) = -80.431 \quad [\text{dB(A)}]$$

$$SN_{ariaa.m}(10^{-6}\Omega) = -81.60 \quad [\text{dB(A)}]$$

$$SN_{ariaa.m}(20\Omega) = -79.80 \quad [\text{dB(A)}]$$

$$SN_{ariaa}(5\Omega) = -82.283 \quad [\text{dB(A)}]$$

$$SN_{ariaa}(43\Omega) = -78.612 \quad [\text{dB(A)}]$$

$$SN_{ariaa.m}(5\Omega) = -81.20 \quad [\text{dB(A)}]$$

$$SN_{ariaa.m}(43\Omega) = -78.40 \quad [\text{dB(A)}]$$

$$SN_{ariaa}(10\Omega) = -81.571 \quad [\text{dB(A)}]$$

$$SN_{ariaa.m}(10\Omega) = -80.70 \quad [\text{dB(A)}]$$

11.3 MCD-WS: Amp2 SN and Gain Calculations - 1/f-Noise Based Version

$$f := 20\text{Hz}, 25\text{Hz}.. 20 \cdot 10^3 \text{ Hz}$$

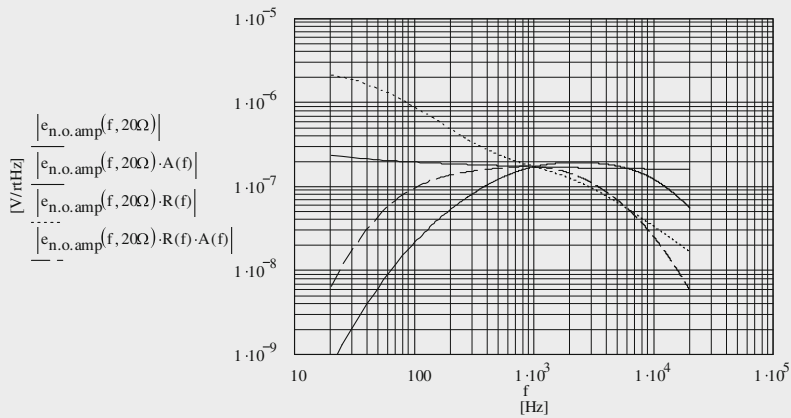


Fig. 11.14 Amp2 output noise voltage densities vs. frequency  
RIAA-equalized + A-weighted + un-weighted

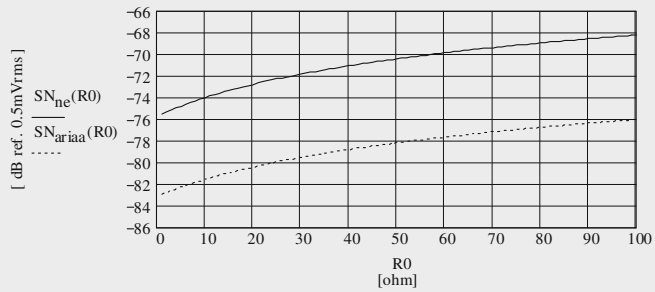


Fig. 11.15 Input referred un-weighted + A-weighted & RIAA-equalized SN vs. R0

## 12.1 Visible and Audible Effects

### 12.1.1 Visible Effects

Before we dive deeper into real listening matters let's have a look at the worst looking frequency and phase responses, generated by the left channel of Engine II and Amp1 & Amp2 via Amp3 only and Amp5 (incl. output transformer). Figure 12.1a shows the measured curves. They are flat according to the goals set in Sect. 1.2. However, there is one exception: the low-frequency response of Amp1. It comes from the deviation already mentioned in Sect. 8.3, Fig. 8.6, and in conjunction with the UBC<sup>1</sup> output resistance of 10.8  $\Omega$ .

To demonstrate the difference Fig. 12.1b shows the curves of the sequence Amp1 via Amp3 & Amp4 and Amp5 + Trafo, however fed directly by the RIAA encoder's output with an output resistance of approximately 0  $\Omega$ . The curves become much more flat.

In Fig. 12.1a the Amp1 curves are the ones that show the biggest deviations from the flatness at 20 Hz and 20 kHz. The frequency responses are located around 0dBV/1 kHz (left ordinate) and the phase responses around 0°/1 kHz (right ordinate). The Amp2 generated curves look very flat.

In Fig. 12.1b the two frequency responses and the two phase responses are hidden by each other. At the low-end of the audio band, they look very much better than the Amp1 ones of Fig. 12.1a. Further down Table 12.4 gives the detailed measurement results.

Figure 12.2 shows the output noise trace of the chain Amp1 + Amp4 + Amp5 + Trafo, input loaded by a 20  $\Omega$  metal film resistor. Based on a typical 3-pham concept this trace should very closely follow the RIAA transfer function.

Definitely not created by the engine in this graph we find a 150 Hz spike. It appears in many other ones of my measurement graphs too. I always thought that

<sup>1</sup>See un-balanced-to-balanced converter in Sect. 15.2.

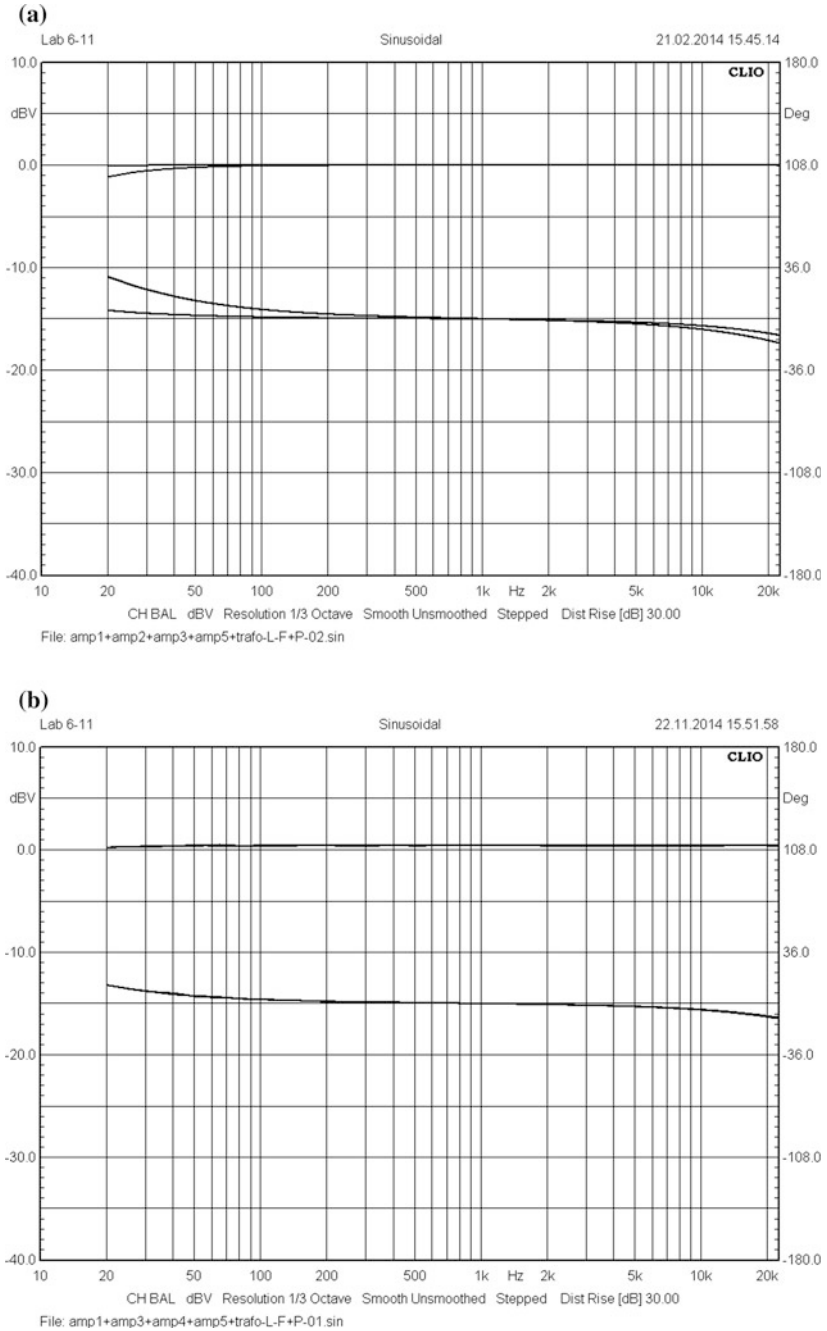


**Fig. 12.1** **a** Frequency and phase response of the left channel's Amps 1 & 2 via Amp3 and Amp5 + Trafo, fed by a generator output resistance of 10.8  $\Omega$ . **b** Frequency and phase response of the left channel's Amp1 via Amp3 and Amp4 and Amp5 + Trafo, fed by a generator output resistance of appr. 0  $\Omega$

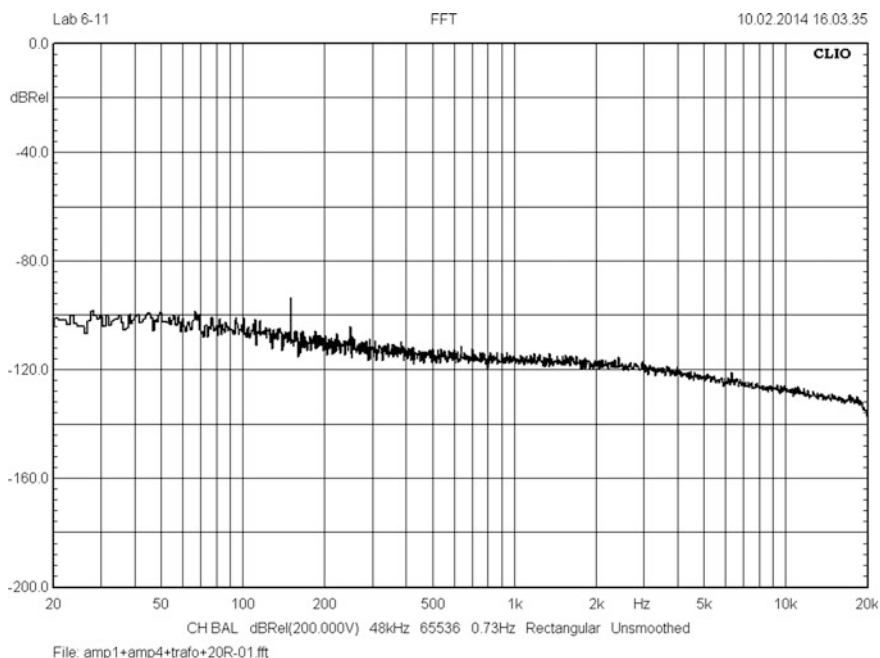


**Fig. 12.2** Engine II output noise voltage density curve of the left channel, input loaded with 20  $\Omega$  and Amp1 + Amp4 + Amp5 + Trafo

one of the many running PSU devices in my lab could generate it. Together with a specialist of the local mains supplier we could identify where it comes from. Only 15 m away from my lab there is a transformer house with a 10 kV/230 V/50 Hz transformer. As long as it runs with full power, the spikes will disappear. In all other cases they will come and go—you never know the rhythm.

I guess, with these frequency and phase response results in conjunction with the amp's rather low noise production the listening tests will become a real challenge.

### 12.1.2 Audible Effects

Studying the above shown graphs will lead to two realizations: it will be hard to hear noise because the majority of the shown noise voltage density values becomes  $< -120$  dBV, and, despite the small deviation from Amp1's frequency response flatness  $< 100$  Hz it will also be hard to identify differences in sound between Amp1 and Amp2.

In the various listening tests, I could go through many different test arrangements with very different source material as well as different loudspeaker and amplifier chains. The basic procedure became always the same: for each loudspeaker situation, the source material had to go through all Engine II offered switching



possibilities. I used the following test records, test noise, headphone, and loud-speaker arrangements in two different rooms, my 16 m<sup>2</sup> lab and my 30 m<sup>2</sup> library.

### 12.1.3 Test Records

Piano	1. “The Köln Concert”, Keith Jarrett, ECM 1064/65ST Live grand piano 2. “Piano”, Martin Vatter, <a href="http://www.martin.vatter.de">www.martin.vatter.de</a> , DMM by Pauler Acoustics Studio grand piano play and direct string treatment by fingers and other measures
Concert	1. “Piano Concert No. 1 in B flat minor”, Tchaikovsky Svatoslav Richter/Herbert von Karajan/Vienna Symphony Orchestra Deutsche Grammophon 138822 Recorded at the Vienna Musikverein building with its stunning acoustic 2. “Moonlight Sonata”, L.v. Beethoven, Wilhelm Kempff, Piano, Deutsche Grammophon LPE 17026, Mono record
Pop etc.	“Saitensprung”, Friedemann, Biber Records, <a href="http://www.in-akustik.com">www.in-akustik.com</a> Plugged and un-plugged percussion and string instruments: guitar & harp
Electronic	“Minimum–Maximum”, Kraftwerk, EMI 0946 3 11828 1 5 Live electronic music at its best; includes Autobahn, Tour de France, etc.

### 12.1.4 Test Noise and Source Equipment

Pink	Via Pink noise generator, <sup>2</sup> RIAA encoder, <sup>3</sup> and un-balanced to balanced converter <sup>4</sup>
Third octave & Bark	45 rpm Deutsche Grammophon test record TM 10 99 109. It offers wobbling frequencies in 27 third octave bands format as well as in 24 Bark bandwidth format
Turntable	Direct driven Pioneer PL-L1000 with tangential tone arm, modified for fully balanced operation
MC	Denon DL-103 No. 2798

<sup>2</sup>TSOS-1 Chap. 10, TSOS-2 Chap. 22.

<sup>3</sup>TSOS-1 Chap. 11, TSOS-2 Chap. 23.

<sup>4</sup>UBC—see Sect. 15.2.

### 12.1.5 Loudspeaker Situation and Headphones

The direct driven lab loudspeakers are located alike the monitoring loudspeakers in a mastering studio (distance LS-ear: max. 1.5 m). Additionally, a center bass unit works down to 15 Hz. It is an improved version of Russel Breden's subwoofer.<sup>5</sup> An active crossover and various kinds of power amps control them all in a 2.1 basic arrangement.

The library room's loudspeaker situation is very much different; however, here I use a 2.1 basic arrangement too. A pair of two small bookshelf loudspeakers can be switched into the arrangement as well as a pair of modified BRAUN LE1 electrostatic loudspeakers,<sup>6,7</sup> (distance LS-ear: max. 2.5 m). They work in the frequency range >100 Hz, filtered by 24 dB Linkwitz/Riley lps and hps. An active KEF B139 in a closed box plays the bass part here.

The head/ear-phones are: AKG 271 Mk II and B&O earphones.

### 12.1.6 Listening Tests

#### 1st Round

No matter which of the eight different amplifier and output transformer alternatives I've been choosing I couldn't hear any difference when playing one of the records from Sect. 12.1.3. I thought that one of the few and rather old mono records I found in my collection could be of additional value because its higher frequencies were all gone by many listening sessions: no chance! Even with headphones, there was no indication of the tiniest difference.

#### 2nd Round

Here I thought that I had to force the Engine II into a worse situation by changing the actual t1-t2 double-triode of the right channel. I took a non-selected old Siemens ECC88 double-triode that has very low noise levels but very different triode characteristics. The SN values do not change but the THD and IMD values became worse. THD = 0.043 %, IMD = 0.26 % (worst case).

Because of the unequal gains of the triodes, the only additional difference I could measure became the fact that the overload margin became worse too.

Like in the first round, from a listening point of view I could not identify any differences.

---

<sup>5</sup>“Roaring subwoofer”, Russel Breden, Electronics (Wireless) World 02-1997, p. 104ff.

<sup>6</sup>“Improved Electrostatic Loudspeaker Power Supply for QUAD ESL57 and BRAUN LE1”, B. Vogel, Electronics (Wireless) World, 02-2006.

<sup>7</sup>“Abenteuer LE1—Restauration der Prof. Rams'schen Design-Legende” “Adventure LE1—Restoration of Prof. Rams' design legend”, B. Vogel, German and English version, Design + Design Nr. 32, 1995, Jo Klatt Design + Design Verlag Hamburg, [www.design-und-design.de](http://www.design-und-design.de).

### 3rd Round

Two years ago, I was coaching a young student at Prof. Seelmann's department of Electronics & Information Technology of the Aalen University, Germany. To get the bachelor degree he was working on a test arrangement with four different kinds of feedback mechanisms in audio pre-amplifiers. He designed four different FET configured three-stage pre-amplifiers,<sup>8</sup> according to an idea I've been presenting in HTGG-1.<sup>9</sup> The aim was to identify differences in sound and to find corresponding explanations, alike the ones Peter Schüller described in the MST, the Mayer-Schüller-Theory.<sup>10</sup>

In an anechoic chamber, we have been listening to a broad range of source material. It was very hard to identify the differences between the four different feedback situations. Only one test signal allowed a clear identification of differences: pink noise.

Therefore, the "killing" test signal for the Engine II should become pink noise via RIAA encoder and an un-balanced to balanced converter. Here, at the first time, I could identify tiny differences, but only when switching the two input amps. There were no differences audible when switching the two central amps 3 and 4 nor when switching the output transformer in and out. Unfortunately, even after this procedure I cannot say what the best situation for the user could be. The differences are simply too small.

A further attack on the amp chains with wobbling frequencies followed. Again, clear differences could not be detected.

### 4th Round

I thought, maybe my wife and some friends and sound specialists could help and identify differences. However, they obtained the same listening results.

---

## 12.2 Measurement Results

### 12.2.1 Noise

This section explains my personal interpretation why I did not identify audible differences between the various amplifier sequences. Two additional graphs show the outstanding low noise voltage generation by the Engine. Practically not contrasting Fig. 12.2. Figure 12.3 shows the Amp2 + Amp3 + Amp5 + Trafo chain's

---

<sup>8</sup>"Audio Amplifier Feedback beats Feedback-free", Florian Ermer, despite the English title the text is written in German and not translated yet, [www.audioexperts.de/audio-technik/554-gegenkopplung-schlaegt-gegenkopplungsfrei.html](http://www.audioexperts.de/audio-technik/554-gegenkopplung-schlaegt-gegenkopplungsfrei.html).

<sup>9</sup>HTGG-1, Chap. 15.

<sup>10</sup>"Maier-Schüller-Theory MST": see my letter to the editor of Linear Audio Vol 4-1 ([www.linearaudio.net/](http://www.linearaudio.net/)) and the PDF document on <http://Burosche.de/audio-technik/509-high-end-2012-klang-2-english.html>.

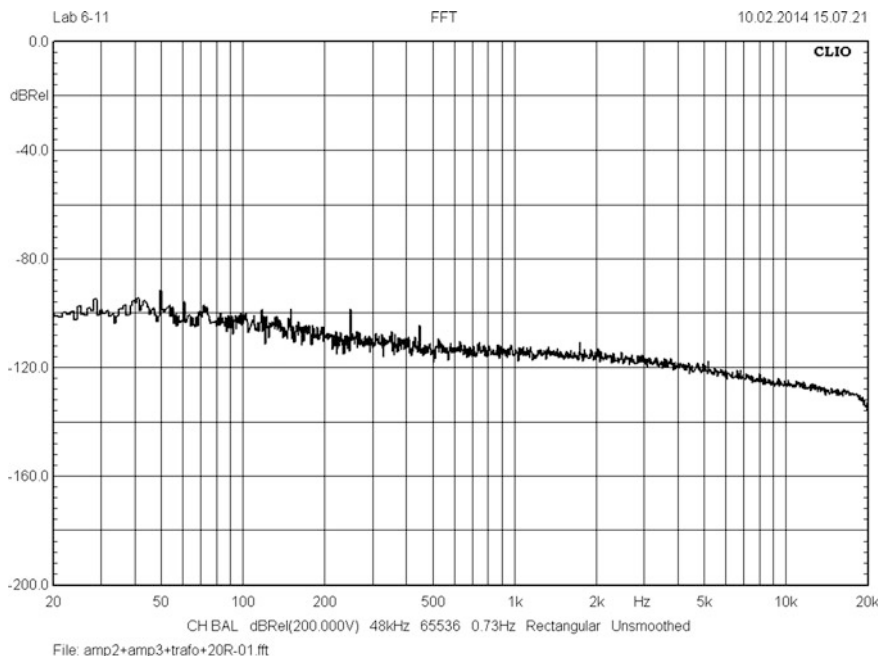


**Fig. 12.3** Engine II output noise voltage density curve of the left channel, input loaded with  $20\ \Omega$  and Amp2 + Amp3 + Amp5 + Trafo

noise voltage density curve, also loaded with  $20\ \Omega$  at its input. However, here comes Amp2 into the game, and the triode driven Amp3 replaces Amp4.

With input shorted via external input another graph, Fig. 12.4, demonstrates the noise performance of the chain Amp3 + Amp5 + Trafo. Now, there is no effect  $>1\ \text{kHz}$  from the  $75\ \mu\text{s}$  time constant because most of this chain's noise is created after the time constant creating section. The same applies to Amp4 instead of Amp3.

At  $1\ \text{kHz}$  the difference of the two curves becomes approximately  $20\ \text{dB}$ . This is roughly the same difference of the measured SNs too: Fig. 12.3:  $-79.9\ \text{dB(A)}$ , Fig. 12.4:  $-99.0\ \text{dB(A)}$ .

### 12.2.2 THD and IMD Matters, Left Channel

The following graphs show the distortion effects of a  $1\ \text{kHz}$  test signal of the left channel only. I have also gone through other test signal frequencies below and above  $1\ \text{kHz}$ . However, the general impression of their spikes  $\geq 2\ \text{dB}$  did not change. Therefore, here, I will concentrate on the  $1\ \text{kHz}$  effects only. The horizontal line in each graph represents the RIAA equalized  $\text{SN}_{\text{riaa}}$  of  $-67.3\ \text{dB}$ . No distortion spike

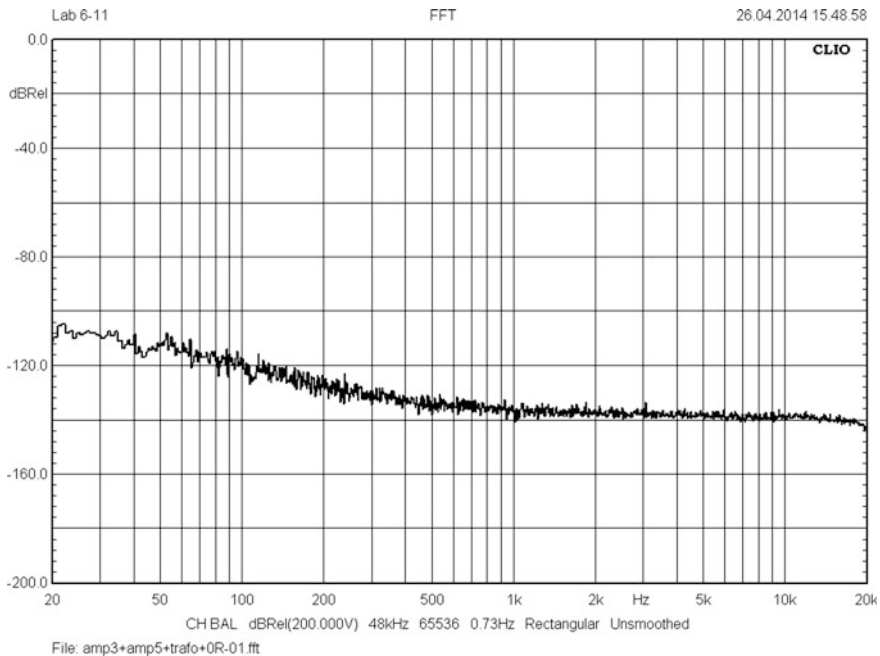


**Fig. 12.4** Engine II output noise voltage density curve of the left channel, external input shorted and Amp3 + Amp5 + Trafo

should cross this line. Otherwise, it becomes noticeable among the mixed noise of the phono-amp and the LP.

I refrain from discussing the before expressed claim about the audibility of distortion spike levels and the level difference between the spike and the  $-67.3$  dB line. However, my personal experience has led to the described conclusion, after the findings of Sect. 15.2 (masking of harmonics by noise) and after many listening tests via loudspeakers and headphones fed by white noise in  $B_{20k}$  and mixed-up with single sinus tones between 50 Hz and 1 kHz.

To create the 1 kHz/0 dBV output signal in Fig. 12.5 I've fed the balanced 1 kHz/0.00159 % generator signal<sup>11</sup> into the triode amp chain Amp1 + Amp3 + Amp5 + Trafo. The d2 and d3 generator levels lie at  $-97.662$  and  $-114.571$  dBV, the corresponding levels of the graph show levels of  $-81.672$  and  $-85.704$  dBV. Transferred into distortion percentages that means 0.0083 and 0.0052 %. Total distortion in  $B_{20k}$  (THD) measures 0.010 % and the level decrease with increasing harmonics order follows the findings of the MST.<sup>12</sup> Theoretically, this path should sound superb.

<sup>11</sup>See Sect. 15.2.

<sup>12</sup>See footnote 9.

In contrast to Fig. 12.5 we have in Fig. 12.6 the Amp3 triode path replaced by Amp4 with op-amps. The 1 kHz test-signal changes its d2/d3 output values to  $-99.131$  and  $-94.738$  dBV, both distortion values now far below the Fig. 12.5 ones, leading to an overall THD of 0.002 %. However, it does not matter, this amp sequence did not sound different to the Fig. 12.5 chain.

Total THD of the Fig. 12.7 amp chain with Amp2 and triode gain stage (Amp2 + Amp3 + Amp5 + Trafo) measures 0.013 %, the d2/d3 levels become  $-78.388$  dBV and  $-86.580$  dBV. Because of the triode's tendency to create stronger equal harmonics the Fig. 12.7 harmonics look similar to the ones of Fig. 12.5; d2 does not affect the sound of this sequence negatively, and d3 also fully disappears in the noise, hence it has no sound disturbing effect. That is why we could not hear any difference to the other amp sequence alternatives.

Now, in Fig. 12.8, things become even stronger after replacement of Amp3 by Amp4, because the d2/d3 spikes ( $-86.376$  dBV and  $-94.327$  dBV, THD = 0.005 %) also fully disappear in the unweighted output referred  $SN_{riaa}$  of  $-67.3$  dBV best-case LP noise. Again, differences to the other amp sequences became inaudible.

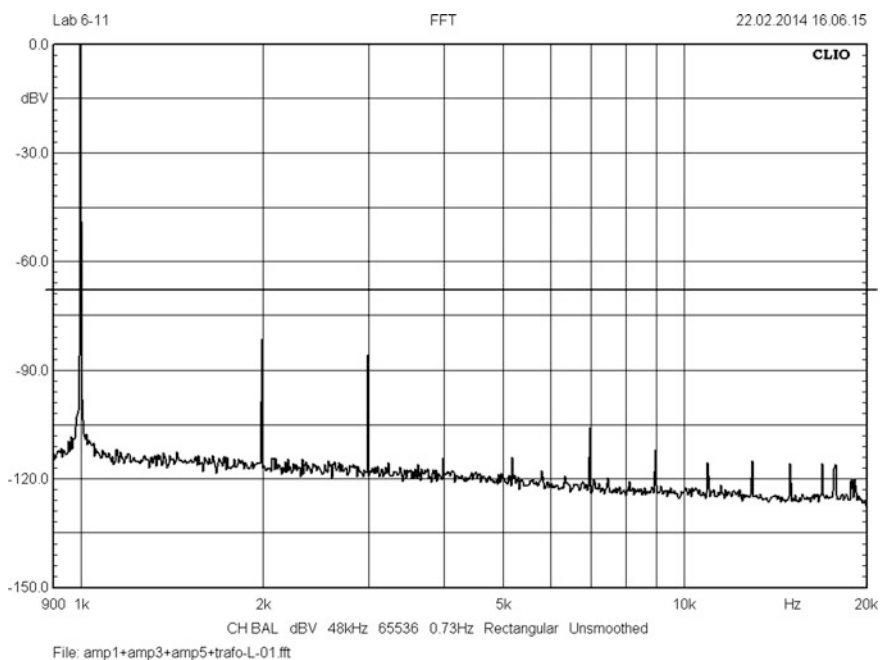


**Fig. 12.5** Left channel's Amp1 + Amp3 + Amp5 + Trafo distortion measurement result of a 1 kHz signal via the central triode path

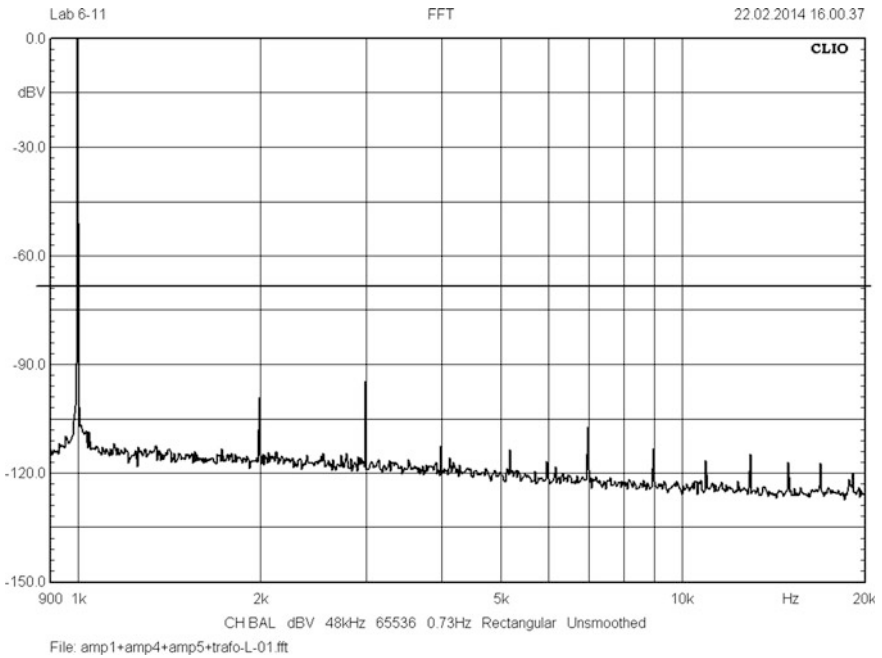


**Fig. 12.6** Left channel's Amp1 + Amp4 + Amp5 + Trafo distortion measurement result of a 1 kHz signal via the central op-amp path

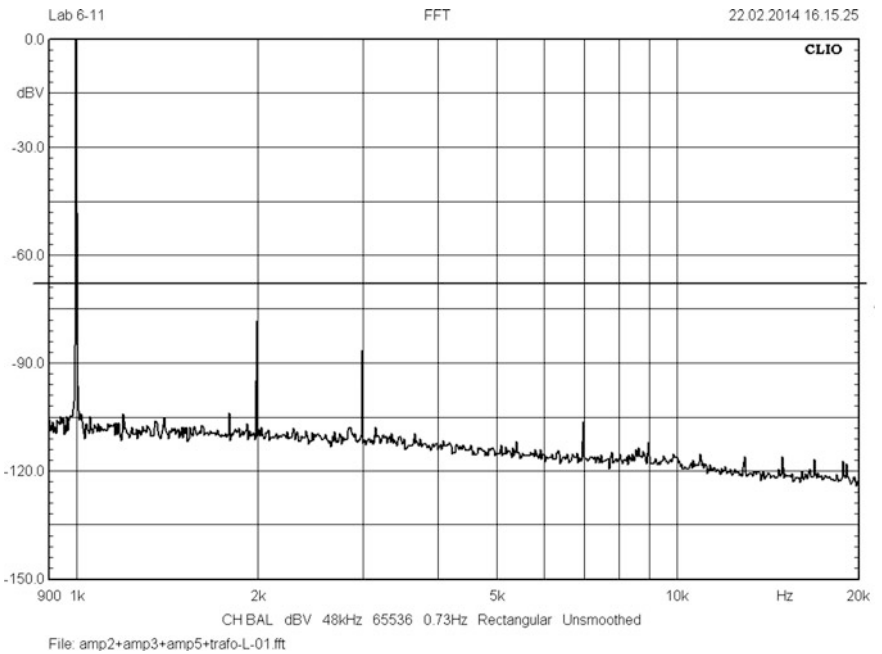


**Fig. 12.7** Same as Fig. 12.5, however, Amp1 is replaced by Amp2

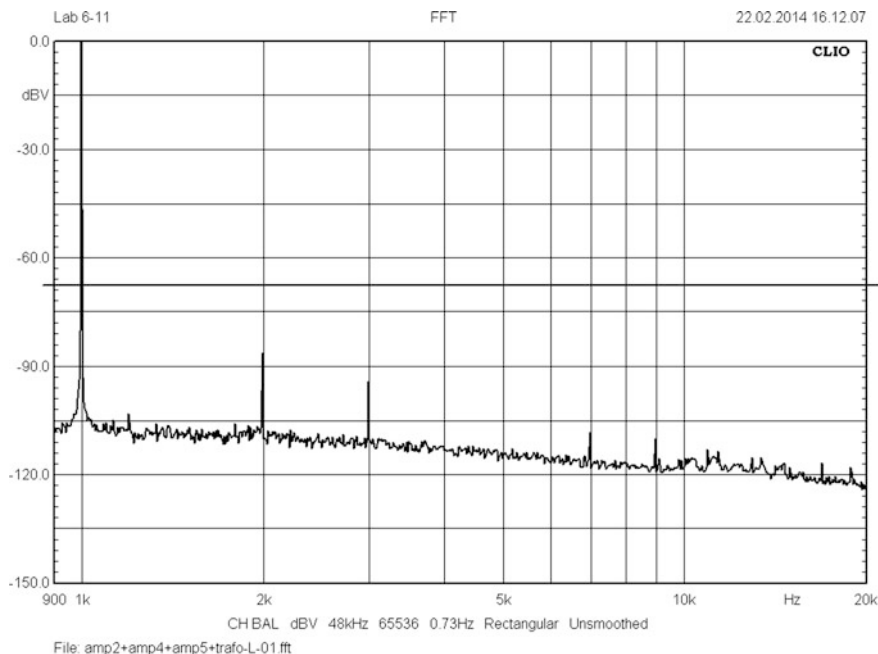


**Fig. 12.8** Same as Fig. 12.6, however, Amp3 is replaced by Amp4

### 12.2.3 THD and IMD Matters, Right Channel

Concerning IMD, the measurement results become always  $<0.01\%$ . ‘Always’ because I have measured all amp sequence possibilities with different frequency pairs with levels set to 20%/80%, such as 8 kHz/250 Hz (DIN), 3 kHz/60 Hz, and 3 kHz/300 Hz.

In the left channel the Amp3’s first E88CC (t1 & t2) is a selected one from JJ with perfectly matched operating conditions at 2 mA/90 V. For right-channel test purposes, I’ve chosen a non-selected but low-noise Siemens NOS ECC88 with rather different operating conditions of its two triode systems. However, P5 of Fig. 2.1 allows trimming to equal gains of t1 & t2.

Compared with the ones of Figs. 12.5 and 12.7 the THD and IMD measurement results look worse: THD = 0.043% (Amp1) and 0.055% (Amp2), IMD  $< 0.01\%$  for 8 kHz/250 Hz but up to 0.026% with the other two frequency pairs.

Only the before mentioned pink-noise test signal (in Sect. 12.1.4) could generate sound differences between the left and the right channel. Music material did not produce audible differences.



## 12.2.4 General THD and IMD Matters

Obviously, the chosen 3-pham concept is a favourable approach to decrease THD and IMD. The 75  $\mu\text{s}$  lp filter, with increasing frequency more and more, suppresses distortion and intermodulation artefacts created by the high-gain input stages. The 318  $\mu\text{s}$  + 3180  $\mu\text{s}$  arrangement creates a further step up to 1/10.

## 12.2.5 Summary Tables and Graphs

I've summed-up the measured findings in four different tables: Table 12.1 gives relevant SNs of different amp sequences, Tables 12.2 and 12.3 play the THD & IMD part, and Table 12.4 shows the generator output resistance dependency of the Amps 1 and 2 frequency and phase responses.

Table 12.1 needs some explanations:

1. Shown in Figs. 12.2 and 12.3, the noise curve of RIAA equalized white noise versus frequency looks like the RIAA transfer curve versus frequency. Thus, when talking about the corresponding SN I always use the subscript 'riaa'; in case of an additional A-weighting, the subscript changes to 'ariaa'. The here used terms  $\text{SN}_o$  (not A-weighted output referred SN) and  $\text{SN}_{o,a}$  (A-weighted output referred SN) indicate something between fully RIAA equalized and half equalized, because with input of Amps 3 and 4 shorted, the 75  $\mu\text{s}$  has practically no effect on the output SN. Hence, the noise curve has no decrease above 1 kHz à la Fig. 12.4 and the RIAA effect comes from the 318  $\mu\text{s}$ /3180  $\mu\text{s}$  network below 1kHz only.
2. With the exception of the reference level, the input referred SNs equal the output referred ones. Automatically, with a gain of 2000 an input referred  $\text{SN}_i$  referenced to 0.5  $\text{mV}_{\text{rms}}/1 \text{ kHz}$  equals an output referred  $\text{SN}_o$  referenced to 1  $\text{V}_{\text{rms}}/1 \text{ kHz}$ . Or, in the case of Amps 3 or 4 plus 5 plus trafo the input reference level is 100  $\text{mV}_{\text{rms}}$  and the gain is 10. Thus, the output referred  $\text{SN}_o$  becomes the input referred  $\text{SN}_i$  too.
3. The same input SN versus output SN mechanism applies to the Sect. 13.3 example amp with a gain of 1000, leading to an overall gain of 10,000. The input reference level becomes thus 0.1  $\text{mV}_{\text{rms}}/1 \text{ kHz}$ .

Note 1: Table 12.4 colours are the colours of Figs. 12.9, 12.10 and 12.11.

Note 2: Further adjustment of Fig. 1.2's P3 and an increase of the capacitance values of Fig. 2.1's C44a–C45b will improve the Amp3 deltas in boxes H-5, H-7, and H-17 to  $\leq(\pm 0.1 \text{ dB})$ . However, my RIAA encoder's<sup>13</sup> exactness is  $\pm 0.1 \text{ dB}$  only!

Note 3: Concerning Amp2 there is no difference to the Table 12.4 values when fed by the RIAA encoder directly (0  $\Omega$ ).

---

<sup>13</sup>See Sect. 14.1.

**Table 12.1** Relevant Engine II SN results

1/A	B	C	D	E	F
2		L channel		R channel	
3	Amp sequence <b>measured</b>	<b>SN.i.ariaa</b>		<b>SN.i.ariaa</b>	
4		Ref. 0.5 mV/1 kHz/20R			
5		dB(A)		dB(A)	
6	Amp1 + Amp3 + Amp5 + o/p-trafo	-81.71		-81.86	
7	Amp1 + Amp4 + Amp5 + o/p-trafo	-81.78		-81.66	
8	Amp2 + Amp3 + Amp5 + o/p-trafo	-79.91		-80.21	
9	Amp2 + Amp4 + Amp5 + o/p-trafo	-79.83		-80.01	
10		<b>SN.o</b>	<b>SN.o.a</b>	<b>SN.o</b>	<b>SN.o.a</b>
11		Ref. 1 V/1 kHz/0R			
12		dBV	dBV(A)	dBV	dBV(A)
13	Amp3 + Amp5 + o/p-trafo	-90.43	-99.00	-90.43	-99.00
14	Amp4 + Amp5 + o/p-trafo	-98.06	-100.82	-98.06	-100.82
15	Amp5 + o/p-trafo	-101.73	-103.50	-101.73	-103.90
16	Amp5 single ended	-101.30	-102.90	-101.30	-102.90
17		<b>SN.i</b>	<b>SN.i.a</b>	<b>SN.i</b>	<b>SN.i.a</b>
18		Ref. 0.5 mV/1 kHz/20R			
19		dB	dB(A)	dB	dB(A)
20	Amp1	-74.00	-76.00	-74.00	-76.00
21	Amp2	-73.13	-75.22	-73.37	-75.34
22					
23	left & right channel & amp sequence <b>calculated</b>	<b>SN.i.ariaa</b>		<b>Deltas</b>	
24		Ref. 0.5 mV/1 kHz/20R		L.meas - calc	
25		dB(A)		dB	
26	Amp1(tr = re) + Amp3 (ds/1 k) + Amp5 + o/p-trafo	-80.89		-0.82	
27	Amp1(tr = re) + Amp4 + Amp5 + o/p-trafo	-80.89		-0.89	
28	Amp2 + Amp3 + Amp5 + o/p-trafo	-80.43		0.52	
29	Amp2 + Amp4 + Amp5 + o/p-trafo	-80.43		0.60	
30		<b>SN.o</b>	<b>SN.o.a</b>		
31		Ref. 1 V/1 kHz/0R			
32		dBV	dBV(A)		
33	Amp3(ds/1 k) + Amp5 + o/p-trafo	-92.87	-100.40	2.44	1.40
34	Amp4 + Amp5 + o/p-trafo	-96.11	-99.94	-1.95	-0.88
35	Amp5 + o/p-trafo	-101.96	-104.01	0.23	0.51
36	Amp5 single ended	-101.24	-103.29	-0.06	0.39

(continued)

**Table 12.1** (continued)

I/A	B	C	D	E	F
37		<b>SN.i</b>	<b>SN.i.a</b>		
38		Ref. 0.5 mV/ 1 kHz/20R			
39		dB	dB(A)		
40	Amp1	-72.62	-74.67	-1.38	-1.33
41	Amp2	-72.80	-74.80	-0.33	-0.42

ds/1 k: data sheet figures and f.c = 1 kHz

tr = re: real data (tr = 11) for the i/p trafo

**Table 12.2** Relevant Engine II THD figures

I/A	B	C	D
2	<b>Left channel via ext. i/p measured ref. i/p:100 mV + o/p:1 V</b>	o/p trafo	
3		Incl.	Excl.
4		%	
5	Amp3 + Amp5	0.011	0.010
6	Amp4 + Amp5	0.002	0.001
7			
8	<b>Left channel via Amp1&amp;2 measured ref. i/p:0.5 mV + o/p:1 V</b>	o/p trafo	
9		Incl.	Excl.
10		%	
11	Amp1 + Amp3 + Amp5	0.010	0.010
12	Amp1 + Amp4 + Amp5	0.002	0.002
13	Amp2 + Amp3 + Amp5	0.013	0.013
14	Amp2 + Amp4 + Amp5	0.005	0.005
15			
16	<b>Right channel via ext. i/p measured ref. i/p:100 mV + o/p:1 V</b>	o/p trafo	
17		Incl.	Excl.
18		%	
19	Amp3 + Amp5	0.040	0.039
20	Amp4 + Amp5	0.002	0.002
21			
22	<b>Right channel via Amp1&amp;2 measured ref. i/p:0.5 mV + o/p:1 V</b>	o/p trafo	
23		Incl.	Excl.
24		%	
25	Amp1 + Amp3 + Amp5	0.043	0.043
26	Amp1 + Amp4 + Amp5	0.002	0.002
27	Amp2 + Amp3 + Amp5	0.055	0.055
28	Amp2 + Amp4 + Amp5	0.014	0.014

**Table 12.3** Relevant Engine II IMD figures

1/A	B	C	D
2	<b>Left channel via Amp1&amp;2 measured ref. i/p:0.5 mV + o/p:1 V 250 Hz/8 kHz + 80 %/20 %</b>	o/p trafo	
3		Incl.	Excl.
4		%	
5			
6		Amp1 + Amp3 + Amp5	0.004
7	Amp1 + Amp4 + Amp5	0.002	0.002
8	Amp2 + Amp3 + Amp5	0.007	0.007
9	Amp2 + Amp4 + Amp5	0.004	0.004
10			
11	<b>Left channel via Amp1&amp;2 measured ref. i/p:0.5 mV + o/p:1 V Other frequency pairs</b>	o/p trafo	
12		Incl.	Excl.
13		%	
14			
15	Amp1 + Amp3 + Amp5: 60 Hz/3 kHz + 80 %/20 %	0.006	0.005
16	Amp2 + Amp3 + Amp5: 300 Hz/3 kHz + 80 %/20 %	0.008	0.008
17	Amp2 + Amp3 + Amp5: 60 Hz/3 kHz + 80 %/20 %	0.007	0.006
18			
19	<b>Right channel via Amp1&amp;2 measured ref. i/p:0.5 mV + o/p:1 V 250 Hz/8 kHz + 80 %/20 %</b>	o/p trafo	
20		Incl.	Excl.
21		%	
22			
23	Amp1 + Amp3 + Amp5	0.008	0.006
24	Amp1 + Amp4 + Amp5	0.006	0.001
25	Amp2 + Amp3 + Amp5	0.010	0.009
26	Amp2 + Amp4 + Amp5	0.008	0.003
27			
28	<b>Right channel via Amp1&amp;2 measured ref. i/p:0.5 mV + o/p:1 V Other frequency pairs</b>	o/p trafo	
29		Incl.	Excl.
30		%	
31			
32	Amp1 + Amp3 + Amp5: 60 Hz/3 kHz + 80 %/20 %	0.012	0.003
33	Amp2 + Amp3 + Amp5: 300 Hz/3 kHz + 80 %/20 %	0.026	0.026
34	Amp2 + Amp3 + Amp5: 60 Hz/3 kHz + 80 %/20 %	0.018	0.009

**Table 12.4** Frequency and phase response measurement results of Amp1 and Amp2, fed by different generator output resistances

1/A	B	C	D	E	F	G	H	I
2	Source	Colours	Unit	20 Hz	1 kHz	20 kHz	Deltas	
3	L-channel						F-E	F-G
4	Amp1 fed directly by RIAA encoder with <b>Ro = 0R</b>							
5	+Amp3	wht	[dBV]	0.544	0.817	0.793	0.273	0.024
6	+Amp3	mag	[°]	10.81	-0.21	-8.63	-11.02	8.42
7	+Amp4	red	[dBV]	0.334	0.463	0.478	0.129	-0.015
8	+Amp4	yel	[°]	10.62	-0.21	-9.26	-10.83	9.05
9								
10	Amp1 fed by RIAA encoder via un-bal/bal-converter with <b>Ro = 10R8</b>							
11	+Amp3	wht	[dBV]	-0.916	0.285	0.256	1.201	0.029
12	+Amp3	mag	[°]	29.95	0.15	-10.85	-29.8	11
13	+Amp4	red	[dBV]	-0.980	0.257	0.221	1.237	0.036
14	+Amp4	yel	[°]	30.14	0.12	-11.37	-30.02	11.49
15								
16	Amp2 fed by RIAA encoder via un-bal/bal-converter with <b>Ro = 10R8</b>							
17	+Amp3	wht	[dBV]	0.388	0.515	0.484	0.127	0.031
18	+Amp3	mag	[°]	5.58	-0.16	-6.05	-5.74	5.89
19	+Amp4	red	[dBV]	0.378	0.440	0.470	0.062	-0.03
20	+Amp4	yel	[°]	5.75	-0.16	-5.49	-5.91	5.33

## 12.3 Conclusions and Final Remarks

Generally, it became a big surprise that by listening to music material my wife, my friends and I could identify neither any big differences nor rather tiny ones (only exception: with pink noise). However, taking into account the fact that many microphone amps produce a certain amount of THD and IMD, mostly not as good as the Engine II figures, and, additionally, power amps and loudspeakers pack another portion of distortion and intermodulation on the complete signal mix, then, we might have an additional explanation for not being far away from the observed listening findings.

Provided that the whole amp chain works with the nominal signal levels between all stages and with the volume knob setting at 14:00 = 2.00 pm in 1 m distance from the loudspeakers there is no audible phono-amplifier generated noise and hum with the DL-103 at the input. My conclusions can thus be summed-up by the following statements:

1. It seems to become a hard job to design different sounding solid-state or triode driven RIAA phono-amps with passive networks, as long as there is no deviation from a flat frequency and phase response in  $B_{20k}$  inside the goals from the

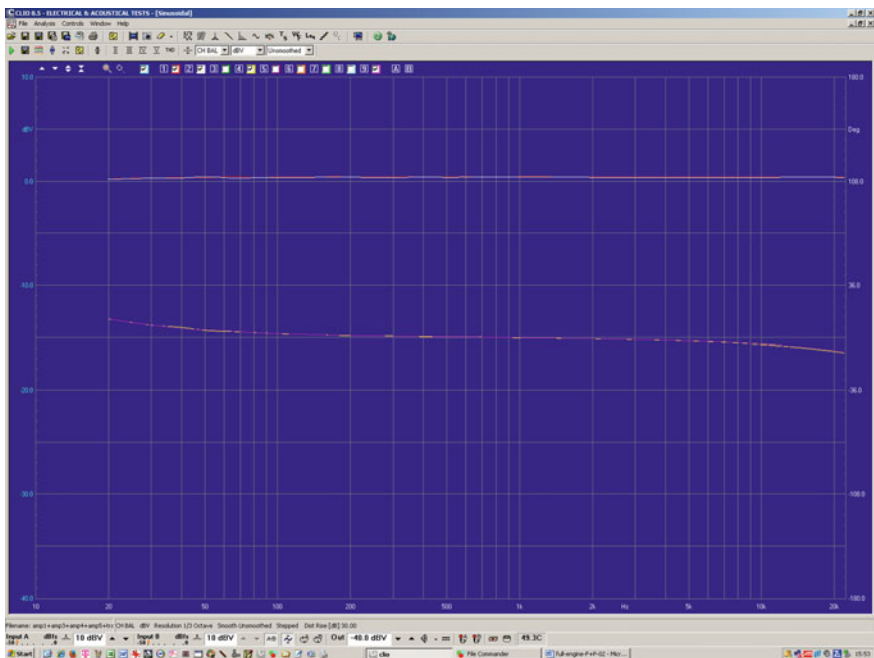


**Fig. 12.9** Frequency and phase responses of Amp1 via Amps 3 & 4, fed by a generator with an output resistance of 0 Ω

beginning, a slew rate always  $>1.8 \text{ V}/\mu\text{s}$ , 1 kHz THD  $< 0.05 \%$ , and IMD  $< 0.01 \%$ .

2. Even the tiny input transformer created  $-1.3 \text{ dB}$  at 20 Hz does not create audible impacts. In addition, other influential factors suppress negative sound impacts caused by any kind of harmonic artefacts too. Here, I'm thinking of the disappearance of these artefacts in the noise level of vinyl records (best case representation by a fictitious horizontal line in the shown THD diagrams at  $\text{SN}_{\text{riaa}} = -67.3 \text{ dB}$  unweighted<sup>14</sup>), and by putting the  $75 \mu\text{s}$  lp at the output of the amp chain's biggest THD and IMD creators, the non-equalized input Amps 1 & 2.
3. Indeed, through disturbing the flatness of the frequency and phase response by playing around with Fig. 1.2's trim pots P1, P3, and P4, from a certain disturbance level on the results will become audible. A flatness deviation of eg  $\pm 2 \text{ dB}$  at 4 kHz can certainly be heard. Then it sounds like changing treble, middle, and/or bass tone controls of the pre-amp that follows the Engine II. The

<sup>14</sup>With  $\text{SN}_{\text{ra}} = \text{SN}_{\text{ar}} - \text{SN}_{\text{r}}$  from TSOS-1, p. 207 or TSOS-2, Chap. 16, Mathcad worksheet 16.2, and the DMM-cut  $\text{SN}_{\text{ariaa}}$  from this book's Sect. 1.B.2 the derivation of the worst case line of  $\text{SN}_{\text{riaa}} = -67.3 \text{ dB}$  looks as follows:  $-71.6 \text{ dB(A)} - (-4.3 \text{ dB}) = -67.3 \text{ dB}$ .

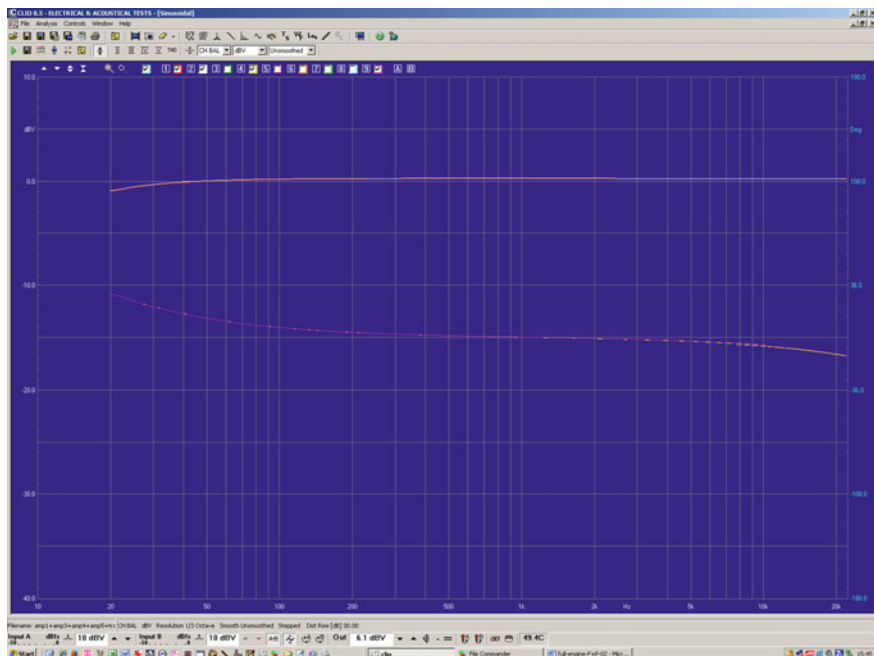


**Fig. 12.10** Frequency and phase responses of Amp1 via Amps 3 & 4, fed by a generator with an output resistance of  $10.8 \Omega$

corresponding threshold level of detecting differences in sound depends on one's personal hearing sensitivity only.

4. Excellent broadband input and/or output transformers do not influence the sound nor do they significantly worsen the noise level of pre-amps. Switching the Amp5 output transformer does not create any audible effect. The corresponding THD and IMD effects are tiny. From a CMRR point of view, transformers are best-in-class components, always outperforming any electronic solution.
5. It seems to me that the other (maybe fundamental) sound influencing differences could come from the basic configuration side of the story: single ended, semi balanced, or fully balanced amplification, with or without overall or purely local or a mixed version of negative feedback.

Principally and not only in case of Engine II, the fully balanced solution seems to be the easiest and most successful way to overcome the many connectivity problems between the various devices of an amp chain from cartridge to loudspeaker. It is a provably better solution than a single ended one and it stands at the beginning of the signal creating process in the recording studios. Because of the high CMRR of the amps even non-shielded TQ2 double-relays from Matsushita /Panasonic do not let in hum and/or other interferences. They provide the all-time balanced switching on the main PCB and on Amp5's PCB.

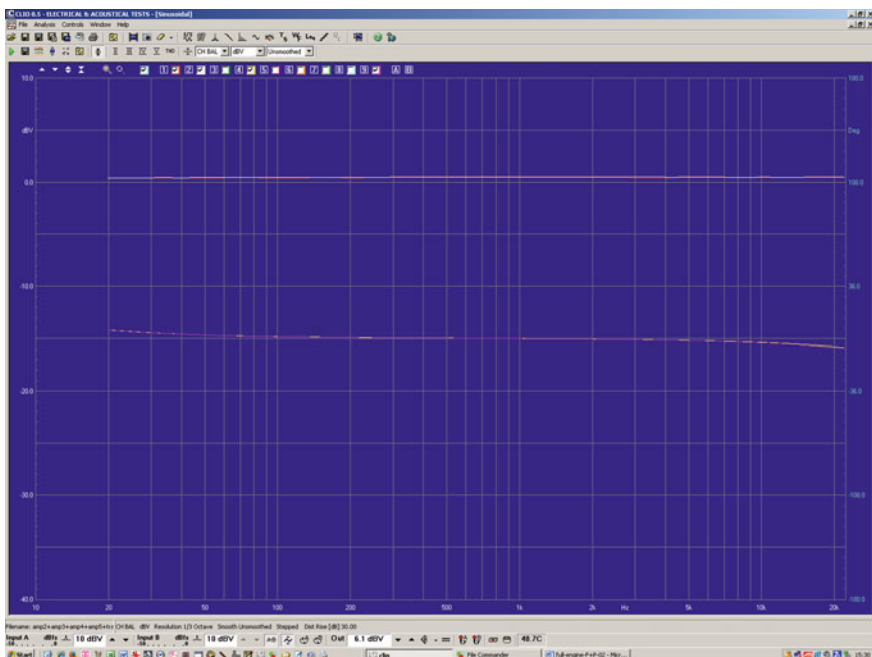


**Fig. 12.11** Frequency and phase responses of Amp2 via Amps 3 & 4, fed by a generator with an output resistance of  $10.8 \Omega$

I guess the recording studio designers really knew and still know how to manage audio signals best. They opted for the balanced way, the one that simply affects nasty influences most.

Not to forget: the passive RIAA networks allow rather easy calculation approaches, frequency response trimming, and easy adaptation to other than RIAA transfer characteristics.

6. Consequently, I think that the main drivers to cover over any differences in sound produced by different phono-amp /pre-amp configurations are the following ones:

- The frequency and phase response flatness in  $B_{20k}$ ,
- The very high un-weighted SN of the phono-amp with input load (for comparison purpose I recommend  $20 \Omega$ ),
- The disappearance of the harmonic and intermodulation artefacts in the mix of LP and phono-amp noise levels.

In the end, if the designers do not follow these conditions, of course, different phono-amps will sound differently. I checked this claim too by listening to the Engine I phono-amps; all four modules were designed according to point 6. from above. It became a hard job to find input signals, which produced a different sounding output. In the period of changing the connections between Engine I and II,



a certain amount of stored listening information gets always lost. After having it done up to ten times, sometimes I could identify tiny differences. However, I was not able to say which result sounded best.

Nevertheless, my favourite phono-amp is the sequence of Amp2 + Amp3 + Amp5 + Trafo—but I have no corresponding rational explanation. It's simply psychology according to my personal (Vogel's) Razor: if you have two devices that sound equal take the one you like best—for many different subjective reasons, including design and integration into one's living space.

---

## **Part II**

# **Knowledge Transfer**

---

## 13.1 Intro

There are many phono enthusiasts having only un-balanced connection possibilities between turntable and amplifier, some are not interested in a variable gain, and others don't mind about a fully balanced amplification chain. In this chapter, I want to demonstrate on how to integrate various Amp1/Amp2-type pre-amp design examples that do not strictly follow the rules of the Engine II approach. However, via the external input and a balanced line we can simply connect these draft pre-amps with Engine II.

What we need here are linear amps with balanced or un-balanced input, balanced output, and no equalization. At least they should fulfil the above-mentioned goals concerning frequency and phase response, overload margin, and SNs. It is not my aim to dive deep into the development of such amps. Many other authors have tackled this issue in depth<sup>1</sup> and their phono-amp circuits without RIAA equalization network and low-noise input section will work well. The only new requirement is the need of a low-noise balanced output section. Douglas Self in his 'Small Signal Audio Design' handbook gives a very good overview on the many different versions. For transformer driven outputs, the Jensen Transformers website shows a broad range of solutions. Professional recording equipment mostly uses them.

The following sections show three extremely to rather low-noise alternatives for MC and MM purposes, two of them derived from the phono-amps already presented in TSOS-1 & TSOS-2.

The first example deals with an un-balanced i/p section and it is BJT driven; the second version is a transformer driven amp with extremely low nominal i/p voltage of  $100 \mu\text{V}_{\text{rms}}/1 \text{ kHz}$  and shows a rather low i/p resistance of appr.  $50 \Omega$ , and the third version shows a fully triode and transformer driven balanced in (MC)/un-balanced in (MM) and balanced out solution.

---

<sup>1</sup>See Sect. 13.5.

Finally, at the end of this chapter in Sect. 13.5 I've added some redesigned phono-amp solutions from other engineers together with my ideas on how we could integrate these solutions into the Engine II concept.

Being in favour of not blowing-up the size of the chapter, the following descriptions concentrate on a few essential and specific issues only.

## 13.2 BJT/Op-Amps Driven MC Input Stage with Un-balanced Input and Balanced Output

The design in Fig. 13.1 is calculated in detail in the following chapter's Mathcad Worksheet MCD-WS 14.1. It is a modified version of a Douglas Self pre-pre-amp design that I have also described in detail in my TSOS-1 and TSOS-2 books as input configuration of the Module 2 phono-amp.

The amp has two trimming pots, P1 and P2 (multi turn). With P1 and input shorted we set the collector current of the 4 paired BJTs to 1.7–2 mA each ( $h_{fe} \geq 500$ ), hence in total max. 8 mA. P2 sets the overall gain, depending on the nominal output voltage of the MC cartridge in conjunction with the nominal output voltage of this amp: 100 mV<sub>rms</sub>. DC-servo OP2 keeps the output of OP3 at 0.00 V.

The gain equations look as follows:

$$\begin{aligned} G_b &= G_{1ub}G_{2b} \\ &= 200 \end{aligned} \quad (13.1)$$

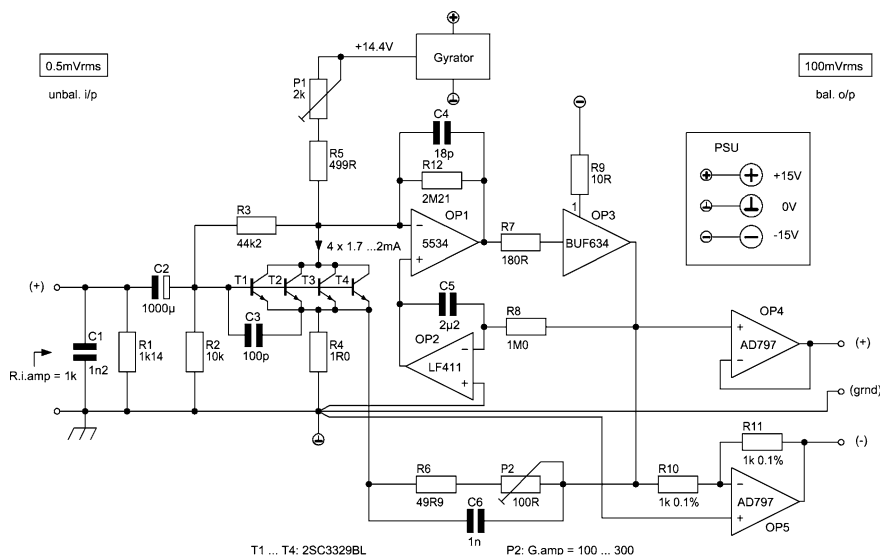


**Fig. 13.1** BJT driven input stage alternative for MC purposes

$$\begin{aligned} G1_{ub} &= 1 + \frac{R5 + P2}{R4} \\ &= 100 \end{aligned} \quad (13.2)$$

$$\begin{aligned} G2_b &= G_{op3} - G_{op4} \\ &= 1 - \left( -\frac{R11}{R10} \right) \\ &= 2 \end{aligned} \quad (13.3)$$

To avoid hum interferences I strongly recommend designing the PCB's ground lines exactly as shown in Fig. 13.1. The emitter current must directly flow back to the ground lead of the PSU.

With a gain of 2 (= bal out/un-bal in) Op-amps 4 & 5 play the balancing output stage. The chosen configuration and op-amps create lowest noise. The negative SN impact of the output stage is 0.01 dB only. Nevertheless, all op-amp types create tiny portions of additional—partly frequency dependent—noise; the worksheet considers it. It also considers all frequency dependent resistor excess noise effects and the frequency dependency of the BJT collector current noise.<sup>2</sup> If needed, additional offset voltage trimming pots (20 k $\Omega$ ) could be inserted into the OP4 & 5 output circuit.

C1 is a polypropylene type and it should be directly located at the input connector, C2 is a Panasonic FC/25 V type, C3 & C4 are ceramic types, C5 is a WIMA MKS2, and C6 could be a simple MKT type.

The Mathcad worksheet calculates graphs (Figs. 14.5 and 14.6) that show a significant increase of the amp's input or output noise voltage density in the low-frequency range. Thus, the calculation of the input referred noise voltage density must be expressed as an average value in  $B_{20k}$ : 312pV/rHz. With input shorted and referenced to 0.5 mV<sub>rms</sub>/1 kHz we can achieve an input referred SN<sub>ariaa.i</sub> of -88.2 dB (A). An input load of 20  $\Omega$  worsens the input referred SN<sub>ariaa.i</sub> to -82.3 dB(A). Consequently, as long as P2 is correctly set to a gain of 200, the output referred SN, which is referenced to 100 mV<sub>rms</sub>/1 kHz, equals the one of the input.

Section 21.5 explains the input section's fundamental equations around T1-T4 and Sect. 21.7 dives into the math of the often seen configuration of an input BJT (or JFET) followed by an op-amp.

---

### 13.3 BJT/Op-Amps Driven MC Input Stage with Balanced Transformer Input and Balanced Output

Figure 13.2 shows the second input amp alternative. It works with a balanced input and with Fig. 13.1 balanced output formed by two AD797s.

---

<sup>2</sup>See Chap. 11, MCD-WS 11.1 & 11.2.

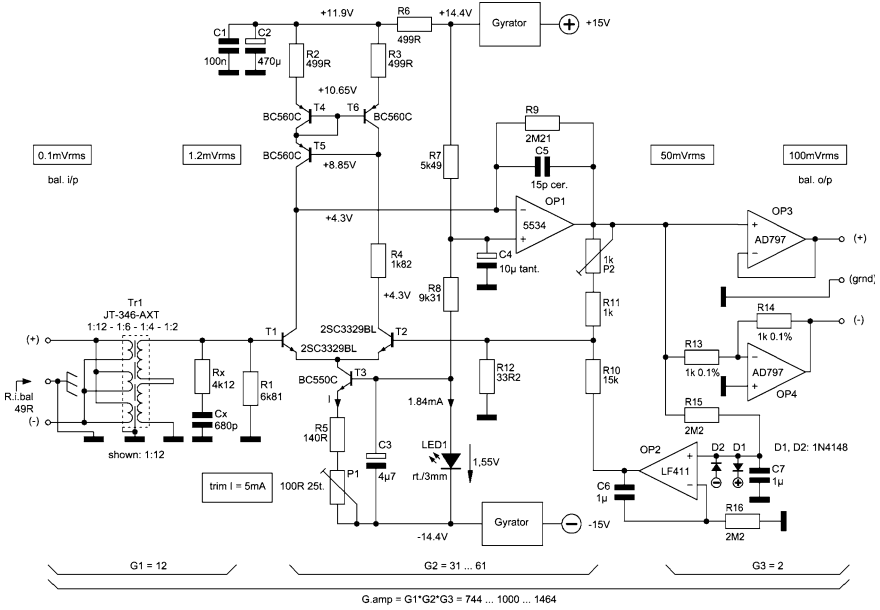


**Fig. 13.2** Balanced transformer input and BJT/Op-Amp driven input stage alternative for low-output MC cartridges

The JT-346-AXT input transformer is set to a turns ratio of  $t_r = 1:12$ , hence  $n = 12$ , thus, with the chosen input resistance of the stage after the transformer ( $R_1$ ), a 1–5  $\Omega$  MC cartridge gets loaded by a load of approximately 49  $\Omega$  (e.g. Audio Note loLtd). This is sufficiently enough for these very low source resistances and low cartridge output levels.

The gain equations look as follows:

$$G_b = G1_b G2_{ub} G3_b = 1000 \tag{13.4}$$

$$G1_b = n = 12 \tag{13.5}$$

$$G2_{ub} = 1 + \frac{R5 + P2}{R4} = \frac{1000}{nG3_b} = 41.67 \tag{13.6}$$

$$\begin{aligned}
 G_{3b} &= G_{op3} - G_{op4} \\
 &= 1 - \left( -\frac{R11}{R10} \right) \\
 &= 2
 \end{aligned} \tag{13.7}$$

I've described the basic design in TSOS-1 & -2, Module 3. The differences come from the balanced output stage around OPs 3 & 4, the absence of the RIAA feedback path, and the collector currents of T1 and T2. I've increased the collector currents to 2.5 mA, hence, we'll get a small input referred improvement over the original design's SN: now, with input shorted, A-weighting, and RIAA equalization the output referred  $SN_{ariaa.o}$  becomes  $-94.3$  dB(A), with input loaded by  $5 \Omega$  we'll get  $SN_{ariaa.o} = -88.7$  dB(A).

Note: The input reference level of  $0.5 \text{ mV}_{rms}/1 \text{ kHz}$  is not realistic for the above-mentioned kind of MC cartridges;  $0.1 \text{ mV}_{rms}/1 \text{ kHz}$  hits reality most. Hence, we must decrease the fantastic looking SN figures by 14 dB! Mathcad Worksheet 14.2 considers the lower reference level. However, these decreased SN figures are still very acceptable, because with input shorted, the average input referred noise voltage density becomes calculated  $170 \text{ pV}/\text{rtHz}$  only.

In the input shorted case the negative SN impact of the output stage with OPs 3 and 4 is  $0.006$  dB only.

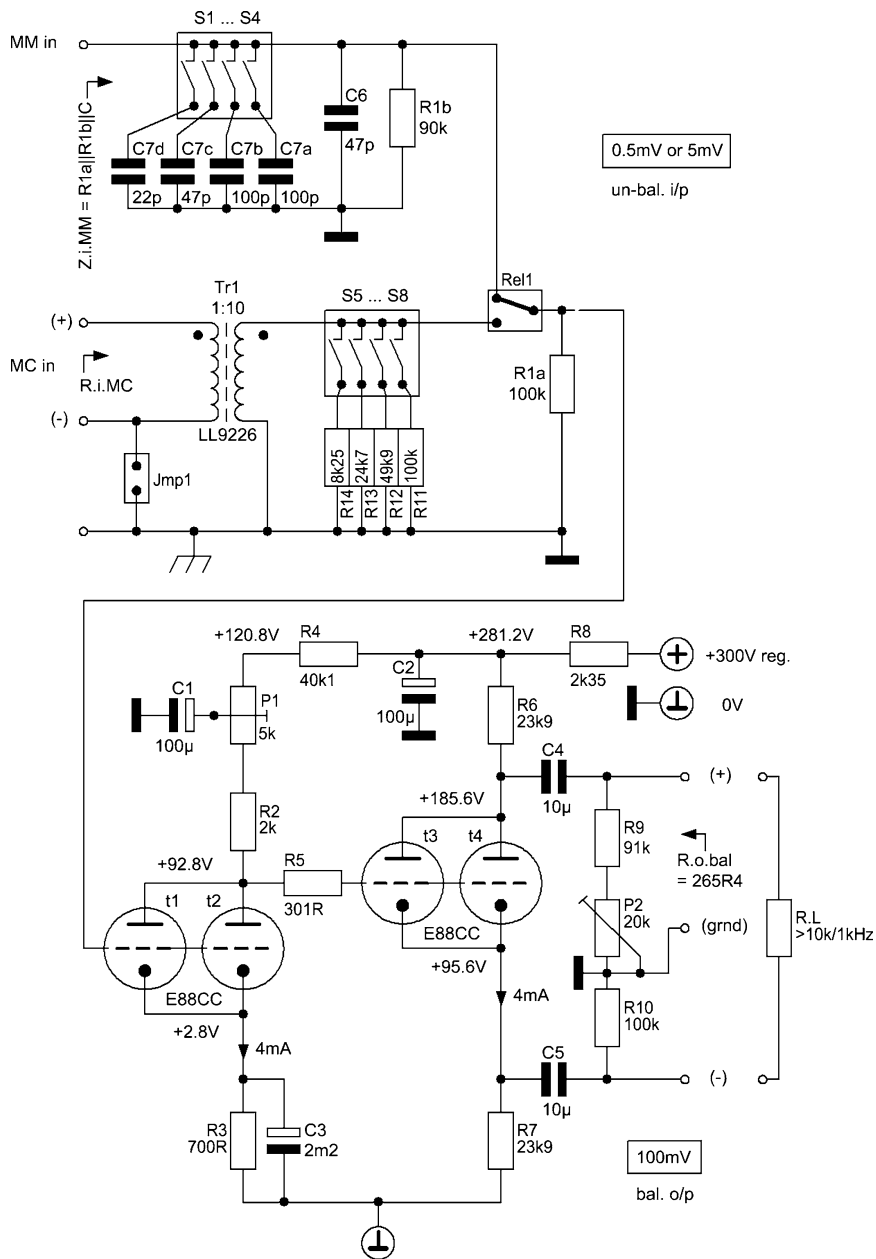
The trimming procedure starts with P1. Its setting should produce  $0.7 \text{ V}$  across R5. Then we feed the input with a  $1 \text{ mV}_{rms}/1 \text{ kHz}$  signal and we trim P2 to  $0.5 \text{ V}_{rms}$  at OP3's output. Automatically, the OP4 output will show the same level with a reversed phase. This procedure yields a balanced output voltage of  $1 \text{ V}_{rms}$ , hence the overall gain becomes 1000. If there would be a need for trimming the output DC level to  $0.00 \text{ V}$  we could add offset voltage trimmers ( $20 \text{ k}\Omega$ ) to OPs 3 & 4.

Because the JT input transformer seems to be no longer part of the Jensen Transformer product range the Lundahl LL9226 becomes a rather good replacement. By choosing the "E" termination alternative, we can set  $tr = 1:20$  or  $n = 20$  (see LL data sheet). With  $R1 = 20 \text{ k}\Omega$ ,  $R11 = 604 \Omega$ , no  $R_x$  and  $C_x$ ,  $R0 = 5 \Omega$  ( $0 \Omega$ ), and P2 set for an overall gain of 1000 we have a calculated  $SN_{ariaa.o} = -74.7$  dB(A) ( $-80.3$  dB(A)), ref  $0.1 \text{ mV}_{rms}/1 \text{ kHz}$ . With input shorted the average input referred noise voltage density becomes  $168.7 \text{ pV}/\text{rtHz}$ .

### 13.4 Fully Triode Driven MC/MM Pre-Amp with Transformer MC-Input and Balanced Output

The fully triode driven version's circuit is given in Fig. 13.3.

It is composed of a low gain CCS (common cathode stage) with a double triode in parallel operation followed by a CPS (concertina or cathodyne phase splitter) with rather low output resistance, however not  $<1 \Omega$ ! Nevertheless, I want to



MC:	$G2 = 11.1$ (P1: 9.4 ... 18)	$G3 = 1.8$	$G.tot.MC = 200$ (170 ... 320)
MM:	$G2 = 11.1$ (P1: 9.4 ... 18)	$G3 = 1.8$	$G.tot.MM = 20$ (17 ... 32)

**Fig. 13.3** Fully triode driven MC/MM input stage alternative with transformer (Lundahl LL9226) MC-input and balanced output



demonstrate here the possibility to create a fully triode and transformer driven MC/MM phono-amp input stage that could also be taken as stand-alone pre-amp, offering an excellent SN performance too.

The question might come-up why I've chosen the parallel operation of t1 and t2 and did not take a single triode that could produce the same  $g_m$  value. First answer: The single triode needs 1 mA more operating current (5 mA) to produce a  $g_m$  of 7 mS at 90 V. It also represents a change of the operating point closer to "A". According to the findings of TSOS-2, Sect. 7.11, Table 17.7, 7 mS seems to be a mutual conductance figure high enough for our purposes here, including the gain stage application of MM amplification by replacing the transformer with a 47 k $\Omega$  resistance and the required paralleled load capacitances, switched by S1–S4. Second answer: I found out that the euphonic harmonics production at the operating point "2 mA/90 V" per triode sounds best in my ears. The parallel operation of t3 and t4 follows the same operating point related arguments.

P1 trims the overall gain from the balanced input to the balanced output. P2 trimming leads to equal 1 kHz output levels to ground. Because the two output resistances to ground differ very much (at the cathode  $R_{o,c} = 750 \Omega$ , at the anode  $R_{o,a} = 18.7 \text{ k}\Omega$ ) the following measurement approach works quite well: we load the balanced o/p by a 10 k $\Omega$  resistance and with two 1 M $\Omega$  (or 10 M $\Omega$ ) input resistance instruments we measure equal amplitudes from anode and cathode to ground.

The CPS is fully described in HTGG-2, Chaps. 10 and 11, and in one of my LTEs<sup>3</sup> to Linear Audio. Its rather low noise production mostly disappears in the noise of the t1, t2 input stage with input load. Figure 13.4 shows the noise model of the amp, configured as an MC phono-amp stage. In case of an MM phono-amp configuration we have to take as input load the noise voltages<sup>4</sup> of the admittances that generate the two input noise voltages  $(e_{n1}(f)^2 + e_{n2}(f)^2)^{0.5}$  as result of the voltage divider effects at the MM input.<sup>5</sup>

MCD Worksheet 14.3 dives deep into the SN calculation course for both versions: MC and MM. The input double triode shows the following low-noise relevant figures:  $f_c \leq 500 \text{ Hz}$ ,  $g_m \geq 3.7 \text{ mS}$  at 2 mA/90 V.<sup>6</sup> Hence, with 20  $\Omega$  input load, and  $n = 10$  the calculated output referred and A-weighted  $SN_{\text{ariaa.o}}$  becomes  $-80.3 \text{ dB(A)}$ .

A change to the transformer configuration of Sect. 13.3 yields an output referred  $SN_{\text{ariaa.o}}$  of  $-73.9 \text{ dB(A)}$ . To get it we need the following component changes:  $R_0 = 5 \Omega$ ,  $n = 20$ , S5–8 and R11–R14 replaced by a new resistance  $R_x = 25 \text{ k}\Omega$ , in conjunction with a low-noise current generator as gain effective anode load P1 must be set to a gain of 1000! (instead of 200). Then, with input shorted, the average input noise voltage density becomes a calculated 221 pV/rtHz.

<sup>3</sup>See on Linear Audio's website '[www.linearaudio.net/letters](http://www.linearaudio.net/letters)' my LTE 'Vol. 0-3' to Stuart Yaniger's article in Vol. 0.

<sup>4</sup>Details see MCD WS 14.4 of next chapter.

<sup>5</sup>See TSOS-1, p. 158, TSOS-2, p. 293.

<sup>6</sup>See TSOS-2 Tables 17.2 and 17.7.

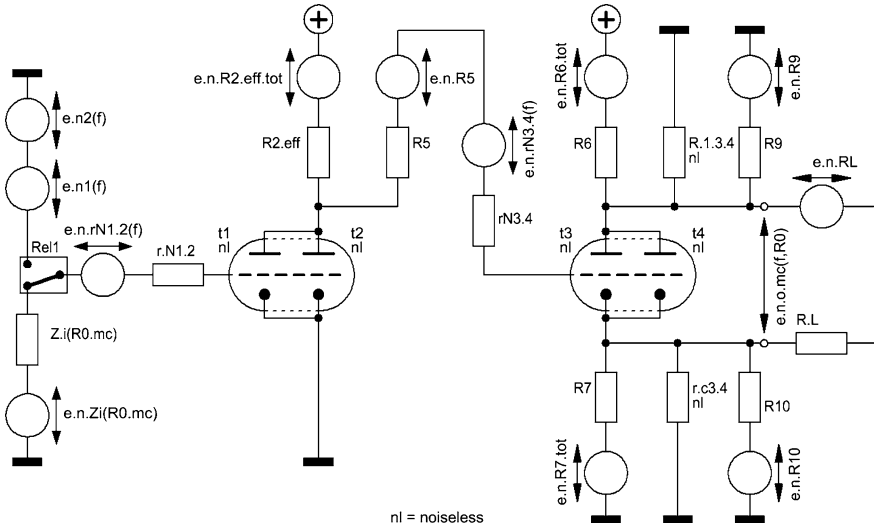


**Fig. 13.4** Noise model of the Fig. 13.3 MC input stage

The same calculation with a Shure V15 V as the input load yields an output referred  $SN_{ariaa.o}$  of  $-82.1$  dB(A). For comparison reasons with the Engine I performance<sup>7</sup> I add the measured V15 V and  $1\text{ k}\Omega$  input load value too:  $-78.1$  dB(A) and  $-78.0$  dB(A).

We obtain the following gain equations<sup>8</sup> for the MC case:

$$G_{b.mc} = G1_{ub}G2_{ub}G3_b \tag{13.8}$$

$$= 200$$

$$G1_{ub} = n \tag{13.9}$$

$$= 10$$

$$G2_{ub} = g_{m1.2}(R2 + P1) \tag{13.10}$$

$$= 11.1$$

$$G3_b = \frac{2\mu \left( \frac{1}{R_{re}} + \frac{1}{0.5R_L} \right)}{r_a + (2 + \mu) \left( \frac{1}{R_{re}} + \frac{1}{0.5R_L} \right)} \tag{13.11}$$

$$= 1.8$$

<sup>7</sup>See TSOS-2 Table 29.2.

<sup>8</sup>Details of the  $G3$  gain equation: see HTGG-2, Chaps. 10 and 11.

## 13.5 Other Development Examples

It might be conspicuous that I do not present my own amp solutions with input sections driven by FETs. The reason is very simple: I never tried to develop them. However, this is not a judgement about the quality of FET driven phono-amps. On the contrary, I think that there are enough excellent solutions on the market. Among them, three very different ones were presented in the past issues of the Linear Audio bookzine. In this section, I want to demonstrate how they could be turned into linear amplifiers, very useful as external or internal Engine II input stages. Choosing them will lead to three main adaptation tasks: to get rid of the RIAA transfer-producing components, to find a balanced output in two cases, and to set the right gain. The next rather condensed sections will show how we can achieve very positive solutions.<sup>9</sup>

### 13.5.1 The Joachim Gerhard Approach<sup>10</sup>

Mr. Gerhard's phono-amp solution is a rather complex amplifier, split into two stages, one linear for the input, and one for the RIAA transfer function performing output. Both stages work in fully differential mode. Resistances separately set their gains. DC servos ensure DC output voltages close to 0 V. The whole design approach and the detailed circuit were published in Linear Audio's Vol. 0, 2010.

Figure 13.5 (top) shows the stripped-down principal circuit without RIAA components and some input (bottom) and other circuit components. Not shown are the DC servos (DCS) for the input and output stages.

The overall differential gain  $G_{\text{tot.b}}$  of this arrangement is split into two gain blocks the following way:

$$\begin{aligned} G_{\text{tot.b}} &= -\frac{V_{\text{o.b}}}{V_{\text{i.b}}} \\ &= G1_b G2_b \\ &= -200 \end{aligned} \quad (13.12)$$

$$\begin{aligned} G1_b &= \frac{V_{\text{o.1st.b}}}{V_{\text{i.b}}} \\ &= 1 + \frac{2Rf1}{RG} \\ &= 100 \end{aligned} \quad (13.13)$$

<sup>9</sup>In the following three sections the several times used term 'roughly calculated SNs' means: application of a HP21 and some rule-of-thumb figures for noise densities close to white noise ( $=\text{low } f_c < 1 \text{ kHz}$ ). They can be found in TSOS-1 and TSOS-2.

<sup>10</sup>Down the Rabbit Hole—Adventure in the Land of Phonostages', Linear Audio Vol. 0, 2010, on <http://www.linearaudio.net>.

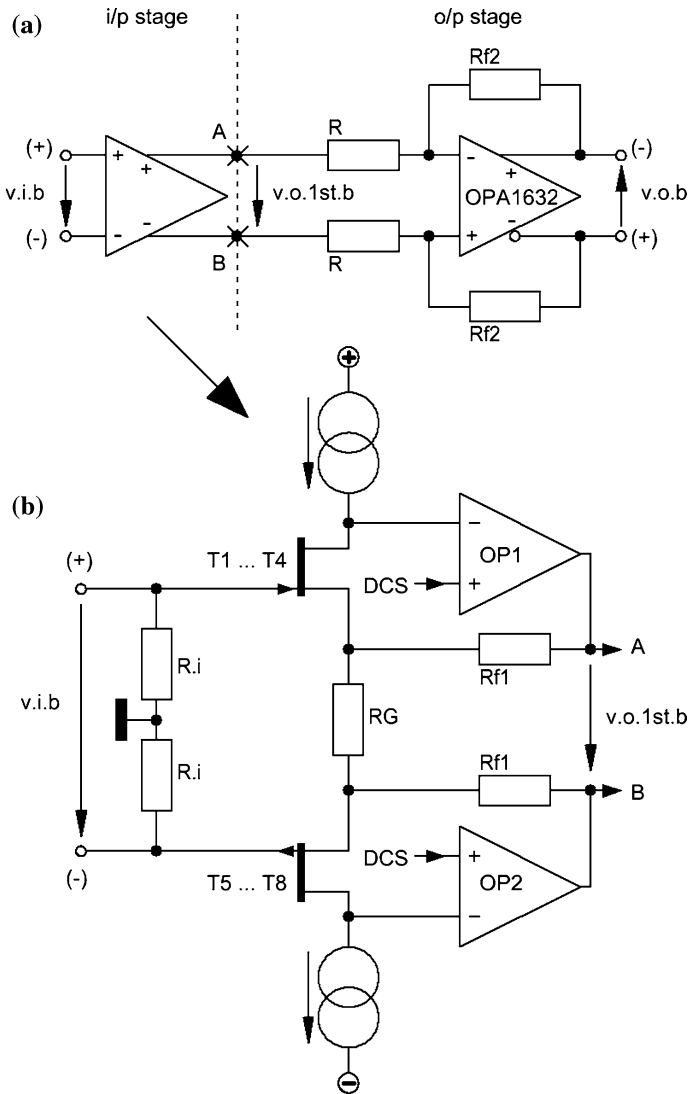


**Fig. 13.5** Principal Joachim Gerhard design with high-Z (Principally, Mr. Gerhard’s low-Z input approach looks the same; details see footnote 11) voltage driven input, turned into a linear input amp for Engine II purposes

$$\begin{aligned}
 G_{2b} &= -\frac{V_{o.b}}{V_{o.1st.b}} \\
 &= -\frac{R_{f2}}{R} \\
 &= -2
 \end{aligned}
 \tag{13.14}$$

$R_G = 2.5 \Omega = R_{11}$  in the Gerhard circuit. If we would set  $G_2 = 2$  then  $R_{f2}$  becomes 2 times  $R$ . With  $R = 440 \Omega (=R_{38}/R_{39})$   $R_{f2}$  becomes  $880 \Omega$ . Because of the rather high gain of the input stage ( $G_1 = 100$ ) the noise production of the output stage is of minor importance.

With  $G_1 = 100$  we get  $R_{f1} = 124 \Omega (=R_{12}/R_{13})$ . If we assume a worst case input referred noise voltage density of  $0.6 \text{ nV}/\sqrt{\text{rtHz}}$  the proposed circuit changes do not negatively touch the general noise behaviour of the Gerhard design, hence, the output referred noise voltage density becomes  $200 \times 0.6 \text{ nV}/\sqrt{\text{rtHz}} = 120 \text{ nV}/\sqrt{\text{rtHz}}$ .

With input shorted and referenced to  $100 \text{ mV}_{\text{rms}}/1 \text{ kHz}$  the non-equalized Fig. 13.5 output referred  $\text{SN}_{\text{ne,o}}$  thus becomes  $-77.0 \text{ dB}$ . If we assume a flat  $F$  and  $P$  in  $B_{20k}$  the output referred RIAA equalized and A-weighted  $\text{SN}_{\text{ariaa,o}}$  yields roughly  $-84.9 \text{ dBV(A)}$ .

With  $20 \Omega$  input load the output referred  $\text{SN}_{\text{ariaa,o}}$  would then decrease to  $-81.3 \text{ dBV(A)}$ . Hence, the shown arrangement would fulfil the Engine II goals. There is another advantage of this type of JFET input stage: with  $2 \times 23.7 \text{ k}\Omega$  the input resistance could be set to  $47.4 \text{ k}\Omega$ , thus, MC cartridges like the Denon DL 103 R could be connected according to its data sheet specs.

This design could work without the output stage too. However, without touching the input stage's noise behaviour and according to (13.14) the output stage offers an elegant possibility of changing the overall gain by simultaneously changing the two  $R_{f2}$  resistances. A bank of several jumpers or a multi-DIP-switch and a set of selected resistors (0.1 %) will make it.

### 13.5.2 The Ovidiu Popa Approach<sup>11</sup>

In detail Mr. Popa's approach, Synaesthesia HP5.1 can be studied on his website <http://www.synaesthesia.ca/LNschematics.html>. It is a pre-pre-amp with a configuration alike the NPN-half of Fig. 13.5 input stage, however with the doubled number of JFETs. The principal circuit is given in Fig. 13.6's input stage. Without increasing the excellent noise voltage situation at the input stage's output the output stage creates the balanced output around OPs 2 and 3 and the two resistors  $R$ . An additional DC-servo ensures DC output voltages close to 0 V (not shown here).

The gain equations look as follows:

$$\begin{aligned} G_{\text{tot,b}} &= \frac{V_{\text{o,b}}}{V_{\text{i,ub}}} \\ &= G_{1\text{ub}} G_{2\text{b}} \\ &= 200 \end{aligned} \tag{13.15}$$

<sup>11</sup>See Mr. Popa's article in Linear Audio Vol. 1, 04-2011, 'On the Noise Performance of Low Noise Input Stage' and the corresponding LTEs on <http://www.linearaudio.net>.

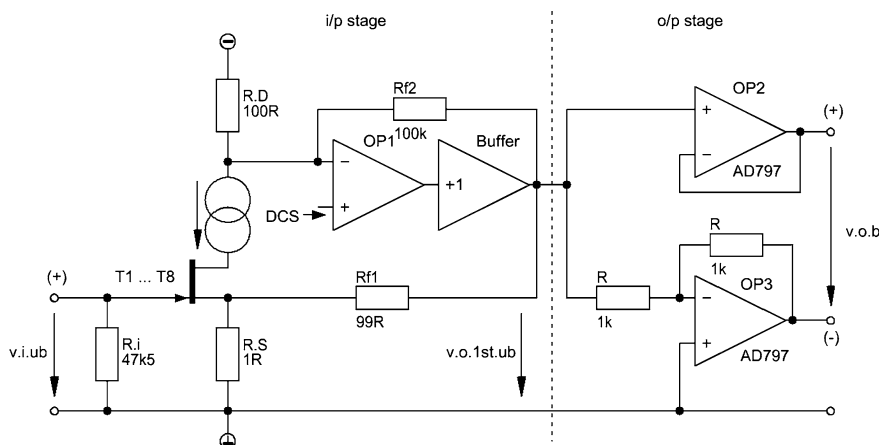


**Fig. 13.6** Principal Ovidiu Popa design with additional and new output stage, turned into a linear input amp for Engine II purposes

$$\begin{aligned}
 G1_{ub} &= \frac{V_{o.1st.ub}}{V_{i.ub}} \\
 &= 1 + \frac{Rf1}{R_S} \\
 &= 100
 \end{aligned} \tag{13.16}$$

$$\begin{aligned}
 G2_b &= \frac{V_{o.v}}{V_{o.1st.ub}} \\
 &= \frac{V_{o.1st.ub} - [-V_{o.1st.ub}(R/R)]}{V_{o.1st.ub}} \\
 &= 2
 \end{aligned} \tag{13.17}$$

With input shorted, an average input noise voltage density of 275 pV/rHz, and referenced to 100 mV<sub>rms</sub>/1 kHz the non-equalized Fig. 13.6 output referred SN<sub>ne.o</sub> thus becomes -82.2 dB. If we assume a flat F and P in B<sub>20k</sub> the output referred RIAA equalized and A-weighted SN<sub>ariaa.o</sub> yields roughly -90.1 dBV(A).

With 20 Ω input load the output referred SN<sub>ariaa.o</sub> would then decrease to -82.8 dBV(A).<sup>12</sup> Hence, the shown arrangement would fulfil the Engine II goals too. Alike the Gerhard design there is an equal advantage of this type of JFET input stage: with 47.5 kΩ as input resistance MC cartridges like the Denon DL 103 R could be connected too.

A variable gain set-up could be performed by copying the method shown in Fig. 13.1.

<sup>12</sup>The complete SN calculations can be found in my LTE to Mr. Popa's Linear Audio article in Vol. 1, on <http://www.linearaudio.net/LTE>

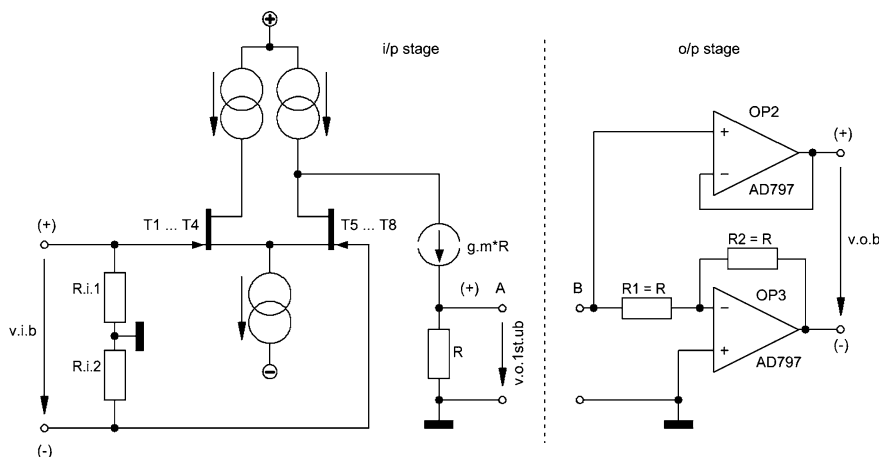


**Fig. 13.7** Principal Bob Cordell design with an additional and new output stage

### 13.5.3 The Bob Cordell Approach<sup>13</sup>

In contrast to the above-described voltage-to-voltage solutions (VV-A) with  $4 \times 2\text{SK}170$  &  $4 \times 2\text{SJ}74$  and  $8 \times \text{BF}862$  JFETs, the Cordell design sets on a high-Z current generating output of his multi-LTP-JFET-input stage with four Dual-JFETs LSK389. Thus, a simple resistor  $R$  at the output can set the gain of this stage. Its value depends on the required gain and the transconductance of the amp; hence, we talk about a transconductance amplifier or VC-A which transfers its input voltage into an output current.

The gain equation thus becomes the following general format:

$$G = g_m R \quad (13.18)$$

At the left side of Fig. 13.7 we find the principal circuit of this stage with a gain of 100 at 1 kHz. On the right side, as balanced signal producing output stage, we find a configuration that equals the one of Fig. 13.6.

The connection of the output stage to the output of the input stage is rather simple: delete  $R$  of the i/p stage ( $=R_{40}$  of Mr. Cordell's design) and connect A & B. Now, the input  $R_1 = R$  of the output stage plays the role of the deleted  $R$  and the feedback  $R_2 = R$  of OP3 sets the gain of OP 3 to "1". Thus, we obtain the following gain equations:

<sup>13</sup>See Mr. Cordell's article in Linear Audio Vol. 4, 09-2012, 'VinyITrak—A full-featured MM/MC phono-preamp' or on [www.cordell.com](http://www.cordell.com).

$$\begin{aligned}
 G_{\text{tot},b} &= \frac{V_{o,b}}{V_{i,b}} \\
 &= G1_b G2_b \\
 &= 200
 \end{aligned} \tag{13.19}$$

$$\begin{aligned}
 G1_b &= \frac{V_{o,\text{st},ub}}{V_{i,b}} \\
 &= g_m R1 \\
 &= 100
 \end{aligned} \tag{13.20}$$

$$\begin{aligned}
 G2_b &= \frac{V_{o,b}}{V_{o,\text{1st},ub}} \\
 &= \frac{V_{o,\text{1st},ub} - \left( -V_{o,\text{1st},ub} \frac{R2}{R1} \right)}{V_{o,\text{1st},ub}} \\
 &= 2
 \end{aligned} \tag{13.21}$$

By making  $R = R1 = R2$  variable by a range of fixed resistors and jumpers, this amp configuration allows setting a broad range of gains, eg from 100–300 with  $R = 890 \Omega$ –2.67 k $\Omega$ .

Mr. Cordell measured an input referred noise voltage density of 0.7 nV/rtHz. If we take it as average value, then, with input shorted, the output referred  $SN_{\text{ne},o}$  becomes  $-74.1$  dB (gain = 200 and reference level = 100 mV<sub>rms</sub>). If we assume a flat F and P in  $B_{20k}$  the output referred RIAA equalized and A-weighted  $SN_{\text{ariaa},o}$  yields roughly  $-82.0$  dBV(A).

With 20  $\Omega$  input load the output referred  $SN_{\text{ariaa},o}$  would then decrease to  $-79.8$  dBV(A). Hence, the shown arrangement would fulfil the Engine II goals too.

---

## 13.6 The Output Stage

The task of the output stages in Figs. 13.1, 13.2, 13.6, and 13.7 lies in the fact of turning an un-balanced signal into a balanced one. A range of other solutions could also do it. However, we need a very low-noise solution here, a solution that does not add more than 0.1 dB noise to the output noise of the preceding gain stage. Each component counts here.

The chosen two-op-amp arrangement does an excellent job. The calculated and measured SN worsening never exceeds the set boundary; even in the extremely low-noise Popa solution, it becomes calculated  $<0.06$  dB.

In the Cordell case, the preceding input stage produces more than a doubled Popa output noise voltage. Hence, the output stage's noise contribution with 6.23 nV/rtHz ( $\equiv -101.1$  dB ref. 0.1 V<sub>rms</sub>) falls below 0.02 dB.



## 13.7 Summary of Results

Table 13.1 shows the most important noise voltage and SN results of the presented draft designs, compared with measured Engine II results.

For a better understanding Table 13.1 needs some additional remarks:

1. Column D shows values of the average noise voltage density in  $B_{20k}$ , hence, including 1/f-noise effects that may exist.
2. Column E transfers Column D values into non-equalized SN (dB) values by referencing them to the nominal signal voltage of  $0.1 V_{rms}$  at the output of the input stages. The contributions of the shown two-op-amp output stages is always  $<0.06$  dB.
3. Column F shows MM usability of the stage, however, with the following adaptations only:

line 9: (yes) with gain reduction to 20, high-Z input equipped with an appropriate MM cartridge load resistance, in conjunction with a long input cable<sup>14</sup>

( $1 \text{ m} \equiv 100\text{--}150 \text{ pF}$ ) the input capacitance could be the bottle-neck:  $C_i \sim 95 \text{ pF}$

line 10: (yes) with the same line 9 arguments;  $C_i \sim 80 \text{ pF}$

line 11: (yes) with Mr Cordell's similar looking MM input stage with a different input LTP.

4. Column G values are Column F values transferred into RIAA equalized and A-weighted SNs,  $i/p$  shorted. Here, because of the input referred SN of the following Engine II stages and according to Figs. 15.3 and 15.4, we can find a noise contribution from the following stages, however, not shown in the table. For example: The amp sequence Amp3 + Amp5 + Trafo has an input referred  $SN_{o,a}$  of  $-99 \text{ dB(A)}$ .<sup>15</sup> It includes the contributions of the RIAA transfer network. Compared with the line 5 and column G value of  $-88.2 \text{ dB(A)}$  we have a difference of only 10.8 dB, thus, with Fig. 15.3 we find an SN worsening of 0.4 dB. If we calculate the whole amp sequence with input shorted the box 5/G value should thus be corrected and reduced by a worsening figure  $W_c(B) = 0.4 \text{ dB}$ .
5. Column H shows the RIAA equalized and A-weighted results. Here, the calculation of a worsening figure makes no sense, because the input load moves the difference of the SN values into a region of  $>16 \text{ dB}$ , hence,  $W_c(B) < 0.1 \text{ dB}$ .
6. Column I shows the gains of the whole RIAA amplifier sequence from input to output.

<sup>14</sup>Remedy: See TSOS-1, p. 144ff, TSOS-2, p. 220ff.

<sup>15</sup>See Table 12.1, line 13, column D.

**Table 13.1** Draft design SNs compared with Engine II results

1/A	B	C	D	E	F	G	H	I	J	K
2	Type or Fig.	i/p characteristic	i/p referred noise voltage density	o/p referred SN <sub>re.o</sub> (i/p shorted)	Usability for MM purposes	Engine II o/p SN <sub>ana.o</sub> (i/p shorted)	Engine II o/p SN <sub>ana.o</sub> (i/p 20 Ω)	Engine II gain	Remarks	Usage
3			calc.	calc.		calc.	calc.			
4			nV/rtHz average	dB		dBV(A)	dBV(A)	times		
5	13.1	4 × NPN BJTs	0.312	-81.1	No	-88.2	-82.3	2,000	MCD-WS 14.1	ub-to-b
6	13.2	n = 12 trafo and i/p load 5 Ω	0.170	-72.4	No	-80.3	-74.7	10,000	MCD-WS 14.2	ub&b-to-b
7	13.3a	4 × E88CC and n = 10 trafo	0.536	-76.4	Yes	-83.0	80.3	2,000	MCD-WS 14.3	ub&b-to-b
8	13.3b	4 × E88CC and i/p like 13.2	0.221	-70.1	No	-78.0	-73.9	10,000	Rough calc.	ub&b-to-b
9	13.5	4 × (NPN and PNP) JFETs	0.500	-77.0	(Yes)	-84.9	-81.3	2,000	Rough calc.	b-to-b
10	13.6	8 × NPN JFETs	0.275	-82.2	(Yes)	-90.1	-82.8	2,000	Rough calc.	ub-to-b
11	13.7	4 × LTP NPN JFETs	0.700	-74.1	(Yes)	-82.0	-79.8	2,000	Rough calc.	ub&b-to-b
12							Meas.			
13	Amp1	n = 10 trafo	0.519	-76.6	No	-84.5	-81.8	2,000	MCD-WS 9.1	ub&b-to-b
14	Amp2	2 × (NPN and PNP) BJTs	0.517	-76.7	No	-83.3	-79.8	2,000	MCD-WS 11.3	b-to-b

7. Column K gives some usage hints:

b-to-b	balanced-in to balanced-out (i/p socket mostly XLR)
ub-to-b	un-balanced-in to balanced-out (i/p socket mostly Cinch or BNC)
ub&b-to-b	un-balanced-in to balanced-out (eg by grounding the XLR pin 3 input with a Neutrik Cinch-XLR adapter), and balanced-in to balanced-out

## Contents

- 14.1 MCD-WS: BJT/Op-Amp Driven MC Input Stage with Un-Balanced Input and Balanced Output
- 14.2 MCD-WS: BJT/Op-Amp Driven MC Input Stage with Balanced Transformer Input and Balanced Output
- 14.3 MCD-WS: Fully Triode Driven MC/MM Pre-Amp with Transformer MC-Input and Balanced Output

**Note 1:** MCD 11 has no built-in unit “rtHz” or “ $\sqrt{\text{Hz}}$ ”. To get  $\sqrt{1 \text{ Hz}}$  based voltage noise and current noise densities the rms noise voltage and current in a specific frequency range  $B > 1 \text{ Hz}$  must be multiplied by  $\sqrt{1 \text{ Hz}}$  and divided by the root of that specific frequency range  $\sqrt{B}$ !

**Note 2:** MCD 11 offers no “dB” unit. This is available from MCD 13 on!

14.1 BJT/Op-Amp Driven Input Stage

BJT/Op-Amp Driven MC input Stage with Un-Balanced Input and Balanced Output :

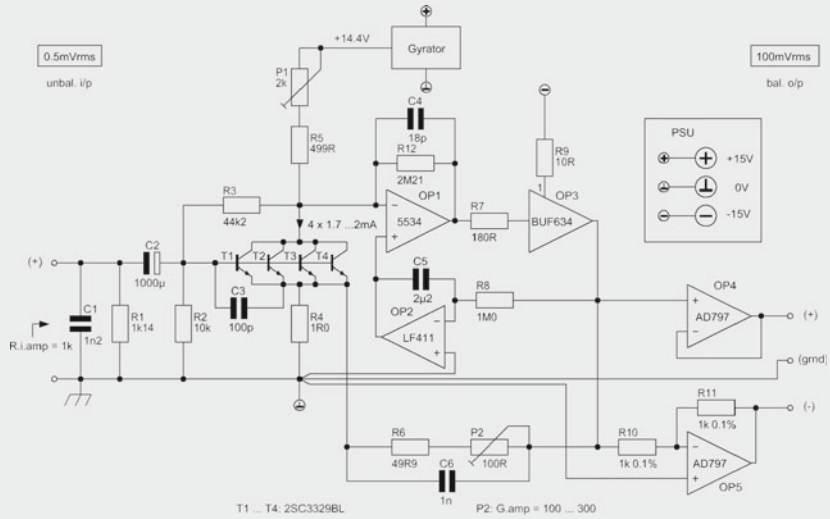


Fig. 14.1 = Fig. 13.1

1. Definition of all meaningful constants, components, etc.:

- $k := 1.38065 \cdot 10^{-23} \cdot \text{V} \cdot \text{A} \cdot \text{s} \cdot \text{K}^{-1}$    
  $q := 1.6021765 \cdot 10^{-19} \text{A} \cdot \text{s}$    
  $T := 300 \cdot \text{K}$    
  $v_{i,nom} := 0.5 \cdot 10^{-3} \text{V}$
- $B_{20k} := 19980 \cdot \text{Hz}$    
  $B_1 := 1 \text{Hz}$    
  $h := 1000 \text{Hz}$    
  $v_{o,nom} := 0.1 \text{V}$
- $R0 := 20 \Omega$    
  $R1 := 1.14 \cdot 10^3 \Omega$    
  $R2 := 10 \cdot 10^3 \Omega$    
  $R3 := 44.2 \cdot 10^3 \Omega$
- $R4 := 1 \Omega$    
  $R5 := 1.3 \cdot 10^3 \Omega$    
  $R6 := 199 \Omega$    
  $R7 := 180 \Omega$
- $R8 := 1 \cdot 10^6 \Omega$    
  $R9 := 10 \Omega$    
  $R10 := 1 \cdot 10^3 \Omega$    
  $R11 := R10$    
  $R12 := 2.21 \cdot 10^6 \Omega$
- $RP_{op4} := \left( \frac{1}{R10} + \frac{1}{R11} \right)^{-1}$    
  $RP_{op4} = 500 \Omega$
- $NI := 31.62 \cdot 10^{-9}$    
  $NI_e := 20 \cdot \log(NI) + 120$    
  $NI_e = -30.001 \text{ [dB]}$
- Note: In the following calculation course I've set  $R5 = R5+P1$ ,  $R6 = R6+P2$  !
- $C1 := 1.2 \cdot 10^{-9} \text{F}$    
  $C2 := 1 \cdot 10^{-3} \text{F}$    
  $C3 := 100 \cdot 10^{-12} \text{F}$    
  $C4 := 18 \cdot 10^{-12} \text{F}$
- $C5 := 2.2 \cdot 10^{-6} \text{F}$    
  $C6 := 1 \cdot 10^{-9} \text{F}$

14.1 BJT/Op-Amp Driven Input Stage

$$\begin{aligned}
 I_C &:= 8 \cdot 10^{-3} \text{ A} & h_{fe} &:= 500 & V_A &:= -160 \text{ V} \\
 V_{CE} &:= 14.4 \text{ V} - R5 \cdot I_C & V_{CE} &:= 4 \text{ V} & V_{BE} &:= 0.7 \text{ V} \\
 V_{R5} &:= I_C \cdot R5 & V_{R5} &:= 10.4 \text{ V} & V_{R4} &:= I_C \cdot R4 & V_{R4} &:= 8 \times 10^{-3} \text{ V} \\
 OP1 &= 5534 & OP2 &= LF411 & OP3 &= BUF634 & OP4 &= AD797 & OP5 &= OP4 \\
 G_{amp} &:= 1 + \frac{R6}{R4} & G_{amp} &= 200 \\
 x &:= 0.17 & f_{c,i} &:= 33750 \text{ Hz} \\
 g_m &:= \frac{q \cdot I_C}{k \cdot T} & g_m &:= 309.454 \times 10^{-3} \text{ S} \\
 r_{bb} &:= \frac{2}{4} \Omega & r_{bb} &= 0.5 \Omega & e_{n,rbb} &:= \sqrt{4 \cdot k \cdot T \cdot B_1 \cdot r_{bb}} & e_{n,rbb} &= 91.016 \times 10^{-12} \text{ V}
 \end{aligned}$$

2. Evaluation of the impedances of the input network as the input load :

f := 10Hz, 20Hz, 20000 Hz

$$Z1(f, R0) := \left( \frac{1}{R0} + 2j \cdot \pi \cdot f \cdot C1 + \frac{1}{R1} \right)^{-1} + \frac{1}{2j \cdot \pi \cdot f \cdot C2} \quad |Z1(h, 20\Omega)| = 19.656 \Omega$$

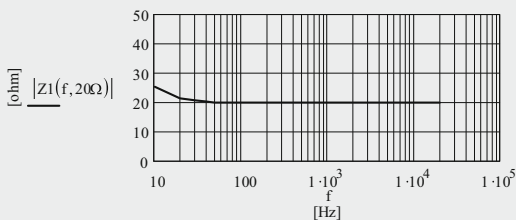


Fig. 14.2  
Impedance of the input network Z1(f)

$$e_{n,Z1}(f, R0) := \sqrt{4 \cdot k \cdot T \cdot B_1 \cdot Z1(f, R0)} \quad |e_{n,Z1}(h, 20\Omega)| = 570.661 \times 10^{-12} \text{ V}$$

3. Evaluation of the impedance of the feedback network :

$$Z2(h) := \left( \frac{1}{R6} + 2j \cdot \pi \cdot h \cdot C6 \right)^{-1} \quad |Z2(h)| = 199 \Omega$$

$$G_{amp}(h) := 1 + \frac{Z2(h)}{R4} \quad |G_{amp}(h)| = 200$$

14.1 BJT/Op-Amp Driven Input Stage

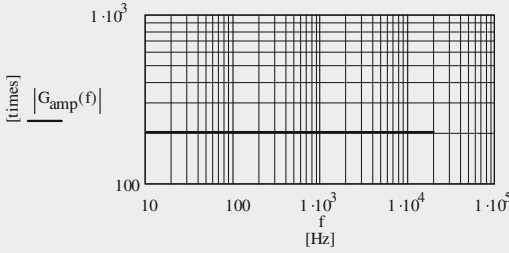


Fig. 14.3a  
Frequency dependent gain

$$\phi_{amp}(f) := \text{atan}\left(\frac{\text{Im}(G_{amp}(f))}{\text{Re}(G_{amp}(f))}\right)$$

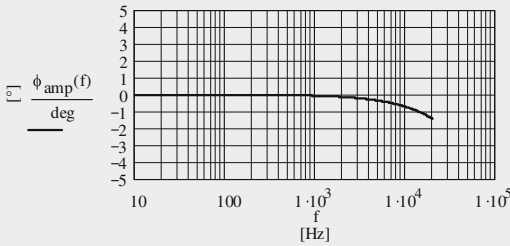


Fig. 14.3b  
Phase response of the gain

4. Calculation of the gain and input resistance of the T1 ... T4 stage :

$$r_{ce} := \left| \frac{V_A}{I_C} \right| \quad r_{ce} = 20 \times 10^3 \Omega$$

$$g_{m,red} := \frac{g_m \left( r_{ce} + R5 \right) \left( h_{fe} - \frac{R4}{r_{ce}} \right)}{h_{fe} \left( r_{ce} + R4 + R5 \right) + g_m \cdot R4 \cdot \left( h_{fe} \cdot r_{ce} + r_{ce} + R5 \right)} \quad g_{m,red} = 239.657 \times 10^{-3} S$$

$$G_{T1.4} := \left| \frac{g_{m,red} R3 - 1}{1 + R3 \cdot \left( \frac{1}{R5} + \frac{1}{r_{ce}} \right)} \right| \quad G_{T1.4} = 284.651$$

$$G_{T1.4,e} := 20 \cdot \log(G_{T1.4}) \quad G_{T1.4,e} = 49.086 \quad [dB]$$

$$r_{be} := \frac{h_{fe}}{g_m} \quad r_{be} = 1.616 \times 10^3 \Omega$$

14.1 BJT/Op-Amp Driven Input Stage

$$r_i := \left[ \frac{1}{R2} + \frac{1}{(r_{be} + h_{fe} \cdot R4) \cdot \left( 1 + g_m \cdot R12 \cdot \frac{R4}{R4 + R6} \right)} + \frac{1}{R3 + \left( \frac{1}{R5} + \frac{1}{r_{ce}} \right)^{-1}} \right]^{-1} \quad r_i = 8.186 \times 10^3 \Omega$$

$$R_{i,amp} := \left( \frac{1}{r_i} + \frac{1}{R1} \right)^{-1} \quad R_{i,amp} = 1000.653 \Omega$$

$$Z_{in}(f) := \left( 2j \cdot \pi \cdot f \cdot C1 + \frac{1}{R_{i,amp}} \right)^{-1} \quad |Z_{in}(h)| = 1.001 \times 10^3 \Omega$$

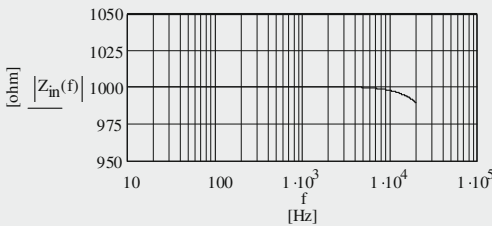


Fig. 14.4  
Input impedance  $Z_{in}(f)$

5. Calculation of the amp's input noise current and voltage :

5.1 Relevant input noise current densities :

$$i_{n,c}(f) := \sqrt{2 \cdot q \cdot I_C \cdot B_1} \cdot \left( 1 + \frac{f_{c,i}}{f} \right)^x \quad i_{n,c}(h) = 92.55 \times 10^{-12} A$$

$$i_{n,i}(f) := \sqrt{\frac{2 \cdot q \cdot I_C}{h_{fe}} \cdot B_1} \cdot \left( 1 + \frac{f_{c,i}}{f} \right)^x \quad i_{n,i}(h) = 4.139 \times 10^{-12} A$$

$$i_{n,R2} := \sqrt{\frac{4 \cdot k \cdot T \cdot B_1}{R2}} \quad i_{n,R2} = 1.287 \times 10^{-12} A$$

$$i_{n,R3} := \sqrt{\frac{4 \cdot k \cdot T \cdot B_1}{R3}} \quad i_{n,R3} = 612.239 \times 10^{-15} A$$

5.2 Relevant resistor noise voltages and currents :

$$e_{N,R4ex}(f) := \sqrt{\left( \frac{\frac{N I_e}{10^{10} \cdot 10^{-12}}}{\ln(10)} \right) \cdot \frac{(I_C \cdot R4)^2 \cdot B_1}{f}} \quad e_{N,R4ex}(h) = 5.272 \times 10^{-12} V$$

$$e_{N,R4} := \sqrt{4 \cdot k \cdot T \cdot R4 \cdot B_{20k}}$$



## 14.1 BJT/Op-Amp Driven Input Stage

Page 5

$$e_{n,R4ex,tof}(f) := \sqrt{e_{N,R4ex}(f)^2 + e_{N,R4}^2 \cdot \frac{B_1}{B_{20k}}}$$

$$e_{n,R4ex,tof}(h) = 128.716 \times 10^{-12} \text{V}$$

$$e_{N,R5ex}(f) := \sqrt{\left( \frac{\frac{N I_e}{10^{10}} \cdot 10^{-12}}{\ln(10)} \right)^2 + \frac{(I_C \cdot R_5)^2 \cdot B_1}{f}}$$

$$e_{N,R5ex}(h) = 6.853 \times 10^{-9} \text{V}$$

$$e_{N,R5} := \sqrt{4 \cdot k \cdot T \cdot R_5 \cdot B_{20k}}$$

$$e_{n,R5ex,tof}(f) := \sqrt{e_{N,R5ex}(f)^2 + e_{N,R5}^2 \cdot \frac{B_1}{B_{20k}}}$$

$$e_{n,R5ex,tof}(h) = 4.641 \times 10^{-9} \text{V}$$

$$e_{n,R6} := \sqrt{4 \cdot k \cdot T \cdot R_6 \cdot B_1}$$

$$e_{n,R6} = 1.816 \times 10^{-9} \text{V}$$

$$e_{n,R7} := \sqrt{4 \cdot k \cdot T \cdot R_7 \cdot B_1}$$

$$e_{n,R7} = 1.727 \times 10^{-9} \text{V}$$

$$e_{n,R8} := \sqrt{4 \cdot k \cdot T \cdot R_8 \cdot B_1}$$

$$e_{n,R8} = 128.716 \times 10^{-9} \text{V}$$

$$e_{n,R10} := \sqrt{4 \cdot k \cdot T \cdot R_{10} \cdot B_1}$$

$$e_{n,R10} = 4.07 \times 10^{-9} \text{V}$$

$$e_{n,R11} := \sqrt{4 \cdot k \cdot T \cdot R_{11} \cdot B_1}$$

$$e_{n,R11} = 4.07 \times 10^{-9} \text{V}$$

$$e_{n,R12} := \sqrt{4 \cdot k \cdot T \cdot R_{12} \cdot B_1}$$

$$e_{n,R12} = 191.35 \times 10^{-9} \text{V}$$

$$i_{n,R5ex}(f) := \frac{e_{n,R5ex,tof}(f)}{R_5}$$

$$i_{n,R5ex}(h) = 3.57 \times 10^{-12} \text{A}$$

$$i_{n,R4ex}(f) := \frac{e_{n,R4ex,tof}(f)}{R_4}$$

$$i_{n,R4ex}(h) = 128.716 \times 10^{-12} \text{A}$$

## 5.3 Noise of op-amps :

OP1 :

$$f_{c,e1} := 6 \text{Hz}$$

$$f_{c,i1} := 8 \text{Hz}$$

$$e_{n,iop1} := 4 \cdot 10^{-9} \text{V}$$

$$e_{n,iop1}(f) := e_{n,iop1} \cdot \sqrt{\frac{f_{c,e1}}{f} + 1}$$

$$i_{n,iop1} := 0.4 \cdot 10^{-12} \text{A}$$

$$i_{n,iop1}(f) := i_{n,iop1} \cdot \sqrt{\frac{f_{c,i1}}{f} + 1}$$

OP2 :

$$f_{c,e2} := 0.1 \cdot 10^3 \text{Hz}$$

$$f_{c,i2} = \text{unknown}$$

$$e_{n,iop2} := 25 \cdot 10^{-9} \text{V}$$

$$e_{n,iop2}(f) := e_{n,iop2} \cdot \sqrt{\frac{f_{c,e2}}{f} + 1}$$

$$i_{n,iop2} := 0.01 \cdot 10^{-12} \text{A}$$

14.1 BJT/Op-Amp Driven Input Stage

$$e_{n.o.op2}(f) := \sqrt{\left[ e_{n.R8} \frac{(2j \cdot \pi \cdot f \cdot C6)^{-1}}{R8} \right]^2 + e_{n.i.op2}(f)^2 \left[ 1 + \frac{(2j \cdot \pi \cdot f \cdot C6)^{-1}}{R8} \right]^2 + \left[ i_{n.i.op2} (2j \cdot \pi \cdot f \cdot C6)^{-1} \right]^2}$$

$$e_{n.o.op2}(h) = 18.184 \times 10^{-9} \text{ V}$$

OP3 :

$f_{c.e3} = \text{unknown}$	$f_{c.i3} = \text{unknown}$	
$e_{n.i.op3} := 4 \cdot 10^{-9} \text{ V}$	$i_{n.i.op3} := 1 \cdot 10^{-12} \text{ A}$	guessed!

OPs 4 & 5 :

$f_{c.e4} := 30 \text{ Hz}$	$f_{c.e5} := f_{c.e4}$	$f_{c.i4} = \text{unknown}$	$f_{c.i5} = \text{unknown}$
$e_{n.i.op4} := 0.9 \cdot 10^{-9} \text{ V}$	$e_{n.i.op4}(f) := e_{n.i.op4} \cdot \sqrt{\frac{f_{c.e4}}{f} + 1}$		
$i_{n.i.op4} := 2 \cdot 10^{-12} \text{ A}$	$i_{n.i.op5} := i_{n.i.op4}$	$e_{n.i.op5}(f) := e_{n.i.op4}(f)$	
Noise gains in the output stage :	$G_{N.op4} := 1$	$G_{N.op5} := 2$	

$$e_{n.o.op4,5}(f) := \sqrt{G_{N.op4}^2 \cdot e_{n.i.op4}(f)^2 + G_{N.op5}^2 \cdot e_{n.i.op5}(f)^2 + e_{n.R10}^2 + i_{n.i.op5}^2 \cdot R11^2 + e_{n.R11}^2}$$

$$e_{n.o.op4,5}(h) = 6.427 \times 10^{-9} \text{ V}$$

5.4 Input referred noise voltage density of T1 ... T4 :

$$e_{n.i.T1,4}(f) := \sqrt{\frac{i_{n.c}(f)^2}{2} + 4 \cdot k \cdot T \cdot r_{bb} \cdot B1}$$

$$e_{n.i.T1,4}(h) = 312.619 \times 10^{-12} \text{ V}$$

$$e_{n.i}(f) := \sqrt{e_{n.i.T1,4}(f)^2 + R4^2 \cdot (i_{n.i}(f)^2 + i_{n.R4ex}(f)^2) + i_{n.R5ex}(f)^2 \cdot \left( R4 + \frac{1}{g_m} \right)^2}$$

$$e_{n.i}(h) = 338.443 \times 10^{-12} \text{ V}$$

$$i_{n.i.amp}(f) := \sqrt{i_{n.i}(f)^2 + i_{n.R2}^2 + i_{n.R3}^2}$$

$$i_{n.i.amp}(h) = 4.378 \times 10^{-12} \text{ A}$$

6. Calculation of the amp's input and output noise voltages :

$G_{0.amp} := g_m \cdot R12$	$G_{0.amp} = 683.892 \times 10^3$
------------------------------	-----------------------------------

$$e_{n.o.tot.0}(f) := \sqrt{\left( \frac{e_{n.i}(f)^2 + \frac{e_{n.i.op1}(f)^2 + e_{n.o.op2}(f)^2}{2}}{G_{T1,4}} \right) \cdot G_{0.amp}^2 + i_{n.R5ex}(f)^2 \cdot R12^2 + i_{n.i.op1}(f)^2 \cdot R12^2 + e_{n.R12}^2 \dots + i_{n.i.op3}^2 \cdot R7^2 + e_{n.R7}^2 + e_{n.i.op3}^2}$$

14.1 BJT/Op-Amp Driven Input Stage

$$e_{n.i.tot}(f) := \frac{e_{n.o.tot,0}(f)}{G_{0,amp}}$$

$$e_{n.o.tot}(f) := \sqrt{(e_{n.i.tot}(f) \cdot G_{amp}(f))^2 + e_{n.R6}^2 + e_{n.o.op4.5}(f)^2}$$

$$e_{n.i.amp}(f) := \frac{e_{n.o.tot}(f)}{G_{amp}(f)}$$

$$e_{n.i.amp}(f, R0) := \sqrt{e_{n.i.amp}(f)^2 + i_{n.i.amp}(f)^2 \cdot Z1(f, R0)^2 + e_{n.Z1}(f, R0)^2}$$

$$e_{n.o.tot,0}(h) = 235.877 \times 10^{-6} V$$

$$e_{n.i.tot}(h) = 344.903 \times 10^{-12} V$$

$$|e_{n.o.tot}(h)| = 69.303 \times 10^{-9} V$$

$$|e_{n.i.amp}(h)| = 346.516 \times 10^{-12} V$$

$$|e_{n.i.amp}(h, 20\Omega)| = 673.147 \times 10^{-12} V$$

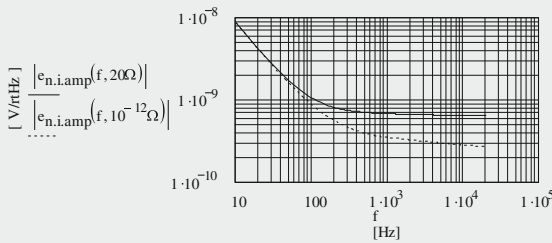


Fig. 14.5  
Frequency and R0  
dependent equivalent input  
noise voltage density for  
two different input loads

7. SN calculations :

$$e_{n.o.amp}(f, R0) := e_{n.i.amp}(f, R0) \cdot G_{amp}(f)$$

$$|e_{n.o.amp}(h, 20\Omega)| = 134.629 \times 10^{-9} V$$

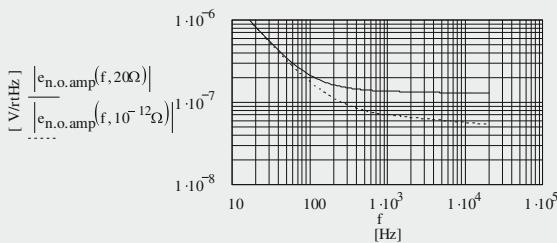


Fig. 14.6  
Frequency and R0  
dependent equivalent  
output noise voltage density  
for two different input loads

14.1 BJT/Op-Amp Driven Input Stage

$$SN_{ne.o}(R0) := 20 \cdot \log \left[ \frac{1}{B_1} \int_{20\text{Hz}}^{20000\text{Hz}} \left( |e_{n.o.amp}(f, R0)| \right)^2 df \right] \cdot \frac{1}{V_{o.nom}}$$

$$SN_{ne.o}(20\Omega) = -74.662 \quad [\text{dB}]$$

Average input referred noise voltage density (R0 dependent) :

$$R0 := 0.001\Omega, 1\Omega .. 100\Omega \qquad SN_{ne.i}(R0) := SN_{ne.o}(R0)$$

$$e_{n.i.amp}(R0) := v_{i.nom} \cdot 10^{\frac{SN_{ne.i}(R0)}{20}} \cdot \sqrt{\frac{B_1}{B_{20k}}}$$

$$e_{n.i.amp}(10^{-12}\Omega) = 312.261 \times 10^{-12}\text{V}$$

$$e_{n.i.amp}(20\Omega) = 653.966 \times 10^{-12}\text{V}$$

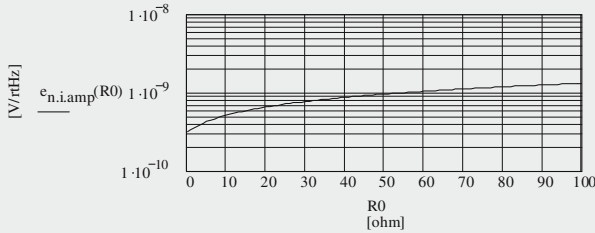


Fig. 14.7  
R0 dependent average input noise voltage density

A-weighting by A(f) :

$$A(f) := \frac{1.259}{1 + \left(\frac{20.6\text{Hz}}{f}\right)^2} \cdot \frac{1}{\sqrt{1 + \left(\frac{107.7\text{Hz}}{f}\right)^2}} \cdot \frac{1}{\sqrt{1 + \left(\frac{737.9\text{Hz}}{f}\right)^2}} \cdot \frac{1}{1 + \left(\frac{f}{12200\text{Hz}}\right)^2}$$

$$SN_{ne.o.a}(R0) := 20 \cdot \log \left[ \frac{1}{B_1} \int_{20\text{Hz}}^{20000\text{Hz}} \left( |e_{n.o.amp}(f, R0)| \right)^2 \cdot (|A(f)|)^2 df \right] \cdot \frac{1}{V_{o.nom}}$$

$$SN_{ne.o.a}(20\Omega) = -76.783 \quad [\text{dB(A)}]$$

14.1 BJT/Op-Amp Driven Input Stage

RIAA equalizing by R(f) :

$$R_{1000} := \left[ \frac{\sqrt{1 + (2 \cdot \pi \cdot 10^3 \text{ Hz} \cdot 318 \cdot 10^{-6} \text{ s})^2}}{\sqrt{1 + (2 \cdot \pi \cdot 10^3 \text{ Hz} \cdot 318 \cdot 10^{-6} \text{ s})^2} \cdot \sqrt{1 + (2 \cdot \pi \cdot 10^3 \text{ Hz} \cdot 75 \cdot 10^{-6} \text{ s})^2}} \right]^{-1} \quad R_{1000} = 9.898$$

$$R(f) := \left[ \frac{\sqrt{1 + (2 \cdot \pi \cdot f \cdot 318 \cdot 10^{-6} \text{ s})^2}}{\sqrt{1 + (2 \cdot \pi \cdot f \cdot 318 \cdot 10^{-6} \text{ s})^2} \cdot \sqrt{1 + (2 \cdot \pi \cdot f \cdot 75 \cdot 10^{-6} \text{ s})^2}} \right] \cdot R_{1000}$$

$$SN_{riaa.o}(R0) := 20 \cdot \log \left[ \frac{\int_{20\text{Hz}}^{20000\text{Hz}} (|e_{n.o.amp}(f, R0)|)^2 \cdot (|R(f)|)^2 \text{ df}}{V_{o.nom}} \right] \quad SN_{riaa.o}(20\Omega) = -71.799 \quad [\text{dB}]$$

$$SN_{ariaa.o}(R0) := 20 \cdot \log \left[ \frac{\int_{20\text{Hz}}^{20000\text{Hz}} (|e_{n.o.amp}(f, R0)|)^2 \cdot (|A(f)|)^2 \cdot (|R(f)|)^2 \text{ df}}{V_{o.nom}} \right] \quad SN_{ariaa.o}(20\Omega) = -82.373 \quad [\text{dB(A)}]$$

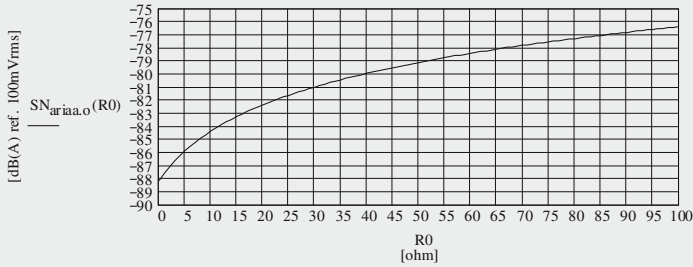


Fig. 14.8 R0 dependent, A-weighted, and RIAA equalized output referred SNs

14.2 BJT/Op-Amp Driven MC Input Stage with Balanced Transformer Input and Balanced Output

BJT/Op-Amp Driven MC Input Stage with Balanced transformer Input and Balanced Output

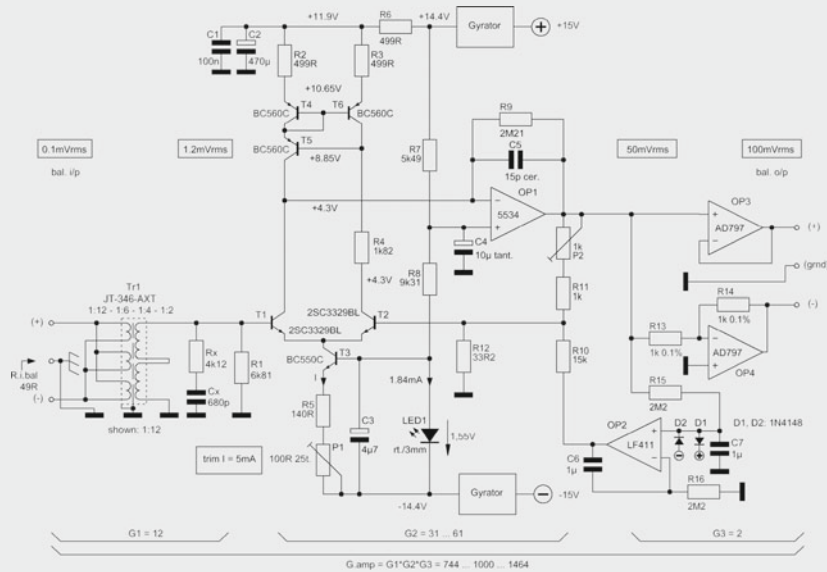


Fig. 14.9 = Fig. 13.2

1. Definition of all meaningful constants, components, etc.:

- $k := 1.38065 \cdot 10^{-23} \cdot \text{V} \cdot \text{A} \cdot \text{s} \cdot \text{K}^{-1}$    
  $q := 1.6021765 \cdot 10^{-19} \text{ A} \cdot \text{s}$    
  $T := 300 \cdot \text{K}$    
  $V_{i,nom} := 0.1 \cdot 10^{-3} \text{ V}$
- $B_{20k} := 19980 \cdot \text{Hz}$    
  $B_1 := 1 \text{ Hz}$    
  $h := 1000 \text{ Hz}$    
  $V_{o,nom} := 0.1 \text{ V}$
- $f := 10 \text{ Hz}, 15 \text{ Hz}, 20 \cdot 10^3 \text{ Hz}$
- $R_0 := 5 \Omega$    
  $R_1 := 6.81 \cdot 10^3 \Omega$    
  $R_2 := 499 \Omega$    
  $R_3 := R_2$    
  $R_4 := 1.82 \cdot 10^3 \Omega$
- $R_6 := 499 \Omega$    
  $R_7 := 5.49 \cdot 10^3 \Omega$    
  $R_8 := 9.31 \cdot 10^3 \Omega$    
  $R_9 := 2.21 \cdot 10^6 \Omega$    
  $R_{10} := 15 \cdot 10^3 \Omega$
- $R_{11} := 1 \cdot 10^3 \Omega$    
  $R_{12} := 33.2 \Omega$    
  $R_{13} := 1 \cdot 10^3 \Omega$    
  $R_{14} := 1 \cdot 10^3 \Omega$    
  $R_{15} := 2.21 \cdot 10^6 \Omega$
- $R_{16} := 2.21 \cdot 10^6 \Omega$    
  $R_x := 4.12 \cdot 10^3 \Omega$
- $NI_e := -30 \text{ [dB]}$    
 $NI := 10^{\frac{NI_e}{20}} \cdot 10^{-6}$    
 $NI = 31.623 \times 10^{-9}$
- Transformer data sheet:   
  $n := 12$    
 $RP := 0.643 \Omega$    
 $RS := 154 \Omega$

## 14.2 BJT/Op-Amp and Transformer Driven Input Stage

Page 2

	$R0_{sec}(R0) := R0 \cdot n^2$	$R0_{sec}(5\Omega) = 720\ \Omega$	optimal transformer load = 6k81	
	$RP_{sec} := RP \cdot n^2$	$RP_{sec} = 92.592\ \Omega$		
	$Rn(R0) := R0_{sec}(R0) + RP_{sec} + RS$		$Rn(5\Omega) = 966.592\ \Omega$	
$C1 := 0.1 \cdot 10^{-6}\text{F}$	$C2 := 470 \cdot 10^{-6}\text{F}$	$C3 := 4.7 \cdot 10^{-6}\text{F}$	$C4 := 10 \cdot 10^{-6}\text{F}$	$C5 := 15 \cdot 10^{-12}\text{F}$
$C6 := 1 \cdot 10^{-6}\text{F}$	$C7 := C6$			
Input load:	$R_{iL}(R0) := \frac{R1 \cdot (R0_{sec}(R0) + RP_{sec} + RS)}{R1 + R0_{sec}(R0) + RP_{sec} + RS}$		$R_{iL}(5\Omega) = 846.449\ \Omega$	
Transistor data:	$T1 = T2 = 2\text{SC3329BL}$	$r_{bb1} := 2\ \Omega$	$r_{bb2} := r_{bb1}$	
	$h_{fe1} := 500$	$h_{fe2} := h_{fe1}$		
	$I_{C1} := 2.5 \cdot 10^{-3}\text{A}$	$I_{C2} := I_{C1}$	$V_{A1} := -160\text{V}$	$V_{A2} := V_{A1}$
	$T3 = \text{BC550C}$	$T4 = T5 = T6 = \text{BC560C}$		
Op-Amps:	$OP1 = 5534$	$OP2 = \text{LF411}$	$OP3 = OP4 = \text{AD797}$	

2. Calculation of the amp's gain and input resistance  $R_i$ :

		succ-apps P1:	$P1 := 347.5\ \Omega$
$G1 := n$	$G2 := 1 + \frac{R11 + P1}{\left(\frac{1}{R10} + \frac{1}{R12}\right)^{-1}}$	$G2 = 41.677$	$G3 := 2$
$G_{amp} := G1 \cdot G2 \cdot G3$			$G_{amp} = 1 \times 10^3$
Note: In the following calculation course $R11p = R11 + P1!$	$R11p := R11 + P1$	$R11p = 1.347 \times 10^3\ \Omega$	
$g_{m1} := \frac{q \cdot I_{C1}}{k \cdot T}$	$g_{m1} = 96.704 \times 10^{-3}\text{S}$		
$r_{be1} := \frac{h_{fe1}}{g_{m1}}$	$r_{be1} = 5.17 \times 10^3\ \Omega$	transformer load:	
$r_{i1} := 2 \cdot r_{be1} \cdot \left(1 + g_{m1} \cdot R9 \cdot \frac{R12}{R11p + R12}\right)$	$r_{i1} = 53.152 \times 10^6\ \Omega$	$\left(\frac{1}{r_{i1}} + \frac{1}{R1}\right)^{-1} = 6.809 \times 10^3\ \Omega$	
$R_i := \left[\left(\frac{1}{r_{i1}} + \frac{1}{R1}\right)^{-1} + RP_{sec} + RS\right] \cdot \frac{1}{n}$		$R_i = 48.998\ \Omega$	

## 14.2 BJT/Op-Amp and Transformer Driven Input Stage

Page 3

3. Calculation of the relevant noise currents and voltages of the whole amp

## 3.1 BJT noise currents :

$$x := 0.5 \quad f_{c,il} := 10\text{-Hz} \quad \text{guessed!} \quad f_{c,i2} := f_{c,il}$$

$$i_{n,c1}(f) := \sqrt{2 \cdot q \cdot I_{C1} \cdot B_1} \cdot \left( \frac{f_{c,il}}{f} + 1 \right)^x \quad i_{n,c1}(h) = 28.445 \times 10^{-12} \text{ A}$$

$$i_{n,b1}(f) := \sqrt{\frac{2 \cdot q \cdot I_{C1} \cdot B_1}{h_{fe1}} \cdot \left( \frac{f_{c,il}}{f} + 1 \right)^x} \quad i_{n,b1}(h) = 1.272 \times 10^{-12} \text{ A}$$

$$i_{n,c2}(f) := i_{n,c1}(f) \quad i_{n,b2}(f) := i_{n,b1}(f)$$

Note: Noise impact of T3 ... T6 ignored!

## 3.2 BJT noise voltages :

$$e_{n,il}(f) := \sqrt{\frac{i_{n,c1}(f)^2}{g_{m1}} + 4 \cdot k \cdot T \cdot B_1 \cdot r_{bb1} + i_{n,b1}(f)^2 \cdot r_{bb1}^2} \quad e_{n,il}(h) = 345.92 \times 10^{-12} \text{ V}$$

$$e_{n,i2}(f) := e_{n,il}(f)$$

## 3.3 Resistor noise voltages :

$$e_{n,RiL}(R0) := \sqrt{4 \cdot k \cdot T \cdot B_1 \cdot R_{iL}(R0)} \quad e_{n,RiL}(5\Omega) = 3.745 \times 10^{-9} \text{ V}$$

$$RP := \left( \frac{1}{R12} + \frac{1}{R10} \right)^{-1} \quad RP = 33.127 \Omega$$

$$e_{n,RP} := \sqrt{4 \cdot k \cdot T \cdot B_1 \cdot RP} \quad e_{n,RP} = 740.835 \times 10^{-12} \text{ V}$$

$$e_{n,R11p} := \sqrt{4 \cdot k \cdot T \cdot B_1 \cdot R11p} \quad e_{n,R11p} = 4.725 \times 10^{-9} \text{ V}$$

$$e_{n,R13} := \sqrt{4 \cdot k \cdot T \cdot B_1 \cdot R13} \quad e_{n,R13} = 4.07 \times 10^{-9} \text{ V}$$

$$e_{n,R14} := \sqrt{4 \cdot k \cdot T \cdot B_1 \cdot R14} \quad e_{n,R14} = 4.07 \times 10^{-9} \text{ V}$$

$$e_{n,R15} := \sqrt{4 \cdot k \cdot T \cdot B_1 \cdot R15} \quad e_{n,R15} = 191.35 \times 10^{-9} \text{ V}$$

$$e_{n,R16} := \sqrt{4 \cdot k \cdot T \cdot B_1 \cdot R16} \quad e_{n,R16} = 191.35 \times 10^{-9} \text{ V}$$



14.2 BJT/Op-Amp and Transformer Driven Input Stage

3.4 Op-Amp noise voltages and currents :

OP1 :

$$f_{c,e1} := 6\text{Hz}$$

$$f_{c,i1} := 8\text{Hz}$$

$$e_{n,iop1} := 4 \cdot 10^{-9}\text{V}$$

$$e_{n,iop1}(f) := e_{n,iop1} \cdot \sqrt{\frac{f_{c,e1}}{f} + 1}$$

$$i_{n,iop1} := 0.4 \cdot 10^{-12}\text{A}$$

$$i_{n,iop1}(f) := i_{n,iop1} \cdot \sqrt{\frac{f_{c,i1}}{f} + 1}$$

Note: Noise impact of OP1 ignored!

OP2 :

$$f_{c,e2} := 0.1 \cdot 10^3\text{Hz}$$

$$f_{c,i2} = \text{unknown}$$

$$e_{n,iop2} := 25 \cdot 10^{-9}\text{V}$$

$$e_{n,iop2}(f) := e_{n,iop2} \cdot \sqrt{\frac{f_{c,e2}}{f} + 1}$$

$$i_{n,iop2} := 0.01 \cdot 10^{-12}\text{A}$$

$$G_{op2}(f) := \left[ 1 + \frac{(2j \cdot \pi \cdot f \cdot C6)^{-1}}{R16} \right]$$

$$|G_{op2}(h)| = 1$$

$$|G_{op2}(0.01\text{Hz})| = 7.271$$

$$e_{n,o,op2}(f) := \sqrt{\left[ e_{n,R15} \cdot \frac{(2j \cdot \pi \cdot f \cdot C7)^{-1}}{R15 + (2j \cdot \pi \cdot f \cdot C7)^{-1}} \right]^2 + e_{n,iop2}(f)^2 + \left[ i_{n,iop2} \cdot \frac{(2j \cdot \pi \cdot f \cdot C6)^{-1} \cdot R16}{(2j \cdot \pi \cdot f \cdot C6)^{-1} + R16} \right]^2 \cdot G_{op2}(f)^2}$$

$$|e_{n,o,op2}(h)| = 26.22 \times 10^{-9}\text{V}$$

$$i_{n,o,op2}(f) := \frac{e_{n,o,op2}(f)}{R10}$$

$$|i_{n,o,op2}(h)| = 1.748 \times 10^{-12}\text{A}$$

OPs 3 & 4 :

$$f_{c,e3} := 30\text{Hz}$$

$$f_{c,e4} := f_{c,e3}$$

$$f_{c,i3} = \text{unknown}$$

$$f_{c,i4} = \text{unknown}$$

$$e_{n,iop3} := 0.9 \cdot 10^{-9}\text{V}$$

$$e_{n,iop3}(f) := e_{n,iop3} \cdot \sqrt{\frac{f_{c,e3}}{f} + 1}$$

$$i_{n,iop3} := 2 \cdot 10^{-12}\text{A}$$

$$i_{n,iop4} := i_{n,iop3}$$

$$e_{n,iop4}(f) := e_{n,iop3}(f)$$

Noise gains in the output stage :

$$G_{N,op3} := 1$$

$$G_{N,op4} := 2$$

$$e_{n,o,op3,4}(f) := \sqrt{G_{N,op3}^2 \cdot e_{n,iop3}(f)^2 + G_{N,op4}^2 \cdot e_{n,iop4}(f)^2 + e_{n,R13}^2 + i_{n,iop4}^2 \cdot R14^2 + e_{n,R14}^2}$$

$$e_{n,o,op3,4}(h) = 6.427 \times 10^{-9}\text{V}$$

14.2 BJT/Op-Amp and Transformer Driven Input Stage

4. Calculation of the amp's input and output noise voltages :

$$e_{n.o.tot}(f,R0) := \sqrt{\left( e_{n.il}(f)^2 + i_{n.bl}(f)^2 \cdot R_{iL}(R0)^2 + e_{n.RiL}(R0)^2 \right) \cdot G2^2 \cdot G3^2 + \left( i_{n.b2}(f)^2 + i_{n.o.op2}(f)^2 \right) \cdot R11P^2 \dots + e_{n.R11P}^2 + e_{n.o.op3.4}(f)^2}$$

$$e_{n.itot}(f,R0) := \frac{e_{n.o.tot}(f,R0)}{G2 \cdot G3}$$

$$e_{n.iamp}(f,R0) := \frac{e_{n.itot}(f,R0)}{n}$$

$$|e_{n.o.tot}(h,5\Omega)| = 326.183 \times 10^{-9} V$$

$$|e_{n.itot}(h,5\Omega)| = 3.913 \times 10^{-9} V$$

$$|e_{n.iamp}(h,5\Omega)| = 326.101 \times 10^{-12} V$$

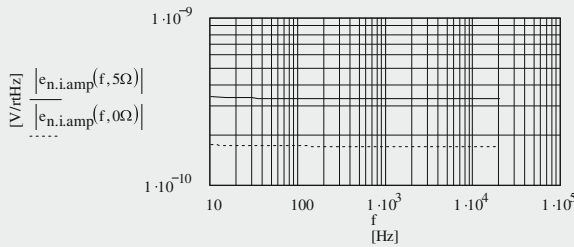


Fig. 14.10  
Input referred noise voltage density based on two different input loads

$$e_{n.o.amp}(f,R0) := e_{n.iamp}(f,R0) \cdot G_{amp}$$

$$|e_{n.o.amp}(h,5\Omega)| = 326.183 \times 10^{-9} V$$

5. SN calculations :

$$SN_{ne.i}(R0) := 20 \cdot \log \left[ \frac{\frac{1}{B1} \int_{20Hz}^{20000Hz} \left( |e_{n.iamp}(f,R0)| \right)^2 df}{v_{i.nom}} \right]$$

$$SN_{ne.i}(10^{-12}\Omega) = -72.383 \quad [dB]$$

$$SN_{ne.i}(5\Omega) = -66.729 \quad [dB]$$

Average input referred noise voltage density (R0 dependent) :

$$R0 := 0.001\Omega, 1\Omega, 100\Omega$$

$$e_{n.iamp}(R0) := v_{i.nom} \cdot 10^{\frac{SN_{ne.i}(R0)}{20}} \cdot \sqrt{\frac{B1}{B20k}}$$

$$e_{n.iamp}(10^{-12}\Omega) = 170.032 \times 10^{-12} V$$

$$e_{n.iamp}(5\Omega) = 326.014 \times 10^{-12} V$$

14.2 BJT/Op-Amp and Transformer Driven Input Stage

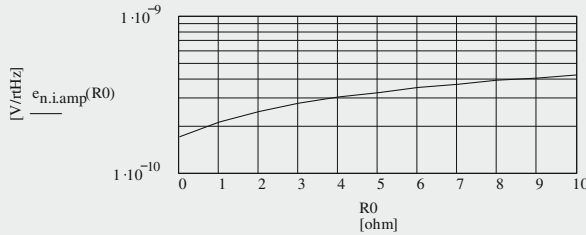


Fig. 14.11  
R0 dependent average  
input noise voltage density

A-weighting by A(f) :

$$A(f) := \frac{1.259}{1 + \left(\frac{20.6\text{Hz}}{f}\right)^2} \cdot \frac{1}{\sqrt{1 + \left(\frac{107.7\text{Hz}}{f}\right)^2}} \cdot \frac{1}{\sqrt{1 + \left(\frac{737.9\text{Hz}}{f}\right)^2}} \cdot \frac{1}{1 + \left(\frac{f}{12200\text{Hz}}\right)^2}$$

$$SN_{ne.o.a}(R0) := 20 \cdot \log \left[ \frac{\sqrt{\frac{1}{B_1} \cdot \int_{20\text{Hz}}^{2000\text{Hz}} \left( |e_{n.o.amp}(f, R0) \right)^2 \cdot (|A(f)|)^2 df}}{V_{o,nom}} \right]$$

$$SN_{ne.o.a}(5\Omega) = -68.773 \quad [\text{dB(A)}]$$

RIAA equalizing by R(f) :

$$R_{1000} := \left[ \frac{\sqrt{1 + \left(2\pi \cdot 10^3 \text{Hz} \cdot 318 \cdot 10^{-6} \text{s}\right)^2}}{\sqrt{1 + \left(2\pi \cdot 10^3 \text{Hz} \cdot 3180 \cdot 10^{-6} \text{s}\right)^2} \cdot \sqrt{1 + \left(2\pi \cdot 10^3 \text{Hz} \cdot 75 \cdot 10^{-6} \text{s}\right)^2}} \right]^{-1} \quad R_{1000} = 9.898$$

$$R(f) := \left[ \frac{\sqrt{1 + \left(2\pi \cdot f \cdot 318 \cdot 10^{-6} \text{s}\right)^2}}{\sqrt{1 + \left(2\pi \cdot f \cdot 3180 \cdot 10^{-6} \text{s}\right)^2} \cdot \sqrt{1 + \left(2\pi \cdot f \cdot 75 \cdot 10^{-6} \text{s}\right)^2}} \right] \cdot R_{1000}$$

$$SN_{riaa.o}(R0) := 20 \cdot \log \left[ \frac{\sqrt{\frac{1}{B_1} \cdot \int_{20\text{Hz}}^{2000\text{Hz}} \left( |e_{n.o.amp}(f, R0) \right)^2 \cdot (|R(f)|)^2 df}}{V_{o,nom}} \right]$$

$$SN_{riaa.o}(5\Omega) = -70.298 \quad [\text{dB}]$$

14.2 BJT/Op-Amp and Transformer Driven Input Stage

$$SN_{ariaa.o}(R0) := 20 \cdot \log \left[ \frac{\sqrt{\frac{1}{B_1} \int_{20\text{Hz}}^{20000\text{Hz}} \left( |e_{n.o.amp}(f, R0) \right)^2 \cdot (|A(f)|)^2 \cdot (|R(f)|)^2 df}}{V_{o.nom}} \right]$$

$SN_{ariaa.o}(0\Omega) = -80.314 \quad [\text{dB(A)}]$

$SN_{ariaa.o}(5\Omega) = -74.659 \quad [\text{dB(A)}]$

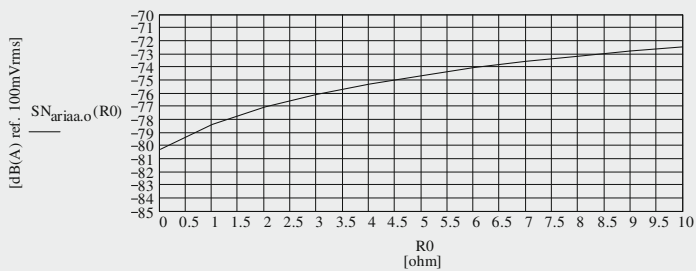


Fig. 14.12 R0 dependent, A-weighted, and RIAA equalized output referred SNs

14.3 Fully Triode Driven Input Stage

Fully Triode Driven MC/MM Pre-Amp with Transformer MC-Input and Balanced Output

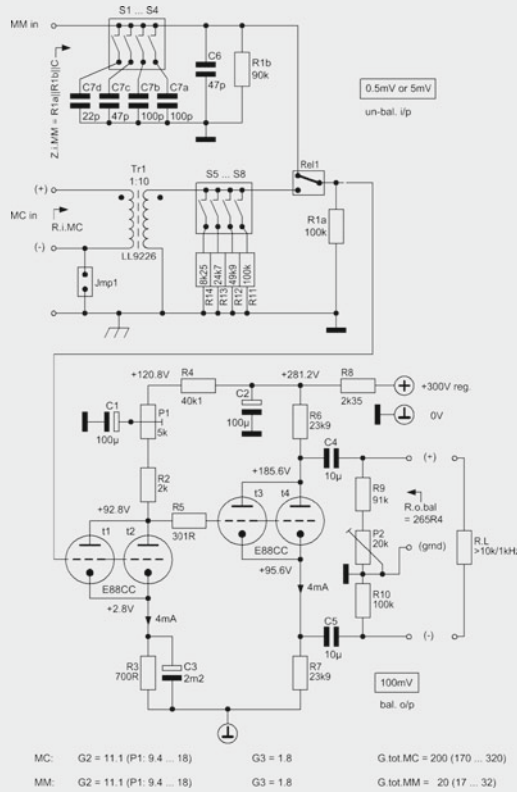


Fig. 14.17 = Fig. 13.6

1. Circuit and component data :

$k := 1.38065 \cdot 10^{-23} \text{V} \cdot \text{A} \cdot \text{s} \cdot \text{K}^{-1}$	$T := 315 \text{K}$	$B_{20k} := 19980 \text{Hz}$	$B_1 := 1 \text{Hz}$	$f_{hp} := 0.5 \text{Hz}$
		$f := 10 \text{Hz}, 15 \text{Hz}.. 20000 \text{Hz}$		$h := 1000 \text{Hz}$
$V_{o,nom} := 100 \cdot 10^{-3} \text{V}$	$V_{i,nom,mm} := 5 \cdot 10^{-3} \text{V}$	$V_{i,nom,mc} := 0.5 \cdot 10^{-3} \text{V}$		
$t_{1,2} = \text{E88CC}$	$I_{a1,2} := 4 \cdot 10^{-3} \text{A}$	$V_{a1,2} := 90 \text{V}$	$V_{g1,2} := -2.8 \text{V}$	
$t_{3,4} = \text{E88CC}$	$I_{a3,4} := 4 \cdot 10^{-3} \text{A}$	$V_{a3,4} := 90 \text{V}$	$V_{g3,4} := -2.8 \text{V}$	

14.3 Fully Triode Driven Input Stage

$R1a := 100 \cdot 10^3 \Omega$	$R1b := 90 \cdot 10^3 \Omega$	$R2 := 2 \cdot 10^3 \Omega$	$R3 := 700 \Omega$	$R4 := 40.1 \cdot 10^3 \Omega$
$R5 := 301 \Omega$	$R6 := 23.9 \cdot 10^3 \Omega$	$R7 := R6$	$R8 := 2.35 \cdot 10^3 \Omega$	$P1 := 5 \cdot 10^3 \Omega$
$R9 := 100 \cdot 10^3 \Omega$	$R10 := R9$			
$V_{R2,P1} := I_{a1,2} \cdot (R2 + P1)$	$V_{R2,P1} = 28 \text{ V}$	$V_{R3} := I_{a1,2} \cdot R3$	$V_{R3} = 2.8 \text{ V}$	
$V_{cc1,2} := V_{a1,2} + V_{R2,P1} + V_{R3}$				$V_{cc1,2} = 120.8 \text{ V}$
		$V_{R6} := I_{a3,4} \cdot R6$	$V_{R6} = 95.6 \text{ V}$	
		$V_{R7} := I_{a3,4} \cdot R7$	$V_{R7} = 95.6 \text{ V}$	
$V_{cc3,4} := V_{a3,4} + V_{R6} + V_{R7}$				$V_{cc3,4} = 281.2 \text{ V}$
$Tr1 = LL9229$	$n := 10$	$Rp := 5 \Omega$	$Rs := 260 \Omega$	Termination alternative "C"

2. Triode valve constants ( $\mu = 29$  selected) :

$\mu_1 := 29$	$g_{m1} := 3.7 \cdot 10^{-3} \text{ S}$	$r_{a1} := \frac{\mu_1}{g_{m1}}$	$r_{a1} = 7.838 \times 10^3 \Omega$
$\mu_2 := 29$	$g_{m2} := 4.1 \cdot 10^{-3} \text{ S}$	$r_{a2} := \frac{\mu_2}{g_{m2}}$	$r_{a2} = 7.073 \times 10^3 \Omega$
$\mu_{1,2} := 29$	$g_{m1,2} := g_{m1} + g_{m2}$	$g_{m1,2} = 7.8 \times 10^{-3} \text{ S}$	
	$r_{a1,2} := \left( \frac{1}{r_{a1}} + \frac{1}{r_{a2}} \right)^{-1}$	$r_{a1,2} = 3.718 \times 10^3 \Omega$	
$\mu_3 := 29$	$g_{m3} := 3.3 \cdot 10^{-3} \text{ S}$	$r_{a3} := \frac{\mu_3}{g_{m3}}$	$r_{a3} = 8.788 \times 10^3 \Omega$
$\mu_4 := 29$	$g_{m4} := 3.7 \cdot 10^{-3} \text{ S}$	$r_{a4} := \frac{\mu_4}{g_{m4}}$	$r_{a4} = 7.838 \times 10^3 \Omega$
$\mu_{3,4} := 29$	$g_{m3,4} := g_{m3} + g_{m4}$	$g_{m3,4} = 7 \times 10^{-3} \text{ S}$	
	$r_{a3,4} := \left( \frac{1}{r_{a3}} + \frac{1}{r_{a4}} \right)^{-1}$	$r_{a3,4} = 4.143 \times 10^3 \Omega$	
$C_{g,c1} := 3.1 \cdot 10^{-12} \text{ F}$	$C_{g,a1} := 1.4 \cdot 10^{-12} \text{ F}$	$C_{a,c1} := 1.75 \cdot 10^{-12} \text{ F}$	
$C_{g,c2} := 3.1 \cdot 10^{-12} \text{ F}$	$C_{g,a2} := 1.4 \cdot 10^{-12} \text{ F}$	$C_{a,c2} := 1.75 \cdot 10^{-12} \text{ F}$	
$C_{g,c1,2} := C_{g,c1} + C_{g,c2}$		$C_{g,c1,2} = 6.2 \times 10^{-12} \text{ F}$	

14.3 Fully Triode Driven Input Stage

$C_{g,a1.2} := C_{g,a1} + C_{g,a2}$	$C_{g,a1.2} = 2.8 \times 10^{-12} \text{F}$	
$C_{a,c1.2} := C_{a,c1} + C_{a,c2}$	$C_{a,c1.2} = 3.5 \times 10^{-12} \text{F}$	$C_{stray1.2} := 2 \cdot 10^{-12} \text{F}$
$C_{g,c3} := 3.1 \cdot 10^{-12} \text{F}$	$C_{g,a3} := 1.4 \cdot 10^{-12} \text{F}$	$C_{a,c3} := 1.75 \cdot 10^{-12} \text{F}$
$C_{g,c4} := 3.1 \cdot 10^{-12} \text{F}$	$C_{g,a4} := 1.4 \cdot 10^{-12} \text{F}$	$C_{a,c4} := 1.75 \cdot 10^{-12} \text{F}$
$C_{g,c3.4} := C_{g,c3} + C_{g,c4}$	$C_{g,c3.4} = 6.2 \times 10^{-12} \text{F}$	
$C_{g,a3.4} := C_{g,a3} + C_{g,a4}$	$C_{g,a3.4} = 2.8 \times 10^{-12} \text{F}$	
$C_{a,c3.4} := C_{a,c3} + C_{a,c4}$	$C_{a,c3.4} = 3.5 \times 10^{-12} \text{F}$	$C_{stray3.4} := 2 \cdot 10^{-12} \text{F}$
$C1 := 100 \cdot 10^{-6} \text{F}$	$C2 := C1$	$C3 := 2.2 \cdot 10^{-3} \text{F}$
		$C4 := 10 \cdot 10^{-6} \text{F}$
		$C5 := C4$
$f_{c1} := 500 \text{Hz}$	$f_{c2} := 1000 \text{Hz}$	$f_{c3} := 3500 \text{Hz}$
		$f_{c4} := 10 \cdot 10^3 \text{Hz}$
$f_{c1.2} := f_{c1} \cdot f_{c2} \cdot \frac{g_{m1} + g_{m2}}{g_{m1} \cdot f_{c2} + g_{m2} \cdot f_{c1}}$	$f_{c1.2} = 678.261 \text{ Hz}$	
$f_{c3.4} := f_{c3} \cdot f_{c4} \cdot \frac{g_{m3} + g_{m4}}{g_{m3} \cdot f_{c4} + g_{m4} \cdot f_{c3}}$	$f_{c3.4} = 5331.882 \text{ Hz}$	

3. Circuit variables, gains, and output resistances :

$R0_{mc} := 20 \Omega$       Shure V15V:       $R0_{mm} := 793 \Omega$        $L0_{mm} := 0.3318 \text{H}$        $R_L := 10 \cdot 10^3 \Omega$

3.1 Gain of second stage (t3 & t4 & output load) :

$R6_{re} := \left( \frac{1}{R6} + \frac{1}{R9} \right)^{-1}$        $R6_{re} = 19.29 \times 10^3 \Omega$

$R7_{re} := \left( \frac{1}{R7} + \frac{1}{R10} \right)^{-1}$        $R7_{re} = 19.29 \times 10^3 \Omega$

$G_{2nd} := \frac{2 \cdot \mu_{3.4} \cdot \left( \frac{1}{R6_{re}} + \frac{1}{0.5 \cdot R_L} \right)^{-1}}{r_{a3.4} + (2 + \mu_{3.4}) \cdot \left( \frac{1}{R7_{re}} + \frac{1}{0.5 \cdot R_L} \right)^{-1}}$        $G_{2nd} = 1.81$

3.2 Output resistance of second stage (t3 & t4) at the anode and cathode :

$R_{1.3.4} := r_{a3.4} + (1 + \mu_{3.4}) \cdot R7$        $R_{1.3.4} = 721.143 \times 10^3 \Omega$

$R_{1.3.4.re} := r_{a3.4} + (1 + \mu_{3.4}) \cdot R7_{re}$        $R_{1.3.4.re} = 582.835 \times 10^3 \Omega$

## 14.3 Fully Triode Driven Input Stage

Page 4

$$R_{o.a3.4} := \left( \frac{1}{R_{1.3.4}} + \frac{1}{R_6} \right)^{-1} \quad R_{o.a3.4} = 23.133 \times 10^3 \Omega$$

$$R_{o.a3.4.re} := \left( \frac{1}{R_{1.3.4.re}} + \frac{1}{R_{6.re}} \right)^{-1} \quad R_{o.a3.4.re} = 18.672 \times 10^3 \Omega$$

$$r_{c3.4} := \frac{r_{a3.4} + R_6}{1 + \mu_{3.4}} \quad r_{c3.4} = 934.762 \Omega$$

$$r_{c3.4.re} := \frac{r_{a3.4} + R_{6.re}}{1 + \mu_{3.4}} \quad r_{c3.4.re} = 781.087 \Omega$$

$$R_{o.c3.4} := \left( \frac{1}{R_7} + \frac{1}{r_{c3.4}} \right)^{-1} \quad R_{o.c3.4} = 899.578 \Omega$$

$$R_{o.c3.4.re} := \left( \frac{1}{R_{7.re}} + \frac{1}{r_{c3.4.re}} \right)^{-1} \quad R_{o.c3.4.re} = 750.69 \Omega$$

## 3.3 Balanced output resistance of second stage (t3 &amp; t4) :

$$R_{o.bal} := \frac{2 \cdot r_{a3.4} \cdot R_{6.re}}{r_{a3.4} + (2 + \mu_{3.4}) \cdot R_{7.re}} \quad R_{o.bal} = 265.442 \Omega$$

## 3.4 Gain (MM) of first stage (t1 &amp; t2 &amp; load-1st = infinite) :

$$G_{amp.mm} := \frac{v_{o.nom}}{v_{i.nom.mm}} \quad G_{amp.mm} = 20$$

$$G_{1st} := \frac{G_{amp.mm}}{G_{2nd}} \quad G_{1st} = 11.049$$

Note: In the following calculation course I set  $R_{2,eff} = R_2 + P1!$

$$G_{1st} = \left| -g_{m1.2} \frac{r_{a1.2} \cdot R_{2,eff}}{r_{a1.2} + R_{2,eff}} \right| \Rightarrow R_{2,eff} := \frac{G_{1st} \cdot r_{a1.2}}{g_{m1.2} \cdot r_{a1.2} - G_{1st}} \quad R_{2,eff} = 2.289 \times 10^3 \Omega$$

$$P1_{eff} := R_{2,eff} - R_2 \quad P1_{eff} = 288.574 \Omega$$

$$G_{1st} := -g_{m1.2} \frac{r_{a1.2} \cdot R_{2,eff}}{r_{a1.2} + R_{2,eff}} \quad G_{1st} = -11.049$$

$$V_{R2,eff} := I_{a1.2} \cdot R_{2,eff} \quad V_{R2,eff} = 9.154 \text{ V}$$



14.3 Fully Triode Driven Input Stage

3.5 Gain (MC) of first stage (t1 & t2 load-1st = infinite & Tr1) :

$$G_{amp.mc} := n \cdot G_{amp.mm} \qquad G_{amp.mc} = 200$$

3.6 Specific capacitances :

$$C6 := 47 \cdot 10^{-12} \text{ F} \qquad C7a := 100 \cdot 10^{-12} \text{ F} \qquad C7b := C7a \qquad C7c := 47 \cdot 10^{-12} \text{ F} \qquad C7d := 22 \cdot 10^{-12} \text{ F}$$

$$C_{i1.2} := (1 - G_{1st}) \cdot C_{g.a1.2} + C_{g.c1.2} + C_{stray1.2} \qquad C_{i1.2} = 41.938 \times 10^{-12} \text{ F}$$

$$C_{o.bal} := C_{g.a1.2} + C_{a.c1.2} + C_{stray1.2} \qquad C_{o.bal} = 8.3 \times 10^{-12} \text{ F}$$

$$r_{c1.2} := \frac{R2_{eff} + r_{a1.2}}{1 + \mu_{1.2}} \qquad r_{c1.2} = 200.217 \ \Omega$$

$$R_{o.c1.2} := \left( \frac{1}{R3} + \frac{1}{r_{c1.2}} \right)^{-1} \qquad R_{o.c1.2} = 155.687 \ \Omega$$

$$C3 := \frac{1}{2 \cdot \pi \cdot f_{hp} \cdot R_{o.c1.2}} \qquad C3 = 2.045 \times 10^{-3} \text{ F}$$

4. Noise voltages and SNs calculations :

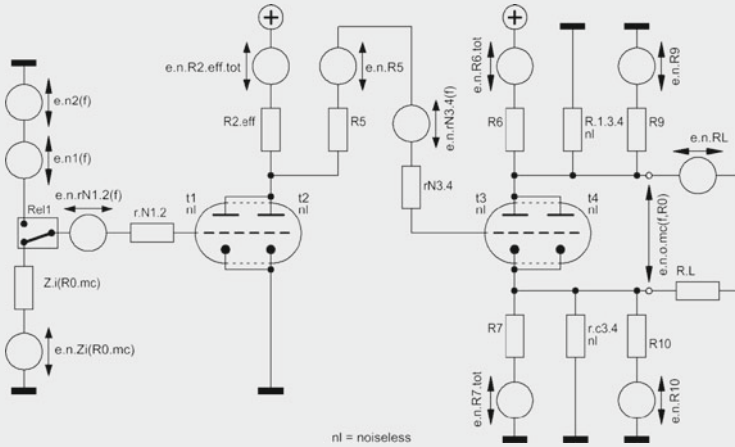


Fig. 14.18 = Fig. 13.7

## 14.3 Fully Triode Driven Input Stage

Page 6

## 4.1 Triodes noise voltages :

$$r_{N1.2} := \frac{3.06}{\mu_{m1.2}}$$

$$r_{N1.2} = 392.308 \Omega$$

$$e_{n,rN1.2}(f) := \sqrt{4 \cdot k \cdot T \cdot B_1 \cdot r_{N1.2} \cdot \sqrt{\frac{f \cdot c_{1.2}}{f} + 1}}$$

$$e_{n,rN1.2}(h) = 3.384 \times 10^{-9} \text{V}$$

$$r_{N3.4} := \frac{3.06}{\mu_{m3.4}}$$

$$r_{N3.4} = 437.143 \Omega$$

$$e_{n,rN3.4}(f) := \sqrt{4 \cdot k \cdot T \cdot B_1 \cdot r_{N3.4} \cdot \sqrt{\frac{f \cdot c_{3.4}}{f} + 1}}$$

$$e_{n,rN3.4}(h) = 6.939 \times 10^{-9} \text{V}$$

## 4.2 Noise voltage of the passive components :

Vishay / Beyschlag MBB 0207

$$NI_e := -30 \text{ [dB]}$$

$$NI := 10^{\frac{NI_e}{20}} \cdot 10^{-6} \text{V} \quad NI = 31.623 \times 10^{-9} \text{V}$$

4.2.1 Effective noise voltage of  $R_L$  :

$$e_{n,R_L} := \sqrt{4 \cdot k \cdot T \cdot B_1 \cdot R_L}$$

$$e_{n,R_L} = 13.189 \times 10^{-9} \text{V}$$

$$e_{n,R_L,eff} := e_{n,R_L} \cdot \frac{R_{o,bal}}{R_L + R_{o,bal}}$$

$$e_{n,R_L,eff} = 341.051 \times 10^{-12} \text{V}$$

4.2.2 Noise voltage of  $R_5$  :

$$e_{n,R_5} := \sqrt{4 \cdot k \cdot T \cdot B_1 \cdot R_5}$$

$$e_{n,R_5} = 2.288 \times 10^{-9} \text{V}$$

4.2.3 Noise voltage of  $R_{0,mc}$  and the input transformer  $Tr1$  :

$$R_{0,mc,sec}(R_{0,mc}) := n^2 \cdot R_{0,mc}$$

$$R_{0,mc,sec}(R_{0,mc}) = 2 \times 10^3 \Omega$$

$$R_{p,sec} := R_p \cdot n^2$$

$$R_{p,sec} = 500 \Omega$$

$$Z_{tr1}(R_{0,mc}) := R_{0,mc,sec}(R_{0,mc}) + R_{p,sec} + R_s$$

$$Z_{tr1}(R_{0,mc}) = 2.76 \times 10^3 \Omega$$

$$Z_i(R_{0,mc}) := \left( \frac{1}{Z_{tr1}(R_{0,mc})} + \frac{1}{R_{1a}} \right)^{-1}$$

$$Z_i(R_{0,mc}) = 2.686 \times 10^3 \Omega$$

$$R_{i,mc} := \frac{R_{1a} + R_s}{n^2} + R_p$$

$$R_{i,mc} = 1.008 \times 10^3 \Omega$$

$$e_{n,Z_i}(R_{0,mc}) := \sqrt{4 \cdot k \cdot T \cdot B_1 \cdot Z_i(R_{0,mc})}$$

$$e_{n,Z_i}(R_{0,mc}) = 6.835 \times 10^{-9} \text{V}$$

14.3 Fully Triode Driven Input Stage

4.2.4 Noise voltage of a V15V cartridge connected to  $R_{i,mm} = R1a||R1b$  :

Assumption :  $C_{cable} := 150 \cdot 10^{-12} F$        $C0 := C_{i1,2} + C6 + C_{cable}$        $C0 = 238.938 \times 10^{-12} F$

$R_{i,mm} := (R1a^{-1} + R1b^{-1})^{-1}$        $R_{i,mm} = 47.368 \times 10^3 \Omega$

$Z0(f) := R0_{mm} + 2j \cdot \pi \cdot f \cdot L0_{mm}$        $|Z0(h)| = 2.23 \times 10^3 \Omega$

$Z0a(f) := \left( \frac{1}{Z0(f)} + 2j \cdot \pi \cdot f \cdot C0 \right)^{-1}$        $|Z0a(h)| = 2.237 \times 10^3 \Omega$

$Z0b(f) := \left( \frac{1}{R_{i,mm}} + 2j \cdot \pi \cdot f \cdot C0 \right)^{-1}$        $|Z0b(h)| = 47.249 \times 10^3 \Omega$

$e_{n,R0,mm} := \sqrt{4 \cdot k \cdot T \cdot B1 \cdot R0_{mm}}$        $e_{n,R0,mm} = 3.714 \times 10^{-9} V$

$e_{n,Ri,mm} := \sqrt{4 \cdot k \cdot T \cdot B1 \cdot R_{i,mm}}$        $e_{n,Ri,mm} = 28.706 \times 10^{-9} V$

$e_{n1}(f) := e_{n,R0,mm} \cdot \frac{Z0b(f)}{Z0(f) + Z0b(f)}$        $|e_{n1}(h)| = 3.661 \times 10^{-9} V$

$e_{n2}(f) := e_{n,Ri,mm} \cdot \frac{Z0a(f)}{Z0a(f) + R_{i,mm}}$        $|e_{n2}(h)| = 1.332 \times 10^{-9} V$

4.2.5 Frequency dependent effective noise voltage of  $R2_{eff}$ ,  $R6$ , &  $R7$ :

$e_{n,R2,eff,ex}(f) := \sqrt{\frac{NI_c}{10} \cdot 10^{-12} \cdot \left( \frac{VR2,eff^2}{f} \right) \cdot B1}$        $e_{n,R2,eff,ex}(h) = 6.033 \times 10^{-9} V$

$e_{n,R2,eff} := \sqrt{4 \cdot k \cdot T \cdot B1 \cdot R2_{eff}}$        $e_{n,R2,eff} = 6.31 \times 10^{-9} V$

$e_{n,R2,eff,tot}(f) := \sqrt{e_{n,R2,eff}^2 + e_{n,R2,eff,ex}(f)^2}$        $e_{n,R2,eff,tot}(h) = 8.73 \times 10^{-9} V$

$e_{n,R6ex}(f) := \sqrt{\frac{NI_c}{10} \cdot 10^{-12} \cdot \left( \frac{VR6^2}{f} \right) \cdot B1}$        $e_{n,R6ex}(h) = 63.001 \times 10^{-9} V$

$e_{n,R6} := \sqrt{4 \cdot k \cdot T \cdot B1 \cdot R6}$        $e_{n,R6} = 20.39 \times 10^{-9} V$

$e_{n,R6,tot}(f) := \sqrt{e_{n,R6}^2 + e_{n,R6ex}(f)^2}$        $e_{n,R6,tot}(h) = 66.219 \times 10^{-9} V$

14.3 Fully Triode Driven Input Stage

$$e_{n,R7.tot(f)} := e_{n,R6.tot(f)}$$

$$e_{n,R10} := \sqrt{4 \cdot k \cdot T \cdot B_1 \cdot R_{10}} \quad e_{n,R9} := e_{n,R10} \quad e_{n,R10} = 41.709 \times 10^{-9} \text{ V}$$

$$e_{n,R7.eff(f)} := \sqrt{e_{n,R7.tot(f)}^2 \cdot \left( \frac{r_{c3.4.re}}{R7 + r_{c3.4.re}} \right)^2 + e_{n,R10}^2 \cdot \left( \frac{R_{o.c3.4}}{R10 + R_{o.c3.4}} \right)^2}$$

$$e_{n,R7.eff(h)} = 2.128 \times 10^{-9} \text{ V}$$

$$e_{n,R6.eff(f)} := \sqrt{e_{n,R6.tot(f)}^2 \cdot \left( \frac{R_{1.3.4.re}}{R6 + R_{1.3.4.re}} \right)^2 + e_{n,R9}^2 \cdot \left[ \frac{\left( R_{1.3.4.re}^{-1} + R6^{-1} \right)^{-1}}{R9 + \left( R_{1.3.4.re}^{-1} + R6^{-1} \right)^{-1}} \right]^2}$$

$$e_{n,R6.eff(h)} = 64.085 \times 10^{-9} \text{ V}$$

4.2.6 Correlated noise voltage of R7 at the anode output, 100% correlated with the one at the cathode :

$$G_{0.cgs3.4} := \left( 1 + \mu_{3.4} \right) \cdot \frac{R_{6.re}}{R_{6.re} + r_{a3.4}} \quad G_{0.cgs3.4} = 24.696$$

$$e_{n,R7.a(f)} := e_{n,R7.eff(f)} \cdot G_{0.cgs3.4} \quad e_{n,R7.a(h)} = 52.562 \times 10^{-9} \text{ V}$$

$$e_{n,R7.corr(f)} := e_{n,R7.a(f)} - e_{n,R7.eff(f)} \quad e_{n,R7.corr(h)} = 50.434 \times 10^{-9} \text{ V}$$

4.2.7 Balanced output noise voltage & SN - MC-case :

$$e_{n,o.2nd(f)} := \sqrt{G_{2nd}^2 \cdot \left( e_{n,R2.eff.tot(f)} \cdot \frac{r_{a1.2}}{r_{a1.2} + R_{2.eff}} \right)^2 + \left( e_{n,R7.corr(f)}^2 + e_{n,R7.eff(f)}^2 + e_{n,R6.eff(f)}^2 \right)}$$

$$e_{n,o.2nd(h)} = 82.163 \times 10^{-9} \text{ V}$$

$$e_{n.o.mc}(f, R_{0.mc}) := \sqrt{\left( e_{n,Z}(R_{0.mc})^2 + e_{n,rN1.2(f)}^2 \right) \cdot G_{1st}^2 \cdot G_{2nd}^2 + e_{n,R5}^2 \cdot G_{2nd}^2 + e_{n,o.2nd(f)}^2 + e_{n,RL.eff}^2} \quad e_{n.o.mc}(h, 20\Omega) = 173.318 \times 10^{-9} \text{ V}$$

$$SN_{ne.o.mc}(R_{0.mc}) := 20 \cdot \log \left[ \frac{\sqrt{\frac{1}{B_1} \cdot \int_{20\text{Hz}}^{2000\text{Hz}} \left( |e_{n.o.mc}(f, R_{0.mc})| \right)^2 df}}{v_{o.nom}} \right]$$

$$SN_{ne.o.mc}(20\Omega) = -73.028 \quad [\text{dB}]$$

14.3 Fully Triode Driven Input Stage

Input noise voltage density (average in B<sub>20k</sub>) with input shorted :

$$e_{n.i.avg.mc} := \frac{\sqrt{\frac{1}{B_{20k}} \cdot \int_{20Hz}^{20000Hz} (|e_{n.o.mc}(f, 0\Omega)|)^2 df}}{G_{amp.mc}} \quad e_{n.i.avg.mc} = 535.767 \times 10^{-12}V$$

A-weighting by A(f) :

$$A(f) := \frac{1.259}{1 + \left(\frac{20.6Hz}{f}\right)^2} \cdot \frac{1}{\sqrt{1 + \left(\frac{107.7Hz}{f}\right)^2}} \cdot \frac{1}{\sqrt{1 + \left(\frac{737.9Hz}{f}\right)^2}} \cdot \frac{1}{1 + \left(\frac{f}{12200Hz}\right)^2}$$

RIAA equalizing by R(f) :

$$R_{1000} := \left[ \frac{\sqrt{1 + (2 \cdot \pi \cdot 10^3 Hz \cdot 318 \cdot 10^{-6} s)^2}}{\sqrt{1 + (2 \cdot \pi \cdot 10^3 Hz \cdot 3180 \cdot 10^{-6} s)^2} \cdot \sqrt{1 + (2 \cdot \pi \cdot 10^3 Hz \cdot 75 \cdot 10^{-6} s)^2}} \right]^{-1} \quad R_{1000} = 9.898$$

$$R(f) := \left[ \frac{\sqrt{1 + (2 \cdot \pi \cdot f \cdot 318 \cdot 10^{-6} s)^2}}{\sqrt{1 + (2 \cdot \pi \cdot f \cdot 3180 \cdot 10^{-6} s)^2} \cdot \sqrt{1 + (2 \cdot \pi \cdot f \cdot 75 \cdot 10^{-6} s)^2}} \right] \cdot R_{1000}$$

$$SN_{ariaa.o.mc}(R_{0mc}) := 20 \cdot \log \left[ \frac{\sqrt{\frac{1}{B_1} \cdot \int_{20Hz}^{20000Hz} (|e_{n.o.mc}(f, R_{0mc})|)^2 \cdot (|A(f)|)^2 \cdot (|R(f)|)^2 df}}{v_{o.nom}} \right]$$

$$SN_{ariaa.o.mc}(20\Omega) = -80.31 \quad [dB(A)]$$

R<sub>0mc</sub> := 0Ω, 1Ω .. 100Ω

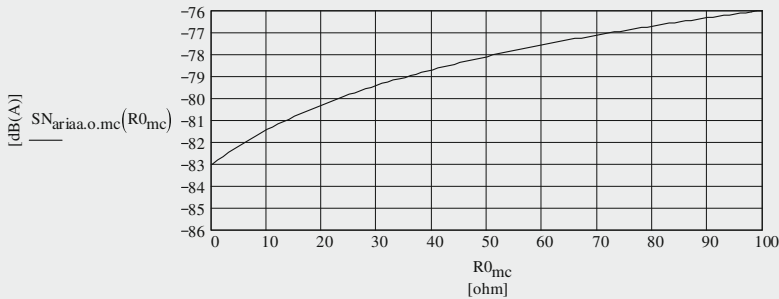


Fig. 14.19 Output referred A-weighted and RIAA equalized SN vs. R<sub>0</sub> of the MC input stage

14.3 Fully Triode Driven Input Stage

4.2.7 Balanced output noise voltage & SN - MM-case

$$e_{n.o.mm}(f) := \sqrt{\left( e_{n1}(f)^2 + e_{n2}(f)^2 + e_{n,rN1,2}(f)^2 \right) \cdot G_{1st}^2 \cdot G_{2nd}^2 \dots + e_{n,R5}^2 \cdot G_{2nd}^2 + e_{n.o,2nd}(f)^2 + e_{n,RL,eff}^2}$$

$$|e_{n.o.mm}(h)| = 127.287 \times 10^{-9} V$$

$$SN_{ne.o.mm} := 20 \cdot \log \left[ \frac{\frac{1}{B_1} \cdot \int_{20Hz}^{2000Hz} (|e_{n.o.mm}(f)|)^2 df}{v_{o,nom}} \right]$$

$$SN_{ne.o.mm} = -65.958 \quad [dB]$$

$$SN_{ariaa.o.mm} := 20 \cdot \log \left[ \frac{\frac{1}{B_1} \cdot \int_{20Hz}^{2000Hz} (|e_{n.o.mm}(f)|)^2 \cdot (|A(f)|)^2 \cdot (|R(f)|)^2 df}{v_{o,nom}} \right]$$

$$SN_{ariaa.o.mm} = -82.141 \quad [dB(A)]$$

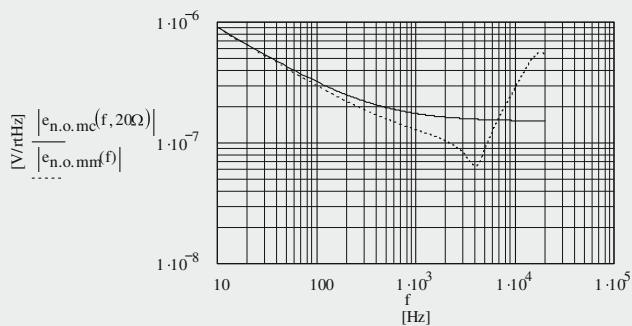


Fig. 14.20 Output noise voltage densities of the two phono-amp input stage versions, inputs loaded

---

## 15.1 Computer Test Equipment

### 15.1.1 Intro

Before we enter into the measurement activities, we need some information about the new measurement system I am using since the middle of the year 2013. It is called Clio 8.5 PCI<sup>1</sup> and it is on Audiomatica's list of discontinued products now. The purchase of this system followed my basic attitude towards very expensive measurement systems like eg the ones of the Audio Precision family: find ways with cost saving approaches to get equally good measurement results. The price of the Clio 8.5 system is roughly a factor of 1/20 smaller than that of the AP system. It works with 18 bit and it runs under WIN XP. It follows the elder 16 bit Clio 6.5 system I've already described in the TSOS books. The basic measurement set-up did not change, however, emphasis lies on the balanced approach here.

The system consists of a small PCI card and two double cables equipped with Cinch connectors. They transfer data between the card and an external measurement Cinch input/Cinch output box, called signal conditioner SC-02. The software itself runs on WIN 2 k and WIN 7 computers, the signal conditioner works with WIN XP only. With this arrangement, the user must measure with WIN XP but could perform the post-measurement work on other computers with more or less modern operating software.

The most important feature of a measurement instrument should be the frequency (F) and phase (P) response. For audio purposes, Clio's F & P is perfect:  $\pm 0.000$  dB and  $\pm 0.000^\circ$  in the  $B_{20k}$  range of 20 Hz–20 kHz.

---

<sup>1</sup>[www.audiomatica.com](http://www.audiomatica.com).

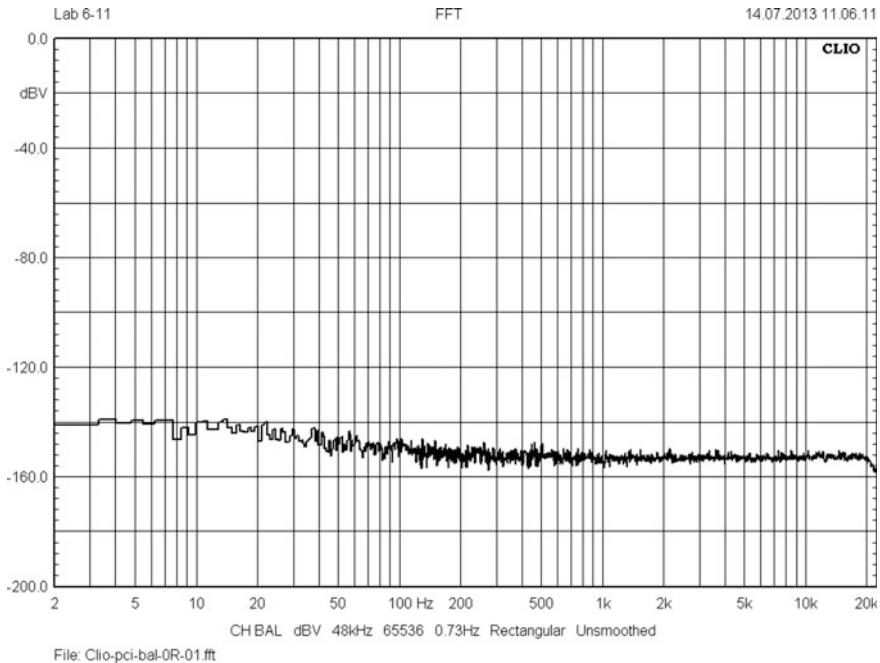


**Fig. 15.1** Input referred noise voltage density curve of the Clío 8.5 measurement system, balanced input shorted

### 15.1.2 Signal-to-Noise Ratio

With the un-balanced (<sub>u</sub>) inputs of the two channels A & B shorted the 18 bits limit the input referred signal-to-noise ratio  $SN_{ne.i.u}$  of each channel to appr.  $6.02 \text{ dB} * 18 = -108.4 \text{ dBV}$  in  $B_{20k}$ . A switch to a balanced (<sub>b</sub>) input configuration yields an  $SN_{ne.i.b}$  of  $-111.8 \text{ dBV}$  in  $B_{20k}$ . With an FFT resolution  $FFT_{res} = 0.73 \text{ Hz}$  Fig. 15.1 shows the frequency range of 2 Hz–20 kHz and the measured noise voltage density curve of the system with its balanced input shorted.

To show the flexibility of the Clío system I add a better looking smoothed version in Fig. 15.2. The FFT size ( $f_s = 65,536$ ) and the sampling rate ( $F_s = 48 \text{ kHz}$ ) are not changed here! Therefore, the smoothed version looks like the one after  $\gg 100$  averages and not alike one with reduced  $f_s$ .<sup>2</sup> Remember: each halving of  $f_s$  would lead to a doubling of  $FFT_{res}$  and it would move up the Fig. 15.1 curve by 3 dB. Practically, the  $1/f$  noise can be ignored; with  $f_{c,e} = 200 \text{ Hz}$  it plays a role in the region of 20 Hz–200 Hz only.

With the given  $SN_{ne.i.b}$  and based on the Chap. 16 findings the best-case difference ‘B’ between the measurement amp’s input SN end the measured output SN of the DUT should always become  $\geq 16 \text{ dB}$  ( $\geq 10 \text{ dB}$ ) for an error (=Worsening

<sup>2</sup>See Fig. 22.6 in TSOS-2.



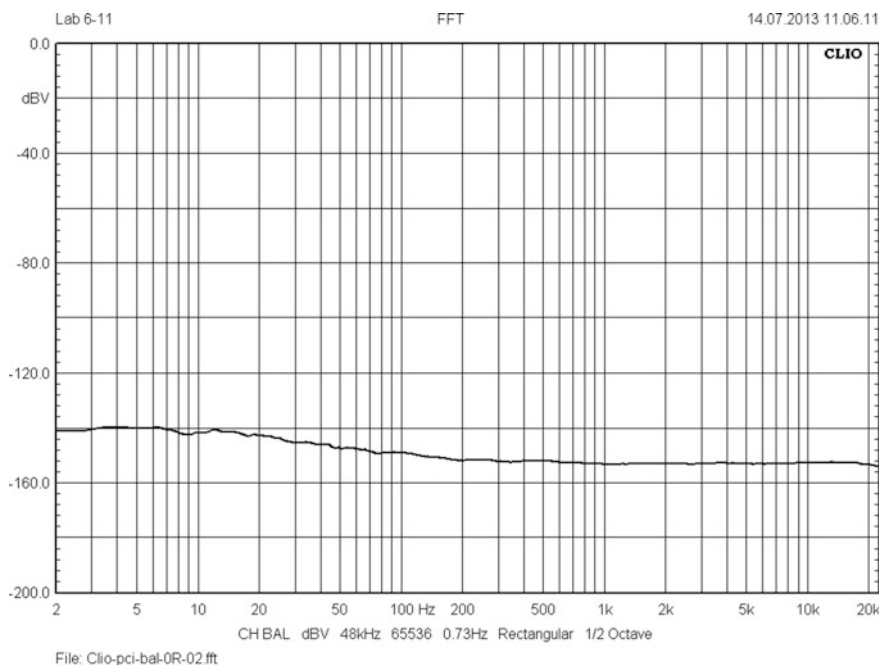


**Fig. 15.2** Same as Fig. 15.1, however, smoothed by 1/2 Octave

Figure  $W_e) \leq 0.1 \text{ dB} (\leq 0.5 \text{ dB})$ .<sup>3</sup> In other words: the DUT’s measured output referred  $SN_{ne.o.b}$  should then become  $\leq -95.8 \text{ dBV} (\leq 101.8 \text{ dBV})$ . Values better than that would include certain additional portions of Clio’s noise. For example, a measured DUT output  $SN_{o.m}$  value of  $-106.8 \text{ dBV}$  creates a  $B = 5 \text{ dB}$  difference to the Clio  $SN_{ne.i.b}$ . Thus, as of Figs. 15.3 and 15.4 it includes  $W_e = 1.2 \text{ dB}$  Clio noise.

Consequently, the real DUT output  $SN_{o.re}$  becomes  $-106.8 \text{ dBV} - 1.2 \text{ dB} = -108 \text{ dBV}$ . Therefore, the Clio system needs very low-noise external measurement amplifiers at its input, allowing to measure DUT output SNs up to  $-120 \text{ dBV}$  (or even better) without Clio impact  $> 0.1 \text{ dB}$ . With a gain of 1000, the balanced-in/balanced-out measurement amp PMMA of Chap. 16 will be able to manage such a challenge.

With the measured output referred  $SN_{o.dut.m} [\text{dBV}]$  of the DUT and the input referred  $SN_{i.ma} [\text{dBV}]$  of the measurement system the creation of the Figs. 15.3 and 15.4 curves is based on the following general equations:

$$W_e(B) = 20 \log \left( \sqrt{10 \frac{SN_{o.dut.m}}{10} + 10 \frac{SN_{i.ma}(B)}{10}} \right) - SN_{o.dut.m} \quad [\text{dB}] \quad (15.1)$$

<sup>3</sup>See Figs. 15.3 and 15.4.

**Fig. 15.3** Worsening figure  $W_e(B)$  as function of the difference  $B$  of two SNs

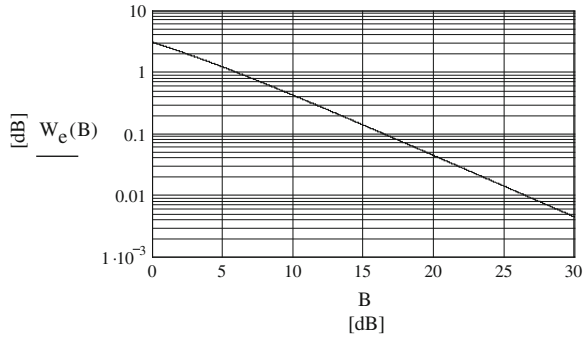
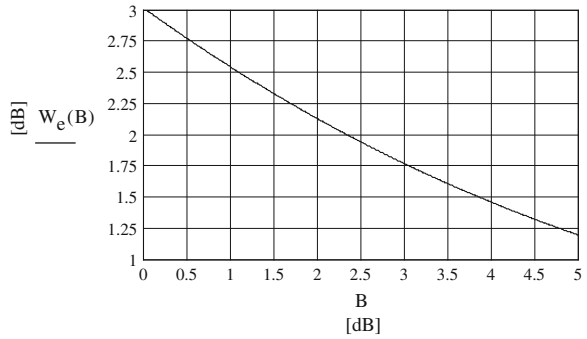


**Fig. 15.4** Zoomed Fig. 15.3 with  $B \leq 5$  dB



$$SN_{i.ma} = 20 \log \left( 10 \frac{SN_{o.dut.m} - B}{20} \right) \quad [dBV] \quad (15.2)$$

$$B = SN_{o.dut.m} - SN_{i.ma} \quad [dB] \quad (15.3)$$

### 15.1.3 Distortion (THD)

The Clio brochure claims a THD level of 0.01 % in  $B_{20k}$ . I have gone through many different THD measurement sessions and I found out that—without big error—Clio’s 1 kHz signal is clean enough for our measurement purposes here. Figure 15.5 shows the spectrum of a 0 dBV output signal fed into one un-balanced input channel; here it is the ‘A’ input. The ‘B’ input looks the same.

Without noise  $N$ , Clio measures  $THD = 0.006 \%$ . A calculation with (15.4) and the levels taken from the Fig. 15.5 graph ( $v_{dl} = 1$  kHz at 0 dBV) yields a THD level of 0.00592 %, a result very close to the rounded three-digit-after-the-decimal-point Clio result. In Sect. 15.2, we will see how this result is improved by passing it through the un-balanced/balanced converter UBC.

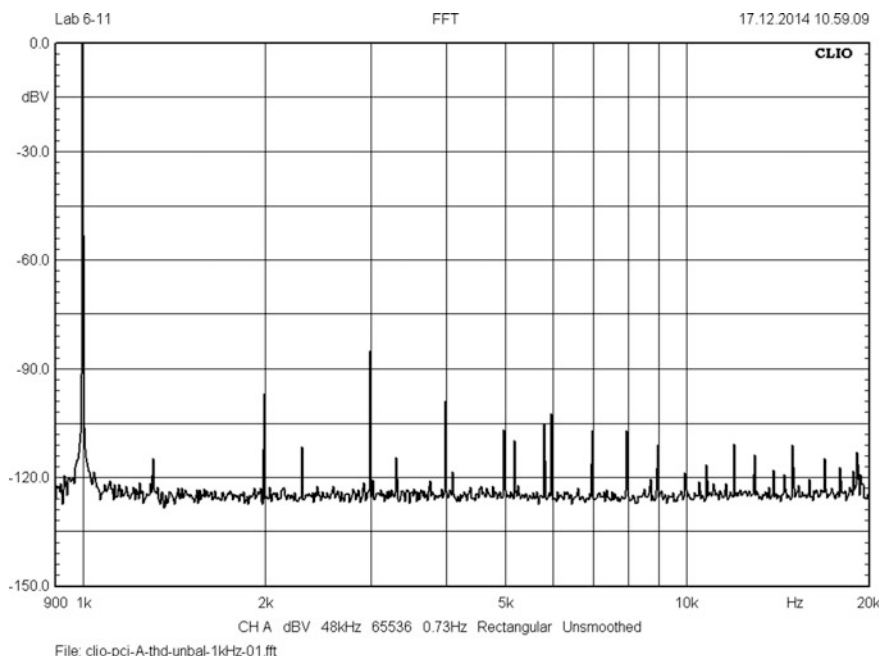


**Fig. 15.5** Clío's 1 kHz 0 dBV signal and its distortion artefacts in  $B_{20k}$

$$\text{THD} = \frac{\sqrt{v_{d2}^2 + v_{d3}^2 + \dots + v_{d20}^2}}{v_{d1}} * 100 \% \quad [\%] \quad (15.4)$$

$$\text{THD} = 20 \log \left( \frac{\text{THD} (\%)}{100 \%} \right) [\text{dB}] \quad (15.5)$$

### 15.1.4 IMD

With its broad range of test signals Clío allows all kinds of IMD measurements. I have tried some of them. Finally, I took the following approach: a high-level low-frequency signal and a low-level high-frequency signal are simultaneously fed into the DUT's input and the output FFT spectrum shows the sidebands around the high-frequency signal. Thus, the amount of sidebands and their levels indicate the total IMD amount produced by the DUT. This approach is the basis of the DIN IMD measurement with its 250 Hz/8 kHz frequency and 4:1 level pair. I also tried two other pairs: 60 Hz/3 kHz and 300 Hz/3 kHz. However, because the results<sup>4</sup> did not drastically change the DIN version became the customary one.

<sup>4</sup>See Table 12.3.

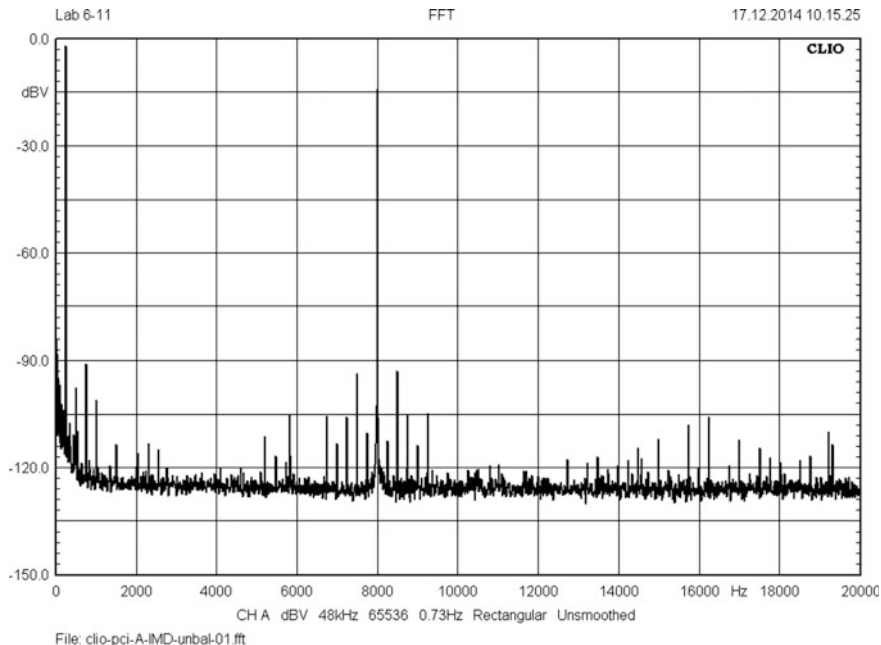


**Fig. 15.6** The Clío IMD measurement result with 250 Hz/8 kHz and 4:1 signal levels

Figure 15.6 shows Clío’s IMD FFT spectrum according to DIN. The SMPTE RP120 approach results look similar to the DIN ones, however based on a different frequency pair: 60 Hz/7 kHz. The DIN result without noise  $N$  becomes  $IMD = 0.0153 \%$ . With the below given equations the calculation result lies very close to the measured one:  $0.0132 \%$ .

With  $f_1 = 250 \text{ Hz}$ ,  $f_2 = 8 \text{ kHz}$ ,  $A = \text{amplitude}$ , and  $n = 2-6$  the equations look as follows:

$$IMD = \sqrt{IMD_{2nd}^2 + IMD_{3rd}^2 + \dots + IMD_{nth}^2} \tag{15.6}$$

$$IMD_{nth} = \frac{A_{(f_2-nf_1)} + A_{(f_2+nf_1)}}{A_{f_2}} \tag{15.7}$$

In Fig. 15.6 the distortion artefacts of the 250 Hz signal  $<6 \text{ kHz}$  and the sideband artefacts around 16 kHz are not part of the measurement result. Here again, the un-balanced/balanced converter UBC will improve the results too.

There is another method to test IMD: the CCIF or ITU-R approach with two different frequencies of equal amplitude and 1 kHz difference, placed in the higher region of  $B_{20k}$ , eg at 14 and 15 kHz or at 19 and 20 kHz. The CCIF IMD result was  $0.0024 \%$ .

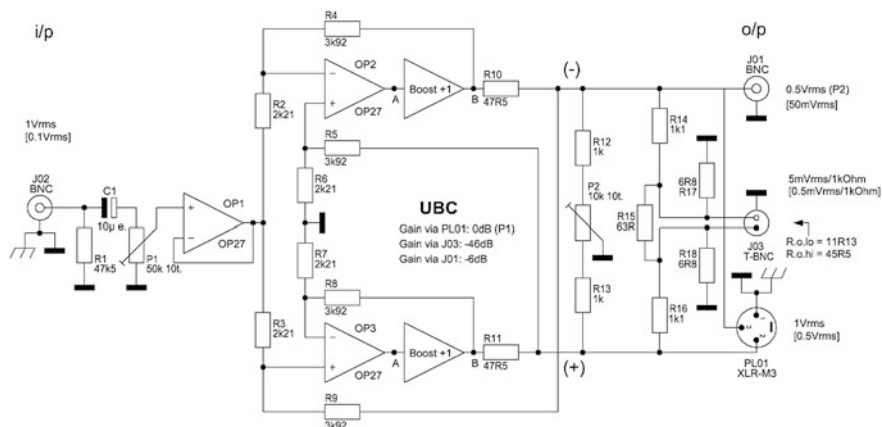


Fig. 15.7 The un-balanced to balanced converter UBC

## 15.2 The Un-Balanced to Balanced Converter UBC

### 15.2.1 Circuit

Although equipped with a balanced input one of the disadvantages of the Clío system is the fact that there is no balanced output. Roughly, 25 years ago, I needed a balanced signal and that is why the then developed UBC in Figs. 15.7 and 15.8 looks a bit old-fashioned with its rather high number of discrete components. Nevertheless, it works sufficiently well and it does not add negative extra signals to the measurement signals we need here. The circuit is a modified version of a transformer replacement for differential line drivers that I found in a 1984 *Wireless World* magazine,<sup>5</sup> and again in Douglas Self's 'Small Signal Audio Design' book.<sup>6</sup> I show a less component-burning booster alternative too; it works well in other configurations (eg Module 2 of TSOS-1 & -2) and according to the respective data-sheet, however, I did not yet test it in the UBC configuration.

The power supply lines of the UBC have  $\pm 15$  V regulated DC voltages and they are further cleaned by gyrators (= C-multipliers).

### 15.2.2 F & P and SN Performance

The frequency (F) and phase (P) response of the UBC is flat in  $B_{20k}$ . With an output signal of 0 dBV via output load = 10 k $\Omega$  at PL01 or of -66 dBV via output

<sup>5</sup>WW 1984–2012, p 73, 'Differential line driver replaces transformer' by S. Whitt.

<sup>6</sup>'Quasi floating balanced output' by Douglas Self, *Small Signal Audio Design*, 2010, p. 387.

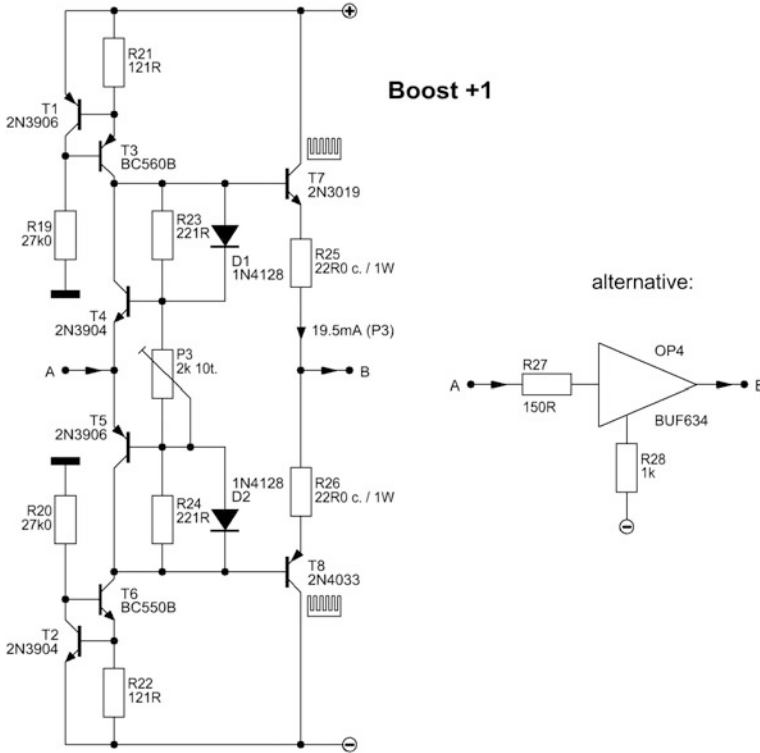


Fig. 15.8 Booster alternatives for Fig. 15.7

load = 1 kΩ at J03 the deviation from the F flatness becomes only -0.001 dB at 20 kHz in both cases.

The deviation from the P flatness shows different pictures at 20 Hz/1 kHz/10 kHz/20 kHz:

- with 0.0 dBV output signal we have a phase of +0.12°/0.00°/-0.67°/-1.21°,
- with -66 dBV output signal we find a phase of +0.54°/0.00°/-1.90°/-3.77°.

If we would assume a -6 dB/oct. hp & lp character +0.54° and -3.77° represent -3 dB corner frequencies of roughly 0.2 Hz and 300 kHz.

With input shorted and because of the still existing noise generator at the input (P1 with appr. 12.25 kΩ noise-effective resistance) the output referred SN at the PL01 output shows an SN<sub>ne.o.re</sub> of -107.9 dBV and -107.7 dBV only,<sup>7</sup> measured with the measurements amps of Chaps. 16 (PMMA) and 17 (PFMA). At the

<sup>7</sup>Calculation results see MCD-WS 18.1; based on the Figs. 15.3 and 15.4 process subscript “<sub>re</sub>” refers to real results.

J03 output we find  $SN_{ne.o.re} = -116.82$  dBV measured with the PFMA and  $SN_{ne.o.re} = -136.16$  dBV measured with the PMMA.<sup>8</sup> These J03 results make no sense because they only reflect the input referred SNs of the measurement amps. The J03 output offers a calculated  $SN_o$  of appr.  $-154.4$  dBV =  $-108.4$  dBV (= calculated PL01 output SN)  $-46$  dB (= voltage divider effect at J03).

The PMMA offers a measured input referred  $SN_{ne.i.m}$  of  $-138.18$  dBV ( $\equiv 0.875$  nV/rtHz). According to Fig. 15.3 and with  $B = 30.27$  dB the original measured result of  $-107.89$  dBV at the PL01 output could be corrected by a tiny  $W_e(B) = 0.004$  dB, hence, we would get  $-107.894$  dBV real  $SN_{ne.o.re}$ . At the J03 output  $B$  becomes  $-16.677$  dB, hence, we can ignore any correction.

The PFMA offers a measured input referred  $SN_{ne.i.m}$  of  $-117.3$  dBV ( $\equiv 9.7$  nV/rtHz). According to Fig. 15.3 and with  $B = 9.99$  dB the original measured result of  $-107.31$  dBV at the PL01 output must be corrected by  $0.41$  dB, hence, we'll get  $-107.72$  dBV real  $SN_{ne.o.re}$ . At the J03 output,  $B$  becomes negative ( $-37.037$  dB), hence, we have nothing to correct.

The approximate difference of 20 dB input referred SN comes from the rather high input referred noise voltage density of the PFMA<sup>9</sup>: calculated 10.6 nV/rtHz average.

### 15.2.3 THD Performance

Provided that UBC's own un-balanced THD level is lower than the one of the preceding generator and if we turn the un-balanced signal into a balanced format the advantages come from the fact that the generator's THD gets damped by the UBC, especially the even harmonics. Therefore, the Fig. 15.9 looks so much better than the one of Fig. 15.5, and with a 1 kHz input signal at 0 dBV the THD level improves by approximately 10 dB to 0.002 %.

Figures 15.10 and 15.11 show what happens with the harmonics by decreasing the input signal to  $-46$  dBV (MM case) or  $-66$  dBV (MC case): nearly all harmonics disappear in the noise mud formed by the noise voltage density level at approximately  $-156$  dBV.

At this point of the survey, it became clear to me that the effective disappearance of harmonics in the DUT's noise level became a major trigger of the Sect. 12.3 conclusions and the integration of the  $SN_{riaa}$  line at  $-67.3$  dBV in the Sect. 12.2.2 graphs.

Of course,

- the results at the J03 output become always better, because this output follows a  $-46$  dB voltage divider, formed by resistors R5, R20, R12, R13, R29,
- the spikes of the IMD measurement result (Fig. 15.6) will disappear in the noise ground too, hence, the astonishing Table 12.3 measurement results should not be very surprising.

<sup>8</sup>Details & calculation results see Chaps. 16 and 18's MCD-WS 18.2.

<sup>9</sup>Details & calculation results see Chaps. 17 and 18's MCD-WS 18.3.

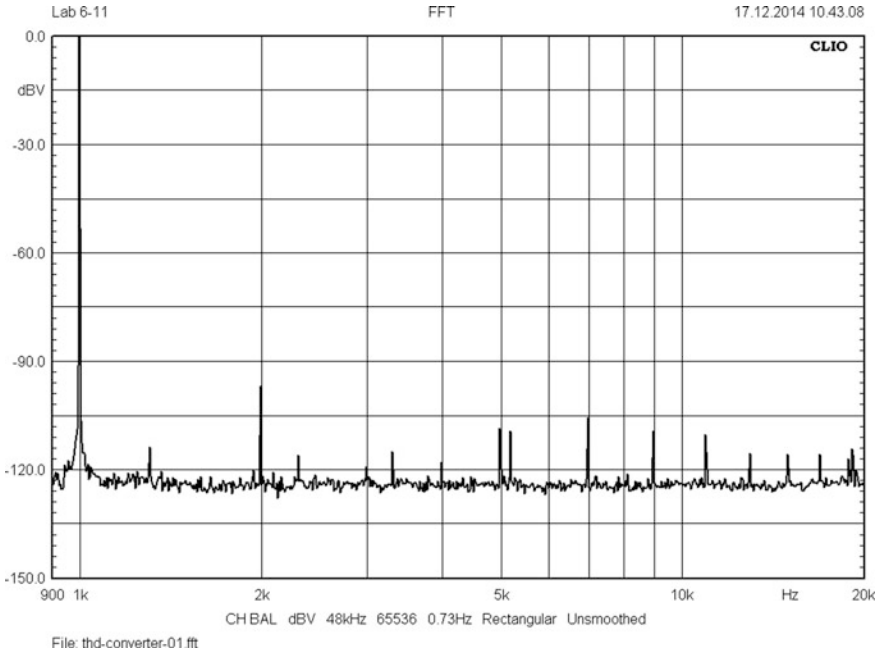


Fig. 15.9 THD at UBC's PL01 output, fed by a 0 dBV/1 kHz signal

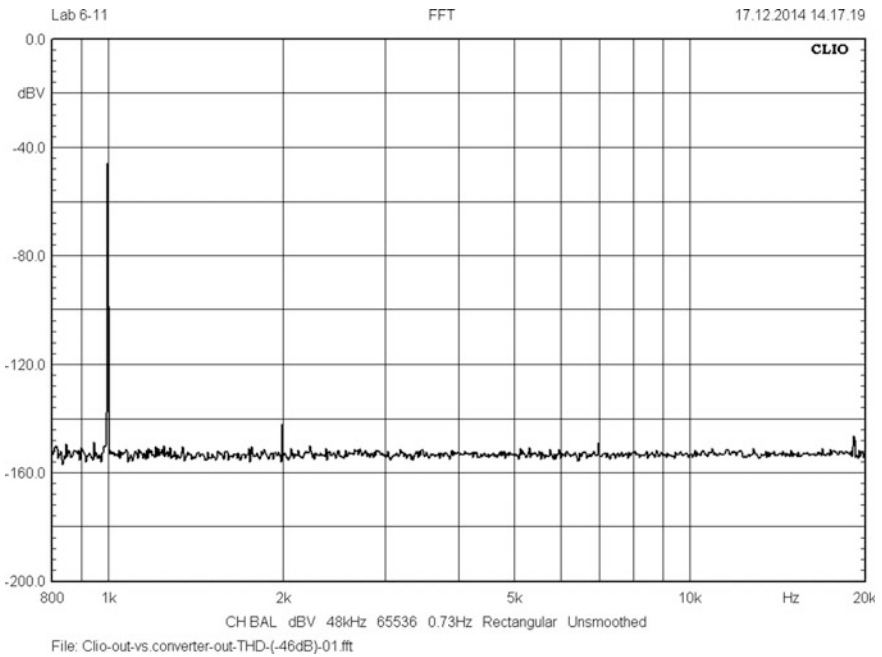
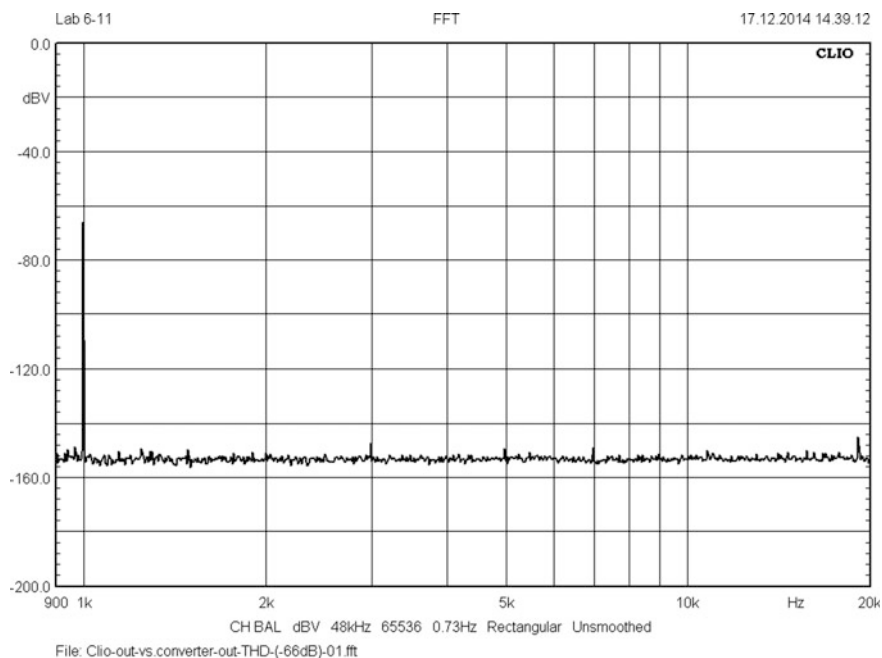


Fig. 15.10 THD at UBC's J03 output, fed by a 0 dBV/1 kHz signal





**Fig. 15.11** THD at UBC's J03 output, fed by a  $-20$  dBV/1 kHz signal

The levels of the noise voltage density grounds of Figs. 15.9, 15.10 and 15.11 show a difference of approximately 28 dB, from  $-125$  dBV to  $-153$  dBV. Two sources produce this difference:

- The above-mentioned voltage divider moves every input signal 46 dB down.
- The then effective input referred noise level of the Clio system moves the noise ground up to the balanced Clio input referred rms noise voltage level of  $-111.8$  dBV or  $-156$  dBV noise voltage density level (see Figs. 15.2 and 15.3). In conjunction with Clio's input noise current, it includes a guessed 3 dB penalty for the yet undefined noise production mechanisms at the Clio input.

### 15.2.4 Output Resistances

The measured UBC's PL01 output resistance  $R_{o,pl01}$  becomes  $45.5 \Omega$ . With the shown components in Fig. 15.7 the output resistance at the J03 output  $R_{o,j03}$  becomes  $11.13 \Omega$ . A change of R15 from  $63 \Omega$  ( $20 \Omega + 43 \Omega$ ) to  $53.2 \Omega$  ( $20 \Omega + 33.2 \Omega$ ) reduces the output resistance to  $10.8 \Omega$ . All measurements were performed with this output resistance; however, instead of  $0.5$  mV<sub>rms</sub> with the shown R15 value the output voltage is  $0.48$  mV<sub>rms</sub> with a  $0.1$  V<sub>rms</sub>/1 kHz input signal.

## 15.3 RIAA Encoder and Trimming

### 15.3.1 Encoder

The Fig. 15.14 encoder circuit goes back to the one I have already published in TSOS-1 & -2,<sup>10</sup> MC output not shown here. For trimming purposes of the RIAA transfer function and to drive the external input we only need a  $50\text{ mV}_{\text{rms}}\text{--}100\text{ mV}_{\text{rms}}$  output level in  $B_{20k}$ . Thus, the inclusion of a jumper across R17 ensures a  $50\text{ mV}_{\text{rms}}/1\text{ kHz}$  signal at the MM output. A further increase of the input voltage to  $2\text{ V}_{\text{rms}}$  will increase the output level by 6 dB.

### 15.3.2 Trimming Actions

Before insertion into the main board's amplification chain, with the help of a special small test-board case (Figs. 15.12 and 15.13) we have to undertake separate trimming processes for Amp1, Amp2, and Amp5, DC offset as well as gain. A first  $B_{20k}$  frequency and phase response, THD and IMD, and overload control check follows by application of the Clio generator + UBC + UBC-J03 output. Additionally, SNs must be measured and crosschecked with the calculation results.

Fed by the Clio frequency sweep generator with very constant output level in  $B_{20k}$  the Fig. 15.14 encoder solution allows the trimming of Fig. 1.2's P1, P3, and P4. The operating level should be set to  $50\text{ mV}_{\text{rms}}\text{--}100\text{ mV}_{\text{rms}}$  at 1 kHz. The encoder plus UBC & PL01 must be connected to the external input of the engine.

The following steps, a look at Fig. 1.2, and Clio's frequency response diagram (sinusoidal analysis) give a guideline through the frequency response trimming, provided that the trimming of Amp3's P7 ensures equal amplitudes at TPs 5 & 6 of Fig. 2.1:

1. We start with Amp3 and P3. At the low-end of  $B_{20k}$  any trimming action of the T1/T3 network gives the perfect anchor point at 20 Hz and P3 moves the found frequency response to a level where it creates a nearly horizontal line towards 1 kHz.
2. Next, P1 comes into the game: with it, we can move the high-end of  $B_{20k}$  to a level position equal to the one at 20 Hz. With perfectly selected component values of the three RIAA networks, we should obtain a rather flat frequency response in  $B_{20k}$ .
3. If the frequency response is not flat enough we repeat the first two steps. However, wrong values of the T1/T3 network cannot be trimmed away.
4. We switch to Amp4 and—alike the process of 1.—with P4 we trim the found frequency response at the low-end of  $B_{20k}$ . Automatically, the already trimmed T2 network will move the frequency response at the high-end of  $B_{20k}$  into a flatness creating position.

<sup>10</sup>TSOS-1: Chap. 12; TSOS-2: Sect. 23.3.

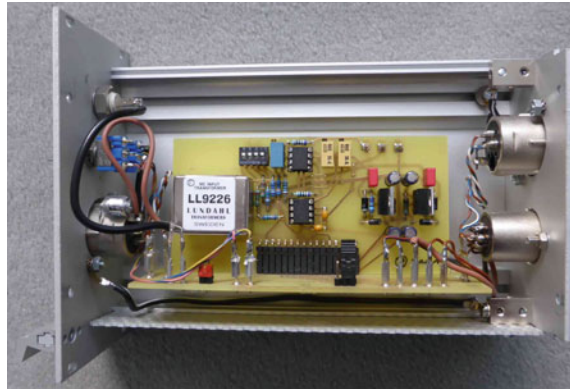


Fig. 15.12 Test-board case with Amp1

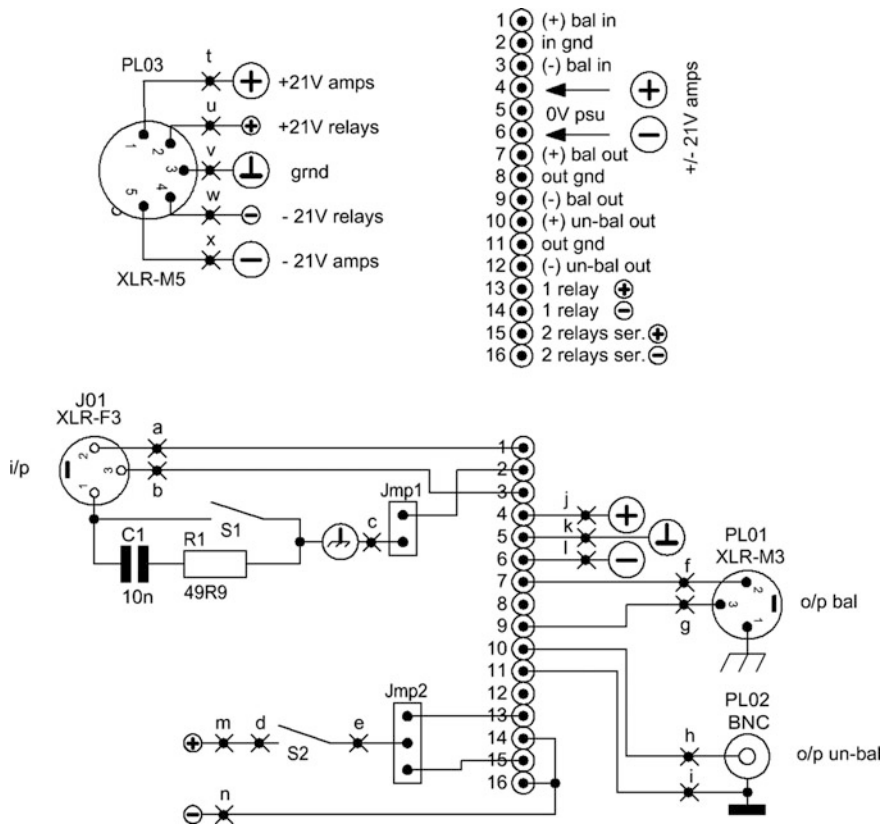
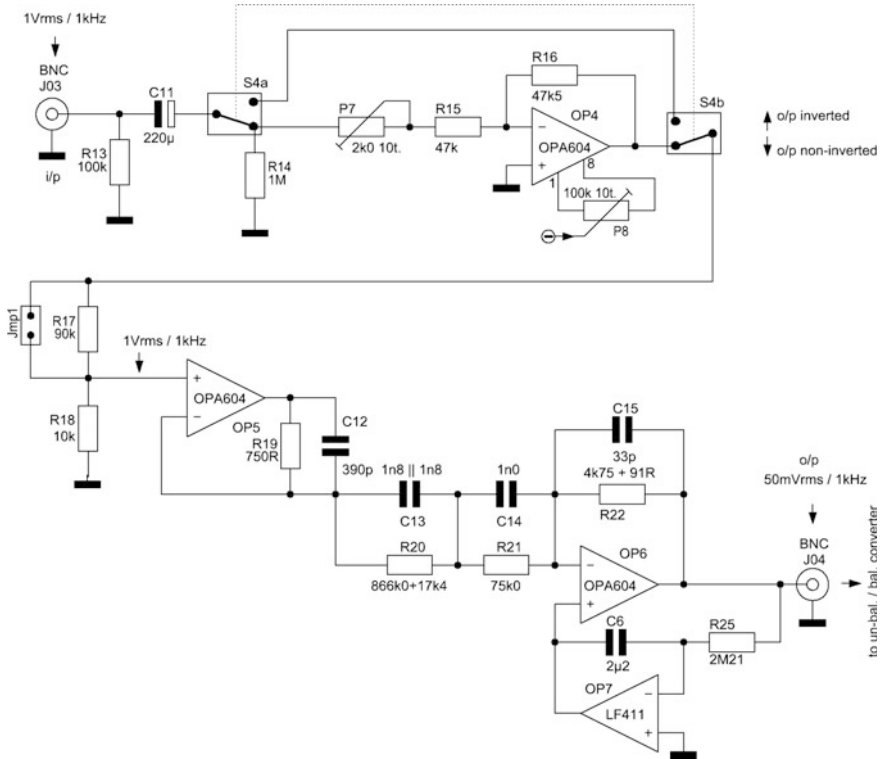


Fig. 15.13 Circuit of the test-board



**Fig. 15.14** RIAA encoder for RIAA transfer function trimming actions via external input of the Engine II

We have two flat frequency responses now with different levels at 1 kHz. Hence, the next step must be the trimming of equal gains for Amps 3 & 4. The gain of Amp3 is fixed because of the chosen components; thus, with a 50 mV<sub>rms</sub>–100 mV<sub>rms</sub>/1 kHz signal at the external input the gain of Amp4 must be trimmed to the Amp3 gain (P9 of Fig. 4.1).

Additionally, all DC offset trim pots of the main board must ensure an output DC level of 0.00 V. It is highly recommended to trim the Fig. 1.2 trim pots of OPs 1 & 2 to 0.00 V output DC-level, because, if not properly trimmed to zero volts, they would additionally influence the triode stage’s anode current.

Before the listening tests can take place the overall frequency and phase responses, the overall THD, IMD, and SN measurements with input loaded become the final check procedures.

---

## 16.1 Intro

The measurement of noise in the balanced world requires special measurement amplifiers (MA). The best case would be one with balanced input and balanced and/or un-balanced output, being capable to feed one of the many computer based measurement solutions (CMS), like eg the Clio system. Then, in this kind of environment, the task of the MA is to lift the DUT noise level far above the input noise level of the CMS. Finally, the CMS reading (in  $-dB$ ) minus the MA gain (in  $dB$ ) will show the output noise level of the DUT. This method allows the measurement of signal and noise levels in the region of  $1 \mu V_{rms}$  balanced, a low-level region nowadays mainly occupied by very high priced audio analyzers from eg Audio Precision or Rohde und Schwarz.

Recently, in stereoplay 2013-03, I read an article on the “NAD M51” DA converter. For me the most astonishing thing was the measurement result of the A-weighted output referred  $SN_{ne.o.a} = -122 \text{ dBV(A)}$ —and hum-free. Based on the FFT diagram in the review, the noise curve shows white noise behaviour with a rather low  $1/f$  noise corner frequency of approximately 350 Hz. I have transferred the Audio Precision SYS 2722 measurement graph into the rough representation of Fig. 16.1.

The 350 Hz corner frequency  $1/f$ -noise effect worsens the otherwise nearly pure white noise signal in  $B_{20k}$  by appr. 0.5 dB. Additionally, the A-weighting effect counts another 2.05 dB. Theoretically, the corresponding purely white noise output signal would thus become  $-122 \text{ dB(A)} + 2.05 \text{ dB} - 0.5 \text{ dB} = -120.45 \text{ dBV}$  (NAD data sheet spec:  $-125 \text{ dB ref. } 2 V_{rms} \equiv -119 \text{ dBV}$ , incl.  $1/f$ -noise, of course). Measured in  $B_{20k}$  this extremely low SN level stands for an average output noise voltage density of 6.72 nV/rtHz. The balanced output resistance shows a measured 141  $\Omega$  (110  $\Omega$  = NAD spec).

---

A shorter version of this chapter was firstly published in Jan Didden’s Linear Audio Vol. 7, 2014-03, ‘A poor man’s measurement amp (PMMA)’.

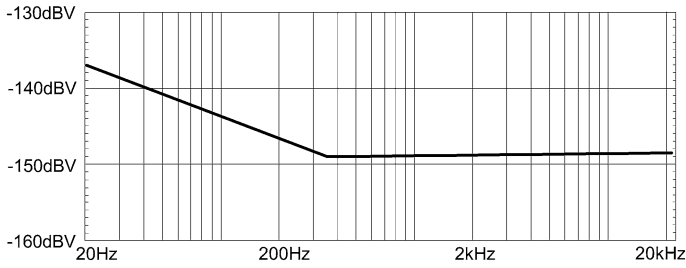


**Fig. 16.1** Output voltage noise density curve of the NAD M51

Nevertheless, the measurement result is not the truth! The above-mentioned SN of  $-122$  dBV(A) includes a certain portion of AP's unweighted input referred  $SN_{i,AP} = -122.4$  dBV of the channel that was used for the measurement. With balanced inputs shorted, stereoplay's four channels in two AP SYS 2722 analyzers, all equipped with 20 kHz brick wall S-AES17 low pass filters, show input referred SNs between  $-122.0$  and  $-122.4$  dBV ( $\equiv -119.0$  dBu to  $-119.4$  dBu in  $B_{22k} = 22$  Hz to 22 kHz with 3rd order lp à la IEC 468).

The identification of a  $1 \mu V_{rms}$  signal spike in an FFT diagram seems not to be a problem, as long as the analyzer's FFT resolution can be set to eg  $\leq 5$  Hz. Depending on the sample rate and FFT size setting and as long as the analyzer's input referred noise voltage density is low enough (practically without impact on the measured signal) the representation of a  $B_{20k}$   $1 \mu V_{rms}$  white noise signal on the screen will show a noise level far lower than  $-120$  dBV. In any case, it should be lower than an average level of  $7.07$  nV/rtHz. Why? See further down in Sect. 16.2.

I do not want to debate what is the 'right' lowest noise level and thus the highest possible SN value of HiFi equipment. In Douglas Self's LA Vol. 5 article,<sup>1</sup> Table 4, we can easily study what we can achieve in that field. Because of their extremely low value all measured figures had to be corrected according to the AP noise impact. To get dBV in  $B_{20k}$  simply subtract  $2.22$  dB +  $0.81$  dB =  $3.03$  dB from the table's dBu values; here,  $0.81$  dB comes from the reduction of the bandwidth ( $0.41$  dB) plus the lp change ( $0.4$  dB) from 3rd ord. Butterworth to the brick wall version).

Thus, I guess an amplifier output referred SN benchmark of  $-120$  dBV in  $B_{20k}$  is still an extreme value and as music listener, I can live with it—even in the quietest moments. However, seen from a development point of view, we have some open questions on an MA that should be capable to measure such extremely low SNs with lowest possible impact on the measurement result. With that in mind, in this chapter I will try to answer at least the following questions:

1. What should be the level of input noise voltage density of an MA with balanced input that causes the low output noise voltage density of a DUT with a measured  $SN_{o,dut,m} = -120$  dBV/ $B_{20k}$  to be off eg  $0.1$  dB maximum only?

<sup>1</sup>Linear Audio Vol. 5, 2013-04, 'A low-noise preamplifier with variable-frequency tone controls', Douglas Self.

2. How does the DUT's output resistance additionally worsens the measurement result and what are the roles of the MA's input resistance  $R_{in}$  and its input noise current density  $i_{n,i}$ ?
3. Based on the following three subgoals how could a rather low budget and easy to built measurement-amp look like?
  - 3.1. Flat frequency and phase response in  $B_{20k}$  ( $\pm 0.02$  dB/ $\pm 10^\circ$ )
  - 3.2. Overall gain: 1000
  - 3.3. Balanced input and balanced/un-balanced outputs
4. How can we calculate the noise performance of that new MA?

We will see further down that the chosen PMMA concept fulfils all above-mentioned goals.

---

## 16.2 The Input Noise Voltage Density Question

Before we start developing the MA and as consequence of the first question and its  $-120$  dBV goal and in order to find the MA's input referred noise voltage density allowed ( $e_{n,i}$ ) we have to go through some math first.<sup>2</sup> The equations for the required MA input referred  $SN_{i,ma}$  look as follows:

With the DUT output  $SN_{o,dut,m}$  [dBV]  $<$   $SN_{i,ma}$  [dBV]<sup>3</sup> and with

$$B = SN_{o,dut,m} - SN_{i,ma} \text{ [dB]} \quad (16.1)$$

we obtain the MA's allowed input referred  $SN_{i,ma}$  as function of B as follows:

$$SN_{i,ma}(B) = 20\log\left(10^{\frac{SN_{o,dut,m} - B}{20}}\right) \text{ [dBV]} \quad (16.2)$$

Application of (16.2) in the following equation will lead to the expression for the allowed impact  $W_e(B)$  [dB] of the MA on the DUT. It should become—in our case here— $0.1$  dB.

$$W_e(B) = 20\log\left(\sqrt{10^{\frac{SN_{o,dut,m}}{10}} + 10^{\frac{SN_{i,ma}(B)}{10}}}\right) - SN_{o,dut,m} \text{ [dB]} \quad (16.3)$$

Figures 16.2a, b show the corresponding graphs.

---

<sup>2</sup>Just to keep the overall picture in one chapter, I repeat Eqs. (15.1)–(15.3) and Figs. 15.3 and 15.4 here.

<sup>3</sup>Here, “ $<$ ” means worse! The other way around ( $>$ ) makes no sense!

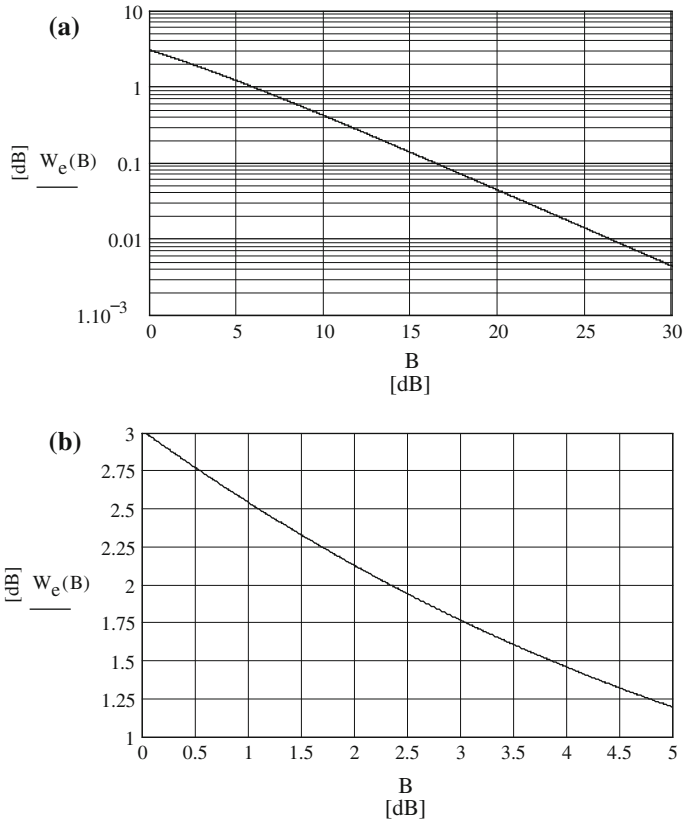


**Fig. 16.2** a Worsening Figure  $W_e(B)$  as function of the difference  $B$  of two SNs. b Zoomed version of Fig. 16.2a for correction purposes of two SNs with values that are close together ( $B \leq 5$  dB)

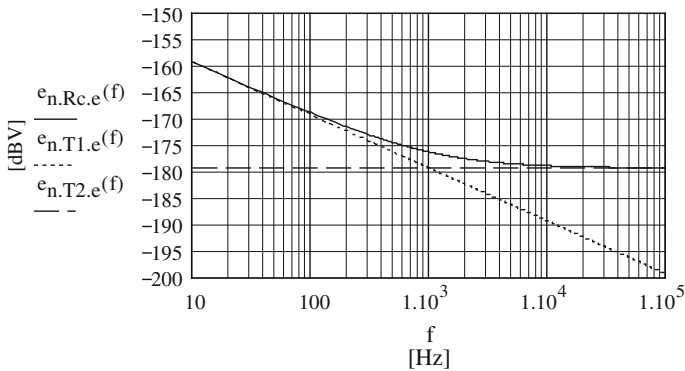


**Fig. 16.3** Noise voltage density situation with a corner frequency of 1 kHz (incl. tangents)



Based on the calculated range of Worsening Figures (y-ordinate), at the allowed Fig. 16.2a value of  $W_e(B) = 0.1$  dB we can now pick-out the delta B (x-ordinate) between the DUT's output referred  $SN_{o,dut}$  and the  $SN_{i,ma}$  of the MA: it becomes 16.33 dB. Hence and in other words: to ensure a  $\leq 0.1$  dB MA impact down to a DUT output SN level of  $-120$  dBV on all kinds of SN measurement in  $B_{20k}$  we need an optimal MA input referred  $SN_{i,ma}$  of  $-136.33$  dBV =  $-120$  dBV - 16.33 dB. Thus, transferred into a white noise voltage density level flat over the complete audio band we need an MA that offers at least a balanced average input noise voltage density  $\leq 1.08$  nV/rtHz, hence, without 1/f-noise corner frequency in  $B_{20k}$ .

If we would, for example, allow a 1/f-noise corner frequency of 1 kHz, the average noise voltage density in  $B_{20k}$  would grow to  $-135.05$  dBV (see Fig. 16.3) and the MA's impact on the DUT's  $SN_{o,dut}$  would also grow to  $W_e(B) = 0.134$  dB. If we would keep the original  $-136.33$  dBV level and we would accept the example corner frequency of 1 kHz, then, to keep an average of 1.08 nV/rtHz in  $B_{20k}$  the white noise region  $> 1$  kHz of the MA's input noise voltage density has to drop from 1.08 nV/rtHz to a balanced 0.93 nV/rtHz.

Thus, to keep things on the safe side and as derived sub-goal for our purposes here the PMMA should offer an input noise voltage density of  $\leq 1$  nV/rtHz average in  $B_{20k}$  with no 1/f-noise corner frequency. The permitted amount of input noise current density is part of the next section's discussion.

## 16.3 The Roles of the MA Input Resistance and Input Noise Current Density

### 16.3.1 Influence of the DUT Output Resistance

I think it is obvious that a voltage divider effect between the DUT's total output resistance  $R_{o,tot}$  and the MA's total input resistance  $R_{in,tot}$  will lead to an improved meter reading of the output referred  $SN_{o,dut,m}$ . This would happen if we would keep the reference level like the one without voltage divider effect.

However, if we would reduce the idle case reference level according to the voltage divider ratio, the measured  $SN_{o,m}$  of the DUT would become the DUT's real one. To get the real  $SN_{o,r}$  with reference to the original reference level (in dBu or dBV) we have to compensate this kind of erroneous improvement by simply adding the magnitude of the voltage divider gain-loss  $G_{loss1,e} = 20\log(G_{loss1})$  to the measured  $SN_{o,m}$ . Hence, we obtain the real  $SN_{o,r}$  as

$$SN_{o,r} = SN_{o,m} + |G_{loss1,e}| \quad (16.4)$$

In Fig. 16.4 the DUT has two kinds of output resistances;  $R_{o1}$  and  $R_{o2}$  represent the real internal output resistance of the DUT. Not taking into account any external noise producing influences, we assume that the whole noise generation of the DUT already covers their internal electronic noise. A typical example for this kind of

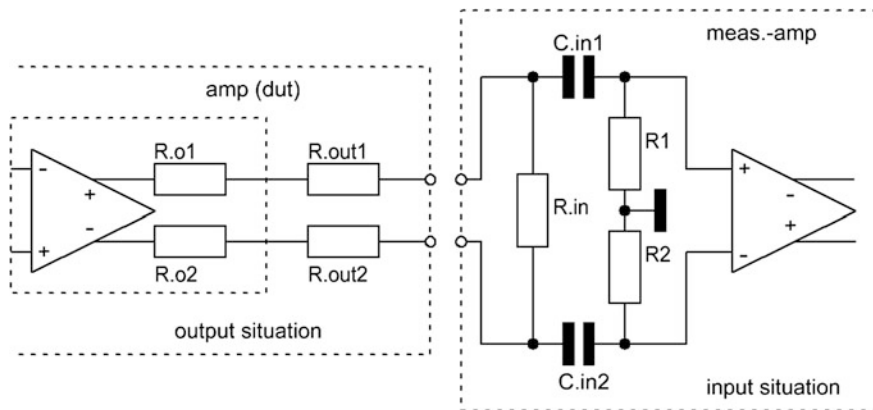


**Fig. 16.4** General output situation of the DUT (left) and balanced input of measurement instrument (right)

output comes from the valve world: the anode output of a common cathode (or common grid) gain stage. In most cases, op-amp outputs offer an output resistance close to 0 Ω, I guess in most cases < 10 Ω in B<sub>20k</sub>.

By bridging the two input capacitances C<sub>in1</sub> & C<sub>in2</sub>, the gain-loss G<sub>loss1.e</sub> thus becomes:

$$G_{\text{loss1.e}} = 20\log\left(\frac{R_{\text{in.tot}}}{R_{\text{o.tot}} + R_{\text{in.tot}}}\right) \tag{16.5}$$

$$\begin{aligned} R_{\text{in.tot}} &= R_{\text{in}} \parallel (R1 + R2) \\ R_{\text{o.tot}} &= R_{\text{o1}} + R_{\text{o2}} + R_{\text{out1}} + R_{\text{out2}} \end{aligned} \tag{16.6}$$

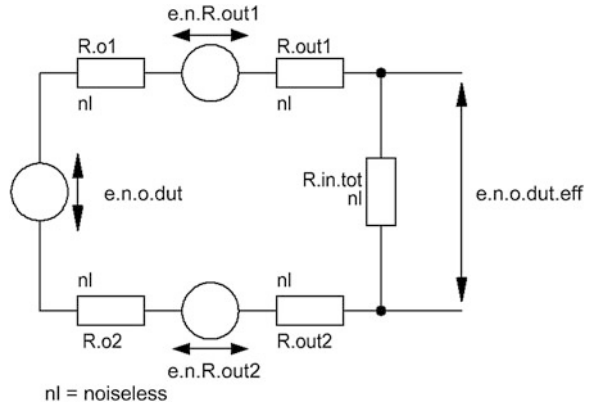
Together with the following cable capacitance, the two resistors R<sub>out1</sub> and R<sub>out2</sub> play an additional low-pass role in cases of very low R<sub>o1</sub> + R<sub>o2</sub>. Many manufacturers put them in place in order to ensure a high-frequency cut far outside B<sub>20k</sub>. In conjunction with the input noise current of the next stage, these DUT internal resistances may produce significant portions of additional noise.

Thus, both kinds of resistances play a role in the gain-loss but can also be significant producers of additional noise.

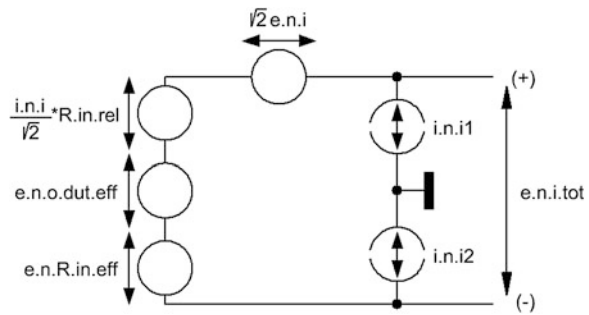
### 16.3.2 The Input Noise Current Density Question

Figure 16.5 shows the situation of the Fig. 16.4 based noise sources. Here, e<sub>n.o.dut.eff</sub> is the DUT’s noise voltage after the voltage divider, however without noise voltage impact of the MA input.

**Fig. 16.5** Effective output noise voltage of the DUT



**Fig. 16.6** The creation of the total input noise voltage of the measurement amp



The noise voltage impact of the MA comes into the game in Fig. 16.6. It is composed of several sources, such as the Fig. 16.5 ones and those of a typical balanced input stage. Here,  $e_{n,i1}$  and  $e_{n,i2}$  are the input noise voltage densities of the MA's input stage, both of equal value  $e_{n,i}$ , series connected, thus increasing their combined value by  $\sqrt{2}$ . The input noise current densities  $i_{n,i1}$  and  $i_{n,i2}$  are both of equal value  $i_{n,i}$ . Also connected in series they decrease their combined value by  $\sqrt{2}$ .

Figure 16.6 shows the result after connecting the DUT output with the MA input: all noise sources form what I call the total input referred noise voltage density  $e_{n,i,tot}$  at the (+) and (-) input of the MA.

For calculation purposes, we need the following equations:

$$e_{n,i,tot} = \sqrt{2e_{n,i}^2 + \left(\frac{i_{n,i}}{\sqrt{2}} R_{in,rel}\right)^2 + e_{n,R,in,eff}^2 + e_{n,o,dut,eff}^2} \quad (16.7)$$

$$\begin{aligned} e_{n,R,in,eff} &= e_{n,R,in,tot} G_{loss2} \\ R_{in,rel} &= R_{in,tot} || R_{o,tot} \\ G_{loss2} &= \frac{R_{o,tot}}{R_{o,tot} + R_{in,tot}} \end{aligned} \quad (16.8)$$

In (16.7), 2nd term, we can see that, as a result of a noise voltage, the input noise current density flows also through the DUT output resistors  $R_{out1}$  and  $R_{out2}$  and resistances  $R_{o1}$  and  $R_{o2}$ . Here, their sum plays by far the major role because of the relatively high value of  $R_{in,tot}$  in  $R_{in,rel}$  [see (16.6) and (16.8)]. According to Fig. 16.5 and with a noiseless  $R_{in,tot}$  we can calculate the 4th term.

The inclusion of  $R_{o1}$  and  $R_{o2}$  into the 2nd term is questionable. Imagine an anode output of a triode with an anode load resistor  $R_a$ . Thus, in case of a bridged cathode resistor (by a capacitance) the output resistance becomes  $R_a \parallel r_a$  ( $r_a$  = internal triode anode resistance). I doubt that the input noise current of the MA will also flow through the triode against the triode's electron current from cathode to anode, hence, from anode to cathode. Consequently, in (16.5) we should take  $R_a$  as the value for  $R_{o1}$  and  $R_{o2}$  (in case of a balanced output stage). As long as the value of  $R_a$  is unknown, we can take the measured or data sheet indicated output resistances of the DUT.

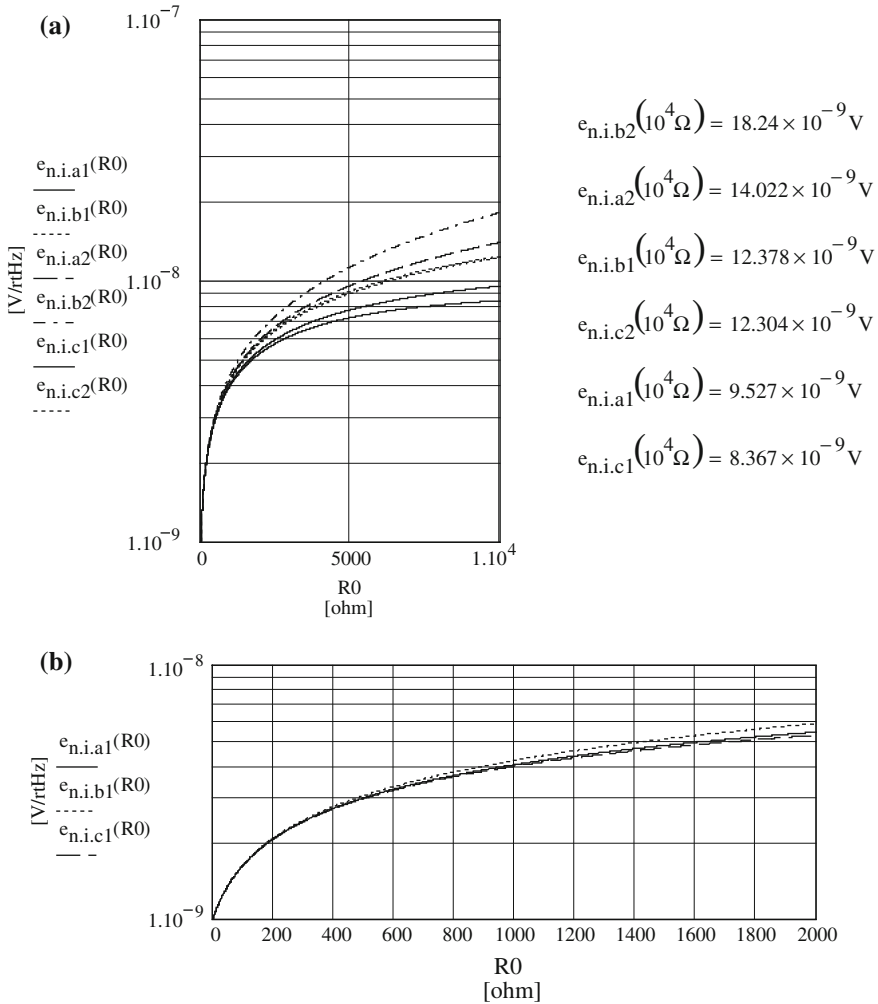
I have calculated a graph that demonstrates the respective relationships. Figure 16.7a shows the additional noise voltage creation if we measure a DUT with output resistances in the range up to 10 k $\Omega$ . Starting point is 1 nV/rtHz and I took three different input noise current density versions: BJT input devices with 1 pA/rtHz (solid and dotted traces and subscript a), 2 pA/rtHz (dashed and dashed-dotted traces and subscript b), and FET input devices with 50 fA/rtHz (dotted and solid traces and subscript c). Additionally, I have chosen two different MA balanced input resistances: 18.182 k $\Omega$  (PMMA and subscript 1) and 200 k $\Omega$  (AP and R&S and subscript 2). At the right-hand scale of Fig. 16.7a I have added the trace values for  $R_o = 10$  k $\Omega$  too. It should allow easier identification of the traces in the left graph.

Figure 16.7b shows the zoomed version for the 18.182 k $\Omega$  MA input resistance case, up to  $R_o = 2$  k $\Omega$  versus the three different input noise current densities.

### 16.3.3 Conclusions

With an MA input resistance of 18.182 k $\Omega$  a look at Fig. 16.7b signals that there is no big difference up to 2 k $\Omega$  output resistance between nearly no input noise current and a rather high one of 2 pA/rtHz. Additionally, for all shown Fig. 16.7a cases up to 2 k $\Omega$  the input resistance difference does not play a major role either. However, we can see that 180  $\Omega$  output resistance doubles the 1 nV/rtHz (= -180 dBV) input noise voltage density goal. With that we no longer can maintain the 0.1 dB worsening goal for the measurement of a 1  $\mu$ V<sub>rms</sub> (= -163 dBV average noise voltage density level) DUT output noise signal. With 2 nV/rtHz (= -174 dBV) the difference B to -163 dBV is only 11 dB; hence, as of Fig. 16.2, the worsening figure grows to 0.33 dB. At eg 1 k $\Omega$  output resistance we obtain thus  $W_e = 1.2$  dB.

To keep both the complexity as well as the required budget of the whole MA circuit as low as possible (Occam's Razor!) I will adequately take the  $W_e$  effects into account and my input noise current density goal for the MA should be set to  $i_{n,i} \leq 1$  pA/rtHz. In such a high gain and low-noise configuration FET input op-amps do not offer any advantage over their BJT counterparts. Although their input noise



**Fig. 16.7** a DUT output resistance versus various MA total input noise voltage variants. b Zoomed version of Fig. 16.7a (for  $R_{in,tot} = 18.182 \text{ k}\Omega$  only)

current impact is marginal, the chance for a very much higher 1/f-noise corner frequency is a given fact. With that in mind the two chosen input noise density values are thus in line with the same values of the un-balanced MA that is already described in Fig. 11.1 (TSOS-1) and Fig. 22.1 (TSOS-2), however, now in a fully balanced mode.

Nevertheless, as input devices for MAs with gains  $\leq 100$  and input noise voltage densities in the range of 3–6 nV/rtHz, FET input op-amps can very well be used, like eg the ones of the OPA627 or OPA827 family. Using those, noise voltage loaded outputs of valve gain stages with high output resistances  $>10 \text{ k}\Omega$  can easily be measured, with a very low MA noise impact on the measured signal.

By changing the MA input resistance to 1 MΩ, or even higher, such a gain stage could also be fit into the PMMA configuration presented here, with only one balanced input stage.

## 16.4 The Final PMMA

### 16.4.1 Principal Circuit Approach

Low complexity means application of rather easy to handle circuits with op-amps or special measurement ICs. I do not know a single IC that offers the specs I want to have; hence, I took the traditional approach by arranging two input op-amps in a balanced in/out configuration and a third one that creates the un-balanced o/p. This is nothing else but the well-know instrumentation amplifier (INA), its principal circuit is given in Fig. 16.8.

Unfortunately, to create  $1 \text{ nV/rtHz} = \sqrt{2} * e_{n,i}$  average input noise voltage density in  $B_{20k}$  I also do not know an op-amp that offers an average input noise voltage density of  $e_{n,i} = 0.707 \text{ nV/rtHz}$  in  $B_{20k}$ . However, the only one I know that offers an input noise current density of  $1 \text{ pA/rtHz}$  also offers  $0.85 \text{ nV/rtHz}$  input noise voltage density in  $B_{20k}$ , the LT1028. To get a lower noise voltage density we must thus work with a paralleled input stage of four op-amps and two additional summing op-amps. Hence, the final MA consists of seven op-amps à la Fig. 16.9.

The resistors Rf1, Rf2, and R should have 0.1 % tolerance. Variable RG1 and RG2 allow the setting of equal gains for each sub input stage up to the output via the summing OPs 5 and 6. We obtain thus a gain  $G_{M,bal} = 1000 \equiv +60 \text{ dB}$  at the balanced output. The common mode gain  $G_{CM,bal}$  of that stage becomes 2, 1 for the input stage with Amp A and Amp B and 2 for the output stage (see Fig. 16.10), hence, the common mode rejection ration CMRR of the PMMA becomes (at least)  $54 \text{ dB} = 20 * \log(G_{M,bal}/G_{CM,bal})$ .

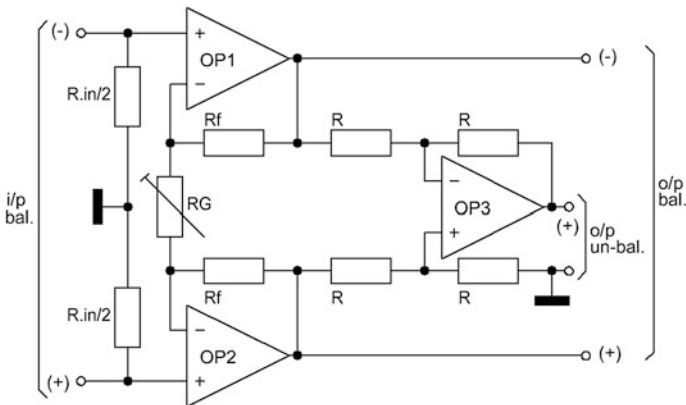
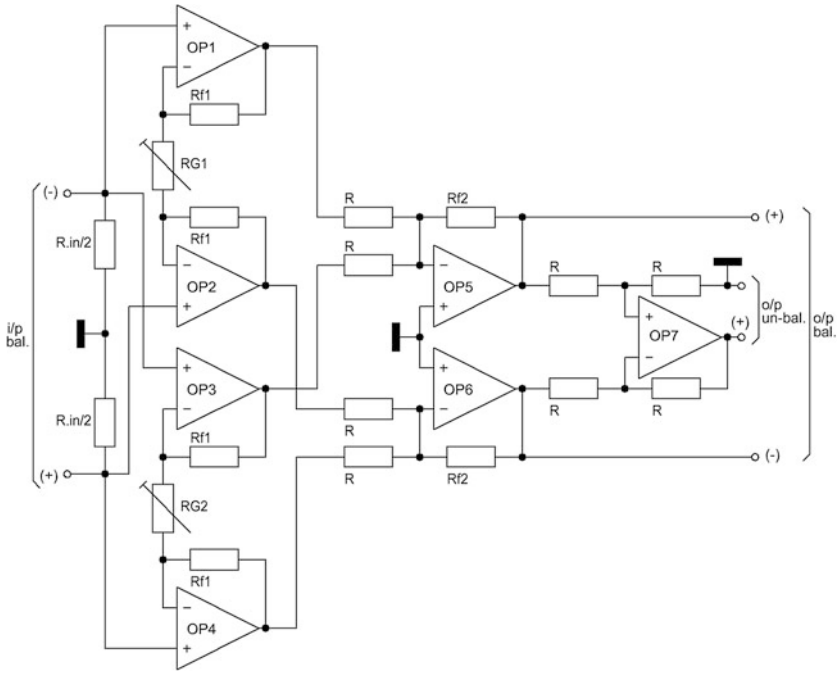
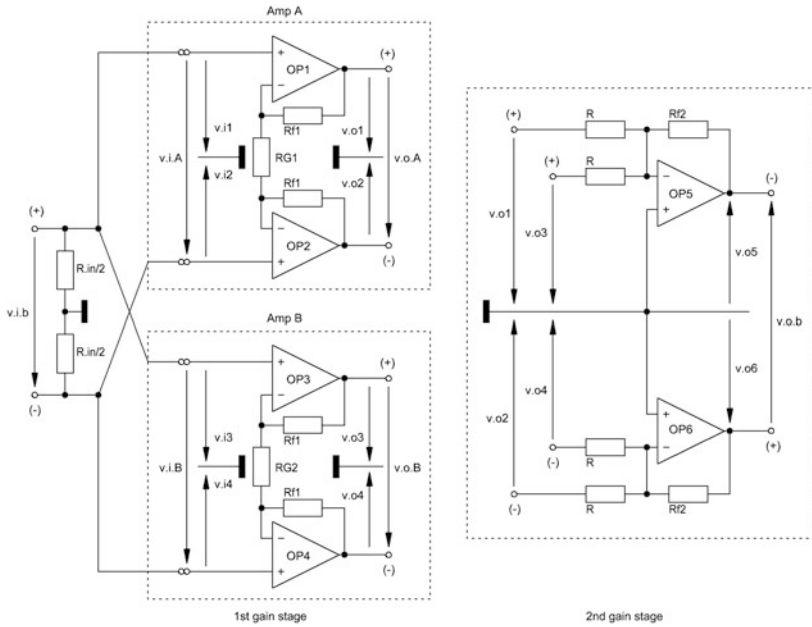


Fig. 16.8 Principal INA circuit



**Fig. 16.9** Principal final MA. (+) and (-) at the *input* and *outputs* indicate the phase relationship



**Fig. 16.10** Relevant circuits for the gain calculation process

OP7 serves as subtractor with a gain of 1. Consequently, the gain  $G_{M,unbal}$  for the PMMA's balanced to un-balanced conversion becomes +60 dB too. Its CMRR offers an additional 60 dB.

### 16.4.2 Gain Calculations

The calculation of the various PMMA gains looks a bit complex. Derived from the Fig. 16.9 principal circuit Fig. 16.10 shows all gain-calculation relevant stages and voltages with the arrows in the right phase direction. To get the balanced gain  $G_M$  from input to output we have to consider several different balanced and un-balanced gains of all gain stages. Additionally, in Fig. 16.10, the first gain stage is composed of the two sub gain stages A and B. Their un-balanced output voltages are summed-up by the second gain stages.

The following equations are the result of the derivation process given in detail in the Mathcad Worksheet MCD-WS 18.2, Point 6:

- The balanced PMMA gain  $G_M$ :

The input gain stage (sub gain stages Amps A and B = 1st gain stage with OP1–OP4) together with the summing output gain stage (=2nd gain stage with OP5 and OP6) form the differential (balanced in/balanced out) PMMA.

- With  $R_{G1} = R_{G2} = R_{G_M}$  the differential overall gain  $G_M$  becomes:

$$\begin{aligned} G_M &= \frac{V_{o,b}}{V_{i,b}} = -1000 \\ &= -2 \left( 1 + \frac{2 R_{f1}}{R_{G_M}} \right) \frac{R_{f2}}{R} \end{aligned} \quad (16.9)$$

- With  $R_{f2} = R$  (recommended) we obtain:

$$G_M = -2 \left( 1 + \frac{2 R_{f1}}{R_{G_M}} \right) \quad (16.10)$$

According to Fig. 16.10, the “-” sign represents a 180° phase inversion.

- The two differential gains  $G_A$  and  $G_B$  of the sub gain stages Amps A and B become:

$$\begin{aligned} G_A &= 1 + \frac{2 R_{f1}}{R_{G_M}} \\ &= 500 \\ G_B &= 1 + \frac{2 R_{f1}}{R_{G_M}} \\ &= 500 \end{aligned} \quad (16.11)$$



- The two gains  $G_{A.ub.1}$  and  $G_{A.ub.2}$  of Amp A's balanced in/un-balanced out sub gain stage path become:

$$\begin{aligned} G_{A.ub.1} &= \frac{V_{o1}}{V_{i,b}} = 250 \\ &= 0.5 G_A \end{aligned} \quad (16.12)$$

$$\begin{aligned} G_{A.ub.2} &= \frac{V_{o2}}{V_{i,b}} = -250 \\ &= -0.5 G_A \end{aligned} \quad (16.13)$$

- The two gains  $G_{B.ub.3}$  and  $G_{B.ub.4}$  of Amp B's balanced in/un-balanced out sub gain stage path become:

$$\begin{aligned} G_{B.ub.3} &= \frac{V_{o3}}{V_{i,b}} = 250 \\ &= 0.5 G_B \end{aligned} \quad (16.14)$$

$$\begin{aligned} G_{B.ub.4} &= \frac{V_{o4}}{V_{i,b}} = -250 \\ &= -0.5 G_B \end{aligned} \quad (16.15)$$

- The gain of the second gain stage with its un-balanced in/un-balanced out becomes:

The second gain stage consists of two inverting and summing op-amps (OP5 and OP6). With  $Rf2 = R$  their gains  $G_{op5}$  and  $G_{op6}$  become  $-1$  for each un-balanced input path. Hence, we obtain the following set of equations:

$$V_{o,b} = V_{o5} - V_{o6} \quad (16.16)$$

$$V_{o5} = -V_{i,b}(G_{A.ub.1} + G_{B.ub.3}) \quad (16.17)$$

$$V_{o6} = -V_{i,b}(G_{A.ub.2} + G_{B.ub.4})$$

=>

$$\begin{aligned} G_M &= \frac{V_{o,b}}{V_{i,b}} \\ &= -(G_A + G_B) \end{aligned} \quad (16.18)$$

### 16.4.3 Noise Calculations—Rule-of-Thumb SN Calculation Approach

Chapter 18's MCD-WS 18.2 gives the full details of the calculation course. However, I'll present the basics of the two noise calculation approaches (rot and detailed) here.

To get a feeling on the output referred SN we will start with a rule-of-thumb (rot) approach. It is based on a single op-amp gain stage in series configuration with a gain of 1000 and input shorted. Figure 16.11 gives the details.

To get  $SN_{o,rot}$  in  $B_{20k}$  and with  $G_M = 1000$  the rot math goes as follows:

$$SN_{o,rot} = 20\log\left(\frac{e_{n,o,rot}}{1V}\right) + 43 \text{ dB [dBV]} \quad (16.19)$$

With the op-amp's  $e_{n,i} = 0.85 \text{ nV}/\sqrt{\text{rtHz}}$  and RG's  $e_{n,RG,rot}$  we obtain the output noise voltage density  $e_{n,o,rot}$ :

$$e_{n,o,rot} = G_M \sqrt{e_{n,i}^2 + e_{n,RG,rot}^2} \quad (16.20)$$

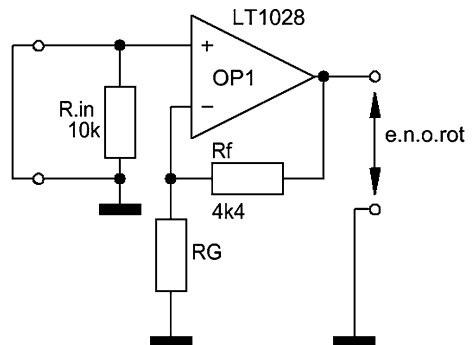
$$RG = \frac{R_f}{G_M - 1} \quad (16.21)$$

$$\begin{aligned} e_{n,RG,rot} &= 0.13 \sqrt{\frac{RG}{\Omega}} \text{ [nV}/\sqrt{\text{Hz}}] \\ &= 0.273 \text{ [nV}/\sqrt{\text{Hz}}] \end{aligned} \quad (16.22)$$

$$e_{n,o,rot} = 893 \text{ nV}/\sqrt{\text{rtHz}} \quad (16.23)$$

Hence,  $SN_{o,rot}$  and the gain stage input referred noise voltage density  $e_{n,i,rot}$  become:

**Fig. 16.11** Circuit for rule-of-thumb SN calculation



$$SN_{o.rot} = -78.0 \text{ dBV} \quad (16.24)$$

$$\begin{aligned} e_{n.i.rot} &= \frac{e_{n.o.rot}}{G_M} \\ &= 0.893 \text{ nV}/\sqrt{\text{Hz}} \end{aligned} \quad (16.25)$$

We have now found the two most important noise based values that show where we should end-up with the PMMA performance.

#### 16.4.4 Noise Calculations—Detailed SN Calculation Approach

The path through the noise calculation jungle of such a gain stage looks rather difficult. However, I will present it in this book because gain stages with lower gain than  $\times 1000$  and other than the shown active and passive components bear many traps. I hope I could avoid most of them.

According to the Fig. 16.9 MA configuration, we have to split the calculation course into three different parts:

- Input stage with OP1–OP4 and composed by differential Amps A and B,
- 2nd and balanced output stage with the two summing stages OP5 and OP6,
- 3rd stage with balanced to un-balanced converter OP7.

Normally, in a  $\times 1000$  MA the influence of the noise of the 2nd and 3rd gain stage can fully be ignored; the 1st stage creates far more noise than the two other stages. However, in configurations with lower gain, the noise impact of the output stage becomes significant. We should know the noise producing mechanism behind this fact. It is also responsible for the increase of the input referred noise voltage density of commercially available INAs, if we set them to low gains.

In contrast to the before mentioned Linear Audio article and the noise calculation approach described there the chosen noise model of one-half of the 1st stage with input shorted is given in Fig. 16.12. The mathematical treatment of the noise voltage of RG and its transfer to the output follows the approach already described in Sect. 4.3. Thus, compared with Table 1 of the original article the calculated results of Tables 16.1 and 16.2 yield a tiny change.

The handling (suppression) of the 100 % correlated noise voltages between the two output leads and ground will be the task of a following amp with balanced input and rather good CMRR.<sup>4</sup> This point is not a problem for the signal path via OP7; with 0.1 % resistances, CMRR of this stage becomes always  $\geq 60$  dB.

Additionally we add an input load  $R_0$ , and, as a reminder, we show the connections to the parallel operating stage with OP3 and 4.

---

<sup>4</sup>See Sect. 16.5.1.

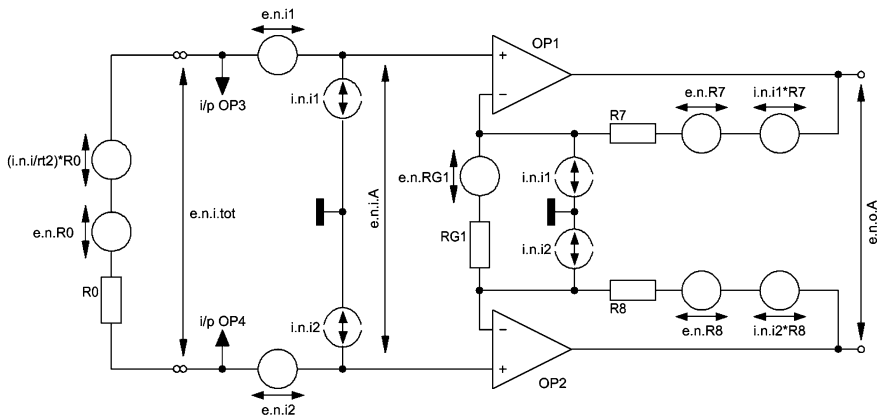


**Fig. 16.12** Noise model of one-half input stage (Amp A with OP1 and OP2)

The noise model of the other half of the input stage (Amp B) looks absolutely the same. By paralleling these two halves, the resultant output noise voltage becomes factor  $\sqrt{2}$  higher.

Paralleling goes via the summing stages OP5 and 6. Figure 16.13 shows the corresponding noise model.

In Fig. 16.15, we find jumpers jmp1–jmp4. They can produce short-circuits at the inputs of the output stage; hence, we can separately check their calculated output noise voltage. Here, RP is the parallel configuration of the input resistors at the (-) input ( $R11||R12, R13||R14$  in Fig. 16.15).

Finally, the well-known subtraction stage in an INA shows its noise model in Fig. 16.14. Here, RP is the parallel configuration of the resistors at the (+) input ( $R17||R19$  in Fig. 16.15).

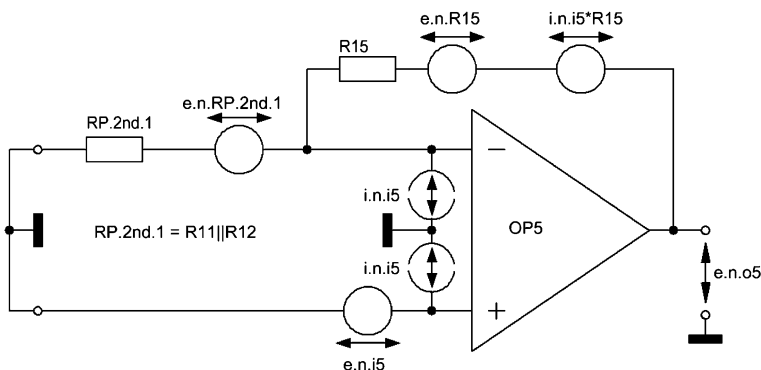


**Fig. 16.13** Noise model of one of the two summing stages (OP5 and OP6)

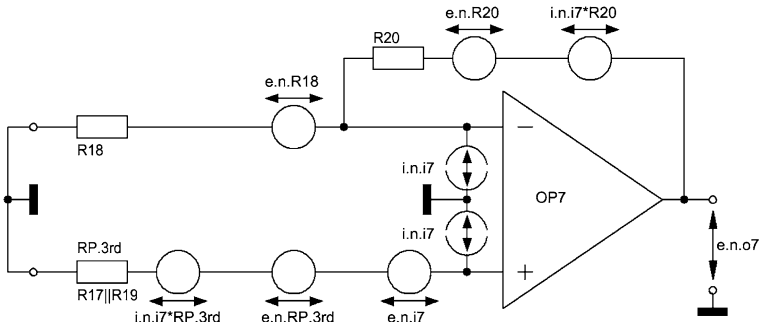


**Fig. 16.14** Noise model of the balanced to un-balanced converter (OP7)

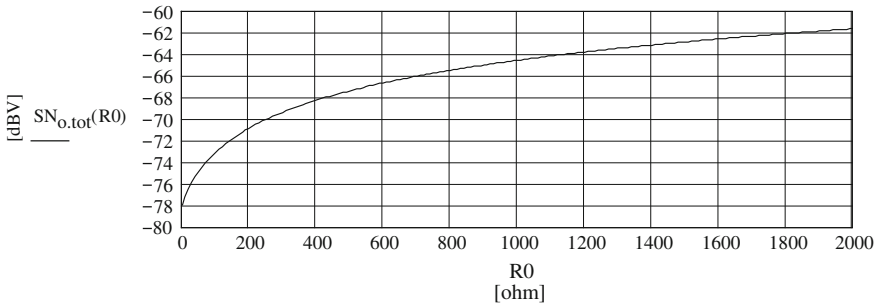


**Fig. 16.15** Input load dependency of the output referred SN

I refrain from filling the pages with a huge amount of equations. The chosen process of output noise voltage calculations follows the block concept: each gain stage’s output noise voltage density becomes multiplied by the gain of the following stages. Then, to get the total output referred noise voltage density  $e_{n,o,tot}$ , we sum-up the un-correlated output noise voltage densities. Division by the gain of the MA will lead to the input referred noise voltage density  $e_{n,i,tot}$ . In addition, the calculation course allows playing around with various values of input load resistances  $R_0$ . To meet the goal from the beginning it should become  $\leq 1$  nV/rtHz with  $R_0 = 0 \Omega$ .

The calculated Fig. 16.15 (= MCD – WS 18.2’s Fig. 18.10) graph of the input load dependent output referred SN shows rather drastically that it would be always better to measure DUT output SNs with DUT output resistances close to  $0 \Omega$ .

To keep the PMMA’s average input noise voltage density in any case  $\leq 1$  nV/rtHz the output resistance should be  $\leq 10 \Omega$ . For consumer products, this becomes rather seldom the case. The final SN determination should always consider these effects.

### 16.5 The Complete PMMA Circuit

Figure 16.16 shows the final and complete built-up PMMA circuit. For a better understanding, the following list gives some hints:

1. The main balanced i/p is J01; it should be used for balanced purpose only. For other purposes, I added J02 and J03; they allow un-balanced application by eg switching S2 and nulling J03. Usage of these inputs may lead to unstable conditions.
2. S1 plays the ground lift, thus, in most cases solving the pin1 problem; based on a Jensen Transformer recommendation, an open S1 and the sequence of R1 and C1 ensure grounding for very high frequencies.
3. R3 and R4 parallel to R2 set the input resistance  $R_{in}$  of 18.182 k $\Omega$ . An attempt to increase R3 and R4 to 100 k $\Omega$  each works too, however the offset-nulling process becomes a nightmare and after each input load change the amp's output shows a tendency to run into the power supply line level. This effect disappears after switching the psu off and on a few seconds later.

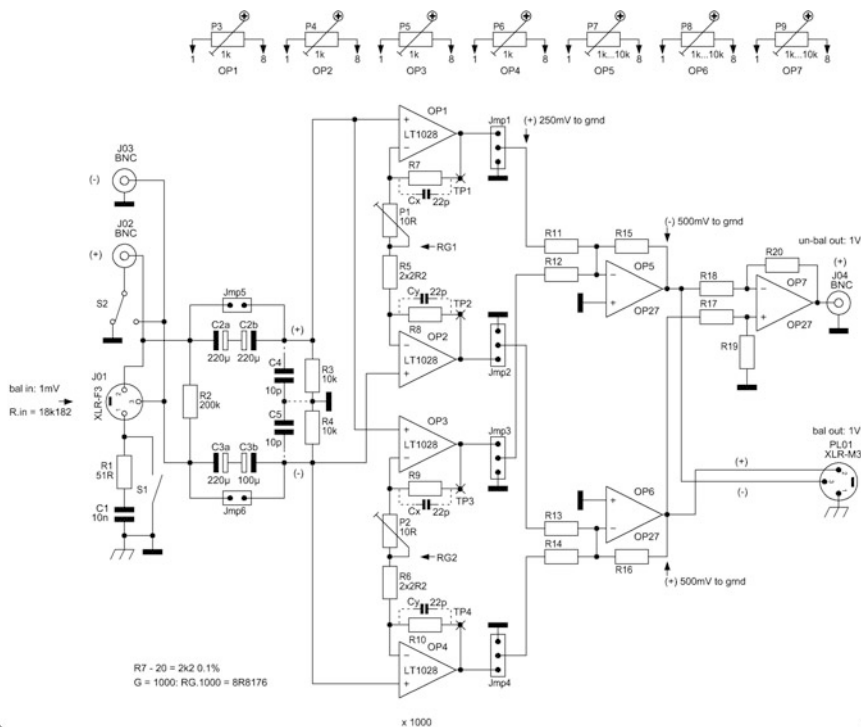
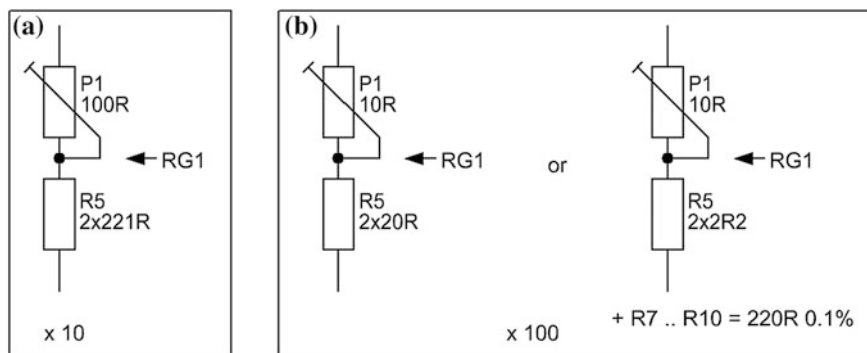


Fig. 16.16 Complete MA circuit



**Fig. 16.17** RG alternatives for gains of **a**  $\times 10$  and **b**  $\times 100$  (for only one input stage)

4. To allow direct amplification jumpers 5 and 6 can bridge the input Cs (C2a + C2b and C3a + C3b). I do not recommend it. It would require a new offset trimming process for each new input load.
5. For easy change to another configuration than the one shown, the two input stages OP1 and OP2 and OP3 and OP4 (including their feedback resistors) are built-up on two separate plug-in PCBs; RG examples for gains of  $\times 10$  and  $\times 100$  are given in Fig. 16.15.
6. A DC voltmeter between TP1 and TP2 or TP3 and TP4 measures the alternately performed offset-nulling of the input stages by P3–P6, hence, after replacing jumpers 1–4 there should be no offset voltage left at outputs PL01 and J04. I must point out that offset-nulling makes sense only after 15 min heating-up the amp with shorted input, and without jumpers 5 and 6. It takes some additional time to get 0.00 V at the outputs.
7. C4, C5, Cx, Cy may be a necessary addition to the circuit; it depends on the PCB layout as well as on the shielding effect of the case; however, in my configuration I only had to pack Cx and Cy on R7–R10, each 22 pF ceramic and selected 1 %.
8. Setting jumpers 1–4 to ground allows easy offset-nulling of OPs 5–7 before the offset-nulling process of the input stages should take place.
9. We feed the PMMA with a 1 kHz/1 mV<sub>rms</sub> balanced input signal. To create a level of 0.5 V<sub>rms</sub> between testpoints T1 and T2 and between T3 and T4 the gains of the two input stages must then be trimmed by P1 and P2; automatically, there will be an output signal of 1 V<sub>rms</sub> at both outputs PL01 and J04.
10. Alternatively, we can measure and trim 0.25 V<sub>rms</sub> between T1 and ground plus T2 and ground and 0.25 V<sub>rms</sub> between T3 and ground plus T4 and ground.
11. In case of a  $\times 10$  or  $\times 100$  gain solution only one input stage will be necessary.
12. Replacement of R3 and R4 by eg 1 M $\Omega$  each and R2 by 2 M $\Omega$  leads to an input resistance of 1 M $\Omega$ , very useful for 1st gain stages with FET op-amps for the measurement of high resistive valve output stages.

13. I've set the input resistance to 18.182 k, a value high enough to measure DUTs with output resistances up to 2 k $\Omega$  balanced. Of course, the measured values have to be corrected for the gain-loss of the voltage to obtain the DUT's actual output referred SN.

---

## 16.6 PMMA Performance

Table 16.1 shows a summary of the main measurement versus calculation results of the MA with gain of  $\times 1000$ . In addition, further down, I show some graphs of the output noise voltage. We see that hum and computer induced spikes will fully disappear if we supply the input with a noise voltage that equals the noise voltage of a resistor  $\geq 1$  k $\Omega$ , which will always be the case with DUT output noise voltages  $\geq 1\mu\text{V}_{\text{rms}}$  in  $B_{20k}$ .

Notes on Figs. 16.18 and 16.19:

- On the y-ordinate the gain (+40.00 dB) of an additional Extra Measurement Amp PFMA<sup>5</sup> and the gain of the measurement filter section (+6.02 dB<sup>6</sup>) are taken into account.
- FFT resolution is 0.73 Hz = sample rate divided by FFT size (length)
- Averaging in all cases: 50
- No computer-induced spikes could be detected. I could not suppress the tiny 150 Hz hum spike that comes in via (my suspicion) the unshielded part of the input XLR plug. It was created by vagabonding hum interferences in my lab<sup>7</sup>; however, with a 1 k $\Omega$  input load the upper traces show that an input noise voltage density signal of 4 nV/rtHz fully hides the spike. The chosen input load simulates a very low-noise amp output ( $\equiv -123.63$  dBV measured), lower than the original  $-120$  dBV goal. Nevertheless, it is really challenging to find the right shielding.
- The heavy lp slope at 20 kHz comes from the 6th order 0.1 dB Chebyshev measurement lp filter. Together with its hp counterpart at 20 Hz, they form a band-pass filter<sup>8</sup> with nearly brick wall character in  $B_{20k}$ .

Figure 16.20 shows the frequency and phase response. At 20 kHz, the frequency response is 0.02 dB lower than at 1 kHz, at 20 Hz there is no difference. Taking into account the phase shift of the signal generator's un-bal to bal converter, we find a  $-5.0^\circ$  phase at 20 kHz versus  $-0.25^\circ$  at 1 kHz; at 20 Hz the phase becomes  $0.15^\circ$ . The un-bal output shows clipping at  $9.9 \text{ V}_{\text{rms}}/1 \text{ kHz}$ , the bal output at  $19.4 \text{ V}_{\text{rms}}$ .

---

<sup>5</sup>see Chap. 17.

<sup>6</sup>see Fig. 11.2 + OP13 (TSOS-1) or Fig. 22.2 + OP13 (TSOS-2).

<sup>7</sup>See my corresponding remarks on Fig. 12.2.

<sup>8</sup>Full calculation in TSOS-2, Chap. 26, MCD-WS 26.2.



**Table 16.1** PMMA performance results

I/A	B	C	D	E	F	G
2	Item	Unit	Rot	Measured	Calculated	Remarks
3	$e_{n.o.tot}$	nV/rtHz	893.0	874.38	892.564	$R_0 = 0 \Omega$
4	$SN_{o.tot}$	dBV	-78.0	-78.14	-77.981	$R_0 = 0 \Omega$
5	EIN	dBV	-138.0	-138.16	-137.976	$EIN = SN_{o.tot} - G_M$
6	$e_{n.o.1st.tot}$	nV/rtHz			892.35	$R_0 = 0 \Omega$
7	$SN_{o.2nd}$	dBV		-110.23	-111.168	$R_0 = 0 \Omega$
8	$SN_{o.3rd}$	dBV		-113.82	-114.811	$R_0 = 0 \Omega$
9	$e_{n.i.tot}$	pV/rtHz	893.0	874.38	892.564	goal $\leq 1$ nV/rtHz, $R_0 = 0 \Omega$
9	ein	dBV	-181.0	-181.17	-180.978	ein = EIN - 43.006 dB

Noise voltages in column F are average values in  $B_{20k}$

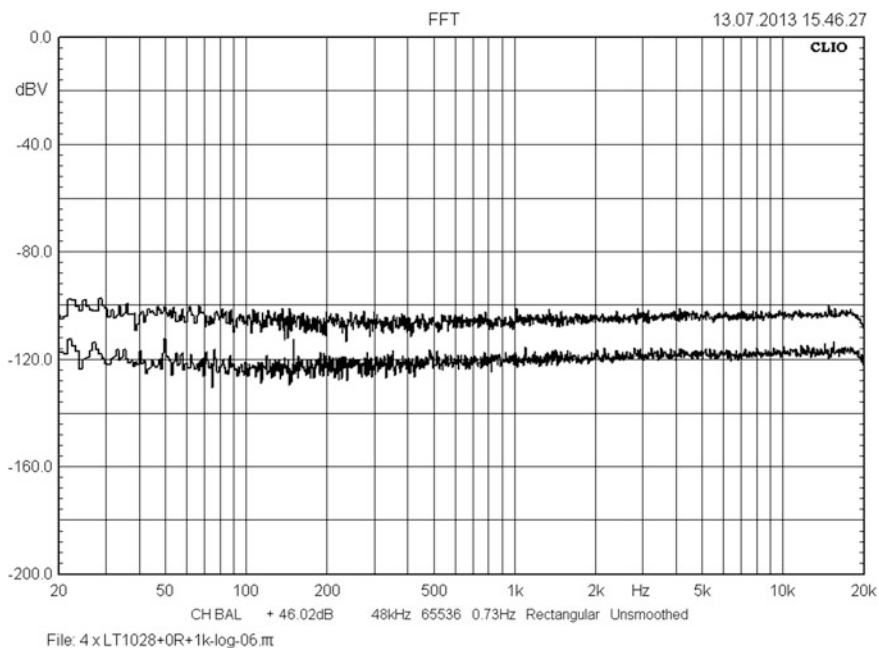


**Fig. 16.18** Output noise voltage density curves, including input  $C_s$  lower trace input shorted, upper trace input loaded with 1 k $\Omega$

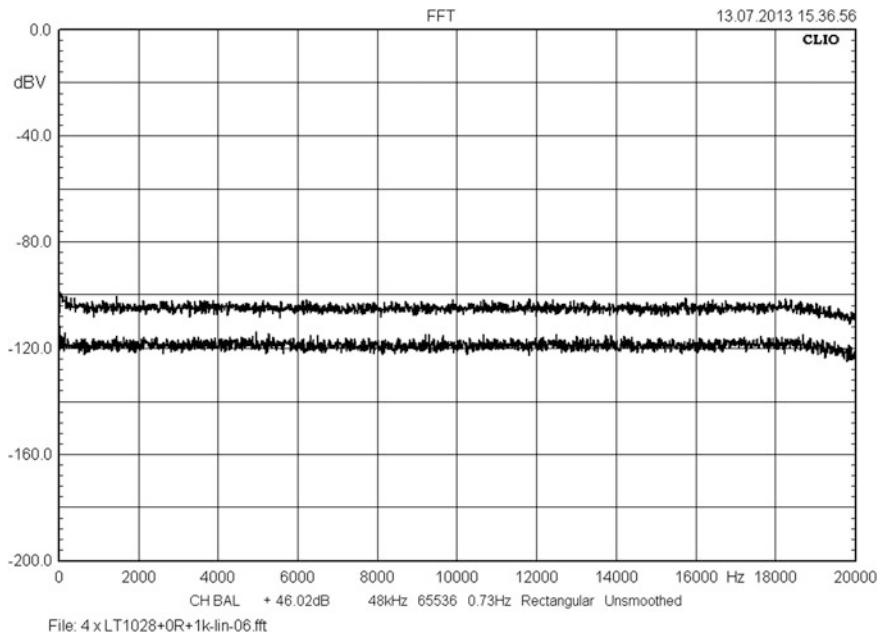


**Fig. 16.19** Same as Fig. 16.18 with linear frequency range

## 16.7 Practical Issues

### 16.7.1 Ground Loop Avoidance and CMRR of a Following Amp

An interruption of the connecting ground or earth or case line between two amplifying balanced devices seems to be one of the most successful measures to avoid ground loops and to increase common-mode rejection.<sup>9</sup> In Chap. 17, the galvanically isolated measurement amplifier PFMA shows how we could fight ground loops, not only for balanced lines, and how we could increase CMRR of the whole measurement set-up by application of an input transformer.

<sup>9</sup>Inter alia: Bill Whitlock on the Jensen Transformers website with

1. 'Balanced Lines in Audio Systems: Fact, Fiction, and Transformers'.
2. 'Interconnection of balanced and un-balanced equipment'.
3. 'A new balanced audio input circuit for maximum common-mode rejection in real-world environments'.

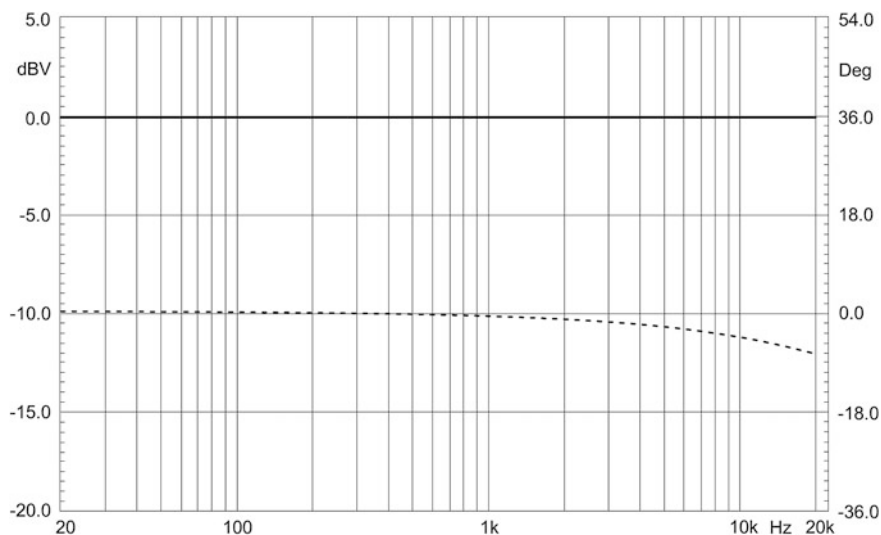


**Fig. 16.20** Frequency (*top*) and phase response (*bottom*) (bal in/bal out)

## 16.7.2 Enclosure

Figures 16.21 and 16.22 demonstrate the final PMMA solution, housed in an Al-box with the following dimensions:  $170 \times 120 \times 55 \text{ mm}^3$ .

In Fig. 16.21, at the right edge of the PCB's top we find the internal PSU ( $\pm 15 \text{ V}$ ), made-up by integrated voltage regulators, fed by a main PSU unit that also could feed all other MAs of my collection by a stable  $\pm 18 \text{ V}$ , as long as there won't be no additional ground loop effect. In this case, a separate  $\pm 18$  to  $\pm 25 \text{ V}$  psu should be used. The op-amp's PSRRs sufficiently suppress any ripple and noise from the supply lines that might enter the op-amp's internal circuits.

On the right PCB of Fig. 16.22 we can see how I packed  $C_x$  and  $C_y$  on the feedback resistors.

## 16.7.3 Room for Improvements

1. I've already mentioned that the MA has a tendency to run very quickly into overload. In such a case switching the psu off-on will lead to a new stable situation. Further efforts are needed to develop a better behaviour.
2. The MA's input stages have no support from a DC servo. Therefore, the DC output level slowly moves up and down, roughly  $\pm 30 \text{ mV}$ .
3. The offset nulling process needs a lot of patience—once performed we will get at least the result of the previous point.

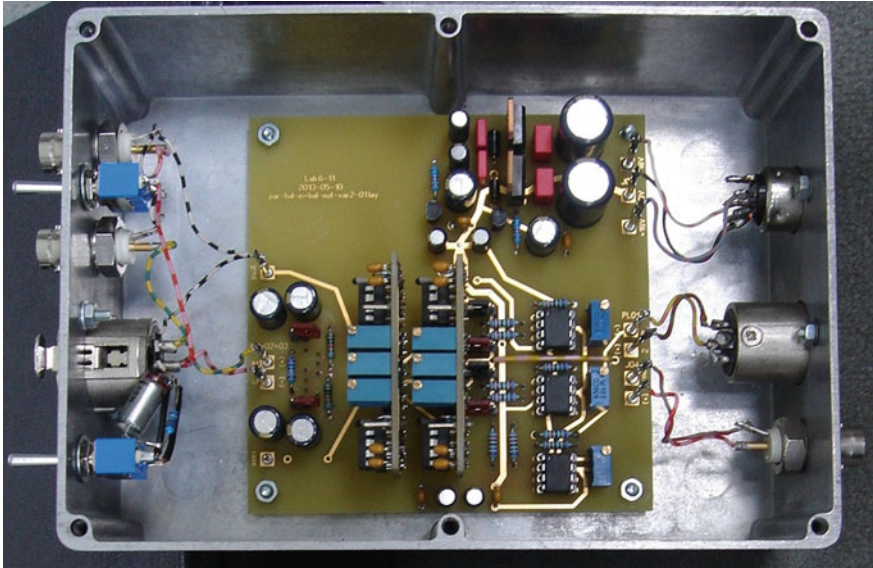


Fig. 16.21 The PMMA in its enclosure

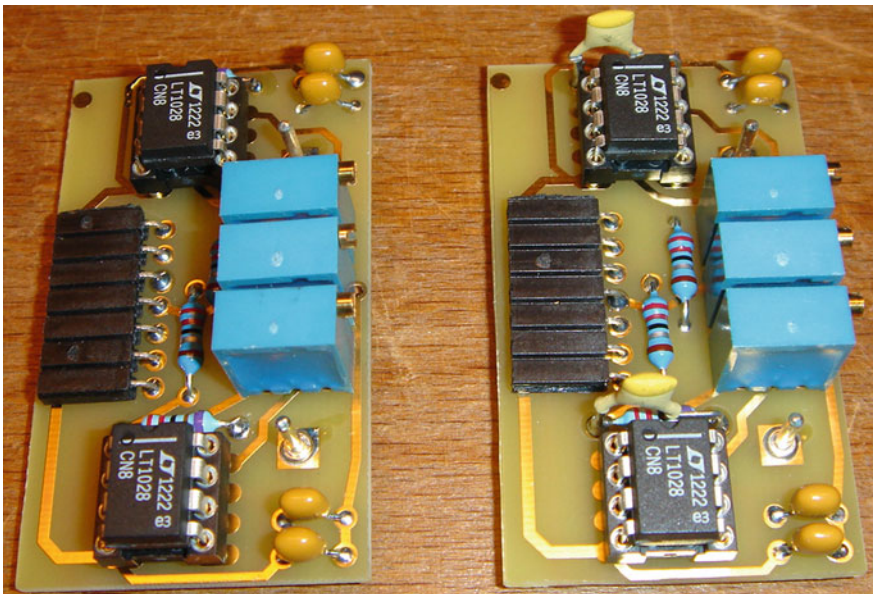


Fig. 16.22 Plug-in input stages of the PMMA

**Table 16.2** Increasing input loads yield increasing differences between measured and calculated output referred SNs

• $SN_o(0 \Omega) = -77.981$ dBV calc. and $-78.14$ dBV measured; $D = -0.16$ dB
• $SN_o(1 \text{ k}\Omega) = -64.570$ dBV calc. and $-63.63$ dBV measured; $D = 0.94$ dB
• $SN_o(2 \text{ k}\Omega) = -61.65$ dBV calc. and $-59.72$ dBV measured; $D = 1.94$ dB

4. Strong shielding of the MA is essential. The chosen AI boxes work quite well in a rather hum-free environment. This is not the case everywhere, especially if the DUT itself produces heavy vagabonding hum interferences, like eg valve driven (power) amps. The MA's balanced input allows rather long lines between the DUT and the MA. The MA could thus be placed a distance away—2 m make no problem.
5. Increasing values of input load resistances lead to increasing differences between the calculated and measured noise production of the MA, the output referred SNs become eg with  $R_{in,rel} = 0 \Omega$  or 1 or 2 k $\Omega$  the values shown in Table 16.2).

My interpretation after having checked the data sheet: at the (+) and (–) inputs of each LT1028 the growing imbalance of the source resistances forces its bias current cancellation mechanism to produce additional noise voltage. It has less common-mode behaviour than it would have in the matched case. Therefore, the op-amp's CMRR becomes increasingly less effective. Hence, this additional un-correlated noise voltage sums-up with the data-sheet spec based one. We can study this effect on the two corresponding LT data sheet graphs.

Unfortunately, there is no indication on how to calculate it. Only interpolation of the above shown Ds will lead to calculation results close to the measured ones. MCD-WS 18.2, Sect. 16.4 gives a rather simple derivation of D as function of the input load; it will ease any required interpolation.

---

## 16.8 Recommendations

In a lowest-noise measurement environment, the PMMA works quite well, as long as we consider the above-described points. The following paragraphs show how we can use it in general.

We can work through the measurement process and the clarification of potential measurement amp impact according to the following example guidelines:

### 16.8.1 DUT Output Resistance $\leq 10 \Omega$

1. Generally, the determination of the whole measurement arrangement's EIN works by shorting the input, by measurement of the output SN, and by subtraction of the measurement arrangement's gain in dB; here, the PMMA's measured input referred rms noise voltage is:  $EIN_m = -138.16 \text{ dBV}$
2. Determination of the DUT's output resistance; here, we assume a very low one:  $R_o \leq 10 \Omega$
3. We measure eg a DUT output referred  $SN_{o,m}$ :  $SN_{o,m} = -130.64 \text{ dBV}$
4. We calculate the difference B:  $B = SN_{o,m} - EIN = 7.52 \text{ dB}$
5. Fig. 16.2a shows the impact  $W_e(B)$ :  $W_e(B) = 0.71 \text{ dB}$
6. The DUT's real output  $SN_{o,r}$  thus becomes:  $SN_{o,r} = SN_{o,m} - W_e(B) = -131.35 \text{ dBV}$

### 16.8.2 DUT Output Resistance $> 10 \Omega$

Depending on the amount of PMMA input noise current  $i_{n,i}$  any  $R_o > 10 \Omega$  will add more or less significant portions of noise voltage, thus, worsening the measurement amp's original EIN to  $EIN_{corr}$  by an equivalent amount in dB, hence, we'll get  $|EIN_{corr}| < |EIN|$ .

Let's check a worst case example with a DUT's total output resistance  $R_o = 2247 \Omega$ ,  $i_{n,i} = 1 \text{ pA}/\sqrt{\text{rtHz}}$ ,  $R_{in,eff} = R_o || R_{in} = 2 \text{ k}\Omega$ :

1. Determination of  $EIN_{corr}$ : by worsening the original EIN ( $-138.16 \text{ dBV}$ ) the PMMA's total input load  $R_{in,eff}$  and input current and voltage noise effect on  $R_o$  lead to an additional input noise voltage density  $e_{n,i,add}$ . With it we can calculate  $EIN_{corr}$  as follows:

$$e_{n,i,add} = \sqrt{(i_{n,i} R_{in,eff})^2 + e_{n,Rin,eff}^2} \quad (16.26)$$

$$\Rightarrow EIN_{add} = -164.757 \text{ dBV} + 43.006 \text{ dB}$$

$$EIN_{corr} = 20 \log \left( \sqrt{10 \frac{EIN_{add}}{10} + 10 \frac{EIN}{10}} \right) \quad (16.27)$$

$$= -121.697 \text{ dBV}$$

$$\Rightarrow e_{n,i,corr} = 5.819 \text{ nV}/\sqrt{\text{Hz}}$$

Crosscheck for (16.27): See Fig. 18.9 on the MCD-WS 18.2. It shows the PMMA's output referred  $SN_{o,tot}$  versus the total input load  $R_o$ . We can pick

$SN_{o,tot}$  for  $R_0 = 2 \text{ k}\Omega$  and we'll get  $-61.693 \text{ dBV}$ . To get  $EIN_{corr}$  we have to subtract the PMMA gain:

$$\begin{aligned} EIN_{corr} &= -61.693 \text{ dBV} - 60 \text{ dB} \\ &= -121.693 \text{ dBV}. \end{aligned}$$

2. We measure eg a DUT output referred  $SN_{o,m}$ :  $SN_{o,m} = -104.38 \text{ dBV}$

3. We calculate  $G_{loss1,e}$ :

$$\begin{aligned} G_{loss1,e} &= 20 \log[R_{in}/(R_{in} + R_o)] \\ &= 20 \log(0.89) \\ &= -1.012 \text{ dB} \end{aligned}$$

4. Interpolation term according to Table 2:  $D = 2.0 \text{ dB}$

5. We obtain  $SN_{o,r}$ :

$$\begin{aligned} SN_{o,r} &= SN_{o,m} + |G_{loss1,e}| - D \\ &= -105.37 \text{ dBV} \end{aligned}$$

6. We calculate the difference B:

$$\begin{aligned} B &= SN_{o,r} - EIN_{corr} \\ &= 16.32 \text{ dB} \end{aligned}$$

7. Fig. 16.2a shows the impact  $W_e(B)$ :  $W_e(B) = 0.1 \text{ dB}$

8. Without PMMA impact the DUT's real output  $SN_{o,dut}$  thus would become:

$$\begin{aligned} SN_{o,dut} &= SN_{o,r} - W_e(B) \\ &= -105.47 \text{ dBV} \end{aligned}$$

### 16.8.3 Summary of Recommendations

Now, we can sum-up all the above given findings into the following main recommendations:

- As long as the DUT output resistance is very low ( $\leq 10 \Omega$ ) the PMMA measures output referred SNs of DUTs up to  $-121.8 \text{ dBV}$  ( $-129.0 \text{ dBV}$ ) in  $B_{20k}$  with an error of  $\leq 0.1 \text{ dB}$  ( $\leq 0.5 \text{ dB}$ ) only.
- To keep the maximum allowed  $0.1 \text{ dB}$  ( $0.5 \text{ dB}$ ) border line and by usage of LT1028 op-amp types any DUT output resistances from  $0 \Omega$  up to  $2.25 \text{ k}\Omega$  (equals  $2 \text{ k}\Omega$  with the paralleled PMMA input resistances) will shift the minimal output referred SNs from measured  $-121.8 \text{ dBV}$  ( $-129.0 \text{ dBV}$ ) to  $-105.5 \text{ dBV}$  ( $-112.7 \text{ dBV}$ ) rounded.

---

## 16.9 Final Notes

- The LT1028 works quite well in an input load environment with nearly equal loads at both inputs. With RGs  $\leq 10 \Omega$  DUT output resistances with values of  $RG \pm 20 - 50 \%$  do not produce much harm. All cases of larger DUT output resistances require additional calculation efforts, making the calculation results less precise.

- Although handicapped by a doubled input noise current, a future project will check the AD797 usability.
- Further CMRR improvement could come from Bruno Putzey’s “optimal input biasing”, given in Fig. 20 of his very interesting article in LA Vol. 5. I have to check this too.
- The nasty DC drift at the outputs (TP1–TP4) of the input stages should be controlled by a well-working DC servo. Maybe it could also be the right measure to suppress the tendency of these stages of sometimes running into overload after an input load change. Then, I guess these measures won’t prevent the MA from getting the RMMA status (Rich Man’s MA).
- Occasionally, in the above given equations we find the term 43.006 dB or its rounded version 43 dB. It is nothing else but  $\sqrt{B_{20k}}$  expressed in [dB] =  $20 \log(\sqrt{19,980 \text{ Hz}})$ , and it stands for the difference between the rms voltage of a white noise signal and its equivalent noise voltage density in  $B_{20k}$ .
- Of course, the chosen expression “worsening figure  $W_e(B)$ ” is nothing else but another approach to express the noise figure  $NF_e$  [dB] of the PMMA. However, in this chapter I use it the chosen way to better underline its influential and negative effect in the measurement process of tiny noise signals.
- Finally, here comes the calculation to find the real A-weighted output referred  $SN_{o,a,NAD,r} = -124.2 \text{ dBV(A)} \pm 0.5 \text{ dB}$  of the NAD M51, without AP analyzer impact, however, in the S-AES17 filter given equivalent noise bandwidth of  $ENB = B_{20k}$ , rounded to one digit after the decimal point:

$$\begin{aligned}
 \rightarrow SN_{o,a,NAD,m} &= -122.0 \text{ dBV(A)} && = \text{measured A-weighted SN of the NAD M51} \\
 &+ 2.05 \text{ dB} && = \text{A = A-weighting based improvement} \\
 \Rightarrow SN_{o,NAD,m} &= -119.95 \text{ dBV} && = \text{output referred SN excl. 1/f-noise,} \\
 &- 0.5 \text{ dB} && = W_{F_e}(f_c) = \text{worsening figure based on the} \\
 &&& \text{1/f-noise corner frequency } f_c = 350 \text{ Hz} \\
 &&& \text{(see LA Vol. 4, p. 19, Fig. 5} \\
 &&& \text{or TSOS-2, Fig. 7.6a in [dB]!)} \\
 \Rightarrow SN_{o,NAD,m,wn} &= -120.45 \text{ dBV} && = \text{output referred SN excl. 1/f-noise,} \\
 &&& \text{hence, theoretically white noise only} \\
 \\
 \rightarrow SN_{i,AP} &= -122.4 \text{ dBV} && = \text{AP SYS 2722 bal. i/p referred} \\
 &&& \text{SN with i/p shorted} \\
 \Rightarrow B &= SN_{o,NAD,m,wn} - SN_{i,AP} \\
 &= -120.45 \text{ dBV} - (-122.4 \text{ dBV}) \\
 &= 1.95 \text{ dB} \\
 \Rightarrow W_e(B) &= 2.2 \text{ dB} && \text{taken from Fig. 16.2b} \\
 \\
 \rightarrow SN_{o,a,NAD,r} &= SN_{o,a,NAD,m} - W_e(B) \\
 &= -122.0 \text{ dBV(A)} - 2.2 \text{ dB} \\
 &= -124.2 \text{ dBV(A)}
 \end{aligned}$$

Note: The AP’s SYS 2722 input referred noise voltage is free of 1/f-noise, hence, if we would calculate B in the A-weighted domain we would create an error that grows for  $f_c > 1 \text{ kHz}$  from appr. 0.5 dB to >5 dB at 20 kHz



---

## 17.1 Intro

The measurement of extremely low noise levels creates problems at many corners of every measurement project. In most cases, the nastiest ones of these come on board with the connections to the CMS. Balanced lines improve things; however, only a galvanically isolated connection helps avoiding ground loops and the penetration of hum interferences into the measurement set-up. Therefore, I strongly recommend the inclusion of a broadband transformer and associated amplification electronic between MA and CMS.

---

## 17.2 Ground Loop Avoidance

For my own measurement purposes, I have developed such an extra measurement amp PFMA around the Jensen Transformers 4:1 type JT-10KB-D. In addition to the galvanic isolation it also offers an outstanding CMRR. The electronic configuration consists of an LT1028C op-amp (gains from transformer input to op-amp output  $\times 5$ —trimmed by P1, or  $\times 50$  with Jmp1 set and trimmed by P3), followed by an un-bal to bal and an un-bal to un-bal converter, each with a gain of 2 (SSM2142 or THAT1646 and OP27 plus a trimmed P2).

Figure 17.1 shows the details. This MA has a flat frequency and phase response in  $B_{20k}$  (see Fig. 17.3) and its input noise voltage density is flat in  $B_{20k}$  (see Fig. 17.2). To keep the input referred SN as good as possible and with its gain of 200 (or 20) OP1 must have outstanding noise voltage and noise current figures. The LT1028C sufficiently fulfils these requirements. The measured PFMA input referred noise production looks as follow: gain  $\times 100$ : 9.641 nV/rtHz (calculated: 10.571 nV/rtHz; gain  $\times 10$ : 10.945 nV/rtHz (calculated 11.647 nV/rtHz). These values are very much smaller than the appr. 900 nV/rtHz of a preceding MA alike the PMMA; hence, there will not be any significant impact on the MA's output noise. Next chapter's MCD-WS 18.3 gives the details.

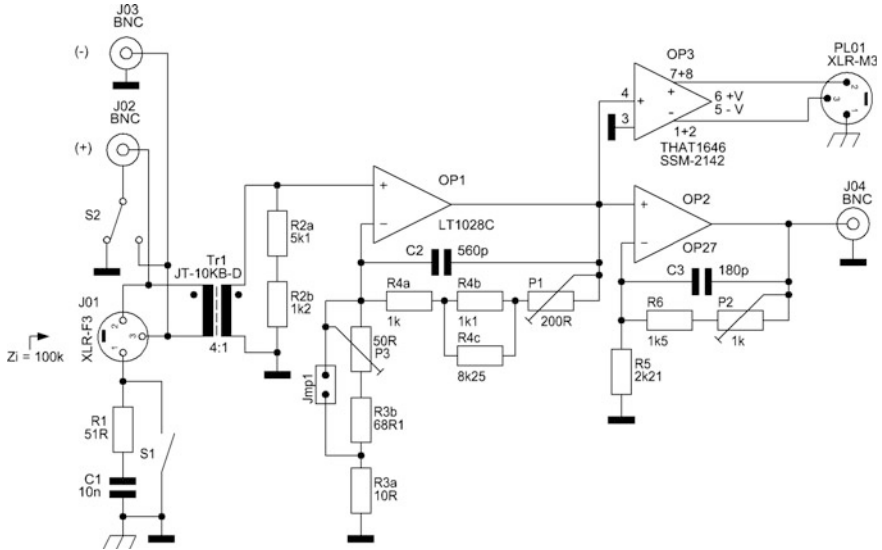


Fig. 17.1 PFMA circuit

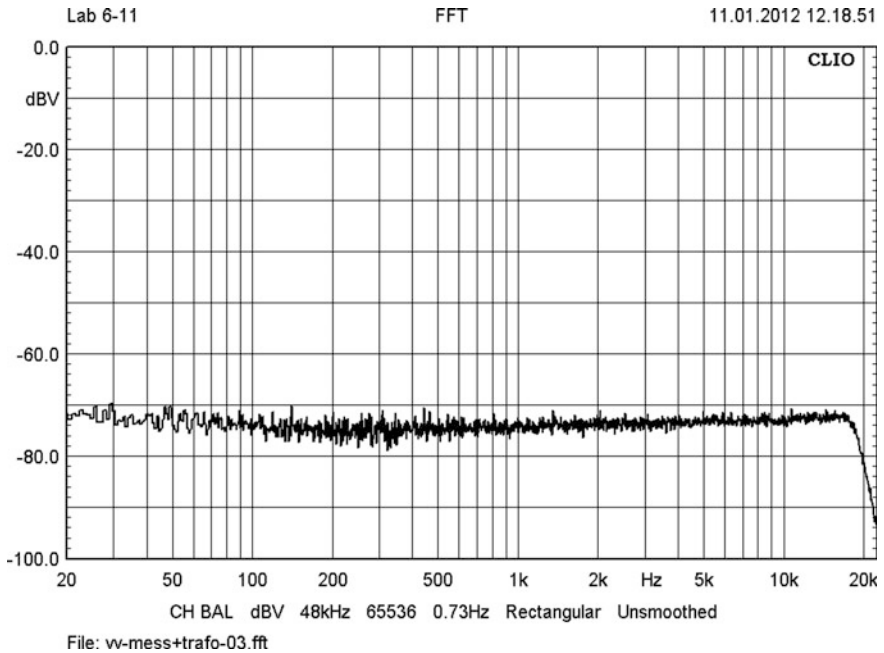


Fig. 17.2 Output noise voltage density of the PFMA, input shorted

The advantage of the MA–PFMA sequence is the fact that the MA can be located very close to the DUT while the PFMA might be located far away, closer to the CMS. The balanced lines and the very high CMRR of the PFMA ensure high immunity against any line induced interference.

### 17.3 Additional PFMA Data

The input XLR socket J01 feeds the input transformer Tr1. The  $tr = 4:1$  relationship of the transformer windings makes  $n = 1/tr$ , hence, 0.25. The input impedance thus becomes approximately  $(R2a + R2b)/(n)^2 = 100\text{ k}\Omega$ . Including the coil resistances,  $Z_i$  increases to a calculated 107 k $\Omega$ .

Referenced to 1 kHz the Fig. 17.3 deviation from a flat F response becomes  $-0.003\text{ dB}$  at 20 Hz and  $-0.003\text{ dB}$  at 20 kHz. We obtain the deviation from a flat P response as follows:  $+2^\circ$  at 20 Hz and  $-13^\circ$  at 20 kHz.

Inputs J02 & J03 ensure direct connection to the transformer input leads. In case of J02 usage we must ground the hot pin of J03, and vice versa. S2 switched into the right position allows an access to the transformer via J02 without any grounding. In this case, J03 must be kept open.

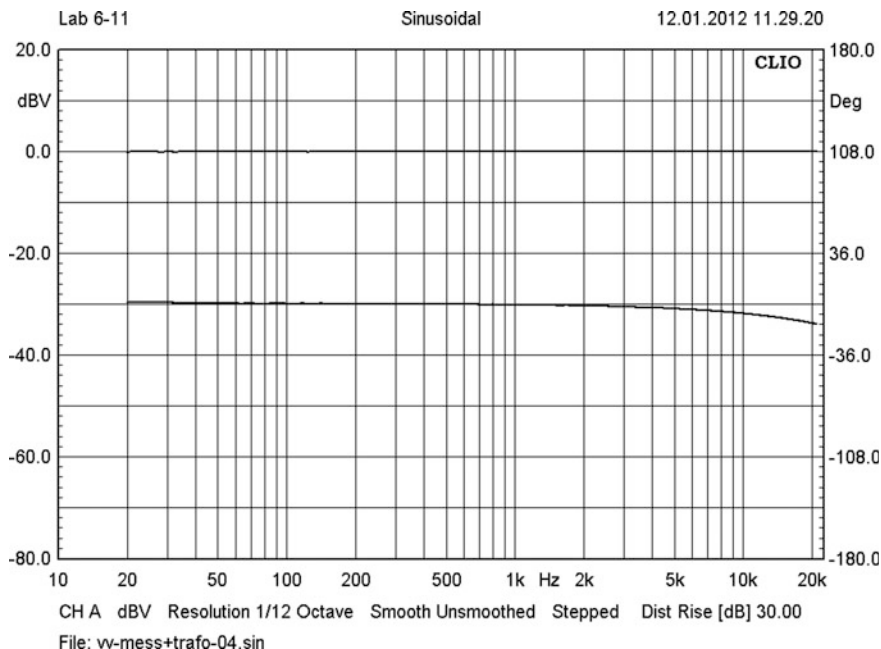


Fig. 17.3 F & P of the PFMA

S1 plays the ground lift, thus, in most cases solving the pin1 problem; based on a Jensen Transformer recommendation, an open S1 and the sequence of R1 and C1 ensure grounding for very high frequencies.

The transformer's CMRR is extremely high; the data sheet claims 120 dB at 60 Hz and 85 dB at 3 kHz.

## 17.4 Gain and SN Calculations

### 17.4.1 Gains

The gain equations of the PFMA are spilt into three different stages: the first gain stage with the transformer Tr1 and its gain  $G_{Tr1}$ , the second one with the LT1028 OP1 and its gain G1, and the third one with the two output gain stages OPs 2 & 3 with equal gains G2. Hence, we obtain the effective gain  $G_{MA}$ —from input to output—as follows:

$$\begin{aligned} G_{MA} &= G_{Tr1}G1G2 \\ &= 100 \text{ or } 10 \end{aligned} \quad (17.1)$$

$$\begin{aligned} tr &= 1 : n \\ &= 4 : 1 \\ &= 1 : 0.25 \end{aligned} \quad (17.2)$$

$$G_{Tr1} = n \quad (17.3)$$

$$\begin{aligned} G1 &= 1 + \frac{R4}{R3a} = \frac{100}{n * 2} = 200 \\ &= 1 + \frac{R4}{R3} = \frac{10}{n * 2} = 20 \end{aligned} \quad (17.4)$$

$$R3 = R3a + R3b + P1 \quad (17.5)$$

$$R4 = R4a + (R4b || R4c) + P2 \quad (17.6)$$

$$\begin{aligned} G2 &= 2 \quad (\text{OP3}) \\ &= 1 + \frac{R6 + P2}{R5} \quad (\text{OP2}) \end{aligned} \quad (17.7)$$

### 17.4.2 Evaluation of Noise Voltages and SNs

The basic situation of the various noise voltage and noise current sources is given in Fig. 17.4. Figure 17.5 shows the circuit that leads to the input load  $R_{i,tot}$  of OP1.

Thus, we'll obtain the effective frequency and  $R0$  dependent input referred noise voltage density  $e_{n,i,MA}(f, R0)$  of the Fig. 17.1 MA as follows:

$$e_{n,i,MA}(f, R0) = \frac{e_{n,o}(f, R0)}{G_{MA}} \tag{17.8}$$

$$e_{n,o}(f, R0) = e_{n,i}(f, R0)G_{amp} \tag{17.9}$$

Here, we need the auxiliary gain  $G_{amp}$ . It becomes:

$$\begin{aligned} G_{amp} &= G1G2 \\ &= 400 \text{ or } 40 \end{aligned} \tag{17.10}$$

The input referred noise voltage density  $e_{n,i1}(f, R0)$  at the input of OP1 in Fig. 17.4 becomes thus:

$$e_{n,i}(f, R0) = \sqrt{e_{n,i1}(f)^2 + i_{n,i1}(f)^2 (RF^2 + R_{i,tot}(R0)^2) + e_{n,RF}^2 + e_{n,Ri,tot}(R0)^2} \tag{17.11}$$

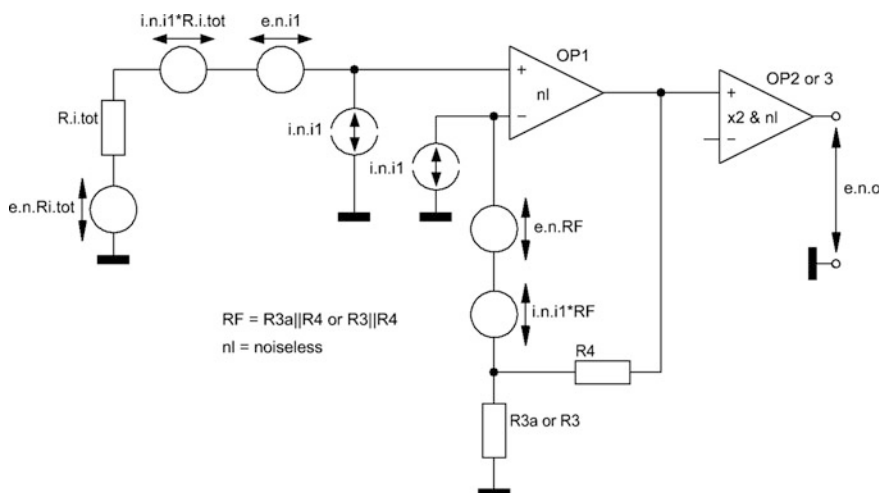


**Fig. 17.4** Noise sources of the PFMA

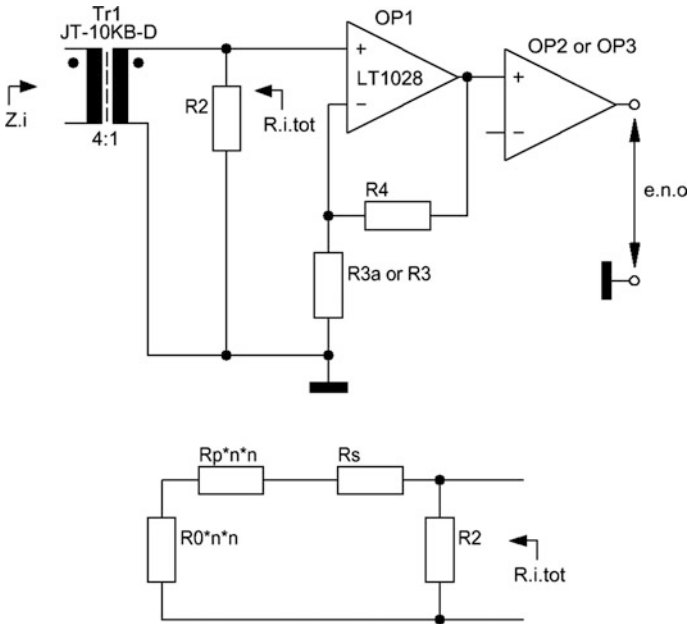
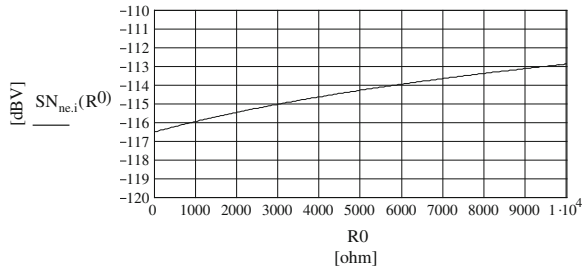


**Fig. 17.5** Evaluation of the OP1 input load

**Fig. 17.6** R<sub>0</sub> dependency of the PFMA's input referred SN



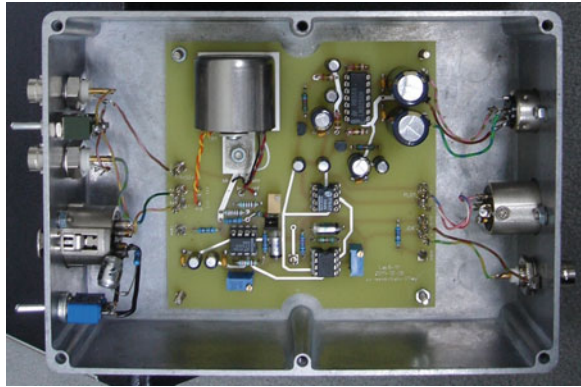
Finally, with Fig. 17.6 showing its R<sub>0</sub> dependency the R<sub>0</sub> dependent input referred SN<sub>ne.i</sub> looks as follows (in [dBV] with v<sub>i.ref</sub> = 1 V<sub>rms</sub>):

$$SN_{ne.i}(R_0) = 20 \log \left( \frac{\sqrt{\frac{1}{B_1} \int_{20\text{Hz}}^{20\text{kHz}} |e_{n.i.MA}|^2 df}}{V_{i.ref}} \right) \quad (17.12)$$

## 17.5 Enclosure

Figure 17.7 demonstrates the final PFMA solution, housed in an Al-box ( $170 \times 120 \times 55 \text{ mm}^3$ ). We find the internal PSU ( $\pm 15 \text{ V}$ ) at the right of the transformer, made-up by integrated voltage regulators, fed by a main PSU unit that also could feed all other MAs of my collection by a stable  $\pm 18 \text{ V}$ , as long as there won't be any additional ground loop effects. In this case, an additional  $\pm 18$  to  $\pm 25 \text{ V}$  PSU should be used. The op-amp's PSRRs sufficiently suppress any ripple and noise from the supply lines that might enter the op-amp's internal circuits.

**Fig. 17.7** PFMA and its enclosure



## Contents

- 18.1 MCD-WS: The UBC
- 18.2 MCD-WS: The PMMA
- 18.3 MCD-WS: The PFMA

**Note 1:** MCD 11 has no built-in unit “rtHz” or  $\sqrt{\text{Hz}}$ . To get  $\sqrt{1\text{Hz}}$  based voltage noise and current noise densities the rms noise voltage and current in a specific frequency range  $B > 1\text{ Hz}$  must be multiplied by  $\sqrt{1\text{Hz}}$  and divided by the root of that specific frequency range  $\sqrt{B}$ !

**Note 2:** MCD 11 offers no “dB” unit. This is available from MCD 13 on!



18.1 MCD-WS: The UBC

Gain and SN calculation of the UBC

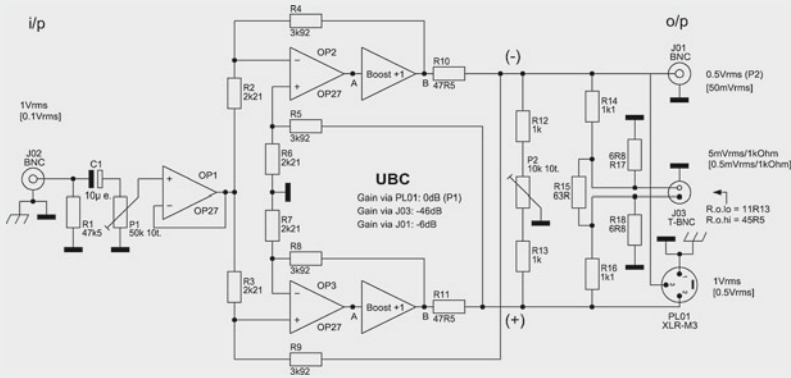


Fig. 18.1 = Fig 15.7

1. Definition of all meaningful constants, components, etc.:

$k := 1.38065 \cdot 10^{-23} \cdot V \cdot A \cdot s \cdot K^{-1}$      $q := 1.6021765 \cdot 10^{-19} \text{ A} \cdot s$      $T := 300 \cdot K$      $V_{i,nom} := 1V$

$B_{20k} := 19980 \cdot \text{Hz}$      $B_1 := 1\text{Hz}$      $h := 1000\text{Hz}$      $V_{o,nom} := 1V$

$f := 10\text{Hz}, 15\text{Hz}, 20 \cdot 10^3\text{Hz}$

$R1 := 47.5 \cdot 10^3 \Omega$      $R2 := 2.21 \cdot 10^3 \Omega$      $R3 := R2$      $R4 := 3.92 \cdot 10^3 \Omega$      $R5 := R4$      $R6 := R2$

$R7 := R2$      $R8 := R4$      $R9 := R4$      $R10 := 47.5 \Omega$      $R11 := R10$

$R12 := 1 \cdot 10^3 \Omega$      $R13 := R12$      $R14 := 1.1 \cdot 10^3 \Omega$      $R15 := 63 \Omega$      $R16 := R14$

$R17 := 6.8 \Omega$      $R18 := R17$

$OP1 = OP27$      $OP2 = OP1$      $OP3 = OP1$      $OP4 = BUF634$      $OP5 = OP4$

$P1 := 50 \cdot 10^3 \Omega$      $P2 := 10 \cdot 10^3 \Omega$      $C1 := 10 \cdot 10^{-6} F$

$R_{L,pl01} := 10 \cdot 10^3 \Omega$      $R_{L,j03} := 1 \cdot 10^3 \Omega$

measured o/p resistance at PL01 :  $R_{o,pl01} := 45.5 \cdot \Omega$

calculated o/p resistance at J03 :  $R_{o,j03} := 2 \cdot \left( \frac{1}{R17} + \frac{1}{0.5 \cdot R15} + \frac{1}{R14 + 0.5 \cdot R_{o,pl01}} \right)^{-1}$   
 $R_{o,j03} = 11.13 \Omega$

18.1 MCD-WS: The UBC

2. Gain and input impedance

$$G_{2nd} := \frac{R4}{R2} \cdot \frac{R4}{R10 + R4} \quad G_{2nd} = 1.75252 \quad G_{1st} := \frac{1}{G_{2nd}} \quad G_{1st} = 0.571$$

via PL01 :

$$G_{p01} := G_{1st} \cdot G_{2nd} \quad G_{p01} = 1$$

$$P1b := P1 \cdot G_{1st} \quad P1b = 28.53 \times 10^3 \Omega \quad P1a := P1 - P1b \quad P1a = 21.47 \times 10^3 \Omega$$

via J03 :

$$G_{j03} := \frac{R_{o,j03}}{R_{o,j03} + R14 + R16} \quad G_{j03} = 5.034 \times 10^{-3}$$

$$G_{j03.e} := 20 \cdot \log(G_{j03}) \quad G_{j03.e} = -45.962 \quad [dB]$$

$$Z_1(f) := \left[ \frac{1}{R1} + \frac{1}{P1 + (2j \cdot \pi \cdot f \cdot C1)^{-1}} \right]^{-1} \quad |Z_1(h)| = 24.359 \times 10^3 \Omega$$

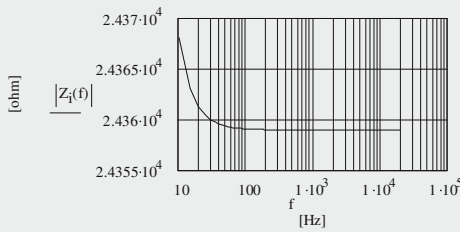


Fig. 18.2  
UBC input impedance

$$\Rightarrow R_i := |Z_1(h)| \quad R_i = 24.359 \times 10^3 \Omega$$

Input load with input shorted:

$$R_{iL} := \left( \frac{1}{P1a} + \frac{1}{P1b} \right)^{-1} \quad R_{iL} = 12.251 \times 10^3 \Omega$$

3. SN calculations

$$RP1 := (R4^{-1} + R2^{-1})^{-1} \quad RP1 = 1.413 \times 10^3 \Omega \quad RP2 := (R5^{-1} + R6^{-1})^{-1} \quad RP2 = 1.413 \times 10^3 \Omega$$

$$e_{n,R4} := \sqrt{4 \cdot k \cdot T \cdot B1 \cdot R4} \quad e_{n,R4} = 8.059 \times 10^{-9} V \quad e_{n,R2} := \sqrt{4 \cdot k \cdot T \cdot B1 \cdot R7} \quad e_{n,R2} = 6.051 \times 10^{-9} V$$

$$e_{n,RP1} := \sqrt{4 \cdot k \cdot T \cdot B1 \cdot RP1} \quad e_{n,RP2} := e_{n,RP1} \quad e_{n,RP1} = 4.839 \times 10^{-9} V$$

$$e_{n,i1} := 3.0 \cdot 10^{-9} V \quad e_{n,i2} := e_{n,i1} \quad e_{n,i3} := e_{n,i1} \quad e_{n,i4} := 4 \cdot 10^{-9} V \quad e_{n,i5} := e_{n,i4}$$

18.1 MCD-WS: The UBC

$$\begin{aligned}
 i_{n,i1} &:= 0.4 \cdot 10^{-12} \text{ A} & i_{n,i2} &:= i_{n,i1} & i_{n,i3} &:= i_{n,i1} & i_{n,i4} &:= 1 \cdot 10^{-12} \text{ A} & i_{n,i5} &:= i_{n,i4} \\
 f_{c,e1} &:= 2.7 \text{ Hz} & f_{c,i1} &:= 120 \text{ Hz} \\
 e_{n,i1}(f) &:= e_{n,i1} \cdot \sqrt{\frac{f_{c,e1}}{f} + 1} & e_{n,i2}(f) &:= e_{n,i1}(f) & e_{n,i3}(f) &:= e_{n,i1}(f) \\
 i_{n,i1}(f) &:= i_{n,i1} \cdot \sqrt{\frac{f_{c,i1}}{f} + 1} & i_{n,i2}(f) &:= i_{n,i1}(f) & i_{n,i3}(f) &:= i_{n,i1}(f) \\
 e_{n,RiL} &:= \sqrt{4 \cdot k \cdot T \cdot B_1 \cdot R_{iL}} & e_{n,RiL} &= 14.247 \times 10^{-9} \text{ V}
 \end{aligned}$$

3.1 Output referred SN via PL01 :

$$e_{n,o,1st}(f) := \sqrt{e_{n,RiL}^2 + e_{n,i1}(f)^2 + i_{n,i1}(f)^2 \cdot R_{iL}^2} \qquad e_{n,o,1st}(h) = 15.456 \times 10^{-9} \text{ V}$$

By ignoring the noise production of the stages around OPs 2 & 3 & Boosters 1 & 2 we'll obtain the noise voltage at the PL01 output as follows:

$$e_{n,o,pl01}(f) := e_{n,o,1st}(f) \cdot G_{2nd} \qquad e_{n,o,pl01}(h) = 27.087 \times 10^{-9} \text{ V}$$

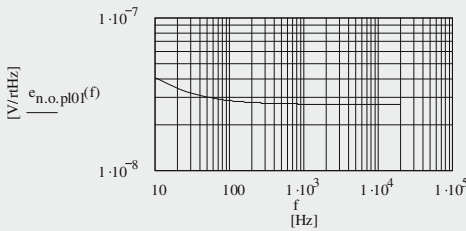


Fig. 18.3  
Output noise voltage density at PL01

$$SN_{ne.o,pl01} := 20 \cdot \log \left[ \frac{\int_{20\text{Hz}}^{20000\text{Hz}} \left( |e_{n,o,pl01}(f)| \right)^2 df}{v_{o,nom}} \right] \qquad SN_{ne.o,pl01} = -108.374 \quad [\text{dBV}]$$

3.2 Output referred SN via J03 :

$$e_{n,o,j03}(f) := e_{n,o,pl01}(f) \cdot G_{j03} \qquad e_{n,o,j03}(h) = 136.344 \times 10^{-12} \text{ V}$$

$$SN_{ne.o,j03} := 20 \cdot \log \left[ \frac{\int_{20\text{Hz}}^{20000\text{Hz}} \left( |e_{n,o,j03}(f)| \right)^2 df}{v_{o,nom}} \right] \qquad SN_{ne.o,j03} = -154.336 \quad [\text{dBV}]$$

## 18.1 MCD-WS: The UBC

Page 4

## 4. Output referred SN calculated and measured with PMMA from MCD-WS 18.2 (lt) :

## 4.1 SN via PL01 :

$$\begin{aligned} \text{From MCD-WS 18.2: } e_{n,iL,avg} &:= 892.564 \cdot 10^{-12} \text{V} & i_{n,iL,avg} &:= 1.042 \cdot 10^{-12} \text{A} & R_{iL} &:= 18.182 \cdot 10^3 \Omega \\ SN_{i,PMMA,m} &:= -138.16 & [\text{dBV}] \\ G_{It} &:= 1000 & G_{It,e} &:= 20 \cdot \log(G_{It}) & G_{It,e} &:= 60 & [\text{dB}] \\ \Rightarrow \\ R_{iL,lt1} &:= \left( R_{iL}^{-1} + R_{o,p01}^{-1} \right)^{-1} & R_{iL,lt1} &:= 45.386 \Omega \\ e_{n,RiL,lt1} &:= \sqrt{4 \cdot k \cdot T \cdot B_1 \cdot R_{iL,lt1}} & e_{n,RiL,lt1} &:= 867.152 \times 10^{-12} \text{V} \\ e_{n,o,lt1}(f) &:= G_{It} \sqrt{\left( e_{n,o,p01}(f)^2 + e_{n,iL,avg}^2 + i_{n,iL,avg}^2 \cdot R_{iL,lt1}^2 + e_{n,RiL,lt1}^2 \right)} & e_{n,o,lt1}(h) &:= 27.115 \times 10^{-6} \text{V} \\ e_{N,o,lt1} &:= \sqrt{\frac{1}{B_1} \int_{20\text{Hz}}^{2000\text{Hz}} \left( |e_{n,o,lt1}(f)| \right)^2 df} & e_{N,o,lt1} &:= 3.817 \times 10^{-3} \text{V} \\ SN_{ne,o,lt1} &:= 20 \cdot \log\left( \frac{e_{N,o,lt1}}{v_{o,nom}} \right) & SN_{ne,o,lt1} &:= -48.364 & [\text{dBV}] \\ SN_{ne,o,p01,lt1} &:= SN_{ne,o,lt1} - G_{It,e} & SN_{ne,o,p01,lt1} &:= -108.364 & [\text{dBV}] \\ \text{measured: } SN_{ne,o,p01,lt1,m} &:= -107.89 & [\text{dBV}] \\ B &:= SN_{ne,o,p01,lt1,m} - SN_{i,PMMA,m} & B &:= 30.27 & [\text{dB}] \Rightarrow & W_e(B) &:= 0.004 & [\text{dB}] \\ SN_{ne,o,p01,lt1,re} &:= SN_{ne,o,p01,lt1,m} - W_e(B) & SN_{ne,o,p01,lt1,re} &:= -107.894 & [\text{dBV}] \end{aligned}$$

## 4.2 SN via J03 :

$$\begin{aligned} R_{iL,lt2} &:= \left( \frac{1}{R_{o,j03}} + \frac{1}{R_{iL}} \right)^{-1} & R_{iL,lt2} &:= 11.123 \Omega \\ e_{n,RiL,lt2} &:= \sqrt{4 \cdot k \cdot T \cdot B_1 \cdot R_{iL,lt2}} & e_{n,RiL,lt2} &:= 429.285 \times 10^{-12} \text{V} \\ e_{n,iL,lt2}(f) &:= \sqrt{e_{n,o,j03}(f)^2 + e_{n,iL,avg}^2 + i_{n,iL,avg}^2 \cdot R_{iL,lt2}^2 + e_{n,RiL,lt2}^2} & e_{n,iL,lt2}(h) &:= 999.84 \times 10^{-12} \text{V} \end{aligned}$$

18.1 MCD-WS: The UBC

$$e_{n.o.lf2}(f) := G_{tr} \cdot e_{n.i.lf2}(f) \qquad e_{n.o.lf2}(h) = 999.84 \times 10^{-9} \text{ V}$$

$$e_{N.o.lf2} := \sqrt{\frac{1}{B_1} \int_{20\text{Hz}}^{2000\text{Hz}} (|e_{n.o.lf2}(f)|)^2 df} \qquad e_{N.o.lf2} = 141.318 \times 10^{-6} \text{ V}$$

$$SN_{ne.o.lf2} := 20 \cdot \log\left(\frac{e_{N.o.lf2}}{V_{o.nom}}\right) \qquad SN_{ne.o.lf2} = -76.996 \quad [\text{dBV}]$$

$$SN_{ne.o.j03.lf2} := SN_{ne.o.lf2} - G_{lf.e} \qquad SN_{ne.o.j03.lf2} = -136.996 \quad [\text{dBV}]$$

measured:  $SN_{ne.o.j03.lf2.m} := -136.02 \quad [\text{dBV}]$

No correction because B becomes negative:

$$B := SN_{ne.o.j03} - SN_{i.PMMA.m} \qquad B = -16.176 \quad [\text{dB}]$$

5. Output referred SN calculated and measured with PFMA from MCD-WS 18.3 (tr) :

5.1 SN via PL01 :

From MCD-WS 18.3:  $e_{n.i.tr.avg} := 10.571 \cdot 10^{-9} \text{ V}$      $i_{n.i.tr.avg} := 260.521 \cdot 10^{-15} \text{ A}$      $R_{i.tr} := 106.9 \cdot 10^3 \Omega$

$$SN_{i.PFMA.m} := -117.30 \quad [\text{dBV}]$$

$$G_{tr} := 100 \qquad G_{tr.e} := 20 \cdot \log(G_{tr}) \qquad G_{tr.e} = 40 \quad [\text{dB}]$$

=>

$$R_{iL.tr1} := (R_{i.tr}^{-1} + R_{o.pl01}^{-1})^{-1} \qquad R_{iL.tr1} = 45.481 \Omega$$

$$e_{n.RiL.tr1} := \sqrt{4 \cdot k \cdot T \cdot B_1 \cdot R_{iL.tr1}} \qquad e_{n.RiL.tr1} = 867.152 \times 10^{-12} \text{ V}$$

$$e_{n.o.tr1}(f) := G_{tr} \cdot \sqrt{(e_{n.o.pl01}(f))^2 + e_{n.i.tr.avg}^2 + i_{n.i.tr.avg}^2 \cdot R_{iL.tr1}^2 + e_{n.RiL.tr1}^2} \qquad e_{n.o.tr1}(h) = 2.909 \times 10^{-6} \text{ V}$$

$$e_{N.o.tr1} := \sqrt{\frac{1}{B_1} \int_{20\text{Hz}}^{2000\text{Hz}} (|e_{n.o.tr1}(f)|)^2 df} \qquad e_{N.o.tr1} = 409.756 \times 10^{-6} \text{ V}$$

$$SN_{ne.o.tr1} := 20 \cdot \log\left(\frac{e_{N.o.tr1}}{V_{o.nom}}\right) \qquad SN_{ne.o.tr1} = -67.749 \quad [\text{dBV}]$$

18.1 MCD-WS: The UBC

$$SN_{ne.o.p01.tr1} := SN_{ne.o.tr1} - G_{tr.e} \qquad SN_{ne.o.p01.tr1} = -107.749 \quad [dBV]$$

measured:  $SN_{ne.o.p01.tr1.m} := -107.31 \quad [dBV]$

$$B := SN_{ne.o.p01.tr1.m} - SN_{i.PFMA.m} \quad B = 9.99 \quad [dB] \Rightarrow W_e(B) := 0.41 \quad [dB]$$

$$SN_{ne.o.p01.tr1.re} := SN_{ne.o.p01.tr1.m} - W_e(B) \qquad SN_{ne.o.p01.tr1.re} = -107.72 \quad [dBV]$$

5.2 SN via J03 :

$$R_{iL.tr2} := \left( \frac{1}{R_{o.j03}} + \frac{1}{R_{i.tr}} \right)^{-1} \qquad R_{iL.tr2} = 11.129 \Omega$$

$$e_{n.RiL.tr2} := \sqrt{4 \cdot k \cdot T \cdot B_1 \cdot R_{iL.tr2}}$$

$$e_{n.i.tr2(f)} := \sqrt{e_{n.o.p01(f)}^2 \cdot G_{j03}^2 + e_{n.i.tr.avg}^2 + i_{n.i.tr.avg}^2 \cdot R_{iL.tr2}^2 + e_{n.RiL.tr2}^2} \qquad e_{n.i.tr2(h)} = 10.581 \times 10^{-9} V$$

$$e_{n.o.tr2(f)} := G_{tr} \cdot e_{n.i.tr2(f)} \qquad e_{n.o.tr2(h)} = 1.058 \times 10^{-6} V$$

$$e_{N.o.tr2} := \sqrt{\frac{1}{B_1} \cdot \int_{20Hz}^{2000Hz} (|e_{n.o.tr2(f)}|)^2 df} \qquad e_{N.o.tr2} = 149.557 \times 10^{-6} V$$

$$SN_{ne.o.tr2} := 20 \cdot \log \left( \frac{e_{N.o.tr2}}{V_{o.nom}} \right) \qquad SN_{ne.o.tr2} = -76.504 \quad [dBV]$$

$$SN_{ne.o.j03.tr2} := SN_{ne.o.tr2} - G_{tr.e} \qquad SN_{ne.o.j03.tr2} = -116.504 \quad [dBV]$$

measured:  $SN_{ne.o.j03.tr2.m} := -116.82 \quad [dBV]$

No correction because B becomes negative:

$$B := SN_{ne.o.j03} - SN_{i.PFMA.m} \qquad B = -37.036 \quad [dB]$$

18.2 MCD-WS: The PMMA

The Very Low-Noise Balanced Measurement Amp PMMA

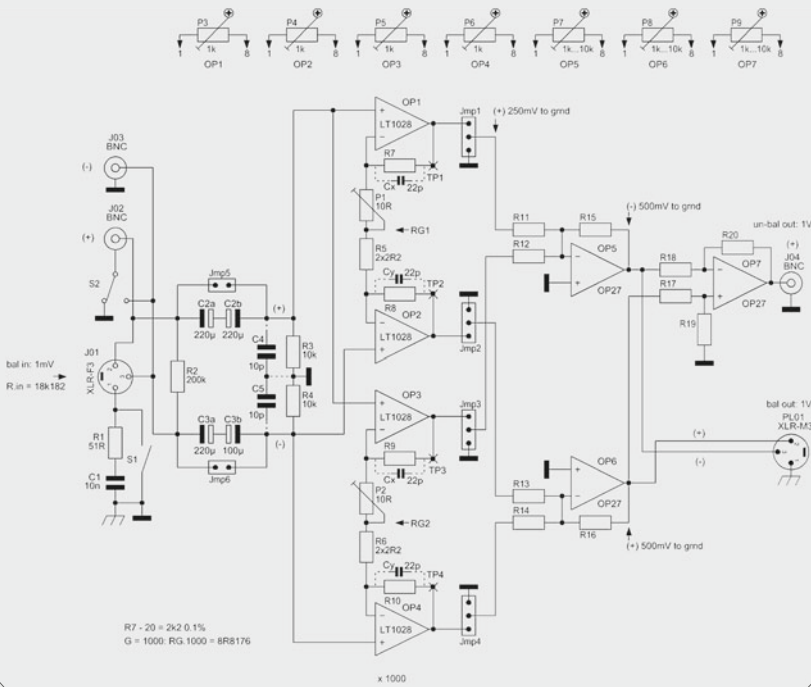


Fig. 18.4 = Fig. 16.15

1. Components :

- OP1 = LT1028C    OP2 = OP3 = OP4 = OP1    OP5 = OP27G    OP6 = OP7 = OP5
- $R0 = R_{o,tot} = R_{o1} + R_{o2} + R_{out1} + R_{out2}$      $R0 := 0\Omega, 10\Omega \dots 2000\Omega$
- $R1 := 51\Omega$      $R2 := 200 \cdot 10^3\Omega$      $R3 := 10 \cdot 10^3\Omega$      $R4 := R3$      $R7 := 2.2 \cdot 10^3\Omega$      $R8 := R7$      $R9 := R7$
- $R_{in,tot} := \frac{R2 \cdot 2 \cdot R3}{R2 + 2 \cdot R3}$      $R_{in,tot} = 18.182 \times 10^3\Omega$      $R7 \dots R20: 0.1\%$      $R := R7$
- The real input load:     $R_{in,rc}(R0) := \frac{R_{in,tot} \cdot R0}{R_{in,tot} + R0}$      $R_{in,rc}(2.247 \cdot 10^3\Omega) = 1999.849\Omega$
- $R10 := R7$      $R11 := 2.2 \cdot 10^3\Omega$      $R12 := R11$      $R13 := R11$      $R14 := R11$      $R15 := R11$      $R16 := R11$
- $R17 := R11$      $R18 := R11$      $R19 := R11$      $R20 := R11$      $R21 := 10\Omega$      $C2 = C3 = 220 \cdot 10^{-6}F$

18.2 MCD-WS: The PMMA

2. Gain :

Note: The complete derivation of the gain equations is shown in 6.!

$$G_M := -1000$$

$$V_{o.ref} := 1 \cdot V$$

Memo for further calculations:  $RG_1 = R_5 + P_1$        $RG_2 = R_6 + P_2$

With  $RG_1 = RG_2 = RG_M$  and equal  $R_s$   $R_7 \dots R_{16}$  and  $R = R_7$  we'll get:

$$G_M = -2 \cdot \left( 1 + \frac{2 \cdot R}{RG_M} \right) = -(G_A + G_B)$$

$$RG_M = \frac{-4 \cdot R}{G_M + 2} = \frac{2 \cdot R}{G_A - 1}$$

$$RG_1 := -4 \cdot \frac{R}{G_M + 2}$$

$$G_A := \left( 1 + \frac{2 \cdot R}{RG_1} \right)$$

$$G_A = 500$$

$$RG_1 = 8.818 \Omega$$

$$RG_2 := -4 \cdot \frac{R}{G_M + 2}$$

$$G_B := \left( 1 + \frac{2 \cdot R}{RG_2} \right)$$

$$G_B = 500$$

$$RG_2 = 8.818 \Omega$$

$$G_{2nd} := -1$$

$$\Rightarrow G_{tot} := (G_A + G_B) \cdot G_{2nd}$$

$$G_{tot} = -1000$$

$$RG_M := RG_1$$

3. Noise and SN :

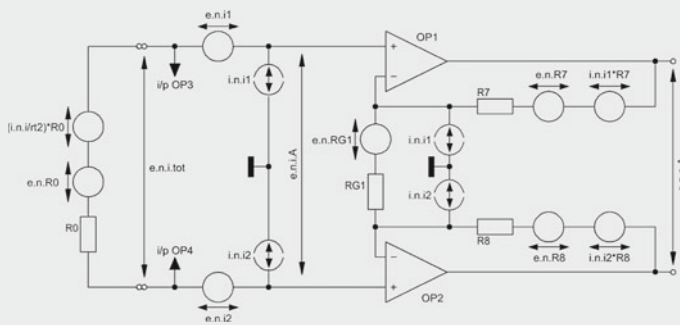


Fig. 18.5 = Fig. 16.12



18.2 MCD-WS: The PMMA

3.1 Noise relevant data :

$$k := 1.38065 \cdot 10^{-23} \text{V} \cdot \text{A} \cdot \text{s} \cdot \text{K}^{-1} \quad T := 300\text{K} \quad B_1 := 1\text{Hz} \quad B_{20k} := 19980\text{Hz} \quad h := 1000\text{Hz}$$

$$f := 10\text{Hz}, 15\text{Hz}, 20 \cdot 10^3 \text{Hz}$$

$$e_{n,i1} := 0.85 \cdot 10^{-9} \text{V} \quad e_{n,i2} := e_{n,i1} \quad e_{n,i3} := e_{n,i1} \quad e_{n,i4} := e_{n,i1} \quad e_{n,i5} := 3.0 \cdot 10^{-9} \text{V} \quad e_{n,i6} := e_{n,i5}$$

$$i_{n,i1} := 1 \cdot 10^{-12} \text{A} \quad i_{n,i2} := i_{n,i1} \quad i_{n,i3} := 1 \cdot 10^{-12} \text{A} \quad i_{n,i4} := i_{n,i1} \quad i_{n,i5} := 0.4 \cdot 10^{-12} \text{A} \quad i_{n,i6} := i_{n,i5}$$

$$f_{c,e1} := 3.5\text{Hz} \quad f_{c,e2} := f_{c,e1} \quad f_{c,e3} := f_{c,e1} \quad f_{c,e4} := f_{c,e1} \quad f_{c,e5} := 2.7\text{Hz} \quad f_{c,e6} := f_{c,e5}$$

$$f_{c,i1} := 250\text{Hz} \quad f_{c,i2} := f_{c,i1} \quad f_{c,i3} := f_{c,i1} \quad f_{c,i4} := f_{c,i1} \quad f_{c,i5} := 120\text{Hz} \quad f_{c,i6} := f_{c,i5}$$

$$e_{n,i1}(f) := e_{n,i1} \cdot \sqrt{\frac{f_{c,e1}}{f} + 1} \quad e_{n,i2}(f) := e_{n,i1}(f) \quad e_{n,i3}(f) := e_{n,i1}(f) \quad e_{n,i4}(f) := e_{n,i1}(f)$$

$$i_{n,i1}(f) := i_{n,i1} \cdot \sqrt{\frac{f_{c,i1}}{f} + 1} \quad i_{n,i2}(f) := i_{n,i1}(f) \quad i_{n,i3}(f) := i_{n,i1}(f) \quad i_{n,i4}(f) := i_{n,i1}(f)$$

$$e_{n,i5}(f) := e_{n,i5} \cdot \sqrt{\frac{f_{c,e5}}{f} + 1} \quad e_{n,i6}(f) := e_{n,i5}(f)$$

$$i_{n,i5}(f) := i_{n,i5} \cdot \sqrt{\frac{f_{c,i5}}{f} + 1} \quad i_{n,i6}(f) := i_{n,i5}(f)$$

$$e_{n,iA}(f) := \sqrt{e_{n,i1}(f)^2 + e_{n,i2}(f)^2} \quad e_{n,iA}(h) = 1.204 \times 10^{-9} \text{V}$$

$$e_{n,iB}(f) := e_{n,iA}(f)$$

$$e_{n,i2nd}(f) := e_{n,i5}(f) \quad i_{n,i2nd}(f) := i_{n,i5}(f)$$

$$RP_{2nd,1} := (R_{11}^{-1} + R_{12}^{-1})^{-1} \quad RP_{2nd,1} = 1.1 \times 10^3 \Omega$$

$$e_{n,R7} := \sqrt{4 \cdot k \cdot T \cdot B_1 \cdot R7} \quad e_{n,R7} = 6.037 \times 10^{-9} \text{V}$$

$$e_{n,R8} := e_{n,R7}$$

$$e_{n,RG1} := \sqrt{4 \cdot k \cdot T \cdot B_1 \cdot RG1} \quad e_{n,RG1} = 382.216 \times 10^{-12} \text{V}$$

$$e_{n,RP,2nd,1} := \sqrt{4 \cdot k \cdot T \cdot B_1 \cdot RP_{2nd,1}} \quad e_{n,RP,2nd,1} = 4.269 \times 10^{-9} \text{V}$$

$$e_{n,R11} := \sqrt{4 \cdot k \cdot T \cdot B_1 \cdot R8} \quad e_{n,R11} = 6.037 \times 10^{-9} \text{V}$$

$$e_{n,R16} := \sqrt{4 \cdot k \cdot T \cdot B_1 \cdot R16} \quad e_{n,R16} = 6.037 \times 10^{-9} \text{V}$$

$$e_{n,Rin,rc}(R0) := \sqrt{4 \cdot k \cdot T \cdot B_1 \cdot R_{in,rc}(R0)} \quad e_{n,Rin,rc}(10\Omega) = 406.924 \times 10^{-12} \text{V}$$

18.2 MCD-WS: The PMMA

3.2 Noise voltage density at the bal o/p of one of the two 1st stages (i/p shorted) :

$$\epsilon_{n.RG1.o} := \epsilon_{n.RG1} \frac{R7 + R8}{RG1} \qquad \epsilon_{n.RG1.o} = 190.726 \times 10^{-9} \text{ V}$$

$$\epsilon_{n.o.A}(f) := \sqrt{\epsilon_{n.iA}(f)^2 \cdot G_A^2 + i_{n.i1}(f)^2 \cdot R7^2 + i_{n.i2}(f)^2 \cdot R8^2 + \epsilon_{n.R7}^2 + \epsilon_{n.R8}^2 + \epsilon_{n.RG1.o}^2}$$

$$\epsilon_{n.o.A}(h) = 631.645 \times 10^{-9} \text{ V}$$

$$\epsilon_{n.o.B}(f) := \epsilon_{n.o.A}(f)$$

3.3 Paralleling of the two i/p stages and the inclusion of an input load R0 :

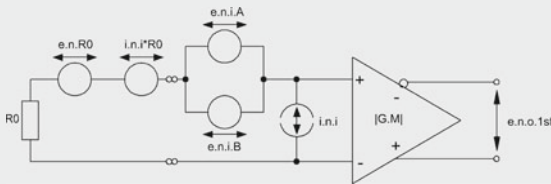


Fig. 18.6  
Noise situation after  
paralleling of two i/p  
stages

$$\epsilon_{n.iA}(f) := \frac{\epsilon_{n.o.A}(f)}{G_A} \qquad \epsilon_{n.iA}(h) = 1.263 \times 10^{-9} \text{ V}$$

$$\epsilon_{n.iB}(f) := \epsilon_{n.iA}(f) \qquad \epsilon_{n.iB}(h) = 1.263 \times 10^{-9} \text{ V}$$

$$\epsilon_{n.o1}(f) := \epsilon_{n.iA}(f) \cdot |G_M| \qquad \epsilon_{n.o1}(h) = 1.263 \times 10^{-6} \text{ V}$$

$$\epsilon_{n.o2}(f) := \epsilon_{n.iB}(f) \cdot |G_M| \qquad \epsilon_{n.o2}(h) = 1.263 \times 10^{-6} \text{ V}$$

$$i_{n.iA}(f) := \sqrt{\left(\frac{1}{i_{n.i1}(f)^2} + \frac{1}{i_{n.i2}(f)^2}\right)^{-1}} \qquad i_{n.iA}(h) = 790.569 \times 10^{-15} \text{ A}$$

$$i_{n.iB}(f) := \sqrt{\left(\frac{1}{i_{n.i3}(f)^2} + \frac{1}{i_{n.i4}(f)^2}\right)^{-1}} \qquad i_{n.iB}(h) = 790.569 \times 10^{-15} \text{ A}$$

$$i_{n.i}(f) := \sqrt{i_{n.iA}(f)^2 + i_{n.iB}(f)^2} \qquad i_{n.i}(h) = 1.118 \times 10^{-12} \text{ A}$$

$$i_{n.i.avg} := \sqrt{\frac{1}{B_{20k}} \int_{20\text{Hz}}^{2000\text{Hz}} (i_{n.i}(f))^2 df} \qquad i_{n.i.avg} = 1.042 \times 10^{-12} \text{ A}$$

18.2 MCD-WS: The PMMA

$$e_{n.o.1st}(f, R0) := \sqrt{\left(\frac{1}{e_{n.o1}(f)^2} + \frac{1}{e_{n.o2}(f)^2}\right)^{-1} + \left(i_{n.i}(f)^2 \cdot R_{in.rc}(R0)^2 + e_{n.Rin.rc}(R0)^2\right) \cdot (|G_M|)^2}$$

$$e_{n.o.1st}(h, 0\Omega) = 893.281 \times 10^{-9} \text{V}$$

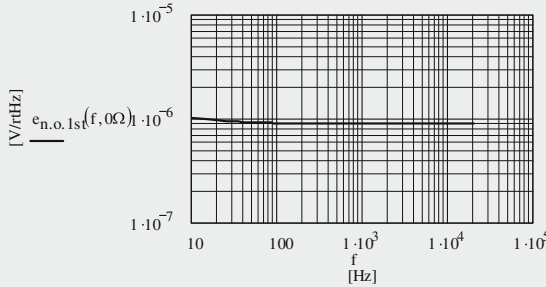


Fig. 18.7  
Output noise voltage density of the whole 1st stage

Average noise voltage density in B<sub>20k</sub> :

$$e_{n.o.1st.avg}(R0) := \sqrt{\frac{1}{B_{20k}} \int_{20Hz}^{2000Hz} \left(|e_{n.o.1st}(f, R0)|\right)^2 df}$$

$$e_{n.o.1st.avg}(0\Omega) = 892.35 \times 10^{-9} \text{V}$$

3.4 Output noise voltage density and SN at the bal o/p of the 2nd stage (OP5 & OP6), i/p shorted

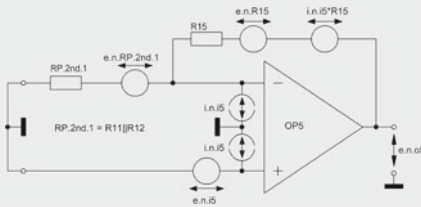


Fig. 18.8 = Fig. 16.13

$$e_{n.o5}(f) := \sqrt{e_{n.i.2nd}(f)^2 \cdot \left(1 + \frac{R16}{RP_{2nd.1}}\right)^2 + e_{n.R16}^2 + i_{n.i.2nd}(f)^2 \cdot R16^2 + e_{n.RP.2nd.1}^2 \cdot \left(\frac{R16}{RP_{2nd.1}}\right)^2}$$

$$e_{n.o5}(h) = 13.836 \times 10^{-9} \text{V}$$

$$e_{n.o6}(f) := e_{n.o5}(f)$$

$$e_{n.o.2nd}(f) := \sqrt{e_{n.o5}(f)^2 + e_{n.o6}(f)^2}$$

$$e_{n.o.2nd}(h) = 19.567 \times 10^{-9} \text{V}$$

## 18.2 MCD-WS: The PMMA

Page 6

$$SN_{o,2nd} := 20 \cdot \log \left[ \frac{\frac{1}{B_1} \cdot \int_{20\text{Hz}}^{20000\text{Hz}} (|e_{n.o.2nd}(f)|)^2 df}{1\text{V}} \right] \quad SN_{o,2nd} = -111.168 \quad [\text{dBV}]$$

$$\text{measured with } R_0 = 0\Omega: \quad SN_{o,2nd,m} := -110.23 \quad [\text{dBV}]$$

3.5 Total input load dependent o/p noise voltage density and the corresponding input and output referred SNs :

$$e_{n.o.tot}(f,R_0) := \sqrt{e_{n.o.1st}(f,R_0)^2 + e_{n.o.2nd}(f)^2} \quad e_{n.o.tot}(h,0\Omega) = 893.495 \times 10^{-9} \text{V}$$

Average noise voltage density in  $B_{20k}$  :

$$e_{n.o.tot.avg}(R_0) := \sqrt{\frac{1}{B_{20k}} \cdot \int_{20\text{Hz}}^{20000\text{Hz}} (|e_{n.o.tot}(f,R_0)|)^2 df} \quad e_{n.o.tot.avg}(0\Omega) = 892.564 \times 10^{-9} \text{V}$$

3.5.1 Balanced i/p and o/p referred SNs :

$$e_{n.i.tot}(f,R_0) := \frac{e_{n.o.tot}(f,R_0)}{|G_M|} \quad e_{n.i.tot}(h,0\Omega) = 893.495 \times 10^{-12} \text{V}$$

Average noise voltage density in  $B_{20k}$  :

$$e_{n.i.tot.avg}(R_0) := \sqrt{\frac{1}{B_{20k}} \cdot \int_{20\text{Hz}}^{20000\text{Hz}} (|e_{n.i.tot}(f,R_0)|)^2 df} \quad e_{n.i.tot.avg}(0\Omega) = 892.564 \times 10^{-12} \text{V}$$

ein and SN evaluation :

$$e_{in} := 20 \cdot \log \left( \frac{e_{n.i.tot.avg}(0\Omega)}{1\text{V}} \right) \quad e_{in} = -180.987 \quad [\text{dBV}]$$

$$e_{N.o.tot}(R_0) := \sqrt{\frac{1}{B_1} \cdot \int_{20\text{Hz}}^{20000\text{Hz}} (|e_{n.o.tot}(f,R_0)|)^2 df} \quad e_{N.o.tot}(0\Omega) = 126.165 \times 10^{-6} \text{V}$$

$$e_{N.i.tot}(R_0) := \sqrt{\frac{1}{B_1} \cdot \int_{\text{Hz}}^{20000\text{Hz}} (|e_{n.i.tot}(f,R_0)|)^2 df} \quad e_{N.i.tot}(0\Omega) = 126.239 \times 10^{-9} \text{V}$$

18.2 MCD-WS: The PMMA

$$SN_{o,tot}(R0) := 20 \cdot \log \left( \frac{e_{N.o,tot}(R0)}{v_{o.ref}} \right)$$

$$SN_{o,tot}(0\Omega) = -77.981 \quad [dBV]$$

measured (R0 = 0Ω):  $SN_{o,tot,m} := -78.14 \quad [dBV]$

$$SN_{i,tot}(R0) := 20 \cdot \log \left( \frac{e_{N.i,tot}(R0)}{v_{o.ref}} \right)$$

$$SN_{i,tot}(0\Omega) = -137.976 \quad [dBV]$$

measured (R0 = 0Ω):  $SN_{i,tot,m} := -138.16 \quad [dBV]$

3.5.2 Equivalent input noise voltage EIN:

$$EIN := SN_{i,tot}(0\Omega)$$

$$EIN = -137.976 \quad [dBV]$$

$$EIN_m := -138.16 \quad [dBV]$$

$$e_{n.i,tot,m} := 10^{\frac{EIN_m - 43.006}{20}} \text{ V}$$

$$e_{n.i,tot,m} = 874.38 \times 10^{-12} \text{ V}$$

3.6 The un-balanced o/p referred SN at OP7's J04 :

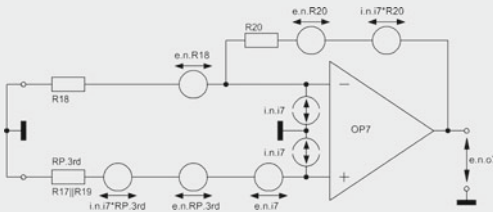


Fig. 18.9 = Fig. 16.14

$$e_{n.i7}(f) := e_{n.i5}(f) \quad i_{n.i7}(f) := i_{n.i5}(f) \quad RP7 := \left( \frac{1}{R17} + \frac{1}{R19} \right)^{-1} \quad RP7 = 1100 \Omega$$

$$e_{n.RP7} := \sqrt{4 \cdot k \cdot T \cdot B_1 \cdot RP7} \quad e_{n.RP7} = 4.269 \times 10^{-9} \text{ V}$$

$$e_{n.R18} := \sqrt{4 \cdot k \cdot T \cdot B_1 \cdot R18} \quad e_{n.R18} = 6.037 \times 10^{-9} \text{ V}$$

$$e_{n.R20} := \sqrt{4 \cdot k \cdot T \cdot B_1 \cdot R20} \quad e_{n.R20} = 6.037 \times 10^{-9} \text{ V}$$

3.6.1 Output noise voltage density and SN (i/p shorted) :

$$e_{n.o7}(f) := \sqrt{\left( e_{n.i7}(f)^2 + i_{n.i7}(f)^2 \cdot RP7^2 + e_{n.RP7}^2 \right) \cdot \left( 1 + \frac{R20}{R18} \right)^2 + e_{n.R18}^2 \cdot \left( \frac{R20}{R18} \right)^2 + e_{n.R20}^2 + i_{n.i7}(f)^2 \cdot R20^2}$$

$$e_{n.o7}(h) = 13.551 \times 10^{-9} \text{ V}$$

18.2 MCD-WS: The PMMA

$$SN_{o7.sh} := 20 \cdot \log \left[ \frac{\frac{1}{B_1} \int_{20\text{Hz}}^{2000\text{Hz}} (|e_{n.o7}(f)|)^2 df}{V_{o.ref}} \right] \quad SN_{o7.sh} = -114.359 \quad [\text{dBV}]$$

measured with  $R_0 = 0\Omega$ :  $SN_{o7.sh.m} := -113.82 \quad [\text{dBV}]$

3.6.2 Output noise voltage and SN with  $i/p$  loaded by the noise of the preceding stages :

$$e_{n.o.ub}(f, R_0) := \sqrt{e_{n.o.tot}(f, R_0)^2 + e_{n.o7}(f)^2} \quad e_{n.o.ub}(h, 0\Omega) = 893.598 \times 10^{-9} \text{V}$$

$$SN_{o.ub}(R_0) := 20 \cdot \log \left[ \frac{\frac{1}{B_1} \int_{20\text{Hz}}^{2000\text{Hz}} (|e_{n.o.ub}(f, R_0)|)^2 df}{V_{o.ref}} \right] \quad SN_{o.ub}(0\Omega) = -77.98 \quad [\text{dBV}]$$

measured :  $SN_{o.ub.m} := -78.14 \quad [\text{dBV}]$

3.7 Graph of the input load dependent output referred SN:

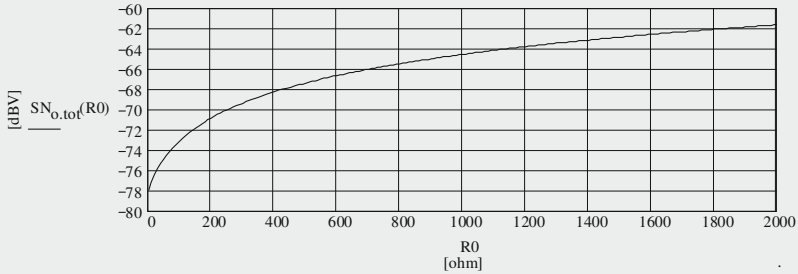


Fig. 18.10 = Fig. 16.15

$$SN_{o.tot}(0\Omega) = -77.981 \quad [\text{dBV}] \quad SN_{o.tot}(2 \cdot 10^3 \Omega) - SN_{o.tot}(0\Omega) = 16.324 \quad [\text{dB}]$$

$$G_{M.e} := 20 \cdot \log(|G_M|) \quad G_{M.e} = 60 \quad [\text{dB}]$$

$$EIN(R_0) := SN_{o.tot}(R_0) - G_{M.e} \quad EIN(2 \cdot 10^3 \Omega) = -121.657 \quad [\text{dBV}]$$

18.2 MCD-WS: The PMMA

3.8. SN calculation by rule-of-thumb (according to Fig. 16.11) :

We assume only one un-balanced LT1028 input stage in series configuration with a gain of  $G_{M,0} = 1000!$

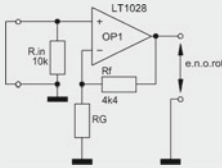


Fig. 18.11 = Fig. 16.11

$G_{M,0} := 1000$	$R_f := 2 \cdot 2 \cdot 2 \cdot 10^3 \Omega$	$e_{n,i} := 0.85 \cdot 10^{-9} V$	$i_{n,i}$ ignored!
$RG := \frac{R_f}{G_{M,0} - 1}$		$RG = 4.404 \Omega$	
$e_{n,RG,rot} := 0.13 \cdot \sqrt{\frac{RG}{\Omega}} \cdot 10^{-9} V$		$e_{n,RG,rot} = 272.827 \times 10^{-12} V$	
$e_{n,o,rot} := G_{M,0} \cdot \sqrt{e_{n,i}^2 + e_{n,RG,rot}^2}$		$e_{n,o,rot} = 893 \times 10^{-9} V$	
$e_{n,i,rot} := \frac{e_{n,o,rot}}{G_{M,0}}$		$e_{n,i,rot} = 893 \times 10^{-12} V$	
$SN_{o,rot} := 20 \cdot \log\left(\frac{e_{n,o,rot}}{1V}\right) + 43$		$SN_{o,rot} = -78$	[dBV]
$EIN_{rot} := SN_{o,rot} - 20 \cdot \log(G_{M,0})$		$EIN_{rot} = -138$	[dBV]
$e_{in,rot} := EIN_{rot} - 43$		$e_{in,rot} = -181$	[dBV]

4. The measurement correction figure D :

$SN_{o,tot}(0 \cdot 10^3 \Omega) = -77.981$	[dBV]	$SN_{o,0R,m} := -78.14$	[dBV]
$SN_{o,tot}(1 \cdot 10^3 \Omega) = -64.57$	[dBV]	$SN_{o,1k,m} := -63.63$	[dBV]
$SN_{o,tot}(2 \cdot 10^3 \Omega) = -61.657$	[dBV]	$SN_{o,2k,m} := -59.72$	[dBV]
$D1 := SN_{o,0R,m} - SN_{o,tot}(0 \cdot 10^3 \Omega)$		$D1 = -0.16$	[dB]
$D2 := SN_{o,1k,m} - SN_{o,tot}(1 \cdot 10^3 \Omega)$		$D2 = 0.94$	[dB]
$D3 := SN_{o,2k,m} - SN_{o,tot}(2 \cdot 10^3 \Omega)$		$D3 = 1.94$	[dB]
$\Rightarrow D(R0) := \frac{R0}{1000\Omega}$			[dB]

18.2 MCD-WS: The PMMA

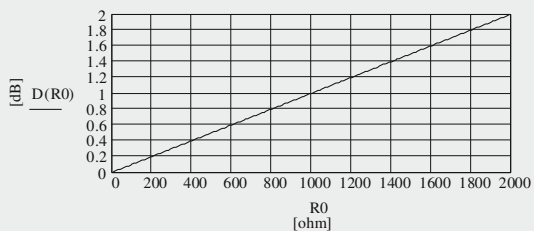


Fig. 18.12 Graph for interpolation purposes of the measurement correction figure D

6. Derivation of the PMMA gain :

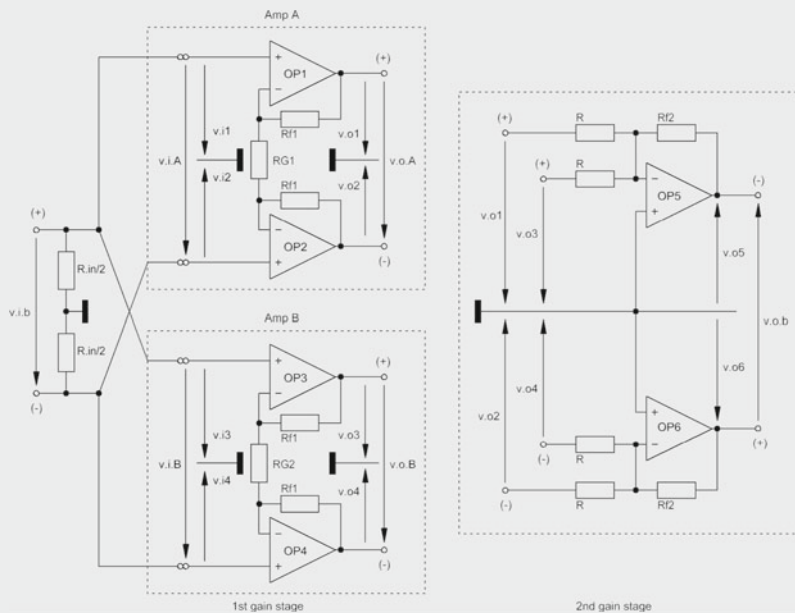


Fig. 18.13 = Fig. 16.10



## 18.2 MCD-WS: The PMMA

Page 11

Differential (balanced) gain of the MA:  $G_M = \frac{v_{o,b}}{v_{i,b}} = \frac{v_{o5} - v_{o6}}{v_{i,b}}$

$$v_{i,b} = v_{o1} - v_{o2} = v_{o3} - v_{o4}$$

$$v_{o,b} = v_{o5} - v_{o6}$$

Un-balanced gain and voltages of the 2nd gain stage with OP5 & OP6:

$$v_{o5} = G_{op5} \cdot (v_{o1} + v_{o3}) \quad G_{op5} = -\frac{Rf2}{R} \quad Rf2 = R \Rightarrow G_{op5} = -1 \Rightarrow v_{o5} = -(v_{o1} + v_{o3})$$

$$v_{o6} = G_{op6} \cdot (v_{o2} + v_{o4}) \quad G_{op6} = -\frac{Rf2}{R} \Rightarrow G_{op6} = -1 \Rightarrow v_{o6} = -(v_{o2} + v_{o4})$$

Differential gains of the two input amps Amp A & Amp B and the gain-setting resistance RG:

$$G_A = \frac{v_{o1} - v_{o2}}{v_{i,b}} = \frac{v_{o1} - v_{o2}}{v_{i1} - v_{i2}} = 1 + \frac{2 \cdot Rf1}{RG1} \quad G_B = \frac{v_{o3} - v_{o4}}{v_{i,b}} = \frac{v_{o3} - v_{o4}}{v_{i3} - v_{i4}} = 1 + \frac{2Rf1}{RG2}$$

$$G_A = G_B \Rightarrow RG1 = RG2 = RG_M \Rightarrow RG_M = \frac{2Rf1}{G_A - 1}$$

Differential ( $G_A, G_B$ ) and balanced / un-balanced gains ( $G_{A,ub}, G_{B,ub}$ ) and voltages of the 1st gain stage with its sub gain stages Amp A and Amp B (OP1 & OP2 and OP3 & OP4):

$$v_{o1} = v_{i,b} \cdot G_{A,ub.1} \quad v_{o2} = v_{i,b} \cdot G_{A,ub.2} \quad v_{o3} = v_{i,b} \cdot G_{B,ub.3} \quad v_{o4} = v_{i,b} \cdot G_{B,ub.4}$$

$$v_{o2} = -v_{o1} \Rightarrow G_A = \frac{2 \cdot v_{o1}}{v_{i,b}} \Rightarrow v_{o1} = 0.5 \cdot G_A \cdot v_{i,b} \Rightarrow G_{A,ub.1} = 0.5 \cdot G_A = 0.5 + \frac{Rf1}{RG_M}$$

$$v_{o1} = -v_{o2} \Rightarrow G_A = \frac{2 \cdot (-v_{o2})}{v_{i,b}} \Rightarrow v_{o2} = -0.5 \cdot G_A \cdot v_{i,b} \Rightarrow G_{A,ub.2} = -0.5 \cdot G_A = -\left(0.5 + \frac{Rf1}{RG_M}\right)$$

$$v_{o4} = -v_{o3} \Rightarrow G_B = \frac{2 \cdot v_{o3}}{v_{i,b}} \Rightarrow v_{o3} = 0.5 \cdot G_B \cdot v_{i,b} \Rightarrow G_{B,ub.3} = 0.5 \cdot G_B = 0.5 + \frac{Rf1}{RG_M}$$

$$v_{o3} = -v_{o4} \Rightarrow G_B = \frac{2 \cdot (-v_{o4})}{v_{i,b}} \Rightarrow v_{o4} = -0.5 \cdot G_B \cdot v_{i,b} \Rightarrow G_{A,ub.4} = -0.5 \cdot G_B = -\left(0.5 + \frac{Rf1}{RG_M}\right)$$

## 18.2 MCD-WS: The PMMA

Page 12

Consequences for the output voltages and the differential gain  $G_M$ :

$$v_{o5} = -v_{i,b} \cdot (G_{A,ub,1} + G_{B,ub,3}) \qquad v_{o,6} = -v_{i,b} \cdot (G_{A,ub,2} + G_{B,ub,4})$$

$$v_{o5} - v_{o6} = v_{i,b} \cdot (-G_{A,ub,1} - G_{B,ub,3} + G_{A,ub,2} + G_{B,ub,4}) = v_{i,b} \cdot (-0.5G_A - 0.5G_B - 0.5G_A - 0.5G_B)$$

$$\Rightarrow v_{o5} - v_{o6} = v_{i,b} \cdot (-G_A - G_B)$$

$$G_M = \frac{v_{o5} - v_{o6}}{v_{i,b}} = -(G_A + G_B) = -2G_A = -2G_B$$

Proof with  $R_{f1} = R_{f2} = R$      $R := 2.2 \cdot 10^3 \Omega$      $R_{f1} := R$      $R_{f2} := R$     and     $G_A := 500$

$$RG := 2 \cdot \frac{R_{f1}}{G_A - 1} \qquad RG = 8.818 \Omega$$

$G_B := G_A$      $G := -(G_A + G_B)$      $G = -1000$

$$G_{A,ub,1} := 0.5 \cdot G_A \qquad G_{A,ub,1} = 250$$

$$G_{A,ub,2} := -0.5 \cdot G_A \qquad G_{A,ub,2} = -250$$

18.3 MCD-WS: The PFMA

The Measurement Amp PFMA with Galvanically Isolated Input (gain = 100)

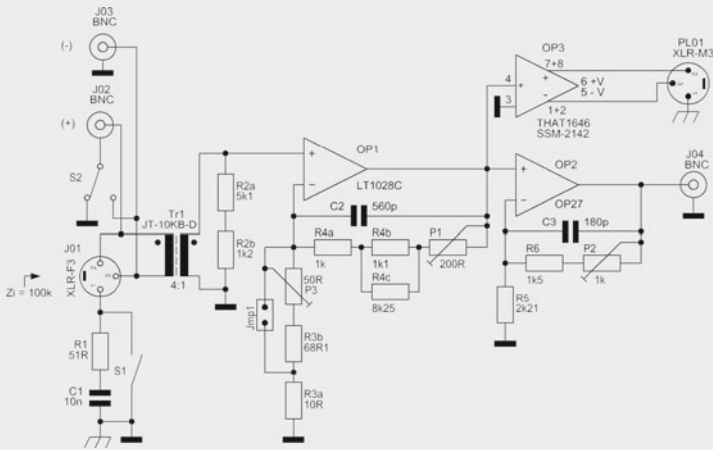


Fig. 18.14 = Fig. 17.1

1. Definition of all meaningful constants, components, etc. :

1.1 Constants, etc. :

$$k := 1.38065 \cdot 10^{-23} \text{V} \cdot \text{A} \cdot \text{s} \cdot \text{K}^{-1} \quad T := 300\text{K} \quad B_1 := 1\text{Hz} \quad B_{20k} := 19980\text{Hz}$$

$$v_{i,\text{ref}} := 1\text{V} \quad f := 10\text{Hz}, 15\text{Hz}, 20 \cdot 10^3\text{Hz} \quad h := 1000\text{Hz}$$

1.2 Transformer :

$$\text{Tr1} = \text{JT-10KB-D} \quad n := \frac{1}{4} \quad n = 0.25$$

$$G_{\text{Tr1,e}} := 20 \cdot \log(n) \text{ [dB]} \quad G_{\text{Tr1,e}} = -12.041 \text{ [dB]} \quad G_{\text{Tr1}} := 10^{\frac{G_{\text{Tr1,e}}}{20}} \quad G_{\text{Tr1}} = 0.25$$

1.3 Gain from i/p to o/p :

$$G_{\text{MA}} = G_{\text{Tr1}} \cdot G_{\text{amp}} \quad G_{\text{amp}} = G_1 \cdot G_2 \quad G_2 = 2$$

$$G_{\text{MA}} := 100 \quad G_1 := \frac{G_{\text{MA}}}{2 \cdot n} \quad G_1 = 200$$

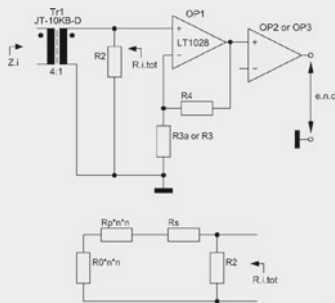
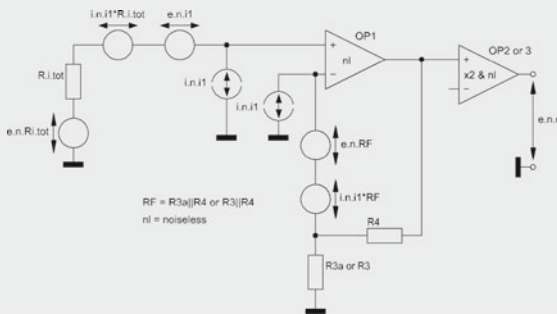
$$G_2 := 2 \quad G_{\text{amp}} := G_1 \cdot G_2 \quad G_{\text{amp}} = 400$$

18.3 MCD-WS: The PFMA

1.4 Components and resistances :

$$\begin{aligned}
 R0 &:= 10^{-12} \Omega & R_p &:= 2.5 \cdot 10^3 \Omega & R_s &:= 225 \Omega & R_{2a} &:= 5.1 \cdot 10^3 \Omega & R_{2b} &:= 1.2 \cdot 10^3 \Omega \\
 R2 &:= R_{2a} + R_{2b} & R2 &:= 6.3 \times 10^3 \Omega & R_{3a} &:= 10 \Omega & & & & \\
 R4 &:= P1 + R_{4a} + \left( \frac{1}{R_{4b}} + \frac{1}{R_{4c}} \right)^{-1} & R4 &:= (G1 - 1) \cdot R_{3a} & & & R4 &:= 1.99 \times 10^3 \Omega \\
 R_{4a} &:= 1 \cdot 10^3 \Omega & R_{4b} &:= 1.1 \cdot 10^3 \Omega & R_{4c} &:= 8.25 \cdot 10^3 \Omega & & & & \\
 P1 &:= R4 - \left[ R_{4a} + \left( \frac{1}{R_{4b}} + \frac{1}{R_{4c}} \right)^{-1} \right] & P1 &:= 19.412 \Omega & & & & & & \\
 \text{Proof:} & & G_M &:= G_{Tr1} \cdot G1 \cdot G2 & G_M &:= 100 & & & & 
 \end{aligned}$$

1.5 Noise calculation relevant feedback and input resistances :



## 18.3 MCD-WS: The PFMA

Page 3

$$RF := \left( \frac{1}{R3a} + \frac{1}{R4} \right)^{-1}$$

$$RF = 9.95 \Omega$$

$$R_{i,tot}(R0) := \left[ \frac{1}{n^2 \cdot (R0 + Rp) + Rs} + \frac{1}{R2} \right]^{-1}$$

$$R_{i,tot}(R0) = 359.495 \Omega$$

$$Z_1 := \frac{(R2a + R2b + Rs)}{n^2} + Rp$$

$$Z_1 = 106.9 \times 10^3 \Omega$$

2. Noise and SN calculations :

$$e_{n,il} := 0.85 \cdot 10^{-9} V \quad f_{c,e1} := 3.5 Hz$$

$$i_{n,il} := 1.0 \cdot 10^{-12} A \quad f_{c,il} := 250 Hz$$

$$e_{n,il}(f) := e_{n,il} \cdot \sqrt{\frac{f_{c,e1}}{f} + 1}$$

$$i_{n,il}(f) := i_{n,il} \cdot \sqrt{\frac{f_{c,il}}{f} + 1}$$

$$i_{n,il,eff}(f) := i_{n,il}(f) \cdot n$$

$$i_{n,il,eff,avg} := \sqrt{\frac{1}{B_{20k}} \cdot \int_{20Hz}^{20000Hz} (i_{n,il,eff}(f))^2 df}$$

$$i_{n,il,eff,avg} = 260.521 \times 10^{-15} A$$

$$e_{n,RF} := \sqrt{4 \cdot k \cdot T \cdot B_1 \cdot RF}$$

$$e_{n,RF} = 406.017 \times 10^{-12} V$$

$$e_{n,Ri,tot}(R0) := \sqrt{4 \cdot k \cdot T \cdot B_1 \cdot R_{i,tot}(R0)}$$

$$e_{n,Ri,tot}(R0) = 2.44 \times 10^{-9} V$$

Noise of OP2 &amp; OP3 ignored!

$$e_{n,i}(f, R0) := \sqrt{e_{n,il}(f)^2 + i_{n,il}(f)^2 \cdot (RF^2 + R_{i,tot}(R0)^2) + e_{n,RF}^2 + e_{n,Ri,tot}(R0)^2}$$

$$e_{n,i}(h, R0) = 2.647 \times 10^{-9} V$$

$$e_{n,o}(f, R0) := e_{n,i}(f, R0) \cdot G_{amp}$$

$$e_{n,o}(h, R0) = 1.059 \times 10^{-6} V$$

$$e_{N,o}(R0) := \sqrt{\frac{1}{B_1} \cdot \int_{20Hz}^{20000Hz} (e_{n,o}(f, R0))^2 df}$$

$$e_{N,o}(R0) = 149.428 \times 10^{-6} V$$

18.3 MCD-WS: The PFMA

$$e_{n.iMA}(f,R0) := \frac{e_{n.o}(f,R0)}{G_{MA}}$$

$$e_{n.iMA}(h,0\Omega) = 10.589 \times 10^{-9} V$$

$$e_{n.iMA.avg}(R0) := \sqrt{\frac{1}{B_{20k}} \int_{20Hz}^{20000Hz} (|e_{n.iMA}(f,R0)|)^2 df}$$

$$e_{n.iMA.avg}(0\Omega) = 10.571 \times 10^{-9} V$$

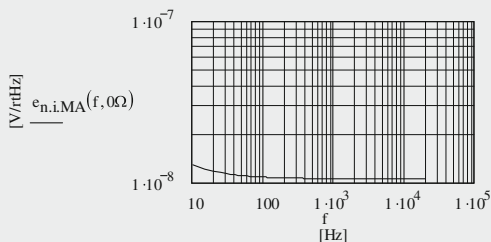


Fig. 18.17  
PFMA input noise  
voltage density vs.  
frequency

$$SN_{ne.i}(R0) := 20 \cdot \log \left[ \frac{\sqrt{\frac{1}{B_1} \int_{20Hz}^{20000Hz} (|e_{n.iMA}(f,R0)|)^2 df}}{v_{i.ref}} \right]$$

$$SN_{ne.i}(R0) = -116.511 \quad [dBV]$$

measured with *i/p* shorted:  $SN_{ne.i.m} := -117.31 \quad [dBV]$

$$SN_{ne.o}(R0) := SN_{ne.i}(R0) + 20 \cdot \log(G_{MA})$$

$$SN_{ne.o}(R0) = -76.511 \quad [dBV]$$

$$R0 := 0.001 \Omega, 50\Omega .. 10 \cdot 10^3 \Omega$$

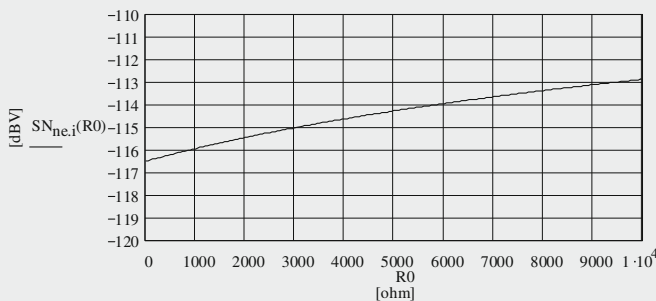


Fig. 18.18 Input referred R0 dependent SN

---

## 19.1 Intro

Attached to a phono-amp input not many different methods allow decreasing the noise production of an MM cartridge. Normally, the following ones help: low input referred noise voltage and noise current of the phono-amp, low values of the cartridge's internal resistance, high internal inductance, etc. However, an obstacle cannot be pushed away by simple means. It's resistor R1 in Fig. 19.1. This figure stands for the principal input situation of the MM cartridge with the input of the phono-amp; Fig. 19.2 moves the situation into its noise model.

In Fig. 19.1 R0 and L0 represent the cartridges impedances, here with the values of a so-called standard model. C1 stands for the phono-amp's input capacitance plus the cable capacitance; the value should hit the cartridge's required capacitance load. R1 is the standard phono-amp input resistance of 47 k $\Omega$ .

Figures 19.3 and 19.4 show the same situation in a balanced input environment.

Because of the complexity of the whole process, we'll start with the noise reduction for the un-balanced amplification first.

---

## 19.2 The Un-Balanced Noise Reduction Approach

### 19.2.1 Basics

The approach goes back to a JAES article,<sup>1</sup> published in 1978. Principally, the authors attack the noise production of a resistor like R1 in Fig. 19.1 by replacing its noise current  $i_{n,R1}$  with a very much lower noise current  $i_{n,R1,red}$ . According to (19.1) a lower resistor noise current would require a higher resistor value  $R1_{new}$ . Without changing the load-effect of R1 by its original value this could be achieved by an adequate resistor synthesis.

---

<sup>1</sup>“Improvement of the Noise Characteristics of Amplifiers for Magnetic Transducers”, Jean M. Hoeffelman & René P. Meys 1978, JAES Vol 28, Nr 12, p. 935 ff.

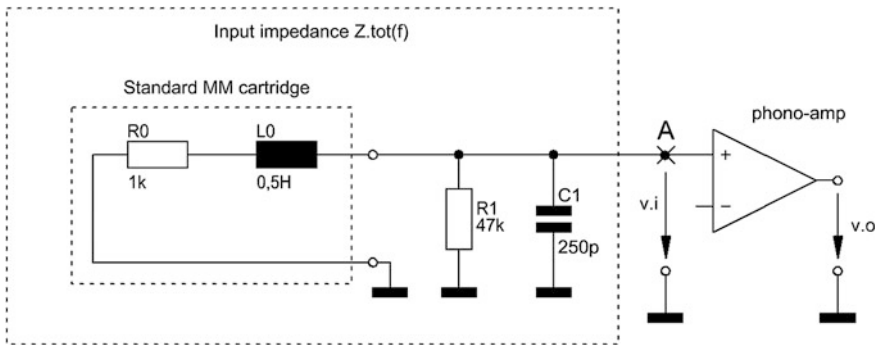


**Fig. 19.1** Principal situation of an MM cartridge attached to an un-balanced phono-amp input

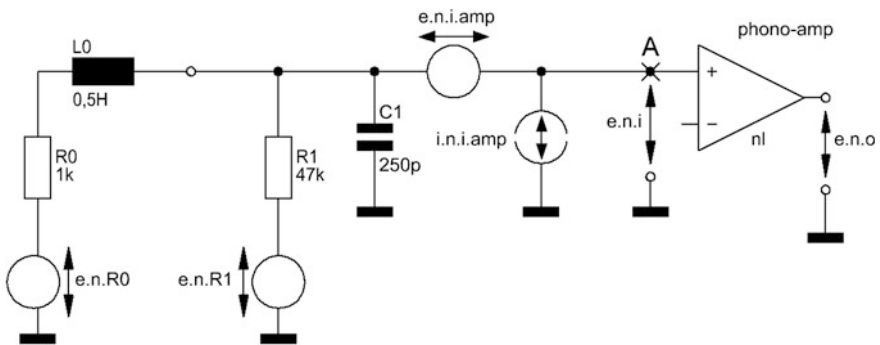


**Fig. 19.2** Noise model of Fig. 19.1

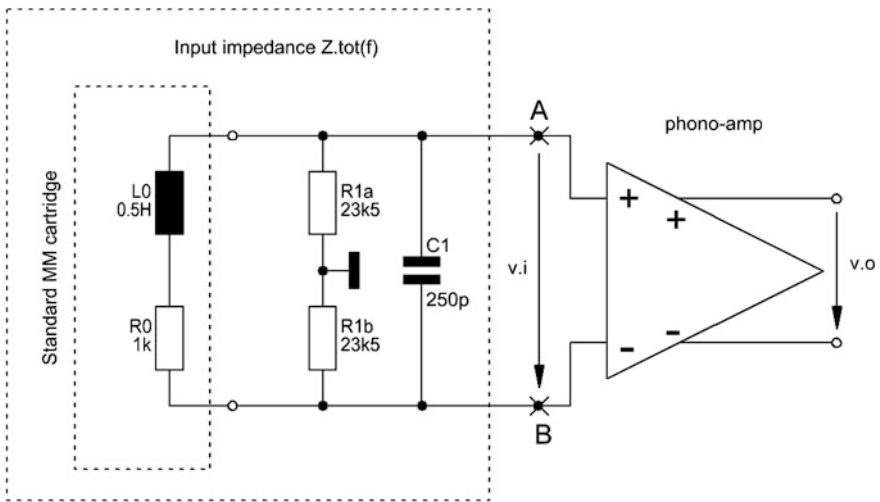


**Fig. 19.3** Principal situation of an MM cartridge attached to a balanced phono-amp input



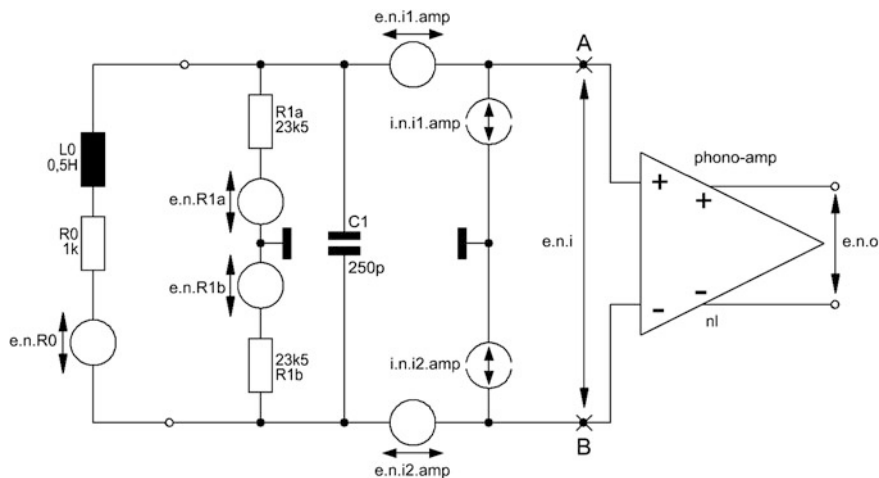


Fig. 19.4 Noise model of Fig. 19.3

$$i_{n.R1} = \sqrt{\frac{4kTB_1}{R1}} \tag{19.1}$$

In a 2003 Electronics World<sup>2</sup> article this new method was firstly adapted to improve the MM phono-amp input referred SN. In this article, Mr van de Gevel named the method ‘resistor cooling’, because in (19.1) a reduction of T would automatically decrease the noise current, and thus we would get an SN improvement effect.

Later on, in 2010, Mr. Douglas Self<sup>3</sup> named the method ‘load synthesis’<sup>4</sup> by electronic means, and I guess this new name in conjunction with his recommended new circuit hits the approach best. In addition, it is rather easy to implement.

What’s missing is a mathematical course with a real MM phono-amp. It should show the expected SN improvement based on the described methods. In the following sections, I will demonstrate two different calculation methods based on the two different synthesis solutions M1 and M2 and I will compare the results with the M3 version, the one with R1 = 47.5 kΩ. The M1 version represents Mr Self’s original idea; M2 shows a variant of M1 by shifting the gain producing part from the output to the input.

Figure 19.5 shows my test MM phono-amp with the input impedance  $Z_{tot}(f)$  and the selectable cartridge loads M1–M3. Jmp1–3 allow the selection of the different input load situations M1–M3 of the MM phono-amp with its circuitry around OPs 3 & 4.

<sup>2</sup>“Noise and Moving-Magnet Cartridges”, Marcel van de Gevel, EW 10-2003, p. 38 ff.

<sup>3</sup>“Small Signal Audio Design”, Chap. 7 p. 197 ff, ‘Electronic Cartridge Loading for Lower Noise’.

<sup>4</sup>Abbreviation for electronic load synthesis: ELS.

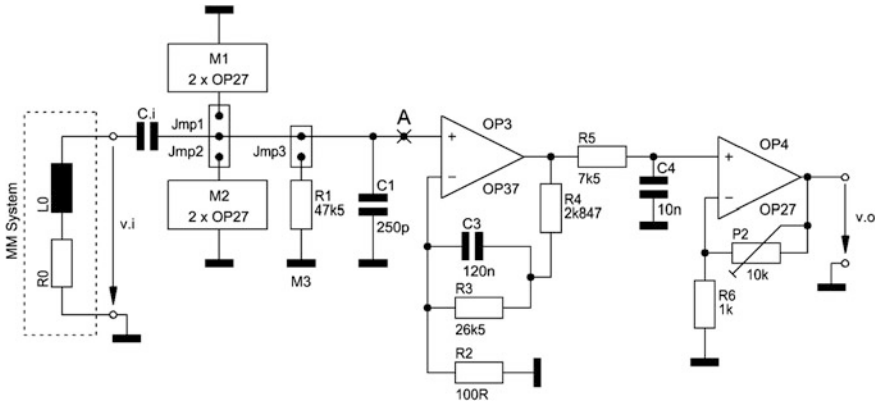


Fig. 19.5 Test MM phono-amp à la Fig. 19.1

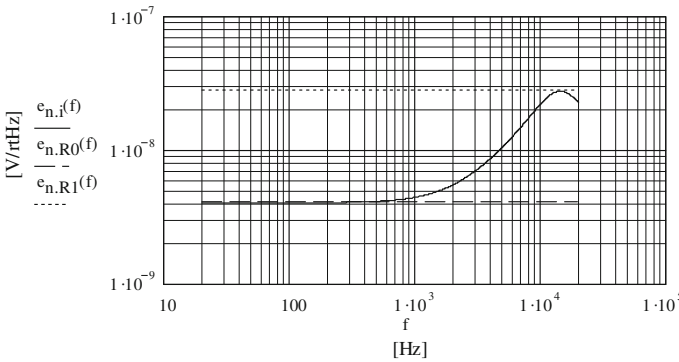


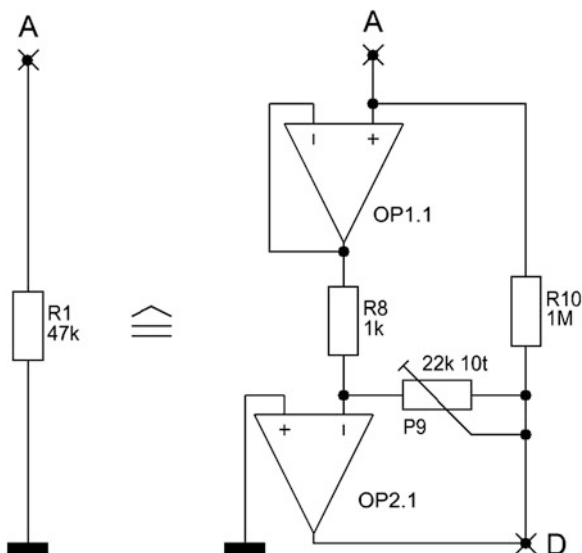
Fig. 19.6 Standard Cartridge noise voltages at the input of the test phono-amp à la Fig. 19.5

With the Standard Cartridge connected to the input Fig. 19.6 shows the various input noise voltages before implementation of an ELS network, hence, M3 with Jmp3 set. The solid curve is the actual one at point A of Fig. 19.5. The dashed trace represents the noise voltage density of R0 and R1's noise voltage density is the dotted trace. The goal is to move the dotted trace in direction of the dashed one, thus, drastically decreasing the solid trace >1 kHz.

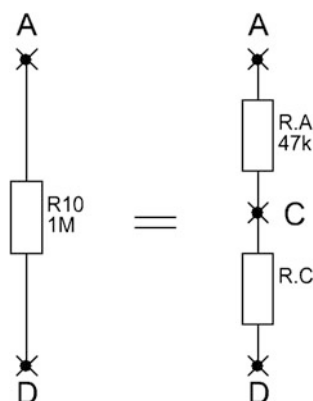
### 19.2.2 The M1 ELS

Figure 19.7 shows the circuit situation with its replacement of the 47 kΩ by an electronic M1 solution around OPs 1.1 & 2.1.

**Fig. 19.7** R1 replaced by an M1 ELS



**Fig. 19.8** R10 split into two sections to produce a virtual ground in-between them



The circuit works as follows<sup>5</sup>:

In Fig. 19.5 Jmp1 must be set. It connects A with the A in Fig. 19.7. Because of its very high input resistance and with a gain of “1” OP1.1 has no load effect for the cartridge and the phono-amp input. With a gain of  $G_{M1}$  at its output the following op amp OP2.1 produces a signal voltage phase shift of 180°. This inverted signal is 100 % correlated to the input signal. It hits the input signal in R10 at point C. This mixing effect is the key effect of the whole circuit. It leads to the Fig. 19.8

<sup>5</sup>Next chapter’s Mathcad worksheet MCD-WS 20.1 gives all details of the example calculations for versions M1–M3, plus, in its Sect. 20.10, the derivation of the here shown equations.

explanation of a new virtual ground at point C where both signals eliminate each other to 0 V. Hence, by choosing the right gain  $G_{M1}$  we can split R10 between A and B into two sections: section 1 between A and C with a resistance  $R_A = 47 \text{ k}\Omega$  and in section 2  $R_C$  between C and D according to (19.2).

$$\begin{aligned} R10 &= (|G_{M1}| + 1)R_A \\ &= R_A + R_C \end{aligned} \quad (19.2)$$

Hence, we obtain  $G_{M1}$  as follows:

$$|G_{M1}| = \frac{R10}{R_A} - 1 \quad (19.3)$$

And the new R10 based noise current looks like:

$$\begin{aligned} i_{n.R1.M1} &= \sqrt{\frac{4kTB_1}{R10}} \\ &\ll i_{n.R1} \end{aligned} \quad (19.4)$$

Expressed in numbers:

- $i_{n.R1.M1} = 128.72 \text{ fA/rtHz}$  instead of  $593.72 \text{ fA/rtHz}$  with M3
- $e_{n.R.A} = 6.05 \text{ nV/rtHz}$  instead of  $27.90 \text{ nV/rtHz}$  with M3

If we would cool R1 to get the same improvement, we would need a temperature of  $T_{M1} = T_{M2} = 14.1 \text{ K} \equiv -259.1 \text{ }^\circ\text{C}$ .

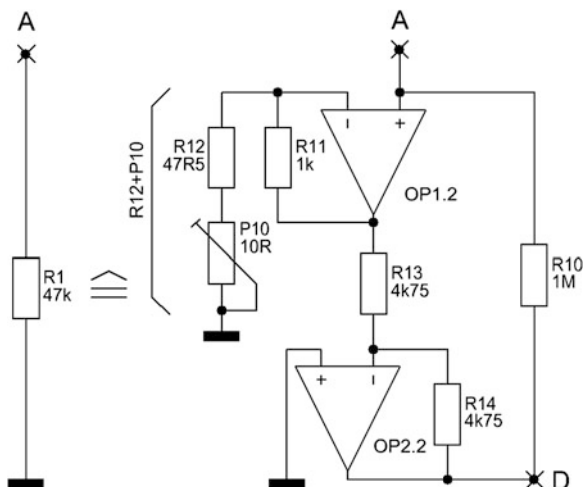
If we would choose  $R10 > 1 \text{ M}\Omega$ , of course, (19.4) would become even better. However, a bigger R10 automatically leads to a bigger gain  $G_{M1}$ . Then, the amplified signal voltage at the output of OP2.1 could run into overload at high frequencies. A rough calculation indicates that a nominal signal input voltage of  $5 \text{ mV}_{\text{rms}}/1 \text{ kHz}$  would become roughly  $50 \text{ mV}_{\text{rms}}$  at  $20 \text{ kHz}$ . Then, a further amplification by  $G_{M1} = 20.277$  would increase it to appr.  $1 \text{ V}_{\text{rms}}$ . Thus, we are appr.  $17.5 \text{ dB}$  far from overload. Consequently,  $1 \text{ M}\Omega$  is a reasonable compromise.

### 19.2.3 The M2 ELS

The M2 ELS version's circuit is given in Fig. 19.9.

Principally, M2 works like M1, without change of the before given equations. P10 sets the arrangement's gain to  $G_{M2} = 20.277$  and R10 is split into two sections, alike Fig. 19.8. In contrast to M1, the M2 version produces a tiny portion less noise.

**Fig. 19.9** R1 replaced by an M2 ELS



### 19.2.4 Results

With a Standard cartridge we gain a calculated difference between the input referred SNs of 0.12 dB only, A-weighted and RIAA equalized, however, the difference to the M3 version becomes 2.66 dB (M1)/2.78 dB (M2). I must point out that the input capacitance C1 plays a significant role too. My standard value is 250 pF, however, with eg 450 pF the differences from above change to 0.13 and 2.78 dB (M1)/2.91 dB (M2).

### 19.2.5 Consequences

The calculations demonstrate that the difference between M1 and M2 becomes ignorable. According to Occam's Razor the M1 approach looks favourable (smaller number of components with practically the same improvement effect).

When thinking of an M1 or M2 implementation we should consider the following remarks concerning the selection of components.

Compared with the Figs. 19.5 and 19.7 components and their values the M1 noise reduction effect will increase with

- decreasing input noise voltage density of the phono-amp
- decreasing R0 and L0 values
- increasing C1 value
- decreasing noise voltage and noise current of OPs 1 & 2
- increasing R10 value

The M1 noise reduction effect will decrease with

- the opposite actions of the before recommended ones, however, on a lower  $SN_{\text{ariaa}}$  basis even a phono-amp with 12 nV/rHz input noise voltage density shows an appr. 1 dB SN improvement

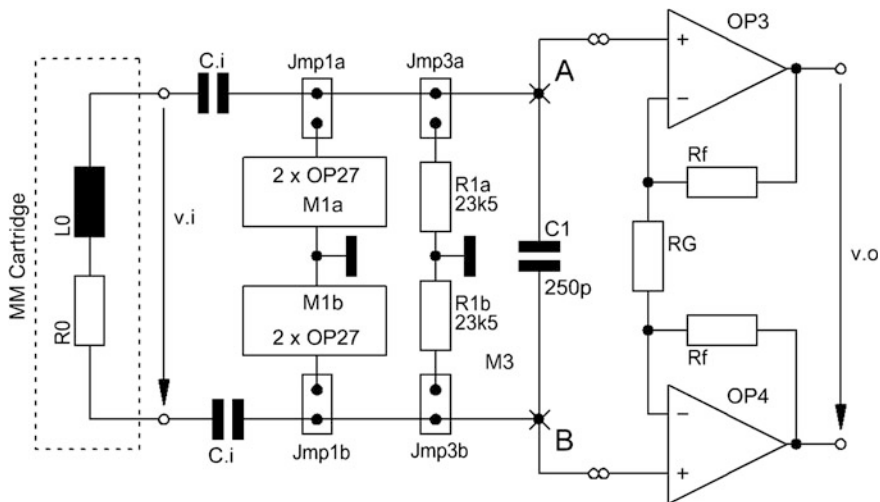


**Fig. 19.10** Input situation of a balanced phono-amp

It makes sense to choose the M2 noise reduction circuit for OPs1 & 2 input noise voltage densities  $>5$  nV/rtHz.

### 19.3 The Balanced Noise Reduction Approach

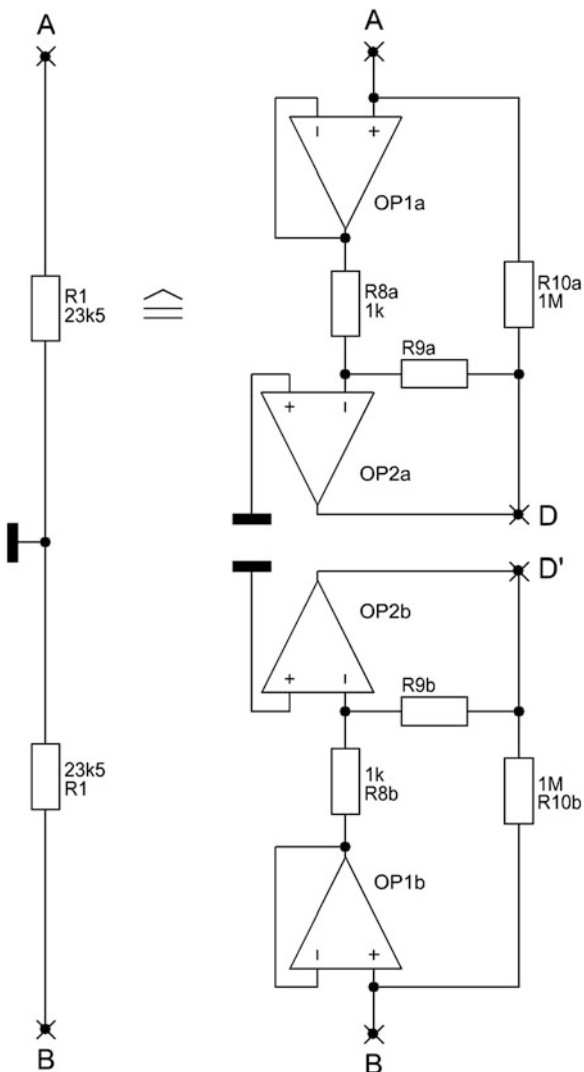
#### 19.3.1 Basics

To check the effectiveness of the chosen noise reduction measure<sup>6</sup> we need a balanced input configuration. For the here presented exercise I've chosen an adapted active input section à la Amp1, shown in Fig. 19.10, however, without RIAA network components. Nevertheless, the RIAA and A-weighting effects will be part of the calculation course. Another simplification comes from the synthesizing parts. I'll concentrate on the M1 mode because I don't see very big advantages of M2 and M1 works with a smaller number of components.

If we set in Fig. 19.10 two jumpers Jmp1a & Jmp1b simultaneously or the two Jmp3a & Jmp3b simultaneously, then, we can simply select between the M1 or M3 mode of the input circuit. Figure 19.11 shows the internal circuits of M1a and M1b. Basically, they look like two versions of the Fig. 19.7 one. However, because of the halving of the input voltage between A and ground (between B and ground too) and without touching the overload performance of the un-balanced version the gain of the OP2a and OP2b stage can nearly be doubled.

<sup>6</sup>See detailed calculation course in MCD-WS 20.2.

**Fig. 19.11** ELS of  $R1a + R1b$



The following equations are essential to understand how the Figs. 19.10 and 19.11 circuits work.<sup>7</sup>

<sup>7</sup>See Chaps. 22 and 23 for further details.

- Gain of a DIF amp with equal op-amps and equal Rf values:

$$\begin{aligned} G_{\text{dif}} &= \frac{V_o}{V_i} \\ &= 1 + \frac{2R_f}{R_G} \end{aligned} \quad (19.5)$$

- Gain of M1a or M1b:

$$G_{M1a} = -\frac{R_9}{R_8} \quad (19.6)$$

$$G_{M1b} = G_{M1a} \quad (19.7)$$

- The value of R10a or R10b:

$$R10a = (|G_{M1a}| + 1)R1a \quad (19.8)$$

$$R10b = R10a \quad (19.9)$$

- The gain  $G_{M1}$  can thus be obtained as follows:

$$|G_{M1a}| = \frac{R10a}{R1a} - 1 \quad (19.10)$$

- And the new R10a or R10b based noise current looks like:

$$\begin{aligned} i_{n,R1a,M1a} &= \sqrt{\frac{4kTB_1}{R10a}} \\ &= i_{n,R1b,M1b} \end{aligned} \quad (19.11)$$

$$i_{n,R1,M1a,b} = \left( \frac{1}{i_{n,R1a,M1a}^2} + \frac{1}{i_{n,R1b,M1b}^2} \right)^{-2} \quad (19.12)$$

- Hence, the new noise current becomes very much smaller than the original one:

$$i_{n,R1,M1a,b} \ll i_{n,R1a} = i_{n,R1b} \quad (19.13)$$

- Thus, the new noise voltage densities become very much smaller too:

$$e_{n,R1,M1ab} = i_{n,R1,M1a,b}(R1a + R1b) \quad (19.14)$$



- Improvements expressed in numbers<sup>8</sup>:
  - $i_{n,R1.M1a,b} = 91.01 \text{ fA/rtHz}$  instead of  $593.72 \text{ fA/rtHz}$  with M3
  - $e_{n,R1.M1a,b} = 4.28 \text{ nV/rtHz}$  instead of  $27.90 \text{ nV/rtHz}$  with M3

The left numbers look smaller than the ones of Sect. 19.2.2. However, compared with the un-balanced case the DIF amps higher input referred noise voltage density will worsen the resultant SNs a bit.

### 19.3.2 Results

With a Standard cartridge we gain a calculated difference of 3.23 dB between the input referred SN of the M1 version and the M3 version, A-weighted and RIAA equalized. I must point out that the input capacitance C1 plays a significant role here too. My standard value is 250 pF, however, with eg 450 pF the differences from above change to 3.5 dB.

### 19.3.3 Consequences

Generally and calculated, the balanced approach yields a better SN improvement than the un-balanced approach, provided that the active devices are of the same type at the same place. There's nothing new apart from the findings already mentioned in Sect. 19.2.5 and, concerning overload, in Sect. 19.2.2.

---

## 19.4 SN Calculations

Compared with the corresponding content of TSOS-1 & TSOS-2 concerning SN calculations there's nothing new in the un-balanced environment. Concerning SN calculations of DIF amps I recommend studying Chaps. 22 and 23.

---

<sup>8</sup>According to MCD-WS 20.2.

## Contents

- 20.1 MCD-WS: The Un-Balanced Version
- 20.2 MCD-WS: The Balanced Version

**Note 1:** MCD 11 has no built-in unit “rtHz” or “ $\sqrt{\text{Hz}}$ ”. To get  $\sqrt{1 \text{ Hz}}$  based voltage noise and current noise densities the rms noise voltage and current in a specific frequency range  $B > 1 \text{ Hz}$  must be multiplied by  $\sqrt{1 \text{ Hz}}$  and divided by the root of that specific frequency range  $\sqrt{B}$ !

**Note 2:** MCD 11 offers no “dB” unit. This is available from MCD 13 on!

20.1 MCD-WS: The Un-Balanced Version

Electronic Load Synthesis ELS - un-balanced version  
 (+ Standard Cartridge + 3 x OP27+1 x OP37)

20.1 Definition of physical constants and frequency ranges :

$T := 300 \cdot K$                        $k := 1.38065 \cdot 10^{-23} \cdot V \cdot A \cdot s \cdot K^{-1}$                        $q := 1.6021765 \cdot 10^{-19} \cdot A \cdot s$   
 $B_{20k} := 19980 Hz$                        $B_1 := 1 Hz$                        $h := 1000 Hz$                        $g := 10^4 Hz$                        $f := 20 Hz, 25 Hz, \dots, 20000 Hz$

20.2 Definition of components, nominal input voltage, and calculation of the input impedance :

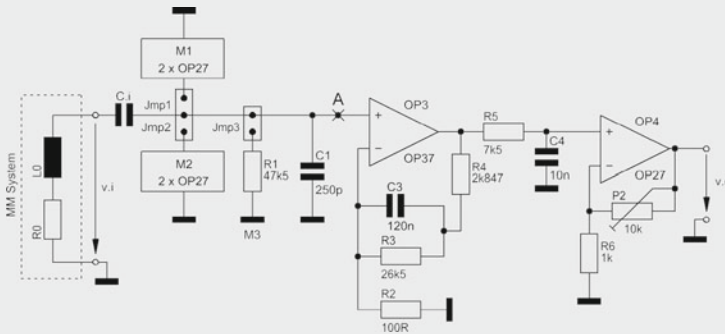


Fig. 20.1 = Fig. 19.5

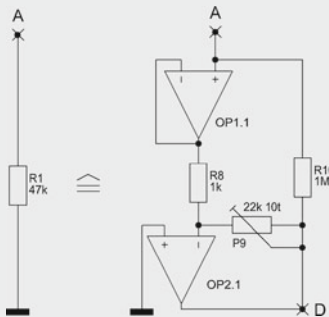


Fig. 20.2 = Fig. 19.7

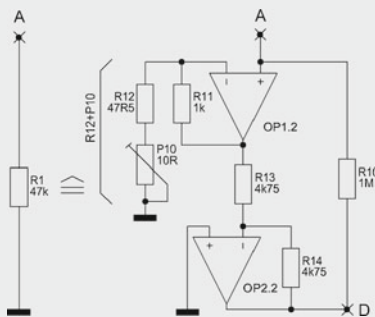


Fig. 20.3 = Fig. 19.9

20.1 MCD-WS: The Un-Balanced Version

$$\begin{aligned}
 R0 &:= 10^3 \Omega & L0 &:= 0.5H & C1 &:= 250 \cdot 10^{-12}F & R1 &:= 47 \cdot 10^3 \Omega \\
 R8 &:= 1 \cdot 10^3 \Omega & R11 &:= 1 \cdot 10^3 \Omega & R12 &:= 47.5 \cdot \Omega & R13 &:= 4.75 \cdot 10^3 \Omega & R14 &:= R13 \\
 R_{A.M1} &:= 47 \cdot 10^3 \Omega & R_{A.M2} &:= R_{A.M1}
 \end{aligned}$$

succ-apps of P9 and P10 will lead to R10= 1.000MΩ

$$\begin{aligned}
 P9 &:= 20.2766 \cdot 10^3 \Omega & G_{M1} &:= \frac{P9}{R8} & G_{M1} &= -20.277 \\
 R10_{M1} &:= R_{A.M1} \cdot (|G_{M1}| + 1) & R10_{M1} &= 1 \times 10^6 \Omega
 \end{aligned}$$

$$P10 := 4.3763 \Omega \quad G_{M2} := \left(1 + \frac{R11}{R12 + P10}\right) \cdot \left(\frac{R13}{R14}\right) \quad G_{M2} = -20.277$$

$$P10 + R12 = 51.876 \Omega \quad R10_{M2} := R_{A.M2} \cdot (|G_{M2}| + 1) \quad R10_{M2} = 1 \times 10^6 \Omega$$

$$\Rightarrow R_C \text{ in both cases :} \quad R_C := R10_{M1} - R_{A.M1} \quad R_C = 953 \times 10^3 \Omega$$

$$Z_{tot1}(f) := \left(\frac{1}{R0 + 2j \cdot \pi \cdot f \cdot L0} + 2j \cdot \pi \cdot f \cdot C1 + \frac{1}{R_{A.M1}}\right)^{-1} \quad |Z_{tot1}(h)| = 3.237 \times 10^3 \Omega$$

$$Z_{tot2}(f) := \left(\frac{1}{R0 + 2j \cdot \pi \cdot f \cdot L0} + 2j \cdot \pi \cdot f \cdot C1 + \frac{1}{R_{A.M2}}\right)^{-1} \quad |Z_{tot2}(h)| = 3.237 \times 10^3 \Omega$$

$$Z_{tot3}(f) := \left(\frac{1}{R0 + 2j \cdot \pi \cdot f \cdot L0} + 2j \cdot \pi \cdot f \cdot C1 + \frac{1}{R1}\right)^{-1} \quad |Z_{tot3}(h)| = 3.237 \times 10^3 \Omega$$

$$v_{i,nom} := 5 \cdot 10^{-3}V$$

$$OP1 = OP27 \quad OP2 = OP27 \quad OP3 = OP37 \quad OP4 = OP27$$

$$f_{c,e1} := 2.7Hz \quad f_{c,e2} := f_{c,e1} \quad f_{c,e3} := 2.7Hz \quad f_{c,e4} := f_{c,e3}$$

$$e_{n,op1} := 3 \cdot 10^{-9}V \quad e_{n,op2} := e_{n,op1} \quad e_{n,op3} := 3 \cdot 10^{-9}V \quad e_{n,op4} := e_{n,op3}$$

$$e_{n,op1}(f) := e_{n,op1} \cdot \sqrt{1 + \frac{f_{c,e1}}{f}} \quad e_{n,op2}(f) := e_{n,op1}(f) \quad e_{n,op3}(f) := e_{n,op3} \cdot \sqrt{1 + \frac{f_{c,e3}}{f}} \quad e_{n,op4}(f) := e_{n,op3}(f)$$

$$f_{c,i1} := 140Hz \quad f_{c,i2} := f_{c,i1} \quad f_{c,i3} := 140Hz \quad f_{c,i4} := f_{c,i3}$$

$$i_{n,op1} := 0.4 \cdot 10^{-12}A \quad i_{n,op2} := i_{n,op1} \quad i_{n,op3} := 0.4 \cdot 10^{-12}A \quad i_{n,op4} := i_{n,op3}$$

$$i_{n,op1}(f) := i_{n,op1} \cdot \sqrt{1 + \frac{f_{c,i1}}{f}} \quad i_{n,op2}(f) := i_{n,op1}(f) \quad i_{n,op3}(f) := i_{n,op3} \cdot \sqrt{1 + \frac{f_{c,i3}}{f}} \quad i_{n,op4}(f) := i_{n,op3}(f)$$

20.1 MCD-WS: The Un-Balanced Version

20.3 Graphs of input impedance ( $Z_{tot1}(f) = Z_{tot2}(f) = Z_{tot3}(f)$  if  $R_A = R1$ ):

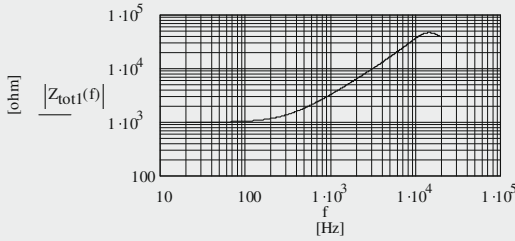


Fig. 20.4  
Input impedance of the Fig. 20.1  
phono-amp input load

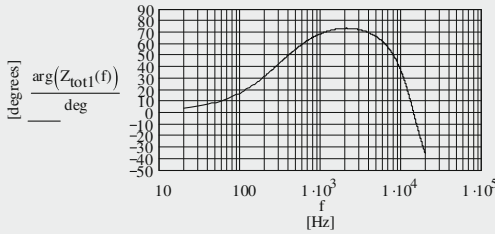


Fig. 20.5  
Phase of the Fig. 20.1 phono-amp  
input load

20.4 Calculation of the noise voltages, currents, and the virtual temperature of the three different input impedance components M1 ... M3 :

$$e_{n.R0} := \sqrt{4 \cdot k \cdot T \cdot R0 \cdot B1}$$

$$e_{n.R0} = 4.07 \times 10^{-9} \text{ V}$$

Version M1 :

$$i_{h.R1.M1} := \sqrt{\frac{4 \cdot k \cdot T \cdot B1}{(|G_{M1}| + 1) \cdot R_{A.M1}}}$$

$$i_{h.R1.M1} = 128.716 \times 10^{-15} \text{ A}$$

$$e_{n.R1.M1} := i_{h.R1.M1} \cdot R_{A.M1}$$

$$e_{n.R1.M1} = 6.05 \times 10^{-9} \text{ V}$$

$$T_{M1} := \frac{e_{n.R1.M1}^2}{4 \cdot k \cdot B1 \cdot R_{A.M1}}$$

$$T_{M1} = 14.1 \text{ K}$$

Version M2 :

$$i_{h.R1.M2} := \sqrt{\frac{4 \cdot k \cdot T \cdot B1}{(|G_{M2}| + 1) \cdot R_{A.M2}}}$$

$$i_{h.R1.M2} = 128.716 \times 10^{-15} \text{ A}$$

## 20.1 MCD-WS: The Un-Balanced Version

Page 4

$$e_{n.R1.M2} := i_{n.R1.M2} \cdot R_{A.M2}$$

$$e_{n.R1.M2} = 6.05 \times 10^{-9} \text{ V}$$

$$T_{M2} := \frac{e_{n.R1.M2}^2}{4 \cdot k \cdot B_1 \cdot R_{A.M2}}$$

$$T_{M2} = 14.1 \text{ K}$$

Version M3 :

$$e_{n.R1.M3} := \sqrt{4 \cdot k \cdot T \cdot R_1 \cdot B_1}$$

$$e_{n.R1.M3} = 27.905 \times 10^{-9} \text{ V}$$

$$i_{n.R1.M3} := \sqrt{\frac{4 \cdot k \cdot T \cdot B_1}{R_1}}$$

$$i_{n.R1.M3} = 593.722 \times 10^{-15} \text{ A}$$

20.5 The input voltage dividers (see TSOS-1 Ch. 4 and TSOS-2 Ch. 13):

$$Z_0(f) := R_0 + 2j \cdot \pi \cdot f \cdot L_0 \quad Z_{1a}(f) := \left( \frac{1}{Z_0(f)} + 2j \cdot \pi \cdot f \cdot C_1 \right)^{-1}$$

with  $R_A$  = synthesized  $R_1$ 

$$Z_{M1}(f) := \left( \frac{1}{R_{A.M1}} + 2j \cdot \pi \cdot f \cdot C_1 \right)^{-1}$$

$$Z_{M2}(f) := Z_{M1}(f)$$

$$e_{n1.M1}(f) := e_{n.R0} \cdot \frac{Z_{M1}(f)}{Z_0(f) + Z_{M1}(f)}$$

$$|e_{n1.M1}(h)| = 3.996 \times 10^{-9} \text{ V}$$

$$e_{n1.M2}(f) := e_{n1.M1}(f)$$

$$e_{n2.M1}(f) := e_{n.R1.M1} \cdot \frac{Z_{1a}(f)}{Z_{1a}(f) + R_{A.M1}}$$

$$|e_{n2.M1}(h)| = 416.599 \times 10^{-12} \text{ V}$$

$$e_{n2.M2}(f) := e_{n2.M1}(f)$$

$$e_{n.i.M1}(f) := \sqrt{\left( |e_{n1.M1}(f)| \right)^2 + \left( |e_{n2.M1}(f)| \right)^2}$$

$$|e_{n.i.M1}(h)| = 4.018 \times 10^{-9} \text{ V}$$

$$e_{n.i.M2}(f) := e_{n.i.M1}(f)$$

with  $R_1$ :

$$Z_{M3}(f) := \left( \frac{1}{R_1} + 2j \cdot \pi \cdot f \cdot C_1 \right)^{-1}$$

20.1 MCD-WS: The Un-Balanced Version

$$e_{n1.M3}(f) := e_{n.R0} \frac{Z_{M3}(f)}{Z0(f) + Z_{M3}(f)} \quad |e_{n1.M3}(h)| = 3.996 \times 10^{-9} \text{ V}$$

$$e_{n2.M3}(f) := e_{n.R1.M3} \frac{Z1a(f)}{Z1a(f) + R1} \quad |e_{n2.M3}(h)| = 1.922 \times 10^{-9} \text{ V}$$

$$e_{n.i.M3}(f) := \sqrt{(|e_{n1.M3}(f)|)^2 + (|e_{n2.M3}(f)|)^2} \quad |e_{n.i.M3}(h)| = 4.434 \times 10^{-9} \text{ V}$$

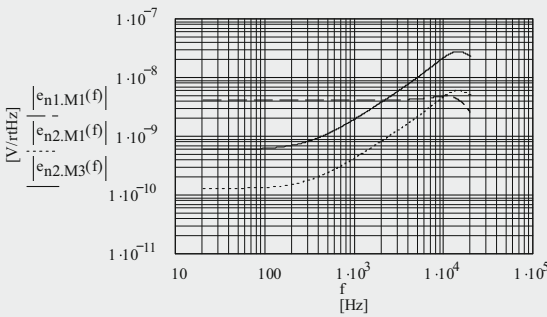


Fig. 20.6  
Noise voltage density  
of the three different  
input voltage dividers

$$e_{n.R0}(f) := e_{n.R0} \quad e_{n.R1}(f) := e_{n.R1.M3}$$

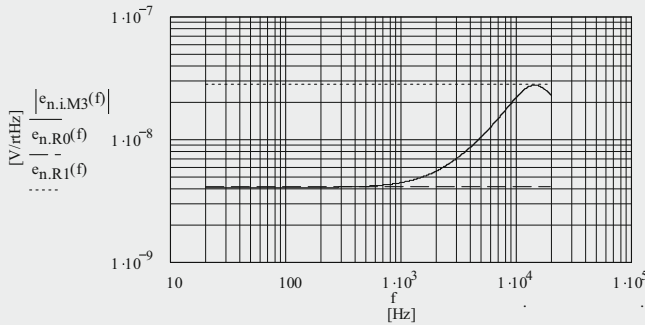


Fig. 20.7 = Fig. 19.6

6. Calculation of the noise effect of RIAA feedback network and the input noise voltage of the phono-amp (noise of OP4 + components = ignorable) :

$$R2 := 100\Omega \quad R3 := 26.5 \cdot 10^3 \Omega \quad R4 := 2.847 \cdot 10^3 \Omega \quad C3 := 120 \cdot 10^{-9} \text{ F}$$

20.1 MCD-WS: The Un-Balanced Version

$$Z3(f) := R4 + \left(2j \cdot \pi \cdot f \cdot C3 + \frac{1}{R3}\right)^{-1} \quad Z4(f) := \left(\frac{1}{R2} + \frac{1}{Z3(f)}\right)^{-1} \quad e_{n,Z4}(f) := \sqrt{4 \cdot k \cdot T \cdot |Z4(f)| \cdot B1}$$

$$e_{n,i.riid}(f) := \sqrt{e_{n,op3}(f)^2 + i_{n,op3}(f)^2 \cdot (|Z4(f)|)^2 + e_{n,Z4}(f)^2} \quad |e_{n,i.riid}(h)| = 3.261 \times 10^{-9} \text{ V}$$

20.7 Calculation of the noise effects of OP1.x and OP2.y :

$$G_{N,op2.1} := -\left(1 + \frac{P9}{R8}\right) \quad G_{N,op2.1} = -21.277$$

$$e_{n,R8} := \sqrt{4 \cdot k \cdot T \cdot B1 \cdot R8} \quad e_{n,R8} = 4.07 \times 10^{-9} \text{ V}$$

$$e_{n,P9} := \sqrt{4 \cdot k \cdot T \cdot B1 \cdot P9} \quad e_{n,P9} = 18.329 \times 10^{-9} \text{ V}$$

$$e_{n.o.op2.1.tot}(f) := \sqrt{\left(|G_{N,op2.1}|\right)^2 \cdot e_{n,op2}(f)^2 + \left(\frac{P9}{R8}\right)^2 \cdot e_{n,R8}^2 + e_{n,P9}^2 + i_{n,op2}(f)^2 \cdot P9^2}$$

$$e_{n.o.op2.1.tot}(h) = 106.338 \times 10^{-9} \text{ V}$$

$$e_{n.o.M1}(f) := \sqrt{e_{n,op1}(f)^2 \cdot (|G_{M1}|)^2 + e_{n.o.op2.1.tot}(f)^2} \quad e_{n.o.M1}(h) = 122.548 \times 10^{-9} \text{ V}$$

$$e_{n.M1.eff}(f) := e_{n.o.M1}(f) \cdot \left| \frac{Z_{tot1}(f)}{R10_{M1} + Z_{tot1}(f)} \right| \quad e_{n.M1.eff}(h) = 396.165 \times 10^{-12} \text{ V}$$

$$e_{n,R11} := \sqrt{4 \cdot k \cdot T \cdot B1 \cdot R11} \quad e_{n,R11} = 4.07 \times 10^{-9} \text{ V}$$

$$e_{n,P10} := \sqrt{4 \cdot k \cdot T \cdot B1 \cdot (R12 + P10)} \quad e_{n,P10} = 927.079 \times 10^{-12} \text{ V}$$

$$e_{n.i.op1.2}(f) := \sqrt{e_{n,op1}(f)^2 + i_{n,op1}(f)^2 \cdot [R11^{-1} + (R12 + P10)^{-1}]^{-2} + \left(\frac{1}{e_{n,R11}} + \frac{1}{e_{n,P10}}\right)^{-1}}$$

$$e_{n.i.op1.2}(h) = 3.137 \times 10^{-9} \text{ V}$$

$$G_{N,op2.2} := -\left(1 + \frac{R14}{R13}\right) \quad G_{N,op2.2} = -2$$

$$e_{n,R13} := \sqrt{4 \cdot k \cdot T \cdot B1 \cdot R13} \quad e_{n,R13} = 8.871 \times 10^{-9} \text{ V} \quad e_{n,R14} := e_{n,R13}$$

$$e_{n.o.op2.2.tot}(f) := \sqrt{\left(|G_{N,op2.2}|\right)^2 \cdot e_{n,op2}(f)^2 + \left(\frac{R14}{R13}\right)^2 \cdot e_{n,R13}^2 + e_{n,R14}^2 + i_{n,op2}(f)^2 \cdot R14^2}$$

$$e_{n.o.op2.2.tot}(h) = 14.057 \times 10^{-9} \text{ V}$$



20.1 MCD-WS: The Un-Balanced Version

$$e_{n.o.M2(f)} := \sqrt{e_{n.i.op1.2(f)}^2 \cdot (|G_{M2}|)^2 + e_{n.o.op2.2.tot(f)}^2} \quad e_{n.o.M2(h)} = 65.146 \times 10^{-9}V$$

$$e_{n.M2.eff(f)} := e_{n.o.M2(f)} \cdot \left| \frac{Z_{tot2(f)}}{R_{10M2} + Z_{tot2(f)}} \right| \quad e_{n.M2.eff(h)} = 210.598 \times 10^{-12}V$$

8. Graph and calculation of the different total input referred noise voltages :

$$e_{n.i.tot.M1(f)} := \sqrt{e_{n.i.riid(f)}^2 + e_{n.i.M1(f)}^2 + e_{n.M1.eff(f)}^2 + (i_{n.op3(f)} \cdot |Z_{tot1(f)}|)^2} \quad |e_{n.i.tot.M1(g)}| = 16.974 \times 10^{-9}V$$

$$e_{n.i.tot.M2(f)} := \sqrt{e_{n.i.riid(f)}^2 + e_{n.i.M2(f)}^2 + e_{n.M2.eff(f)}^2 + (i_{n.op3(f)} \cdot |Z_{tot2(f)}|)^2} \quad |e_{n.i.tot.M2(g)}| = 16.574 \times 10^{-9}V$$

$$e_{n.i.tot.M3(f)} := \sqrt{e_{n.i.riid(f)}^2 + e_{n.i.M3(f)}^2 + (i_{n.op3(f)} \cdot |Z_{tot3(f)}|)^2} \quad |e_{n.i.tot.M3(g)}| = 26.72 \times 10^{-9}V$$

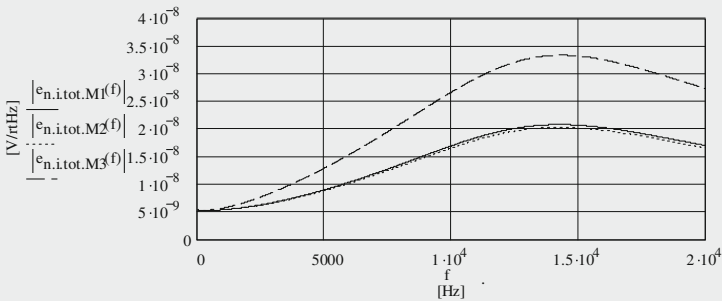


Fig. 20.8 Total input noise voltage densities at the input of the phono-amp (A)

9. Calculation of SNs : .

9.1 Non-equalized :

$$SN_{ne.M1} := 20 \cdot \log \left[ \frac{\sqrt{\frac{1}{B_1} \int_{20Hz}^{2000Hz} (|e_{n.i.tot.M1(f)}|)^2 df}}{v_{i.nom}} \right] \quad SN_{ne.M1} = -67.133 \quad [dB]$$

20.1 MCD-WS: The Un-Balanced Version

$$SN_{ne.M2} := 20 \cdot \log \left[ \frac{\sqrt{\frac{1}{B_1} \int_{20\text{Hz}}^{2000\text{Hz}} \left( |e_{n.i.tot.M2}(f) \right)^2 df}}{v_{i.nom}} \right] \quad SN_{ne.M2} = -67.338 \quad [\text{dB}]$$

$$SN_{ne.M3} := 20 \cdot \log \left[ \frac{\sqrt{\frac{1}{B_1} \int_{20\text{Hz}}^{2000\text{Hz}} \left( |e_{n.i.tot.M3}(f) \right)^2 df}}{v_{i.nom}} \right] \quad SN_{ne.M3} = -63.181 \quad [\text{dB}]$$

$$SN_{ne.D1} := SN_{ne.M1} - SN_{ne.M3} \quad SN_{ne.D1} = -3.952 \quad [\text{dB}]$$

$$SN_{ne.D2} := SN_{ne.M2} - SN_{ne.M3} \quad SN_{ne.D2} = -4.157 \quad [\text{dB}]$$

$$SN_{ne.D3} := SN_{ne.M2} - SN_{ne.M1} \quad SN_{ne.D3} = -0.205 \quad [\text{dB}]$$

9.2 RIAA-equalized :

$$R_{1000} := \left[ \frac{\sqrt{1 + \left( 2 \cdot \pi \cdot 10^3 \text{Hz} \cdot 318 \cdot 10^{-6} \text{s} \right)^2}}{\sqrt{1 + \left( 2 \cdot \pi \cdot 10^3 \text{Hz} \cdot 3180 \cdot 10^{-6} \text{s} \right)^2} \cdot \sqrt{1 + \left( 2 \cdot \pi \cdot 10^3 \text{Hz} \cdot 75 \cdot 10^{-6} \text{s} \right)^2}} \right]^{-1} \quad R_{1000} = 9.898$$

$$R(f) := \left[ \frac{\sqrt{1 + \left( 2 \cdot \pi \cdot f \cdot 318 \cdot 10^{-6} \text{s} \right)^2}}{\sqrt{1 + \left( 2 \cdot \pi \cdot f \cdot 3180 \cdot 10^{-6} \text{s} \right)^2} \cdot \sqrt{1 + \left( 2 \cdot \pi \cdot f \cdot 75 \cdot 10^{-6} \text{s} \right)^2}} \right] \cdot R_{1000}$$

$$SN_{riaa.M1} := 20 \cdot \log \left[ \frac{\sqrt{\frac{1}{B_1} \int_{20\text{Hz}}^{2000\text{Hz}} \left( |e_{n.i.tot.M1}(f) \right)^2 \cdot (|R(f)|)^2 df}}{v_{i.nom}} \right] \quad SN_{riaa.M1} = -78.114 \quad [\text{dB}]$$

$$SN_{riaa.M2} := 20 \cdot \log \left[ \frac{\sqrt{\frac{1}{B_1} \int_{20\text{Hz}}^{2000\text{Hz}} \left( |e_{n.i.tot.M2}(f) \right)^2 \cdot (|R(f)|)^2 df}}{v_{i.nom}} \right] \quad SN_{riaa.M2} = -78.202 \quad [\text{dB}]$$

$$SN_{riaa.M3} := 20 \cdot \log \left[ \frac{\sqrt{\frac{1}{B_1} \int_{20\text{Hz}}^{2000\text{Hz}} |e_{n.i.tot.M3}(f)|^2 \cdot (|R(f)|)^2 df}}{v_{i.nom}} \right] \quad SN_{riaa.M3} = -75.979 \quad [\text{dB}]$$

20.1 MCD-WS: The Un-Balanced Version

$$SN_{riaa.D1} := SN_{riaa.M1} - SN_{riaa.M3} \qquad SN_{riaa.D1} = -2.135 \qquad [dB]$$

$$SN_{riaa.D2} := SN_{riaa.M2} - SN_{riaa.M3} \qquad SN_{riaa.D2} = -2.223 \qquad [dB]$$

$$SN_{riaa.D3} := SN_{riaa.M2} - SN_{riaa.M1} \qquad SN_{riaa.D3} = -0.088 \qquad [dB]$$

9.3 Non-equalized but A-weighted :

Definition of A-filter frequencies and transfer function:

$$f_1 := 20.6Hz \quad f_2 := f_1 \quad f_3 := 107.7Hz \quad f_4 := 737.9Hz \quad f_5 := 12200Hz \quad f_6 := f_5 \quad f_G := 1000Hz$$

$$v_{1000} := \left[ \sqrt{1 + \left(\frac{f_1}{f_G}\right)^2} \right]^2 \cdot \sqrt{1 + \left(\frac{f_3}{f_G}\right)^2} \cdot \sqrt{1 + \left(\frac{f_4}{f_G}\right)^2} \cdot \left[ \sqrt{1 + \left(\frac{f_5}{f_6}\right)^2} \right]^2 \qquad v_{1000} = 1.259$$

$$A(f) := v_{1000} \left[ \frac{1}{\sqrt{1 + \left(\frac{f_1}{f}\right)^2}} \right]^2 \cdot \frac{1}{\sqrt{1 + \left(\frac{f_3}{f}\right)^2}} \cdot \frac{1}{\sqrt{1 + \left(\frac{f_4}{f}\right)^2}} \cdot \left[ \frac{1}{\sqrt{1 + \left(\frac{f}{f_5}\right)^2}} \right]^2$$

$$SN_{a.M1} := 20 \cdot \log \left[ \frac{\sqrt{\frac{1}{B_1} \cdot \int_{20Hz}^{2000Hz} \left( |e_{n.i.tot.M1}(f)| \right)^2 \cdot (|A(f)|)^2 df}}{v_{i.nom}} \right] \qquad SN_{a.M1} = -71.028 \qquad [dB(A)]$$

$$SN_{a.M2} := 20 \cdot \log \left[ \frac{\sqrt{\frac{1}{B_1} \cdot \int_{20Hz}^{2000Hz} \left( |e_{n.i.tot.M2}(f)| \right)^2 \cdot (|A(f)|)^2 df}}{v_{i.nom}} \right] \qquad SN_{a.M2} = -71.219 \qquad [dB(A)]$$

$$SN_{a.M3} := 20 \cdot \log \left[ \frac{\sqrt{\frac{1}{B_1} \cdot \int_{20Hz}^{2000Hz} \left( |e_{n.i.tot.M3}(f)| \right)^2 \cdot (|A(f)|)^2 df}}{v_{i.nom}} \right] \qquad SN_{a.M3} = -67.289 \qquad [dB(A)]$$

$$SN_{a.D1} := SN_{a.M1} - SN_{a.M3} \qquad SN_{a.D1} = -3.739 \qquad [dB]$$

$$SN_{a.D2} := SN_{a.M2} - SN_{a.M3} \qquad SN_{a.D2} = -3.93 \qquad [dB]$$

$$SN_{a.D3} := SN_{a.M2} - SN_{a.M1} \qquad SN_{a.D3} = -0.191 \qquad [dB]$$

20.1 MCD-WS: The Un-Balanced Version

9.4 RIAA-equalized and A-weighted :

$$SN_{ariaa.M1} := 20 \cdot \log \left[ \frac{\sqrt{\frac{1}{B_1} \int_{20\text{Hz}}^{20000\text{Hz}} (|e_{n.i.tot.M1}(f)|)^2 \cdot (|A(f)|)^2 \cdot (|R(f)|)^2 df}}{v_{i.nom}} \right]$$

$SN_{ariaa.M1} = -81.405 \quad [\text{dB(A)}]$

$$SN_{ariaa.M2} := 20 \cdot \log \left[ \frac{\sqrt{\frac{1}{B_1} \int_{20\text{Hz}}^{20000\text{Hz}} (|e_{n.i.tot.M2}(f)|)^2 \cdot (|A(f)|)^2 \cdot (|R(f)|)^2 df}}{v_{i.nom}} \right]$$

$SN_{ariaa.M2} = -81.525 \quad [\text{dB(A)}]$

$$SN_{ariaa.M3} := 20 \cdot \log \left[ \frac{\sqrt{\frac{1}{B_1} \int_{20\text{Hz}}^{20000\text{Hz}} (|e_{n.i.tot.M3}(f)|)^2 \cdot (|A(f)|)^2 \cdot (|R(f)|)^2 df}}{v_{i.nom}} \right]$$

$SN_{ariaa.M3} = -78.745 \quad [\text{dB(A)}]$

$SN_{ariaa.D1} := SN_{ariaa.M1} - SN_{ariaa.M3} \quad SN_{ariaa.D1} = -2.66 \quad [\text{dB}]$

$SN_{ariaa.D2} := SN_{ariaa.M2} - SN_{ariaa.M3} \quad SN_{ariaa.D2} = -2.78 \quad [\text{dB}]$

$SN_{ariaa.D3} := SN_{ariaa.M2} - SN_{ariaa.M1} \quad SN_{ariaa.D3} = -0.12 \quad [\text{dB}]$

20.1 MCD-WS: The Un-Balanced Version

10. Derivation of the reduced noise voltage of the nominal input load of 47kΩ:

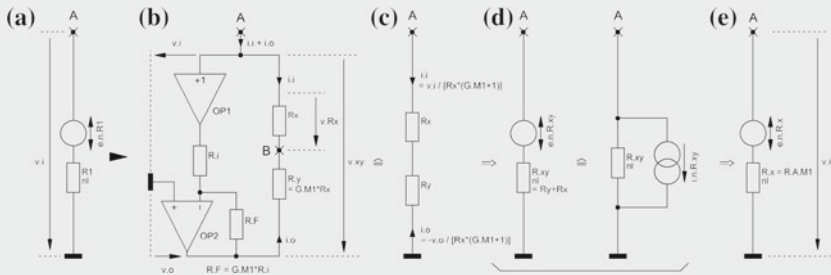


Fig. 20.9 Derivation sequence

Fig. 20.9 a)

$$v_i := v_{i,nom} \quad R_1 := 47 \cdot 10^3 \Omega \quad e_{n,R1} := \sqrt{4 \cdot k \cdot T \cdot B_1 \cdot R_1} \quad e_{n,R1} = 27.905 \times 10^{-9} V$$

$$i_{n,R1} := \frac{v_i}{R_1} \quad i_{n,R1} = 593.722 \times 10^{-15} A$$

$$i_{L,nom} := \frac{v_i}{R_1} \quad i_{L,nom} = 106.383 \times 10^{-9} A$$

Fig. 20.9 b)

we choose  $R_1 = 1k\Omega$  and an overload-friendly gain  $|G_{M1}| \sim 20$ :  $R_1 := 1 \cdot 10^3 \Omega$   $G_{M1} := -20$

Fig. 20.9 c)

If  $R_x := 47 \cdot 10^3 \Omega$  then  $R_y$  becomes  $R_y := |G_{M1}| \cdot R_x$   $R_y = 940 \times 10^3 \Omega$

Fig. 20.9 d)

$$R_{xy} := R_x + R_y \quad R_{xy} = 987 \times 10^3 \Omega$$

succ-apps of  $R_F$  should lead to an easier-to-handle  $R_{xy} = 1M\Omega$  and the final value for  $G_{M1}$ :  $R_F := 20.2766 \cdot 10^3 \Omega$

$$G_{M1} := -\frac{R_F}{R_1} \quad G_{M1} = -20.277 \quad R_{xy} := R_x \cdot |G_{M1}| + R_x \quad R_{xy} = 1 \times 10^6 \Omega$$

=>  $R_y := R_{xy} - R_x$   $R_y = 953 \times 10^3 \Omega$

20.1 MCD-WS: The Un-Balanced Version

The value of  $G_{M1}$  must equal the ration of  $i_o / i_i$ , hence:

$$v_o := v_i \cdot |G_{M1}| \quad v_o = 101.383 \times 10^{-3} \text{V}$$

$$i_i := \frac{v_i}{(|G_{M1}| + 1) \cdot R_x} \quad i_i = 5 \times 10^{-9} \text{A} \quad i_o := \frac{-v_o}{R_x \cdot (1 + |G_{M1}|)} \quad i_o = -101.383 \times 10^{-9} \text{A}$$

$$\Rightarrow \quad \left| \frac{i_o}{i_i} \right| = 20.277 \quad i_{res1} := i_i + i_o \quad i_{res1} = -96.383 \times 10^{-9} \text{A}$$

$$i_{res2} := \frac{v_i}{(|G_{M1}| + 1) \cdot R_x} + \frac{-v_i \cdot |G_{M1}|}{R_x \cdot (1 + |G_{M1}|)} \quad i_{res2} := \frac{-v_i \cdot (|G_{M1}| - 1)}{R_x \cdot (|G_{M1}| + 1)} \quad i_{res2} = -96.383 \times 10^{-9} \text{A}$$

$$\Rightarrow \quad i_{res1} = i_{res2}$$

Fig. 20.9 e) & d)

$$v_{R.xy} := i_{res1} \cdot R_x \cdot (|G_{M1}| + 1) \quad v_{R.xy} = -96.383 \times 10^{-3} \text{V}$$

$$v_{R.x} := i_{res1} \cdot R_x \quad v_{R.x} = -4.53 \times 10^{-3} \text{V}$$

$$\frac{v_{R.x}}{v_{R.xy}} = \frac{R_x}{R_{xy}} \quad R_x := R_{xy} \cdot \frac{v_{R.x}}{v_{R.xy}} \quad R_x := R_{A.M1} \quad \Rightarrow \quad R_{A.M1} = 47 \times 10^3 \Omega$$

$$e_{n.R.xy} := \sqrt{4 \cdot k \cdot T \cdot B_1 \cdot R_{xy}} \quad e_{n.R.xy} = 128.716 \times 10^{-9} \text{V}$$

=> noise voltage approach to get the noise voltage of the synthesized 47kΩ resistor :

$$\frac{e_{n.R.x}}{e_{n.R.xy}} = \frac{R_x}{R_{xy}} \quad e_{n.R.x} := \frac{R_x}{R_{xy}} \cdot e_{n.R.xy} \quad e_{n.R.A.M1} := e_{n.R.x} \quad \Rightarrow \quad e_{n.R.A.M1} = 6.05 \times 10^{-9} \text{V}$$

=> noise current approach to get the noise voltage of the synthesized 47kΩ resistor:

$$i_{n.xy} := \sqrt{\frac{4 \cdot k \cdot T \cdot B_1}{R_{xy}}} \quad i_{n.xy} = 128.716 \times 10^{-15} \text{A} \quad e_{n.R.x} := i_{n.xy} \cdot R_x \quad \Rightarrow \quad e_{n.R.x} = 6.05 \times 10^{-9} \text{V}$$

$$\text{vs. } e_{n.R1} := 29.7 \cdot 10^{-9} \text{V}$$

20.2 MCD-WS: The Balanced Version

Electronic Load Synthesis ELS - balanced version  
(+ Standard Cartridge + 2 x OP27)

1. Definition of physical constants and frequency ranges :

$T := 300 \cdot K$                        $k := 1.38065 \cdot 10^{-23} \cdot V \cdot A \cdot s \cdot K^{-1}$                        $q := 1.6021765 \cdot 10^{-19} \cdot A \cdot s$   
 $B_{20k} := 19980 \text{ Hz}$                        $B_1 := 1 \text{ Hz}$                        $h := 1000 \text{ Hz}$                        $g := 10^4 \text{ Hz}$                        $f := 20 \text{ Hz}, 25 \text{ Hz}.. 20000 \text{ Hz}$

2. Definition of components, nominal input voltage, and calculation of the input impedance :

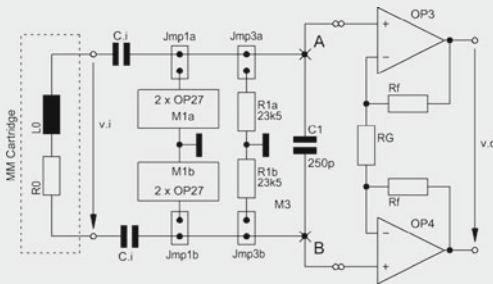


Fig. 20.10 = Fig. 19.10

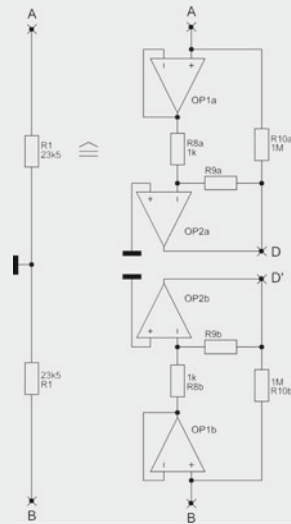


Fig. 20.11  
= Fig. 19.11

$R0 := 10^3 \Omega$                        $L0 := 0.5 \text{ H}$   
 $C1 := 250 \cdot 10^{-12} \text{ F}$   
 $R1a := 23.5 \cdot 10^3 \Omega$                        $R1b := R1a$   
 $R8a := 1 \cdot 10^3 \Omega$                        $R8b := R8a$   
 succ-apps of G leads to  $R10a = 1 \text{ M}\Omega$   
 $G_{M1a} := -41.56$                        $G_{M1b} := G_{M1a}$   
 $R9a := R8a \cdot |G_{M1a}|$                        $R9a = 41.56 \times 10^3 \Omega$   
 $R9b := R9a$   
 $R10a := (|G_{M1a}| + 1) \cdot R1a$   
 $R10a = 1 \times 10^6 \Omega$                        $R10b := R10a$

20.2 MCD-WS: The Balanced Version

$$Z_{tot1}(f) := \left( \frac{1}{R0 + 2j \cdot \pi \cdot f \cdot L0} + 2j \cdot \pi \cdot f \cdot C1 + \frac{1}{R1a + R1b} \right)^{-1} \quad |Z_{tot1}(h)| = 3.237 \times 10^3 \Omega$$

OP1b = OP1a                      OP2b = OP2a                       $v_{i,nom} := 5 \cdot 10^{-3} V$   
 OP1a = OP27                      OP2a = OP27                      OP3 = OP37                      OP4 = OP27  
 $f_{c,e1} := 2.7 Hz$                        $f_{c,e2} := f_{c,e1}$                        $f_{c,e3} := 2.7 Hz$                        $f_{c,e4} := f_{c,e3}$   
 $e_{n,op1} := 3 \cdot 10^{-9} V$                        $e_{n,op2} := e_{n,op1}$                        $e_{n,op3} := 3 \cdot 10^{-9} V$                        $e_{n,op4} := e_{n,op3}$   
 $e_{n,op1}(f) := e_{n,op1} \cdot \sqrt{1 + \frac{f_{c,e1}}{f}}$                        $e_{n,op2}(f) := e_{n,op1}(f)$                        $e_{n,op3}(f) := e_{n,op3} \cdot \sqrt{1 + \frac{f_{c,e3}}{f}}$                        $e_{n,op4}(f) := e_{n,op3}(f)$   
 $f_{c,i1} := 140 Hz$                        $f_{c,i2} := f_{c,i1}$                        $f_{c,i3} := 140 Hz$                        $f_{c,i4} := f_{c,i3}$   
 $i_{n,op1} := 0.4 \cdot 10^{-12} A$                        $i_{n,op2} := i_{n,op1}$                        $i_{n,op3} := 0.05 \cdot 10^{-12} A$                        $i_{n,op4} := i_{n,op3}$   
 $i_{n,op1}(f) := i_{n,op1} \cdot \sqrt{1 + \frac{f_{c,i1}}{f}}$                        $i_{n,op2}(f) := i_{n,op1}(f)$                        $i_{n,op3}(f) := i_{n,op3} \cdot \sqrt{1 + \frac{f_{c,i3}}{f}}$                        $i_{n,op4}(f) := i_{n,op3}(f)$

3. Graphs of input impedance  $Z_{tot1}(f)$ :

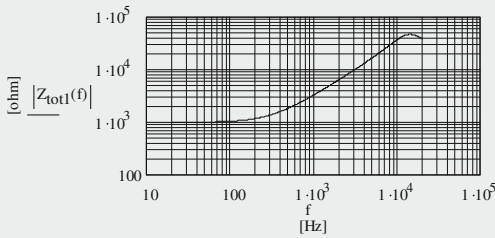


Fig. 20.12  
Input impedance of the Fig. 20.1  
phono-amp input load

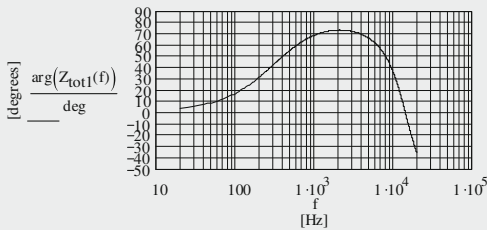


Fig. 20.13  
Phase of the Fig. 20.12 phono-amp  
input load



## 20.2 MCD-WS: The Balanced Version

Page 3

4. Calculation of the noise voltages & currents of the input impedance components M1 & M3 :

$$e_{n,R0} := \sqrt{4 \cdot k \cdot T \cdot R0 \cdot B1}$$

$$e_{n,R0} = 4.07 \times 10^{-9} \text{ V}$$

Version M1 :

$$i_{n,R1a.M1a} := \sqrt{\frac{4 \cdot k \cdot T \cdot B1}{(|G_{M1a}| + 1) \cdot R1a}} \quad i_{n,R1b.M1b} := i_{n,R1a.M1a} \quad i_{n,R1a.M1a} = 128.706 \times 10^{-15} \text{ A}$$

$$i_{n,R1.M1a.b} := \sqrt{\left( \frac{1}{i_{n,R1a.M1a}^2} + \frac{1}{i_{n,R1b.M1b}^2} \right)^{-1}} \quad i_{n,R1.M1a.b} = 91.009 \times 10^{-15} \text{ A}$$

$$e_{n,R1a.M1a} := i_{n,R1a.M1a} \cdot R1a \quad e_{n,R1b.M1b} := e_{n,R1a.M1a} \quad e_{n,R1a.M1a} = 3.025 \times 10^{-9} \text{ V}$$

$$e_{n,R1.M1a.b} := \sqrt{e_{n,R1a.M1a}^2 + e_{n,R1b.M1b}^2} \quad e_{n,R1.M1a.b} = 4.277 \times 10^{-9} \text{ V}$$

Version M3 :

$$e_{n,R1.M3a.b} := \sqrt{4 \cdot k \cdot T \cdot (R1a + R1b) \cdot B1} \quad e_{n,R1.M3a.b} = 27.905 \times 10^{-9} \text{ V}$$

$$i_{n,R1.M3a.b} := \sqrt{\frac{4 \cdot k \cdot T \cdot B1}{R1a + R1b}} \quad i_{n,R1.M3a.b} = 593.722 \times 10^{-15} \text{ A}$$

5. The input voltage dividers (see TSOS-1 Ch. 4 and TSOS-2 Ch. 13):

$$Z0(f) := R0 + 2j \cdot \pi \cdot f \cdot L0 \quad Z1a(f) := \left( \frac{1}{Z0(f)} + 2j \cdot \pi \cdot f \cdot C1 \right)^{-1}$$

with R1a &amp; R1b= synthesized:

$$Z_{M1}(f) := \left( \frac{1}{R1a + R1b} + 2j \cdot \pi \cdot f \cdot C1 \right)^{-1}$$

$$e_{n1.M1}(f) := e_{n,R0} \cdot \frac{Z_{M1}(f)}{Z0(f) + Z_{M1}(f)} \quad |e_{n1.M1}(h)| = 3.996 \times 10^{-9} \text{ V}$$

$$e_{n2.M1}(f) := e_{n,R1.M1a.b} \cdot \frac{Z1a(f)}{Z1a(f) + R1a + R1b} \quad |e_{n2.M1}(h)| = 294.556 \times 10^{-12} \text{ V}$$

$$e_{n.i.M1}(f) := \sqrt{\left( |e_{n1.M1}(f)| \right)^2 + \left( |e_{n2.M1}(f)| \right)^2} \quad |e_{n.i.M1}(h)| = 4.007 \times 10^{-9} \text{ V}$$

20.2 MCD-WS: The Balanced Version

with  $R1a+R1b$ :

$$Z_{M3}(f) := \left( \frac{1}{R1a + R1b} + 2j \cdot \pi \cdot f \cdot C1 \right)^{-1}$$

$$e_{n1.M3}(f) := e_{n.R0} \frac{Z_{M3}(f)}{Z0(f) + Z_{M3}(f)}$$

$$|e_{n1.M3}(h)| = 3.996 \times 10^{-9} \text{ V}$$

$$e_{n2.M3}(f) := e_{n.R1.M3a.b} \frac{Z1a(f)}{Z1a(f) + R1a + R1b}$$

$$|e_{n2.M3}(h)| = 1.922 \times 10^{-9} \text{ V}$$

$$e_{n.i.M3}(f) := \sqrt{\left( |e_{n1.M3}(f)| \right)^2 + \left( |e_{n2.M3}(f)| \right)^2}$$

$$|e_{n.i.M3}(h)| = 4.434 \times 10^{-9} \text{ V}$$

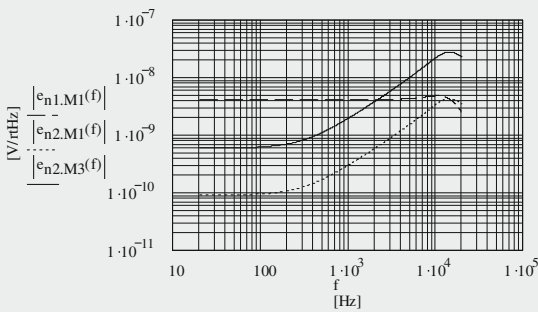


Fig. 20.14  
Noise voltage density  
of the three different  
input voltage dividers

$$e_{n.R0}(f) := e_{n.R0}$$

$$e_{n.R1.M3a.b}(f) := e_{n.R1.M3a.b}$$

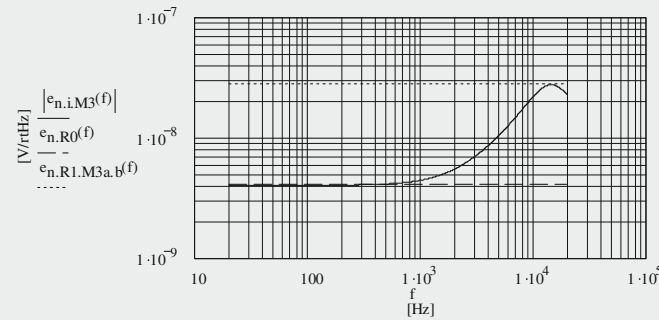


Fig. 20.15 = Fig. 19.12

## 20.2 MCD-WS: The Balanced Version

Page 5

6. Calculation of the input noise voltage of the phono-amp  
(noise of RIAA section + components = ignorable):

$$RG := 100\Omega \quad R_f := 1 \cdot 10^3\Omega \quad G_{DIF} := 1 + 2 \cdot \frac{R_f}{RG} \quad G_{DIF} = 21$$

$$RG_f := \left( \frac{1}{RG} + \frac{1}{R_f} \right)^{-1} \quad RG_f = 90.909\Omega$$

$$e_{n,RG,f} := \sqrt{4 \cdot k \cdot T \cdot B_1 \cdot RG_f} \quad e_{n,RG,f} = 1.227 \times 10^{-9} \text{ V}$$

$$e_{n,i3,4}(f) := \sqrt{e_{n,op3}(f)^2 + e_{n,op4}(f)^2} \quad e_{n,i3,4}(h) = 4.248 \times 10^{-9} \text{ V}$$

$$i_{n,i3,4}(f) := \sqrt{\left( \frac{1}{i_{n,op3}(f)^2} + \frac{1}{i_{n,op4}(f)^2} \right)^{-1}} \quad i_{n,i3,4}(h) = 37.749 \times 10^{-15} \text{ A}$$

$$e_{n,i,tot3,4}(f) := \sqrt{e_{n,i3,4}(f)^2 + i_{n,i3,4}(f)^2 \cdot RG_f^2 + e_{n,RG,f}^2} \quad e_{n,i,tot3,4}(h) = 4.422 \times 10^{-9} \text{ V}$$

7. Calculation of the noise effects of OP1a,b and OP2a,b :

$$G_{N,op2a} := -\left( 1 + \frac{R9a}{R8a} \right) \quad G_{N,op2a} = -42.56$$

$$e_{n,R8a} := \sqrt{4 \cdot k \cdot T \cdot B_1 \cdot R8a} \quad e_{n,R8a} = 4.07 \times 10^{-9} \text{ V}$$

$$e_{n,R9a} := \sqrt{4 \cdot k \cdot T \cdot B_1 \cdot R9a} \quad e_{n,R9a} = 2.624 \times 10^{-8} \text{ V}$$

$$e_{n,o,op2a,tot}(f) := \sqrt{\left( |G_{N,op2a}| \right)^2 \cdot e_{n,op2}(f)^2 + \left( \frac{R9a}{R8a} \right)^2 \cdot e_{n,R8a}^2 + e_{n,R9a}^2 + i_{n,op2}(f)^2 \cdot R9a^2} \quad e_{n,o,op2a,tot}(h) = 214.397 \times 10^{-9} \text{ V}$$

$$e_{n,o,op2b,tot}(f) := e_{n,o,op2a,tot}(f)$$

$$e_{n,o,M1a}(f) := \sqrt{e_{n,op1}(f)^2 \cdot \left( |G_{M1a}| \right)^2 + e_{n,o,op2a,tot}(f)^2} \quad e_{n,o,M1a}(h) = 248.099 \times 10^{-9} \text{ V}$$

$$e_{n,o,M1b}(f) := e_{n,o,M1a}(f)$$

$$e_{n,o,M1}(f) := \sqrt{2} \cdot e_{n,o,M1a}(f) \quad e_{n,o,M1}(h) = 350.866 \times 10^{-9} \text{ V}$$

$$e_{n,M1,eff}(f) := e_{n,o,M1}(f) \cdot \left| \frac{Z_{tot1}(f)}{R10a + R10b + Z_{tot1}(f)} \right| \quad e_{n,M1,eff}(h) = 567.373 \times 10^{-12} \text{ V}$$

20.2 MCD-WS: The Balanced Version

8. Graph and calculation of the different total input referred noise voltages :

$$e_{n.i.tot.M1}(f) := \sqrt{e_{n.i.tot.3.4}(f)^2 + e_{n.i.M1}(f)^2 + e_{n.M1.eff}(f)^2 + (i_{n.i.3.4}(f) \cdot |Z_{tot}(f)|)^2}$$

$$|e_{n.i.tot.M1}(g)| = 9.685 \times 10^{-9} V$$

$$e_{n.i.tot.M3}(f) := \sqrt{e_{n.i.tot.3.4}(f)^2 + e_{n.i.M3}(f)^2 + (i_{n.i.3.4}(f) \cdot |Z_{tot}(f)|)^2}$$

$$|e_{n.i.tot.M3}(g)| = 22.58 \times 10^{-9} V$$

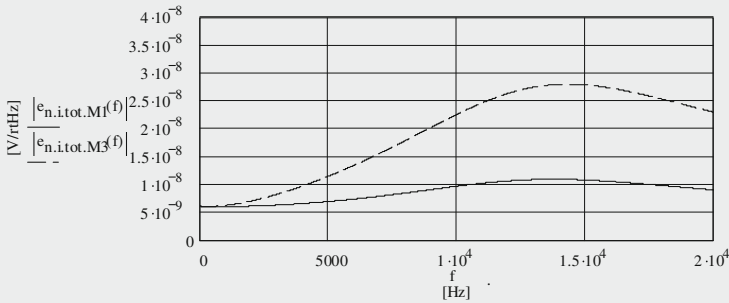


Fig. 20.16 Total input noise voltage densities at the input of the phono-amp (points A-B)

9. Calculation of SNs :

9.1 Non-equalized :

$$SN_{ne.M1} := 20 \cdot \log \left[ \frac{\sqrt{\frac{1}{B_1} \int_{20Hz}^{20000Hz} (|e_{n.i.tot.M1}(f)|)^2 df}}{v_{i.nom}} \right]$$

$$SN_{ne.M1} = -71.94 \quad [dB]$$

$$SN_{ne.M3} := 20 \cdot \log \left[ \frac{\sqrt{\frac{1}{B_1} \int_{20Hz}^{20000Hz} (|e_{n.i.tot.M3}(f)|)^2 df}}{v_{i.nom}} \right]$$

$$SN_{ne.M3} = -64.627 \quad [dB]$$

$$SN_{ne.D1} := SN_{ne.M1} - SN_{ne.M3}$$

$$SN_{ne.D1} = -7.313 \quad [dB]$$

20.2 MCD-WS: The Balanced Version

9.2 RIAA-equalized :

$$R_{1000} := \left[ \frac{\sqrt{1 + (2 \cdot \pi \cdot 10^3 \text{ Hz} \cdot 318 \cdot 10^{-6} \text{ s})^2}}{\sqrt{1 + (2 \cdot \pi \cdot 10^3 \text{ Hz} \cdot 3180 \cdot 10^{-6} \text{ s})^2} \cdot \sqrt{1 + (2 \cdot \pi \cdot 10^3 \text{ Hz} \cdot 75 \cdot 10^{-6} \text{ s})^2}} \right]^{-1} \quad R_{1000} = 9.898$$

$$R(f) := \left[ \frac{\sqrt{1 + (2 \cdot \pi \cdot f \cdot 318 \cdot 10^{-6} \text{ s})^2}}{\sqrt{1 + (2 \cdot \pi \cdot f \cdot 3180 \cdot 10^{-6} \text{ s})^2} \cdot \sqrt{1 + (2 \cdot \pi \cdot f \cdot 75 \cdot 10^{-6} \text{ s})^2}} \right] \cdot R_{1000}$$

$$SN_{riaa.M1} := 20 \cdot \log \left[ \frac{\int_{20\text{Hz}}^{20000\text{Hz}} \left( \frac{1}{B_1} \right) \cdot |e_{n.i.tot.M1}(f)|^2 \cdot (|R(f)|)^2 \text{ df}}{v_{i,nom}} \right] \quad SN_{riaa.M1} = -78.593 \quad [\text{dB}]$$

$$SN_{riaa.M3} := 20 \cdot \log \left[ \frac{\int_{20\text{Hz}}^{20000\text{Hz}} |e_{n.i.tot.M3}(f)|^2 \cdot (|R(f)|)^2 \text{ df}}{v_{i,nom}} \right] \quad SN_{riaa.M3} = -76.307 \quad [\text{dB}]$$

$$SN_{riaa.D1} := SN_{riaa.M1} - SN_{riaa.M3} \quad SN_{riaa.D1} = -2.285 \quad [\text{dB}]$$

9.3 Non-equalized but A-weighted :

Definition of A-filter frequencies and transfer function:

$$f_1 := 20.6\text{Hz} \quad f_2 := f_1 \quad f_3 := 107.7\text{Hz} \quad f_4 := 737.9\text{Hz} \quad f_5 := 12200\text{Hz} \quad f_6 := f_5 \quad f_G := 1000\text{Hz}$$

$$v_{1000} := \left[ \sqrt{1 + \left(\frac{f_1}{f_G}\right)^2} \right]^2 \cdot \left[ \sqrt{1 + \left(\frac{f_3}{f_G}\right)^2} \right]^2 \cdot \left[ \sqrt{1 + \left(\frac{f_4}{f_G}\right)^2} \right]^2 \cdot \left[ \sqrt{1 + \left(\frac{f_6}{f_5}\right)^2} \right]^2 \quad v_{1000} = 1.259$$

$$A(f) := v_{1000} \left[ \frac{1}{\sqrt{1 + \left(\frac{f_1}{f}\right)^2}} \right]^2 \cdot \left[ \frac{1}{\sqrt{1 + \left(\frac{f_3}{f}\right)^2}} \right]^2 \cdot \left[ \frac{1}{\sqrt{1 + \left(\frac{f_4}{f}\right)^2}} \right]^2 \cdot \left[ \frac{1}{\sqrt{1 + \left(\frac{f}{f_5}\right)^2}} \right]^2$$

20.2 MCD-WS: The Balanced Version

$$SN_{a.M1} := 20 \cdot \log \left[ \frac{\sqrt{\frac{1}{B_1} \int_{20\text{Hz}}^{2000\text{Hz}} (|e_{n.i.tot.M1}(f)|)^2 \cdot (|A(f)|)^2 df}}{v_{i.nom}} \right] \quad SN_{a.M1} = -74.965 \quad [\text{dB(A)}]$$

$$SN_{a.M3} := 20 \cdot \log \left[ \frac{\sqrt{\frac{1}{B_1} \int_{20\text{Hz}}^{2000\text{Hz}} (|e_{n.i.tot.M3}(f)|)^2 \cdot (|A(f)|)^2 df}}{v_{i.nom}} \right] \quad SN_{a.M3} = -68.628 \quad [\text{dB(A)}]$$

$$SN_{a.D1} := SN_{a.M1} - SN_{a.M3} \quad SN_{a.D1} = -6.337 \quad [\text{dB}]$$

9.4 RIAA-equalized and A-weighted :

$$SN_{ariaa.M1} := 20 \cdot \log \left[ \frac{\sqrt{\frac{1}{B_1} \int_{20\text{Hz}}^{2000\text{Hz}} (|e_{n.i.tot.M1}(f)|)^2 \cdot (|A(f)|)^2 \cdot (|R(f)|)^2 df}}{v_{i.nom}} \right] \quad SN_{ariaa.M1} = -82.659 \quad [\text{dB(A)}]$$

$$SN_{ariaa.M3} := 20 \cdot \log \left[ \frac{\sqrt{\frac{1}{B_1} \int_{20\text{Hz}}^{2000\text{Hz}} (|e_{n.i.tot.M3}(f)|)^2 \cdot (|A(f)|)^2 \cdot (|R(f)|)^2 df}}{v_{i.nom}} \right] \quad SN_{ariaa.M3} = -79.433 \quad [\text{dB(A)}]$$

$$SN_{ariaa.D1} := SN_{ariaa.M1} - SN_{ariaa.M3} \quad SN_{ariaa.D1} = -3.226 \quad [\text{dB}]$$

---

## 21.1 Intro

In my TSOS books, I've demonstrated the usage of a certain kind of MC phono-amp input stage, composed by a CE configured BJT that is followed by an op-amp, principally according to Fig. 5.6b in TSOS-2 and Fig. 3.23b in TSOS-1. However, I didn't show an exact method to calculate the gain of the chosen BJT input stage that drives the Module 2 phono-amps (four BJTs in parallel operation). In addition, the given noise calculation equations were based on white noise only.

Now, this chapter will give equations

- to calculate the gain of a range of different CE configured BJT input stages, including the one of Module 2,
- to calculate frequency dependent BJT noise voltages for 1/f-noise corner frequencies  $f_c > 0$  Hz.

Before we enter into the details of the input stages, and to prepare the handling of the frequency dependency, we have to repeat some BJT basics in Sect. 21.2.<sup>1</sup>

---

## 21.2 BJT—Bipolar Junction Transistor—Basics

### 21.2.1 Equations for Low Frequency Small Signal Calculations

All given equations are based on the Fig. 21.1 NPN BJT device model and a chosen operating point. The use of PNP devices requires inversed supply voltages and the turn over of electrolytic capacitors only.

---

<sup>1</sup>T/S, Chap. 2, and my own derivations are the main sources of this chapter's equations (see Appendix 2).

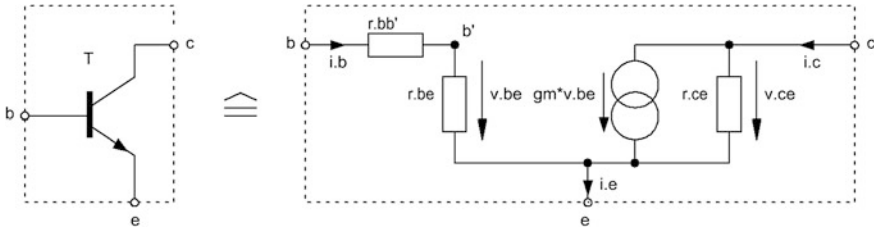


**Fig. 21.1** BJT model for low-frequency small signal calculation purposes

- Mutual conductance  $g_m$  expressed in terms of DC collector current  $I_C$ , Boltzmann's constant  $k$ , absolute temperature  $T$  and the electron charge  $q$ :

$$g_m = \frac{qI_C}{kT} \quad (21.1)$$

- Small signal current gain  $h_{fe}^2$  expressed in terms of the DC current gain  $h_{FE}^3$  (=suitable approach on the small signal field):

$$h_{fe} \cong h_{FE} \quad (21.2)$$

- Base-emitter resistance  $r_{be}$  expressed in terms of small signal current gain  $h_{fe}$  and mutual conductance  $g_m$ :

$$r_{be} = \frac{h_{fe}}{g_m} \quad (21.3)$$

- Collector-emitter resistance  $r_{ce}$  expressed in terms of Early voltage  $V_A^4$  and the operating collector current  $I_C$ :

$$r_{ce} = \frac{V_A + V_{CE}}{I_C} \quad (21.4)$$

$$V_{A,npn} = 30 \text{ V to } 150 \text{ V} \quad (21.5)$$

$$V_{A,pnp} = -30 \text{ V to } -75 \text{ V}$$

<sup>2</sup>Also called  $\beta$  in some regions of the world.

<sup>3</sup>Also called  $B$  in some regions of the world.

<sup>4</sup>Usually,  $V_A$  is not indicated in data sheets; it must be guessed or determined with the help of the output characteristics chart (see T/S, p. 36).  $V_{CE}$  can be ignored in cases of  $V_A \gg V_{CE}$ .



### 21.2.2 Circuit Parameter Based Formulae

All given formulae are based on the common emitter configuration (e).

- Mutual conductance  $g_m$ :

$$g_m = \frac{h_{21,e}}{h_{11,e}} = y_{21,e} = \frac{h_{fe}}{h_{ie}} \tag{21.6}$$

- Small signal current gain  $h_{fe}$ :

$$h_{fe} = h_{21,e} = \frac{y_{21,e}}{y_{11,e}} \tag{21.7}$$

- Base-emitter Resistance  $r_{be}$ :

$$r_{be} = h_{11,e} = \frac{1}{y_{11,e}} = h_{ie} \tag{21.8}$$

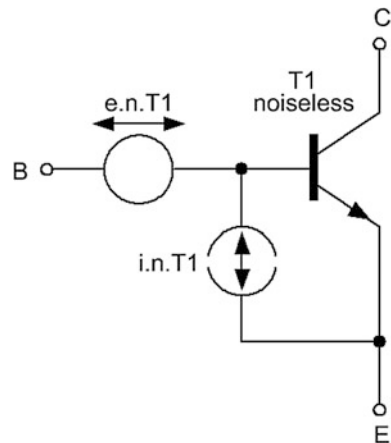
- Collector-emitter resistance  $r_{ce}$ :

$$r_{ce} = \frac{h_{11,e}}{h_{11,e}h_{22,e} - h_{12,e}h_{21,e}} = \frac{1}{y_{22,e}} = \frac{h_{ie}}{h_{ie}h_{oe} - h_{re}h_{fe}} \tag{21.9}$$

### 21.2.3 Noise of a BJT—Frequency Independent Version

- Equivalent noise model (Fig. 21.2):

Fig. 21.2 BJT noise model



- Equivalent input noise voltage density  $e_{n,T1}$ :

$$e_{n,T1} = \sqrt{e_{n1,T1}^2 + i_{n,T1}^2 r_{bb'}^2 + e_{n,rbb'}^2} \quad (21.10)$$

$$e_{n1,T1} = kT \sqrt{\frac{2}{qI_C}} B_1 \quad (21.11)$$

$$e_{n,rbb'} = \sqrt{4kTr_{bb'}} B_1 \quad (21.12)$$

$$B_1 = 1 \text{ Hz} \quad (21.13)$$

- Equivalent input noise current density  $i_{n,T1}$ :

$$i_{n,T1} = \sqrt{2q \frac{I_C}{h_{fe}}} B_1 \quad (21.14)$$

### 21.2.4 Noise of a BJT—Frequency Dependent Version

Many BJTs show significant low-frequency noise (flicker or 1/f-noise). It is part of the collector current, hence, part of the base current too. With that in mind, the key equations of Sect. 21.2.3 change to the following ones:

- Equivalent input noise voltage density  $e_{n,T1}(f)$ :

$$e_{n,T1}(f) = \sqrt{e_{n1,T1}^2 + i_{n,T1}(f)^2 r_{bb'}^2 + e_{n,rbb'}^2} \quad (21.15)$$

- Equivalent input noise current density  $i_{n,T1}(f)$  with the 1/f-noise corner frequency  $f_{c,i}$ :

$$i_{n,T1}(f) = \sqrt{2q \frac{I_C}{h_{fe}}} B_1 \sqrt{1 + \frac{f_{c,i}}{f}} \quad (21.16)$$

Note:  $f_{c,i}$  is not given in data sheets. However, some manufacturers show noise current versus frequency noise charts that allow a graphical evaluation of  $f_{c,i}$ . Others give frequency-based charts with information about a range of noise figures NF versus resistor input load and collector current. Here, the evaluation of  $f_{c,i}$  follows the rather complex math approach that is described in detail in this book's Chaps. 10 and 11.

### 21.2.5 Noise of a Resistor R

- Noise voltage density:

$$e_{n,R} = \sqrt{4kTRB_1} \quad (21.17)$$

- Noise current density:

$$i_{n,R} = \sqrt{\frac{4kT}{R}} B_1 \quad (21.18)$$

- Excess noise—average and thus frequency independent version for a chosen frequency bandwidth of interest:

With  $NI$  = resistor noise index in [ $\mu$ V/decade/ $1V_R$ ] or in [dB] with  $NI_e = 20 \log(NI) + 120$  (see resistor data sheet),  $V_R$  = DC voltage across  $R = I_C * R$ , and  $d$  = number of decades in  $B$  = frequency bandwidth of interest we'll obtain the average excess noise voltage density  $e_{n,Rex}$  in  $B$ :

$$e_{n,R,tot} = \sqrt{e_{n,R}^2 + e_{n,Rex}^2} \quad (21.19)$$

$$e_{n,Rex} = NI \sqrt{d} V_R \sqrt{\frac{B_1}{B}} \quad (21.20)$$

- Excess noise—frequency dependent version:

$$e_{n,R,tot}(f) = \sqrt{e_{n,R}^2 + e_{n,Rex}(f)^2} \quad (21.21)$$

$$e_{n,Rex}(f) = \sqrt{\left( \frac{NI_e}{10 \frac{10}{10} 10^{-12}} \right) \left( \frac{V_R^2}{f} \right) B_1} \quad (21.22)$$

### 21.2.6 Noise Factor & Noise Figure

- Noise Factor NF:

$$NF = \frac{\sqrt{e_{n,T1}^2 + i_{n,T1}^2 R_0^2 + e_{n,R0}^2}}{e_{n,R0}} \quad (21.23)$$

- Noise Figure  $NF_e$ :

$$NF_e = 20 \log(NF) \quad (21.24)$$

Note: In case of frequency dependent calculations, the frequency of interest should be 1 kHz.

### 21.2.7 Signal-to-Noise Ratios SN

With the input and output referred reference voltages  $v_{i.ref}$  and  $v_{o.ref}$  we obtain the SNs in  $B = f_{hi} - f_{lo}$ . Here,  $B_1 = 1$  Hz and  $e_{n,i}(f)$  stands for the frequency dependent input noise voltage density of a gain stage. The same applies to the SN of the output noise voltage density  $e_{n,o}(f)$ :

- Input referred  $SN_i$ :

$$SN_i = 20 \log \left( \frac{\sqrt{\frac{1}{B_1} \int_{f_{lo}}^{f_{hi}} |e_{n,i}(f)|^2 df}}{v_{i.ref}} \right) \quad (21.25)$$

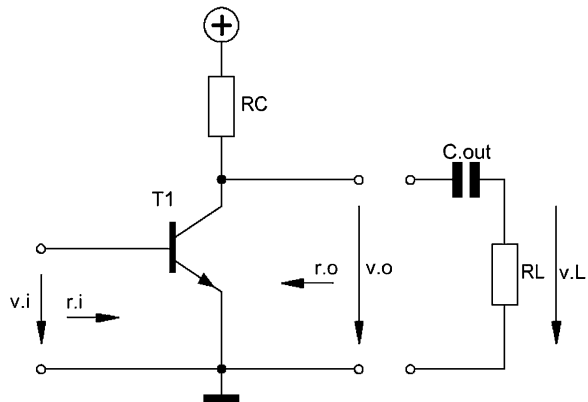
- Output referred  $SN_o$ :

$$SN_o = 20 \log \left( \frac{\sqrt{\frac{1}{B_1} \int_{f_{lo}}^{f_{hi}} |e_{n,o}(f)|^2 df}}{v_{o.ref}} \right) \quad (21.26)$$

## 21.3 Basic ( $b$ ) $CE_b$ Circuit

See Fig. 21.3.

**Fig. 21.3** Basic common emitter circuit CE



### 21.3.1 Idle Gains $G_b$ and $G_{b,rot}$

$$G_b = -\frac{V_o}{V_i} \quad (21.27)$$

$$\begin{aligned} G_b &= -h_{fe} \frac{RC \parallel r_{ce}}{r_{be}} = -\frac{h_{fe}}{r_{be}} \left( \frac{1}{RC} + \frac{1}{r_{ce}} \right)^{-1} \\ &= -g_m \left( \frac{1}{RC} + \frac{1}{r_{ce}} \right)^{-1} = -\frac{qI_C}{kT} \left( \frac{1}{RC} + \frac{1}{r_{ce}} \right)^{-1} \end{aligned} \quad (21.28)$$

$G_{b,rot}$  ( $RC \ll r_{ce}$ ):

$$G_{b,rot} \approx -g_m RC \quad (21.29)$$

### 21.3.2 $G_b(RL) = RL$ Dependent Gain $G_b$

$$G_b(RL) = -g_m \left( \frac{1}{r_{ce}} + \frac{1}{RC} + \frac{1}{RL} \right)^{-1} \quad (21.30)$$

$C_{out}$  without negative frequency and phase response effect!

### 21.3.3 Input Resistance $r_i$ (O/P Open)

$$r_i = r_{be} \quad (21.31)$$

### 21.3.4 Output Resistance $r_{o,o}$ (I/P = Open)

$$r_{o,o} \approx RC \quad (21.32)$$

### 21.3.5 Output Resistances $r_{o,s}$ and $r_{o,s,rot}$ (I/P = Shorted)

$$r_{o,s} = r_{ce} \parallel RC \tag{21.33}$$

$r_{o,s,rot}$  ( $r_{ce} \gg RC$ ):

$$r_{o,s,rot} \approx RC \tag{21.34}$$

### 21.3.6 Operating Gains $G_{op}(R0, RL)$ and $G_{ops}(f, R0, RL)$

As of Fig. 21.4 inclusion of the bias setting input resistors R1 & R2 leads to the operating input resistance  $r_{i,ops}$  and output resistance  $r_{o,ops}$ :

$$r_{i,ops} = r_i \parallel R1 \parallel R2 \tag{21.35}$$

$$r_{o,ops} = r_{o,s} \tag{21.36}$$

If  $C_{in}$  and  $C_{out}$  do not hurt the flat frequency and phase response in the bandwidth of interest, the corresponding frequency independent equations look as follows:

$$\begin{aligned} G_{op}(R0, RL) &= \frac{v_o(R0, RL)}{v_0} \\ &= G_i(R0)G_bG_o(RL) \\ &= G_i(R0)G_b(RL) \end{aligned} \tag{21.37}$$

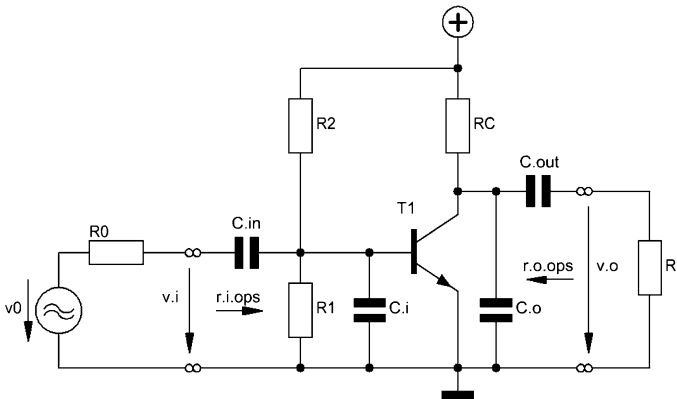


Fig. 21.4  $CE_b$ 's operational model

$$G_b(\text{RL}) = G_b G_o(\text{RL}) \quad (21.38)$$

$$G_i(\text{R0}) = \frac{r_{i,\text{ops}}}{r_{i,\text{ops}} + \text{R0}} \quad (21.39)$$

$$G_o(\text{RL}) = \frac{\text{RL}}{r_{o,\text{ops}} + \text{RL}} \quad (21.40)$$

Via inclusion of the Miller-capacitance-effect for  $C_i$  and  $C_o$ , the frequency dependent version becomes thus:

$$\begin{aligned} r_{i,\text{ops}}(f) &= (z_i(f) \parallel \text{R1} \parallel \text{R2}) + (2j\pi f C_{\text{in}})^{-1} \\ z_i(f) &= r_i \parallel C_i \end{aligned} \quad (21.41)$$

$$\begin{aligned} r_{o,\text{ops}}(f) &= z_{o,s}(f) + (2j\pi f C_{\text{out}})^{-1} \\ z_{o,s}(f) &= r_{o,s} \parallel C_o \end{aligned} \quad (21.42)$$

$$\begin{aligned} G_{\text{ops}}(f, \text{R0}, \text{RL}) &= \frac{v_o(f, \text{R0}, \text{RL})}{v0} \\ &= G_i(f, \text{R0}) G_b G_o(f, \text{RL}) \\ &= \frac{r_{i,\text{ops}}(f)}{r_{i,\text{ops}}(f) + \text{R0}} G_b \frac{\text{RL}}{r_{o,\text{ops}}(f) + \text{RL}} \\ &= G_i(f, \text{R0}) G_b(f, \text{RL}) \end{aligned} \quad (21.43)$$

$$C_i = C_{\text{be}} + C_{\text{bc}}(1 - G_b(\text{RL})) \quad (21.44)$$

$$C_o = C_{\text{ce}} + C_{\text{bc}} \quad (21.45)$$

### 21.3.7 Noise—Frequency Independent Version

Figure 21.5 is Fig. 21.4 transferred into a circuit that shows all noise relevant sources:

With input and output not loaded, the input noise voltage density  $e_{n,i}$  becomes:

$$e_{n,i} = \sqrt{e_{n,T1}^2 + \frac{e_{n,\text{RC,tot}}^2}{G_b^2}} \quad (21.46)$$

TSOS-1 & TSOS-2 explain the calculation of the BJTs input referred noise voltage density  $e_{n,T1}$ . The frequency independent calculation of the noise voltage density of RC looks as follows:

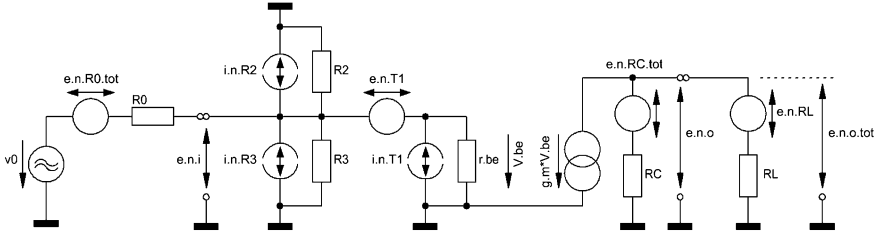


Fig. 21.5 Fig. 21.4 with all relevant noise sources

$$e_{n.RC.tot} = \sqrt{e_{n.RC}^2 + e_{n.RCex}^2} \tag{21.47}$$

$$e_{n.RC} = \sqrt{4kTRCB_1} \tag{21.48}$$

With NI = resistor noise index (see resistor data sheet),  $V_{RC}$  = DC voltage across RC, and d = number of decades in B = frequency bandwidth of interest we'll obtain the average excess noise voltage density  $e_{n.RCex}$ :

$$e_{n.RCex} = \frac{NI\sqrt{d}V_{RC}}{\sqrt{B}} \tag{21.49}$$

The input referred noise current density becomes:

$$i_{n.i} = \sqrt{i_{n.T1}^2 + i_{n.RA}^2 + i_{n.RB}^2} \tag{21.50}$$

$$i_{n.R} = \sqrt{\frac{4kT}{R}} B_1 \tag{21.51}$$

With all shown noise sources included, the output referred noise voltage density  $e_{n.o}$  thus becomes:

$$e_{n.o.tot}(R0, RL) = \sqrt{e_{n.i}^2 G_b(RL)^2 + e_{n.R0.tot}(R0)^2 G_{op}(R0, RL)^2 + e_{n.RL}^2 \left(\frac{RL}{r_{o,s} + RL}\right)^2} \tag{21.52}$$

$$e_{n.R0.tot}(R0) = \sqrt{e_{n.R0}(R0)^2 + i_{n.i}^2 R0^2} \tag{21.53}$$



### 21.3.8 Noise—Frequency Dependent Version

Based on Fig. 21.5, the above given equations, and the frequency related Sects. 21.2.4 and 21.2.5, the frequency dependent output referred noise voltage density  $e_{n.o.tot}(f)$  becomes:

$$e_{n.o.tot}(f, R0, RL) = \sqrt{e_{n.i}(f, RL)^2 G_b(RL) + e_{n.R0.tot}(f, R0) G_{ops}(f, R0, RL) + e_{n.RL}^2 \left( \frac{RL}{z_{o.s}(f) + RL} \right)^2} \tag{21.54}$$

$$e_{n.i}(f, RL) = \sqrt{e_{n.T1}(f)^2 + \frac{e_{n.RC.tot}(f)^2}{G_b(RL)^2}} \tag{21.55}$$

The calculation of  $e_{n.RC.tot}(f)$  follows the rules given in Sect. 21.2.5. Section 21.2.7 gives the equations to calculate SNs.

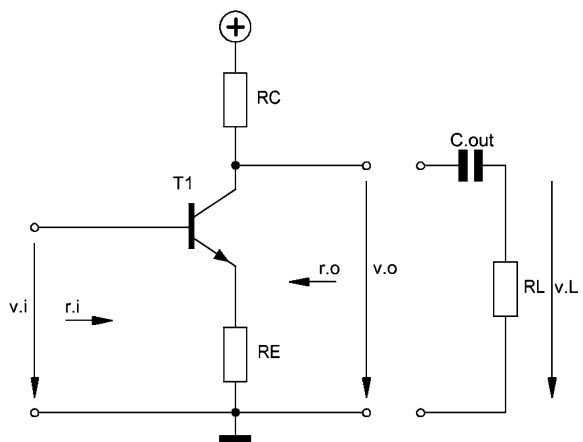
## 21.4 CE Circuit CE<sub>cf</sub> with Current Feedback

See Fig. 21.6.

### 21.4.1 Gains $G_{cf}$ and $G_{cf.rot}$

$$G_{cf} = - \frac{V_o}{V_i} \tag{21.56}$$

**Fig. 21.6** Common emitter circuit CE<sub>cf</sub> with cf via RE



$$\begin{aligned}
 G_{cf} &= -\frac{g_m RC(h_{fe} r_{ce} - RE)}{h_{fe}(r_{ce} + RE + RC) + g_m RE r_{ce} + g_m RE(r_{ce} + RC)} \\
 &= -\frac{RC(h_{fe} r_{ce} - RE)}{\frac{kT}{qI_C} h_{fe}(r_{ce} + RE + RC) + RE(h_{fe} r_{ce} + r_{ce} + RC)}
 \end{aligned} \tag{21.57}$$

$G_{cf}$  and application of the reduced mutual conductance  $g_{m,red}$ :

$$\begin{aligned}
 g_{m,red} &= g_m \frac{G_{cf}}{G_b} \\
 &= \frac{g_m(r_{ce} + RC) \left( h_{fe} - \frac{RE}{r_{ce}} \right)}{h_{fe}(r_{ce} + RE + RC) + g_m RE(h_{fe} r_{ce} + r_{ce} + RC)}
 \end{aligned} \tag{21.58}$$

Hence:

$$G_{cf} = -g_{m,red} RC \tag{21.59}$$

With  $RE \ll RC \ll r_{ce}$  we obtain  $g_{m,red,rot}$  and  $G_{cf,rot,1}$ :

$$g_{m,red,rot} \cong \frac{g_m}{1 + g_m RE} \tag{21.60}$$

$$G_{cf,rot,1} \approx -g_{m,red,rot}(RC \parallel r_{ce}) \tag{21.61}$$

$G_{cf,rot,2}$  ( $h_{fe} \gg 1$ ):

$$G_{cf,rot,2} \approx -\frac{g_m RC}{1 + g_m RE} \tag{21.62}$$

$G_{cf,rot,3}$  (like  $G_{cf,rot,2}$  plus  $g_m RE \gg 1$ ):

$$G_{cf,rot,3} \approx -\frac{RC}{RE} \tag{21.63}$$

#### 21.4.2 Input Resistances $r_i$ and $r_{i,rot}$ (O/P Open)

$$r_i = r_{be} + RE \frac{(1 + h_{fe})r_{ce} + RC}{r_{ce} + RE + RC} \tag{21.64}$$

$r_{i,rot}$  ( $r_{ce} \gg RC, RE; h_{fe} \gg 1$ ):

$$r_{i.rot} \gg r_{be} + h_{fe}RE \quad (21.65)$$

### 21.4.3 Output Resistances $r_{o,o}$ and $r_{o,o.rot}$ (I/P = Open)

$$r_{o,o} = (r_{ce} + RE) \parallel RC \quad (21.66)$$

$r_{o,o.rot}$  ( $r_{ce} \gg RC$ ):

$$r_{o,o.rot} \approx RC \quad (21.67)$$

### 21.4.4 Output Resistances $r_{o,s}$ and $r_{o,s.rot}$ (I/P = Shorted)

$$r_{o,s} = \left[ r_{ce} \left( 1 + \frac{h_{fe} + \frac{r_{be}}{r_{ce}}}{1 + \frac{r_{be}}{RE}} \right) \right] \parallel RC \quad (21.68)$$

$r_{o,s.rot.1}$  ( $r_{ce} \gg r_{be}$ ;  $h_{fe} \gg 1$ ):

$$r_{o,s.rot.1} \approx \left[ r_{ce} \frac{h_{fe}RE + r_{be}}{RE + r_{be}} \right] \parallel RC \quad (21.69)$$

$r_{o,s.rot.2}$  ( $r_{ce} \gg RC$ ):

$$r_{o,s.rot} \approx RC \quad (21.70)$$

### 21.4.5 Operating Gains $G_{op}(R0, RL)$ and $G_{ops}(f, R0, RL)$

As of Fig. 21.7 inclusion of the bias setting input resistors  $R1$  &  $R2$  leads to the operating input resistance  $r_{i,ops}$  and output resistance  $r_{o,ops}$ :

$$r_{i,ops} = R1 \parallel R2 \parallel r_i \quad (21.71)$$

$$r_{o,ops} = r_{o,o} \quad (21.72)$$

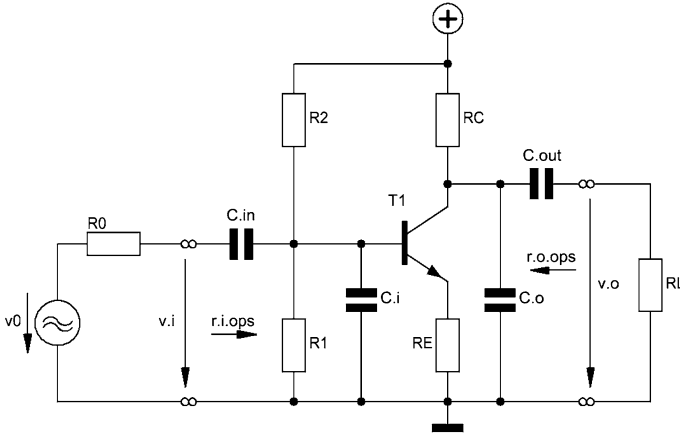


**Fig. 21.7**  $CE_{cf}$ 's operational model

If  $C_{in}$  and  $C_{out}$  do not hurt the flat frequency and phase response in the bandwidth of interest, the corresponding frequency independent equations look as follows:

$$\begin{aligned} G_{op}(R0, RL) &= \frac{v_o(R0, RL)}{v0} \\ &= G_i(R0)G_{cf}G_o(RL) \\ &= G_i(R0)G_{cf}(RL) \end{aligned} \quad (21.73)$$

$$G_{cf}(RL) = G_{cf}G_o(RL) \quad (21.74)$$

$$G_i(R0) = \frac{r_{i,ops}}{r_{i,ops} + R0} \quad (21.75)$$

$$G_o(RL) = \frac{RL}{r_{o,ops} + RL} \quad (21.76)$$

Via inclusion of the Miller-capacitance-effect for  $C_i$  and  $C_o$ , the frequency dependent version becomes thus:

$$\begin{aligned} r_{i,ops}(f) &= (z_i(f) \parallel R1 \parallel R2) + (2j\pi f C_{in})^{-1} \\ z_i(f) &= r_i \parallel C_i \end{aligned} \quad (21.77)$$

$$\begin{aligned} r_{o,ops}(f) &= z_{o,s}(f) + (2j\pi f C_{out})^{-1} \\ z_{o,s}(f) &= r_{o,s} \parallel C_o \end{aligned} \quad (21.78)$$

$$\begin{aligned}
 G_{\text{ops}}(f, R_0, RL) &= \frac{v_o(f, R_0, RL)}{v_0} \\
 &= G_i(f, R_0)G_{\text{cf}}G_o(f, RL) \\
 &= \frac{r_{i,\text{ops}}(f)}{r_{i,\text{ops}}(f) + R_0} G_{\text{cf}} \frac{RL}{r_{o,\text{ops}}(f) + RL} \\
 &= G_i(f, R_0)G_{\text{cf}}(f, RL)
 \end{aligned}
 \tag{21.79}$$

$$C_i = \frac{C_{\text{be}}}{1 + g_m RE} + C_{\text{bc}}(1 - G_{\text{cf}}(RL))
 \tag{21.80}$$

$$C_o = \frac{C_{\text{ce}}}{1 + g_m RE} + C_{\text{bc}}
 \tag{21.81}$$

### 21.4.6 Noise and SN

According to Fig. 21.8 the noise voltage and SN calculations follow the rules given in Sects. 21.3.7 and 21.3.8. Additionally, the following exception has to be taken into account: the emitter resistance RE creates an additional noise voltage. Thus, in (21.10) and (21.15) it will increase the noise voltage of T1 as follows:

$$e_{n,T1}(f) = \sqrt{e_{n1,T1}^2 + i_{n,T1}(f)^2 R_{\text{BE}}^2 + e_{n,R,\text{BE}}^2}
 \tag{21.82}$$

$$R_{\text{BE}} = r_{\text{bb}'} + RE
 \tag{21.83}$$

$$e_{n,R,\text{BE}} = \sqrt{4kTB_1 R_{\text{BE}}}
 \tag{21.84}$$

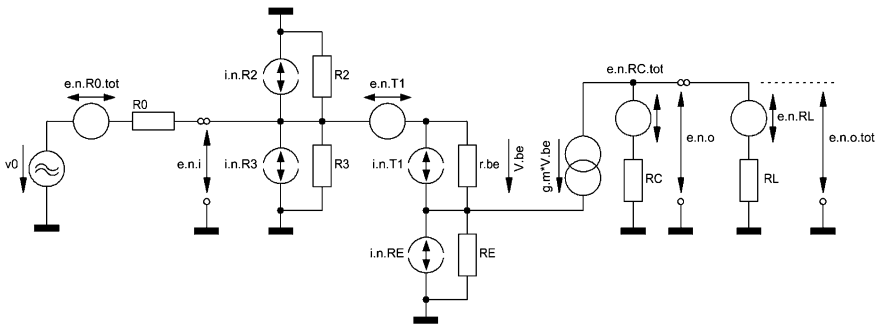


Fig. 21.8 Noise model of Fig. 21.7 with all relevant noise sources

If the excess noise of RE becomes significant we have to consider it too. By addition of RE Fig. 21.5 changes to Fig. 21.8.

## 21.5 CE Type 2 Circuit CE<sub>vcf2</sub> with Voltage Feedback and Current Feedback

### 21.5.1 Gain G<sub>vcf2</sub>

Systematically, with the reduced mutual conductance  $g_{m,red}$  of Sect. 21.4.1 the gain equation of Fig. 21.9 can be derived from the evolution of the Fig. 21.10 circuits and their gain equations.

Figure 21.10a shows a CE<sub>vfl</sub> gain stage Type1 with a voltage feedback via R2. In Fig. 21.10b we reduce R1 to 0Ω and add R3; hence, we'll have a CE<sub>vf2</sub> Type 2 now. The next step is the inclusion of RE. It leads to a CE<sub>vcf2</sub> Type 2. The CE<sub>vfl</sub> Type 1 is Fig. 21.9 including R1, however, not shown here.

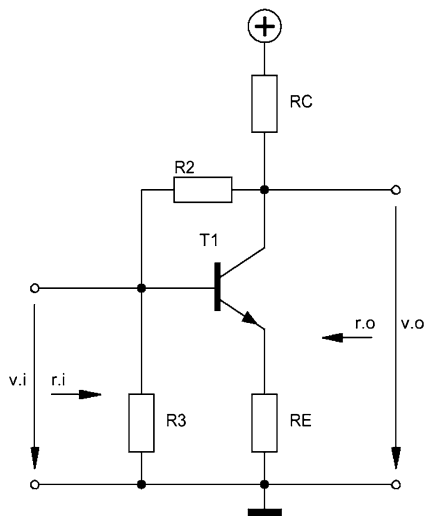
The gain G<sub>vfl</sub> of Fig. 21.10a becomes:

$$G_{vfl} = - \frac{g_m R2 - 1}{1 + g_m R1 \left(1 + \frac{1}{h_{fe}}\right) + \left(R1 + R2 + R1 R2 \frac{g_m}{h_{fe}}\right) \left(\frac{1}{RC} + \frac{1}{r_{ce}}\right)} \quad (21.85)$$

As of Fig. 21.10b we set R1 = 0 Ω in the equation above. The gain G<sub>vf2</sub> thus becomes:

$$G_{vf2} = - \frac{g_m R2 - 1}{1 + R2 \left(\frac{1}{RC} + \frac{1}{r_{ce}}\right)} \quad (21.86)$$

**Fig. 21.9** Common emitter circuit CE<sub>vcf2</sub> with vf via R2 and cf via RE



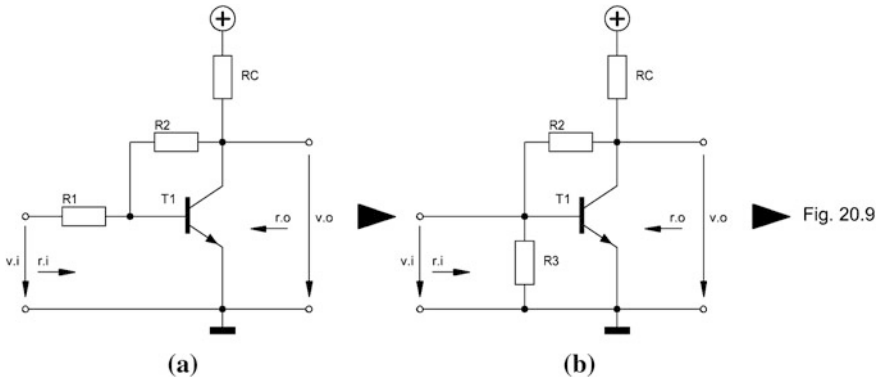


**Fig. 21.10** Derivation of the gain equation for Fig. 21.9

Here,  $R_3$  plays no role in the gain equation. A further inclusion of  $R_E$  into the Fig. 21.10b circuit and application of  $g_{m,red}$  leads to the gain  $G_{v_{cf2}}$  of Fig. 21.9 as follows:

$$G_{v_{cf2}} = - \frac{g_{m,red} R_2 - 1}{1 + R_2 \left( \frac{1}{RC} + \frac{1}{r_{ce}} \right)} \tag{21.87}$$

**21.5.2 Input Resistance  $r_i$  (O/P Open)**

$$r_i = \left[ \frac{1}{R_3} + \frac{1}{r_{be} + h_{fe} R_E} + \frac{1}{R_2 + \left( \frac{1}{RC} + \frac{1}{r_{ce}} \right)^{-1}} \right]^{-1} \tag{21.88}$$

**21.5.3 Output Resistance  $r_{o,s}$  (I/P Shorted)**

$$r_{o,s} = (r_{ce} + R_E) \parallel RC \parallel R_2 \tag{21.89}$$

### 21.5.4 Output Resistance $r_{o,o}$ (I/P Open)

$$r_{o,o} = (r_{ce} + RE) \parallel RC \parallel \frac{r_{be}(R3 + R2) + R1R2}{r_{be} + R3(1 + h_{fe})} \tag{21.90}$$

### 21.5.5 Other Equations

All other equations, already similarly given in the previous sections, can be derived by application of the following additions:

$$R3_{eff} = R3 \parallel R0 \tag{21.91}$$

$$RC_{eff} = RC \parallel RL \tag{21.92}$$

### 21.5.6 Noise and SN

Figure 21.11 shows the Fig. 21.9 noise model.

The major difference to the Fig. 21.8 noise model comes from the treatment of R2. However, because of the rather difficult math T/S recommends the application of the equations for  $e_{n,i}$  and  $i_{n,i}$  according to TSOS-1, p. 51f and TSOS-2, p. 70. These equations lead to the input referred noise voltage density and noise current density equations of Sect. 21.3.7 plus the ones of Sect. 21.4.6. Thus, we obtain for the here presented gain stage the input referred noise voltage density in the R0, RL, and frequency dependent format as follows:

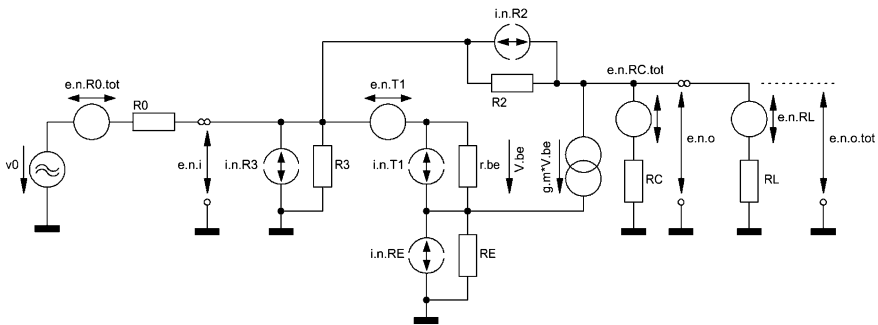


Fig. 21.11 Noise model of the Fig. 21.9 CE<sub>vcf2</sub> gain stage



$$e_{n.i.tot}(f, R0, RL) = \frac{e_{n.o.tot}(f, R0, RL)}{G_{vcf2}(RL)} \quad (21.93)$$

$$e_{n.o.tot}(f, R0, RL) = \sqrt{\begin{aligned} &e_{n.i}(f)^2 G_{vcf2}(RL) \\ &+ e_{n.R0.tot}(f, R0) G_{ops}(f, R0, RL) \\ &+ e_{n.RL}^2 \left( \frac{RL}{Z_{o.s}(f) + RL} \right)^2 \end{aligned}} \quad (21.94)$$

$$e_{n.i}(f, RL) = \sqrt{e_{n.T1}(f)^2 + \frac{e_{n.RC.tot}(f)^2}{G_{vcf2}(RL)^2}} \quad (21.95)$$

$$e_{n.T1}(f) = \sqrt{e_{n1.T1}^2 + i_{n.T1}(f)^2 R_{BE}^2 + e_{n.R.BE}^2} \quad (21.96)$$

$$R_{BE} = r_{bb'} + RE \quad (21.97)$$

$$e_{n.R0.tot}(f, R0) = \sqrt{e_{n.R0}(R0)^2 + i_{n.i}(f)^2 R0^2} \quad (21.98)$$

$$Z_{o.s}(f) = r_{o.s} \parallel C_o \quad (21.99)$$

$$C_o = \frac{C_{ce}}{1 + g_m RE} + C_{bc} \quad (21.100)$$

$$i_{n.i}(f) = \sqrt{i_{n.T1}(f)^2 + i_{n.RA}^2 + i_{n.RB}^2} \quad (21.101)$$

The calculation of the frequency dependent  $e_{n.RC.tot}(f)$  follows the rules shown in Sect. 21.2.5. Section 21.2.7 gives the equations to calculate SNs.

## 21.6 Correction of a TSOS-1 and TSOS-2 Gain Result

Now, with the shown equations, we can calculate the gain of the example gain stage of TSOS-1, Fig. 3.26 and TSOS-2 Fig. 5.9: We obtain

$$G_{vcf} = 46.97 \text{ dB} \quad (21.102)$$

The result is very close to the simulated one of (3.91) and (5.23) in the TSOS books:

$$G_s = 47.0 \text{ dB} \quad (21.103)$$

## 21.7 The CE in Series Configuration with an Op-Amp

### 21.7.1 Basics

The headline's closed loop circuit arrangement is shown in the principal circuit of Fig. 21.12. The working gains of this arrangement look as follows (we ignore the value of R.DCS here):

$$\begin{aligned} G_{\text{amp}} &= \frac{V_o}{V_i} \\ &= 1 + \frac{Z_{f1}}{R_E} \end{aligned} \quad (21.104)$$

$$G_{\text{ops}} = G_i G_{\text{amp}} \quad (21.105)$$

$$G_i = \frac{R_{in}}{R_0 + R_{in}} \quad (21.106)$$

Because of the very low output resistance,  $R_L$  does not influence the gains. In the RIAA amp case  $Z_{f1}$  could be one or all RIAA time constants producing network(s). In most cases,  $Z_{f2}$  should be chosen as high valued resistor  $R_{f2} \geq 100 \text{ k}\Omega$  with a small capacitor  $C_{f2}$  (10pF–47pF) parallel to it. The values heavily depend on the stability and the bandwidth of the whole arrangement. To find the right values for each circuit we have to go through a trial and error process or via pSpice. All my designs work well with  $2.2 \text{ M}\Omega \parallel 12\text{pF}$ – $22\text{pF}$  and a 5534A as OP1. DCS in Fig. 21.12 means DC servo voltage, or a fixed DC voltage that sets

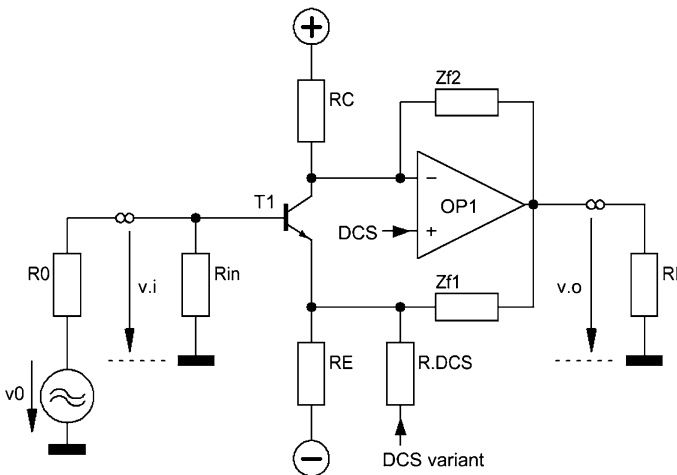


**Fig. 21.12** Principal circuit of a closed loop arrangement with a BJT followed by an op-amp

the collector DC voltage of T1. If we chose a fixed voltage at the (+) input of OP1 the DCS input works via  $R_{DCS}$  and a corresponding servo circuit.

With the well know general gain equation for op-amps in mind the exactness of the working gain equations depend on the idle gain  $G_0$  of the T1 + OP1 pair. Therefore, with a gain of 1000 and an error of less than 1 % it should become  $G_0 > 100,000$ .<sup>5</sup> This gain  $G_0$  is composed by the mutual conductance of T1 and Zf2 as follows:

$$G_0(f) = | -g_{m1}Zf2(f) | \quad (21.107)$$

Simplified and not frequency dependent version:

$$G_0 = | -g_{m1}Rf2 | \quad (21.108)$$

With  $\beta = RE/(RE + Zf1(f))$  the working frequency dependent and closed loop gain  $G(f)$  thus becomes:

$$G_{amp}(f) = \frac{G_0(f)}{1 + G_0(f)\beta(f)} \quad (21.109)$$

Hence, for a gain  $G_0 \geq 10^5$  and  $Rf2 = 2.2 \text{ M}\Omega$  we need  $g_m \geq 45.5 \text{ mS}$ . The Module 2 phono-amp with 4 paralleled BJTs and a collector current  $I_C = 6.7 \text{ mA}$  creates  $g_m = 259 \text{ mS}$ , Amp2's  $g_m$  becomes  $170.2 \text{ mS}$  with  $I_C = 4.4 \text{ mA}$ .

Only the input stage and the input load should generate the counting noise of the phono-amp. Hence, at least the input stage's gain should have a value that its input referred noise voltage times the gain makes the noise of the following gain stages ignorable. This contribution allowed<sup>6</sup> discussion has led to my recommendation of an input stage gain  $\geq 37.5 \text{ dB}$ .

Nevertheless, the next section explains the calculation process of the input referred noise voltage in full detail, no matter if the op-amp stage does add noise or not.

## 21.7.2 Noise and SN

We assume a  $CE_{vcf2}$  input à la Fig. 21.9, no noise from the DCS variants and resistive feedback paths of the amp and OP1, hence,  $Rf1$  and  $Rf2$  instead of  $Zf1$  and  $Zf2$ . In case of an RIAA network, we take the value of the magnitude of the  $Zf1$  impedance at 1 kHz. According to  $Rf2$ , there should be no difference between  $Zf2$ 's magnitude at 1 kHz and the  $Rf2$  resistor value.

<sup>5</sup>'Intuitive IC OP Amps', 1984, Thomas M. Frederiksen, National's Semiconductor Technology Series.

<sup>6</sup>Details see TSOS-1, Chapter 3.2, TSOS-2, Chapter 5.4.

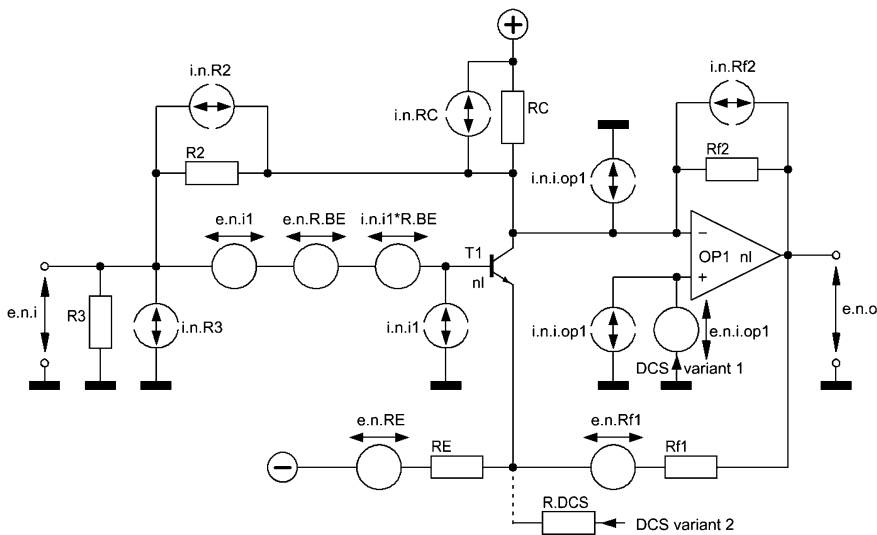


**Fig. 21.13** Frequency independent noise model of the modified Fig. 21.12 amp

Figure 21.13 shows the frequency independent noise model of the modified Fig. 21.12 amp. Nevertheless, the frequency dependency will be part of the equation paragraphs.

We obtain the general equations for the input referred noise voltage density  $e_{n,i}(f)$  as follows:

$$e_{n,i}(f) = \sqrt{\frac{e_{n,i1}(f)^2 + e_{n,R,BE}^2 + i_{n,i1}(f)^2 R_{BE}^2}{|G_{vcf2.1}|^2 + \frac{i_{n,RC}(f)^2 + i_{n,i.op1}(f)^2 + i_{n,Rf2}^2}{g_{m1}^2}}} \tag{21.110}$$

$$e_{n,i1}(f) = \frac{i_{n,C1}(f)}{g_{m1}} \tag{21.111}$$

$$i_{n,i1}(f) = \frac{i_{n,C1}(f)}{h_{fe1}} \tag{21.112}$$

$$R_{BE} = r_{bb1'} + \left( \frac{1}{RE} + \frac{1}{Rf1} \right)^{-1} \tag{21.113}$$

Thus, the output referred noise voltage density looks like:

$$e_{n,o}(f) = e_{n,i}(f)G_{amp} \tag{21.114}$$

With an input load  $R_0$   $i_{n,i}(f)$  comes into the game. We obtain the amp's input noise voltage density as follows:

$$i_{n,i}(f) = \sqrt{i_{n,i1}(f)^2 + i_{n,R2}^2 + i_{n,R3}^2} \quad (21.115)$$

Hence, the input loaded amp increases the output referred noise voltage density by the noise of  $R_0$  the following way:

$$e_{n.o.amp}(f, R_0) = G_{amp} \sqrt{e_{n,i}(f)^2 + i_{n,i}(f)^2 R_0^2 + e_{n,R0}(R_0)^2} \quad (21.116)$$

Provided that one of the two DCS variants is chosen and their output noise voltage might influence the amp's noise production in a countable way we can add this noise voltage density to the one of OP1 in (21.110) (=variant 1) or we take variant 2 and change the above shown equations as follows ( $_{dcs2}$ ):

$$e_{n.o.amp.dcs2}(f, R_0) = G_{amp} \sqrt{e_{n,i}(f)^2 + i_{n,i}(f)^2 R_0^2 + e_{n,R0}(R_0)^2 + e_{n.o.dcs2}(f)^2 (Rf1R_{DCS})^2} \quad (21.117)$$

Here,  $e_{n.o.dcs2}(f)$  must include the noise of  $R_{DCS}$ .

$$e_{n.i.amp.dcs2}(f) = \frac{e_{n.o.amp.dcs2}}{G_{amp}} \quad (21.118)$$

Normally, DCSs have an lp transfer character with very low corner frequencies. That's why we can assume ignorable tiny influences.

The SN calculations follow the equations of Sect. 21.2.7.

## 22.1 Intro

I use the terminus technicus DIF-amp or DIFA for amplifiers with a differential input and a differential output. Their differential gain  $G_{\text{dif}}$  follows the rule:

$$G_{\text{dif}} = \frac{V_{o1} - V_{o2}}{V_{i1} - V_{i2}} \tag{22.1}$$

Another expression for  $G_{\text{dif}}$  could be:

$$G_{\text{dif}} = \frac{V_{\text{dif.o}}}{V_{\text{dif.i}}} \tag{22.2}$$

Here, according to Fig. 22.1 the signal voltages on the right side of (22.1) are the ones between the input or output leads and ground. In addition, the ones with subscript 2 have a 180° phase shift to the ones with subscript 1.

The voltages of (22.2) are the ones between the input leads and between the output leads. With equal values for the input voltages  $v_{i1}$  and  $v_{i2}$  but opposite phase we obtain:

$$\begin{aligned} V_{i2} &= -V_{i1} \\ V_{o2} &= -V_{o1} \end{aligned} \tag{22.3}$$

Hence,

$$G_{\text{dif}} = \frac{2V_{o1}}{2V_{i1}} = \frac{V_{o1}}{V_{i1}} = \frac{V_{o2}}{V_{i2}} \tag{22.4}$$

In the following sections I'll concentrate on two different DIFA types only: the DIFA-OPA and the DIFA-IC. These types serve phono-amp needs best.

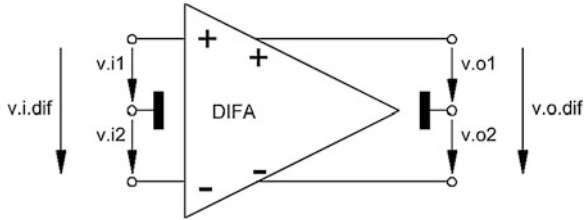
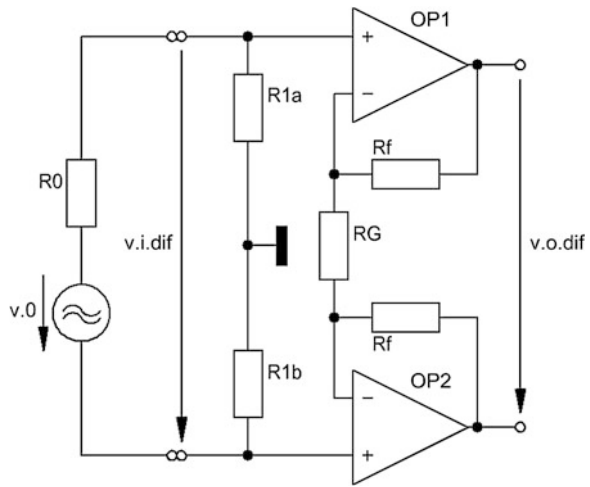


**Fig. 22.1** Situation of the signal voltages in a DIFA

**Fig. 22.2** General DIF-OPA circuit with input load



## 22.2 The DIFA-OPA<sup>1</sup>

### 22.2.1 Basics

Shown in Fig. 22.2 the DIFA-OPA consists of two op-amps and a handful of passive components. There is no phase shift between input and output signal voltages and the general appearance is alike the one of the input stage of an instrumentation amplifier type 2.<sup>2</sup>

With equal valued resistors  $R_f$  and equal valued resistors  $R_1$  in Fig. 22.2 the gain equations for the differential gain  $G_{dif}$  and the operational gain  $G_{dif.ops}$  look as follows:

<sup>1</sup>eg Amp1 of Chaps. 8 and 9.

<sup>2</sup>See TSOS-1 Sect. 3.6 or TSOS-2 Chap. 9.

$$\begin{aligned} G_{\text{dif}} &= \frac{V_{\text{o,dif}}}{V_{\text{i,dif}}} \\ &= 1 + \frac{2R_f}{R_G} \end{aligned} \quad (22.5)$$

$$\begin{aligned} G_{\text{dif,ops}} &= \frac{V_{\text{o,dif}}}{v_0} \\ &= G_{\text{dif}} G_i \end{aligned} \quad (22.6)$$

$$G_i = v_0 \frac{R1a + R1b}{R0 + R1a + R1b} \quad (22.7)$$

The CMRR thus becomes:

$$\text{CMRR} = \frac{G_{\text{dif}}}{G_{\text{cm}}} \quad (22.8)$$

$$G_{\text{cm}} = 1 \quad (22.9)$$

### 22.2.2 Noise Calculations Version 1

Without R1a and R1b Fig. 22.3 gives all relevant DIF-OPA noise sources. The noise effects of the two input resistors  $R1a + R1b = R1$  can be combined with the noise of R0 as follows:

$$R0_{\text{eff}} = R0 || R1 \quad (22.10)$$

$$e_{\text{n,R0,eff}} = \sqrt{\left( \frac{1}{e_{\text{n,R0}}^2} + \frac{1}{e_{\text{n,R1}}^2} \right)^{-1}} \quad (22.11)$$

There are two versions to get the Fig. 22.2 input referred noise voltage density  $e_{\text{n,i,tot}}$ .

Version 1: According to Fig. 22.3 we obtain the frequency independent output noise voltage density  $e_{\text{n,o,tot1}}$  as follows:

$$e_{\text{n,o,tot1}} = \sqrt{G_{\text{dif}}^2 \left( e_{\text{n,i1}}^2 + e_{\text{n,i2}}^2 + e_{\text{n,R0,eff}}^2 + R0_{\text{eff}}^2 \left( \frac{1}{i_{\text{n,i1}}^2} + \frac{1}{i_{\text{n,i2}}^2} \right)^{-1} \right) + e_{\text{n,Rf}}^2 \left( \frac{2R_f}{R_G} \right)^2 + 2e_{\text{n,Rf}}^2 + (i_{\text{n,i1}}^2 + i_{\text{n,i2}}^2) R_f^2} \quad (22.12)$$



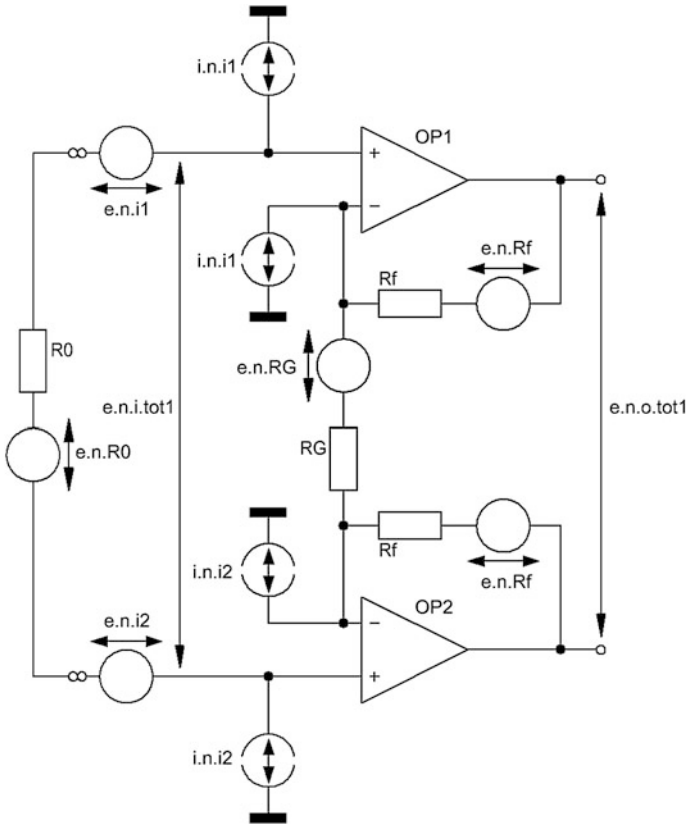


**Fig. 22.3** Relevant noise sources of Fig. 22.2

Thus,  $e_{n.i.tot1}$  becomes:

$$e_{n.i.tot1} = \frac{e_{n.o.tot1}}{G_{dif}} \tag{22.13}$$

### 22.2.3 Noise Calculations Version 2

Version 2 requires an adapted Fig. 22.3, shown in Fig. 22.4.

Without detour via the output, with  $e_{ni1} = e_{n.i2}$  and  $i_{n.i1} = i_{n.i2}$  the input referred noise voltage density can thus be calculated directly:

$$e_{n.i.tot2} = \sqrt{e_{n.i}^2 + e_{n.R0,eff}^2 + e_{n.RG,f}^2 + i_{n.i}^2 (R0_{eff}^2 + RG_f^2)} \tag{22.14}$$

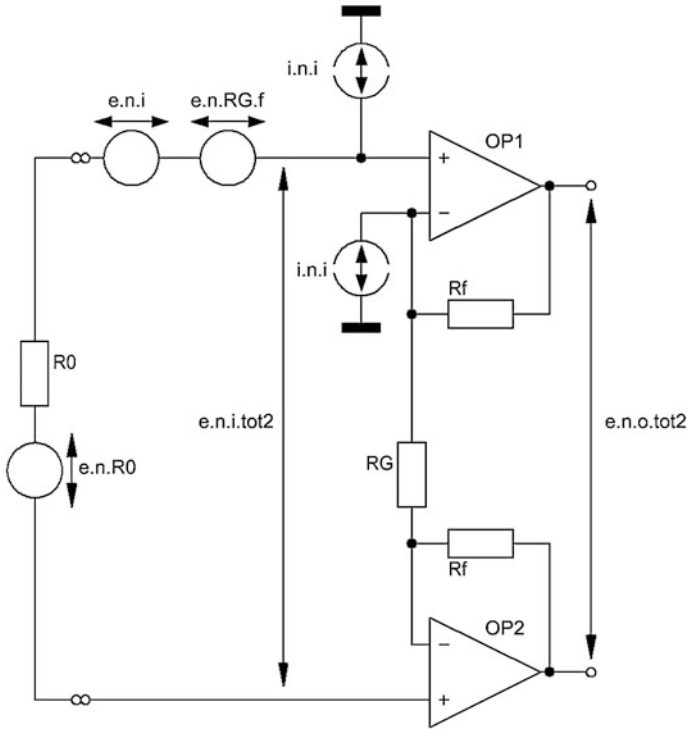


Fig. 22.4 Adapted Fig. 22.3

$$e_{n.i} = \sqrt{e_{n.i1}^2 + e_{n.i2}^2} \tag{22.15}$$

$$= \sqrt{2} i_{n.i1}$$

$$i_{n.i} = \sqrt{\left(\frac{1}{i_{n.i1}^2} + \frac{1}{i_{n.i2}^2}\right)^{-1}} \tag{22.16}$$

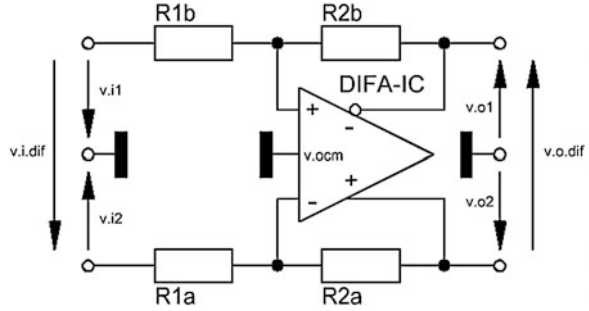
$$= \frac{i_{n.i1}}{\sqrt{2}}$$

$$RG_f = RG \parallel (2Rf) \tag{22.17}$$

A short math exercise yields:

$$e_{n.i.tot1} = e_{n.i.tot2} \tag{22.18}$$

**Fig. 22.5** Typical amplifier circuit with a DIFA-IC



### 22.2.4 Noise Calculations Version with One Input Lead Grounded

If we ground one input lead the noise current through  $R_{0\text{eff}}$  changes to  $i_{n,i1}$  and (22.14) changes to:

$$e_{n.i.\text{tot}2.\text{grd}} = \sqrt{e_{n,i}^2 + e_{n,R0.\text{eff}}^2 + e_{n,RG.f}^2 + i_{n,i1}^2 R_{0\text{eff}}^2 + i_{n,i}^2 R_G^2} \tag{22.19}$$

Hence, we'll always get:

$$e_{n.i.\text{tot}2} < e_{n.i.\text{tot}2.\text{grd}} \tag{22.20}$$

Because of the always existing 1/f-noise of op-amps next chapter's MCD-WS 23.1 gives frequency dependent example calculations for all versions.

## 22.3 The DIFA-IC<sup>3</sup>

### 22.3.1 Basics

A completely different DIF approach works with an intelligent arrangement of two shunt configured op-amps in such a way that the differential output signal voltage has a 180° phase shift to the differential input signal voltage (see Fig. 22.5).

With equal valued resistors  $R1a = R1b$  and  $R2a = R2b$  the gain  $G_{\text{dif}}$  of this arrangement becomes:

$$G_{\text{dif}} = -\frac{R2a}{R1a} \tag{22.21}$$

<sup>3</sup>eg in Sect. 13.5.1 Joachim Gerhard's solution.

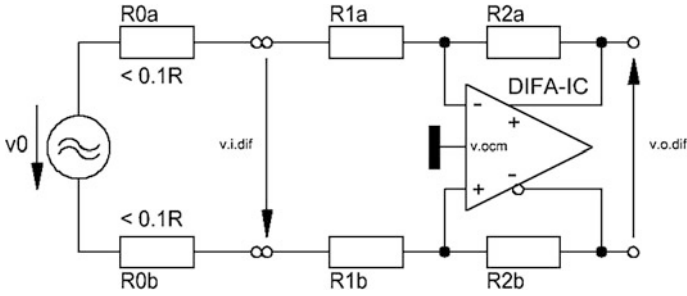


**Fig. 22.6** DIFA-IC with input load

And we obtain its noise gain  $G_{N,dif}$  as follows:

$$G_{N,dif} = |G_{dif}| + 1 \tag{22.22}$$

This type of amplifier IC topology creates one specific problem: any change of its input resistors  $R1a$  and  $R1b$  will lead to other than the calculated gain results. A typical change will occur with output resistances of preceding gain stages  $>0 \Omega$ . The ideal situation is given in Fig. 22.6 and  $R0a$  and  $R0b$  both equal but  $>0 \Omega$  will change (22.21) as follows:

$$G_{dif2} = -\frac{R2a}{R1a + R0a} \tag{22.23}$$

In any case,  $|G_{dif2}| < |G_{dif}|$ !

Concerning CMRR the data sheet specs are the only source.

### 22.3.2 Noise Calculations Version 1

Basically, in Version1 the noise calculations follow the recommendations of Texas Instruments.<sup>4</sup> However, with a lot of math rearrangements<sup>5</sup> the equation to calculate the output referred noise voltage density  $e_{n,o,dif}$  of Fig. 22.7 could be simplified. We obtain thus  $e_{n,o,dif}$  in the frequency dependent format:

$$e_{n,o,dif1}(f) = \sqrt{\frac{e_{n,i}(f)^2(1 + |G_{dif}|)^2}{+2 \left[ i_{n,i}(f)^2 R2a^2 + e_{n,R1a}^2 |G_{dif}|^2 + e_{n,R2a}^2 \right]}} \tag{22.24}$$

<sup>4</sup>“Fully-Differential Amplifiers”, TI Application Report SLOA054D.

<sup>5</sup>See Chap. 23 and the derivation in MCD-WS 23.3.

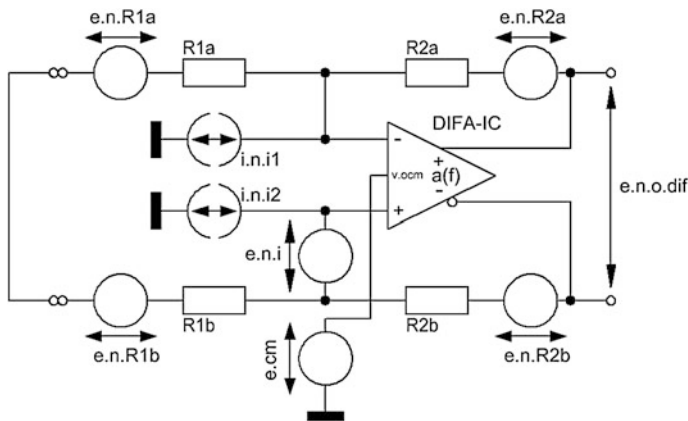


**Fig. 22.7** Noise sources of a DIFA-IC

The input referred noise voltage density becomes:

$$e_{n.i.dif1}(f) = \frac{e_{n.o.dif1}(f)}{G_{N.dif}} \tag{22.25}$$

$e_{n.i}$ ,  $i_{n.i}$ , and their 1/f-noise corner frequencies must be picked from the data sheets.

By application of the specific noise voltage summing method any noise voltage  $e_{n.prec}(f)$  from a preceding gain stage must be multiplied with  $|G_{dif}|$  and be added to  $e_{n.o.dif1}(f)$  to get the new output noise voltage density  $e_{n.o.tot.dif1}(f)$ , hence,

$$e_{n.o.tot.dif1}(f) = \sqrt{|G_{dif}|^2 e_{n.prec}(f)^2 + e_{n.o.dif1}(f)^2} \tag{22.26}$$

In the above given equations there is no term concerning the noise voltage  $e_{n.cm}(f)$  of the common mode input. It can be ignored as long as it is grounded. However, any DC servo that works via the  $v_{ocom}$  input adds the noise voltage of the servo too, hence, it must be multiplied with  $G_{N.dif}$  and be added by an additional term squared in (22.24).

### 22.3.3 Noise Calculations Version 2

A look back to TSOS-2's MCD-WS 12.16 and Sect. 8.7 (see  $e_{n.i.shu}$ ) allows calculating the input referred noise voltage density of such a double shunt configured op-amp arrangement by an equivalent approach. Thus,  $e_{n.i.dif2}(f)$  becomes:

$$e_{n.i.dif2}(f) = \sqrt{e_{n.i}(f)^2 + 2 \left[ (i_{n.i}(f)RP1)^2 + e_{n.RP1}^2 \right]} \tag{22.27}$$

$$RP1 = R1a||R2a \quad (22.28)$$

We obtain the output referred noise voltage density  $e_{n.o.dif2}(f)$  as follows:

$$e_{n.o.dif2}(f) = G_{N.dif} e_{n.i.dif1}(f) \quad (22.29)$$

Thus,<sup>6</sup>

$$\begin{aligned} e_{n.o.dif1}(f) &= e_{n.o.dif2}(f) \\ e_{n.i.dif1}(f) &= e_{n.i.dif2}(f) \end{aligned} \quad (22.30)$$

and

$$e_{n.o.tot.dif2}(f) = \sqrt{|G_{dif}|^2 e_{n.prec}(f)^2 + e_{n.o.dif2}(f)^2} \quad (22.31)$$

---

<sup>6</sup>See MCD-WS 23.2.

## Contents

- 23.1 MCD-WS: DIFA-OPA
- 23.2 MCD-WS: DIFA-IC

**Note 1:** MCD 11 has no built-in unit “rtHz” or “ $\sqrt{\text{Hz}}$ ”. To get  $\sqrt{1 \text{ Hz}}$  based voltage noise and current noise densities the rms noise voltage and current in a specific frequency range  $B > 1 \text{ Hz}$  must be multiplied by  $\sqrt{1 \text{ Hz}}$  and divided by the root of that specific frequency range  $\sqrt{B}$ !

**Note 2:** MCD 11 offers no “dB” unit. This is available from MCD 13 on!

23.1 MCD-WS: DIFA-OPA

DIF-Amp with Op-Amps (DIFA-OPA) and input loaded with R0

1. Gain and Noise Calculations :

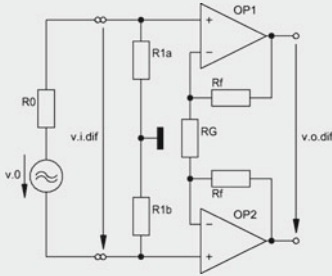


Fig. 23.1 = Fig. 22.2

$k := 1.38065 \cdot 10^{-23} \text{V} \cdot \text{A} \cdot \text{s} \cdot \text{K}^{-1}$	$T := 300 \cdot \text{K}$	$B_1 := 1 \text{Hz}$	$B_{20k} := 19980 \text{Hz}$	$h := 1000 \text{Hz}$
$f := 20 \text{Hz}, 25 \text{Hz}, 20 \cdot 10^3 \text{Hz}$			$v_{i,nom} := 5 \cdot 10^{-3} \text{V}$	
$OP1 = OP27$	$OP2 = OP1$			
$e_{n,il} := 3.0 \cdot 10^{-9} \text{V}$	$e_{n,i2} := e_{n,il}$	$f_{c,e1} := 2.7 \text{Hz}$	$e_{n,il}(f) := e_{n,il} \cdot \sqrt{\frac{f_{c,e1}}{f} + 1}$	
$i_{n,il} := 0.4 \cdot 10^{-12} \text{A}$	$i_{n,i2} := i_{n,il}$	$f_{c,il} := 140 \text{Hz}$	$i_{n,il}(f) := i_{n,il} \cdot \sqrt{\frac{f_{c,il}}{f} + 1}$	
			$i_{n,i2}(f) := i_{n,il}(f)$	
$R0 := 12 \cdot 10^3 \Omega$	$Rf := 10 \cdot 10^3 \Omega$	$RG := 100 \Omega$		
$e_{n,RG} := \sqrt{4 \cdot k \cdot T \cdot B_1 \cdot RG}$			$e_{n,RG} = 1.287 \times 10^{-9} \text{V}$	
$e_{n,Rf} := \sqrt{4 \cdot k \cdot T \cdot B_1 \cdot Rf}$			$e_{n,Rf} = 12.872 \times 10^{-9} \text{V}$	
$e_{n,R0} := \sqrt{4 \cdot k \cdot T \cdot B_1 \cdot R0}$			$e_{n,R0} = 14.1 \times 10^{-9} \text{V}$	
$G_{dif} := 1 + 2 \cdot \frac{Rf}{RG}$			$G_{dif} = 201$	



23.1 MCD-WS: DIFA-OPA

1.1 Output referred approach (= Version 1) :

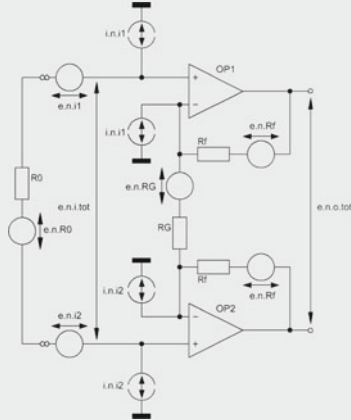


Fig. 23.2 = 22.3

$$e_{n.o.tot1}(f) := \sqrt{G_{dif}^2 \left[ e_{n.i1}(f)^2 + e_{n.i2}(f)^2 + e_{n.R0}^2 + \left( \frac{1}{i_{n.i1}(f)^2} + \frac{1}{i_{n.i2}(f)^2} \right)^{-1} \cdot R0^2 \right] + e_{n.RG}^2 \cdot \left( \frac{2 \cdot Rf}{RG} \right)^2 + 2 \cdot e_{n.Rf}^2 + 2 \cdot i_{n.i1}(f)^2 \cdot Rf^2}$$

$$e_{n.o.tot1}(h) = 3.059 \times 10^{-6} V$$

$$e_{n.i.tot1}(f) := \frac{e_{n.o.tot1}(f)}{G_{dif}}$$

$$e_{n.i.tot1}(h) = 15.22 \times 10^{-9} V$$

1.2 Input referred approach (= Version 2) :

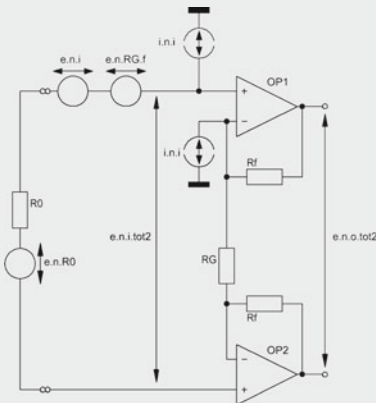


Fig. 23.3 = Fig. 22.4

23.1 MCD-WS: DIFA-OPA

$$e_{n,i}(f) := e_{n,il}(f) \cdot \sqrt{2} \qquad i_{n,i}(f) := \frac{i_{n,il}(f)}{\sqrt{2}}$$

$$RG_f := \left( \frac{1}{RG} + \frac{1}{2 \cdot Rf} \right)^{-1} \qquad RG_f = 99.502 \, \Omega$$

$$e_{n,RG,f} := \sqrt{4 \cdot k \cdot T \cdot B_1 \cdot RG_f} \qquad e_{n,RG,f} = 1.284 \times 10^{-9} \, V$$

$$e_{n,itot2}(f) := \sqrt{e_{n,i}(f)^2 + i_{n,i}(f)^2 \cdot (RG_f^2 + R0^2) + e_{n,RG,f}^2 + e_{n,R0}^2} \qquad e_{n,itot2}(h) = 15.22 \times 10^{-9} \, V$$

$$e_{n,o,tot2}(f) := G_{dif} \cdot e_{n,itot2}(f) \qquad e_{n,o,tot2}(h) = 3.059 \times 10^{-6} \, V$$

Hence,  $e_{n,o,tot2}(f) = e_{n,o,tot1}(f) \qquad e_{n,i,tot2}(f) = e_{n,i,tot1}(f)$

1.3 One input lead grounded :

$$e_{n,itot2,grd}(f) := \sqrt{e_{n,i}(f)^2 + i_{n,il}(f)^2 \cdot R0^2 + i_{n,i}(f)^2 \cdot RG_f^2 + e_{n,RG,f}^2 + e_{n,R0}^2} \qquad e_{n,itot2,grd}(h) = 15.645 \times 10^{-9} \, V$$

$$e_{n,o,tot2,grd}(f) := G_{dif} \cdot e_{n,itot2,grd}(f) \qquad e_{n,o,tot2,grd}(h) = 3.145 \times 10^{-6} \, V$$

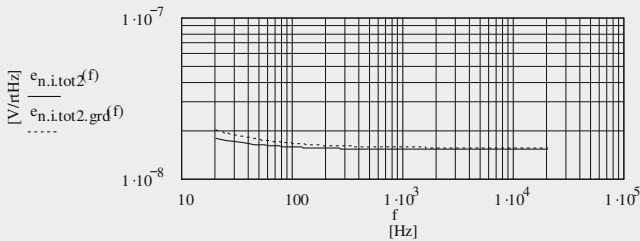


Fig. 23.4 Input referred and input loaded noise voltage densities of the fully differential input and the grounded input

Hence,  $e_{n,o,tot2,grd}(f) > e_{n,o,tot2}(f)$

23.1 MCD-WS: DIFA-OPA

2. SN calculations :

$$SN_{ne2} := 20 \cdot \log \left[ \frac{\sqrt{\frac{1}{B_1} \cdot \int_{20\text{Hz}}^{2000\text{Hz}} (|e_{n.i.tot2}(f)|)^2 df}}{v_{i.nom}} \right] \quad SN_{ne2} = -67.346 \quad [\text{dB}]$$

$$SN_{ne2.grd} := 20 \cdot \log \left[ \frac{\sqrt{\frac{1}{B_1} \cdot \int_{20\text{Hz}}^{2000\text{Hz}} (|e_{n.i.tot2.grd}(f)|)^2 df}}{v_{i.nom}} \right] \quad SN_{ne2.grd} = -67.124 \quad [\text{dB}]$$

Hence,  $|SN_{ne2}| > |SN_{ne2.grd}|$

23.2 MCD-WS: DIFA-IC

DIF-Amps with ICs (DIFA-IC)

1. Gain and Noise Calculations :

Example DIFA-IC = OPA1632

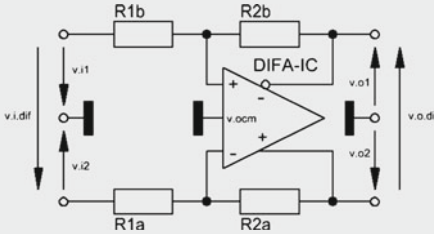


Fig. 23.5 = 22.5

$$k := 1.38065 \cdot 10^{-23} \text{ V} \cdot \text{A} \cdot \text{s} \cdot \text{K}^{-1} \quad T := 300 \cdot \text{K} \quad B_1 := 1 \text{ Hz} \quad B_{20k} := 19980 \text{ Hz} \quad h := 10^3 \text{ Hz}$$

$$f := 20 \text{ Hz}, 25 \text{ Hz}, 20 \cdot 10^3 \text{ Hz}$$

$$e_{n,i} := 1.3 \cdot 10^{-9} \text{ V} \quad f_{c,e} := 0.6 \cdot 10^3 \text{ Hz} \quad e_{n,i}(f) := e_{n,i} \sqrt{\frac{f_{c,e}}{f} + 1} \quad e_{n,i}(h) = 1.644 \times 10^{-9} \text{ V}$$

$$i_{n,i} := 0.4 \cdot 10^{-12} \text{ A} \quad f_{c,i} := 2 \cdot 10^3 \text{ Hz} \quad i_{n,i}(f) := i_{n,i} \sqrt{\frac{f_{c,i}}{f} + 1} \quad i_{n,i}(h) = 692.82 \times 10^{-15} \text{ A}$$

$$R1a := 1 \cdot 10^3 \Omega \quad R2a := 200 \cdot 10^3 \Omega \quad R1b := R1a \quad R2b := R2a$$

$$G_{\text{dif}} := \frac{R2a}{R1a} \quad G_{\text{dif}} = -200$$

$$G_{N,\text{dif}} := |G_{\text{dif}}| + 1 \quad G_{N,\text{dif}} = 201$$

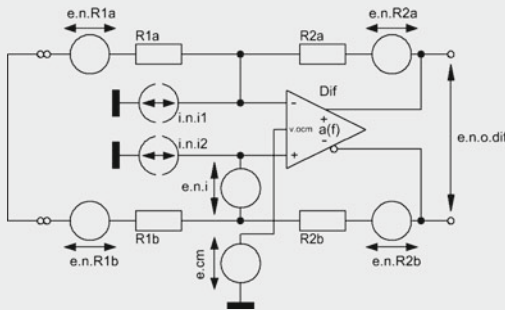


Fig. 23.6 = Fig. 22.6

23.2 MCD-WS: DIFA-IC

1.1 Output referred approach (= Version 1) :

$$\begin{aligned}
 e_{n,R1a} &:= \sqrt{4 \cdot k \cdot T \cdot R1a \cdot B1} & e_{n,R1b} &:= e_{n,R1a} & e_{n,R1a} &= 4.07 \times 10^{-9} \text{ V} \\
 e_{n,R2a} &:= \sqrt{4 \cdot k \cdot T \cdot R2a \cdot B1} & e_{n,R2b} &:= e_{n,R2a} & e_{n,R2a} &= 57.564 \times 10^{-9} \text{ V} \\
 e_{n,o,dif,o}(f) &:= \sqrt{e_{n,i}(f)^2 \cdot G_{N,dif}^2 + 2 \cdot \left[ i_{n,i}(f)^2 \cdot R2a^2 + e_{n,R1a}^2 \cdot \left( |G_{dif}| \right)^2 + e_{n,R2a}^2 \right]} & & & & (1) \\
 e_{n,o,dif,o}(h) &= 1.216 \times 10^{-6} \text{ V} \\
 e_{n,i,dif,o}(f) &:= \frac{e_{n,o,dif,o}(f)}{G_{N,dif}} & & & & e_{n,i,dif,o}(h) = 6.052 \times 10^{-9} \text{ V}
 \end{aligned}$$

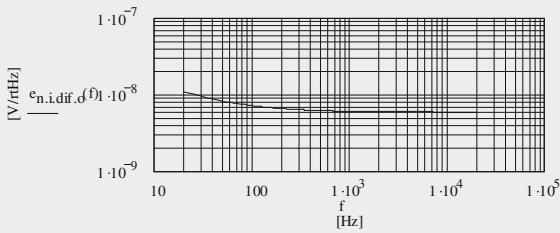


Fig. 23.7 Input referred differential noise voltage density, input shorted or output resistance of preceding gain stage -0R

1.2 Input referred approach (= Version 2) :

$$\begin{aligned}
 RP1 &:= \frac{R1a \cdot R2a}{R1a + R2a} & RP2 &:= RP1 & RP1 &= 995.025 \text{ } \Omega \\
 e_{n,RP1} &:= \sqrt{4 \cdot k \cdot T \cdot B1 \cdot RP1} & e_{n,RP2} &:= e_{n,RP1} & e_{n,RP1} &= 4.06 \times 10^{-9} \text{ V} \\
 e_{n,i,dif,f}(f) &:= \sqrt{e_{n,i}(f)^2 + 2 \cdot \left( i_{n,i}(f)^2 \cdot RP1^2 + e_{n,RP1}^2 \right)} & & & e_{n,i,dif,f}(h) &= 6.052 \times 10^{-9} \text{ V} \\
 e_{n,o,dif,f}(f) &:= e_{n,i,dif,f}(f) \cdot G_{N,dif} & & & e_{n,o,dif,f}(h) &= 1.216 \times 10^{-6} \text{ V} \\
 \Rightarrow & & e_{n,o,dif,o}(f) &= e_{n,o,dif,f}(f) & \text{ and } & e_{n,i,dif,o}(f) = e_{n,i,dif,f}(f)
 \end{aligned}$$

2. SN calculations :

$$SN_{ne} := 20 \cdot \log \left[ \frac{\frac{1}{B1} \cdot \int_{20\text{Hz}}^{20000\text{Hz}} \left( |e_{n,o,dif,o}(f)| \right)^2 df}{v_{o,nom}} \right] \qquad SN_{ne} = -75.422 \quad [\text{dBV}]$$

23.2 MCD-WS: DIFA-IC

3. Derivation of (1) via TI-SLOA054D :

$$G_{dif} = -\frac{v_{o,dif}}{v_{i,dif}} \quad v_{i,dif} = v_{i1} - v_{i2} \quad v_{o,dif} = v_{o1} - v_{o2} \quad v_{o,cm} = 0$$

$$B1 := \frac{R1a}{R1a + R2a} \quad B1 = 4.975 \times 10^{-3} \quad B2 := \frac{R1b}{R1b + R2b} \quad B2 = 4.975 \times 10^{-3}$$

$$B1 = B2 \quad \Rightarrow \quad B := B1$$

$$G_{dif} = -\left( \frac{1-\beta}{\beta} \cdot \frac{1}{1 + \frac{1}{a(f)\beta}} \right) \quad a(f) \gg 1 \quad \Rightarrow \quad G_{dif} := -\frac{1-\beta}{\beta} \quad G_{dif} = -200$$

$$RA := \frac{R1a \cdot R2a}{R1a + R2a} \quad RA = 995.025 \, \Omega \quad RB := \frac{R1a \cdot R2b}{R1a + R2b} \quad RB = 995.025 \, \Omega$$

$$\Rightarrow \quad RA = RB$$

$$e_{n,R1a} := \sqrt{4 \cdot k \cdot T \cdot R1a \cdot B1} \quad e_{n,R1b} := e_{n,R1a} \quad e_{n,R1a} = 4.07 \times 10^{-9} \text{ V}$$

$$e_{n,R2a} := \sqrt{4 \cdot k \cdot T \cdot R2a \cdot B1} \quad e_{n,R2b} := e_{n,R2a} \quad e_{n,R2a} = 57.564 \times 10^{-9} \text{ V}$$

$$e_{n,i} := 1.3 \cdot 10^{-9} \text{ V} \quad i_{n,i} := 0.4 \cdot 10^{-12} \text{ A} \quad e_{cm} := 0 \text{ V}$$

in case of  $B1 \neq B2$  any noise voltage  $e_{cm} > 0 \text{ V}$  at the common mode input would play a role, however, with 1% resistances the factor  $(B1-B2)$  makes it still ignorable and the respective term in the equation below becomes ignorable too. But, the noise voltage of DC servos that work via the  $v_{ocm}$  input must be added by an additional term.

$$e_{n,o,dif} = \sqrt{\frac{(2 \cdot e_{n,i})^2 + (2 \cdot i_{n,i} \cdot RA)^2 + (2 \cdot i_{n,i} \cdot RB)^2 + [2 \cdot e_{n,R1a} \cdot (1-\beta)]^2 + [2 \cdot e_{n,R1a} \cdot (1-\beta)]^2 + [2 \cdot e_{cm} \cdot (B1 - B2)]^2}{(2 \cdot \beta)^2} + e_{n,R2a}^2 + e_{n,R2b}^2} \dots$$

$$e_{n,o,dif1} := \sqrt{\frac{(2 \cdot e_{n,i})^2 + (2 \cdot i_{n,i} \cdot RA)^2 + (2 \cdot i_{n,i} \cdot RB)^2 + [2 \cdot e_{n,R1a} \cdot (1-\beta)]^2 + [2 \cdot e_{n,R1a} \cdot (1-\beta)]^2}{(2 \cdot \beta)^2} + e_{n,R2a}^2 + e_{n,R2b}^2} \quad (2)$$

$$e_{n,o,dif1} = 1.189 \times 10^{-6} \text{ V}$$

$$G_{N,dif1} = \frac{1}{\beta} \quad G_{N,dif1} = 201 \quad e_{n,i,dif1} := \frac{e_{n,o,dif1}}{|G_{dif}|} \quad e_{n,i,dif1} = 5.944 \times 10^{-9} \text{ V}$$

23.2 MCD-WS: DIFA-IC

3.1 First symplification of (2) :

$$e_{n.o.dif2} := \sqrt{\frac{e_{n.i}^2 + 2 \cdot (i_{n.i} \cdot RA)^2 + 2 \cdot [e_{n.R1a} \cdot (1 - \beta)]^2}{\beta^2} + 2 \cdot e_{n.R2a}^2} \quad e_{n.o.dif2} = 1.189 \times 10^{-6} \text{V} \quad (3)$$

$$SN_{ne2} := 20 \cdot \log \left( \frac{e_{n.o.dif2} \cdot \sqrt{\frac{B_{20k}}{B_1}}}{v_{o.nom}} \right) \quad SN_{ne2} = -75.492 \quad [\text{dBV}]$$

3.2 Frequency dependent version of (3) :

$$f_{c.e} := 0.6 \cdot 10^3 \text{Hz} \quad e_{n,i}(f) := e_{n.i} \cdot \sqrt{\frac{f_{c.e}}{f} + 1} \quad e_{n,i}(h) = 1.644 \times 10^{-9} \text{V}$$

$$f_{c.i} := 2 \cdot 10^3 \text{Hz} \quad i_{n,i}(f) := i_{n.i} \cdot \sqrt{\frac{f_{c.i}}{f} + 1} \quad i_{n,i}(h) = 692.82 \times 10^{-15} \text{A}$$

$$e_{n.o.dif3}(f) := \sqrt{\frac{e_{n,i}(f)^2 + 2 \cdot (i_{n,i}(f) \cdot RA)^2 + 2 \cdot [e_{n.R1a} \cdot (1 - \beta)]^2}{\beta^2} + 2 \cdot e_{n.R2a}^2} \quad e_{n.o.dif3}(h) = 1.216 \times 10^{-6} \text{V} \quad (4)$$

$$e_{n.i.dif3}(f) := \frac{e_{n.o.dif3}(f)}{|G_{dif}|} \quad e_{n.i.dif3}(h) = 6.082 \times 10^{-9} \text{V}$$

Second simplification of (2) :

Second simplification and usage of the term  $G_{dif} = R_{2a}/R_{1a}$  leads to equation (1) at the beginning of this worksheet

---

## 24.1 Intro

I guess this chapter stands for the end of my journey through the jungle of low-noise phono-amps and associated issues. Rather often, I've been asked about my personal ranking of things that ensure optimal sound reproduction of vinyl records. The today's answer is not easy; however, I would like to rank the following two tools among the top positions:

- I know people still running rather old turntables (made in the sixties of last century), old tape recorders (eg Revox A77 or one of the BRAUN TG series) and old FM tuners from manufacturers around the world. Moreover, they are happy, they restore, and they collect these things. I also own an old BRAUN PCS 52 E turntable with SME II tonearm and a Shure V15 IV cartridge. Sometimes, just to check its correct working, I listen to it and I'm always surprised about its still excellent sound reproduction. Of course, a change to one of the other cartridges I own needs the application of a tracking force measurement instrument. Section 24.2 shows the one I use.<sup>1</sup>
- The quality of the sources that create the sound we're listening to heavily depends on the quality of the making process. Hence, we're talking about the groove-making or cutting technology which is—after the mix is hopefully well done—the most sensitive part of the whole LP making process.

From time to time, a cutting lathe from eg Neumann needs a quality check and re-trimming of its parameters, especially those of the cutting head. This is the moment where special test and calibration records (TCRs) enter the scene. In TSOS-1 and TSOS-2, I gave some remarks on the issue and I gave a sad look into the future of the availability of modern test records for cutting lathe calibration

---

<sup>1</sup>Pictures: Courtesy Jo Klatt, Design+Design, Hamburg, Germany.



**Fig. 24.1** BRAUN tracking force measurement instrument



purposes. Later on, I became very surprised about the fact that there are collectors of test records, especially of those excellent ones produced by the former DDR (German Democratic Republic—GDR). For collector and potential duplication purposes, in Sect. 24.3 I add tables of all known test records of the ex-GDR, DIN and Deutsche Grammophon Gesellschaft.

**Fig. 24.2** The BTFMI in action



---

## 24.2 The BRAUN Tracking Force Measurement Instrument

The BRAUN Tracking Force Measurement Instrument (BTFMI) is a rather rare thing to get and—very surprising—we cannot find it in the Braun+Design Tax booklet.<sup>2</sup> Otherwise, this booklet covers everything BRAUN ever produced, incl. actual collector prices.

The BTFMI is a typical 1962 Prof. Rams design and it is impressive because of his simple but very effective usage. In addition, compared with an electronic instrument, the pond scale shows very exact values of the cartridge's tracking force.

This instrument is a must-have for every design-oriented LP enthusiast and—because of its eye-catching appearance, exactness, and clever simplicity—it exceeds all modern battery powered electronic. Of course, that's why—despite its yesterday look—it should not be regarded as old stuff (Figs. 24.1 and 24.2).

---

## 24.3 Professional Test and Calibration Records

By accident, some years ago (2013) I stumbled over a stereoplay advertisement about the search for test records. I thought this could be a good chance to learn more about test records in general—and I asked the owner of the advertisement for information about his goals and his collection. I knew very well that the western

---

<sup>2</sup>Braun+Design Tax, Edition 2013, ISBN 978-3-9811106-6-1.

**Table 24.1** TCRs of the Deutsche Grammophon Gesellschaft<sup>a</sup>

A: 17 cm TCRs <sup>b</sup>	
• 10 01 941	Turntable check and adjustments
• 10 01 942	Wow and Flutter tests with 5 kHz
• 10 01 944	Wow and Flutter tests with 3 kHz
• 11 01 495	Tests of stereo replay equipment
• 11 01 496	Disque de contrôle pour appareils stéréophoniques
• 11 01 497	Tests of setting up stereo equipment
B: 33 cm TCRs <sup>c</sup>	
• 10 99 008	Wow and Flutter tests with 5 kHz
• 10 99 010	Wow and Flutter tests with 3 kHz
• 10 99 011	IMD tests with 400 Hz/4 kHz, 4:1 level ratio
• 10 99 014	Demonstration of the audibility of linear distortions
• 10 99 103	1 kHz test tone 0 dB/−20 dB—stereo and mono—33 1/3 and 45 rpm
• 10 99 106	Frequency sweep à la DIN 45 547 (16 kHz–20 Hz)
• 10 99 108	Difference tone measurements à la CCIR—sweep between 1 and 20 kHz with 400 Hz difference
• 10 99 109	Loudspeaker measurements with wobbled frequencies in 1/3 octave and Bark bands
• 10 99 111	General frequency response in 30 Hz–20 kHz and reference tone measurements
• 10 99 112	Reference, trackability and frequency
• 16 41 001	Test signals to check consumer stereo equipment

<sup>a</sup>Old version's numbers: without the first two digits

<sup>b</sup>German versions only, except 11 01 496 and 11 01 497

<sup>c</sup>Also in English: 10 99 112

world produced a huge range of different TCRs, eg Deutsche Grammophon Gesellschaft in Table 24.1 and the ones based on DIN in Table 24.2. Quite often, in discussions about it I was confronted with the opinion that the TCRs of the ex-GDR must have been the best ones, if not so, at least they showed equal quality compared with the best ones of the western world (incl. Japan).

A German collector has sent me Table 24.3 listing of his still not complete collection. For further completion, he is searching for a handful of missing TCRs. It is thrilling to read his additional—yet not published—extensive explanation of real-life test record applications.

Old stuff? Of course not! Regular testing and calibration of the cutting lathe parameters requires new, unused, or seldom used TCRs. They are essential for keeping the LP production quality as high as possible. As long as there are increasing LP market shares the production of high quality test and calibration records for private usage becomes essential too.

**Table 24.2** DIN TCRs<sup>a</sup>

• DIN 45 541	Frequency response—stereo and mono 33 1/3 rpm
• DIN 45 542	Distortion measurements 33 1/3 and 45 rpm
• DIN 45 543	Frequency sweep 20 Hz–20 kHz and crosstalk tests
• DIN 45 544	Rumble measurement à la DIN 45 539—stereo and mono 33 1/3 rpm
• DIN 45 545	Wow and Flutter—33 1/3 and 45 rpm
• DIN 45 549	Trackability

<sup>a</sup>German versions only**Table 24.3** TCRs of the VEB-Deutsche Schallplatten<sup>a</sup>

• LB 13	TCR <sup>b</sup> for wow and flutter tests with 3150 Hz for 16 2/3, 33 1/3, 45, 78 rpm
• LB 21	TCR—single record to adjust go and stop of an automatic tone arm drive
• LB 22	TCR for controlling the starting point on 25 cm records
• LB 23	TCR for controlling the starting point on 30 cm records
• LB 24	=LB 21
• LB 27	TCR for skating compensation—without grooves
• LB 41	TCR with sweep frequency 20 Hz–20 kHz
• LB 42	TCR with sweep frequency 31.5 Hz–16 kHz
• LB 48	TCR with different music examples and test tones
• LB 49	TCR for production purposes of all kinds of turntables, music and single test tones
• LB 107	TCR with music and single test tones for early stereophonic tests
• LB 108	TCR with different music examples and test tones
• LB 138	TCR for trackability tests, 315 Hz, 94 μm lateral
• LB 202	TCR for distortion tests with 315 Hz and 3150 Hz difference tone recordings
• LB 203	TCR for production of cartridge purposes: crosstalk measurement, cartridge transfer characteristic, frequency response
• LB 207	TCR for crosstalk and level measurements with a 1 kHz single tone
• LB 208	TCR for the error of the vertical tracking angle
• LB 209	TCR to check the correct adjustment of the headshell/cartridge installation
• LB 210	TCR for frequency response and crosstalk tests in the range of 20 Hz–20 kHz
• LB 211	TCR for frequency response and crosstalk tests in the range of 20 Hz–20 kHz
• LB 212	TCR for frequency response tests in the range of 20 Hz–20 kHz
• LB 237	TCR for trackability tests with a 10 kHz burst signal
• LB 238	TCR for trackability tests with 315 Hz and 100 μm lateral
• LB 239	TCR for rumble tests

<sup>a</sup>Listing: courtesy Ulrich Neef, Plauen, Germany<sup>b</sup>TCR Test and calibration record

According to the vinyl-cutting specialist Mr Daniel Krieger from SST Brügge-mann,<sup>3</sup> Frankfurt, Germany, the quality of cutting lathe TCRs is still a major issue and their availability yet not satisfyingly solved. The problem: There is no light-pattern measurement instrument<sup>4</sup> available allowing to test fresh master cut signals according to their velocity specs, eg DIN 0 dB at 1 kHz with 8 cm/s/1 kHz. Obviously, all instruments disappeared after the CD conquered the music industry. All other frequencies on a TCR are referenced to this signal.

Today, it's not a problem to cut test signals and frequency sweeps on test records. There are many different ones available. However, without an exact reference signal they can be used for customer purposes only. It's nothing for cutting lathe calibrations.

---

## 24.4 Final Note

When talking about good sounding audio equipment for reproduction purposes I think the design of audio equipment devices and their integration into an existing living environment plays a major satisfying and personal quality-defining role too. But, this is a question of subjectivity and—concerning expenses—courage for the gap, and, in my mind, not a question of the objectively measured quality of products. In this respect, our personal Razor should guide us and not third parties!

---

<sup>3</sup>[www.sst-ffm.de](http://www.sst-ffm.de).

<sup>4</sup>Details see JAES Vol. 5 1957, 'The calibration of disc recordings with light-pattern measurement', P.E. Axon & W.K.E. Geddes.

---

## Appendix 1

### List of Mathcad Worksheets

- 3.1 MCD-WS The Triode Gain Stage Amp3 with RIAA Networks
- 5.1 MCD-WS The Solid-State Gain Stage Amp4 with RIAA Networks
- 7.1 MCD-WS The Op-Amp + Transformer Driven Output Stage Amp5
- 9.1 MCD-WS The Transformer + OP-Amp Driven Amp1 (Real Data)
- 9.2 MCD-WS The Transformer + OP-Amp Driven Amp1 (Data Sheet Data)
- 11.1 MCD-WS Evaluation of the 1/f-Noise Corner Frequency of a 2SA1316 BJT
- 11.2 MCD-WS Evaluation of the 1/f-Noise Corner Frequency of a 2SC3329 BJT
- 11.3 MCD-WS Amp2 SN and Gain Calculations—1/f-Noise Based Version
- 14.1 MCD-WS BJT/Op-Amps Driven MC Input Stage with Un-Balanced Input and Balanced Output
- 14.2 MCD-WS BJT/Op-Amps Driven MC Input Stage with Balanced Transformer Input and Balanced Output
- 14.3 MCD-WS Fully Triode Driven MC/MM Input Stage with Transformer MC-Input and Balanced Output
- 18.1 MCD-WS The UBC (Un-Balanced-to-Balanced Converter)
- 18.2 MCD-WS The PMMA (Fully-Differential Measurement Amp)
- 18.3 MCD-WS The PFMA (Galvanically Isolated Measurement Amp)
- 20.1 MCD-WS The Un-Balanced Version (MM Noise Reduction)
- 20.2 MCD-WS The Balanced Version (MM Noise Reduction)
- 23.1 MCD-WS DIFA-OPA (Differential Amps)
- 23.2 MCD-WS DIFA-IC (Differential Amps)

---

## Appendix 2

### Useful Literature and Web Sites

#### Books

“Electronic Circuits, Handbook for Design and Application”

U. Tietze, C. Schenk, 2nd Edition, Springer 2008

ISBN 978-3-540-00429-5

Abbreviation in this book: **T/S**

It is the translated version of the 12th German edition of “Halbleiter-Schaltungstechnik”, 2002, ISBN 3-540-42849-6 (13th edition in 2010)

The accompanying CD-ROM also covers data sheets and simulation softwares like MicroSim V8.0

“Low-Noise Electronic System Design”

C. D. Motchenbacher, J. A. Connelly, John Wiley & Sons 1993

ISBN 0-471-57742-1

Abbreviation in this book: **M/C**

“Self on Audio”

Douglas Self, Newnes 2000

ISBN 0 7506 4765 5

Abbreviation in this book: **D/S**

“Small Signal Audio Design”

Douglas Self, Focal Press, Elsevier 2010

ISBN 978-0-240-52177-0

“Intuitive IC OP Amps”

Thomas M. Frederiksen, National’s Semiconductor Technology Series 1984

“How to Gain Gain”

Burkhard Vogel, Springer 2013, 2nd edition

ISBN 978-3-642-33032-2

Abbreviation in this book: **HTGG-2**

“The Sound of Silence”

Burkhard Vogel, Springer 2008, 1st edition

ISBN 978-3-540-76884-5

Abbreviation in this book: **TSOS-1**

“The Sound of Silence”

Burkhard Vogel, Springer 2011, 2nd edition

ISBN 978-3-642-19773-4

Abbreviation in this book: **TSOS-2**

## Web Sites

[www.tubedata.info/](http://www.tubedata.info/)

This web site covers nearly all valve data sheets

[www.sengpielaudio.com/](http://www.sengpielaudio.com/)

This web site covers sound studio and audio calculations in English and German

[www.7a.biglobe.ne.jp/yosh/recspecs.htm](http://www.7a.biglobe.ne.jp/yosh/recspecs.htm)

“Personal notes on record specifications”

Website with a great collection on IEC/DIN audio specs

## Magazines

Electronics World (ex Wireless World, ex Electronics and Wireless World)

[www.electronicsworld.co.uk](http://www.electronicsworld.co.uk)

Elektor Electronics

[www.elektor.de](http://www.elektor.de) (D)

[www.elektor.com](http://www.elektor.com) (UK)



Linear Audio

[www.linearaudio.net](http://www.linearaudio.net) (NL)

Tube CAD Journal

[www.tubecad.com](http://www.tubecad.com) (US)

# Index TSOS-1

(Subjects and Personality's Names)

## Symbols

$\mu$ A723 197, 311  
1/f-noise 19, 59, 92  
2N2905A 197  
2N3055 197  
2N4403 193  
2SC2546E 29, 38, 124, 158ff  
2SJ74 56  
2SK170 56ff  
2SK289 67  
3rd octave 126  
3rd octave band measurement 153

## Numbers

5532 187ff  
5534 186ff  
7308 299

## A

absolute room temperature 183  
active solution 241ff  
active-passive solution 238ff  
AD536 155, 279ff  
AD797 123, 314  
Adam, Wilfried 54, 155, 291  
admittances 156  
AEG-Telefunken 75  
A-filter transfer function 164  
AMP 155, 165  
amplifier noise model 18  
AN-104 135, 149, 157  
AN-222 159, 160  
AN-346 240  
ANSI 291  
anti-aliasing filter 291  
anti-RIAA transfer 9,11, 279, 295  
anti-RIAA transfer function 10, 135  
argument 157  
A-weighting 112  
A-weighting filter CCIR 279ff

A-weighting filter NAB 297ff  
A-weighting filters 182, 183

## B

balanced 86  
balanced (b) solutions 250  
balanced cable connections 299  
balanced in/balanced out 251  
balanced in/un-balanced out 251  
base spreading resistance 36,54,159ff  
Bateman, Cyril 200  
Baxandall, P. J. 159  
BC212B 135, 144  
benchmark 182  
BFW16A 124, 193  
BJT 36, 119  
BJT noise model 36  
BNC 168, 305  
Boltzmann's constant 21, 157, 183  
Brüggemann, Albert 82, 126, 324  
BUF603 297  
BUVO 187

## C

Cale, JJ 324  
cartridge equivalent model 154  
cartridge loading capacitor 168  
cascode 66  
cathode input resistance 76  
CCIR 291, 295  
CE gain stage noise model 51  
CE stage 48  
Chebyshev 155, 292  
cinch 305  
Clapton, Eric 324  
CLIO 40 279  
CLIO 6.5, 6.5 151, 155, 279ff  
CLIO AD converter 291  
Connelly, J. A. 17  
contribution allowed 42ff  
cooling 169  
correction factor 140  
CS gain stage 63ff  
Cu 126  
Cu master 128 ff  
cutting technologies 125

**D**

Dael, J. W. van 164, 245  
 degrees 157  
 Denon DL-103 3, 121, 181, 197  
 Deutsche Grammophon Gesellschaft 5, 168  
 deviation 13, 233, 246ff  
 DMM (technology) 125, 140, 141, 325  
 DOSE 186  
 draft design 104

**E**

E188CC 299  
 Early voltage 69  
 ELC-131D 155  
 Elector Electronics 81, 151, 155, 245  
 ELMA 311  
 Emerick, Geoff 299  
 engine diagram 304  
 Epcos 200  
 equivalent transformer circuit 110, 189  
 example calculations 52, 70, 76, 89,  
     91, 99, 100, 111  
 excess noise 34, 52  
 experience electronics 187

**F**

fab 4 (The Beatles) 299  
 FETs 55ff  
 FFT 190, 281, 319ff  
 filter bank 291ff  
 fisher electronic 305  
 flicker noise 19  
 formulae method 247ff  
 Frederiksen, Th. M. 86, 291  
 Friedemann 324  
 full speed 324

**G**

gain loss of the transformer 109ff  
 Gevel, Marcel van 150, 154, 161  
 groove 3

**H**

half speed 324  
 headers 314  
 heaters 85  
 HM 412 155  
 Hood, John Linsley 229  
 HP 331 A 155  
 hum 83ff, 298, 305, 319

**I**

IEC 11, 182, 314  
 impedance measurement 151  
 impedance network 156  
 impedance transfer 108  
 in-amp 93ff  
 in-amp IC circuitry topologies 102ff  
 in-amp IC topology type 1 102  
 in-amp IC topology type 2 103  
 in-amp noise model 95ff  
 in-amp type 2 topology 251  
 INA103 102  
 inductance 54,181  
 insertion loss 234 ff

**J**

J113A 144  
 J37 (Studer tape recorder) 299  
 JAES 7  
 Jensen 187 ff  
 Jensen Transformers 107  
 JFET noise model 58  
 JFETs 55,119,120  
 JLH 229  
 Johnson noise 21  
 Jones, Morgan 81  
 JT-346-AX 123ff  
 JT-346-AXT 314  
 JT-347-AXT 124  
 jumpers 314

**K**

Kay, Sharon x  
 Kruithof, J. A. 164, 245

**L**

L-Com 305  
 lacquer (technology) 125  
 LF356 144  
 Linn Linto 182 ff  
 LM317/337 197  
 LM394 32,161,193  
 logarithmic converter 285 ff  
 low-noise BJTs 45 ff  
 low-noise measurement pre-amplifier 154  
 low-noise valves 74  
 low-noise vinyl records 324  
 low-noise in-amp 104  
 LT1028 155, 285  
 Lundahl 187

**M**

M44G 150, 168  
 magnitude 156  
 manufacturer's data 150  
 Massey, Howard 299  
 MAT02 44,124,193  
 MathCad 149 ff  
 MC cartridge 3, 181  
 MC cartridge noise 182ff  
 MC phono-amp 304  
 MC phono-amp noise 182ff  
 McCormick, Tom 55  
 MCD 149ff  
 measurement amp 158, 165, 279, 285  
 measurement filters 279  
 microphones 299  
 Miller capacitance 64  
 Miller-C 122, 230ff, 236ff  
 MM cartridge 3, 149ff  
 MM cartridge data 150  
 MM cartridge noise 154ff  
 MM phono-amp 190, 304  
 module 1 304, 309, 321ff  
 module 2 304, 311, 320, 324  
 module 3 304, 313  
 Mogami 193  
 Motchenbacher, C. D. 17  
 MOTHER 126, 136  
 Mu-metal 86  
 mutual conductance 38, 68

**N**

NAB 291, 295  
 NAB-A-Filter 155  
 Neumann 127  
 Neumann phono-amp PUE 74 135  
 Neumann PUE 7 144, 169  
 Neumann VMS-80/DMM 127  
 Neutrik 193  
 noise contribution 42, 314  
 noise current 18, 59  
 noise current sources parallel-connected 23  
 noise current sources series connected 23  
 noise factor 28, 43  
 noise figure 28, 60, 61  
 noise figure approach 112  
 noise gain 92  
 noise index 34  
 noise measurement system 279  
 noise model 79  
 noise resistance 72  
 noise spectrum 85

noise voltage 18, 59, 72, 73  
 noise voltage approach 111  
 noise voltage densities 201  
 noise voltage sources parallel-connected 23  
 noise voltage sources series-connected 22  
 Nordholt, E. H. 7  
 Nyquist 21, 183

**O**

Okhams's Razor 49, 154  
 op-amp noise model 88, 90  
 op-amps 86  
 OP27 19ff, 31, 89, 91, 197  
 OPA604 151, 296  
 OPA627 313, 314  
 optimal source resistance 30, 62, 116  
 Ortofon RMA-297 127  
 Ortofon Rondo 197  
 Ortofon Samba 123  
 overload 236

**P**

Panasonic (FC/25V) 197  
 paralleling 24  
 passive solution 228ff  
 Pauler, Günter 126, 325  
 peak velocity 168  
 phase angle 156  
 phase measurement 151  
 phono-amps 6ff, 140ff  
 Pikatron 187ff  
 potential-free 299  
 power supply 192, 197, 289, 304, 311  
 pre-amps 3, 313  
 pre-pre-amp 3  
 primary 110  
 pSpice 13,153  
 PSU 1 ... 3 304  
 PSU-4 305  
 purpose 3

**Q**

Quad 84

**R**

radians 157  
 RCA 305  
 rectifier 285ff  
 reduced mutual conductance 63

relay control 318  
 resistor noise 21  
 results 167, 196, 200, 235, 303, 319  
 RIAA 5  
 RIAA decoder 295  
 RIAA encoder 295  
 RIAA equalization 155, 165  
 RIAA networks 227  
 RIAA phono amp engine 303ff  
 RIAA time constant 227  
 RIAA transfer 5, 9, 11, 183, 190, 193,  
     197, 227, 279, 295ff  
 RIAA transfer function 10, 163, 227  
 Ricker, Stan 324  
 RTA 190

## S

Schenk, C. 17  
 secondary 110  
 Self, Douglas 17,184ff, 196  
 sensitivity 168  
 sequece 26  
 Sergeant Pepper's 299  
 series configuration 87  
 series mode 245  
 S-filter 185ff, 285, 294  
 Sheingold, D. H. 86, 161  
 Sherwin, Jim 149, 157  
 shot noise 291  
 shunt configuration 87  
 shunt mode 243  
 Shure V15 V MR 3, 5, 314  
 Signal-to-Noise Ratio 33  
 SME 3012 127  
 Smith, L. 86, 161  
 SN by simple means 183  
 SN calculations 162  
 SN-factors 184  
 solid-state approach 193  
 SON 126  
 sound 197, 200, 324  
 Sowter187ff  
 spectral noise voltage density 290, 323ff  
 SRPP 66,81ff, 236  
 SSM2017 103, 313ff  
 SSM2210 32, 105, 193  
 stereoplay 84ff  
 Stockfisch Records 126, 325  
 stray-C 230ff  
 Studer 299

succ-apps method 245ff  
 sum of two SNs 139

## T

Talema toroidal transformer 197  
 tape recorder 299  
 Taylor, E. F. 190  
 Taylor, F. 294  
 Teldec 126, 140  
 Telefunken 71, 135ff  
 temperature 169  
 test circuit for i/p capacitances 196  
 test record 5, 168  
 test terminal 282  
 THAT 300 104  
 THAT 320 104  
 Tietze, U. 17  
 transfer factor 138  
 transformer driven MC phono-amp 190ff  
 transformer equations 108ff  
 transformer noise model 108ff  
 transformer solution 187  
 transformers 106ff  
 TSD15 (EMT) 127  
 Tube CAD Journal 82  
 tubes 71  
 turns ratio 106  
 Twin-BNC 193, 305

## U

U87 (microphone) 299  
 un-balanced (ub) solutions 228ff

## V

V15II 127  
 V15III 150  
 V15IV 150  
 V15V 136  
 valve noise model 71  
 valve power supplies 83  
 valves 71, 119  
 VALVO 75  
 velocity 125, 181  
 Vierzen, R. M. van 7  
 vinyl record 3, 125ff  
 vinyl record noise 126ff  
 Vitilec 305  
 VMS-80/DMM 127

**W**

Walker, H. P. 149, 243  
weighted 69  
weighting filters 33  
Whitlock, Bill 299  
Williams, A. 294  
WIMA MKP4/10 200

wiring 193  
wobble speed 298  
worst case 139

**X**

XLR 305

# Index TSOS-2

(Subjects and Personality's Names)

## Symbols

$\pi$ -model (BJT) 55  
 $\pi$ -network (power supplies) 144  
 $\mu$ A723 337, 680  
 $\mu$ -F 368ff  
 $\mu$ -follower 122, 131ff, 193, 368ff, 375  
1/f-corner-frequency 33, 102ff  
1/f-noise 31ff, 66, 77ff, 97ff, 160, 293, 396, 621  
2N3055 337  
2N2905A 337  
2N4403 63ff, 333  
2-pham 368ff, 383  
2-pham (example) 391ff  
2SA1083E, F 63ff  
2SA1316BL 65ff, 690  
2SB737S 63ff  
2SC2546E, F 44, 57ff, 63ff, 73, 82ff, 195, 293ff, 689  
2SC3329BL 65ff, 690  
2SC550 33  
2SJ74 77, 83  
2SK170 77ff, 82ff  
2SK389 83, 89, 194  
3-pham 368ff  
3-pham (example) 397ff  
3rd octave 202, 286ff, 383  
26dB boundary 414  
45° modulation, modulated 5, 18ff  
45°/45° modulation 18ff  
6BK8 101  
6SN7 108  
6J5 108  
6KX8 140  
7DJ6 97  
12AU7 108, 367, 372  
12AT7 108, 372  
12AX7 108, 372  
20Hz hp 687

## Numbers

2549 (Mogami) 332, 677  
5532 (op-amp) 327

5534 ( " ) 325  
6276 (pentode) 101  
6922 (double-triode) 97, 108ff, 372  
7308 (double-triode) 601  
10 99 112 (test record) 5, 303

## A

absolute temperature 292, 322  
AC/DC-conversion 613  
active anode load 368  
active devices 40  
active-passive 2-step solution 519  
active 1-step solution 522  
Adam, Wilfried 59, 74, 289, 573, 615  
admittances 290  
Adventure: Noise 283  
AD53 290, 560, 576  
AD745 6  
AD797 198, 622, 677, 687  
A-DIN certified 586  
AEG 106  
A-filter 102, 367  
A-filter transfer 299  
A-filter-weighting 83  
AI-box 300  
AI plug-in box 8  
AMP 300ff  
amps 3ff  
amplifier chain 3  
amplifier noise model 32  
amplifying stages 41  
AN-104 (Nat. Sem.) 204, 283, 292  
AN-222 (Nat. Sem.) 293, 332, 680  
AN-346 (Nat. Sem.) 520  
Analog Devices 34ff, 175, 290  
analog meter 576  
analog solution 643  
Analogue Dialogue 296  
anode current 690  
anode load 122  
anode load resistance 110  
anode power lines 141f  
ANSI 50, 102, 299, 559  
arm (circuits) 560, 613  
anti-alias filter 588, 591, 602  
anti-alias filter (CLIO) 595  
anti-phase 18  
anti-RIAA (ARIAA) 341, 634, 642  
anti RIAA transfer 9, 204, 597ff  
anti RIAA transfer function 9ff

Application hints (National Semic.) 605  
 argument 291  
 arm circuits 613f  
 ARIAA 634, 644  
 ARIAA network 642  
 AS040 186, 329  
 audio analyzer 118  
 audio band 33  
 AUDIOMATICA Srl 286, 595, 643  
 Audio Precision 584, 619, 628, 643  
 audio spectrum 51  
 Audio.TST 619  
 average noise voltage density 7  
 averaging 329  
 average 35  
 average noise resistance 139  
 average spectral noise voltage density 102  
 average reading meter 560, 570  
 average single frequency component 581  
 A-weighting 50, 152, 566, 617ff  
 A-weighting term 186  
 A-weighting application (silly) 609ff  
 A-weighting filters 320ff, 593  
 A-weighted SN 299

## B

B32652 (capacitor) 340  
 balanced amplifier 122  
 balanced cable connections 600  
 balanced gain stage 134f  
 balanced input 7  
 balanced solutions (RIAA network) 531  
 band-pass filter (hum figure) 636  
 base 55  
 base spreading resistance 55ff, 74f  
 Bateman, C. 340  
 Baxandall, P. J. 55, 293  
 BC109C 579  
 BC212B 205, 220  
 BD 679, 680 300  
 benchmarks 320  
 Berliner, Emil 17  
 BFW16A 64, 198f, 333  
 bin(s) 582  
 bin width 588  
 bipolar junction transistor 6, 55ff  
 BJT 6, 32, 55ff  
 BJT noise model 55  
 blocks 402ff  
 Bloehbaum, F. 95  
 BNC connectors 300, 676  
 Boltzmann's constant 6, 100, 292, 322  
 BRAUN 621  
 brick wall filter 602ff

Brüggemann 144  
 btb-elektronik (internet) 738  
 BUF634 336  
 buffer 336  
 Burr-Brown 176, 220  
 Butterworth 559ff, 591, 605ff, 687  
 Butterworth band-pass 602, 604  
 BUVO 327ff  
 bypassed 86, 109ff  
 bypassed cathode resistor 121  
 bypassing capacitance 102

## C

cable capacitance 93  
 calculated deviation (2- & 3-pham) 397, 399  
 calculation approach (2- & 3-pham) 385ff  
 calculation approachA (2- & 3-pham examples) 401ff  
 calculation by blocks (2-pham) 402ff  
 calculation by blocks (3-pham) 404ff  
 calculation method(s) (valves) 379, 407  
 Cale, JJ 703  
 calibration process 220  
 calibration record 20  
 camouflage(s) 583  
 capacitance load of MM cartridge 88  
 capacitors 39  
 cartridge equivalent circuit 18  
 cartridge equivalent model 287f  
 cartridge impedance 285  
 cascoded gain stage 89ff  
 cascoded SRPP 91  
 cathode current sink 134  
 cathode follower 21, 368ff  
 cathode input resistance 107  
 cathode resistance noise 107  
 cartridge 3  
 CCA 122, 374ff, 402  
 CCIR 468-(Filter) 290, 559, 586, 633, 642  
 CCIR-1kHz 566  
 CCIR-2kHz 566  
 CCIR-A-Filter 593  
 CCG 120ff  
 CCS 368ff  
 CCSCF 368ff, 409  
 CE stage 67  
 CF 128ff, 368ff  
 CFA 128ff, 591  
 Chebyshev 559ff, 605ff, 23, 641  
 Chebyshev hp 289, 324, 622, 641  
 cinch 676  
 circuit worsening factor 140  
 circuitry topology (in-amp) 174ff  
 Clapton, E. 703



- CLIO 286ff, 560ff
  - CLIO noise performance 576
  - coil inductance 45, 319
  - coil resistance 183, 327
  - coil turns 328
  - coil windings 183
  - collector 55
  - collector current 32ff, 45, 58f, 82
  - common anode 95
  - common base 60
  - common cathode 95
  - common cathode stage 95, 108, 368ff
  - common collector 60
  - common drain 77
  - common emitter 60
  - common gate 77
  - common grid 95
  - common plate 95
  - common source 77
  - comparison (measurement results) 610
  - Connelly, J. A. 31, 66, 737
  - constant current generator (valve) 120ff
  - contribution allowed 61ff, 88, 560
  - confusion 565ff
  - cooling 304
  - corner frequency 81, 85, 88, 97ff, 367ff, 602ff
  - corner frequency changing factor 104
  - correction factor (cartridges) 217
  - correction factor(s) 602ff
  - correlated 36, 134, 631
  - cross-section 18ff
  - CS-configuration 86
  - CSRPP 91
  - CSV60 621
  - Cu layer 214
  - Cu master 202
  - Cu material 214
  - current feedback 67ff
  - current feedback op-amps 153
  - current noise index 50, 372, 409f
  - current mirror 329
  - current sink 134
  - customer confusion 586ff
  - cutting (vinyl) 9
  - cutting modulations 17ff
  - cutting possibilities vii
  - cutting process 9
  - cutting technologies 201
- D**
- Dael, J. W. van 299, 526, 528
  - Dangerous Music 632
  - Darlington transistors 300
  - data sheet 19, 33
  - DC power supply 576
  - DC resistance 19
  - decade 50
  - Decca 203
  - decode 9
  - decoder 559
  - decoding 10
  - decoding mode 12
  - decoding process 9
  - decoding transfer function 11
  - degrees (converted from rad) 291
  - definite frequency bandwidth 297
  - Denon 3, 20ff
  - Denon GmbH 21, 26
  - derivation (arm vs. rms) 570
  - Deutsche Grammophon Gesellschaft 5, 303
  - deviation 14ff, 404, 512ff
  - deviation area 637
  - deviation (CCIR transfer) 597
  - deviation tolerance 637
  - differential amplifier 122
  - differential gain stage 134f
  - differentiation 75
  - differentiator 12
  - digital meter 576
  - digitisation 319
  - DIN 5
  - DIN-IEC 651 559, 586
  - DIN EN 61672-1 586
  - DIN 0dB (level) 22, 25, 185, 303
  - DIN 45405 559, 586ff
  - DIN 45535/6 11
  - DIN standard 8
  - direct metal mastering (DMM) 201
  - distortion analyzer 290
  - distortion artefacts 142, 631
  - DL-103 3, 20ff, 185, 319, 337, 690
  - DL-103R 25f
  - DL series (Neutrik) 676
  - DMM 201, 220ff, 703
  - DMM process 202
  - Dolby arm approach 612ff
  - Dolby, R. 566, 593
  - DOSE 324ff
  - draft design (in-amp) 177f
  - draft design (JFET) 93
  - draft design (valve) 151
  - D/S 31
  - double-triode(s) 110ff, 368ff
  - drain 77
  - drain current 32

**E**

E88C 375  
 E88CC 97, 105, 108ff, 372  
 E188CC 601  
 ear 3  
 Early voltage 91  
 EC8010 414  
 EC92 375  
 ECC81 108, 372  
 ECC82 108, 367, 372  
 ECC83S 108, 372  
 ECC88 97, 7f, 17  
 ECC808 140  
 ECF80 621  
 Edison, Alva 17  
 EF86 101  
 EL84T 134  
 ELC-131-D 290  
 electron (elementary) charge 100  
 Elector Electronics 101, 176, 286, 289, 739  
 Electronics World x, 101, 739  
 Elektor 176, 299, 526, 739  
 ELMA 679  
 Emerick, G. 601  
 Emerson 332  
 emitter 55  
 emitter bulk resistor 55  
 emitter resistor 55  
 EMT TSD15 203, 214  
 ENB 138, 322  
 encode 9  
 encoder 559  
 encoding mode 12  
 engine 671ff  
 engine diagram 672f  
 engine functions 672ff  
 engine performance 693ff  
 Engineering Note 1.2 565  
 Epcos (capacitor) 340  
 equalization 297  
 equalization factor 322  
 equalized 49, 299  
 equalizing effects 5, 49  
 equalizing network 559  
 equivalent circuit(s) 35ff, 182, 327  
 equivalent gate noise current density 80  
 equivalent grid noise current density 95f  
 equivalent noise bandwidth viii, 138, 322, 566ff, 602ff  
 equivalent noise current density BJT 56  
 equivalent noise current density triode 96  
 equivalent input noise sources 32  
 equivalent input rms noise voltage EIN 99

equivalent noise voltage density BJT 56  
 equivalent noise voltage density JFET 78  
 equivalent noise voltage density (opa) 153  
 equivalent noise voltage density triode 95  
 equivalent noise resistance (triode) 96f  
 ESCORT 290  
 essentials 1  
 Etna E1 418  
 EU standard 8  
 Everest C3 418  
 example calculation 71ff, 75, 92ff, 108ff  
 example calculation (in-amp) 171ff  
 example calculation series config. 157  
 example calculation shunt config. 159  
 example calculation (transformer) 184ff  
 example 2-pham 391ff  
 example 3-pham 397ff  
 example phono-amps (calc. approach) 391ff  
 example phono-amp (hum figure) 634ff  
 EXCEL 14, 287  
 excess noise 50ff, 71ff, 86, 107ff, 409  
 experience electronics 327  
 exponent change 582

**F**

fab 4 (Beatles) 601  
 Fairchild 680  
 FEG viii, 332  
 FET(s) 6, 32, 77ff  
 FFT analyzer 118  
 FFT approach 622, 627  
 FFT diagram(s) 367f, 583ff  
 FFT measurement 329, 573, 579ff  
 FFT measurement methods viii  
 FFT noise measurement 579ff  
 FFT resolution 579  
 FFT size(s) 579, 627  
 field effect transistor 6, 77ff  
 filter approach 622, 624  
 filter bank 1 591ff  
 filter bank 2 604ff  
 fischer elektronik 676  
 flank modulation 18ff, 215, 303  
 flicker noise 33, 97, 329  
 FM stations 31  
 formulae method 528  
 forward transfer admittance 80  
 fourth time constant (20Hz) 376  
 fourth time constant (>20kHz) 526  
 Frederiksen, Th. M. 153, 593, 738  
 frequency 32  
 frequency response 10, 180, 693ff  
 frequency test record 5

Friedemann, W. 703  
 full-speed mastering 201, 703  
 fully active solution (RIAA) 506  
 fully active-passive solution (RIAA) 506  
 fully passive solution (RIAA) 506  
 Future Equipment Service viii

## G

gain 86  
 gain loss 183  
 gain rate 560  
 gain setting options (in-amps) 165f  
 gain stage calculation 71ff, 85f  
 gate 77  
 gate cut-off current 80  
 gate-drain-capacitance 87  
 general noise effects 31  
 Gerhard, J. 689  
 Gevel, M. van 284, 288, 296  
 Glowing GainMaker 109, 134  
 golden ears 414  
 grain size 214  
 graphs (o/p noise voltage density) 342f  
 graphs (performance) 693ff  
 Green, L. 287  
 grid load resistance 112  
 grid resistor(s) 691  
 grooves 3  
 groove depth 18ff  
 groove width 18ff, 203  
 guarantee 139  
 Gundry, K. 566, 593  
 gyrators 300

## H

half-speed mastering 201, 703  
 Hameg 290  
 Handbook of Linear Applications 220  
 hard disk 562  
 head shell 3  
 headers 687  
 heating effect, equivalent 32  
 heater(s) 141, 144  
 HF measurement amp 622ff  
 HF measurement instrument 639ff  
 high-end 31, 319  
 high-price 31  
 high-Z 131  
 Highlights 15 - 18 217  
 Hitachi 44  
 HM 412 290  
 Hood, J. L. 508, 737

How to Gain Gain (HTTG) 107, 738  
 HP 331A 290, 560  
 HR2000 560  
 HTTG 107f  
 hum vii, 118, 141ff, 617ff  
 hum artefact(s) 138, 617ff, 639  
 hum content 144  
 hum figure vii, 144, 559, 589,  
 hum figure (linear amps) 617ff  
 hum figure (phono-amps) 631ff  
 hum-free 6, 586  
 hum-infected 586, 631  
 hum interference(s) 6, 600, 639  
 hum spectrum 624  
 hum spikes 589

## I

ideal filter 602  
 ideal situation 14  
 idle gain 136  
 idle output voltage 144  
 idle voltage 19  
 IEC 11, 297, 320, 376  
 IEC 20Hz hp 671  
 IEC 651 586  
 IEC/CD 1672 299  
 impedances 39  
 INA103 174  
 in-akustik 703  
 in-amp(s) 165ff  
 in-amp noise model 165ff  
 in-amp IC topology 174ff  
 indicator(s) 560  
 inductance(s) 19, 39  
 inductance of MC cartridge 195, 319  
 influence of temperature 304  
 input load 320  
 input noise current 77  
 input noise resistance 79, 285  
 input network 291  
 input network impedance 414  
 input possibilities 411  
 input referred 33  
 input referred noise voltage density 92, 121  
 input resistance 45, 65, 285, 300, 324ff  
 input resistance (cathode) 107  
 input section 677  
 input sensitivity 6  
 insertion loss 511ff, 560, 576, 579  
 integrated amplifier 617  
 internal resistance 20ff  
 inverse RIAA transfer 634  
 ISCE 565

ITU 566, 612  
 ITU-T J.16 633, 25  
 ITU-R 486 586

## J

J113A 220  
 J37 (Studer) 601  
 JAES 6, 221, 566, 593, 601  
 JAN double-triodes 418  
 Jensen Transformers 152, 180, 185f, 197f,  
 327ff, 412, 601, 677, 679, 687f  
 JFET 77ff  
 JFET gain stage 87  
 JFET noise model 79  
 JFETs parallel connected 194  
 JJ electronics viii, 108ff, 372  
 jogis-roehrenbude 101  
 Jones, Morgan 108, 122, 131, 328, 369, 375,  
 417, 738  
 Johnson noise 35, 107  
 JT-10KB-DPC 677  
 JT-123-SPLC 679  
 JT-346-AX or AXT 152, 197, 337, 687  
 JT-347-AXT 180, 186, 198  
 JT-44K-DX 185ff  
 junction field effect transistors 77ff  
 jumper settings 686

## K

Kay, Sharon x  
 Kelvin 292  
 kernel (BJT) 55  
 Kruihof, J. A. 299, 526, 528

## L

lacquer technology 201, 703  
 lateral modulated, modulation 5, 17  
 L-com 332, 676  
 LF356 220  
 linear amps 591, 617  
 Linear Applications Databook 204, 283, 292f  
 Linear Audio 95, 689, 739  
 line input transformer 677  
 lin/log-converter 614  
 Linn Linto 320ff  
 LL9226 329  
 LM317 337  
 LM337 337  
 LM394 61ff, 71, 296, 333  
 load capacitance 19, 284, 304  
 load resistance 19

locations (hum) 639  
 lowest-noise 31, 95  
 low-frequency noise 31, 367  
 log-converter 560, 576  
 long-tailed pair 60, 66, 134, 329  
 loudness pot 337  
 lowest-noise 92, 95, 100, 146, 151, 176f  
 lowest-noise in-amps 177  
 low-frequency noise 367, 375, 381, 397, 413ff  
 low-noise 6  
 low-noise BJTs 192  
 low-noise measurement pre-amp 289  
 low-noise triodes 150, 379, 415  
 low-noise valves 105, 121, 139  
 low-noise vinyl records 703  
 low-pass filter (30Hz) 593  
 low-pass filter sections 611  
 low-Z 131  
 LP records 201  
 LT1028 289, 573, 622  
 Lundahl 180, 327f

## M

M44G 304  
 magnetic shielding 144  
 magnitude 12  
 mains interferences 142, 332  
 mains transformers 142  
 manufacturer 17  
 manufacturer selected triodes 407  
 Massey, H. 601  
 master (Cu) 202  
 mastering 201  
 MAT02/03 61, 63ff, 333, 337  
 Mathcad ix, 14, 283  
 mathematical model 290, 302  
 Mathew, D. 619  
 Mathsoft 283  
 Matsushita 679  
 maxi records 201  
 maximal SNs (records) 216  
 maximal stage gain allowed 88  
 maximum deviation 591  
 maxi ix  
 MC cartridge 3ff, 19, 81ff, 411  
 MC cartridge classification 181  
 McCormick, T. 59, 74  
 MC encoding situation 598  
 MC phono-amp 330, 336  
 M/C 31  
 measurement amp(s) 300, 559ff, 573ff  
 measurement confusion 565ff  
 measurement equipment

- (HF in phono-amps) 633
  - measurement filter(s) 559, 591ff
  - measurement methods 566
  - measurement results (relationships) 568f
  - measurement results (comparisons) 610
  - measurement set-up 561, 624
  - measurement standards 566
  - measurement system
    - noise performance 576ff
  - measurement tools 289
  - measurement set-up 75, 561
  - measurement set-up (hum figure) 624
  - mechanic arrangement 378
  - metal film resistor(s) 51, 691
  - Metzler, B. 628, 737
  - microphone pre-amps 591
  - Microsoft 287
  - MicroSim ix
  - Miller capacitance 87f, 152
  - MKP (capacitor) 340, 372
  - MKT (capacitor) 340, 372
  - MM cartridge 3ff, 19, 65, 83ff, 92, 284ff, 411
  - MM encoding situation 598
  - MM phono-amp 330, 411
  - modulation possibilities vii
  - modules 1 - 4 672ff, 679ff, 694ff
  - module 3 viii
  - Mogami 332, 677
  - mono 17f
  - monophonic purposes 25
  - monophonic records 18
  - monophonic signal 22
  - morphological box 381
  - Motchenbacher, C. D. 31, 66, 737
  - MOTHER 202
  - Motorola 205
  - mud effects 583
  - Mu-metal 144
  - Musical Fidelity XLP 326, 333
  - mutual conductance of BJT 69
  - mutual conductance of JFET 91
  - mutual conductance (anode) 100
  - mutual conductance (cathode) 100
  - mutual conductance (minim. required) 410
  - mutual conductance of triode 97ff, 690
  - mutual conductance of pentode 100
- N**
- NAB 50, 559
  - NAB/ANSI 299
  - NAB-A-filter 289
  - National Semiconductor 48, 204, 605
  - negative valve effects 148f
  - Neumann (GmbH) 152, 202, 220
  - Neumann PUE 74 203ff, 220ff, 304
  - Neumann U87 601
  - Neutrik 332, 676
  - NF (calculations) 62, 145, 410
  - noise (cathode resistance) 107
  - noise (general effects) 31ff
  - noise basics 29ff
  - noise calculations (triodes) 101ff
  - noise contribution 61
  - noise currents 33
  - noise current density 34ff, 56ff, 80, ff, 96, 120, 153, 173ff, 199
  - noise current source(s) 32ff, 55
  - noise density 33
  - noise density frequency band 292
  - noise factor 43ff
  - noise figure 43ff, 82ff, 6, 7
  - noise figure approach (trafo) 184ff
  - noise figure calculation process 17
  - noise floor (records) 202
  - noise floor (FFT diagrams) 583
  - noise-free 32
  - noise gain 163
  - noise generator(s) 559, 573, 579ff
  - noise index NI 50
  - noise in BJTs 55ff
  - noise in instrumentation amps 165ff
  - noise in JFETs 77ff
  - noise in MC phono-amps 319ff
  - noise in MM cartridges 283ff
  - noise in op-amps 153ff
  - noise in transformers 179ff
  - noise in valves 95ff
  - noise issues 9, 31
  - noiseless amplifier 291
  - noise level (records) 202
  - noise measurement methods vii
  - noise measurement results (different methods) 566ff
  - noise measurement system 559ff
  - noise model 32, 56ff, 59, 70, 95f, 118f
  - noise model (in-amps) 165ff
  - noise model (measurement amp) 292ff
  - noise model (op-amp) 155ff
  - noise model series configuration 157f
  - noise model shunt configuration 158f
  - noise of capacitors 39
  - noise of inductances 39
  - noise of triode driven phono-amps 367ff
  - noise of vinyl records 201ff
  - noise performance 46, 343
  - noise power 43, 49
  - noise resistance 96f

Noise Specs Confusing? 204  
 noise voltages 33  
 noise voltage approach (trafo) 184ff  
 noise voltage density 36ff, 57ff, 77ff, 113ff  
 noise voltage density plots (valves) 146ff  
 noise voltage of the MOTHER 214  
 noise voltage source 32ff, 55  
 nominal data 21  
 nominal input voltage 179  
 nominal internal resistance 21  
 nominal output load 21  
 nominal output voltage 21, 179  
 non-equalized 297, 633ff  
 non-inverting configuration 154  
 non-selected 117  
 non-weighted 633  
 Nordholt, E. H. 66, 221  
 noval 108  
 Nyquist, M. 36, 292, 627  
 Nyquist frequency 582, 588

**O**

octal 108  
 octave-band analysis 283  
 Okham's Razor x, 67, 131, 288  
 op-amp 6, 33  
 OP27 33ff, 61f, 337, 634  
 OPA604 285  
 OPA627 683  
 operating frequency bandwidth 292  
 operating gain 42  
 operating output level 333  
 operating point 372  
 operational amplifier 6  
 operational SN 333  
 optimal (optimum) collector current 75, 336, 688f  
 optimal input load 75  
 optimal (optimum) source resistance viii, 46, 75, 84, 161  
 optimisation process 141  
 optimal (optimum) collector current 75, 688  
 optimum source resistance 46f, 84f, 161f  
 Ortofon RMA-297 203  
 Ortofon Rondo 337  
 Ortofon Samba 198  
 oscillation prevention resistor 112, 372  
 output capacitance 87  
 output current noise 134  
 output impedance 42  
 output load 109, 385  
 output power 49  
 output resistance 110, 136

output section 687  
 output voltage 19ff  
 overload(ing) ix, 9, 89, 174, 283, 289, 328, 332, 507, 516, 520, 615

**P**

Panasonic (FC) 336ff  
 paralleling 40f, 105, 373, 375  
 parallel-connected 37f  
 parallel operation 108ff  
 Parametric Technology Corp. 283  
 passive 1-step solution 507  
 passive 2-step solution 515  
 passive RIAA (transfer) network 89, 369ff  
 Pauler Acoustics 202f, 703  
 Pauler, Günter 202f  
 PCC88 97  
 peak value 32  
 peak velocity 5, 22ff, 201  
 pentode 95, 100, 109  
 pentode noise resistance 100f  
 pentode noise voltage 101f  
 phase angle(s) 286, 341  
 phase measurement 285  
 phase relationship 109  
 phase response 180, 693ff  
 phase shift 69  
 phono-amp 3  
 phono-amp noise 6  
 phono amplification 3  
 physical constants 32  
 Pikatron 180, 327f  
 pin-1 problem 677  
 pink noise 33, 117, 367, 559, 579ff  
 pink noise generator 579ff  
 PL504 621  
 platter 3  
 plug-in box 8  
 ponderé 587  
 pop-corn-noise 367  
 Potchinkov, A. 738  
 potential-free 677  
 power amplifier 617  
 power supply(s) 74, 84, 141ff, 300, 331f, 337ff, 369f, 520, 576, 671f, 676, 679ff  
 power-supply-unit 329, 369ff  
 plug-in box 8  
 pre-amps 3ff  
 pre-pre-amp(s) 3ff, 319, 411  
 primary 179, 183, 327  
 professional audio (magazine) 632  
 pSpice simulation 16, 67, 220, 287  
 PSU 690

PSU 1 - 5 672ff  
 PUE 74 203ff  
 purpose 3, 6f

## Q

Q & A (transformer) 190ff  
 Q & A (2- & 3-pham) 389  
 Quad 24P 142ff  
 quadratic equation 57, 283, 294f  
 quasi-peak 290, 393, 560, 566ff, 586,  
 596, 612, 633, 642

## R

rabbit hole 689  
 radians 291  
 random 31  
 Rauschmessungen 101  
 rbb' calculation 295  
 RCA 676  
 real situation 14  
 Record Industry Ass. of America 9  
 record reference levels vii  
 rectifier 560, 576  
 red noise 102, 367  
 reduced mutual conductance 86  
 reference level(s) vii, 5, 17ff203  
 reference point 12  
 reference test record 5  
 reference voltage 102  
 regulated power supply 144  
 relay control 688  
 relay drivers 688  
 relationships (measurement results) 568f  
 relationship (SNs) 417  
 resistor-capacitor network 194  
 resistor excess noise 50ff  
 resistor noise 35ff  
 results 302ff, 327, 333, 341,  
 379, 413, 610  
 results ( $\mu$ -F 2- & 3-pham calculated) 386f  
 results (example triode phams) 407f  
 results (hum figure) 622f  
 results (hum figure in phono-amps) 633, 639,  
 642  
 results (module 3) 689  
 results (test gain-stages) 382  
 reverse-transfer-capacitance 87  
 RG58 677  
 RG176 332  
 Rhode & Schwarz 290, 560, 602, 643  
 RIAA x, 5, 9, 283ff  
 RIAA curve 367

RIAA decoder 597ff  
 RIAA decoding function 505  
 RIAA encoder 597ff  
 RIAA equalized 7, 92, 633  
 RIAA equalization 83, 300  
 RIAA equalizing term 186  
 RIAA feedback network 336  
 RIAA-Isierung 299, 526, 528  
 RIAA network(s) 151, 340, 369, 372, 376, ff,  
 505ff, 691  
 RIAA transfer 5, 9ff, 14, 220, 283, 298,  
 322, 505ff  
 RIAA transfer circuit 299  
 RIAA weighting 9ff, 2  
 Ricker, S. 703  
 ripple rejection 680  
 rms velocity 201  
 RMS voltmeter 290  
 Robinson, D. 566, 593  
 Roehren 101  
 Roehren Taschen Tabelle 106  
 Rohm 66  
 role of 2nd gain-stage 414  
 rotary switch 573, 679  
 RTA measurement 329  
 rule(s) of thumb 143, 300414  
 rule of thumb (FFT diagrams) 579  
 rumble 204ff, 220, 289

## S

sample frequency 581  
 sample rate 581, 627  
 schematic 16  
 Schenk, C. 737  
 scope 290  
 secondary 179, 183, 327ff  
 sensitivity 6, 220, 289, 303,  
 319, 622, 628, 631, 642, 672  
 sequence 12, 36ff, 61, 143, 164, 169, 177,  
 195, 287, 327, 368, 372, 569, 587,  
 611f, 634f  
 selection 62ff, 106, 217ff  
 selected low-noise 116  
 Self, Douglas ix, 31, 67, 322ff, 620, 737  
 Semiconduct. Handbook (Telefunken) 205  
 sengpielaudio (internet) 738  
 Sennheiser electronic 202  
 Sennheiser UPM 550 203  
 sequence-connected 36ff  
 sequence of two amplifying stages 41ff  
 Sergeant Pepper's ... 601  
 series configuration 153ff  
 series mode (RIAA feedback) 526

- S-filter 323ff, 367, 573, 593
  - Shannon 588
  - Sheingold, D. H. 153, 296
  - Sherwin, J. 204, 283, 292
  - shielded cable 332
  - shot noise 102, 152, 388, 395
  - shunt configuration 154ff
  - shunt regulated push-pull see SRPP
  - shunt mode (RIAA feedback) 524
  - Shure 3, 284
  - Shure M44G 284
  - Shure V15 III 203, 284
  - Shure V15IV 284
  - Shure V15V (MR) 203, 205ff, 284ff, 687
  - sidebands 631
  - Siemens (capacitor) 340, 372
  - signal-to-noise ratio (SN) ix, 5, 32ff, 49, 66, 72, 114, 139, 158f, 186f, 283, 297ff, 586, 617ff, 633ff
  - signal modulation 27
  - signal track 20
  - silly (A-weighting) 609ff
  - single ix
  - single records 201
  - singleton 77, 83f
  - skin effect 287
  - SME 3009 203
  - SME 3012 203
  - SME connector 300
  - Smith, L. 153, 297
  - smoothing effect 300, 388, 413
  - SN by simple means 321ff
  - SN calculation (vinyl record) 204
  - SN calculation rules 321ff
  - SN (calculations) 49, 145, 297
  - SN-delta 321
  - SN guessing (via FFT) 590
  - SN measurements 102
  - SN of the MOTHER 213
  - SN relationship(s) 417
  - socket (valve) 378
  - soft start 689
  - solid-state devices 6
  - Solid Tube Audio 417, 738
  - solving approach 57
  - SON(S) 202
  - sound (& measurement & pressure) 332, 337, 340, 505, 586f, 601, 609, 618, 629, 676703
  - source 77
  - source resistor 85
  - source resistance (cartridge) 319
  - Sowter 180, 327f
  - specifications (MM cartridges) 284
  - spectral noise density 153, 202
  - spectral noise current density 34
  - spectral noise voltage density 34, 52, 108, 114
  - spot noise 367
  - Springer web site [www.springer.com](http://www.springer.com)
  - SRPP gain stage (JFET) 88f
  - SRPP gain stage (valve) 120, 126ff, 374ff
  - SRPP (valve) 120f, 368
  - SSM2210 63ff, 198f, 333, 337
  - SSM2017 174f, 683
  - SSM2220 63ff
  - SST Brüggemann 144, 202ff, 703
  - stamper 202
  - standard cartridge 303
  - step-up transformer 7, 151, 180ff, 319
  - stereo 18
  - stereo equalizer 418
  - stereoplay 142, 217ff, 320, 341, 586, 631f, 739
  - Stockfish Records 202f, 703
  - stray-C 508, 511, 517
  - Studer 601
  - succ-apps 375, 404, 410
  - succ-apps approach (RIAA) 512
  - successive approximation (RIAA) 512
  - subsonic 289
  - sum of A-weighted SNs 216f
  - sum of two SNs 217, 683
  - summary (on FFT measurement) 581f
  - summary (on hum figure) 628
  - summary (on measurement methods) 571
  - summary (on MM cartridges) 305
  - summary (on valves) 415ff
  - summary tables 703f
  - suppression of noise 134
- T**
- Talema 337
  - tangents 98
  - Taylor, E. F. 329
  - Taylor, F. 595, 738
  - Teldec 203, 206ff, 217, 220, 222
  - Telefunken (+ Decca) 203, 205
  - Telefunken Labor Buch 95, 738
  - Texas Instruments 176
  - temperature 32, 62, 332, 340
  - temperature (influence of) 304
  - test and calibration record 20ff
  - test circuit (capacitances) 336
  - TESTfactory 586, 631
  - test gain-stage(s) 372
  - test magazines 333
  - test record 5, 19ff, 303



test terminal 560ff  
Texas Instruments 66  
That Corporation 66  
That 300 63ff, 177  
That 320 63ff, 177  
That 1648 687  
thermal noise 31  
Thorens TEP3800 632  
threshold voltage 89ff  
third octave 202ff  
Tietze, U. 737  
time constants 9ff, 14, 340, 405, 505, 519, 526  
toroidal transformer 300, 337  
Toshiba 65  
TQ2-12V relay 679  
trackability test record 5, 303  
transfer factor (cartridges) 214  
transfer function 49  
transfer function producing networks 591  
transfer of impedances 181  
transfer plot 9  
transformer 7  
transformer capacitance 183  
transformer classification 181  
transformer equation (ideal) 181ff  
transformer equation (real) 183ff  
transformer frequency response 180  
transformer inductance 183  
transformer input situation 412  
transformer phase response 180  
transformer solution 327ff  
triode constants 110, 123, 135, 402, 416  
triode constants data 135  
triode driven 151, 367ff, 672, 691  
triode equation 111  
triode noise model 95f  
triode noise production 135  
triode noise resistance 96, 410  
triode noise voltage 97ff  
triodes 95ff, 367ff  
T/S 31  
TSD15 (EMT) 203, 214  
TSR-1005 21  
TSR-1007 23  
Tube CAD Journal 101, 739  
tube data (internet) 738  
tubes 95ff  
turns ratio 179  
turn-table 3  
Twin-BNC 332, 676

**U**

un-balanced - balanced conversion 681  
un-balanced input 7  
un-balanced solutions (RIAA network) 506  
un-bypassed 86, 107, 109ff, 369  
un-bypassed cathode resistor 107, 121  
un-loaded 109  
uncorrelated 36, 291  
un-equalized 634  
UPGR 290, 560ff, 602  
US standard 8

**V**

valve control figure 97  
valve constants 375, 379  
valve manufacturers 139  
valve manufacturing industry 105  
valve noise model 95f  
valve power supplies 141ff  
valves 6, 95ff  
Valves Pocket Book 106  
Valvo 106  
van den Hul 201  
velocity 19ff, 201ff, 214  
vertical modulation 17  
Vierzen, R. M. van 66, 221  
vinyl record ix, 201ff, 520, 617, 703  
vinyl record noise 201ff  
vinyl record reference levels vii, 17ff  
Vishay 51, 410  
Vitelec 332, 676  
VMS-80/DMM 202, 212  
voltage divider(s) 42, 74, 112f, 118f, 189, 196, 221, 292f, 327, 391, 399, 416, 511ff, 576, 597  
voltage feedback 67ff  
voltage feedback op-amps 153  
voltage potential 50, 369  
volume knob 31  
V15III 203  
V15V (MR) 3, 204, 396, 414, 687ff

**W**

Walker, H. P. 219, 283, 524  
Warner Music Group 203  
weighted 49  
weighted SN calculations 92  
weighting filters 49, 596  
weighting factor 322  
Weinzierl, S. 738

WEKA Media Publishing 586  
white-noise 33, 103  
white-noise based (meas. results) 568  
white-noise character 214  
white-noise generator 580  
white-noise level 620  
white-noise region 80, 96  
Whitlock, B. 601  
Williams, A. 595, 738  
Wilson current mirror 329  
WIMA (polypropylene capacitor) 340, 372  
WIN98 560  
wiring 332  
Wireless World x  
wobble speed 600f  
Wonneberg, F. 738  
worsening factor 102, 140  
worsening figure 140

worst case SNs (records) 215ff  
wyciwym viii  
wyciwym approach (final) 607ff

**X**

XLR 332, 676

**Y**

Yageo 372

**Z**

Zwicky, F. 381  
Zwicky approach 381ff  
Zwicky matrix 382

# Index TSOS-E

(Subjects and Personality's Names)

## Numbers & Symbols

1:1 83  
1:10 101  
1/f-noise  
- Amp1 23,  
- Amp2 128ff, 132ff  
- Amp4 58  
- BJT 341, 344  
- CMS 234  
- DIFA 370, 372  
- other input stages 201  
- PMMA 247, 251, 274  
180° 53  
19" 5  
19" 3 UH-42 HP 11ff  
19" 3 UH-84 HP 11ff  
2SA1316 BL 125ff  
2SC3329 BL 125ff, 190  
2SJ74 199  
2SK170 199  
2-pham 6  
3-pham 7, 165  
317 (LM) 15  
337 (LM) 15  
2798 168  
5534 125, 188ff  
6922 21  
7308 21

## A

Aalen (university) 170  
Abbreviations xvii  
absolute temperature 342  
AD797 188ff, 274  
admittance(s) 193  
AES (UK) 58  
AKG 169  
AI-box 269ff, 281  
alternatives (input resistors) 141  
Amp1 6, 101ff, 101ff  
- CMRR 103f  
- gain calculation 102f

- noise calculation 104f  
- SN calculation 105  
Amp2 6  
- CMRR 127  
- gain calculation 125ff  
- noise calculation 127ff  
- SN calculation 137ff  
Amp3 6, 21ff  
- CMRR 21  
- gain calculation 25f  
- noise calculation 27f  
- SN calculation 27f  
Amp4 6, 49ff  
- CMRR 49, 55f  
- gain calculation 52ff  
- noise calculation 56ff  
- SN calculation 60f  
Amp5 6, 25, 28, 83ff  
- CMRR 86  
- gain calculation 83f  
- noise calculation 86f  
- SN calculation 89  
amp  
- central 7ff  
- differential 365ff  
- input 7  
- microphone 49  
- sequence 51  
- -stage, no-noise 23  
amplifier  
- chain(s) 167f  
- differential 52  
- instrumentation 53  
- measurement 247, 275  
- transconductance 199  
amplifying devices 6  
anode 193  
anode output 252, 254  
Analog Devices 49, 128  
anechoic chamber 170  
Appendices xv  
AP 248, 254, 274  
AP system 233  
arrangement(s), loudspeaker 168  
artefacts  
- distortion 238  
- harmonic 183  
- intermodulation 183  
- sideband 238  
Atwell, Bob 49

audible effects 167ff  
 audio band 128, 155  
 Audiomatica 233  
 Audio Note 190  
 Audio Precision 233, 247  
 auxiliary (PFMA gain) 279  
 average  
 - (noise voltage) 61  
 - density value 28  
 - level 248  
 - value 189  
 averaging 266  
 A-weighted 5, 28, 51, 61, 89, 140, 247,  
 274, 312, 317  
 A-weighting 104  
 A-weighting function 28, 61

## B

balanced  
 - fully vii, 5  
 - gain 26, 54  
 - input capacitance(s) 8  
 - input load 58  
 - inputs 5  
 - line 277  
 - output noise 88  
 - outputs 5  
 Bark 168  
 base-emitter resistance 342  
 base-spreading resistance 130ff  
 basic consideration(s) 6  
 bass control 181  
 BC550C 190  
 BC560C 190  
 Beethoven, Ludwig van 168  
 benchmark 248  
 BF862 199  
 Biber Records 168  
 BJT driven 4, 187f  
 BJT noise model 128ff  
 BJT(s) 21, 28, 125ff, 254, 341ff  
 block, gain 195  
 block diagram 5  
 BNC 203  
 B & O 169  
 board, main 6  
 Boltzmann 342  
 booster(s) 126f, 239  
 BRAUN 169, 385ff  
 BRAUN+Design Tax 385, 387  
 BRAUN PCS 52 E 385  
 BRAUN TG 385

Breden, Russel 169  
 brick wall 248  
 broadband 6  
 BTFMI 387f  
 budget, low 249  
 BUF634 188  
 Burosch, Klaus 23  
 Butterworth 248

## C

cable capacitance 252, 307  
 calibration records 385ff  
 capacitance, input 307, 313, 317  
 calculation, NF 134ff  
 capacitance, Miller 349ff  
 capacitance(s) 9, 201, 307  
 capacitance(s), balanced input 8  
 capacitance, cable 252, 307  
 cartridge, standard 310ff, 317  
 case(s) 5, 11ff  
 case, insertion 11  
 cathode 193  
 - follower 9  
 - load 26  
 - output 252  
 - resistor 254  
 cathodyne phase splitter  
 CCIF 238  
 CCS 191  
 CCSCF 21  
 CCSi 25, 28  
 CE (BJT) 341ff  
 center section 6  
 central amp 7ff  
 ceramic 8, 141  
 CF 21  
 CF gain 26f  
 CGS 25, 28  
 channel, left 11  
 channel, right 11  
 Chebyshev 266  
 Cinch 203  
 CLIO 30, 51, 89, 233ff, 243  
 clipping 23, 49  
 closed-loop 137  
 CMR 64  
 CMRR 181  
 - Amp1 103f  
 - Amp2 127  
 - Amp3 21, 25  
 - Amp4 49, 55f, 61  
 - Amp5 86

- PMMA 256, 258, 261, 268
- PFMA 275, 278
- DIFA 366, 371
- CMRR, lousy 51
- CMS 247, 275
- CM voltage 89, 103
- C-multiplier(s) 239
- Cohen, Graeme John 58
- coil(s) 101
- coil resistance(s) 277
- collector
  - current 25, 342
  - current, operating (DC) 132
  - -emitter resistance 342
  - noise current 130, 189
- common
  - cathode stage 191, 252
  - emitter (CE) 341ff
  - grid stage 28, 191, 252
  - mode gain 256
  - mode input 372
  - mode rejection ratio 6
- comparisons 3, 6
- complementary (BJTs) 125ff
- concertina phase splitter 191
- condition(s), equal 6
- connection, input 7
- Connelly, J. A. 59, 393
- consideration(s), basic 6
- concept, general 5
- configuration 5
- constant current sink 25
- constants, physical xxv
- Contents ix
- converter, DA (NAD) 247
- converter, un-balanced to balanced 105
- cooling, resistor 309
- corner frequencies (1/f-noise) 25, 58, 128ff
- correlated, noise voltage(s) 25, 28, 59, 61ff, 102, 261
- Cordell, Bob 199ff
- CPS 191, 193
- C-R-C chain 20
- current, collector 25, 342
- current, DC 21
- current, emitter 189
- current gain, DC 130, 342
- current gain, operating 132
- current generator 21
- current sink (constant) 21, 25
- cutting head 385
- cutting lathe 385, 390

**D**

- DA converter (NAD) 247
- data sheet data 130ff
- DC current 21, 125
- DC current gain 130, 342
- DC resistance 101
- DCS 195
- DC servo 108, 195ff, 269, 274, 372
- DC voltage 125
- decade(s) 345
- DDR 386
- Denon 104, 168
- density, noise current all chapters
- density, noise voltage all chapters
- dependent, frequency 10
- Design + Design 169, 385
- designer(s) 183
- Deutsche Grammophon 168
- Deutsche Grammophon (TCRs) 386ff
- development examples 195ff
- deviation 24
- deviation (calculated) 51
- devices, amplifying 6
- Didden, Jan 23, 247
- DIF (amp) 21, 25, 64, 316f, 365ff
- DIFA 365ff
- DIFA-IC 365
- DIFA-OPA 365ff
- DIFCF 26
- DIFCF, noise calculation 27f
- DIFCF, SN calculation 27f
- DIF gain 25ff
- differential
  - amplifier 52, 365ff
  - gain 52f, 195, 258, 365ff, 365ff, 370
  - gain stage 21
  - mode (fully) 195
  - output 25. 54
  - o/p resistance 24
- DIN 5, 126, 237f
- DIN (TCRs) 386ff
- distortion 236ff
  - artefacts 238
  - level 5f
  - low- 6
  - spike level 23
- DL-103 (Denon) 104, 168
- DL-103 R 197ff
- DMM 186
- DMM cut 5
- double-relay(s) 181

double triode 14, 20f, 28, 169  
 draft design(s) 187ff  
 dual JFET 199  
 DUT 234ff, 241, 247ff, 252ff, 263, 277

## E

E188CC 21  
 E88CC 21ff, 175, 192  
 Early voltage 342  
 ECC88 169, 175  
 ECM 168  
 effects, audible 167ff  
 effects, visible 165ff  
 EIN 272f  
 Elektor 394  
 electron charge 342  
 Electronics (Wireless) World 169, 394  
 Elektronik 49  
 ELS 309ff  
 emitter current 189  
 emitter load(s) 137  
 ENB 274  
 enclosure (PMMA) 269, 281  
 encoder, RIAA 165, 168, 243  
 Engine I vii, 6, 21, 183  
 Engine II viii, 3ff, 6, 183  
 Engine II results, summary 176ff  
 environment, low resistive 125  
 equal condition(s) 6  
 equalized, non- 23  
 equivalent noise model (BJT) 343  
 equivalent noise source(s) 130  
 Ermer, Florian 170  
 ESL 57 169  
 euphonic harmonics 193  
 EW 309  
 examples, development 195ff  
 excess noise (resistor) 345  
 extension, TSOS vii  
 external input viii, 5, 187

## F

FC 63V 24  
 female, strip connectors 84  
 FET(s) 170, 195ff, 254  
 FFT diagram 20, 23, 248  
 FFT resolution 234, 248, 266  
 FFT size 234, 248, 266  
 Figures (listing) xxvii  
 filter, measurement 266  
 fisher (company) 11  
 flat 5

flatness 24  
 flexibility 7  
 flicker-noise 128ff, 344  
 Floru, Fred 58  
 FM tuners 385  
 Focal Press 125  
 Frederiksen, Thomas M. 393  
 frequencies, high 7  
 frequency dependent 10, all chapters  
 frequency independent 10, all chapters  
 frequency response(s) 5, 105ff, 165ff  
 Friedemann 168  
 front 13f  
 fully balanced vii  
 fully passive 5, 7

## G

gain  
 - Amp1 102f  
 - Amp2 125ff  
 - Amp3 25f  
 - Amp4 52ff  
 - Amp5 83f  
 - balanced 26, 54  
 - BJT 347ff  
 - (BJT driven) 188f, 341ff  
 - block(s) 195  
 - CF 26f  
 - common mode 256  
 - current 342  
 - (Cordell) 199f  
 - DIF 25ff  
 - differential 52f, 195, 258, 365ff, 370  
 - (Gerhard) 195  
 - idle (BJT) 347ff  
 - loss 103  
 - -loss 251f  
 - noise 371  
 - (noise reduction) 312, 316  
 - nominal 5, 125  
 - operating (BJT) 348ff  
 - (PFMA) 275, 278  
 - (PMMA) 258  
 - (Popa) 197f  
 - overall 125, 249  
 - transformer 103  
 - (transformer driven) 190  
 - (triode driven) 194  
 galvanically isolated 7, 275ff  
 galvanic isolation 275  
 GDR 386  
 German Democratic Republic 386  
 generator, current 21

generator output resistance 103, 105ff  
 Gerhard, Joachim 195ff, 370  
 Gevel, Marcel van de 309  
 goals 3f  
 goal, worsening 254  
 ground  
 - lead, PSU 189  
 - lift(s) 15, 278  
 - line 189  
 - loop 268, 275  
 grounded grid 25  
 grounding 15  
 gyrator(s) 239

## H

half (N, P) 133ff  
 harmonic(s) 241  
 harmonic artefacts 183  
 harmonics, euphonic 193  
 headphone 168f  
 heater PSU, triode 18  
 heater supplies 20  
 Herbert, Gary K. 58  
 HiFi equipment 248  
 high frequencies 7  
 high-frequency (cut) 252  
 high-quality 6  
 high-Z 196, 199, 201  
 hints (PMMA) 264ff  
 Hoeffelman, Jean M. 307  
 HP21 195  
 HP5.1 197  
 HTGG-2 394  
 hum 6, 266  
 hum-free 247  
 hum interference(s) 188, 266

## I

### IC, measurement 256

idle gain (DIF) 26  
 idle gain(s) BJT 347ff  
 IEC 468 248  
 IMD 6, 23, 51, 89, 169, 171ff, 181, 237f  
 impedance, input load 139  
 improvements 269  
 INA 53, 256, 261  
 independent, frequency 10  
 Index TSOS-1 397  
 Index TSOS-2 403  
 Indices xv

input  
 - alternative 7  
 - amp 7  
 - capacitance(s) 8f, 307, 313, 317  
 - common mode 372  
 - connection 7  
 - current 49  
 - external viii, 5  
 - load 23, 104  
 - load, balanced 58  
 - load impedance 139  
 - reference level 191  
 - resistance(s) BJT 347ff  
 - resistance(s) 7, 103, 137, 249, 251ff  
 - resistors (alternatives) 141  
 - section 6  
 - stage, paralleled 256  
 - transformer 101, 181  
 - voltage divider 51  
 - voltage, transformer 101  
 insertion case 11  
 instrumentation amplifier(s) 53, 256, 357  
 integrated stabilizing circuit 20  
 interference(s), hum 189, 266  
 intermodulation artefacts 183  
 intermodulation level 6  
 isolated, galvanically 7  
 isolation, galvanic 275  
 ITU-R 238

## J

JAES 307  
 Jarrett, Keith 168  
 Jensen Transformers Inc. 84, 187,  
 268, 275, 278  
 JFET(s) 197ff  
 JFET driven 4, 197  
 JFET, dual 199  
 JJ 175  
 JT-10-KB-D 275  
 JT-346-AXT 190  
 jumper(s) 262, 314

## K

Karajan, Herbert von 168  
 Kempff, Wilhelm 168  
 kernel (BJT) 130f  
 Kirkwood, Wayne 58  
 Klatt, Jo 169, 385  
 Kraftwerk 168  
 Krieger, Daniel 390

**L**

LA 274  
 lathe, cutting 385, 390  
 LE 1 169  
 LED 11  
 left channel 11  
 level, average 248  
 level, output 83  
 light-pattern measurement instrument 390  
 linear amps 5  
 linear amps 187  
 linear amp stage(s) 5  
 Linear Audio 15, 23, 170, 193, 195ff,  
 247f, 395  
 Linkwitz 169  
 listening test(s) 167ff  
 list of figures xxvii  
 list of tables xxxvii  
 LF411 188ff  
 LL9226, Lundahl 101, 191  
 LSK389 199  
 load, cathode 26  
 load-effect 307  
 load resistor 254  
 load(s), emitter 137  
 load synthesis 309  
 loss, gain 013  
 loudspeaker 169  
 loudspeaker arrangement(s) 168  
 loudspeaker chain(s) 167f  
 low budget 249  
 low-distortion 6  
 low-end (audio band) 165  
 low-hum 20  
 low-noise 6, 20, 49  
 low-pass role 252  
 low resistive environment 125  
 low-THD 49  
 low-Z 196  
 LP vinyl record 5  
 LT783KC 20  
 LT1028 102, 256ff, 271, 275, 278  
 LTE(s) 193, 198  
 LTP 201  
 Lundahl 103  
 Lundahl LL9226 101, 191

**M**

MA 247ff, 252ff, 275  
 magnitude 9, 251  
 main board 6, 12, 20, 84  
 main board wiring 19  
 mains connections 15

mains interferences 20  
 main PCB 15ff  
 margin, overload 5  
 Mathcad worksheet(s) viii  
 mathematical sizes xxv  
 Matsushita 181  
 Mayer-Schüller-Theory 170  
 MC cartridge load(s) 101ff  
 MC cartridge(s) viii, 3  
 MC pre-amp 125  
 MC purposes 5ff, 29, 187  
 measurement amplifier 247, 275  
 measurement filter 266  
 measurement IC 256  
 measurement instrument, light-pattern 390  
 measurement instrument, tracking force 385ff  
 Measurement tools 233ff  
 Meys, René P. 307  
 microphone amp(s) 49, 58, 180  
 middle control 181  
 Miller capacitance 349ff  
 mix (noise levels) 183  
 MKS 189  
 MKT 189  
 MM cartridge(s) viii 4, 307ff  
 MM purposes 5, 29, 187  
 MM, standard model 307f  
 mode, differential (fully) 195  
 model, operational (BJT) 354ff  
 model(s), noise (BJT) 356ff  
 Module 4 21  
 Module 2 125ff, 188, 341  
 Mono record 168  
 MST 170  
 Motchenbacher, C. D. 59, 393  
 Musikverein (Vienna) 168  
 mutual conductance 131, 193, 342  
 mutual conductance, reduced 137

**N**

N (noise) 236ff  
 NAD M51 247, 274  
 Neef, Ulrich 389  
 network, R-C 101  
 network(s), RIAA 6  
 Neumann 385  
 Neutrik 203  
 NF(s) 29, 62, 104f, 274, 344  
 NF charts 132ff  
 NF calculation 134ff  
 NF-picking 137, 140  
 NF values 132ff  
 N-half 133ff



- noise
  - (BJT) 349ff
  - calculation(s) 56ff, 86f, 127ff
  - calculation, DIFCF 27f
  - current all chapters
  - current, collector 130
  - factor 345
  - figure 29, 62, 344, 346
  - flicker- 128ff
  - gain 371
  - index (resistor) 345ff
  - low- 6
  - model(s), BJT 128ff, 343, 355ff
  - model (PMMA) 261ff
  - model (triode driven) 194
  - pink 168ff, 175
  - red 130
  - reduction 307ff
  - results 170f
  - shot 130
  - sources (DIFA-IC) 372
  - sources (DIFA-OPA) 368f
  - source(s), equivalent 130
  - test 168
  - voltage(s) 27f, 279
  - voltage density all chapters
  - voltage, correlated 25, 28, 61ff, 102, 261
  - voltage, un-correlated 28, 59f
  - white 23, 128
- nominal gain 5, 125
- nominal output level 83
- nominal signal level 6
- non-equalized 23
- no-noise amp-stage 23
- no-noise arrangement 62
- non-shielded 181
- NOS 23, 175
- NPN 341
- NPN-half 197
  
- O**
- Occam's Razor 254, 313
- OP27 51, 102, 275
- OPA1632 54
- OPA627 6, 51, 255
- OPA827 255
- op-amp driven 4
- op-amp output 252
- op-amps, quadruple 49
- operating collector current (DC) 132
- operating current gain 132
- operating gain (BJT) 348ff
- operational gain (DIFA) 366f
- operational model (BJT) 354ff
- o/p resistance, differential 24
- o/p resistance(s) 24
- oscillation, wild 109, 141
- output
  - anode 252, 254
  - cathode 252
  - differential 25, 54
  - level 83
  - level, nominal 83
  - load, transformer 101
  - op-amp 252
  - resistance 7f, 10, 29, 49, 243, 247, 251ff, 272f
  - resistance, generator 103, 105ff,
  - resistance(s) (BJT) 347ff
  - resistance(s), triode 7, 193
  - stage(s) 49, 200
  - transformer 6, 83, 88, 165
  - un-balanced 83
  - voltage swing 49, 52
  - voltage, transformer 101
- overall gain(s) 125, 249
- overload 312
  - (PMMA) 269
  - goal 7, 23
  - margin 5, 23, 49, 83
  - question 7
  - requirement 6
  - situation 126
  - threat 126
- overview, Engine II 3
  
- P**
- pair, value 134
- Panasonic 24, 181
- Panasonic FC 189
- paralleled input stage 256
- parallel operation 193
- passive, fully 5ff
- Pauler acoustics 168
- PCB(s) 11ff, 84, 109, 141, 181
- PCB, main 15ff
- PCI 233
- PCS 52 E, BRAUN 385
- performance (PMMA) 266ff
- PFMA 240f, 266, 268, 275ff
- P-half 133ff
- pham, 2- 6
- pham, 3- 7, 165
- phase

- response(s) 5, 105ff, 165ff
- shift 53, 365f
- splitter, cathodyne 191
- splitter, concertina 191
- piano 168
- picture(s) 11ff
- pink noise 168ff, 175
- Pioneer 168
- phenomenon, transient 127, 141
- phono-amps 6
- physical constants xxv
- PL-L 1000 168
- plugged-in 12ff
- plug-in 84
- PMMA 235, 240f, 247ff, 254ff, 264ff, 275
- PNP 341
- point(s) 5
- polypropylene 189
- Popa, Ovidiu 197ff
- post-measurement work 233
- pot, trimming 7
- power supply 5, 84f
- pre-amp(s) 29, 61, 181, 187ff
- pre-amp, MC 125
- pre-pre-amp 197
- primary 104
- printed circuit board(s) 12ff
- PSRR 269, 281
- PSU 5, 11ff, 15, 167, 281
  - ground lead 189
  - (PMMA) 269
  - soli-state 16
  - triode 17
  - triode heater 18
- psychology 184
- Putzey, Bruno 274

## Q

- Quad 169
- quadruple op-amps 49

## R

- Rams, Prof. 169, 387
- ratio, common mode rejection 6
- ratio, signal-to-noise 5
- Razor, Occam's 254, 313
- Razor (personal) 390
- Razor (Vogel's) 184
- R-C network 101
- rear 13ff
- record, Mono 168
- record(s), calibration 385ff

- record specifications 394
- record(s), test 168, 385ff
- recording studio 183
- red noise 130
- reduced mutual conductance 137
- reduction, noise 307ff
- reference level, input 191
- reference signal 390
- regulated 5
- relay(s) 6
- requirements 5
- resistance(s)
  - base-emitter 342
  - base-spreading 130ff
  - collector-emitter 342
  - input 7, 103, 137, 249, 251ff
  - coil 277
  - output 7f, 10, 243, 247, 251ff, 272f
  - output (BJT) 347ff
- resistor, cathode 254
- resistor cooling 309
- resistor, load 254
- response, frequency 5
- response, phase 5
- result(s) (draft designs) 201ff
- results, Engine II 176ff
- results, noise 170f
- Revox A77 385
- RIAA
  - encoder 165, 168, 244
  - equalized 5, 62, 140, 312, 317
  - equalization 104
  - network(s) 6, 24, 49
  - transfer 104
  - transfer function 5f, 26f, 54f
  - voltage divider 51
- Richter, Svatoslav 168
- right channel 11
- Riley 169
- ringing 141
- RMMA 274
- Rohde und Schwarz (R&S) 247
- role, low-pass 252
- roughly 195
- R&S 254
- rule-of-thumb 195, 260

## S

- S-AES17 248, 274
- sample rate 234, 266
- Schaltungstips 49
- Schenk, C. 393
- Schüller, Peter 170

SC-02 233  
 secondary 104  
 section, center 6  
 section, input 6  
 Seelmann, Prof. 170  
 Self, Douglas 125, 187f, 239, 248, 309, 393  
 sengpielaudio 394  
 sequence 7  
 sequence, amp 51  
 sequence connected 9  
 servo, DC 108, 195ff, 269, 274, 372  
 shielding 266, 271  
 shot noise 130  
 Shure viii  
 Shure V15 IV 385  
 Shure V15 V 194  
 sideband artefacts 238  
 Siemens 169, 175  
 signal chain 5  
 signal conditioner 233  
 signal level, nominal 6  
 signal path(s) 7, 9  
 signal-to-noise ratio(s) 5, 234ff, 346  
 single ended 101, 181  
 single-ended intermediate vii  
 sink, current (constant) 21, 25  
 situation, overload 125  
 size(s), mathematical xxv  
 slew rate 5, 181  
 SLOA054D (TI) 371  
 slope 130ff  
 slope figure 130ff  
 small signal 341f  
 SME II 385  
 SMPTE RP120 238  
 SN 5  
 SN (BJT) 346  
 SN calculation(s) 60f, 86f, 137ff, 260ff, 279f, 317  
 SN calculation, DIFCF 27f  
 SN improvement figure 23  
 solid-state 7  
 solid-state PSU 16  
 sound 6, 167ff  
 source(s) 6  
 spike(s) 165f, 241, 266  
 spike level, distortion 23  
 SSM2142 275  
 SSM2210 128  
 SST Brüggemann 390  
 stabilizing circuit 20  
 stacked 20  
 standard cartridge 310ff, 317

standard Model, MM 307f  
 stereo (use) 11  
 stereoplay 247, 387  
 strip connectors, female 84  
 studio, recording 183  
 sub-net 7  
 subtractor(s) 53, 56, 59f  
 subtraction stage 262  
 subwoofer 169  
 succ-apps 137  
 successive approximation 137  
 summing stage 262  
 summary results, Engine II 176ff  
 switchable 6  
 switches 20  
 switching possibilities 13  
 symbols xvii  
 synthesis, load 309  
 SYS 2722 248, 274

## T

tables (listing) xxxvii  
 Tchaikovsky 168  
 TCR(s) 385ff  
 temperature (T) 130, 309  
 temperature, absolute 342  
 test-board (case) 244f  
 test(s), listening 167ff  
 test noise 168  
 test point(s) 125  
 test record(s) 168, 385ff  
 Texas Instruments 371  
 THAT Corp. 58  
 THAT1646 275  
 THD 6, 23, 89, 169, 171ff, 181, 236ff  
 THD + N 23  
 THD performance (UBC) 241ff  
 Third octave 168  
 thread, overload 126  
 TI Application 371  
 Tietze, U. 393  
 time constant(s) 7f, 51  
 tonearms 3  
 tools, measurement 233ff  
 Toshiba 124, 132  
 TQ2 181  
 tracking force (measurement instrument) 385ff  
 Trafo 23  
 transconductance 13  
 transconductance amplifier 199  
 transfer function, RIAA 5f, 26f, 55  
 transformer(s) 7, 182

- driven 4, 187
- gain 103
- house 167
- input 101, 181
- input voltage 101
- output 6, 83, 88, 165
- output voltage 101
- output load 101
- transient phenomenon 127, 141
- transit frequency (BJT) 128
- treble control 181
- Trimming 233ff, 244ff
- trimming possibilities 5
- trimming procedure 191
- trimming pot 7
- triode 254
  - driven 187
  - heater PSU 18
  - output resistance 7
  - PSU 17
  - system(s) 21, 23
- TSOS extension vii
- TSOS-1 3, 394
- TSOS-2 3, 394
- tubecad 395
- tubedata 394
- turns ratio(s) 102ff, 190
- turntable(s) 3, 168
- Tyler, Les 58

## U

- un-balanced vii
  - connectors viii
  - inputs 5
  - output 83, 88f
  - to balanced converter 105, 168
- UBC 105, 165, 236ff, 239ff
- un-correlated, noise voltage 28, 59f

## V

- value pair 134
- valve 7

- valve driven 4
- Vatter, Martin 168
- VC-A 199
- VEB-Deutsche Schallplatten 389
- velocity 5, 390
- Vienna Symphony Orchestra 168
- Vierfach Op-Amps 49
- vinyl vii
- visible effects 165ff
- voltage divider 243, 252
  - effect(s) 105, 193, 251
  - input 51
  - RIAA 51
- voltage swing, output 52
- volume knob 180

## W

- Walton, John 15
- white noise 23, 128, 247f, 341
- Whitlock, Bill 268
- Whitt, S. 239
- wild oscillation 109, 141
- WIMA 189
- WIN 2k 233
- WIN 7 233
- WIN XP 233
- winding(s) 277
- Wily-Interscience 59
- Wireless World 239, 394
- wiring, main board 19
- wobbling 168ff
- Worsening Figure 201, 234ff, 250f, 254, 272ff
- worsening goal 254

## X

- x (slope figure) 130ff
- XLR 203, 266, 277

## Y

- y (slope figure) 132ff
- Yaniger, Stuart 193